

# **Tectonics and sedimentation of early continental collision in the Eastern Mediterranean (Northwest Syria).**

Mathew Francis Hardenberg

BSc (Hons)(Lon), MSc (Abdn)



Thesis submitted for the degree of Doctor of Philosophy

University of Edinburgh

2003

## **Declaration**

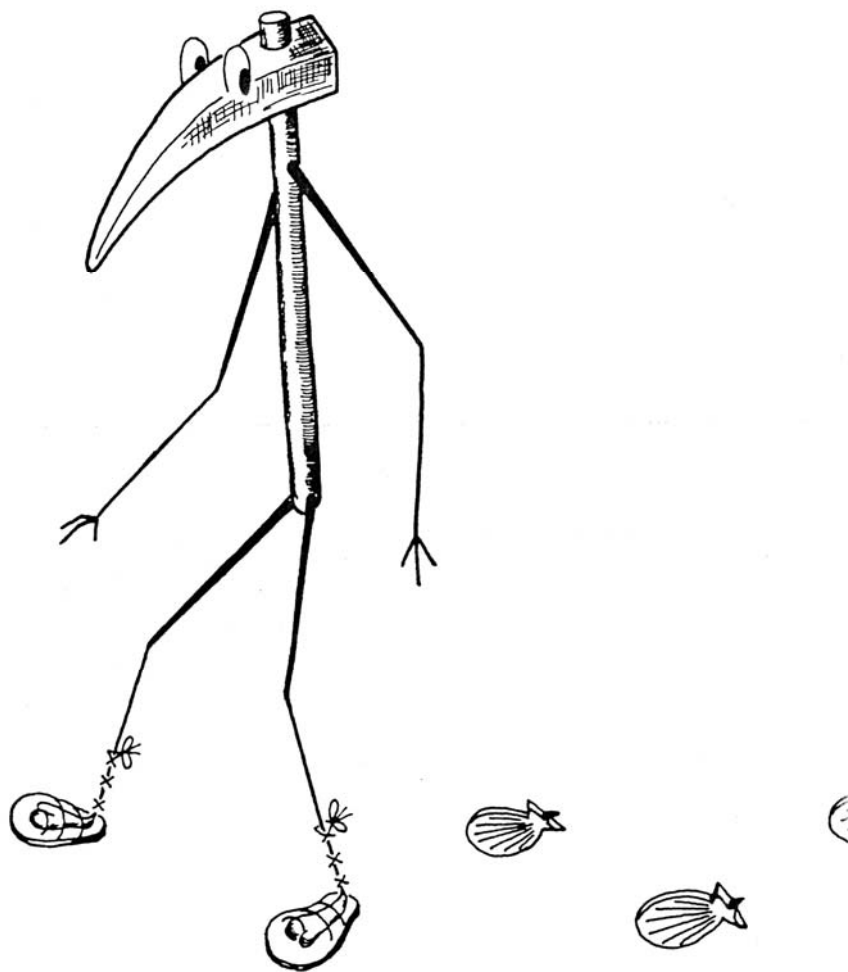
I declare that this thesis is my own work unless explicitly stated, and that all other contributions have been acknowledged.

Mat Hardenberg, 2003

*"One never notices what has been done;*

*One can only see what remains to be done."*

*Marie Curie, in a letter to her brother (1894).*



ANON

## Abstract

The northeastern margin of the African plate, in the Latakia region of northwest Syria, has an important bearing on the closure and collisional history of the Tethys Ocean in the Eastern Mediterranean region. This field-based study focuses on the Tertiary geology of the Nahr El-Kabir basin and provides new insights on the sedimentation, biochronology, structure and regional tectonics of the area.

Three unconformity-bound megasequences of Late Cretaceous to Tertiary age are identified, which were strongly influenced by tectonic processes: 1. Late Maastrichtian-Mid Eocene; 2. Miocene; 3. Late Miocene (Messinian)-Late Pliocene. Megasequence 1 was initiated by a Late Maastrichtian-age marine transgression over Maastrichtian-emplaced ophiolitic rocks and melange (Baer Bassit Massif). Water depths increased in the Palaeocene, giving rise to outer-shelf-depth carbonate deposition, rich in planktic foraminifera. Marine high productivity is reflected in common diagenetic chert formation. Nummulite-rich carbonates accumulated on a shallower shelf during Early-Mid Eocene time. Shallowing of marine conditions, coupled with tectonic instability, culminated in emergence, followed by a Late Eocene-Oligocene hiatus. Megasequence 2 is spatially restricted to the Nahr El-Kabir Graben and begins with Early Miocene carbonate deposition of mainly pelagic facies. In the Middle Miocene, there was an increasing input of basin margin-derived high-density turbidites and debris flows. Minor ongoing tectonism was followed by regression during the Messinian salinity crisis. Megasequence 3 begins with the accumulation of mainly laminated gypsum, followed by gypsum debris flows and selenitic gypsum. Initial Pliocene transgression led to shallow-marine, open-shelf muddy sedimentation, shallowing up, prior to the Late Pliocene into marls and bioclastic carbonates. Late Pliocene-Quaternary time was marked by progressive uplift, marine and continental terracing and erosion.

A Maastrichtian to Paleogene submerged shelf succession on the Arabian Platform culminated in a regional hiatus during the Late Eocene-Oligocene. Early Neogene rifting led to development of a transtensional basin (the Nahr El-Kabir Graben, a probable half graben). Strike-slip deformation (probably sinistral) and regional uplift followed during Late Neogene-Quaternary time.

The Miocene Nahr El-Kabir Graben developed along an important, inferred, transform fault system. The resulting El-Kabir Lineament demarcates the northern margin of the African Plate (Arabian sub-plate). The El-Kabir Fault links southwestwards with the southern Cyprus active margin and northeastwards with the Dead Sea Transform Fault and, thus, represents an important, previously unrecognised, segment of the Africa-Eurasia plate boundary.



## Acknowledgements

To get to a third degree without a holding down a real job for any length of time, I have relied on the help and support of many people. Over the last 3 years, the following, have made an immense difference to life and work:

I would like to *thank* Alastair Robertson for his endless patience, guidance and exemplary, not to mention timely, reviews of my work. As my supervisor you have challenged, motivated and expanded my desire to learn, throughout my time at Edinburgh University.

To John Dixon, I would also like to extend my *thanks* not only for your encouragement, but also for sending me on every overseas fieldtrip possible, that may or may not have had anything to do with Mediterranean or Tertiary geology. Marcel Bou-Dagher Fadel (UCL) and Sylvia Gardin (Paris) are *thanked* profusely for their dating of foraminifera and nannofossils, enabling an accurate timeframe for this work.

Fieldwork in Syria was very kindly permitted and supported by the General Establishment of Geology & Mineral Resources, Ministry of Petroleum and Mineral Resources, Damascus. Everybody I met from the Establishment extended such open friendship and hospitality; I am indebted to you all. *Thank you* to Dr Mohammed Talal Ballani, the General Director, for all your help to Khalil Al-Riyami, Dan Howard and myself. Dr's Mohammed Ali Humaidi and Mahamood Al-Ahmed, you provided excellent hospitality in Damascus, Latakia and Qaastal Maaf, making the fieldwork practical. Dr Hasan Abu Romieh and Randa Mohamed, *thank you* for supplying and setting up the seismology survey in the project area. Dr Adnan Al-Hafez and your team of fieldwork geologists, *thanks* for your excellent discussions and tour of the Ghab Graben. Adnan Tawil, *thank you*. Having survived my driving almost every road, track and pathway in northwest Syria with you over three field-seasons, I can count you as a true friend; you also had the sense to leave the car before the accident. I wish you and your new wife the best of happiness.

Syria Shell PD, provided logistical support for the project with sample transport and vehicles, which aided enormously the amount of fieldwork possible. *Thank you* to business managers Dr's Jan Beijering and Hans Bachmann, for your support. Dr's Nimir Arab, Georges Schoelcher and Maarten Lechner of the exploration staff, *thank you* for your help, interest and challenging discussions. I sincerely hope this work is useful. Haythem Betanjaneh, *thank you* for guiding me through the maze of car hire and ensuring my samples reached Edinburgh before me.

To NERC and the British Geological Society, *thanks* for your support throughout and especially with print submission of this thesis.

Long periods away from home and an inability to speak more than 50 words in Arabic were irrelevant, *thanks* to the friendship, amazing hospitality and food of Feras, Kalil, Samir and their families at Balloran village. To eat grilled chicken, or have coffee and narjilleh, by the lake on a warm night, whilst almost crying with laughter, night after night, is something I will never forget. I wish you all the best in life, congratulations on your forthcoming marriages and hope to visit again soon.

Edinburgh Royal Infirmary, Edinburgh Diabetic Clinic and Mountains for Diabetics are all *thanked* on a massive scale for literally picking me up, getting me back on my feet and then encouraging me to get out and on with an active life after my last field season. *Thanks* also to my friend Ed, cohort of many an adventure and munro, for giving up your snacks when I need them and providing haute cuisine in a tent, half way up a mountain.

In Edinburgh, I have been ably fed, watered, entertained and X-boxed by Theo and Christina, my flatmates. Khalil, Noah, Matt, Theo, Sarah and Sam made up the Tethyan Research Team (aka 'Club Med') during my time and it has been fun. *Thank you* also to girlfriends R, S, N and S for your company, a PhD is a selfish activity; I'm sorry things didn't work out and I hope you are all happy. During writing, I was challenged to stay late into the evening, writing 'just another page' by Solveigh, although as she was expecting, I felt it my duty to lose. *Congrats* to you, Richard and welcome Aneirin!

To Wind, Sand & Stars, *thank you* for repeatedly inviting me back to lead in the Sinai Desert, dragging me away from the relentless sunshine of Scotland, and having faith in my trip leading skills, especially after my diabetes.

Lastly, my biggest *thank you* is to my family. *Thank you* for getting me this far in life and for all your love, encouragement and support.

## Contents of thesis:

### ***Chapter 1 – Project introduction***

Introduction	1
Regional geography	1
Geological and plate tectonic setting	1
• <i>Figure 1.4</i> New geological map ( <b>pull-out version in Appendix 2</b> )	5
Summary of the plate tectonic setting of the Baer Bassit Ophiolite	9
Project aims	12
Project database and Arabic names	13
Thesis style	18
• <i>Figure 1.11</i> Key to figures ( <b>pull-out version in Appendix 2</b> )	19

### ***Chapter 2 – Literature review and previous work***

Previous work on the northwest of Syria	20
The mapping of Syria by the Russians	20
The Cretaceous succession and earlier units	21
Maastrichtian	22
The Paleogene	24
Danian	24
Palaeocene and Eocene	28
Palaeocene-Lower Eocene	29
Middle Eocene	30
Oligocene	32
The Neogene	33
Aquitania	39
Burdigalian	39
Helvetian (Langhian-Serravallian)	40
Tortonian	41
Helvetian-Tortonian undifferentiated	41
Messinian	41
Pliocene	42
Continental Pliocene	47
Quaternary	47
Supplementary data and structural synthesis	48
Tectonics	50
Summary and critic of previous work	55

### ***Chapter 3 – Sedimentology of the Tertiary successions***

Sedimentology and stratigraphy	57
Project biostratigraphy	57
Project time-slices	58
Biostratigraphic studies	59
Pelagic foraminifera	59
Nannofossils	61

Methodology of fieldstudies	63
Sedimentary rocks and time slices	66
Basement rocks	67
Time-slice 1 Maastrichtian to Lower Eocene	69
Time-slice 2 Middle Eocene	82
Time-slice 3 Aquitanian transgressive limestones	91
Time-slice 4 Burdigalian transgressive limestones	99
Time-slice 5 Langhian bioclastic limestone	104
Time-slice 6 Langhian-Serravallian debris flows	105
Time-slice 7 Serravallian-Tortonian regressive limestones	135
Time-slice 8 Messinian evaporites	136
Time-slice 9 Pliocene transgressive marls	141
Time-slice 10 Pliocene transgressive marls and eruptives	149
Time-slice 11 Pliocene regressive sandstones	152
Time-slice 12 Quaternary	152
Point counting	161
Diagenesis	163

#### ***Chapter 4 – Structural geology of the NW of Syria***

Structural data – Introduction	167
Structural data from fieldwork	167
Remote sensing	170
Regions in structural detail	179
El-Kabir Lineament	179
Offshore Latakia	193
Banyas	205
Jus Ash-Shaghour	209
Southern margin of the El-Kabir Graben	215
Faulting within the graben	224
Strike-slip faulting and Riedal shears	230
Summary	233

#### ***Chapter 5 – Regional geology of the Eastern Mediterranean***

Introduction	235
Polis Graben, Cyprus	235
Hatay Graben, Turkey	241
Adana Basin, Turkey	245
Ghab Graben, Syria	248

#### ***Chapter 6 – Discussion of results and tectonic models***

Introduction	257
Sedimentary processes and environments	257
Time-slice analysis	260
Palaeogeography	284
Structural history with relation to sedimentology	291
Supplementary data	293

Neotectonics	297
Geological history of northwest Syria	303
Tectonic implications	308
Tectonic evolution of the Latakia area, especially the El-Kabir Lineament	308
Comparison to regional geology of the Eastern Mediterranean	319
Diachronous collision?	319

## ***Chapter 7 – Project conclusions***

Conclusions	323
Diachronism	324
Wider applicability of results	326

## ***References***

## ***Appendix 1 – Project biostratigraphy***

## ***Appendix 2 – Pull-out geological map, location map and key***

## ***Appendix 3 – Fieldwork localities***

## Introduction

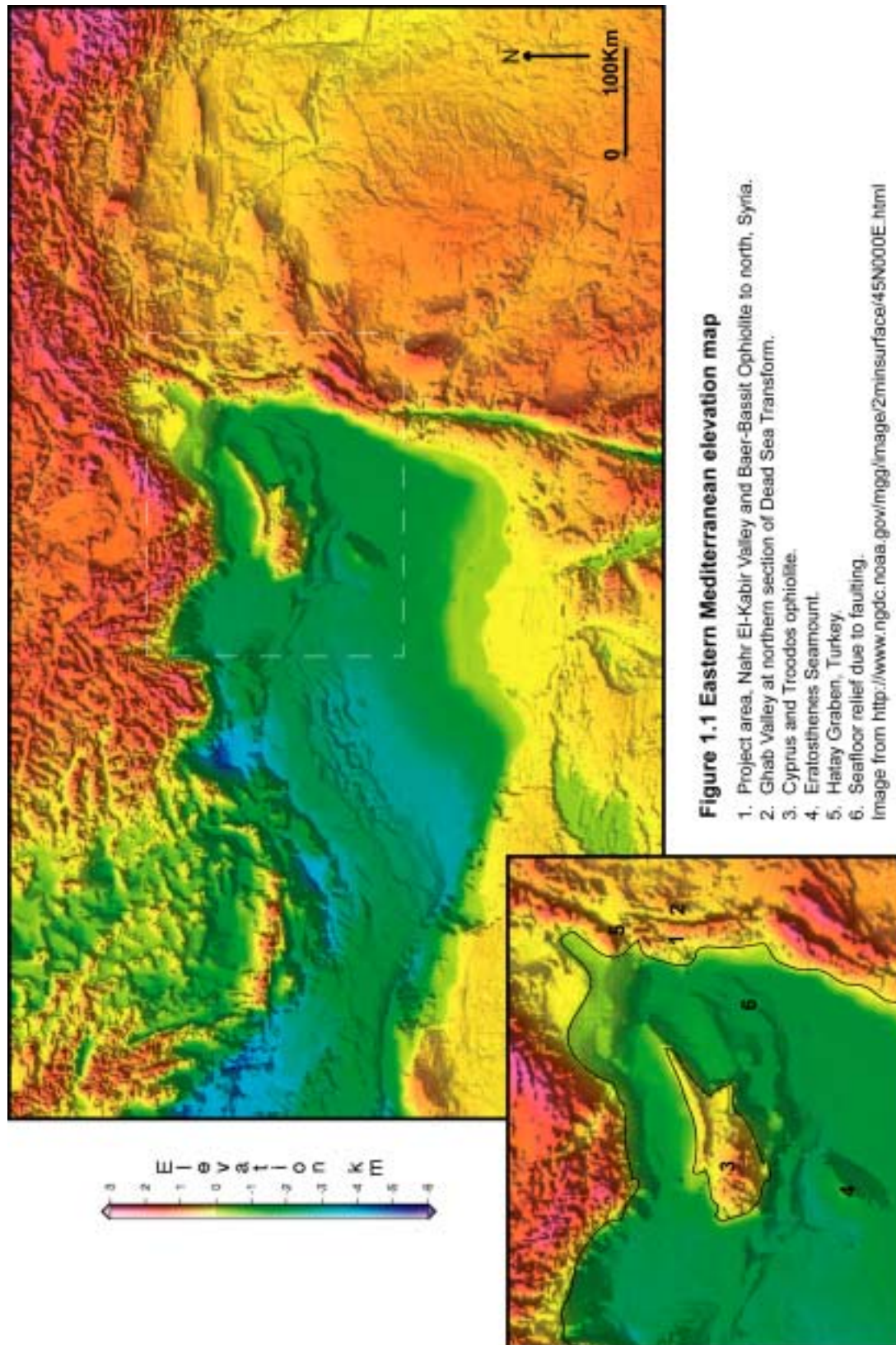
The study area of this project is the coastal strip of Syria bordering the Mediterranean Sea between Lebanon and Turkey (Figure 1.1). The town of Banyas in the south (35km north of Lebanon) and the village of Kassab, on the border with Turkey to the north (approximately 80km to the north of Banyas) mark the maximum extent of fieldwork carried out. Inland, fieldwork was also carried out as far east as the Dead Sea Transform Fault (approximately 40km from the coast), and thus the project area covered approximately 3200km<sup>2</sup> (Figure 1.2).

### *Regional geography*

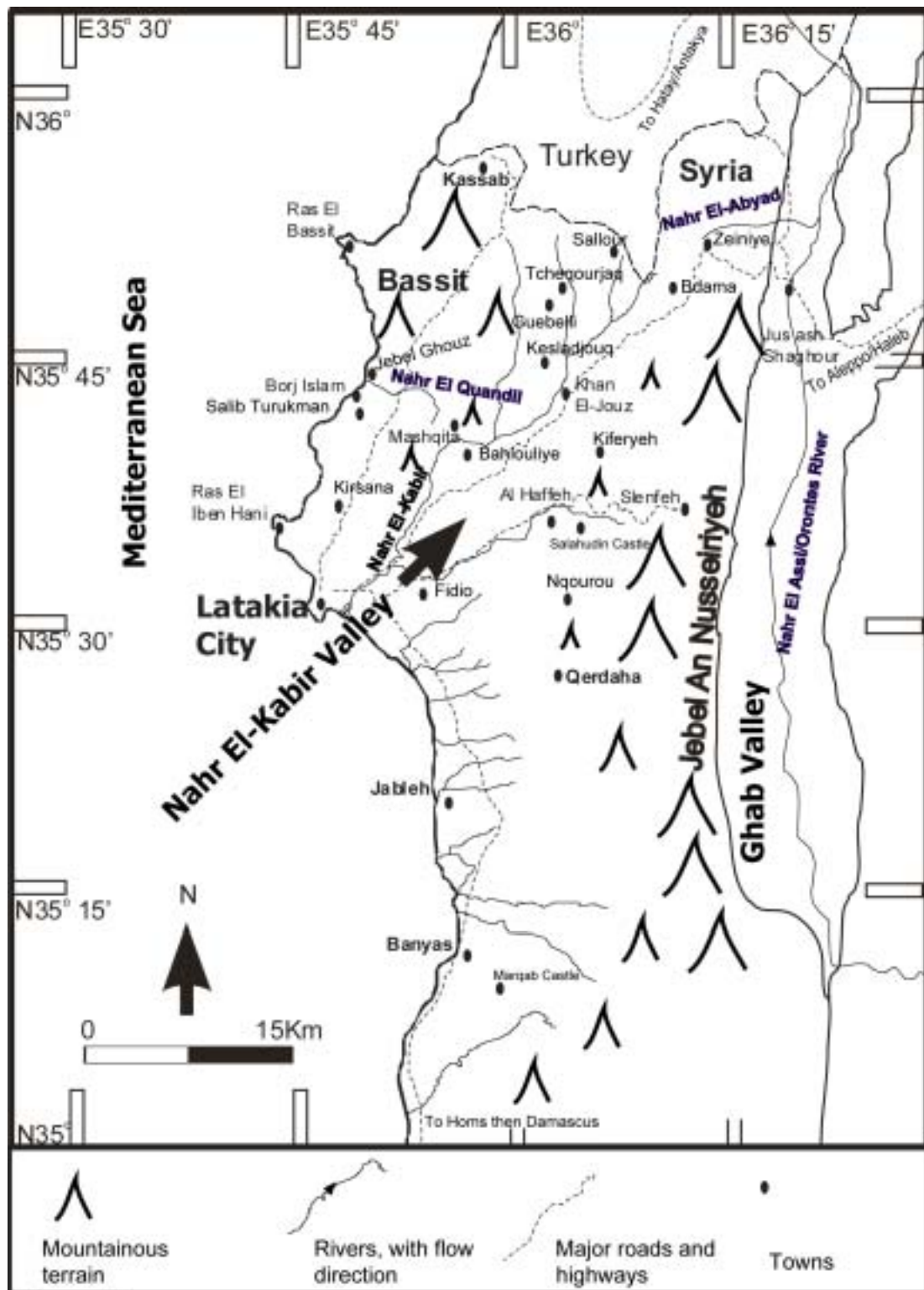
Two mountain ranges dominate the area, rising from the extensive flat plains around the port of Latakia, the major city in the region (Figure 1.2). The 'Baer Bassit Massif' (see glossary Chapter 1) extends northeastwards along the coast from Latakia City for some 40km and rises gradually to an average height of 1000m above sea level. The highest point, Jebel Aqraa, 1700m, straddles the border. In contrast, the Jebel An-Nassuriyeh Mountains run from north to south for over 60km, approximately 10-15km inshore. This mountain range is asymmetrical, rising gradually from the west, with an almost vertical relief to the east; it averages 1300-1600m in height along the elongate ridge crest. Two depressions are also prominent in the topography: the 10-15km wide Nahr El-Kabir River Valley and the Ghab Valley. The Nahr El-Kabir Valley trends northeast-southwest and narrows to the northeast from the coast and Latakia City, dividing the Baer Bassit Massif and the Jebel An-Nassuriyeh Mountains. The geology of the Nahr El-Kabir Valley and the Tertiary outcrops on the two mountain ranges forms the main focus of this project. The Ghab Valley, to the east, is discussed in more detail in Chapter 5, as it is regionally important.

### *Geological and plate tectonic setting*

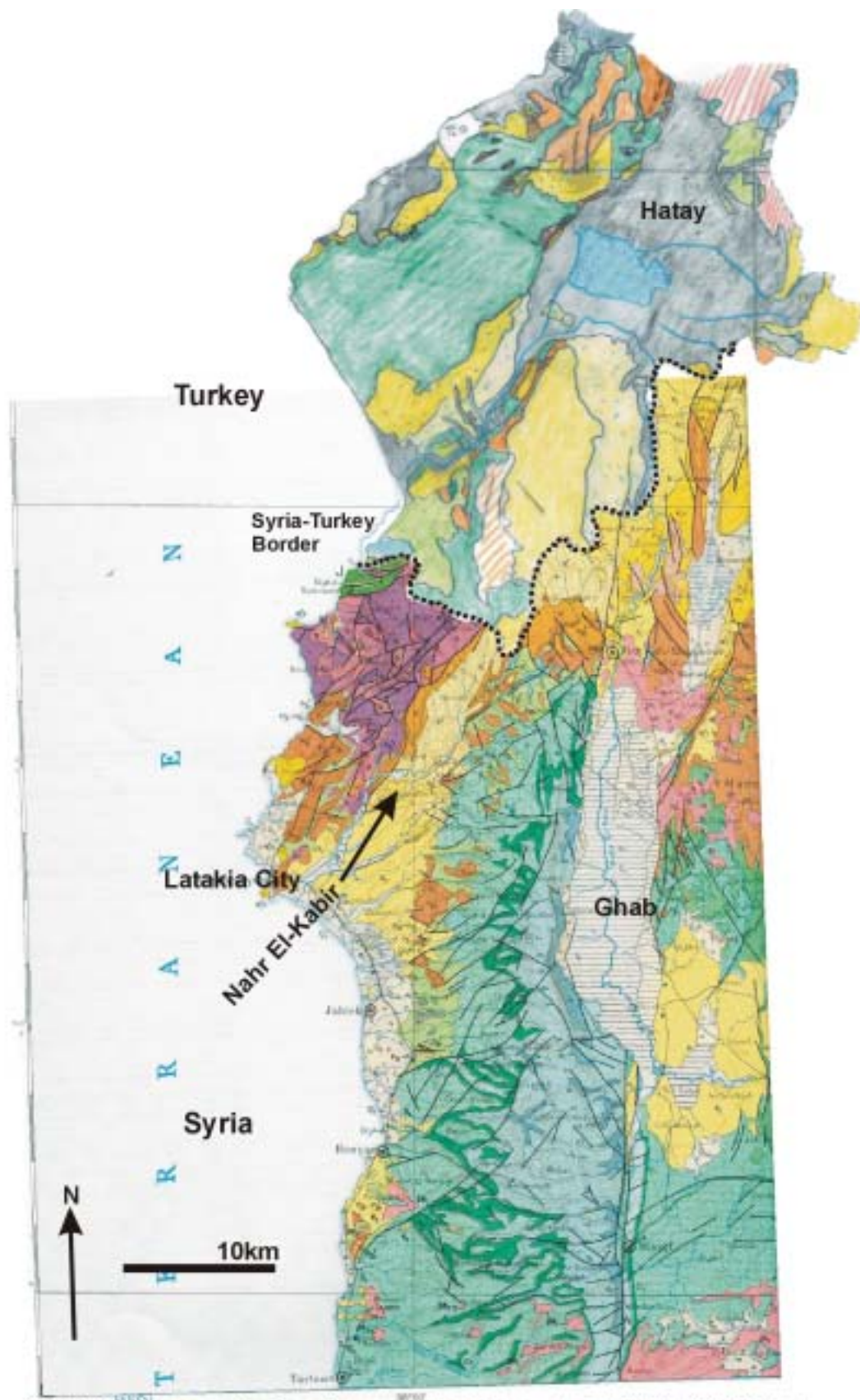
Some of the earliest work on the northwest Syria was carried out by Dubertret (1932, 1933 and 1954). He systematically identified the 'roche verte' (i.e. green serpentinite; part of the Baer Bassit Ophiolite) and compiled the first published geological map of both Syria and Lebanon (Dubertret, 1954). Ponikarov et al. (1963, 1966) built on this work, as this Soviet team mapped the whole of Syria at 1:200 000 scale and established the stratigraphy and biostratigraphy of the region (discussed in detail in Chapter 2)(Figure 1.3 & updated in this study, Figure 1.4). Their work also put forward the idea that the rocks seen in the Baer Bassit region (termed Massif) were unusual compared to the rocks of similar age at Jebel An-







**Figure 1.2** Project area location map, showing major towns, villages and topography (see also pull-out version, Appendix 2).



**Figure 1.3** A composite view of the maps by Ponikarov et al. (1966)(1:500 000) and Piskin (1985)(1:50 000) of NW Syria and Turkey. See Figure 1.4 for explanations of units.



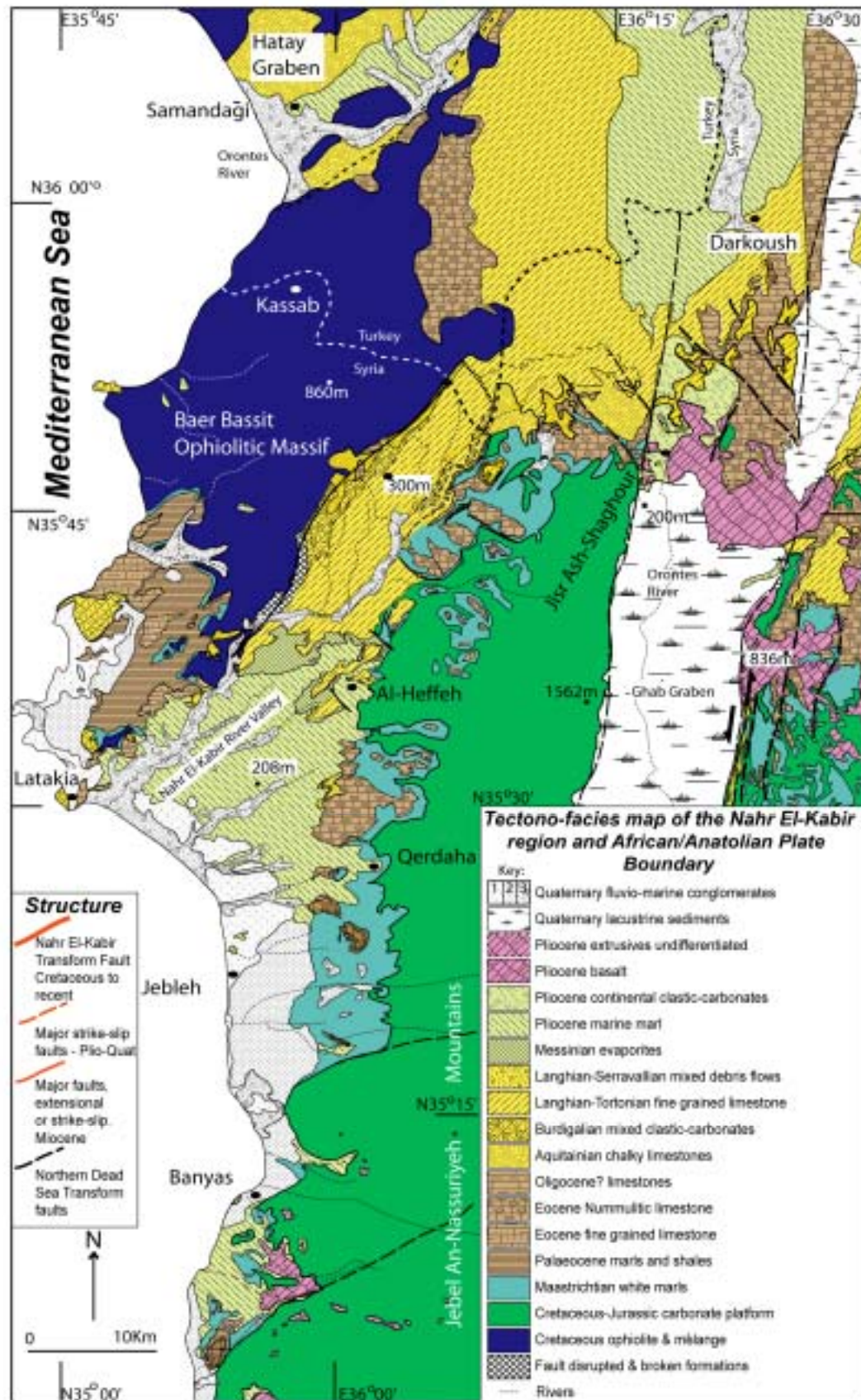
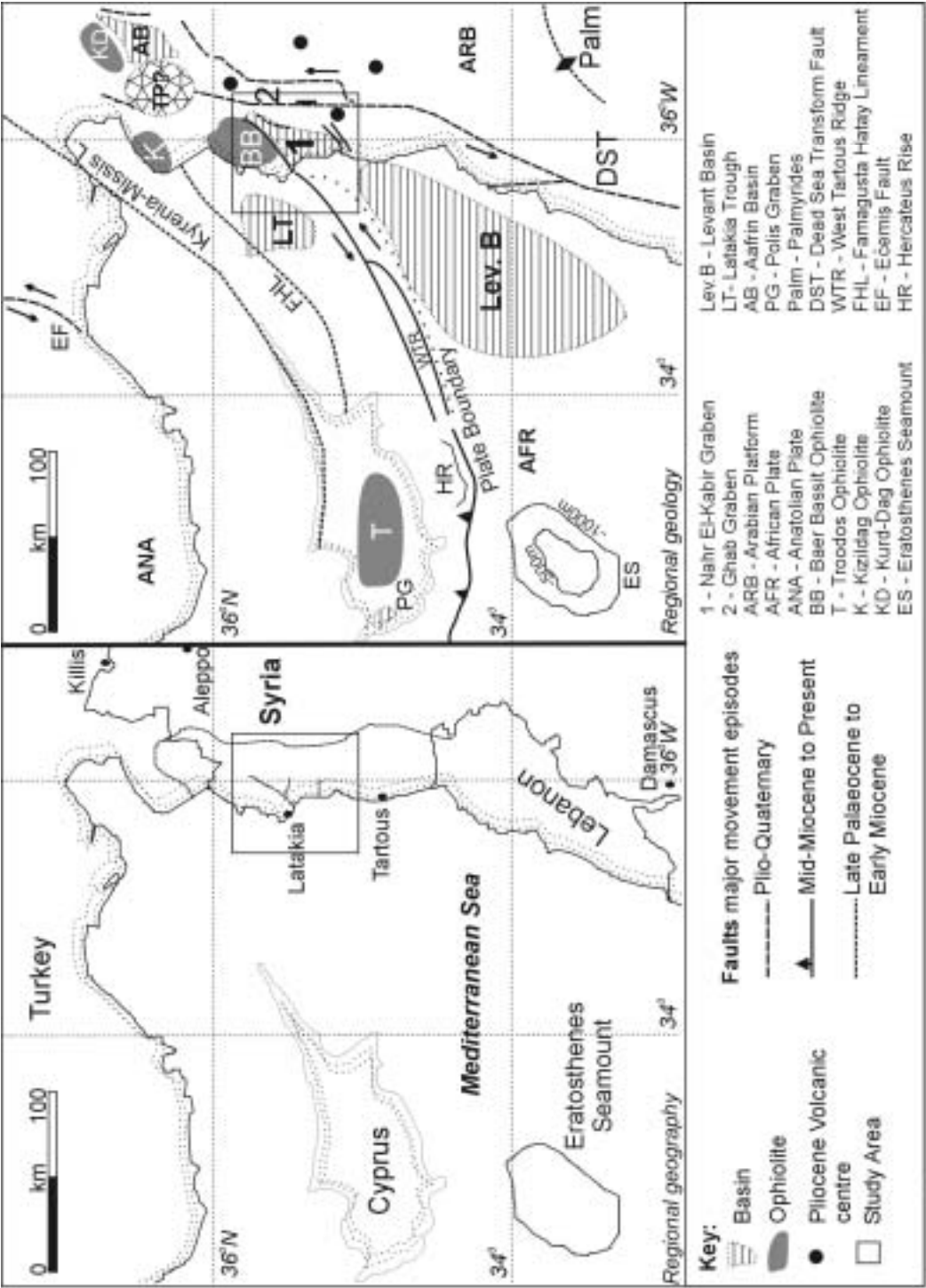


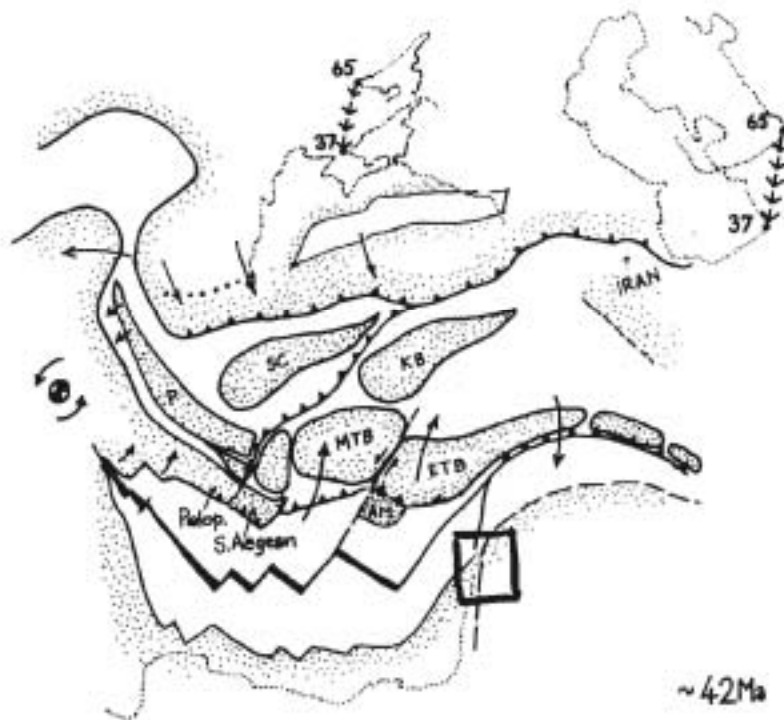
Figure 1.4 Reinterpreted & redrawn geological map of project area, this study. Full interpretation on pull-out map.

Nassuriyeh Mountains, some 20km to the south; a “Precambrian” volcanic-sedimentary assemblage close to a Jurassic-Cretaceous-Jurassic platform. They inferred that the Baer Bassit Massif must have been emplaced due to gravity sliding and that the overlying Maastrichtian to Recent cover was neoautochthon. The Baer Bassit Massif and the “roche verte” of Dubertret (1932) were formally recognised as ophiolitic fragments by Parrot (1977) and suggestions relating to subduction, accretion and obduction of the Baer Bassit Ophiolite were developed. By 1984, the concepts of plate tectonics, ophiolites and transform faults had been applied across the Eastern Mediterranean area and were published as a set of thematic papers (Dixon & Robertson, 1984). These works started to explore the possibilities of distinct palaeogeographic settings of the continental plates and the Tethys Ocean in the region (Figure 1.5). It also introduced concepts of change through time in the geological setting, which was absent previously (Figure 1.6) (Robertson and Dixon, 1984)

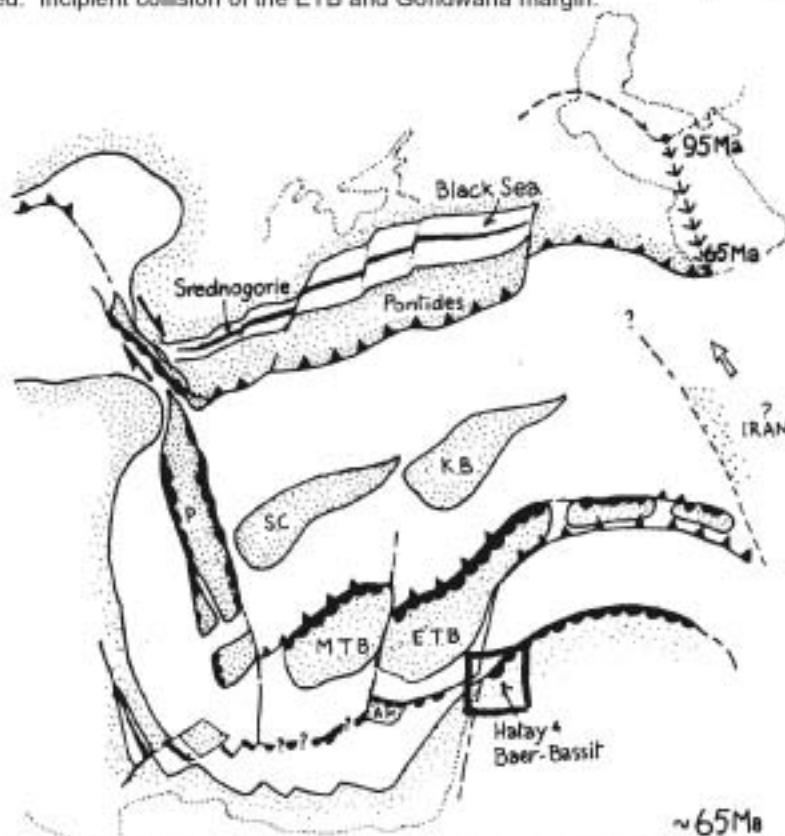
A geological history could then be hypothesised: 1. Delaune-Meyère (1984) suggested that the sedimentary rocks she found within the Baer Bassit Massif showed that rifting had started in the Late Triassic and correlated the Baer Bassit region with similar units in Antalya (southern Turkey) and Cyprus. 2. This part of the northern margin of Pangea supercontinent (later Gondwana) was also said to have existed continuously through Jurassic and Cretaceous times. 3. Parrot (1977) and Delaune-Meyère (1984) inferred that compression started by Late Cretaceous time as they recognised that the Baer Bassit Massif was an ophiolite. Ricou (1971) identified the “peri-arabic crescent”, a chain of Late Cretaceous ophiolites obducted over a 15Ma period, from Cyprus to Oman, including Baer Bassit. 4. Ricou (1971) and other French workers related the ophiolite emplacement to continental collision and obduction occurred onto the African Plate as the Tethys Ocean (Neotethys) closed. 5. Delaloye & Wagner (1984) tried to quantify this movement, suggesting that the African Plate had moved northwards towards Eurasia at a speed of 3-4  $\text{cm y}^{-1}$  and that 900-1200km of the Neotethyan Ocean had been lost, although this does account for the full picture. Robertson (1998), developed these ideas further and related the episodes of Triassic rifting, the Jurassic-Cretaceous passive margin and the Latest Cretaceous-Paleogene units to closure/collision of the Tethys in the Eastern Mediterranean margin. His work was further extended for the Baer Bassit Ophiolite by Al-Riyami (2000) & Al-Riyami et al. (2001). This tectonic summary for the Baer Bassit region is given below, as it is a useful starting point for this project (Figure 1.7).



**Figure 1.5** Location map of the northeastern Mediterranean Sea, showing the project area and interpreted tectonic features (Benarvarham et al., 1995; Robertson, 1998; Vidal et al., 2000)



**Figure 1.6 B.** Late Eocene tectonic setting from Robertson and Dixon (1984). Project area boxed. Incipient collision of the ETB and Gondwana margin.



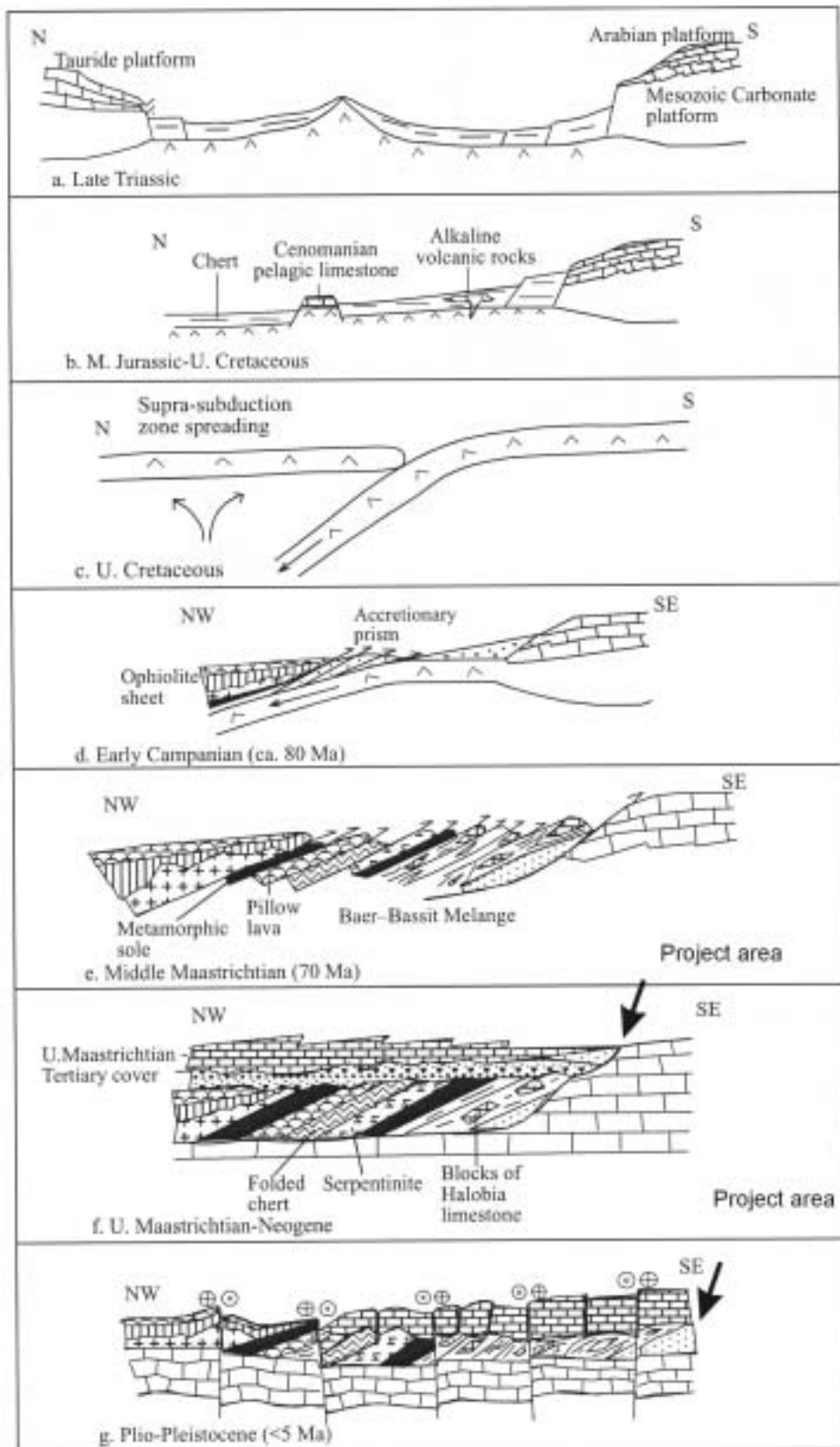
**A.** Latest Cretaceous tectonic setting from Robertson and Dixon (1984). Project area is boxed. P- Pelagonian Block, SC - Sakaraya Continent, KB - Kirsehir Block, MTB - Menderes Tauride Block, ETB - East Tauride Block, AM- Alanya Massif.

Despite the extensive work on the ophiolite-related units and the sedimentary-tectonic history of the overlying Tertiary successions remained largely neglected, although excellent mapping by Ponikarov et al. (1966) and biostratigraphical studies by Krashenninnikov (1971, 1994) has been carried out, see Chapter 2. The initial stage of continental convergence had been demonstrated, but there was then a gap in the geological knowledge for 45-60Ma until the latest Miocene to Plio-Quaternary structuration and break-up of the African and Arabian plates (based on studies in Syria and offshore by: Ivanov et al., 1992; Domas, 1994; BenAvraham et al., 1995; Devyatkin et al., 1997; Vidal et al., 2000 A&B; Brew et al., 2001). This understudied time interval is debatably when continental collision occurred also in SE Turkey (Yilmaz, 1983; Aktas & Robertson, 1984; Robertson, 1998) and would have occurred in northwest Syria. So far, only the thesis by Al-Riyami (2000, a student of our Edinburgh University Tethyan Research Group) and later papers (Al-Riyami et al., 1999, 2001), has investigated the tectonics of emplacement of Baer Bassit and its post-obduction structuration.

Obvious problems remain to be solved in this region relating to the formation of a wide, Early Tertiary marine basin after ophiolite emplacement and sub-aerial uplift, then further development of a narrow basin throughout the Late Tertiary. The later occurs both pre and post the splitting of the African and Arabian plates (Dead Sea Transform Faulting, Dubertret, 1932; Delaloye and Wagner, 1984; Quennell, 1984; Domas, 1994; Brew et al., 2001), whilst the region is in a continuously tightening collision zone.

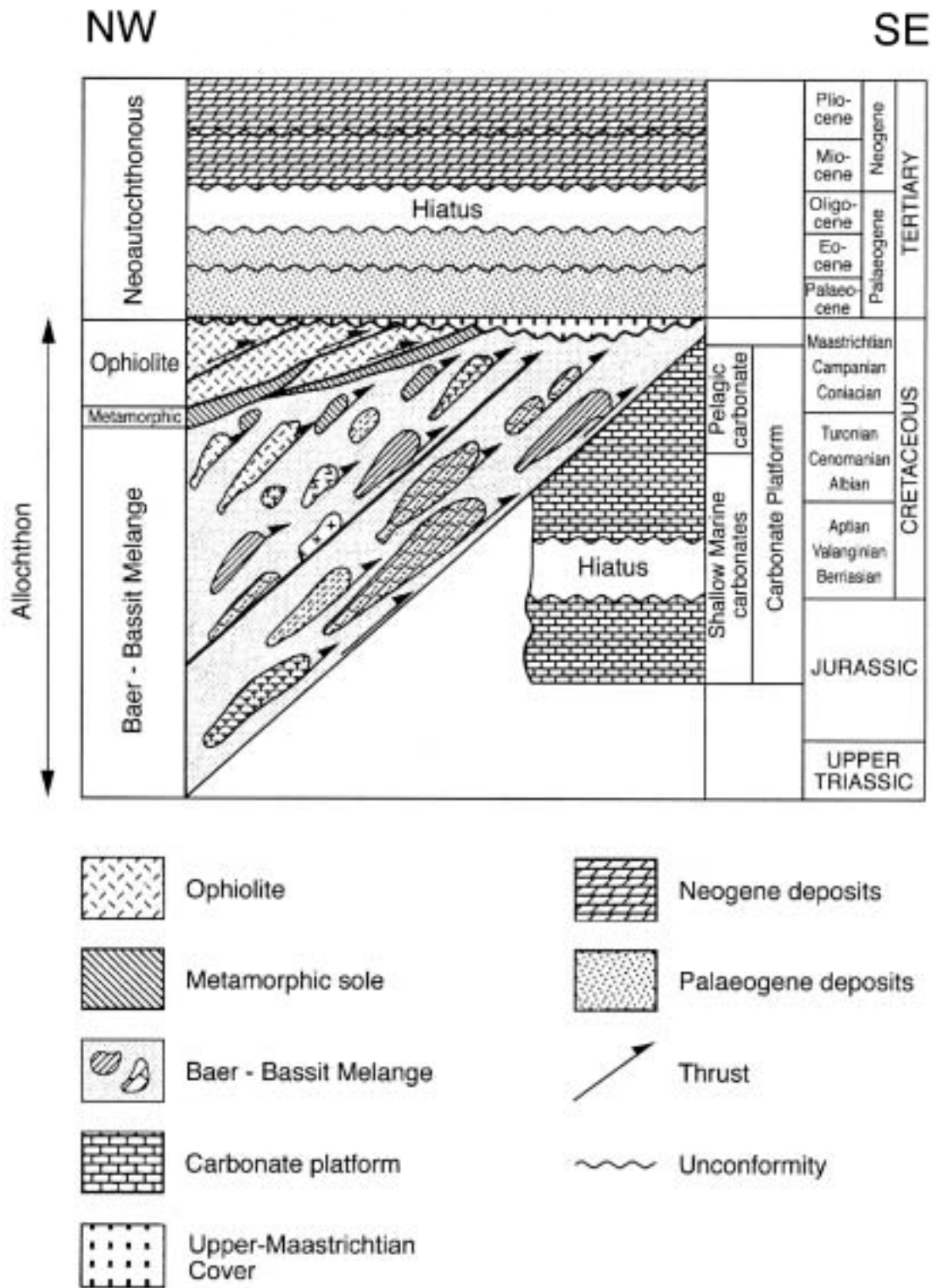
### ***Summary of the tectonic setting of the Baer Bassit Ophiolite and NW Syria***

Khalil Al-Riyami (PhD, Edinburgh University, 2000) has recently completed the most thorough tectonic synthesis of pre-Tertiary events along the Anatolian/African plate margins of NW Syria, through his work investigating the Baer Bassit Ophiolitic Massif (Figure 1.7). He reported that there was no preserved evidence of initial continental rifting in the Arabian passive margin and that the oldest units seen in the Baer Bassit Ophiolitic Massif are of Upper Triassic age. These comprise alkali basalt and deep-water pelagic sediments, indicative of deep-water rift setting. During the Upper Triassic to Middle Jurassic, deep-sea sediments were deposited on a deep-water basinal slope, along the southern margin of a small Neotethyan basin. Throughout the Middle Jurassic to Early Cretaceous a deep-sea



**Figure 1.7** The changing plate tectonic setting of the Anatolian and African/Arabian plates from the Triassic to Recent, according to Al-Riyami (2000) and Al-Riyami et al. (2002). The approximate project area is marked.





**Figure 1.8** The tectonostratigraphy of the Baer Bassit Massif and Tertiary cover sequence. From Al-Riyami (2000).

setting below the carbonate compensation depth (CCD) is likely as no carbonate input is present. A seamount setting is considered to be very likely for a separate volcanic sedimentary unit of Middle Jurassic to Early Cretaceous age. By the Middle Cretaceous, carbonate sediments were accumulating along the Arabian passive margin, often redeposited through submarine channels. During the Late Cretaceous the Baer Bassit Ophiolite is considered to have formed, with the Neotethyan Ocean above a northward dipping subduction zone. During the latest Cretaceous (Maastrichtian), the Baer Bassit Ophiolite was accreted and finally emplaced on to the Arabian passive margin (African plate). Individual thrust sheets were strongly imbricated during emplacement process and are believed to form a wedge of material overlying the ramp, thickening seaward.

After emplacement of the Baer Bassit Ophiolite, the area became emergent briefly as fluvial sediments are found. However, during the Maastrichtian the region was rapidly transgressed and an Early Tertiary carbonate platform was established. Throughout the Palaeocene to the Middle Eocene, the region continued to be in a submerged shelf setting. The Late Eocene to Oligocene was marked by an unconformity that can be related to final suturing (collision) of the Neotethys Ocean to the north possibly with the Eastern Tauride Block (Robertson, 1998, Al-Riyami et al., 2000)(also see Chapter 6, this work). This collision was thought to have caused the up-doming of Jebel Aqraa (Syria-Turkey border) and large-scale, low-amplitude folding of the Palaeogene cover on the Baer Bassit Massif; more regionally it was also responsible for the inversion of the Syrian Arc, Palmyra and the Euphrates Graben (Chaimov, 1992; Searle, 1994; Alsdorf et al.; 1995). After this collision the Miocene to Late Pliocene was marked by another marine transgression and non-marine Quaternary deposition (Figure 1.8). During this Miocene to Recent time, strike-slip faulting occurred throughout the northern and central areas of the Baer Bassit Massif, although the timing was not constrained, due to a lack of sedimentary cover in their study region. Al-Riyami (2000) mapped two sets of strike-slip faults (both sinistral and dextral), orientated NE-SW and NW-SE and suggested that these extended offshore and might represent the Anatolian/African plate boundary and its connection to the Dead Sea Transform Fault.

This synthesis forms the starting point for my investigations into the post-ophiolitic tectonic history.



### ***Project Aims***

The aims of this project were four-fold and relate to improving the understanding of early continental collision in the Eastern Mediterranean region and its application worldwide:

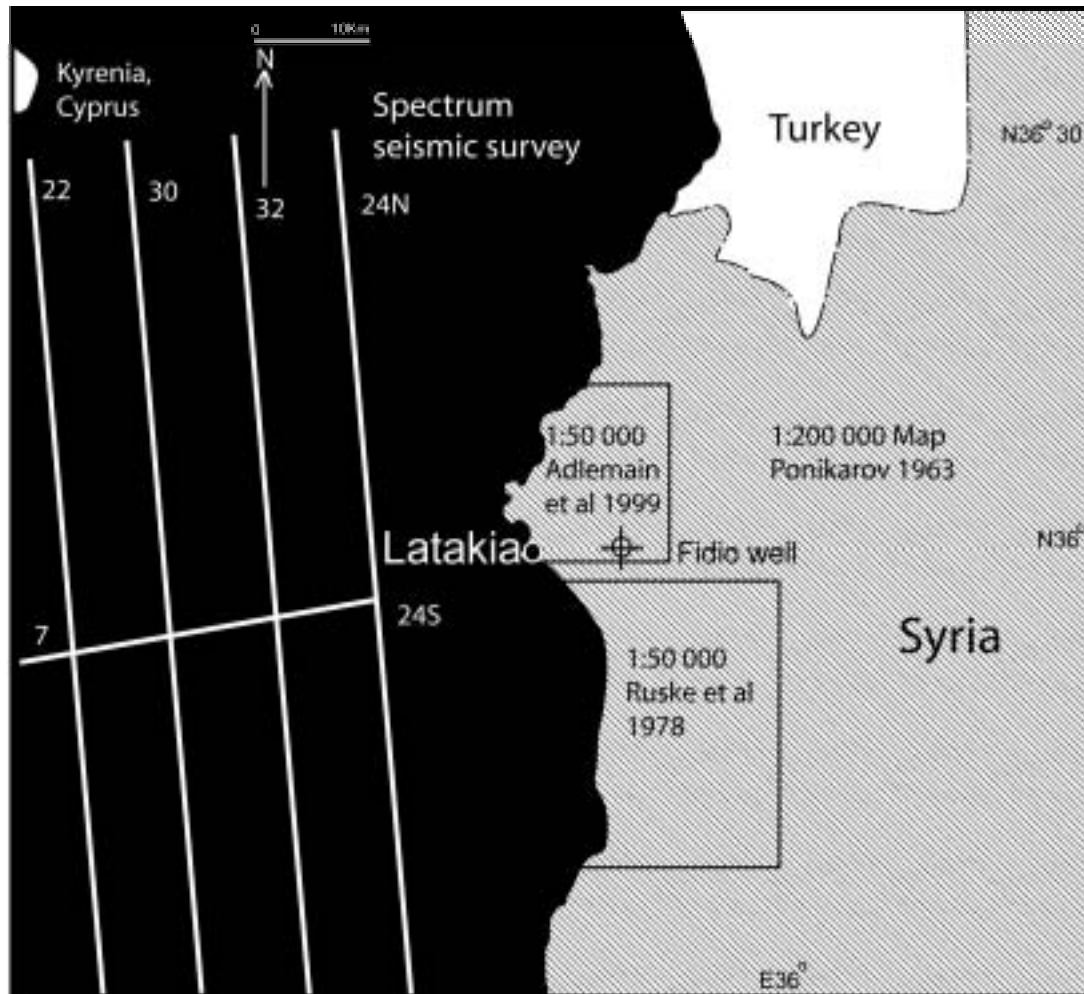
1. To determine, based on detailed field studies, the sedimentological and tectonic relationships of the final closure of the Tethys Ocean (post-ophiolitic obduction) within a continent-continent collisional setting using evidence from the African plate margin, rather than the Anatolian plate, which is more deformed.
2. To examine the tectonic-sedimentary implications of the potentially diachronous nature of such collisions in relation to the location within a collision zone. The northwest margin of Syria is ideally situated between the Zagros Mountains (full collision) and the Eastern Mediterranean (incipient collision) (Robertson, 1998).
3. To apply modern sedimentary rock facies descriptions and remote sensing data to build on the the sedimentary rock cataloguing and mapping by Ponikarov et al. (1966). This would provide, for the first time, a comprehensive geological picture both onshore and offshore, of the region and allow assessment of the tectonic events in the region.
4. To draw possible inferences applicable to collisional processes worldwide.

### ***Project Database and Arabic Names***

This project is primarily based on field data and observations made over three field seasons, between late 1999 and late 2001. In total about 5 months of fieldwork was carried out.

#### **Geological maps**

Geological maps of the region were difficult to come by. The field area was mapped by a Russian team between 1957 and 1963, as was Syria as a whole (Ponikarov et al. 1963) and these maps were published at the 1:500 000 and 1:200 000 scale at that time in the Soviet Union. The Baer Bassit ophiolite was also mapped at 1:50 000 during the same study by Kazmin and Kulakov (1968). Re-mapping of various parts of the field area has since been carried out (Figure 1.9). In 1978, Ruske et al. published maps at 1:50 000 for the area between the coast and Qerdaha City to Banyas Town and in 1999, a provisional 1:50 000 map by Adjemian J. and Khatoun A. was completed for the Baer Bassit Massif to Latakia City area, although no accompanying reports for either could be found. The Ponikarov et al. (1963)



**Figure 1.9** Geological map and seismic dataset localities, showing the extent and coverage

maps at 1:500 000 and 1:200 000 were very kindly made available by the Syrian General Establishment of Geology and Mineral Resources, as were photocopies of the other maps mentioned above.

### Topographical maps

Topographic maps at 1:50 000 scale covering most of the region were obtained commercially in Damascus and are predominantly in Arabic. The Arabic, when transliterated into English has numerous possible spellings and this work has tried to use the currently acceptable form and closest phonetic sound (though Latakia City can also be spelt Lattakia, Latiqueieh or Al-Latheqieh). The cartographic work for these maps and all the geological maps dates from an original French survey in 1924 (by the French army, updated in 1943 by Dubertret). Since

that time the population of the area has risen dramatically and new towns, villages and roads have been created. Large parts of the Nahr El-Kabir Valley are now very intensively cultivated, as this region and the Ghab Graben provide most of Syria's population with fresh produce. Access to low-lying areas, certain roads, railway lines, quarries and borders was restricted, due to agricultural, forestry and security reasons, even if these were the only outcrops available and permission letters from the Establishment of Geology were presented. For these reasons this project used the Global Positioning System (WGS84 map datum) and a relative distance to the nearest large, easily identifiable settlement to locate most of the outcrops and localities visited. Magnetic variation is also absent from most of the maps; although this is quite small in this region. In 1924 the magnetic variation was  $+1^{\circ}8'$ , increasing to  $+2^{\circ}48'$  by 1963 and  $+3^{\circ}48'$  at the end of 2001. The shift between the original Russian map (Ponikarov et al. 1963) and this study is therefore insignificant.

#### Localities and field data

During the course of this fieldwork some 427 localities and outcrops were investigated. At each site fieldwork was carried out to place the locality in context and numerous samples, photographs, sketches and field measurements were taken. This represents a substantial database of geological information, which was supplemented on return from the field by laboratory analysis (i.e. thin sectioning).

#### Seismic and offshore data

Spectrum Energy and Information Technology Limited very kindly made available 5 lines from their 2D 1975 Eastern Mediterranean survey for interpretation. By modern standards the seismic data are basic, being only 48 channel, but this is currently the best resolution released data and of much higher quality than previous research cruise surveys (i.e. Krasheninnikov and Hall, 1994). The survey starts approximately 15km offshore from Latakia and the north-south line spacing is in the order of 10km. The offshore region covered is shown by Figure 1.9. Offshore well data does exist in Iskenderun Bay and onshore in the Latakia region of the Nahr El-Kabir Valley but none of these data have been formally released by the Syrian and Turkish companies (Al-Furat and the Turkish Petroleum Organisation) or the relevant government ministries involved. Therefore, subsurface interpretation has had to be by extrapolation of surface features. One well at Fidjo, near Latakia, has been sketched in the paper by Dzhabur (1985). This well is discussed fully in

Chapters 2, 3, 4 & 6, although it should be noted from the outset that the interpretation presented in this paper (Dzhabur, 1985) is un-correlatable with any other published work or field locality.

Subsidiary information and remote sensing data

Satellite image data, digital bathymetric and topographic data, can now be freely downloaded for this area of the Middle East from the United States National Oceanic and Atmospheric Association website (<http://www.noaa.gov> and also [www.nima.mil](http://www.nima.mil)) (Figures 1.1 & 1.10). This includes 10m resolution SPOT monochrome satellite images (bought from the French by the United States Defence Department) and basic 5' digital elevation models. The bathymetric models have proved to be an invaluable resource in correlating large scale seismic features across the Eastern Mediterranean seafloor and there has also been some success in using satellite images to identify features seen in the field across the Syrian-Turkish border.

Arabic names and text

Place names in this thesis are based on the Russian 1:200 000 map (Ponikarov et al. 1963), printed in English for the Syrian government. The names were originally transliterated by the French Army survey in 1924 and often have a hint of "Gallic" in them, but most are very close to the colloquial Arabic spoken in this region. Therefore, the majority of names have already been anglicised in printed literature and are preserved here for clarity. The only major name change is Latakia (Latakia City) from Al-Latheqieh on the map, as more recent texts use this spelling. 'Lattakia' (with 2 t's, the geological feature) is sometimes confusing as it refers to the offshore basin north east of Latakia City, but has in some literature been used in error to describe onshore areas. Therefore, Laṭakia (with one t) refers to the city and onshore sites in this thesis and Lattakia (with 2 t's) to the offshore. The pronunciation of all the anglicised arabic words is phonetic and relates to the Levantine colloquial Arabic spoken throughout Syria rather than modern standard Arabic.

*Major places of interest:*

Latakia - major trading port town, regional capital city

'Ras Shamera/Ugarit' - birthplace of music 2000BC, first earthquakes recording Banyas,

Jableh and Tartous - Large port towns and oil facilities south of Latakia



**Figure 1.10** SPOT monochrome satellite imagery of the northwest of Syria. Dark colours indicates water or heavy vegetation. ([www.nima.gov](http://www.nima.gov))

Qerdaha - Syrian President's family town

Bassit, Kassab, Qaastal Maaf – towns in the ophiolitic region north of Latakia.

Jisr Ash Shaghour - major town in the Ghab Graben (a pull-apart basin of the Dead Sea

Transform fault, approximately 40Km due east of Latakia)

Dimashq, Demashq, Al-Cham – Damascus, Syrian capital city

Antioch – regional name for this area north to Antakya/Hatay in Turkey

*Geographical names:*

Nahr – river

Kabir – big

Jabal, jebel, gebel – mountain

*Conventions and terms used throughout this project (see also Figure 1.2):*

Baer Bassit Massif (later defined as the Baer Bassit Ophiolitic Massif) – The region and rock units associated with the Baer Bassit Ophiolite and its emplacement.

Nahr El-Kabir Valley (later Graben) – main river valley trending NE-SW to Latakia City.

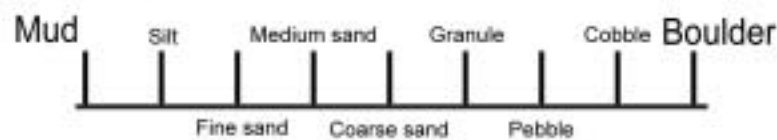
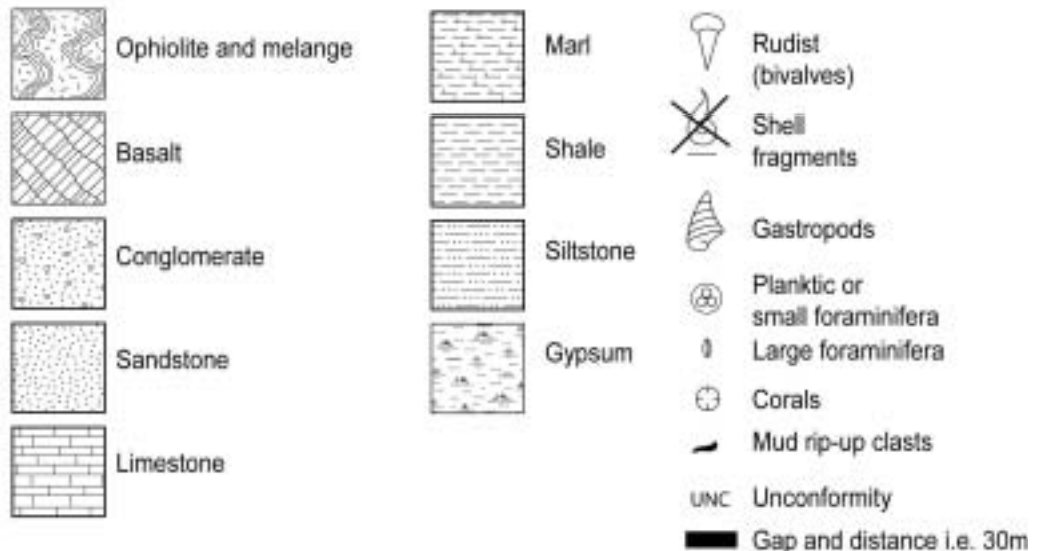
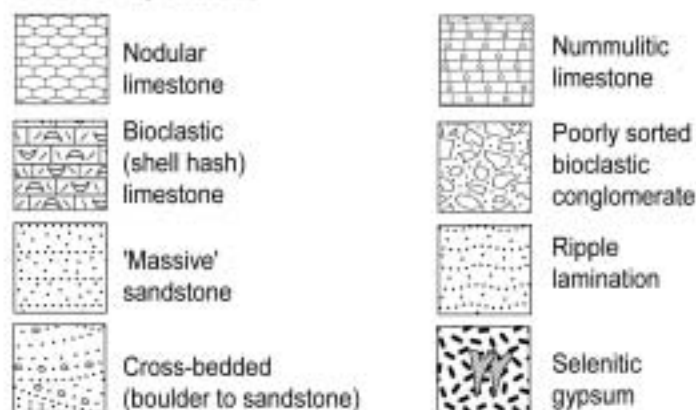
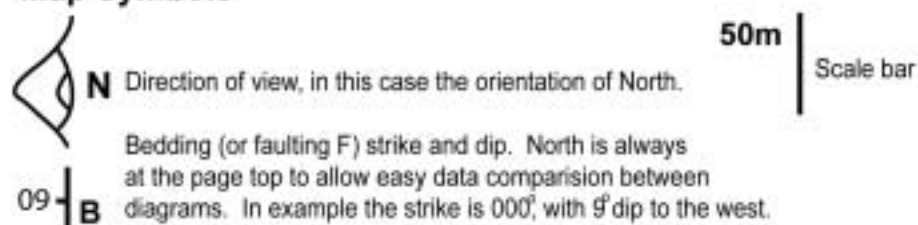
Ghab Valley (later Graben) – main valley trending N-S, some 40km inshore and parallel to it, associated with the Dead Sea Transform Fault.

Jebel An-Nassuriyeh Mountains – the mountain range trending N-S, 15km inshore and parallel to it.

Graphical conventions – Figure 1.11 is the key to all figures presented throughout the thesis.

## ***Thesis Style***

This PhD thesis has been aimed at presenting the geological data and new interpretations in the most user friendly format, not only for the reader, but also for practical use by the Syrian Establishment of Geology and Syria Shell. As such, substantial effort has been given to graphical means of presentation (i.e. new maps, Figure 1.4), rather than relying solely on text based descriptions.

**Grain size****Lithological symbols****Facies symbols****Map Symbols**

**XPL, PPL** Refer to crossed polarised and plain polarised light microscopy

**Figure 1.11** Key to diagrams, logs and maps used throughout this thesis (unless otherwise given)

## Literature Review

### *Previous work on the northwest of Syria*

Seismological events and mineral exploration have been recorded historically in Syria since 2000BC, but it was Dubertret (1932, 1933 & 1954) (see Chapter 1) who was as one of the pioneers of geological research in the area. He described the stratigraphy, mapped parts of Syria and Lebanon and discovered the “roches verte” (Baer-Bassit Ophiolite; Parrot, 1977). Since his work, the primary source of field data has come from the Soviet mapping team (Ponikarov et al., 1963, 1966 and 1967). They recorded and mapped the geology systematically. A summary of their work and more recent additions (Krashenninnikov 1971, 1994) and corrections form the basis of the literature for this project.

### *The mapping of the Syria by the Russians*

The Russian regional geological maps (see Figure 1.3, Ponikarov et al. 1963) were based on three years of fieldwork by Soviet geologists in the early 1960's and a series of monographs explaining the maps was published in 1966 (Ponikarov et al. 1966 and 1967). The majority of their work focused on the Baer-Bassit Massif (an ophiolite later recognised by Parrot, 1977, and Delaunay-Mayère et al. 1984) and a relatively brief explanation was given of the post-ophiolitic sequences (termed neoautochthon throughout their and later Soviet literature). It is this “neoautochthon” which forms this research project. The Soviet report is characterised by a working biostratigraphy and lithologic cataloguing.

The following section is a summary of the key descriptive aspects set out in their mapping report, relevant to this project area, and I will also outline the regional post-ophiolitic stratigraphy and the, then, level of understanding of the geological setting by the Russian workers. This summary is needed to clarify the geology of the region, as their work is a translation from Russian and numerous advances in sedimentology, tectonics and stratigraphy have superseded many of the initial results as reported by them. Descriptive phrases such as ‘aphanitic limestones’, ‘buried into the relief’ and ‘basal’ (Ponikarov et al. 1966), have been reinterpreted respectively as e.g. fine-grained limestones, deposited on karst or weathered surfaces and the rocks at the base of a succession. No major field-based research work on the neoautochthonous successions have been published since this Russian work, so it is an invaluable starting point for this project.



The majority of their sedimentary rock descriptions are lithological and also detail the foraminiferal assemblages identified for each period. Krasheninnikov updated and redrafted various logs and maps in his summary of Syrian geology (1971) and an updated biostratigraphy (Krasheninnikov, 1994) is used here, as it is based on more modern species names (discussed fully in Appendix 1). Krasheninnikov (1971 & 1994) also carried out much of the original microfossil dating work in Ponikarov et al. (1966). Later sections will discuss the re-mapping of essential aspects of the geology and the interpretation of the sedimentology of the area and results from this project (see Chapters 3, 4 & 6).

All quotes and information in this section are from Ponikarov et al. (1966 and 1967) unless otherwise indicated. Stage names are given first as they appear on the map and reports by Ponikarov et al., (1963, 1966 and 1967) and then in the updated format by Krasheninnikov (1971 & 1994), where appropriate, to provide clear reference for the reader. Where outcrops were distinguished geographically (i.e. the Paleogene), the reference descriptions have been highlighted to focus on those near the Baer-Bassit Massif or the Jebel An-Nassuriyeh Mountains (see Figure 1.2).

### ***The Cretaceous succession and earlier units***

The work of Ponikarov et al. (1966) details rocks of various ages from the Triassic to recent in this region, although at the time of publication, ophiolites and other major tectonic features were not properly identified or dated as such (see summary Chapter 1). The Baer-Bassit Massif was recorded as being an unusual sequence of “Precambrian igneous rocks”, emplaced into position due to “gravity sliding” processes. It was more recently established that the Baer-Bassit Massif is an ophiolite that was emplaced during the Maastrichtian (Parrot, 1977; Delauyne-Mayere, 1984; Robertson, 1998; Al-Riyami et al., 1999, 2002; Howard, 2000), and so the cover rocks studied in this project are younger, but often contain fragments from these older rocks.

The Baer-Bassit Ophiolite was believed to have been emplaced from the north as the area to the south forms part of the large, coherent, Anatolian Plate. This direction of emplacement was later confirmed by Whitechurch (1977) and Al-Riyami & Robertson (2002). The ophiolite is not an intact sequence (Parrot, 1977 & Al-Riyami et al., 1999, 2002), but is a heavily deformed complex of basic volcanic and plutonic rocks, deep marine pelagic rocks and melange (fragments of pre, syn and post ophiolitic lithologies, pervasively mixed), (Al-Riyami & Robertson, 2002). The ophiolite was fragmented and emplaced onto the

Jurassic to Late Cretaceous continental carbonate platform margin of the African plate (Ponikarov et al., 1966; Delauney-Mayere et al., 1984; Al-Riyami et al., 2002). Therefore, this project concentrates on the Maastrichtian to present rocks, starting immediately after emplacement.

### ***Maastrichtian, Upper Unit ( $Cr_2m^b$ )***

The Upper Maastrichtian was recognised as an individual unit across the whole of the northwest of Syria apart from the southern margin of the Nahr El-Kabir Valley (see below 'Maastrichtian Undifferentiated')(Figure 2.1). North of Latakia City it was reported to be characterised by a glauconitic basal bed (less than 20m thick) followed by a thick sequence of clayey, chalky limestone. This succession was recorded as resting on the Baer-Bassit ophiolitic rocks with a sharp angular unconformity.

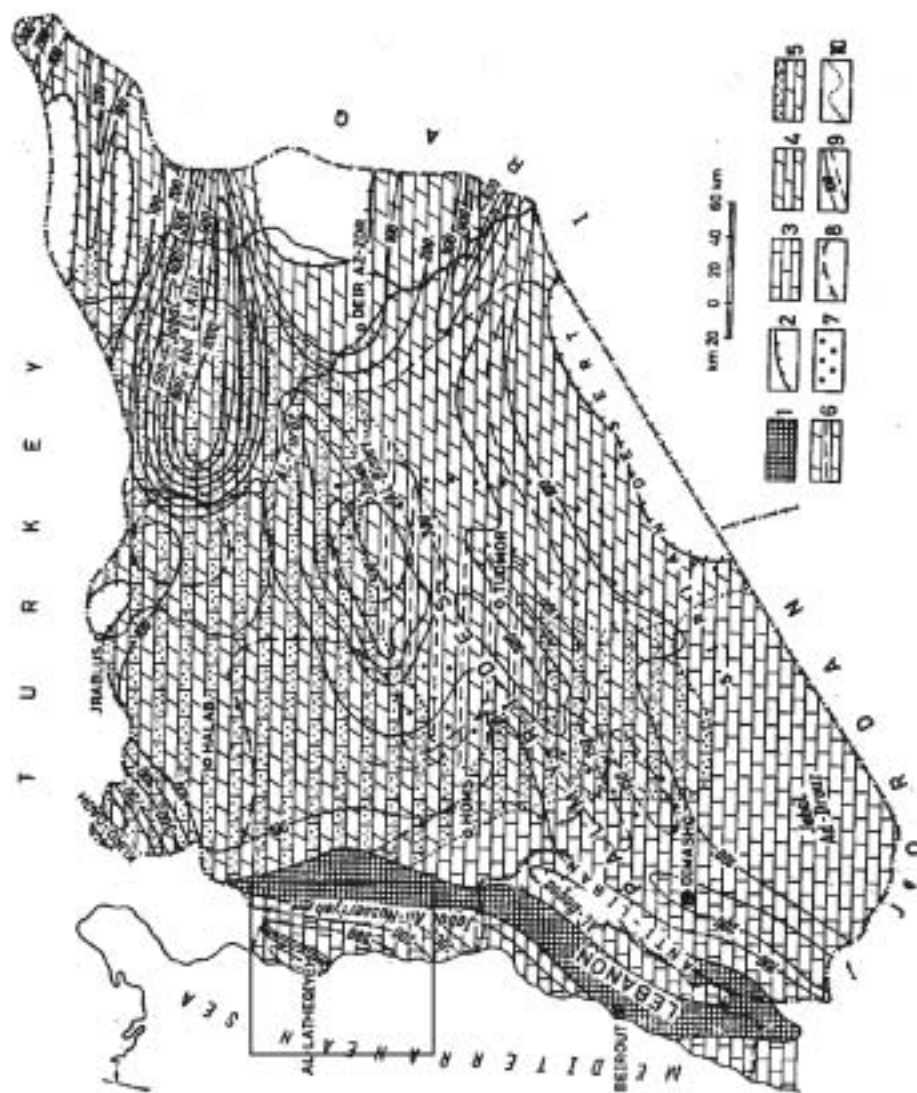
In detail, the basal bed of this succession was described as clastic clast rich and to be comprised of ophiolitic rocks. Al-Riyami et al. (1999), described this as a fluvial to marine facies, which passed into the typical clayey, chalky, limestone lithology as described by Ponikarov et al. (1966). The Upper Maastrichtian succession was recorded as 15-60m thick and passed into the Lower Palaeocene succession without a noticeable lithological change.

### ***Maastrichtian, undifferentiated ( $Cr_2m$ )***

Undifferentiated Maastrichtian sedimentary rocks were found to be exposed in the Jebel An-Nassuriyeh foothills running north south on the eastern margin of the Nahr El-Kabir Valley. These were specified to comprise clayey foraminiferal limestones and marls, lying unconformably on Cenomanian-Turonian neritic carbonate rocks. A distinct basal bed, 0.5-2m thick, containing glauconite and phosphatic material was noted to be generally present, though at the village of Mzeraa this bed was reported to be 40-45m thick.

Three informal members were assigned to the unit from descriptions of the sediments between the towns of Qerdaha and Nahr As-Saneh:

- ≠ The lowest unit was reported as 225m thick of light grey, foraminiferal, clayey limestone, which weathered a bright white colour.
- ≠ Overlying, the middle unit was noted to be 45m thick, blue-grey marl, intercalated with thin (<1m) clayey limestone beds. Rare concretions of barite were also noted.



**Figure 2.1** Maastrichtian and Danian (Lower Palaeocene) outcrop map from Ponikarov et al. (1967). Project area highlighted. 1- no outcrop at present day, 2- areas of no sedimentation, 3- limestone, 4-marl, 5- limestone and marl, 6- clay and clayey marl, 7-phosphate horizons, 8- Danian succession boundary, 9- isopach lines, 10- lithology boundaries. I

€ The topmost section was described as two units totalling 45m thickness. The lower section was noted as marl, intercalated with limestone. The upper section was reported to be light grey, clayey, foraminiferal limestone with large (2-10cm) barite spheres. Ponikarov et al. (1966) reported that Paleogene and then Neogene sediments transgressively overlie the Maastrichtian succession. This was inferred as having led to an increased amount of erosion towards the axial part of the Jebel An-Nassuriyeh Mountains. The maximum thickness of the succession was indicated to be 315m, as found at the logged site detailed above, reducing to just tens of metres at other sites. No further information or logs were given, however.

### ***The Paleogene***

The Paleogene was mapped as four distinct units by Ponikarov et al., (1963, 1966), based on a scheme then in use by Soviet micropalaeontologists (see Appendix 1) (Figure 2.2).

#### ***1. Lower Palaeocene, Danian (Cr<sub>2d</sub>) – P1<sub>abc</sub>, P2***

##### ***Baer-Bassit Massif***

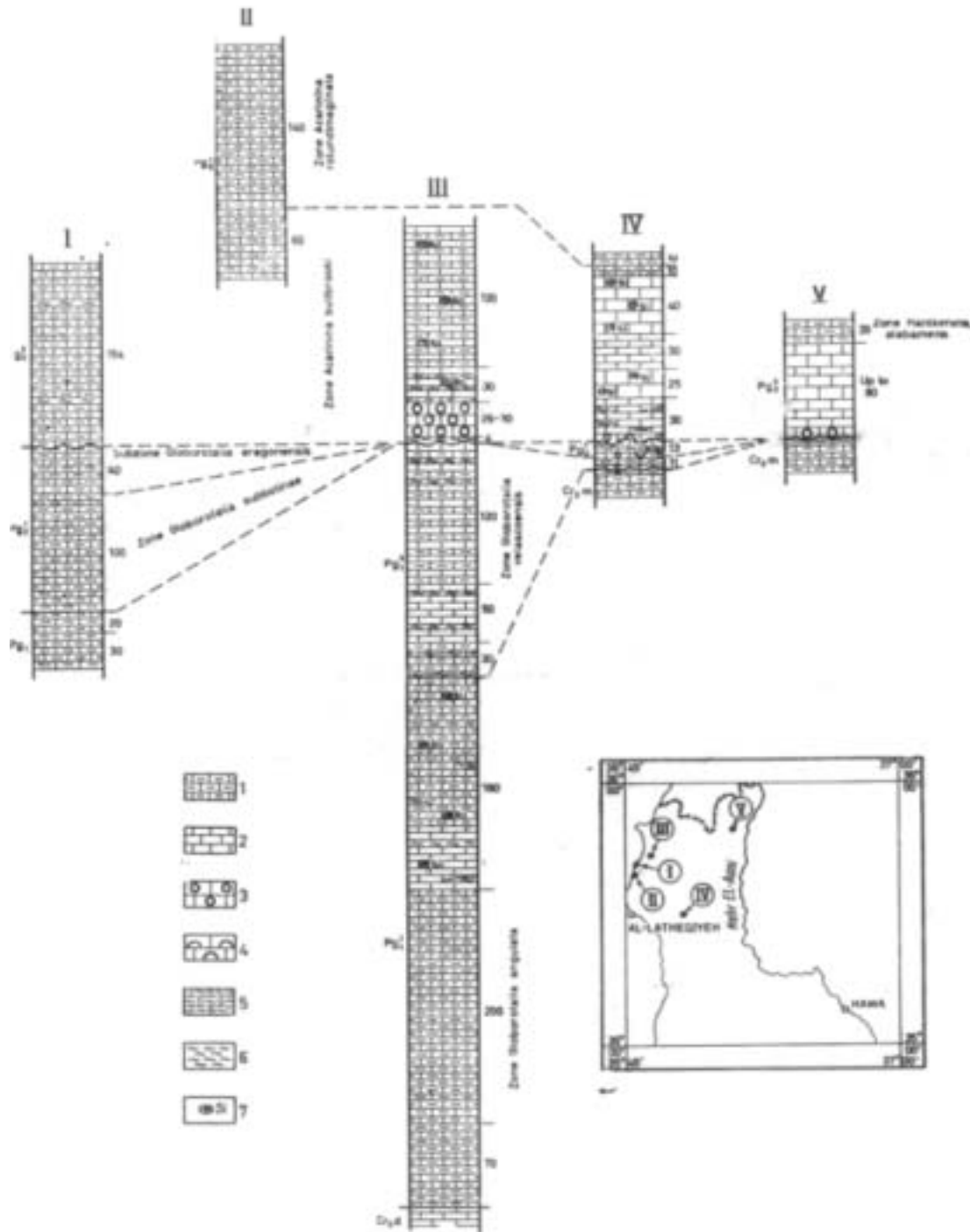
The mapped Danian unit was reclassified by Krasheninnikov (1994) as Lower Palaeocene from the Upper Cretaceous age of the original mapping, notwithstanding the fact that the unit was identified only at Sahl, north of Latakia and then only using foraminifera.

Krasheninnikov et al. (1996) later stated that the lowest Danian stage (*Parvularugoglobigerina eugubina* zone) was missing entirely in Syria due to transgression.

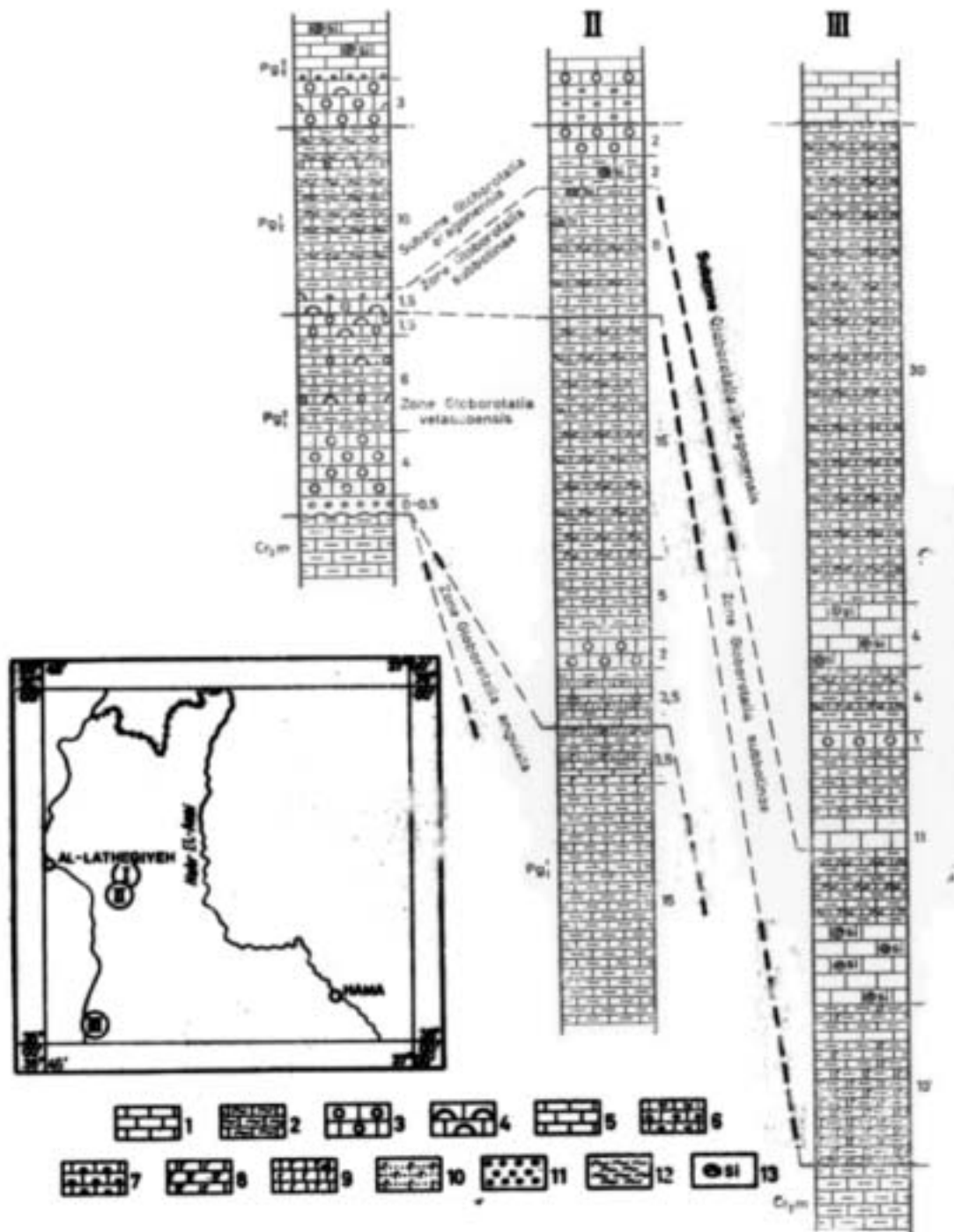
Three zones were identified:

- € The lowest unit was named as the '*Eoglobigerina* zone' and was reported as comprising of 20m of light-gray clayey foraminiferal limestone.
- € Overlying this was 40m of the '*Globigerina pseudobulloides* and *G. triloculinoidea* zone'. A clayey, foraminiferal, poorly bedded limestone alternating with firm foraminiferal limestone.
- € The topmost zone that Ponikarov et al. (1966) named was the '*Planorotalia compressa* zone'. It was reported to be 25-35m thick of foraminiferal, poorly bedded, dark grey marl.

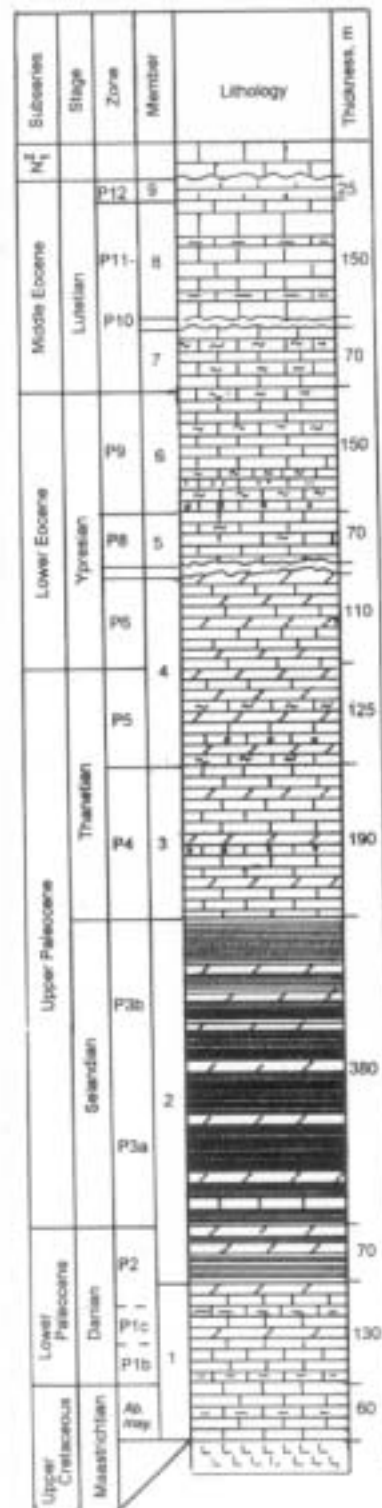
It is unclear as to how these three zones fit into the current four-fold subdivision (P1A to P2, Berggren et al., 1995) of the Lower Palaeocene as few foraminiferal species were recorded. Again, no obvious lithological transition into the Upper Palaeocene succession was noted.



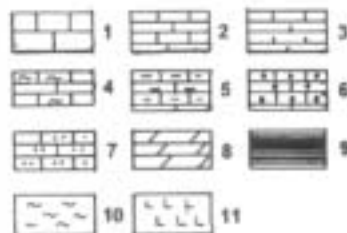
**Figure 2.2** Correlation logs of the Palaeogene sections in the Latakia area and Jebel An-Nassuriyeh. From Ponikarov et al. (1966), poor original copy. 1- clayey limestone, 2- limestone, 3- Nummulitic limestone, 4- algal limestone, 5- silicified arenaceous limestone, 6- chert, 7- chert concretions.



**Figure 2.3** Correlation logs of the Palaeocene and Lower Eocene sections on the Jebel An-Nassuriyah Mountains, from Ponikarov et al. (1966), poor original copy. 1- clayey limestone, 2- silicified limestone, 3- Nummulitic limestone, 4- algal limestone, 5- limestone, 6- conglomerate-like limestone, 7- limestone with phosphorite nodules, 8- clayey, glauconitic limestone, 9- glauconitic limestone, 10- glauconite sandstone, 11- conglomerate, 12- chert, 13- chert concretions.



**Figure 2.4** Composite Palaeogene log from Krasheninnikov (1994). 1- thick-bedded limestones, 2- thin bedded limestones, 3- chalky limestones, 4- silicified limestones, 5- clayey limestones, 6- organogenic limestones, 7- limestones with detrital material, 8- marls, 9- dark argillites, 10- chert, 11- ophiolite rocks. Foraminiferal zones; refer to those given in Chapter 4 and Appendix.



## ***Palaeocene and Eocene***

The Palaeocene and Eocene successions were mapped as two lithostratigraphical units on the geological map of Ponikarov et al. (1966), as lithology variations were not obvious, and a lithological break was inferred at the Middle Eocene succession (Figures 2.3 and 2.4). These mapped units were of Palaeocene-Lower Eocene and the Middle Eocene age. The mapped units were then divided into descriptive sections in Ponikarov et al. (1966), based on the foraminiferal assemblages.

### ***2. Palaeocene-Lower Eocene (Pg<sub>1</sub>-Pg<sub>2</sub><sup>1</sup>)***

#### ***Baer-Bassit Massif***

The Palaeocene-Lower Eocene succession was reported as reaching a maximum thickness of 790m overlying the Baer-Bassit ophiolite (Ponikarov et al. 1966). Sedimentation was inferred to continue from the Danian without a lithological change, but some units were poorly exposed and were identified by drilling or in scattered outcrops (i.e. Lower Eocene, see Figure 2.5). Moving easterly across the ophiolite, the Lower Eocene succession was recorded as pinching out and was noted to be deeply eroded at the base of the overlying Middle Eocene succession. A break in sedimentation prior to the Middle Eocene succession was inferred.

#### ***Jebel An-Nassuriyeh***

The Palaeocene-Lower Eocene succession was only mapped south of the Latakia City latitude, on the flanks of the Jebel An-Nassuriyeh mountains, where it formed a much thinner unit than in the Baer-Bassit region, only 10's of metres thick. Impersistent beds of nummulitic and bioclastic limestone were noted to exist with large quantities of the calcareous algae "*Lithothamnium*", as well as glauconitic sands and phosphorite nodules. The unit was mapped as directly overlying the Maastrichtian succession and being overlain transgressively by facies of the Middle Eocene succession.

Ponikarov et al. (1966) suggested that the disparity between the sediments and sediment thicknesses on the Baer-Bassit Massif and Jebel An-Nassuriyeh Mountains was due to uplift inferred in the Jebel An-Nassuriyeh area. They did not, however, explain the phenomenon or date this uplift, but they simply state that transgression occurred and that the sediment facies appear to show a shallowing of water depths. Later this hypothesis was strongly contested by Brew et al. (2000), as they dated the uplift event as a Plio-Quaternary



feature occurring as the Dead Sea Transform fault propagated through the area (see Chapters 5 & 6).

#### Lower Palaeocene ('*Globorotalia angulata* zone')

##### *Baer-Bassit Massif*

The Lower Palaeocene was recorded as a thick succession by Ponikarov et al. (1966). They divided the succession into three units:

- € The lowermost 70m, were described as dark-grey and green-grey marls.
- € These were overlain by some 200m of light grey, clayey, foraminiferal limestones, alternating with dark-grey marls.
- € The limestone and marls were noted to be capped by a further 180m of foraminiferal, clayey limestones and marls, with intercalated beds and lenses of chert.

The above description relates to sites drilled on the Baer-Bassit Massif. Further south on the Jebel An-Nassuriyeh, the Lower Palaeocene was only reported to be found at Safarquiyyeh village (15km southeast of Latakia) on a small, faulted tectonic block (18m thick). The lithologies recorded were dark grey marls, becoming glauconitic sandstones and bioclastic and detrital limestones further up the succession. No *Nummulites* foraminifera were recorded.

#### Upper Palaeocene (*Globorotalia velascoensis* zone)

##### *Baer-Bassit Massif*

A thickness of 200m of Upper Paleocene sediments was recorded by Ponikarov et al. (1966). The exact locations of the measurements were not given, but the information was implied to be from composite measurements along the Nahr El-Quandil River, bordering the Baer-Bassit Massif.

Ponikarov et al. (1966) divided the succession into 3 units, the lowermost 30m being of clayey, foraminiferal limestone and silicified limestones. Grains of serpentinite, chert, and the large foraminifera *Nummulites deserti*, *N. solitarius* and *Discocyclina douvillei* were noted. The lower unit was overlain by 50m of light grey, foraminiferal, bioclastic and detrital limestone with chert nodules. These two units were overlain by the last unit in the succession, which was recorded as a further 120m of limestone and clayey limestones with chert. The Palaeocene foraminifera (*Nummulites solitarius* and *Nummulites deserti*), were noted to be mixed with *Nummulites planulatus*, of Lower Eocene association, although no further inferences were given as to this occurrence.

*Jebel An-Nassuriyeh*

To the south, on the Jebel An-Nassuriyeh Mountains, the Lower Palaeocene was mapped as outcropping between the towns of Qerdaha and Jebleh, although the thickness was not given. At these localities Ponikarov et al. (1966) noted that the succession commenced with either conglomerates or glauconitic calcareous sandstones and limestones. *Nummulites frassi* and *N. deserti* were recognised, as was *Discocyclina nummulitica* and *D. archiaci*, in the overlying foraminiferal, clayey limestones. At the top of the sequence *Nummulites planulatus* (Lower Eocene association) was recorded and again, no further inferences were given for the mixed foraminiferal assemblage.

## Lower Eocene

(*Globorotalia subbotinae* zone and *Globorotalia aragonensis* subzone)

*Baer-Bassit Massif*

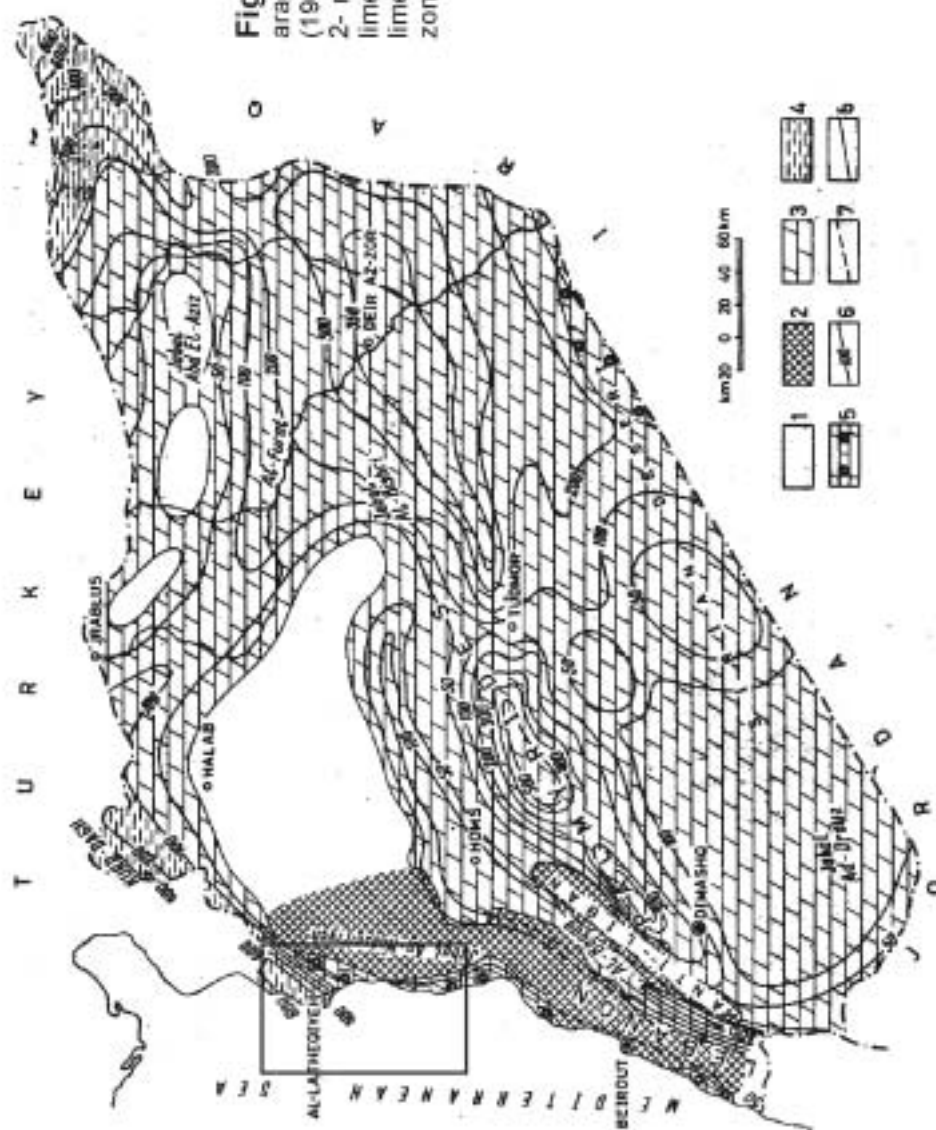
This zone was reported, based on drilling at Salib Turukman, north of Latakia, by Ponikarov et al. (1966). They noted that this succession contained grey to blueish-grey marls and clayey limestones. The lower 100m they assigned to their '*Globorotalia subbotinae* zone' and the top 40m to the '*Globorotalia aragonensis* zone', although no sedimentological break was noticed.

*Jebel An-Nassuriyeh*

The Lower Eocene succession was mapped on the Jebel An-Nassuriyeh Mountains south of the towns of Safarqiyeh and Banyas by Ponikarov et al. (1966). They reported that the succession reached a maximum thickness of 65m south of Banyas, but was normally found to be much thinner. No description of the sedimentary rocks was given. A list of the important foraminifera was produced to place the succession in the two zones described above, including various species of *Nummulites* and *Discocyclina* (see Appendix 1).

**3. Middle Eocene ( $Pg_2^2$ )**

Sedimentary rocks of Middle Eocene age were found by Ponikarov et al. (1966) near Latakia City (Baer-Bassit Massif), on the Jebel An-Nassuriyeh Mountains and to the east of the Ghab Valley. The succession was split biostratigraphically into three zones, which were difficult to differentiate in the field. These three zones were reported as (oldest to youngest): 'the *Acarinina Bullbrookii* Zone', 'the *Acarinina Rotundimarginata* Zone' and 'the *Hantkenina Alabamensis* zone'. The foraminiferal framework these zones were based upon was updated and modified by Krasheninnikov (1994) as they do not correlate to modern standards (see Appendix 1). The sedimentary rock descriptions, although not updated are still useful.



**Figure 2.5** Palaeocene-Lower Eocene (Globorotalia aragonensis zone) outcrop map from Ponikarov et al. (1967). Project area within box. 1- no sediments, 2- no sediments at present day, 3- marl and clayey limestone, 4- marl and clay, 5- marl and bioclastic limestone, 6- isopach lines, 7- isopach lines in eroded zones, 8- lithology boundaries.

*Baer-Bassit Massif*

Near the city of Latakia, Ponikarov et al. (1963 and 1966) recorded the Middle Eocene succession above the Lower Eocene with traces of erosion. The topmost unit (*'Acarinina pentacamerata zone'*) of the Lower Eocene succession was noted as being absent. The Middle Eocene-age sedimentary rocks were introduced as monotonous and the description was limited to friable and less friable foraminiferal limestones, containing grey and brown chert and with occasional “nummulites-like” foraminifera.

The *'Acarinina bullbrooki zone'* was observed in a borehole at the village Borj Islam and in outcrop on the southern margin of the Nahr El-Qandil River. In the borehole, the thickness recorded was 60m, whereas at outcrop some 175-180m of the succession was observed. Only at the Nahr El-Qandil River locality was the base of the unit recorded as 25-30m of massive detrital limestone, containing species of *Nummulites* (see Appendix 1). The *'Acarinina rotundimarginata zone'* was not reported to contain any *Nummulites* and a thickness of 140m was recorded. The rocks assigned to the *'Hantkenina alabamensis zone'* were inferred as being heavily eroded in Pre-Neogene times and were found only near the city of Latakia and Salib Turukman village. In outcrop, they attained a maximum thickness of 30m, but thinned rapidly further inland. The sedimentary rocks seen at these localities were recorded as clayey limestones with yellow and grey flints and some sandy clayey limestones. *Nummulites* foraminifera were noted to be present (see Appendix 1). Near the Nahr El-Kabir Valley, the sediments were observed to overlies the Baer-Bassit Massif ophiolitic rocks.

*Jebel An-Nassuriyeh*

In contrast to the Middle Eocene succession on the Baer-Bassit Massif, Ponikarov et al. (1966) recorded that the main lithology seen on the Jebel An-Nassuriyeh Mountains was nummulitic limestones. The rock descriptions indicate that the majority of the succession comprised 'massively laminated' (25-50m thick), fine-grained limestones with chert and abundant *Nummulites* foraminifera. Locally the base of some these limestones was characterised by glauconitic grains and limestone pebbles. The Middle Eocene succession was described as cutting down into the underlying Lower Eocene and Maastrichtian rocks with an uneven profile such that erosion increased to the east. The maximum thickness recorded was at the village of Nqourou (125m), encompassing both the *'Acarinina bullbrooki zone'* and the *'Acarinina rotundimarginata zone'*.

At the village of Btendra, the *Nummulites* and bivalve species found indicated a late Middle Eocene or even Upper Eocene age for the rocks at the top of the succession. At this site and further north towards Adasiyeh village, this unit was reportedly unconformably overlain by a further 20m of massive, clayey, chalky limestone, entraining blocks of older rocks. The '*Hantkenina alabamensis* zone' was recognised at this locality by Ponikarov et al. (1966) from the clayey limestones in the matrix, although the zonation does not obviously correlate with the evidence given for the Btendra village locality. The top of the succession was recognised only from foraminiferal studies as it appeared to be overlain by the lithologically similar Aquitanian succession.

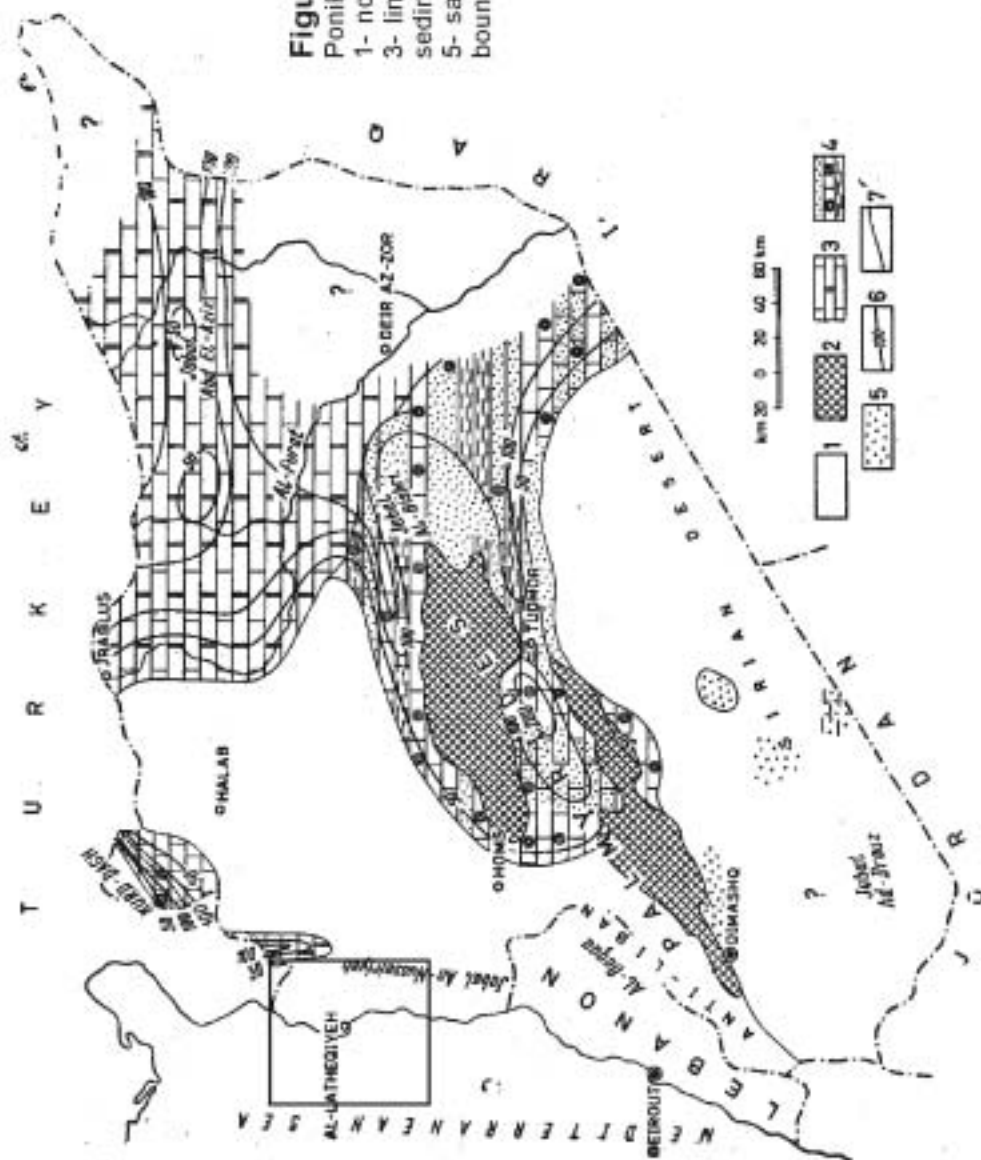
#### **4. Oligocene (*Pg<sub>3</sub>*)**

Oligocene sediments were not found within the Nahr El-Kabir Valley outcrops investigated by Ponikarov et al. (1966) and were mapped only east of Jus Ash-Shaghour, in the Ghab Valley (Figure 2.6).

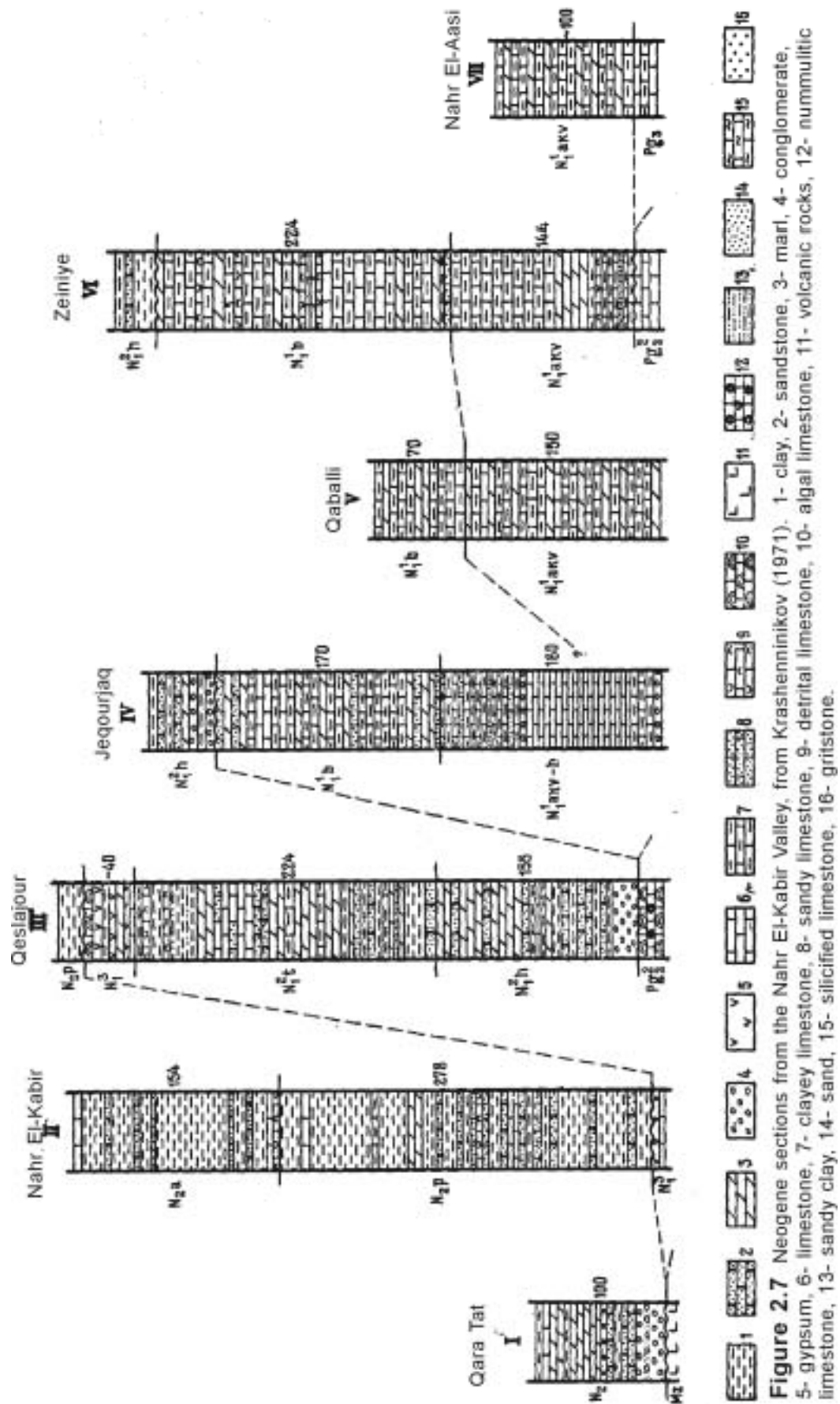
The Nahr El-Kabir Valley was commercially drilled in the 1970's by the Syrian Oil Company near the town of Fidjo (5km southeast of Latakia) and although the data have never been officially released, some of these results were included in the paper by Dzhabur (1985). He identified a horizon of Oligocene age in this borehole. In the sketch log he presented, the Oligocene limestones (123m thick) appeared to rest unconformably on the Cretaceous, giving a total post-Cretaceous thickness of 2157m. However, the data presented amounted to only one rudimentary sonic well log. No supporting biostratigraphy and sedimentological information was given, thus, these findings cannot be confirmed.

#### ***The Neogene***

Ponikarov et al. (1966) described the Neogene sediments as having very variable facies, but being lithologically monotonous. However, the report does not catalogue the facies or give sedimentological information. The map (Ponikarov et al. 1963) does not completely subdivide the area into time stages but groups stages based on obvious changes in lithology (Figures 2.7, 2.8, 2.9 and 2.10).

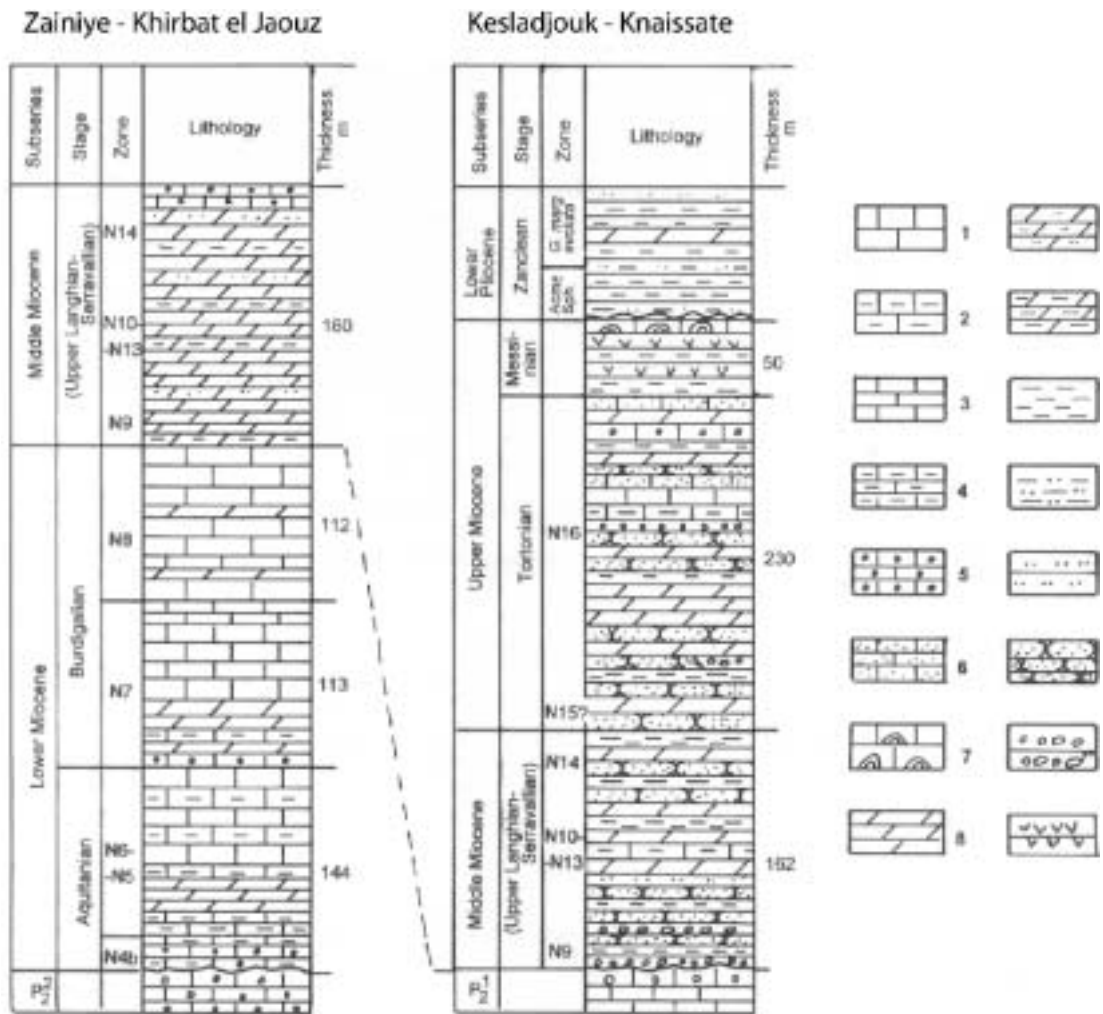


**Figure 2.6** Oligocene outcrop map of Syria, from Ponikarov et al. (1967). Project area highlighted.  
 1- no sedimentation, 2- no sediments at present day,  
 3- limestone, dolomite and marl, 4- "shallow water  
 sediments", sandstone, clay and "reef" limestone,  
 5- sandstone, 6- isopach lines, 7- lithology  
 boundaries



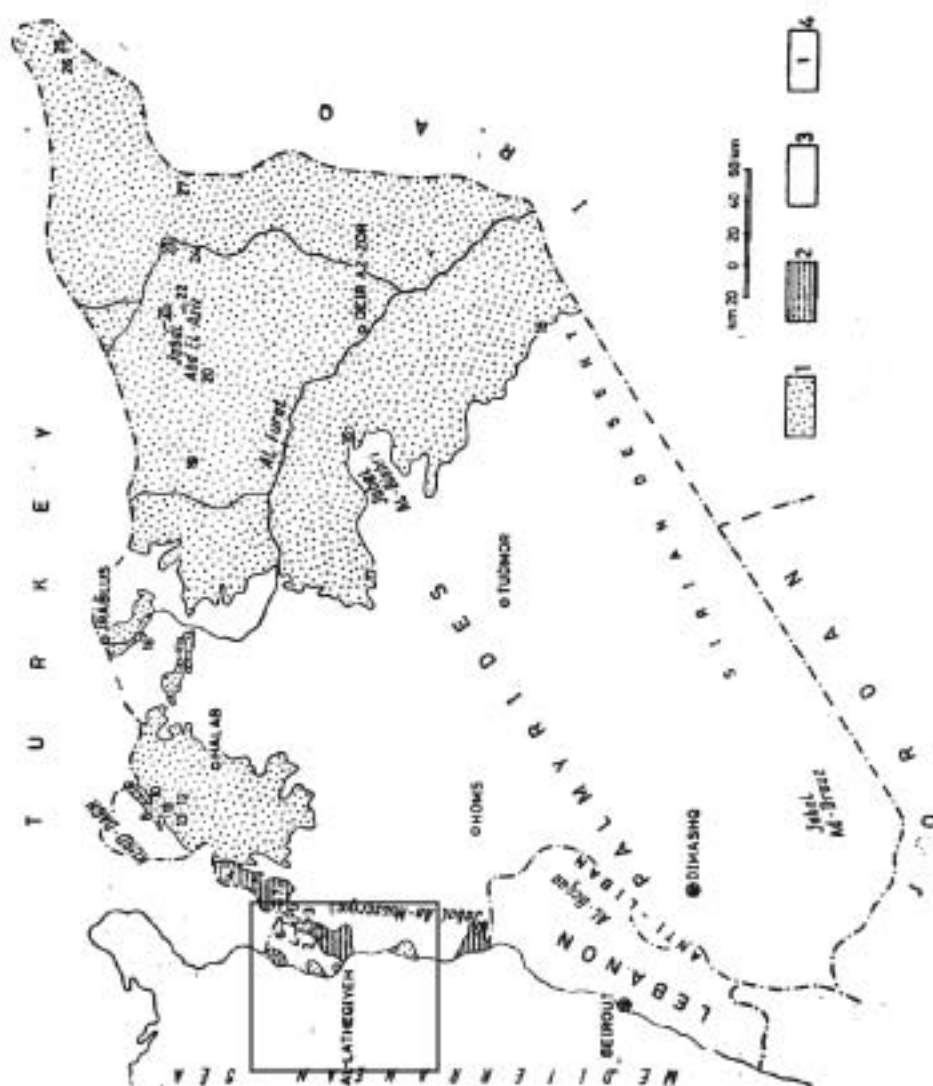
**Figure 2.7** Neogene sections from the Nahr El-Kabir Valley, from Krashenninikov (1971). 1- clay, 2- sandstone, 3- marl, 4- conglomerate, 5- gypsum, 6- limestone, 7- clayey limestone, 8- sandy limestone, 9- detrital limestone, 10- algal limestone, 11- volcanic rocks, 12- nummulitic limestone, 13- sandy clay, 14- sand, 15- silicified limestone, 16- gritstone.



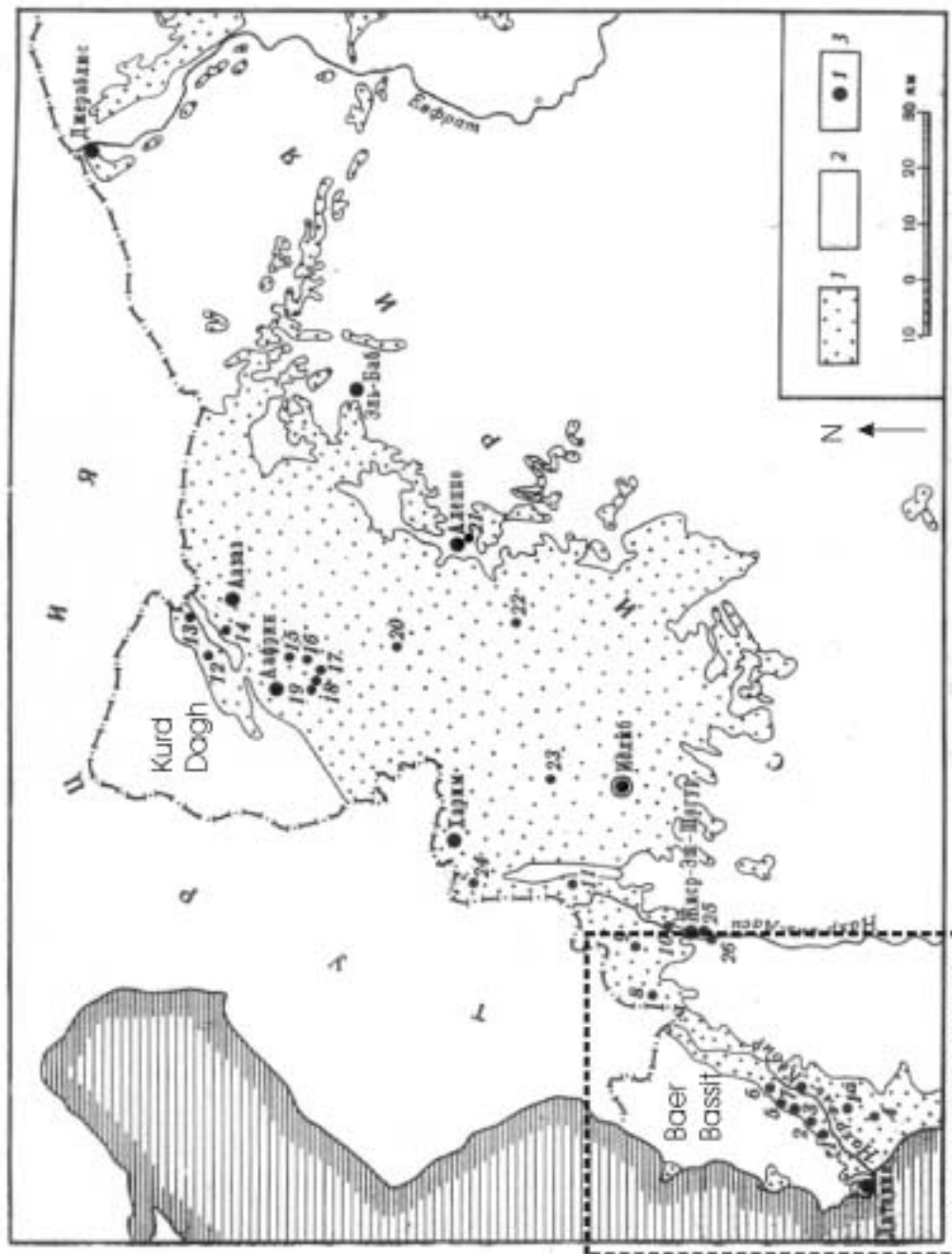


**Figure 2.8** Composite logs of the Neogene deposits found within the Nahr El Kabir Valley (right) and those further north (left), from Krashenninikov (1994). 1- chalky limestones, 2- clayey limestones, 3- soft and hard, fine-grained limestone, 4- clayey limestones (2), 5- organogenic limestones, 6- sandy limestones, 7- algal limestones, 8- marls, 9- silty marls, 10- clayey marls, 11- calcareous clays, 12- silty clays, 13- silt, 14- sandstones, 15- conglomerates, 16- gypsum. Refer to Chapter 4 and Appendix for foraminiferal zones.





**Figure 2.9** Outcrop map of Neogene rocks, from Ponikarov et al. (1967). Project area within the marked box. 1- areas of marine Miocene rocks, 2- areas of marine Pliocene rocks, 3- no Neogene age rocks, 4- location of Neogene logged sections (see Figure 2.7).



**Figure 2.10**

Map of Neogene exposures in northwest Syria (1), (2) no outcrops, (3) log locality. Highlighted box is the area for this project. Numbers refer to log localities in Figure 2.7 (1-7). From Krashennnikov (1971).

### ***Aquitanian ( $N_{1akv}$ ) – Lower Miocene – $N_4?$ , $N_5$***

The Aquitanian sediments were reported to commence with a sharp unconformity on the underlying Eocene succession and were recorded as outcropping solely within the Nahr El-Kabir Valley region and the Ghab Valley (Ponikarov et al., 1966). Variation in the succession was recorded from the northern to southern margins of the Nahr El-Kabir Valley and it was also noted that the Aquitanian sedimentary rocks were difficult to differentiate from the Eocene successions as they could be lithologically similar. Basal rudaceous rocks were said to be often absent and the Aquitanian succession was specified as being overlain by the Burdigalian succession with apparently no erosion, or by the Middle Miocene/Pliocene successions with a sharp unconformity.

The Aquitanian succession on the southern margin of the Nahr El-Kabir Valley was noted to comprise monotonous, white, unclearly bedded, clayey, foraminiferal limestone and marls by Ponikarov et al. (1966). The limestone lithologies were also catalogued as being intercalated with rare and thin sandstones, sandy marls and detrital limestone. The unit was said to reach a maximum thickness of 125-145m thickness, thinning to the south to 40-50m. At the village of Khan El Jouz, large blocks of Eocene nummulitic limestone were noted to be entrained within the sediments. Ponikarov et al. (1966) suggested that these blocks might have slid into the margins of a shallow Neogene sea.

Ponikarov et al. (1966) recorded a slight variation in the Aquitanian sediments on the northern margin of the Nahr El-Kabir Valley. The sediments were also described as monotonous, clayey, mostly unclearly bedded, limestone alternating with marl, but they also noted that rare, thin, non-persistent beds of polymict sandstone were also present, as was yellow detrital limestone. At Qaballi village the succession was recorded to reach its maximum thickness of 150m, from an average of about 80m.

### ***Burdigalian ( $N_{1b}$ ) – Lower Miocene***

The Burdigalian succession was reported to crop out on both the northern and southern margins of the Nahr El-Kabir Valley. Considerable differences in the sedimentary rocks between these margins was reported by Ponikarov et al. (1966). At the southern margin, the succession was noted to comprise of homogenous carbonate sediments, exhibiting a clear contact on the underlying Aquitanian, although the lithological change was recorded as being slight. In contrast, the northern margin sedimentary rocks were mapped as abutting directly onto the Baer-Bassit Massif and were said to comprise terrigenous conglomerates

and sandstones. Ponikarov et al. (1966) stated that all the Burdigalian facies overlie the lower units without erosion, except for those suggested by a basal conglomerate found only in the northwest of the Nahr El-Kabir Valley. The top of the Burdigalian succession was recorded to be overlain by units that were deeply eroded into it. Ponikarov et al. (1966), stated that “facies differences recorded during the Aquitanian became more pronounced in the Burdigalian”, although they did not expand on this description. The Burdigalian succession was split into two informal units.

Near Adasiyeh village, to the north of the Nahr El-Kabir Valley, the Burdigalian succession was recorded as reaching its maximum thickness of 220m (Ponikarov et al. 1966). No unconformity to the underlying Aquitanian succession was noted, or a major lithological change. The lower part of the succession was described as white to light grey, clayey, limestone and marls, whilst the upper part of the sequence was dominated by detrital limestones.

Within and on the southern margin of the Nahr El-Kabir Valley these distinctions were specified as being more prominent. The lower unit was noted to reach 160m thickness and to comprise of thinly bedded clays, laminated clayey limestone and limestone conglomerates. The upper unit was described as poorly bedded clayey limestone and marls, interbedded with lenses of sandstone and gravel and contained *Chlamys*, *Pecten* and *Ostrea*. This unit was noted to reach an average thickness of 155-170m and the maximum recorded thickness (330m) was at Jeqourjaq village, close to the Baer-Bassit Massif. This locality is a working asphalt pit, now belonging to the Syrian Establishment of Geology.

Ponikarov et al. (1966) also noted that the Burdigalian succession thinned to less than 100m thickness at the village of Khan El-Jouz (6km SE of Jeqourjaq) and was only 18m thick a further 20km to the southeast.

### ***Helvetian ( $N_1h$ ) – Langhian/Serravallian – Middle Miocene***

In the coastal region, north of Latakia, the Middle Miocene sediments were mapped as a small, single unit by Ponikarov et al. (1963). Krasheninnikov (1994) later revised the stage designation ‘Helvetian’ to Middle Miocene.

Ponikarov et al. (1966) recorded that this Middle Miocene succession was overlying directly the Cretaceous and Paleogene rocks on the margins of the Nahr El-Kabir Valley. The unconformity was noted to be at a low angle and varying amounts of erosion were

recorded. Occasionally the succession was also noted to commence with a conglomerate or infilled a pre-existing karst palaeotopography.

The succession was described as comprising of monotonous bioclastic and detrital limestone lithologies, with the facies being changeable. Macrofossils were also recorded, including gastropods, bivalves (*Clamys*), echinoids (*Clypeaster*) coral, algae and numerous foraminifera. The unit was logged as varying between 1-20m thickness.

### ***Tortonian ( $N_1t$ )***

The Tortonian succession was not individually mapped in the Nahr El-Kabir Valley by Ponikarov et al. (1966) and was only recorded to the east of the Ghab Valley.

### ***Helvetian-Tortonian Undifferentiated ( $N_1h-t$ ), Langhian to Tortonian undifferentiated***

The Middle Miocene sedimentary rocks of the Nahr El-Kabir Valley were mapped as one unit by the original Russian survey (Ponikarov et al. 1966) although they did divide the succession into two indistinct units for descriptive purposes. Overall, the succession was reported to reach a maximum thickness of 410m, although they specified a lower unit as being 155m thick and an upper as 225m thick.

The succession was noted to commence with a sharp unconformity and deposition occurred onto what was suggested as an eroded palaeotopography in the underlying successions. At the top of the succession, the transition from the Middle to the Upper Miocene was described being one of two possible processes: either a regression or erosive transgression by the overlying Pliocene succession.

The undifferentiated nature of the mapping of the Middle and Upper Miocene succession was chronicled by Ponikarov et al. (1966) as being due to rapid facies changes that led to problems identifying individual stratigraphic stages. They stated that some localities were fixed by the age of foraminifera they found, but they did not catalogue these reference localities.

The lithology of the units was described as alternating conglomerates, polymict sandstones, bioclastic detrital limestones, marls and sandy calcareous clays. The whole succession was reported to show considerable facies variation, although again no details were given. Near the village of Sallour, at the northernmost and narrowest end of the Nahr El-Kabir Valley, conglomerates were noted to dominate the succession. Further south, as the

valley widened, clays and marls were recorded as the dominant lithology. To the north of the Nahr El-Kabir Valley, in the Abyad River valley (Baksariyeh village), conglomerate was entirely absent.

### ***Messinian ( $N_1^3$ )***

The Russian study was completed before the hypothesis of the Messinian Salinity Crisis (MSC) was developed in the Mediterranean by Hs et al. (1973, 1977). Withstanding this, Ponikarov et al. (1963) had regarded the depositional environment as normal marine regressing to lacustrine and hypersaline.

They recorded that the succession commenced above an erosive unconformity, which removed some of the Upper Miocene successions. Three localities were cited by Ponikarov et al. (1966), each having a distinct Messinian succession. At the town of Al-Haffeh, a 30-35m thick unit of gypsum was recorded. It was stated that clays laterally replaced this gypsum locally. Five kilometres to the west, near the village of Fadreh, Ponikarov et al. (1966), reported that the succession commenced with 3-6m of shelly ("Serpula") limestones. The limestones were impersistent and contained oval blocks of almost pure shell hash up to 8m in diameter. These blocks were overlain by 25m of gypsum intercalated with sporadic and impersistent beds of limestone, marls, sandstone and stromatolitic limestone. Moving a further 5km south, the gypsum and shelly limestone were absent, leaving a section comprising only of alternating clays, marls and stromatolitic limestone. Foraminifera normally associated with Pliocene age rocks were found towards the top of the succession at this last locality.

### ***Pliocene ( $mN_2$ ) - Marine Pliocene***

The marine Pliocene succession recorded in the Nahr El-Kabir Valley was dated as Plaisancian i.e. Lower Pliocene, by Ponikarov et al. (1966). Since that time, Krashenninnikov (1994) has updated the stratigraphy and reported the presence of both Upper Pliocene and Lower Pliocene strata at this locality.

Rocks of Pliocene age were recorded by Ponikarov et al. (1966) in four major areas near the present coastline and distinct lithologies were catalogued at each site. At every locality, it was stated that the Pliocene succession either eroded the underlying strata or overlay a karst surface. The areas reported were: 1, the Nahr El-Kabir Valley, 2, on the Baer-Bassit Massif, 3, on the western slope of the Jebel An-Nassuriyeh Mountains and 4, near

Banyas town. The unit was reported to reach a maximum thickness of 460m, presumably in the Nahr El-Kabir Valley (Figures 2.11, 2.12 and 2.13).

### *1 Nahr El-Kabir Valley Pliocene*

This succession was divided into two units by Ponikarov et al. (1966). The lower unit was recorded as 230m thick and marl dominated, whilst the upper unit contained more arenaceous sediments and reached a maximum thickness of 180m. The sedimentary rocks were described as grey, dark grey to blue grey calcareous to arenaceous clays. They were also noted to contain horizons 2-18m thick of bedded, arenaceous, bioclastic, detrital limestone and oyster limestone. The limestones were unconsolidated and were replaced laterally by loose, poorly cemented calcareous sandstones. Ponikarov et al. (1966) specified that over 200 species of molluscs could be found in the succession.

### *2 On the Baer-Bassit Massif*

Two small outcrops were mapped overlying the Baer-Bassit Massif. The first was near the coast at the village of Ras El Bassit, approximately 100m above present sea level. The second was reported to occur much further inland near the Balloran reservoir, at a height of over 300m above the present sea level. Each succession consisted of a lower unit of coarse conglomerates and sandstones, fining upwards to clays, siltstones and marls. The overlying top unit was recorded as being bioclastic limestone. The maximum thickness given for the succession was 100m at Ras El Bassit village.

### *3 Western slope of Jebel An Nassuriyeh, near Qerdaha*

The Pliocene succession recorded by Ponikarov et al. (1966) near the Jebel An-Nassuriyeh Mountains, was inferred as being proximal with respect to the faults mapped in that area. The sedimentary rocks were described as being rudaceous, with both conglomerates and breccias. The conglomerates were noted to contain poorly rounded clasts, whilst the breccias were recorded to consist of large blocks of calcareous material and Eocene Nummulitic limestone. The breccias reached a maximum thickness of 50m and were described as being “reefal”. Away from the faults the lower part of the Pliocene succession consisted of “unfossiliferous reef limestones”, forming prominent mounds in the topography up to 50m high.

#### *4 Near Banyas town*

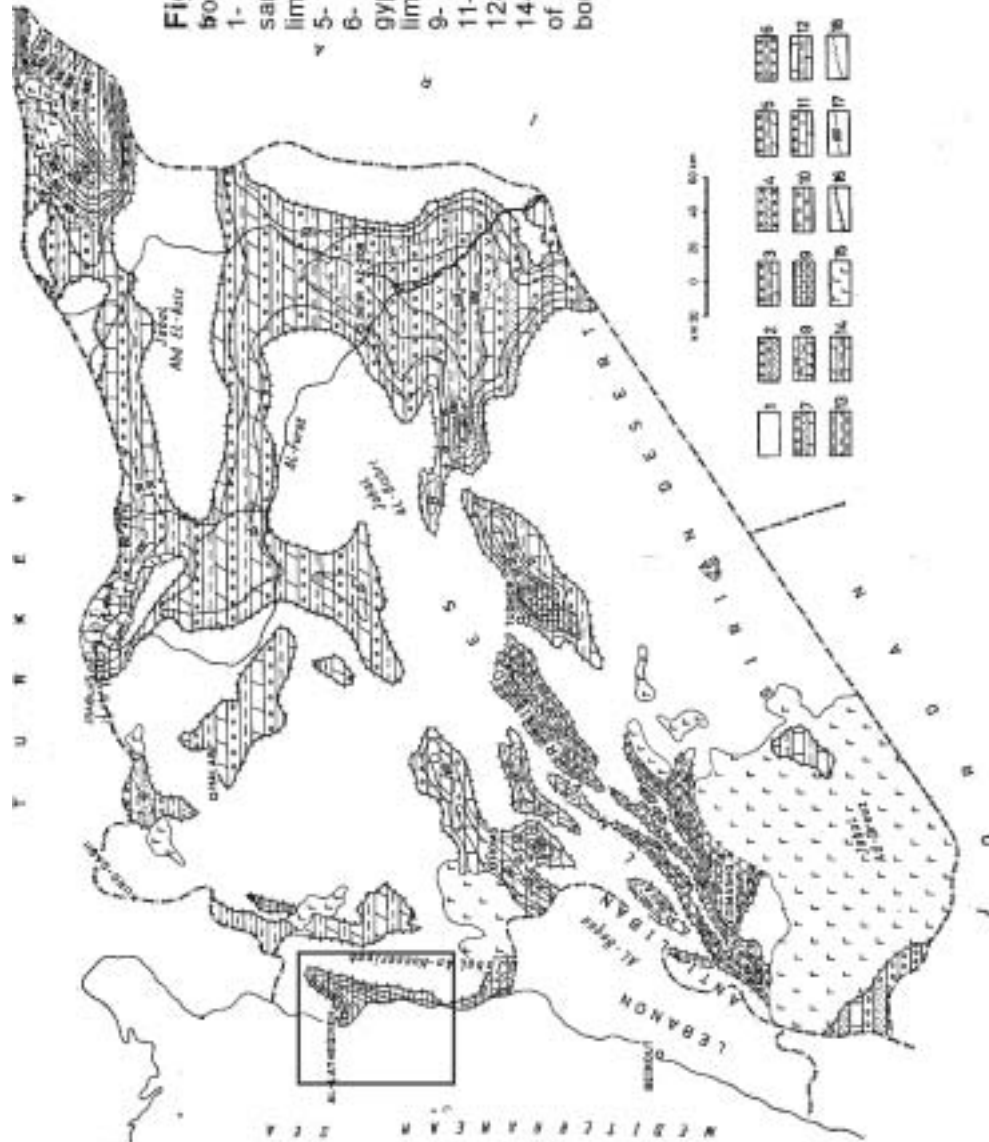
Basic tuff breccias and pyroclastic rocks were mapped near Banyas town by Ponikarov et al. (1963, 1966). The volcanic suite of rocks was reported to overly the Paleogene and Cretaceous successions by infilling an existing weathered surface. The maximum thickness recorded was 150m, although it was noted that the average thickness was 50m. The tuffs and tuff breccias were described as friable black rocks, weathering a rusty-brown colour. The pyroclastic rocks were reported to contain clasts of varying sizes of olivine basalt, dark coloured volcanic glass and ash.

A series of “dipping strata” or “cross bedded strata” was noted throughout and this layering was recorded to steepen moving upwards in the succession. It was stated that this might have been an artifact of cone eruptions, though no eruptive centres were found. The pyroclastic rocks were also reported to contain lenses and beds of Pliocene marine sediments. North of the town of Banyas, the Pliocene was present in a palaeo-valley and consisted of yellowish-green coloured marls and clays overlying the tuff succession. It was also stated that sheets of Pliocene basalt overlie the tuff rocks at other, unspecified, localities. Devyatkin et al. (1997) reported an age of  $4.35 \pm 0.22$  Ma for the basalts from lead isotope dating.

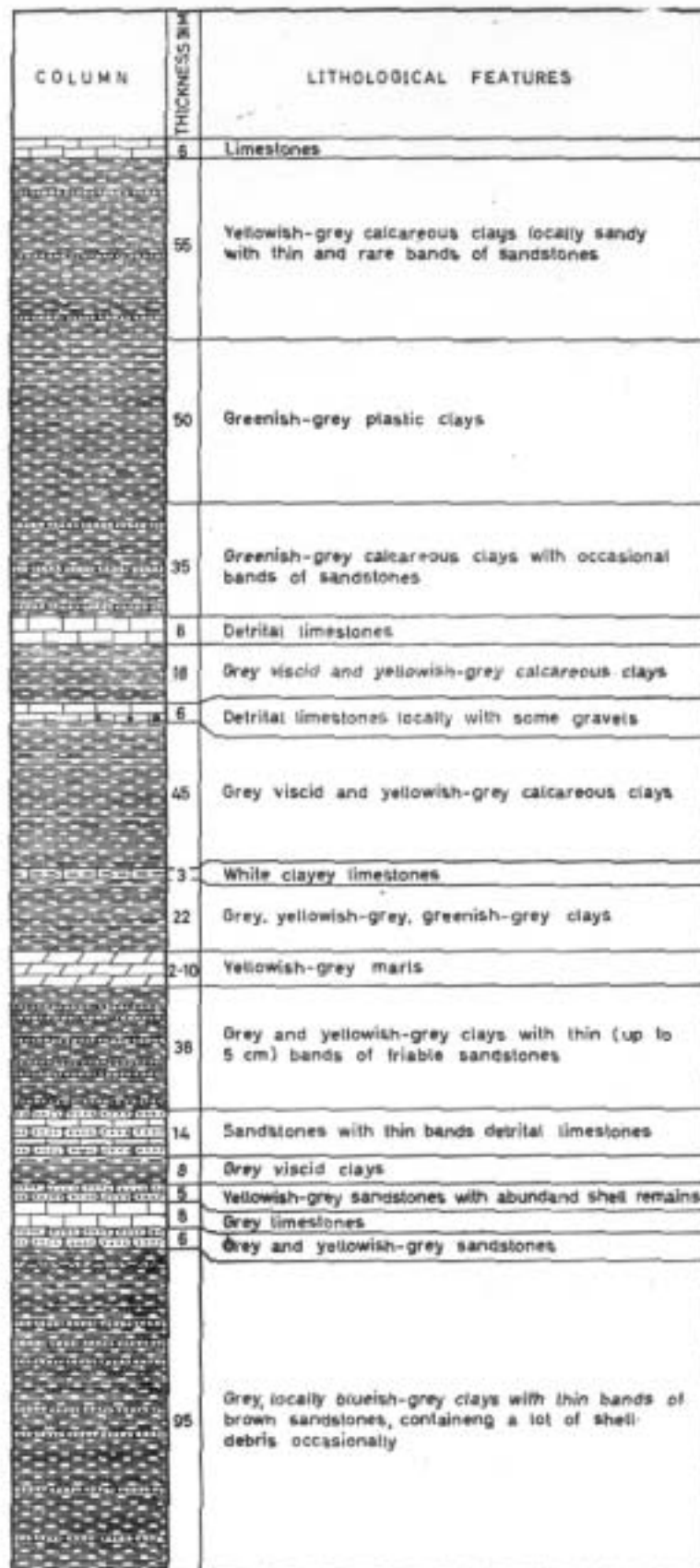
#### ***Pliocene (cN<sub>2</sub>) – Continental Pliocene***

Lacustrine marls and gravels were found only to the east of the project area, in the Ghab Valley, by Ponikarov et al. (1966). The succession was drilled at three localities across the valley to ascertain the complete sequence and they calculated that the complete unit reached a maximum thickness of 150m. One well was thought to have penetrated the base of the unit, reaching rocks of latest Cretaceous age. Coarse material at the base of the succession was reportedly overlain by “plastic” marl containing fresh water molluscs (see Chapter 5).

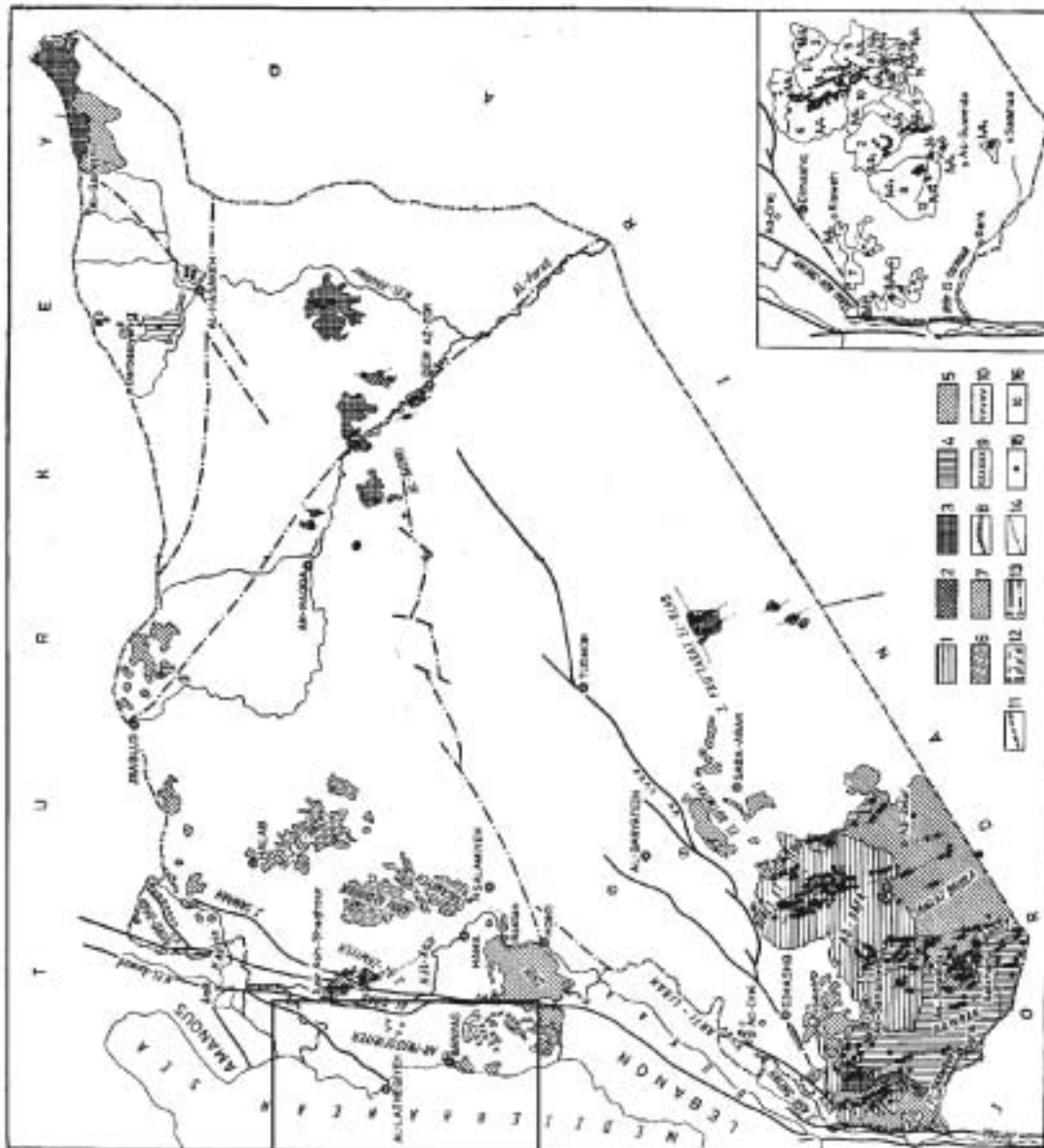




**Figure 2.11** Outcrop map of Pliocene sediments, from Ponikarov et al. (1967). Project area highlighted. 1- land, 2- lacustrine conglomerate, clay and sandstone, 3- lacustrine conglomerate, clay and limestone, 4- lacustrine conglomerate and sandstone, 5- lacustrine conglomerate, clay, marl and sandstone, 6- lacustrine conglomerate, sandstone, clay and gypsum, 7- lacustrine conglomerate, sandstone and limestone, 8- marine limestone marl and tuff, 9- lacustrine limestone, 10- lacustrine conglomerate, 11- lacustrine conglomerate, limestone and marl, 12- lacustrine limestone and clay, 13- marine clay, 14- lacustrine marl and clay, 15- basalt, 16- shoreline of sea basin (lake), 17- isopach lines, 18- lithology boundaries.



**Figure 2.12** Composite log of Pliocene age deposits from the Nahr El-Kabir Valley, from Ponikarov et al. (1966).



**Figure 2.13** Map of volcanism in Syria, from Ponikarov et al. (1967). 1- recent basalt, 2- Upper Quaternary basalt, 3- Middle Quaternary basalt, 4- Lower Quaternary basalt, 5- Pliocene basalt, 6- Upper Miocene basalt, 7- Middle Miocene basalt, 8- Lower Eocene basalt, 9- Upper Cretaceous basalt, 10- Lower Cretaceous basalt, 11- Middle Jurassic basalt, 12- hypabyssal basaltic rocks a) Quaternary, b) Pliocene, c) Miocene, 13- faults, 14- faults feeding channels of lava, 15- cones of extinct volcanoes, 16- numbers of recent basalt sheets.

### ***Quaternary (Q<sub>1</sub>-Q<sub>4</sub>)***

The Quaternary was split into four distinct units due to the assigned marine or fluvial nature of the sediments (Ponikarov et al. 1966). The rocks were mapped as covering a large part of the low-lying region of the Nahr El-Kabir Valley, reaching a maximum height above the current sea level of 215m. The four-fold divisions were: 1, Q<sub>1</sub> Lower Quaternary, 2, Q<sub>1-2</sub> Lower and Middle Quaternary, 3, Q<sub>3</sub> Upper Quaternary and 4, Q<sub>4</sub> Recent (Figure 2.14).

#### **Q<sub>1</sub> The Lower Quaternary**

These deposits were thought to form the two highest terraces above the Mediterranean at about 80m above present sea level, although above Jebleh town deposits were said to be at 120m and even extended up to 215m above sea level. The sediments were marine or proluvial (fluvio-marine), mainly conglomerates and yellowish grey organogenous-detrital limestone. The marine unit thickness reached 7m and comprise well rounded, sub-spherical to spherical clasts, pebbles and grains as well as the limestone. The shelly limestones were interbedded with sandstone and overlies Plaisancian and Astian (now termed Piacenzian) rocks, indicating a Calabrian age.

#### **Q<sub>1-2</sub> The Lower and Middle Quaternary**

Ponikarov et al. (1966) recorded unfossiliferous and fossiliferous marine sediments containing pebbles of limestone and chert in five terraces between 80m and 5m above present sea level. They also noted a more widespread yellow and brown fossiliferous sandstone, with cross bedding that seemed to be syndeformed and infilled topographic lows. The sandstones contained fragments of *Pecten*, *Ostrea*, corals and echinoids (Ponikarov et al. 1966). Upper Paleolithic flint implements were found near Latakia in these sediments.

#### **Q<sub>3</sub> Upper Quaternary**

The Upper Quaternary sediments were noted to be dominated by several genetic types of sediments: alluvium, proluvium, deluvium, lacustrine sediments and marine sediments (Ponikarov et al., 1966). The fluvial deposits were recorded to be found close to the current fluvial system and reached thicknesses of 2-11m. Near the Jebel An-Nassuriyeh Mountain foothills a red clay was found (20-30m thick), which was dated as 6-8000 years old, utilising pottery and tool fragments.

#### Q<sub>4</sub> Recent

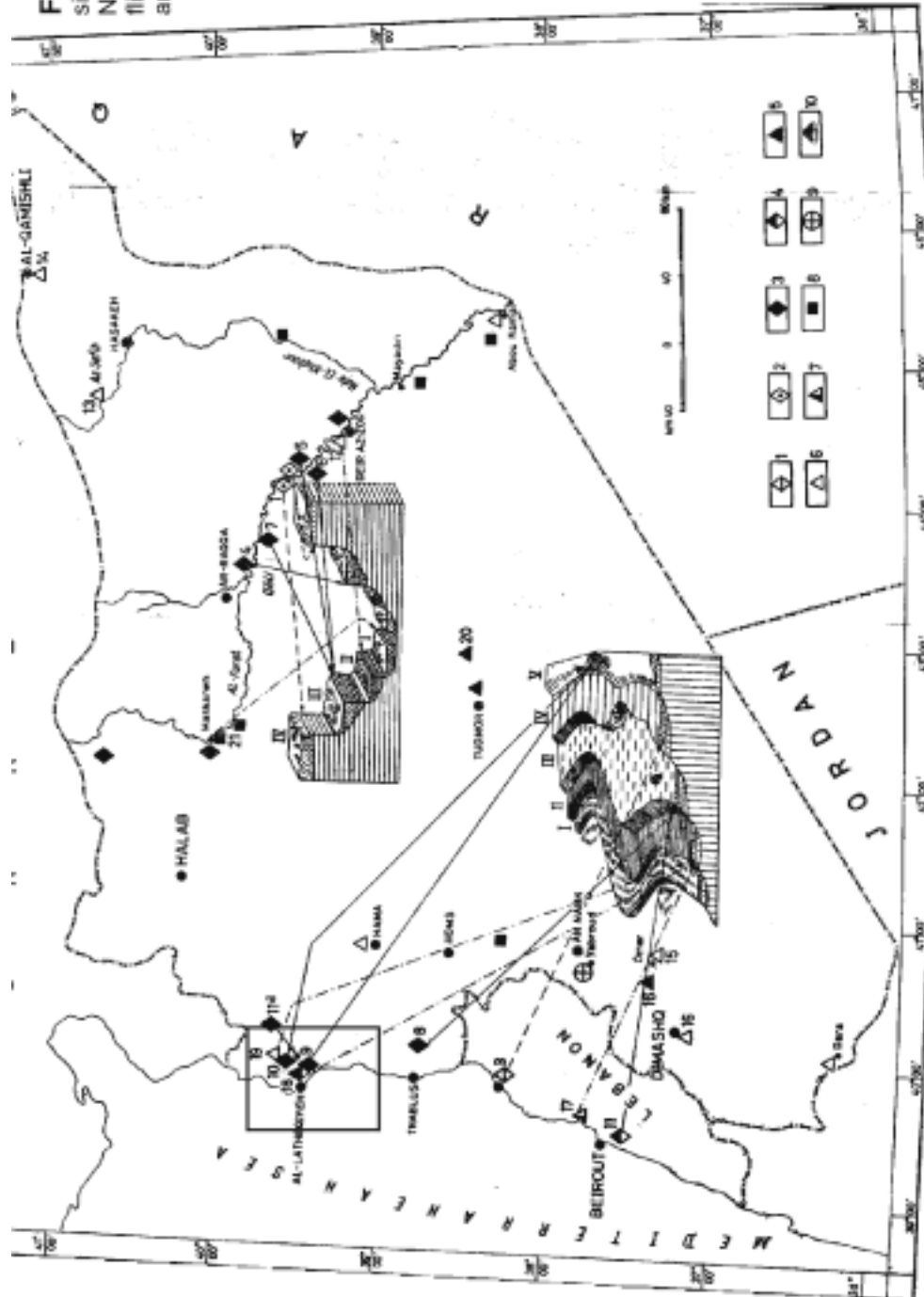
Recent sediments in this area were recorded as a mixture of alluvial, lacustrine and aeolian sediments, with the alluvial and aeolian deposits being specific to the Nahr El-Kabir Valley. Coarse gravel and sandy loams were also found in all river valleys and wadis. Sand dunes were found just north and south of Latakia along the coast, reaching 5m in height and up to 1km broad, to the 'coastal benches' (marine terraces). In the Ghab Valley, synchronous deposits were lacustrine.

#### ***Supplementary data and structural synthesis***

One of the major aims of the Russian work (Ponikarov et al. 1966) was to assess Syria for exploitable resources and much of their work details the location of water supplies, building stone and hydrocarbon shows. Their work is currently being updated and supplemented by a large-scale resources project by the Establishment of Geology, Damascus and is only briefly discussed here.

During the Russian study, magnetic and gravimetric data was acquired for Syria. The magnetic profile covers the Latakia region (see Figure 2.15), although unfortunately the gravimetric profile does not. The profile shows an irregular negative magnetic trend over the Baer Bassit Massif, increasing in value to the ridge of the Jebel An-Nassuriyeh Mountains. No further explanation was given.

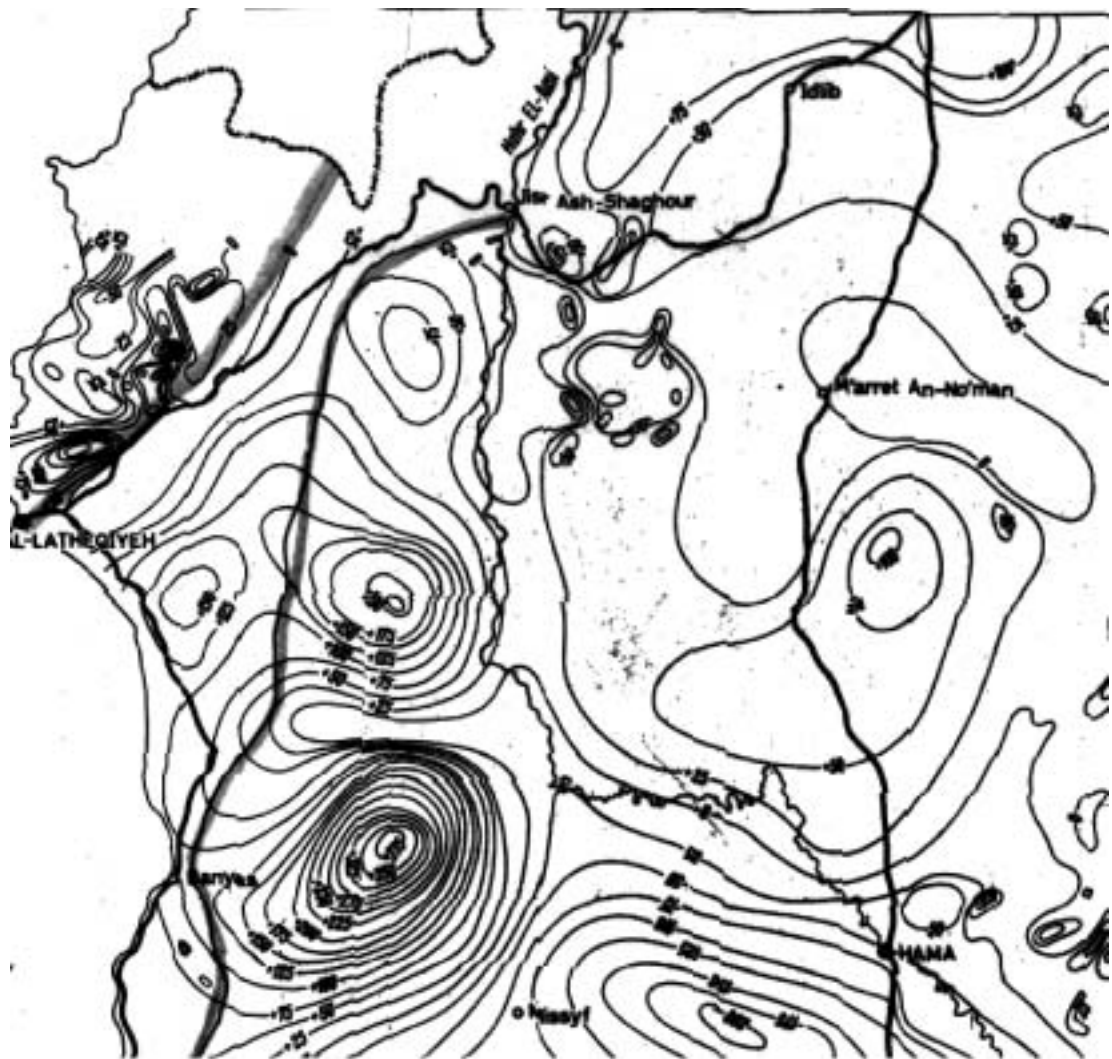
**Figure 2.14** Quaternary terrace sites from Ponikarov et al. (1967). Numbers 1-10 refer to findings of flint tools. Project area highlighted and terracing shown.



## Tectonics (also see Chapter 4)

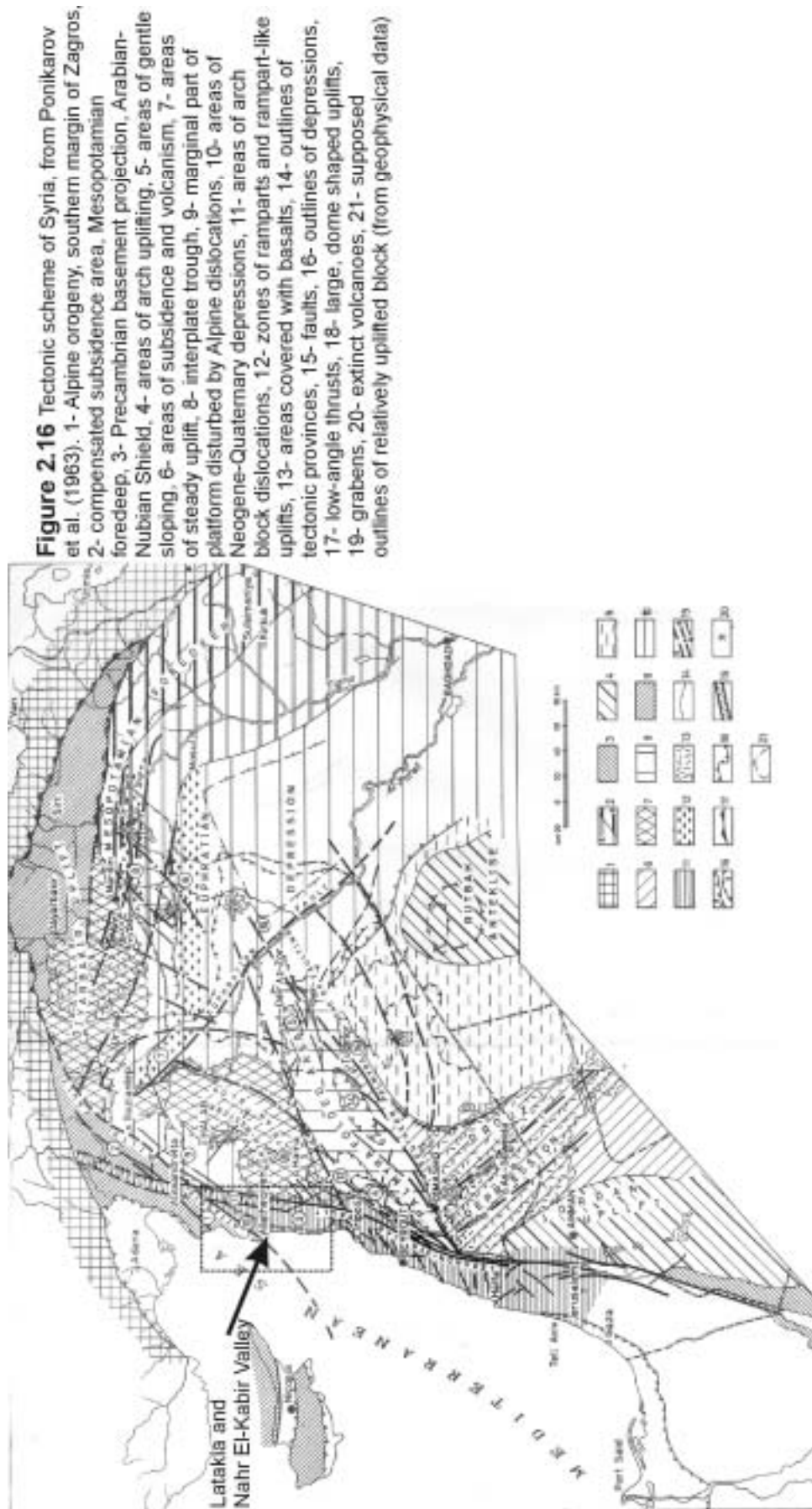
The basic elements of the tectonics in northwest Syria were recorded by Ponikarov et al., (1966 and 1967) as they form the most prominent topographic features (the Baer Bassit Massif, the Nahr El-Kabir Valley, the Jebel An-Nassuriyeh Mountains and the Ghab Valley)(Figures 2.16 and 2.17). However, there were gaps in their knowledge of the essential processes and in the timing of events and a complete tectonic synthesis was not put forward:

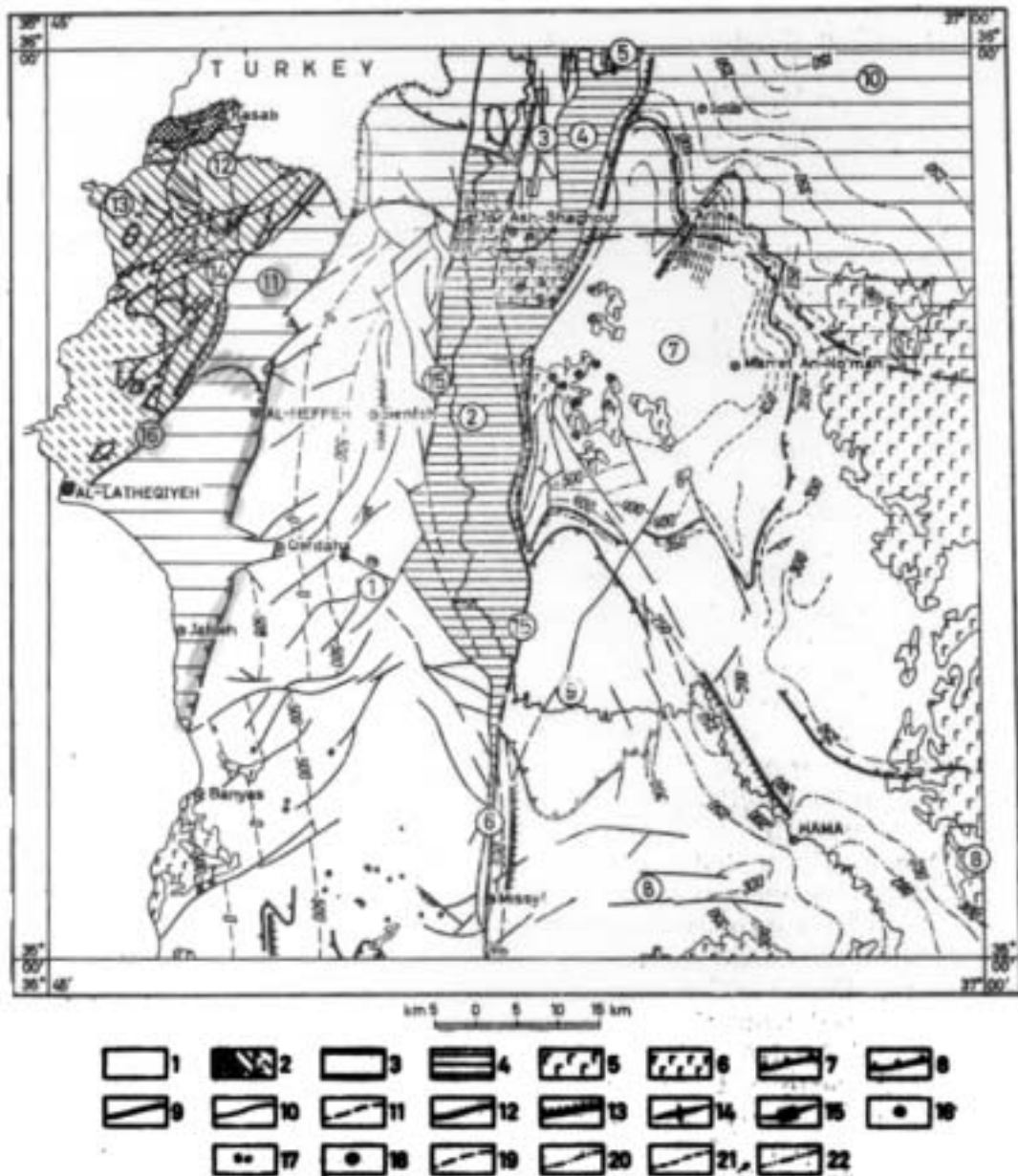
- € The Nahr El-Kabir Valley was recognised as a Miocene filled “depression”, a 6-8km wide “trench” running northeast to southwest. Dips were reported as sub-horizontal except near the “Latakia geosuture” (Figure 2.18).
- € The “Latakia-Killis Fault” (also “Latakia geosuture”) was recognised as a thrust fault bordering the Baer Bassit Massif. It was noted to connect the Latakia region to the town of Killis in southern Turkey (and the Kurd Dagh Ophiolite), some 150km to the northeast. Ponikarov et al. (1966 and 1967) reports that the fault is buried under Paleogene and Neogene deposits but local uplift occurs near the fault (massif margin) due to compression from the uplift of the Jebel An-Nassuriyeh Mountains.
- € The Baer Bassit Massif was recognised as being of “ophiolitic formation”, but the method of emplacement was unclear and the intense structuration and mass of ages encouraged the Russian team to conclude that the massif must be something unusual.
- € The Jebel An-Nassuriyeh Mountains were regarded as a “one-sided horst with a gentle anticlinal bend in the part near the (Dead Sea Transform) fault” (Ponikarov et al. 1966 and 1967). Two series of “ruptures” (faults) were recognised as “dissecting” the mountain range; one with a northeast trend and one with a northwest trend. The northeasterly trending faults appeared to have downthrown the northwestern limbs (hanging walls) by considerable throws (10’s to 100’s metres). The northwestern faults in contrast were found to be less numerous and have much less throw, dropping the northeastern limbs. No timing was given for the faulting and uplift.
- € The Dead Sea Transform Fault (Quenell, 1953) was recognised as a major rift fault at the time of mapping by Ponikarov et al. 1966 (termed “Lebanon-Syria fault”). It was thought to be responsible for the formation of the Ghab Graben and gravimetric surveys suggested to Ponikarov et al. (1967). that 2-3km’s of Pliocene sediments were present within.



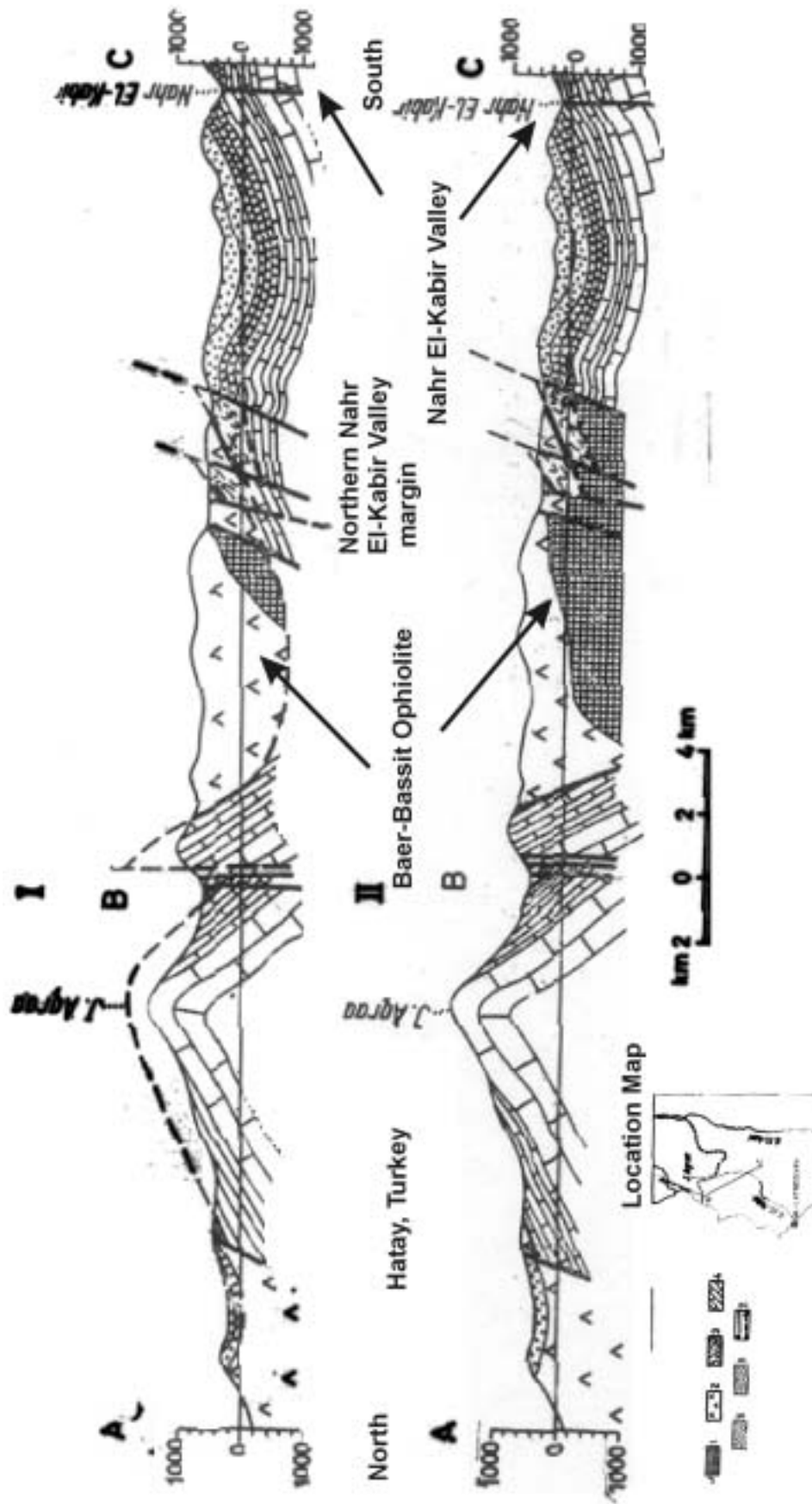
**Figure 2.15** Magnetic map of the northwest of Syria from Shatsky et al. (1966). Isolines are at 25 gammas and the Nahr El-Kabir Valley is highlighted. The Baer Bassit Massif is shown with negative magnetic trend, whilst the Jebel An-Nassuriyah Mountains show a strong positive trend. No gravimetric data were recorded over this area at the time of mapping.







**Figure 2.17** Tectonic map of the Latakia region, from Ponikarov et al. (1966), poor original. 1- region of relatively stable uplift, 2- marginal part of platform disturbed by Alpine movements, 3- Neogene depressions filled with marine deposits, 4- Pliocene troughs filled with continental deposits, 5- Upper Miocene basalts, 6- Pliocene basalts and tuff breccia, 7- boundaries of depressions and troughs, 8- contours of anticlines and synclines, 9- faults of deep seated occurrence, 10- faults, 11- faults supposedly under Pliocene deposits, 12- overthrusts, 13- flexures, 14- anticline folds, 15- coffer shaped anticline folds, 16- volcanoes of Pliocene age, 17- stocks of Pliocene basic rocks, 18- volcanic vents of Upper Jurassic-Lower Cretaceous age, 19- Cretaceous structure contours, 20- Campanian structure contours, 21- Middle Eocene structural contours, 22- Helvetian (Middle Miocene) structural contours.



**Figure 2.18** From Ponikarov et al. (1986). Two alternative cross sections through the Baer-Bassit Ophiolite and the northern margin of the Nahr El-Kabir Valley. The Tertiary sediments in this project are shown only as three units on the far right of this sketch, gently folded into a syncline and abutting a mass of thrust faults on the southern margin of the ophiolite.

## Summary and critic of previous work

The Russian field studies and regional reports (Ponikarov et al., 1966, Krasheninnikov, 1971 and 1994) and (Krasheninnikov et al. 1996) resulted in the following main conclusions:

- ≠ They were the first to systematically geologically map Syria and identify the major ages, rock units and lithologies throughout, within the constraints of knowledge at that time.
- ≠ They established the stratigraphic framework of Syria and applied this scheme, based mainly on planktonic foraminifera, to the country as a whole (including the area studied in this project).
- ≠ Within the project area the main findings were:
  1. The Baer Bassit Ophiolitic Massif was identified as a special rock unit, overlain by a separate series of marine, carbonate successions starting in the Maastrichtian through to the Middle to Late Eocene.
  2. These Maastrichtian to Eocene successions were found on the Baer-Bassit Massif as a complete sequence and at the Jebel An-Nassuriyeh Mountains as much thinner, often incomplete successions, separated locally by minor unconformities.
  3. Eocene sediments were markedly different between the localities on the Baer-Bassit Massif (fine, chalky limestones) and the Jebel An-Nassuriyeh Mountains (nummulitic limestones, which are similar to those found in the remainder of northern Syria). The Middle Eocene was the last unit seen before a widespread erosional episode covering Middle/Late Eocene and the Oligocene periods.
  4. The Aquitanian succession was found to be lithologically similar to the Eocene sedimentary rocks, but was only found within the Nahr El-Kabir Valley. It showed a sharp unconformity to the underlying successions and variation between the north and south margins of the Nahr El-Kabir Valley.
  5. The Burdigalian showed markedly more variation in lithology on the north and south margins of the Nahr El-Kabir Valley than the Aquitanian succession. Terrestrial input was recorded from the Baer Bassit Massif, leading to the only recorded erosional surface on the Aquitanian succession. In contrast, the southern margin was dominated by bioclastic and detrital limestone.
  6. The Langhian-Serravallian-Tortonian successions were found in two areas and only identified as an undifferentiated unit. On the Baer Bassit Massif, a single outcrop of

bioclastic limestone was recorded. In the second area, the Nahr El-Kabir Valley, the successions extend northwards from Bahlouliyah village to the Turkish border and had two key characteristics. In the Nahr El-Kabir Valley itself, the successions predominantly comprise bioclastic limestone and conglomerates, whereas to the north, marly limestone was the main component. The Tortonian was not individually identified in the Nahr El-Kabir Valley.

7. Gypsum, intercalated with limestones, was found in Messinian age sedimentary rocks of the Nahr El-Kabir Valley.
8. The Pliocene succession consisted of two units of limestone and sandstone in the Nahr El-Kabir Valley and limestone and basalt near Banyas. The eruptive age of the basalt was  $4.35 \pm 0.22\text{Ma}$  (Devyatkin et al., 1997) (i.e. the Lower Pliocene). Sandstones were noted to cap the Pliocene marly limestones and numerous species of marine gastropods were found.
9. The Quaternary was split into four units based on terracing found in the Nahr El-Kabir Valley. The highest two (up to 200m above sea level), had marine influence and the lower two were indicative of fluvial and alluvial processes.
10. Ideas relating to the regional structure were put forward based on the important topographical features.

Whilst the Russian work stands as a comprehensive and generally accurate piece of geological mapping, there are large gaps in their results. These are specifically: ideas relating to the environments of deposition, sedimentary processes, sediment reworking, sedimentary architecture, sediment facies, structural geology and the overall tectonic picture of the region. In almost every succession described, these topics were not covered. For a more complete understanding of the area and its importance for early continental collision in the Eastern Mediterranean region, much more study was undertaken and this is discussed in the following chapters.

## Sedimentology and stratigraphy

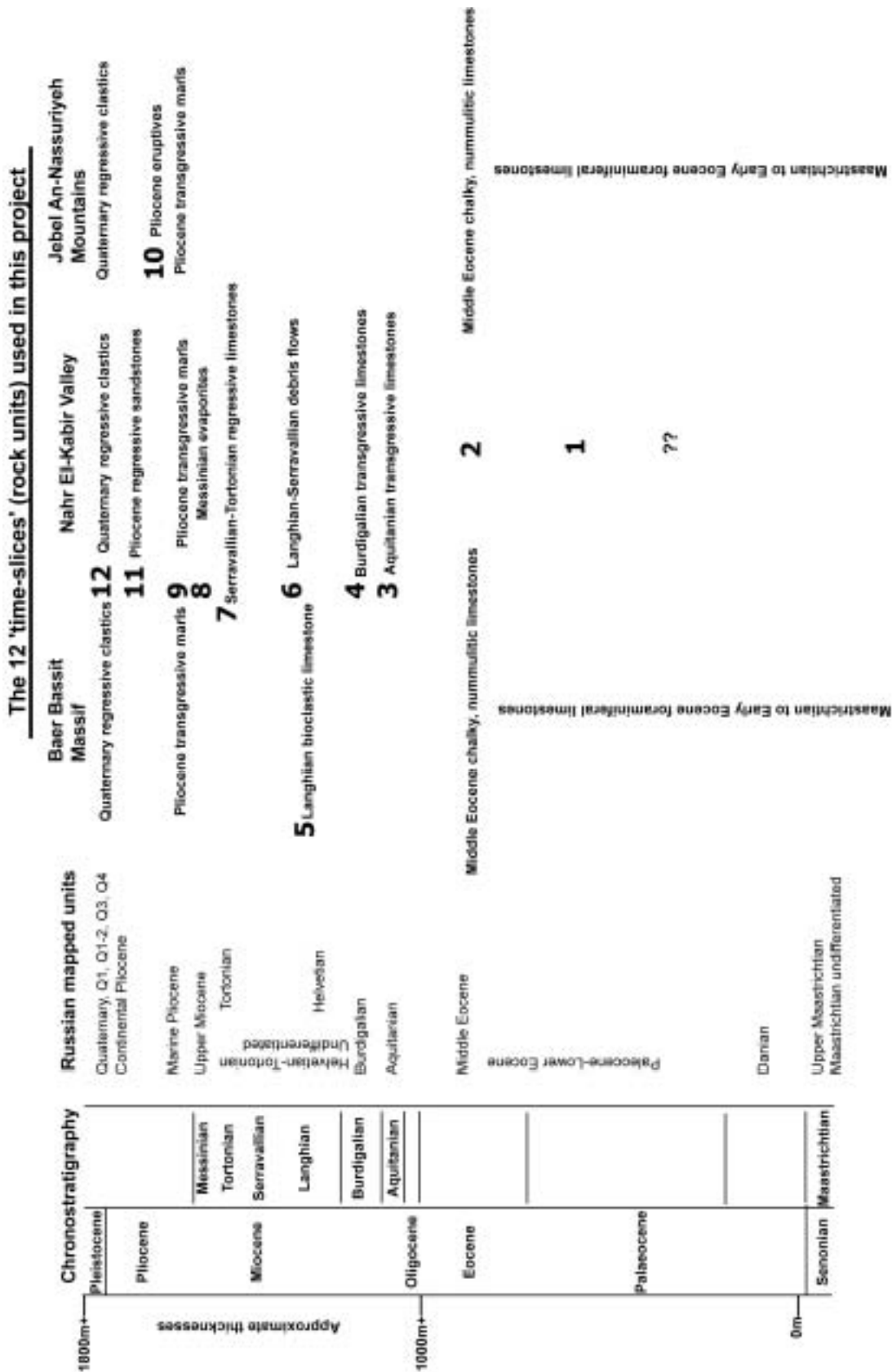
Reading the Russian mapping report (Ponikarov et al. 1966) and examining the rock units in the field, it is immediately obvious that the lithostratigraphic mapping and descriptions, although detailed, miss much of the geological picture. Each rock unit has marked lateral and vertical variation, which has not been previously explained fully. No benefit to this work would be gained from a formal definition of the formations (naming formations has been left to the Syrian Geological Survey)(see biostratigraphy, below).

The sedimentary facies are closely linked with the structural evolution of the area and this aspect needs to be explained at the onset for clarity (Chapter 4 details the structure of the area). This chapter explains the rock relationships, the facies present and the processes involved. To this end, this chapter will also put forward local interpretations of the rock units as twelve 'time-slices', then Chapters 6 and 7 will put these into a regional framework. Chapter 6 will also develop the concept that three 'megasequences' of Tertiary deposition occurred prior to the Quaternary in the Nahr El-Kabir Valley region. It will also explain the tectonostratigraphy, present a new facies map of the region and discuss the palaeogeography by combining the sedimentological and structural information.

The twelve 'time-slices' used in this study are shown in Figure 3.1. These take account of the most marked components of the sedimentary rock record of northwest Syria. Each 'time-slice' is described with regard to the facies, microfacies and facies variation. The lateral and vertical facies variation provides the basis for interpretations and regional comparisons. In general, the 'time-slices' link closely to known chronostratigraphic boundaries.

### *Project biostratigraphy*

The Tertiary biostratigraphy used here was developed by Ponikarov et al. (1963, 1966, 1967) and updated by Krasheninnikov (1971, 1994). It is based on a planktonic foraminifera zonal scheme developed in Russia (see Appendix 1). As such, it is very detailed, but often quite difficult to correlate with current international standards (i.e. Berggren et al. 1995). It can therefore, strictly, only be regarded as a local stratigraphy. Gastropods (Jaquet, 1933), pollen and spores (Simakova, 1993) and diatoms (Devyatkin et al. 1994) have also been used to subdivide Late Neogene successions where foraminiferal data were insufficient, although



**Figure 3.1** Project time-slices, relating the sedimentology of the project area to the regional stratigraphy developed by Ponikarov et al. (1963)

these studies are chronostratigraphically restricted (Appendix 1). The difficulties in correlating to the worldwide biostratigraphical schemes are due also in part to the evidence of the semi-isolated nature of the Mediterranean basin during the Late Tertiary. Worldwide eustatic curves (i.e. Haq et al. 1988), which can sometimes be used as proxies for major stratigraphic events, are also problematic in this region (see Chapter 6).

For this project, foraminiferal and nannofossil samples were sent to Marcel BouDagher-Fadel (University College, London)(20 samples) and Silvia Gardin (Paris)(10 samples), respectively, for dating. The preliminary results are broadly in agreement with the dating of the Russian map units (Ponikarov et al. 1963) (Figure 3.1). Work is ongoing with both micropalaeontologists to publish a user-friendly biostratigraphy with regional microfossil zonations, tied to the tectonic events, for Cyprus, Lebanon and Syria.

### Biostratigraphic studies

For this project, originally two PhD's were envisaged; this project was to look at the structure and sedimentology, whereas a parallel project was to update the biostratigraphy and date the units which were poorly identified or undifferentiated. Ultimately, this second project changed the emphasis of its research. The other project (also NERC funded) was carried out by Dan Howard at University College, London. Dan Howard chose to carry out biostratigraphic studies relating to the genesis and emplacement of the Baer Bassit Ophiolitic Massif and carried out only a reconnaissance study of the Tertiary. This meant that for this project, I had to make considerable use of the Russian biostratigraphy (Ponikarov et al., 1967; Krashenninnikov, 1971 & 1994), testing its accuracy as far as possible. Specialist studies (see below), determined that the Russian framework was robust enough to allow detailed sedimentological and stratigraphical studies of the area (Figure 3.2). However, the absence of dedicated biostratigraphy within the project has led to a lack of information regarding faunal community structure and diversity, palaeosynecological interrelationships and growth-form strategies. Further work is underway with the two micropalaeontologists detailed below to address this shortcoming.

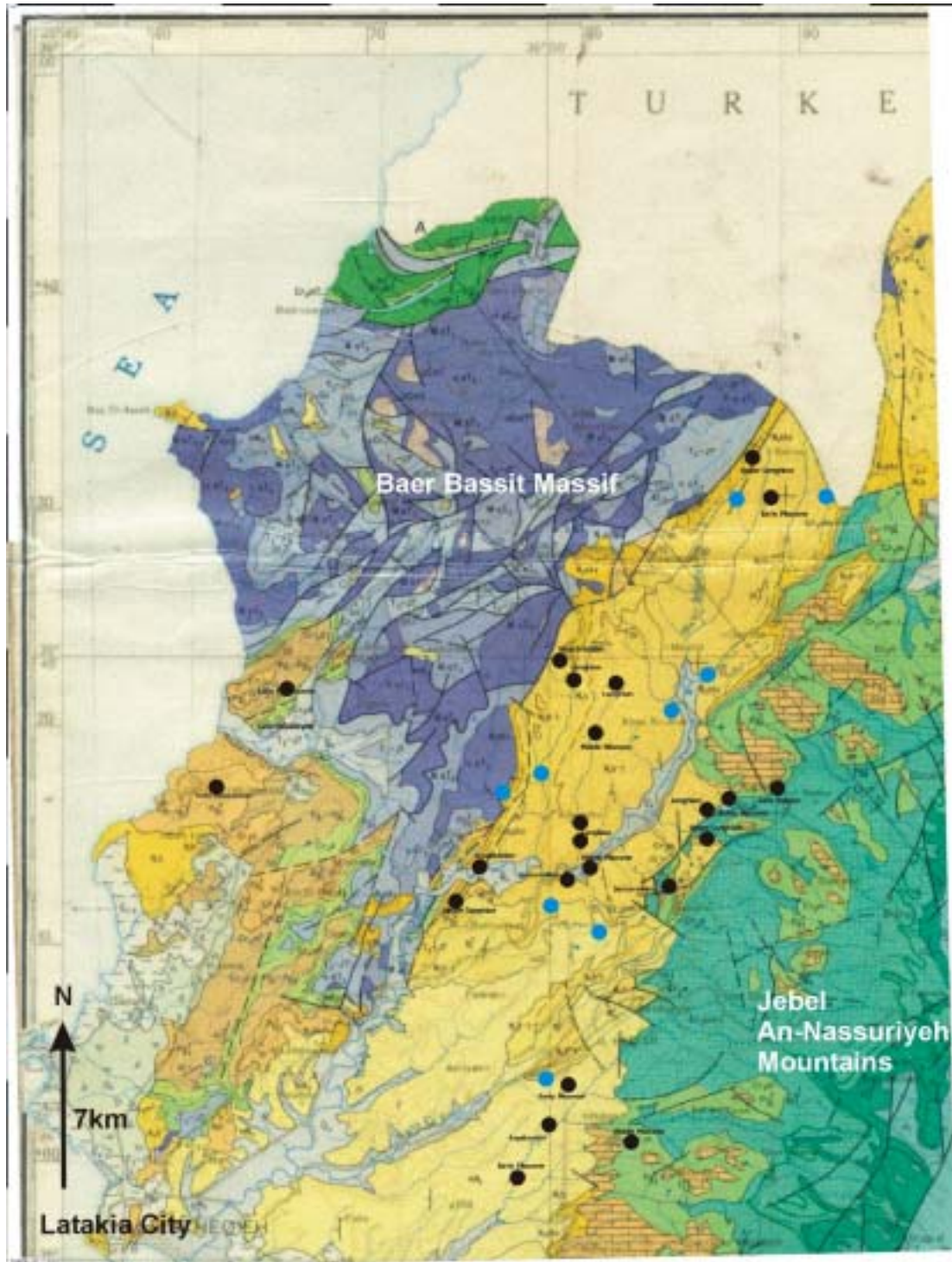
### Pelagic foraminifera

In this study, pelagic foraminifera were studied in thin section and sent for expert identification by Marcel BouDagher-Fadel, who has regional expertise in foraminiferal



identification from Lebanon and Cyprus. She is currently preparing a new, regional pelagic foraminiferal biostratigraphy for the Tertiary.

The thin section samples sent to Marcel BouDagher-Fadel were in the main from relatively hard carbonate samples to survive the sectioning process. Dan Howard (University College, London) also took numerous soft samples for Palaeocene whole



**Figure 3.2** Sample localities for foraminifera ● and nannofossil ● dating. The foraminiferal sites were chosen to assess the Early and Late Tertiary, from both margins of the Nahr El-Kabir Valley. Nannofossil samples were chosen to assess the amount of reworking in the centre of the valley. The samples were sent for expert analysis to Marcel BouDagher-Fadel and Silvia Gardin, respectively (see main text).

foraminiferal extraction, although results from his work were not available at the time of writing.

Marcel's work has allowed for differentiation to the stage and occasionally sub-stage level (i.e. Serravallian to Late Serravallian) for the samples taken, which is enough detail for the purposes of this work (Table 3.3 and Figure 3.2). Reworking of sediments was obvious in the field and in thin section (see later, this chapter), but was hardly mentioned in any of the Russian studies.

This extreme reworking of the microfossils may limit the accuracy of the dating. Further specialist studies may be needed in the future, especially with regard to interpretations of water depths derived from benthic to planktonic foraminiferal ratios (in thin section). For these reasons, the inferred environment from the microfauna (in thin section), is separated from results based on the complete study of each time-slice in the field.

### Nannofossils

Ten nannofossil smear slides were prepared in the department for key localities within the Tertiary successions of the Nahr El-Kabir Valley. They were sent to Silvia Gardin (Université Pierre et Marie Curie, Paris) who very kindly agreed to assess them and has shown interest in examining them further. Her findings are that the mapped ages given by Ponikarov et al. (1967) are in the main accurate, but that large amounts of Cenomanian, Maastrichtian, Eocene and Oligocene flora is also present in the majority of samples (Table 3.4 and Figure 3.2). This is accounted for by the intensive reworking of the sediments in the Nahr El-Kabir Valley (see later, this chapter), related to uplift of the Jebel An-Nassuriyeh Mountains (see Chapter 4).

				<i>Planktonic Foraminifera and other biomarkers identified by Marcel BouDagher-Fadel (University College, London)</i>
Cenozoic	Quaternary			No sample recorded
	Pliocene	Late		No sample recorded
		Early		<i>Globigerinoides sp.</i> , <i>Orbulina sp.</i> , <i>Sphaeroidinellopsis subdehiscens</i> , <i>Sphaeroidinella dehiscens</i> , <i>Dentoglobigerina altispira</i> , <i>Operculinella sp.</i>
	Neogene	Messinian		No sample recorded
		Tortonian		No sample recorded
	Miocene	Serravallian		<i>Globorotalia praemenardii</i> , <i>Orbulina bilobata</i> , <i>Orbulina universa</i> , <i>Orbulina suturalis</i> , <i>Dentoglobigerina altispira</i> , <i>Globigerinoides obliquus</i> , <i>Sphaeroidinellopsis sudehiscens</i> , <i>Globigerina sp.</i> , <i>Orbulina sp.</i> , <i>Globigerinoides sp.</i> , <i>Bulimina sp</i> <i>Globoquadrina sp.</i> <i>Valvulineria sp.</i> , <i>Nodosaria sp.</i> , <i>With some small benthic foraminifera</i> ; <i>Bulimina sp.</i> <i>Cycloclypeus sp.</i> , <i>Amphistegina sp.</i> , <i>Elphidium sp.</i> plus ostracod and rodophytes fragments.
		Langhian		<i>Orbulina bilobata</i> , <i>Orbulina universa</i> , <i>Dentoglobigerina altispira</i> , <i>Globigerina decoraperta</i> , <i>Globigerinoides quadrilobatus</i> , <i>Praeorbulina glomerosa</i> , <i>Praeorbulina transitoria</i> , <i>Globigerinoides trilobus</i> , <i>Globorotalia peripheroronda</i> , <i>Globorotalia mayeri</i>
			Burdigalian	
		Aquitanian		<i>Rotalia sp.</i> , <i>Miogypsinella sp.</i> , <i>Miogypsinoides sp.</i> , <i>Operculina sp.</i> , <i>Lepidocyclina stratifera</i> , <i>Lepidocyclina (Nephrolepidina)</i>
	Palaeogene	Oligocene		No sample recorded
		Eocene	Late	<i>Victoriella sp.</i> , <i>Fabiania sp.</i> , <i>Discocyclina sp.</i> , <i>Rotalia sp.</i> , <i>Operculina sp.</i>
			Middle	
		Palaeocene	Early	
Late			<i>Morozovella velascoensis</i> , <i>Morozovella uncinata</i> , <i>Planorotalites pseudomenardii</i> , <i>Subbotina pseudobulloides</i> , <i>Globorotalia aequa</i> , <i>Assilina sp.</i>	
Cretaceous	Senonian	Early	No sample recorded	
		Maastrichtian	<i>Subbotina pseudobulloides</i> , <i>Morozovelle uncinata</i> , <i>Morozovella velascoensis</i> , <i>Glorotalia aequa</i> , <i>Rugoglobigerina rotundata</i> , <i>Planohedbergella sp.</i> , <i>Globotruncana sp.</i> , <i>Rugoglobigerina sp.</i> , <i>Hedbergella sp.</i> , <i>Spiroplecta sp.</i> , <i>Globotruncana stuarti</i> , plus Ostracods	
Mesozoic				

**Table 3.3** Foraminiferal species identified by Marcel BouDagher-Fadel from samples collected during this project (BouDagher-Fadel et al. 1998, 1999, 2000 A&B).

<b>Time period</b>	<b>Diagnostic nannofossils</b>	<b>Supplementary fauna and remarks</b>
<b>Early Pliocene</b>	<i>Pseudoemiliana lacunosa</i> , <i>Discoaster calcaris</i> , <i>D. broweri</i> , <i>D. asymmetricus</i> , <i>D. surculus</i> , <i>Syracosphaera pulchra</i> , <i>Calcidiscus macintyreii</i> , <i>Umbilicosphaera rotula</i> . Sphenoliths are absent.	Common reworked Cretaceous and Paleogene taxa. Ascidian spicules present.
<b>Late Miocene- Early Pliocene</b>	<i>Calcidiscus leptoporous</i> , <i>Calcidiscus mcintyreii</i> , <i>C. tropicus</i> , <i>Helicosphaera mediterranea</i> , <i>Sphenolithus moriformis</i> , <i>S. cf. S. abies</i> , <i>Sciphosphaera apsteini</i> , <i>Discoaster surculus</i> , <i>D. variabilis</i> , <i>D. exilis</i> , <i>Umbilicosphaera jafari</i> , <i>U. rotula</i> , <i>Sphenolithus abies</i> , <i>Sciphosphaera cylindrica</i>	Abundant Ascidian spicules. Reworked nannofossils outnumber those <i>in situ</i> – mainly from Paleogene (Danian to Late Oligocene). Cretaceous taxa also present.
<b>Late Miocene</b>	<i>Calcidiscus leptoporous</i> , <i>Calcidiscus mcintyreii</i> , <i>C. tropicus</i> , <i>Reticulofenestra gelida</i> , <i>Helicosphaera carteri</i> , <i>Sphenolithus moriformis</i> , <i>Sphenolithus cf. S. abies</i> .	Abundant Ascidian spicules. Common reworked Eocene and Oligocene taxa ; rare reworked Cretaceous taxa. Discoasters absent (unusual), very proximal setting?
<b>Miocene</b>	<i>Calcidiscus leptoporous</i> , <i>Calcidiscus mcintyreii</i> , <i>Helicosphaera carteri</i> , <i>Reticulofenestra gelida</i> , <i>Discoaster exilis</i> group, 6-rays overgrowth <i>discoasters</i> spp.	Rare reworked Cretaceous and Eocene taxa. Coccoliths are very small size – restricted environment?

**Table 3.4** Nannofossil species identified by Silvia Gardin, from initial Nahr El-Kabir Valley samples.

### ***Methodology of sedimentological field studies***

The sedimentary rocks of the project area were intensively studied (utilising more than 400 field localities, 300 samples over three field seasons), with samples, field sketches, logs and measurements taken to shed light on the sediments and processes. On return from the field, the samples were cut for further hand inspection and those of most interest were thin sectioned for standard polarised light microscopy.

## Stratigraphic and sedimentological terminology

Much of the previous work carried out in the region (Chapters 1 and 2) has used old or unspecific terminology to describe stratigraphic units (e.g. Upper Serravallian) or the sedimentology and structure (e.g. ‘massively laminated beds’ and ‘geosuture’). Throughout the field-studies many sedimentological and structural features had to be re-examined due to inaccurate terminology in previous work. This thesis uses up to date terminology to improve clarity of discussion and to conform to modern international standards.

For example, the Upper Serravallian is referred to as the Late Serravallian and bedding or lamination is defined in Table 3.5. Structural terms are also updated in Chapter 4 onwards.

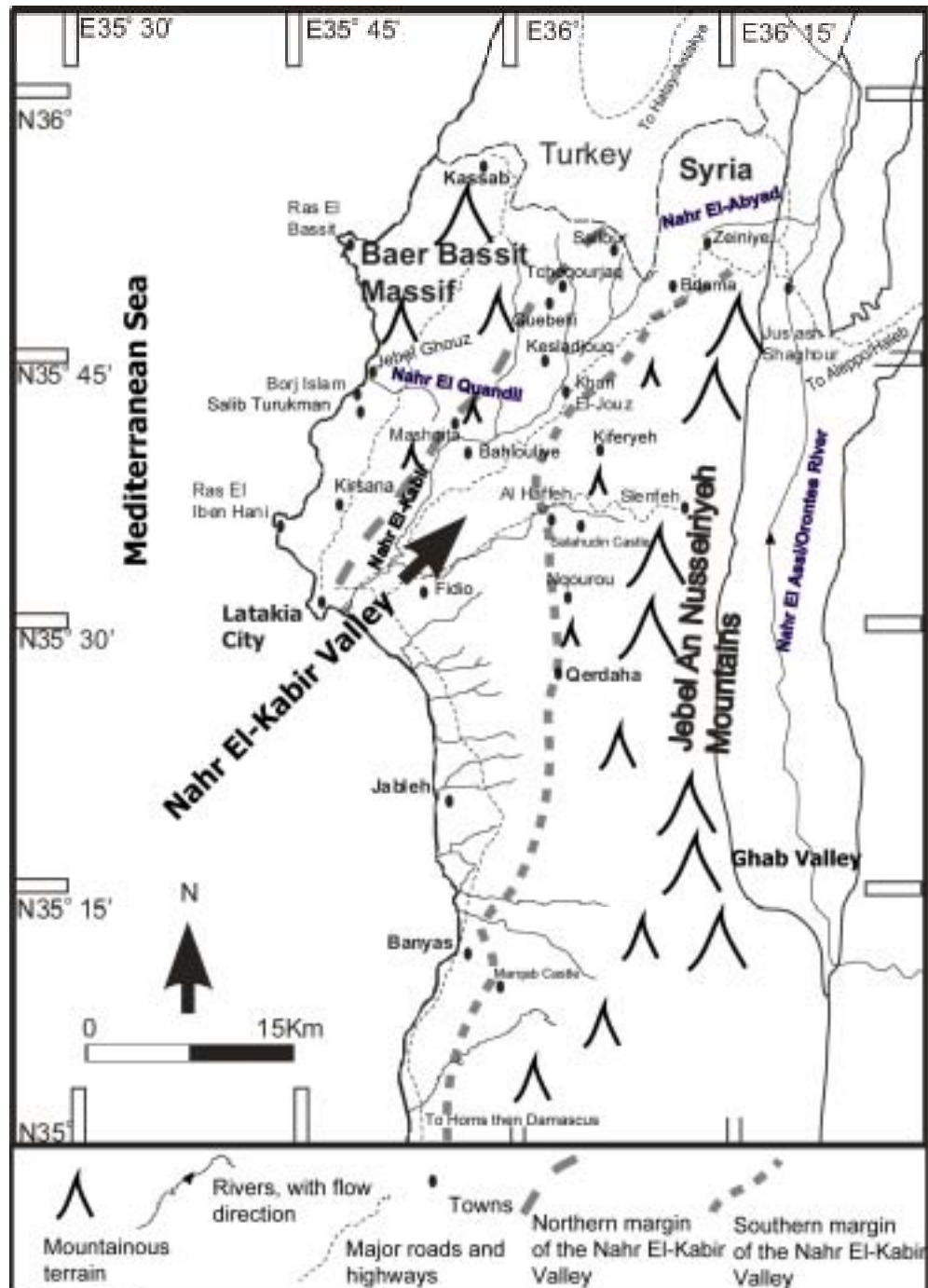
<b>Beds</b>	<b>Laminae</b>
Very thick beds	Very thick laminae
--1000mm--	--30mm--
Thick bed	Thick laminae
--300mm--	--10mm--
Medium bed	Medium laminae
--100mm--	--3mm--
Thin bed	Thin laminae
--10mm	--1mm--
Very thin bed	Very thin laminae

**Table 3.5** Terminology for thickness of beds and laminae, from Tucker (1991).

## Sedimentological descriptions and localities

Each of the twelve time-slices is described in detail in the following sections. The facies are described, as is the lateral variation (in geographical trend), where required. Figure 3.6 illustrates the geography of the region (the Baer-Bassit Massif, Nahr El-Kabir Valley, etc). When describing the margins of the Nahr El-Kabir Valley, the terms north and south margin refer to specific areas. The ‘northern margin’ is the region directly south of the Baer Bassit Massif (and the El-Kabir Lineament; see Chapter 4). The ‘southern margin’ refers to the region bordering the northern extent of the Jebel An-Nassuriyeh Mountains, between Bdama

Village in the north and Banyas Town in the south. 'North of the Nahr El-Kabir Valley', is a reference to the Nahr El-Abyad region and 'on the Baer Bassit Massif' is the region between the Nahr El-Qandil and Latakia City.



**Figure 3.6** Project area location map, showing major towns, villages and topography

## Sedimentary rocks and time-slices

### *Basement rocks, the Cretaceous and earlier-age platform limestones*

Previous studies (Ponikarov et al., 1963, 1966, 1967; Krashennnikov, 1971; Mouty, 1997; Leonov, 2000) have examined the Jurassic-Cretaceous carbonate platform that forms the Jebel An-Nassuriyeh Mountains (and the northern Arabian Platform margin) and, as such, they are not directly part of this project. However, the uppermost part of the succession appears to be the source of much of the reworked material in the Nahr El-Kabir Valley and therefore, warrants description (see later in this chapter and Chapter 6).

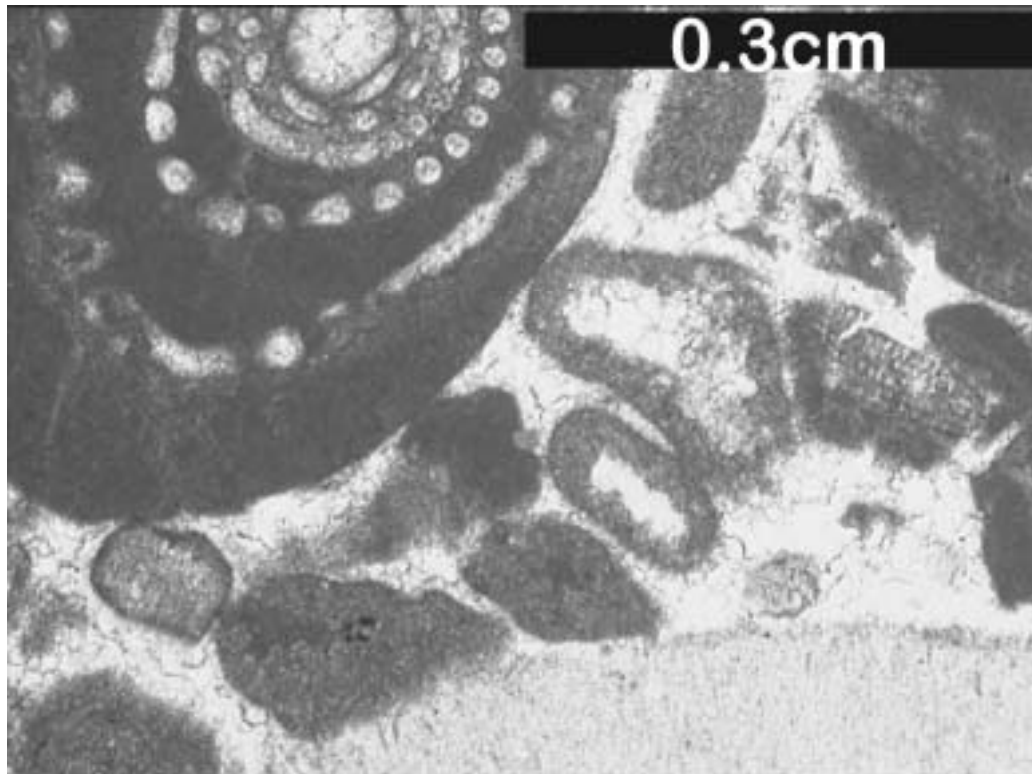
The Cretaceous platform limestones are remarkably homogenous across the Jebel An-Nassuriyeh Mountains with little facies change throughout the succession. Figure 3.7A shows a typical thin section through the hard, sparitic grainstone. Bryozoan, peloids, algal material and shell fragments make up most of the limestone, which is typically medium thickness bedded (10-25cm thick), in subtly fining-upwards beds. These beds are not planar bedded but appear to have undulations and are folded. Bedding gradually becomes thin (2-10cm) towards the top of the succession, but remains a mix of sparitic grainstones. Black chert is present as nodules throughout the upper part of the unit. Almost no terrestrial material was found within the Cretaceous samples examined from the Jebel An-Nassuriyeh Mountains. The grains and matrix are almost entirely carbonate.

The Jurassic-Cretaceous platform sediments form a continuous unit with only minor internal unconformities. The Maastrichtian universally overlies the Cretaceous sediments with a break in sedimentation, but, no erosive unconformity on the Jebel An-Nassuriyeh Mountains unless the contact is structural.

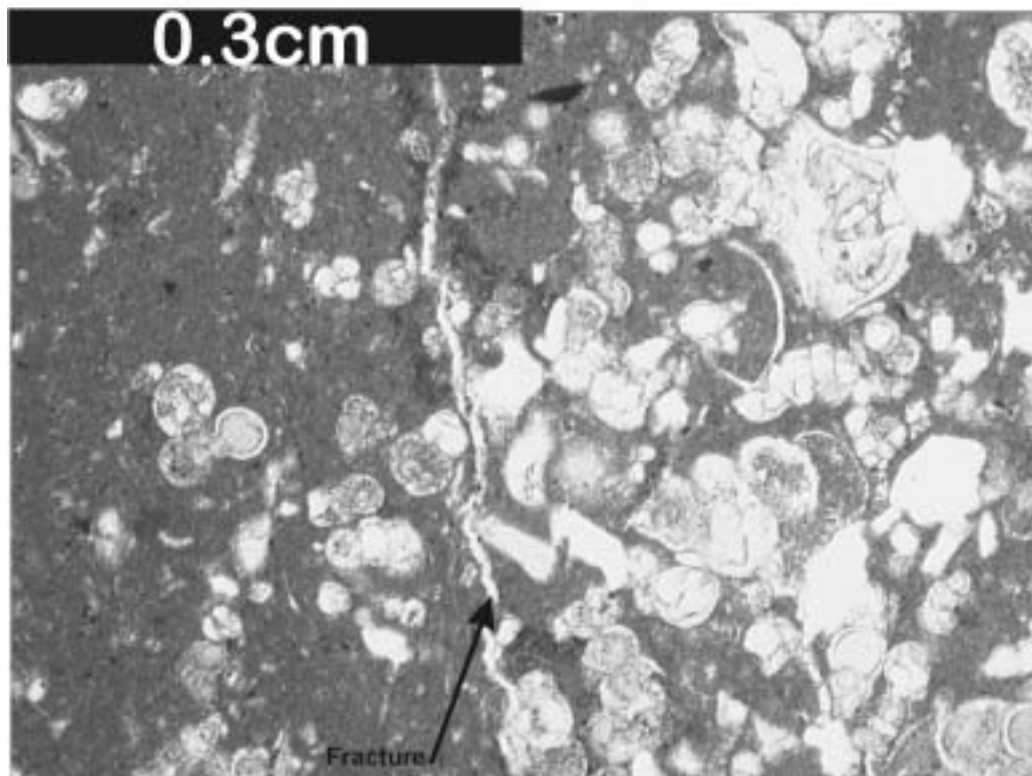
### *Interpretation and depositional processes*

The Cretaceous limestones were deposited as part of a neritic carbonate platform, and as such, contain many features indicative of shallow, marine conditions (e.g. fauna, peloids and a lack of terrestrial material). However, slumped beds (probably syn-depositional, seen near Al-Haffeh and Banyas Towns) and carbonate mass flow beds, indicate gravity reworking processes were active. Deposition probably occurred into deeper (outer?) shelf-depth water as pelagic foraminifera are common.





**Figure 3.7 A** Cretaceous grainstone from Jebel An-Nassuriyeh. Alveolinid foraminifera, peloids, algal material and shell fragments in a sparite cement. PPL



**B.** Maastrichtian foraminiferal wackestone and packstone from the Nahr El-Kabir valley southern margin. Rapid facies change mid-slide due to possible minor depositional condition changes. Partial dissolution due to fracturing. PPL



Contemporaneous and earlier sediments from the Baer Bassit Ophiolitic Massif (the Anatolian Plate margin) were studied in detail by Al-Riyami (2000), for his PhD thesis. His descriptions for these ophiolitic and melange rocks (i.e. mainly basic volcanic and plutonic rocks, deep-water pelagic sedimentary rocks, neritic carbonate rocks) are used herein, as many of these lithologies were redeposited within the younger sediments within the Nahr El-Kabir region (see later this chapter and Chapter 6).

### ***Time-slice 1, Maastrichtian to Early Eocene foraminiferal limestones***

#### *Introduction*

Foraminiferal limestones and marls of Maastrichtian to Early Eocene-age are well exposed and are found in two main areas within the project region (Figure 3.6, also see pull-out maps):

1. On the Baer Bassit Ophiolitic Massif.
2. Along the western margin foothills of the Jebel An-Nassuriyeh Mountains.

The mapped successions (Ponikarov et al. 1966) are regarded as one 'time-slice' in this work, as continuous sedimentation took place on the Baer Bassit Massif. Sedimentation was not continuous on the Jebel An-Nassuriyeh Mountains, as breaks in the succession are inferred (see below). Based on the mapping by Ponikarov et al. (1963, 1966), the above 'time-slice' is regarded by them as a series of homogeneous units, divisible into a maximum of four successions, mainly on biostratigraphic evidence (i.e. Maastrichtian, Danian, Lower Paleocene and Upper Paleocene-Lower Eocene). They stated that sedimentary transitions between some of these successions could not reliably be identified in the field. During this project, the field-studies built on their accurate mapping and the extent of any facies heterogeneity could be explored.

In general, the sediments on the Baer Bassit Massif show the most continuous successions, with every unit present. On the Jebel An-Nassuriyeh Mountains, the outcrops are much less prominent and the successions appear to be condensed. There are numerous, localised unconformities present on the Jebel An-Nassuriyeh Mountains localities and considerable facies variation. As the Baer Bassit Massif and the Jebel An-Nassuriyeh Mountains represent separate tectonic blocks (i.e. Anatolian Plate and Arabian Platform; see Chapter 6), the sedimentary rock variations are vital to assess the tectonic setting of the Early Tertiary.

Maastrichtian to Early-Eocene-age sedimentary rocks are characterised by white to light grey marls, shales and chalky limestones. Little, if any clastic material is present and the units are thinly laminated to thickly bedded. These units appear to be relatively undisturbed throughout, with only a few exceptions (detailed below).

### Maastrichtian-age sedimentary rocks

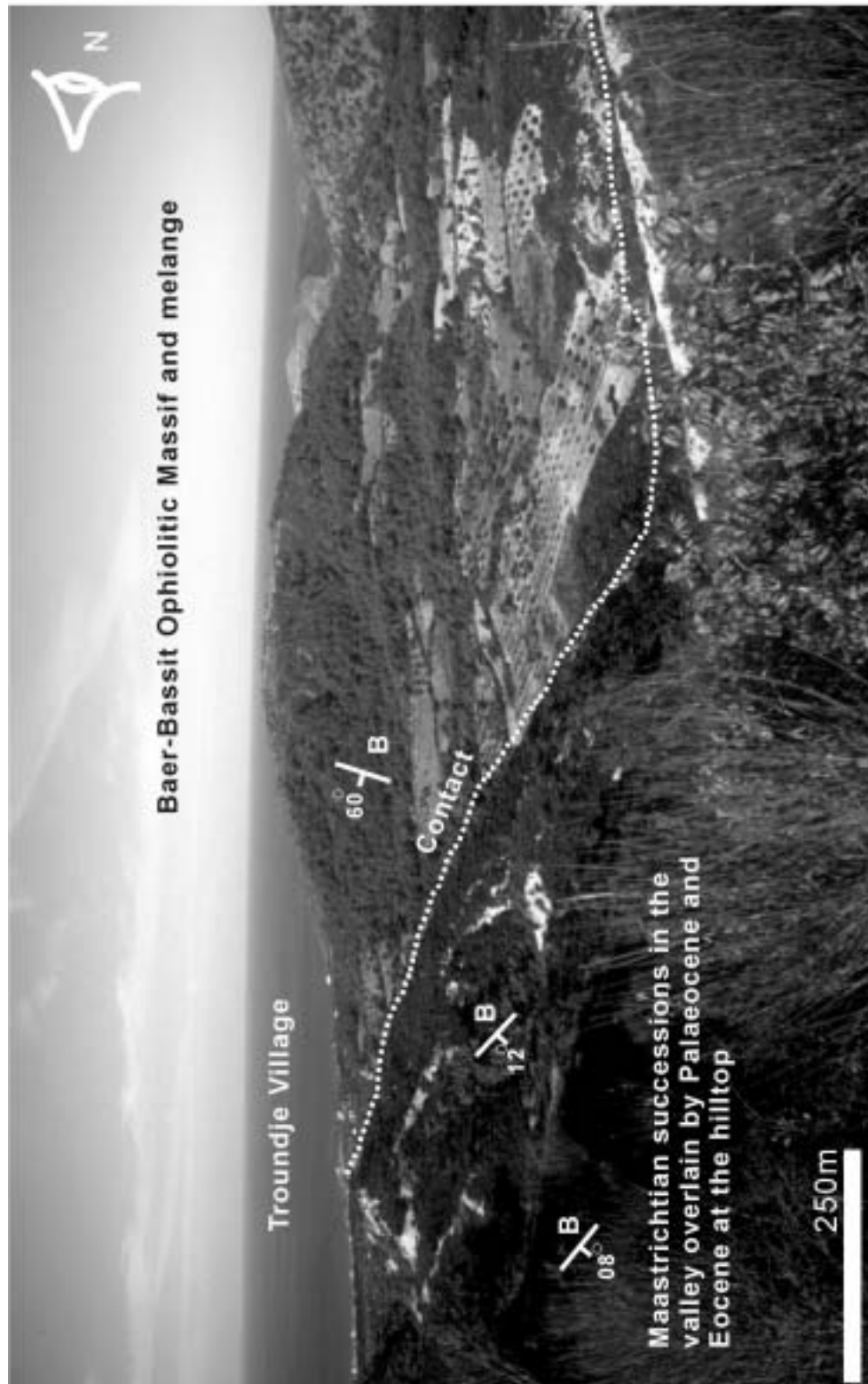
#### *The Baer Bassit Massif*

On the Baer Bassit Massif, Al-Riyami (2000) reported that the succession commences with fluvial sandstones and conglomerates of Maastrichtian-age. A section similar to his was found during this project, 10km north of the Nahr El-Qandil River, at the northern margin of a broad, shallow syncline, where the ophiolitic contact is preserved (Figure 3.8). The section commences with a boulder conglomerate of ophiolitic massif fragments in a cherty, sandy matrix (Figure 3.9). The conglomerate is overlain by 30m of unfossiliferous, fining-upwards, sandy sediment before marly limestone commences. The uppermost unit is typical chalky limestone of Maastrichtian-age in the region. Therefore, this section shows a sedimentary transition during marine transgression. Further south, on the southern margin of the Nahr El-Qandil River valley, sandstone is not seen but foraminifera-rich siltstones and red and green coloured clays appear instead. These lithologies are overlain by foraminiferal wackestones and packstones. The foraminifera present are predominantly planktonic. On the remainder of the Baer Bassit Massif Maastrichtian-age sediments are not obvious and no exposure of greater than 30m thick was seen.

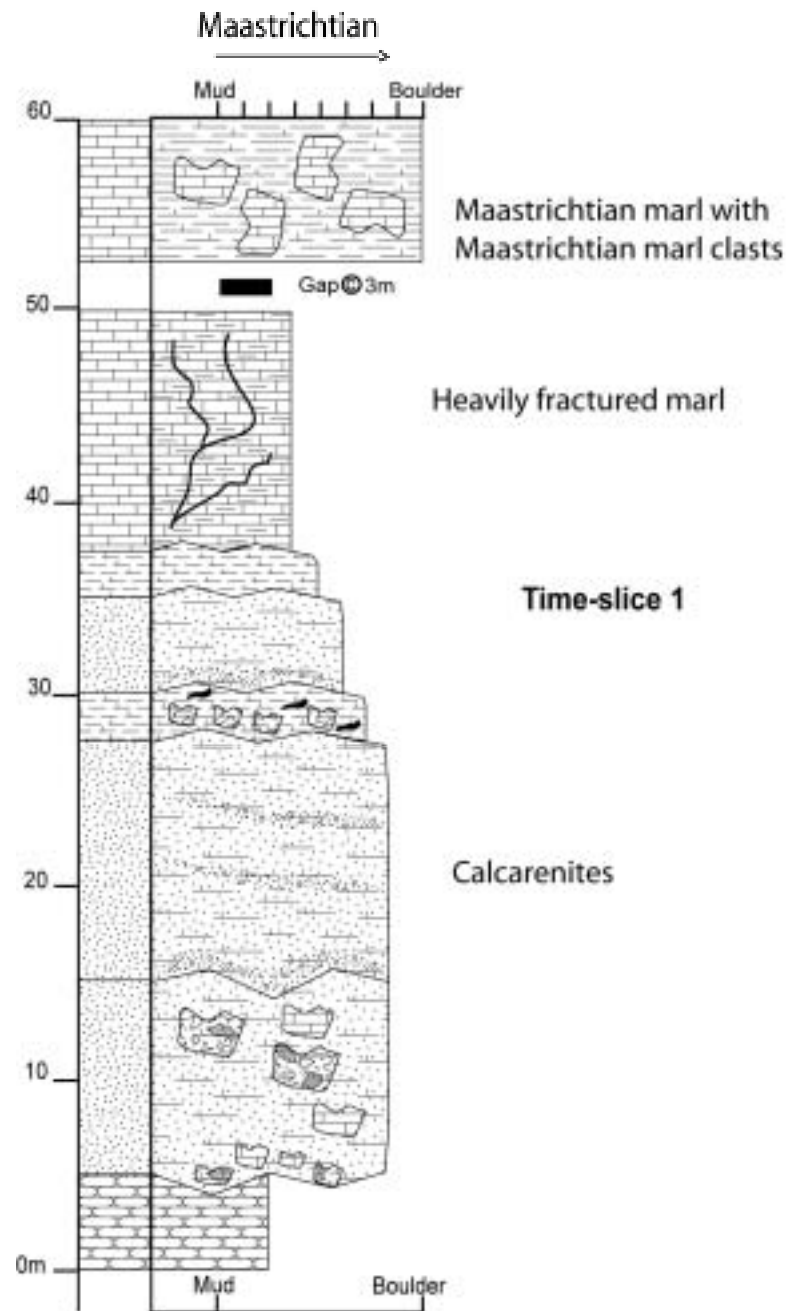
#### *The Jebel An-Nassuriyeh Mountains*

Most of the Maastrichtian-age sedimentary rocks are foraminiferal wackestones and occasionally packstones. In outcrop they weather a conspicuous white to light grey colour. Lamination is always at a millimeter to 1cm scale. Figure 3.7B shows typical Maastrichtian-age wackestones from close to the top of the succession on the Jebel An-Nassuriyeh Mountains.

The base of the Maastrichtian succession is poorly exposed on the Jebel An-Nassuriyeh Mountains. Glauconite-rich beds are found near the centre of the range (see also Chapter 2), as a very thin unit (<10m) and are associated with (<30cm) medium thickness, cross-laminated beds that pinch-out to the north and south. They are directly overlain by white, foraminiferal wackestone. At other localities, glauconite is not apparent and the



**Figure 3.8** The contact between the Baer-Bassit Ophiolitic Massif and the post-emplacement cover sequences, at Troundje Village, 45km NNE of Latakia City. In the field, the ophiolite is easily recognisable by its purple and red colour, in comparison with the near white of the Maastrichtian and Palaeocene successions. The Palaeocene at this locality and further south is gently folded. This photograph shows the northernmost limb of the syncline which terminates 10km south in the Nahr El-Qandil River valley.



**Figure 3.9** Maastrichtian succession overlying ophiolitic melange at Omyatour Village, 2Km north of Jebel Ghouz.

majority of the sediments found are in thinly laminated, planar beds. Maastrichtian-age sediments do, however, infill what appears to be a palaeotopography in the top of the Cretaceous basement succession. There is no evidence of down-cutting or erosion; the Maastrichtian sedimentary rocks overlie an undulating top surface of the Cretaceous (averaging 8-10m wavelength, 1m amplitude). The Maastrichtian-age beds can be seen to pinch out against the undulating succession. Ponikarov et al. (1966) logged a 315m thickness of Maastrichtian sediment. This thickness has been impossible to corroborate, as most outcrops are typically less than 10m thick. From composite measurements carried out in this study, a more realistic maximum would be 150-200m.

#### *Preliminary interpretation of Maastrichtian-age sediments*

The Maastrichtian-age sediments show a fairly rapid transition from sub-aerial to fully marine conditions on the Baer Bassit Massif. The variation in facies at the base of the unit may indicate that the Baer Bassit Ophiolitic Massif was never totally emergent, but dipped to the west, as in the present setting.

Little variation is seen in the Jebel An-Nassuriyeh Mountain exposures, although the absence of glauconite could indicate a distal deeper-water setting. Planktic-rich foraminiferal wackestones and packstones, are prominent, indicating a fairly deep-water platform setting. Marcel BouDagher-Fadel indicated that in her experience the packstones would be from an outer shelf environment (2 samples), which agrees with the field evidence.

The contact between the Maastrichtian and older Cretaceous platform rocks is unconformable, as shown by infilling of a pre-existing Cretaceous topography. There is no indication of sub-aerial exposure on the Jebel An-Nassuriyeh Mountains. The formation of a palaeotopography on the uppermost part of the Cretaceous succession may be related to emplacement of the Baer Bassit Ophiolitic Massif that occurred further north and related updoming or warping of the platform.

Having investigated the complete unit, it is likely that the Baer Bassit Massif area represented a drowned platform abutting the Jebel An-Nassuriyeh area. Some palaeotopography may have existed here at this time as glauconite locally formed (only in water depths of 20-200m and is only found at the base of the succession). There is very little evidence of depositional instability throughout the Maastrichtian succession.

## Palaeocene

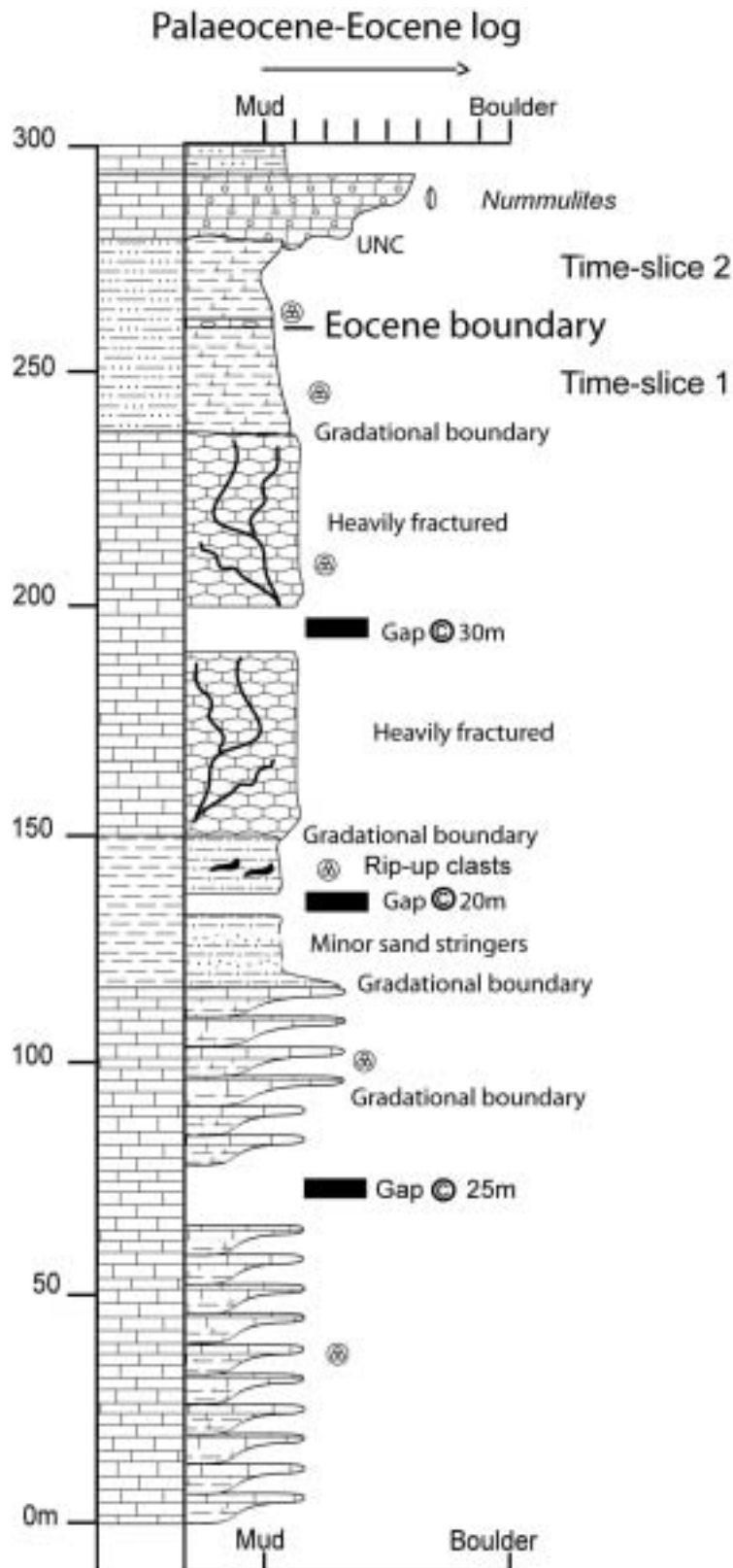
Palaeocene-age rocks are represented by a mix of foraminiferal wackestones and packstones. Wackestones predominate on the Jebel An-Nassuriyeh Mountains and in the lowermost Palaeocene sections on the Baer Bassit Massif (Figure 3.10). The contact between the Palaeocene-age strata and the Maastrichtian is often indistinct and was primarily identified by colour change (white to grey, Figure 3.8). No evidence of erosion was seen. A thickness of 5-600m of Palaeocene sedimentary rocks were recorded on the Baer Bassit Massif. In contrast, less than 150m thickness was observed on the Jebel An-Nassuriyeh Mountains.

In comparison to Maastrichtian-age lithologies, many of the Paleocene wackestones show evidence of current activity during deposition as grains are orientated preferentially (i.e. Figure 3.33, grains 'follow' the circular shape of foraminifera such as *Globigerinids*). Calcite spar infilling of foraminifera and of pore spaces (moldic porosity) is common, as is an earlier stage of bitumen infilling, although the timing is unconstrained. Fine-sand size grains of chert are fairly common within the Baer Bassit samples, but intercalated chert beds are rare.

### *Baer Bassit Massif*

The Palaeocene contact with the Maastrichtian succession is poorly defined on the Baer Bassit Massif and was ascertained only by foraminifera dating. In the lowermost sections, grey foraminiferal wackestones are intercalated with occasional graded, light coloured, carbonate-rich, thin to medium thickness beds (Figure 3.11). Intercalated beds of hard foraminiferal packstones comprise entirely of carbonate material (inferred to be gravity derived, see below). Overlying the wackestones are 80m of dark shales and mudstones, without any carbonate material. The shales then give way upwards to cyclical limestone and marly carbonates for the remainder of the unit (Figure 3.12). A 50cm thick, very finely laminated shale caps the succession ('paper shale').

Clastic clasts of detrital chert, carbonate nodules, calcarenites (with pebbles), asymmetrical ripples with bifurcating crests, convoluted beds, burrows (*Thalassinoides*) and pyritised fossils were observed within isolated exposures of the uppermost Palaeocene succession on the Baer Bassit Massif.

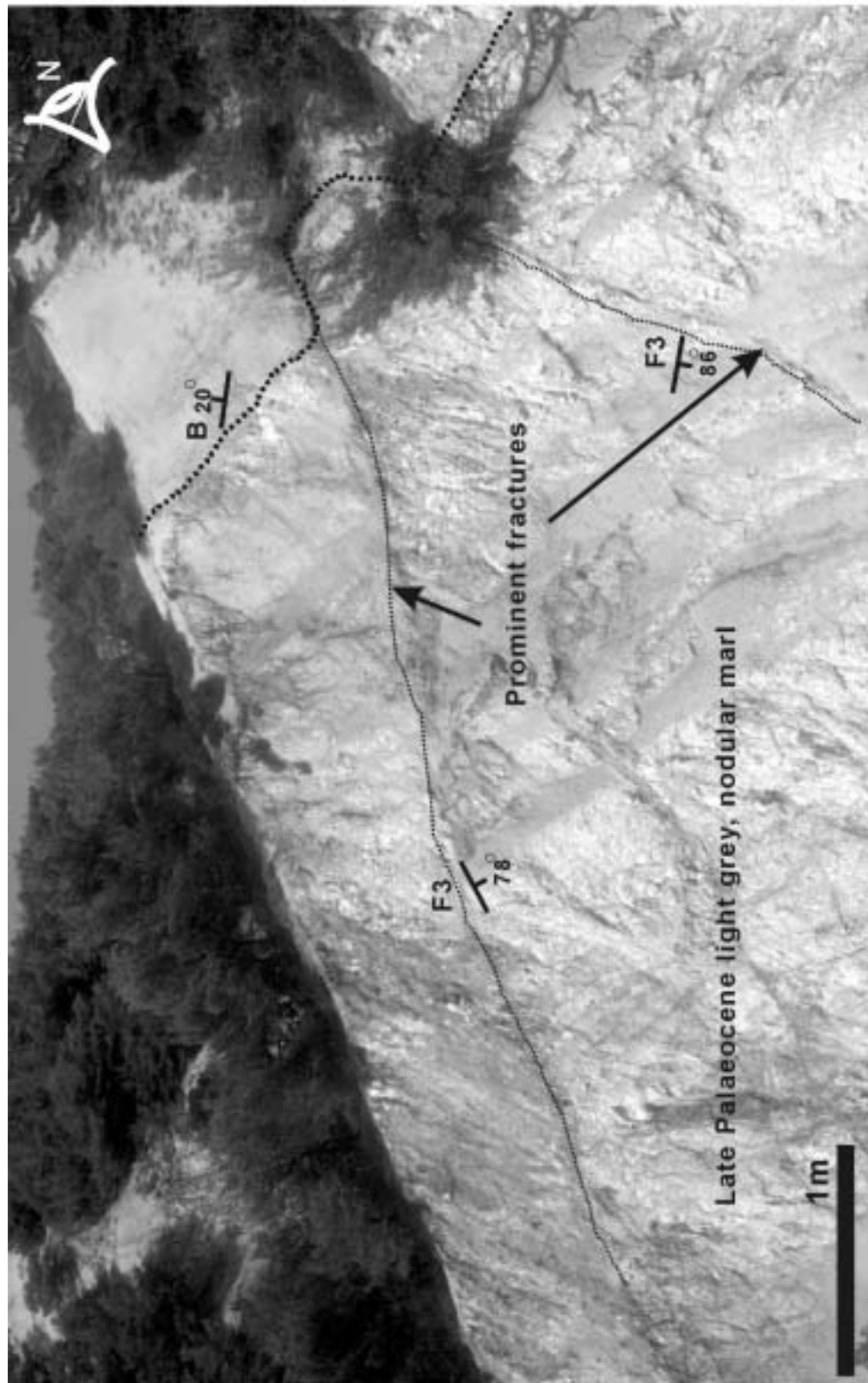


**Figure 3.10** Palaeocene-Early Eocene succession log, from the Nahr El Qandil River valley.



**Figure 3.11** Early Palaeocene exposures of marl, thinly laminated wackestone (and thin turbiditic limestone beds, see text). This unit forms the southern limb of the shallow syncline terminating at Trondje Village 10km to the north. This exposure has also been cut by normal faults.





**Figure 3.12** Late Palaeocene nodular marl, close to hard, silicified Eocene marker bed with nummulitic foraminifera, approximately 150m stratigraphically above the previous locality (Fig 3.11). The outcrop is heavily fractured in two prominent orientations and has well developed zones of fault gouge reflecting the soft lithology.

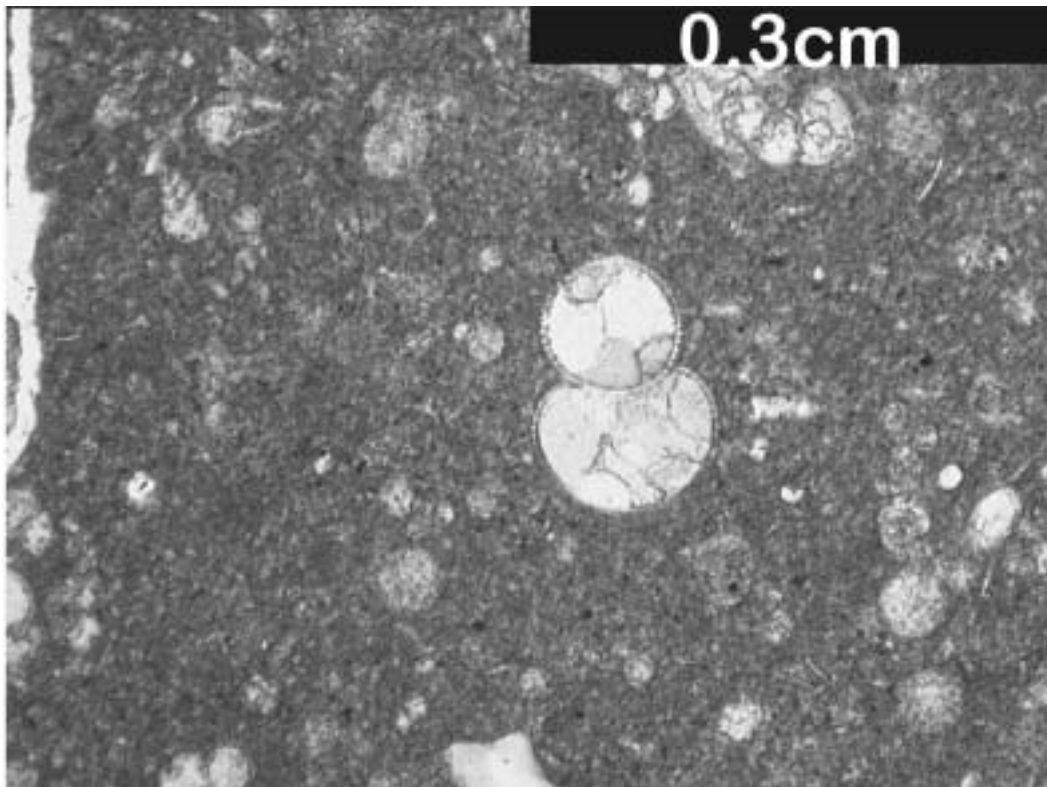
*Jebel An-Nassuriyeh*

Palaeocene-age sediments are not present north of Qerdaha Town on the Jebel An-Nassuriyeh Mountains (central to the range, see pull-out maps). Near Banyas Town, in the southernmost exposures they reach a maximum thickness of 100-150m, thinning to the north. Typically the Palaeocene-age rocks are grey wackestones, with carbonate concretions (nodular 'doggers') and are indistinctly bedded. In outcrops near Qerdaha Town, the unit is <20m thick and is comprised silty and thinly bedded to laminated, intercalated limestone and marl. In both areas the Eocene is observed to overlie the succession erosively (Figures 3.13, 3.14 and 3.15).

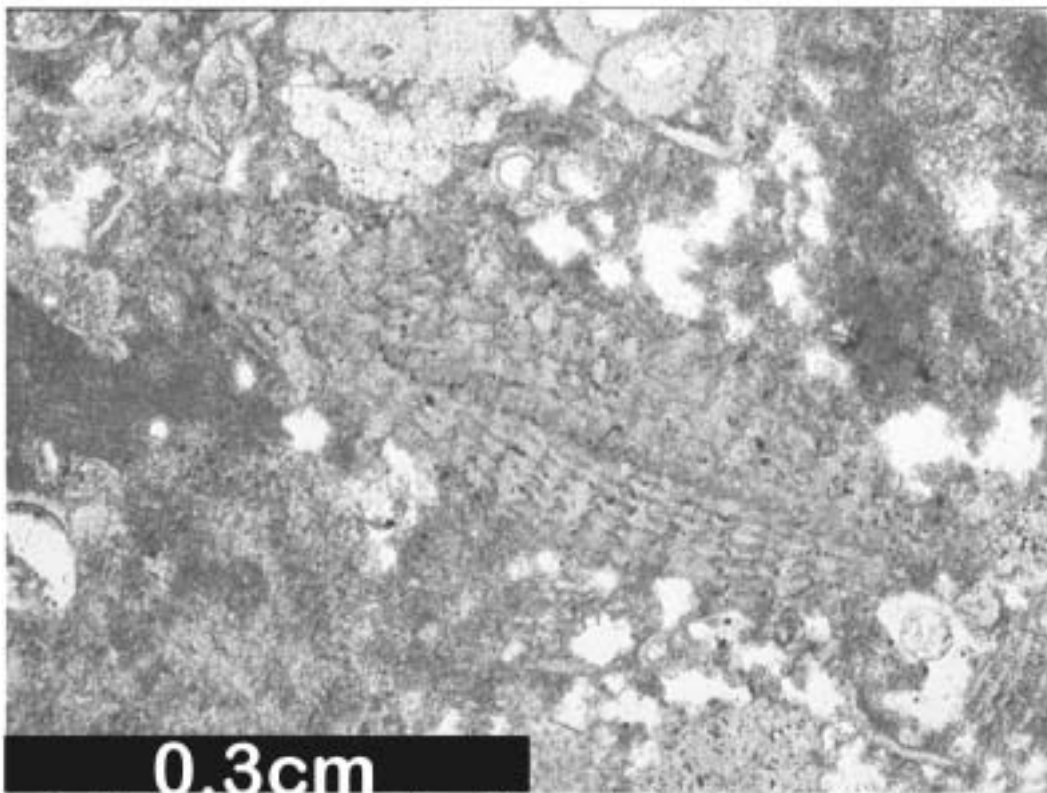
*Preliminary interpretation of Palaeocene-age sediments*

The submerged, neritic marine conditions found during the Maastrichtian are interpreted to have prevailed for much of the Palaeocene, perhaps shallowing slightly later. Input of clastic material indicates erosion of an uplifted area, either the Baer-Bassit Massif and/or the Jebel An-Nassuriyeh region, although sub-aerial exposure is unlikely to have been major, as clastic input is very limited. Mass flow deposits are common throughout the Palaeocene, especially at the base of the succession, but clastic material is sparse, suggesting distal deposition. Overall, Palaeocene-age sediments have a very high planktic to benthic foraminiferal ratio indicating an outer shelf setting is likely. Marcel BouDagher-Fadel suggested that sedimentation rates were probably rapid (3 samples), but did not specify a setting.

A major feature of the Palaeocene is the difference in sediment thicknesses between the Baer Bassit Massif (600m) and the Jebel An-Nassuriyeh (150m). On the Baer Bassit Massif the section appears complete from the Maastrichtian through to Early Eocene-age. Only the Late Palaeocene could be positively identified on the Jebel An-Nassuriyeh Mountains and then only in the south, so that erosion or non-deposition of the Early Palaeocene is likely. No sedimentological evidence of a break or transgression at the re-commencement of deposition could be found however (see Chapter 6).



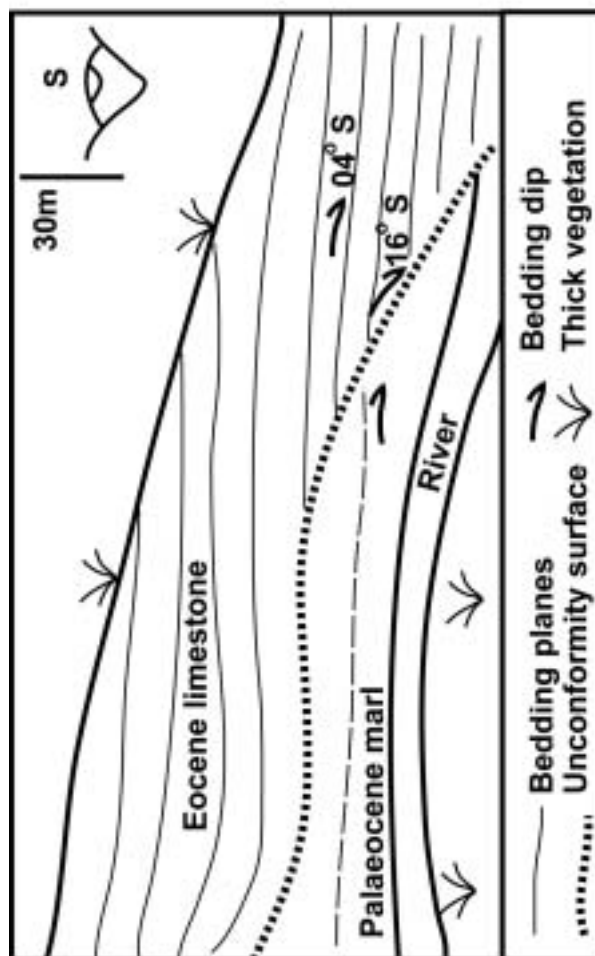
**Figure 3.13 A** Early to Middle Palaeocene wackestone from the Baer Bassit Massif. *Milogypsinoides* foraminifera, with later dissolution and sparitic cement. Very minor chert fragments. XPL



**B.** Early Eocene wackestone from the northern margin of the Nahr El-Kabir Valley. *Nummulites* (pos. *Discocyclina*) foraminifera visible. Minor dissolution. PPL.



**Figure 3.14** 10km due south of Banyas. A quarry view of the Eocene succession overlying the condensed Palaeocene succession. The Palaeocene is grey and marly, with carbonate concretions. The succession is condensed to 100-200m thick and dips gently to the southeast. It is overlain by chalky Eocene limestone with siliceous concretions, with trace fossils and burrows. This overlying succession dips gently ( $<5-10^\circ$ ) to the west. The outcrop is heavily fractured in a NW-SE orientation.



**Figure 3.15** The Eocene/Palaeocene unconformable contact seen in a river cutting at Safarqiyeh Village, near Banyas town. Both Palaeocene successions appear to be condensed in comparison with those seen on the Baer-Bassit Massif; the Eocene sediments appear to onlap a pre-existing Palaeocene surface.

## Early Eocene

Early Eocene-age strata comprise sediments similar to those of the Late Palaeocene, predominantly wackestones and packstones. They are typically chalky, lighter in colour and contain less marl than the Palaeocene sediments.

### *Baer Bassit Massif*

On the Baer Bassit Massif the Eocene-age strata form alternating, thin to medium bedded, foraminiferal wackestones, packstones and grainstones. A 10cm-thick chert bed marks the transition from Palaeocene to Eocene-age strata in many localities in this region (dated by Marcel BouDagher-Fadel), but no erosion was apparent. *Nummulites* and *Discocyclina* foraminifera are the most common large foraminifera throughout the Eocene-age strata and the occurrence of these benthic foraminifera increases towards the top of the succession. An erosive unconformity is observed at many localities prior to the uppermost, Middle Eocene-age nummulites-rich unit.

### *Jebel An-Nassuriyeh*

On the Jebel An-Nassuriyeh Mountains near Banyas Town, Early Eocene wackestones and packstones crop out in much thinner exposures (a maximum thickness of 200m is calculated, rather than the 600-700m on the Baer Bassit Massif). They unconformably overlie the Palaeocene succession either by erosion (Figure 3.14) or erosion followed by onlap (Figure 3.15). In outcrop, the Eocene-age strata are white, thinly planar bedded, chalky limestones with laminated silicified intercalations. Middle Eocene-age nummulitic sparitic packstones unconformably overlie the thin, chalky limestones on the southern margin of the Nahr El-Kabir Valley.

### *Preliminary interpretation of Early Eocene-age sediments*

Early Eocene-age facies are very similar to those observed within the Palaeocene and depositional environments were probably similar. Slightly higher ratios of benthic to planktonic foraminifera (Marcelle BouDagher-Fadel) indicates slightly shallower water conditions than the outer shelf.

Ponikarov et al. (1963) mapped the Paleocene and Early Eocene as one unit, due to the lack of identifying features. The questions relating to the thickness discordance

applicable to the Palaeocene are also relevant to the Early Eocene. In this study some features were found to help differentiate the Palaeocene and Eocene successions, but exposure was insufficient to remap the unit.

#### Summary of time-slice 1

Time-slice 1 forms a continuous sedimentary succession on the Baer Bassit Massif. Figures 3.16, 3.17a and 3.17b, show the facies variation from logged samples and identify a subtle shallowing of water depth. Time-slice 1, on the Jebel An-Nassuriyeh Mountains, shows similar facies, but contains two major unconformities.

Therefore, time-slice 1 indicates that a rapid drowning of the region occurred in the north (Baer Bassit), followed by a slow shallowing of water depth, hypothesised from outer shelf to perhaps inner shelf depths.

#### ***Time-slice 2, Middle Eocene chalky, nummulitic limestones***

Middle Eocene sediments crop out over the entire field area with the exception of the Nahr El-Kabir Valley (overlain by Neogene). Three facies of Middle Eocene-age sediments are observed and each is restricted geographically; 1, those overlying the ophiolitic complex at Baer Bassit, 2, the southern and western margin to the Jebel An-Nassuriyeh Mountains and 3, the vast desert plains to the East of the Ghab Valley. This study is mainly concerned with facies 1 & 2, although those further inshore provide a useful comparison. Each unit unconformably overlies older units with apparent erosion.

#### ***Baer Bassit Massif***

On the Baer Bassit Massif, rocks of Middle Eocene-age are well exposed, capping the successions along the northern coastline. They comprise grey marls and white-yellow, chalky limestones with occasional large foraminifera, especially *Nummulites*. Dark brown chert is commonly intercalated with marl layers. The chalky limestones are foraminiferal wackestones and very occasionally packstones or grainstones (Figure 3.18), although these are rare except in the uppermost part of the succession. Lime mud is the primary component of the lowermost part of the succession with rare clastic clasts of detrital chert derived from the Baer Bassit Ophiolitic Massif. Macrofossils and rock-forming bioclasts are also rare, only the foraminifera form a significant component. In the uppermost part of the succession the



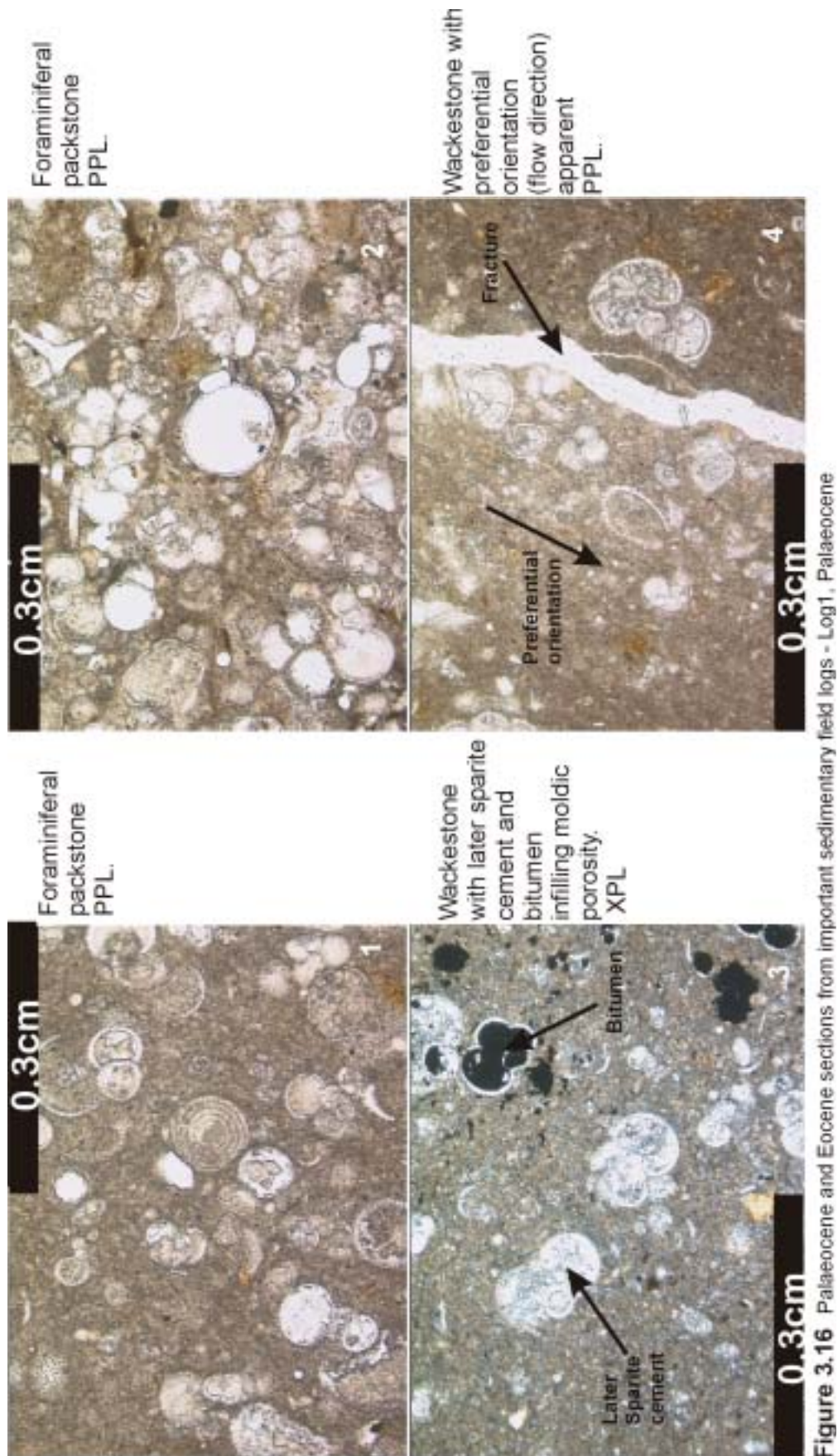
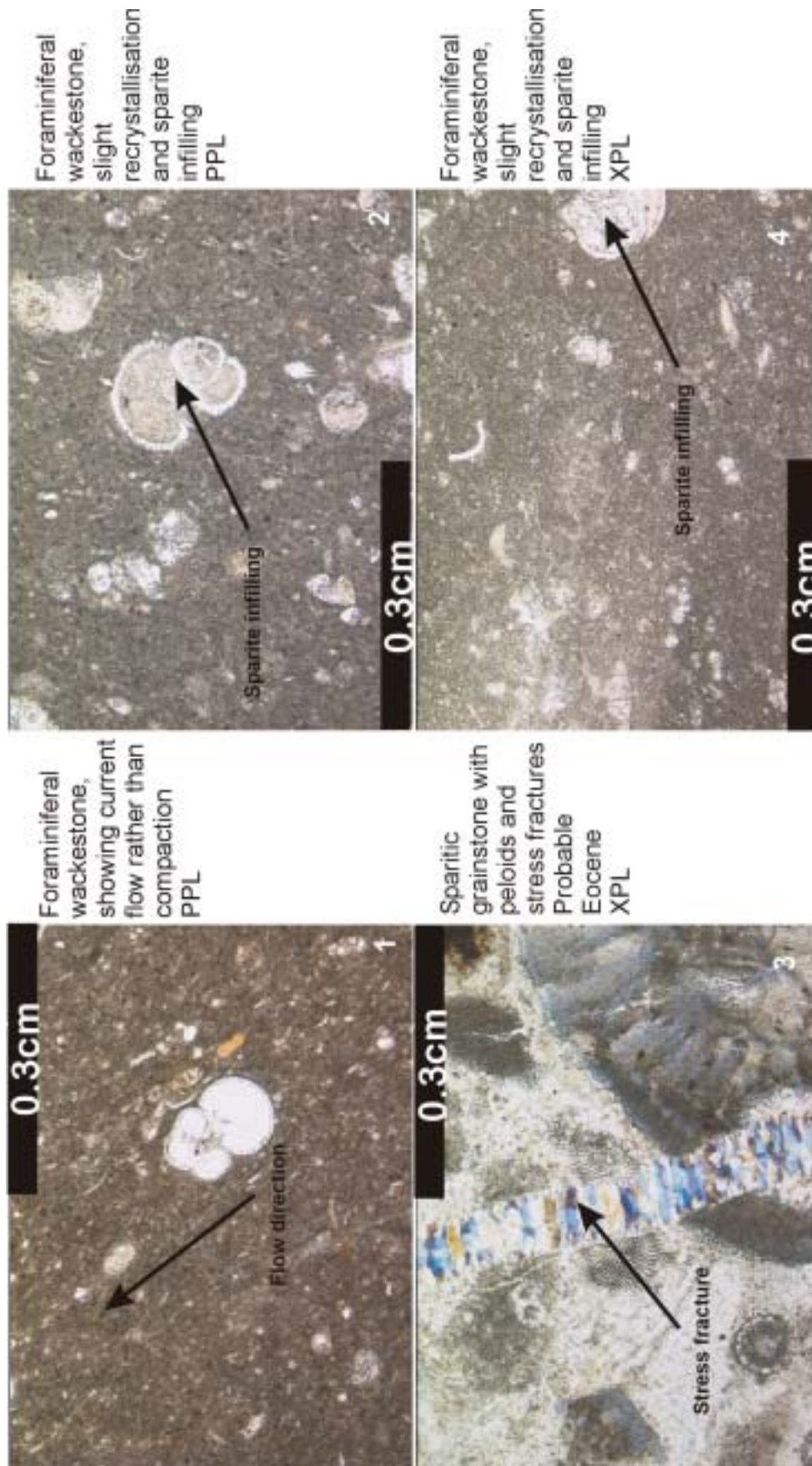
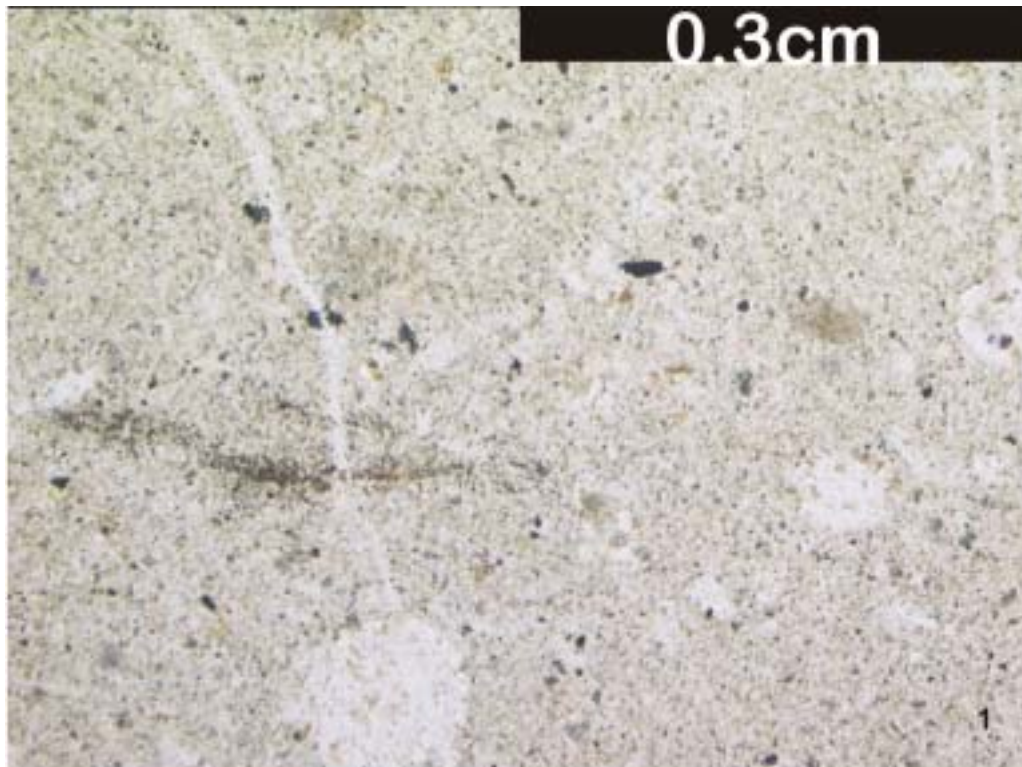


Figure 3.16 Palaeocene and Eocene sections from important sedimentary field logs - Log1, Palaeocene

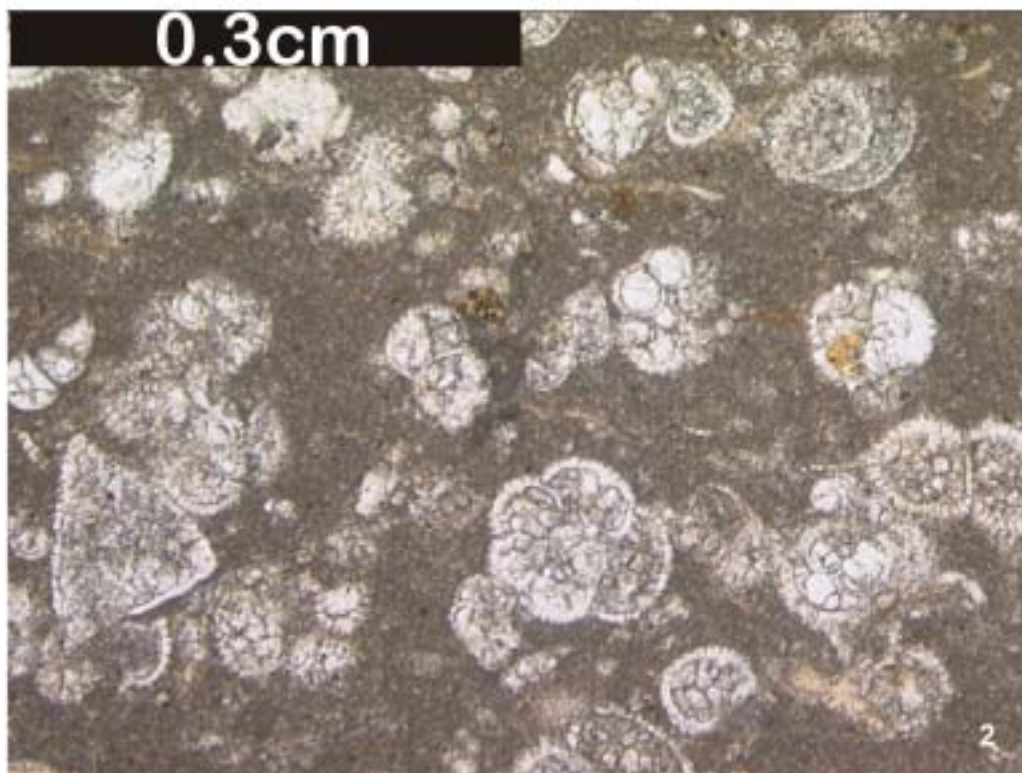




**Figure 3.17a** Palaeocene and Eocene sections from major sedimentary field logs - Log2, Palaeocene to earliest Eocene.



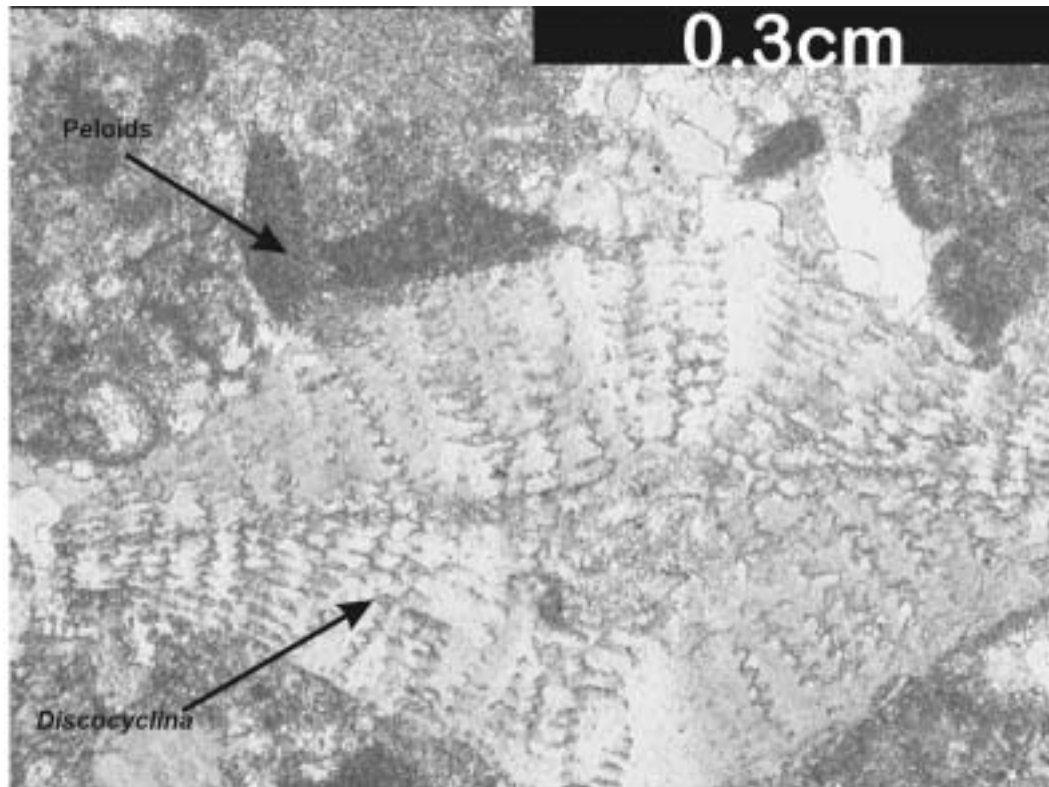
Confirmed Eocene cherty facies; Eocene marker bed, dated by Marcel BouDagher-Fadel. Complete dissolution and recrystallisation. PPL



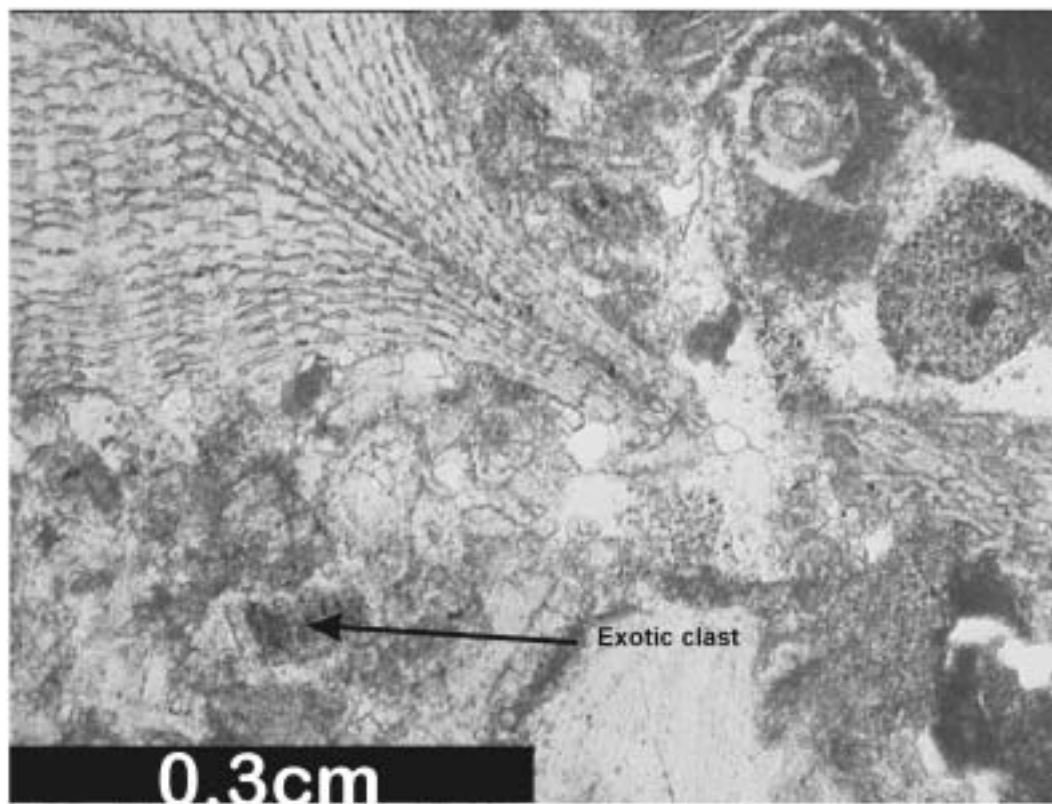
Foraminiferal packstone, highest Eocene strata seen in the region - probably Middle Eocene. PPL.

**Figure 3.17b** Palaeocene and Eocene sections from main sedimentary field logs - Log3, Palaeocene to earliest Eocene





**Figure 3.18 A** Eocene 'Nummulitic' sparitic packstone, with peloids and micritic infilling. XPL.



**B** Nummulitic grainstone with microbial (algal) material and exotic clasts, possibly ophiolite derived. PPL.

proportion of binding carbonate material (algal), peloids and ophiolitic massif clasts increases considerably and bioclastic packstones and grainstones are common.

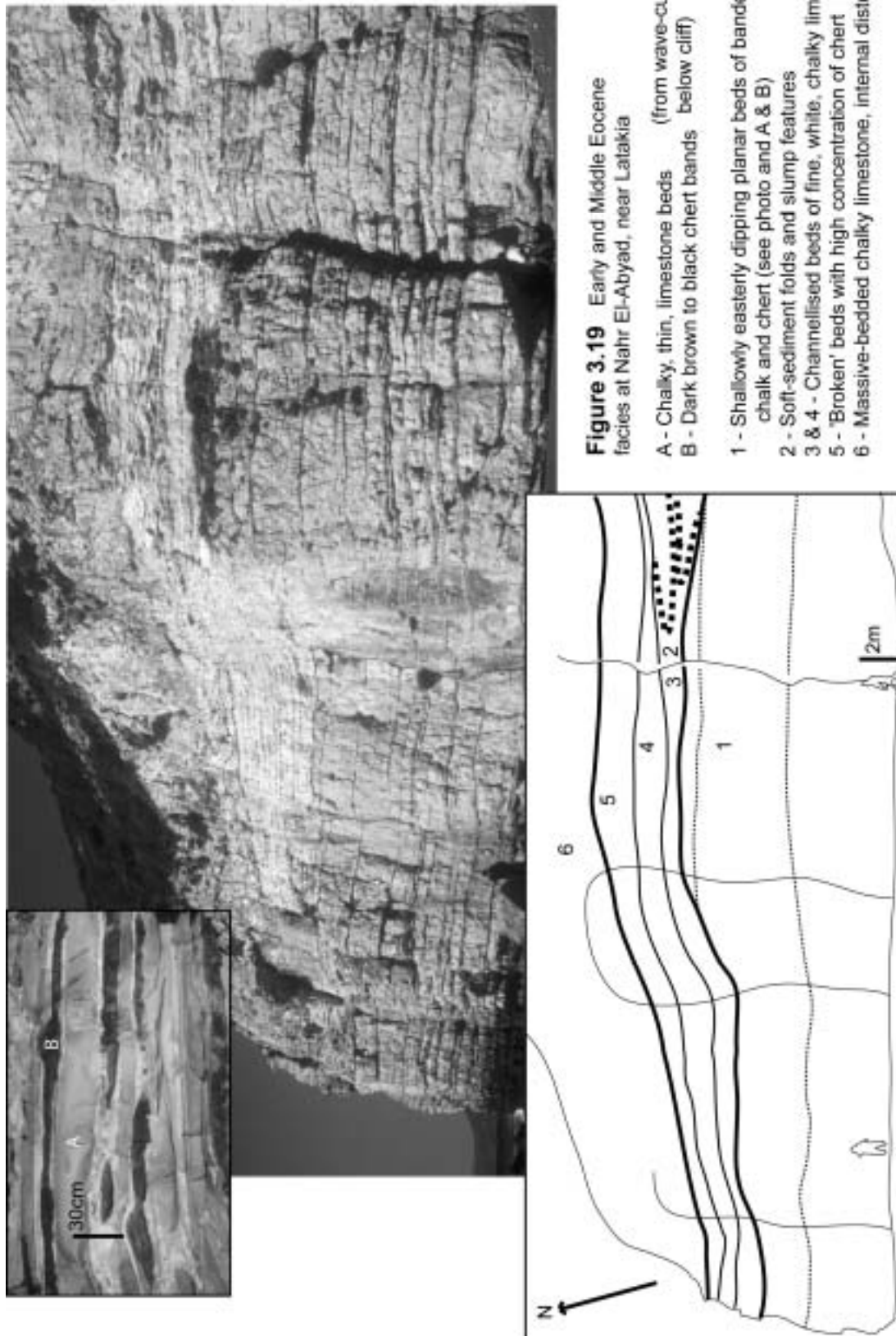
In the lowermost part of the succession, symbiotic algae coatings (pers.comm Dan Howard, 1999, represents the photic zone) were observed within the chalk-rich beds, on the *Alveolina*, *Nummulites* and *Discocyclina* foraminifera. *Thalasinoides* burrows are also present indicating bioturbation. The chalks become increasingly silty up succession and chalk beds pinch and swell. Intercalated marls are continuous and planar bedded.

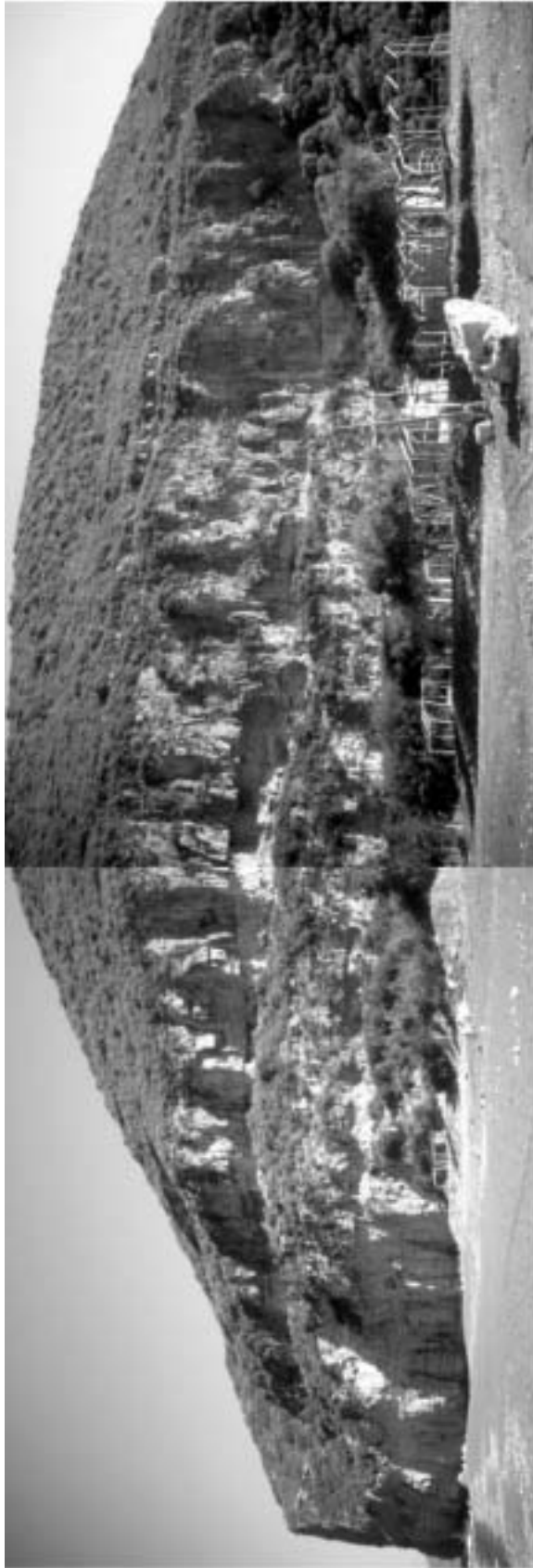
In large cliff exposures north of Borj Islam Village (Nahr El-Qandil River valley) the sedimentary architecture of the unit is well exposed (Figures 3.19 and 3.20). These show that Middle Eocene chalks are grouped on three scales. Individual beds are thinly to thickly bedded (10-50cm thickness); these beds are organised as packages of beds on a 2-5m scale and the packages form 'channel-like' features, repeating throughout the cliff exposure (75-100m thick). The 'channel-like' features can occasionally be seen to pinch-out laterally over distances of up to 500m and often down-cut into the 'channels' below, removing them partially. Folding and distortion of individual beds and of complete packages of beds are common, often with undisturbed lamination above and below each disturbed unit.

Near Latakia City, Middle Eocene-age sediments are devoid of *Nummulites* and consist of intercalated, medium bedded, chalky wackestones and marl, in equal quantities. Each layer exhibits prominent planar striations and laminations (see Chapter 4). The beds are intensively deformed and conjugate folded, suggesting slumping due to proximity to a major fault (see Chapters 4, 6 and Tucker et al. 1990).

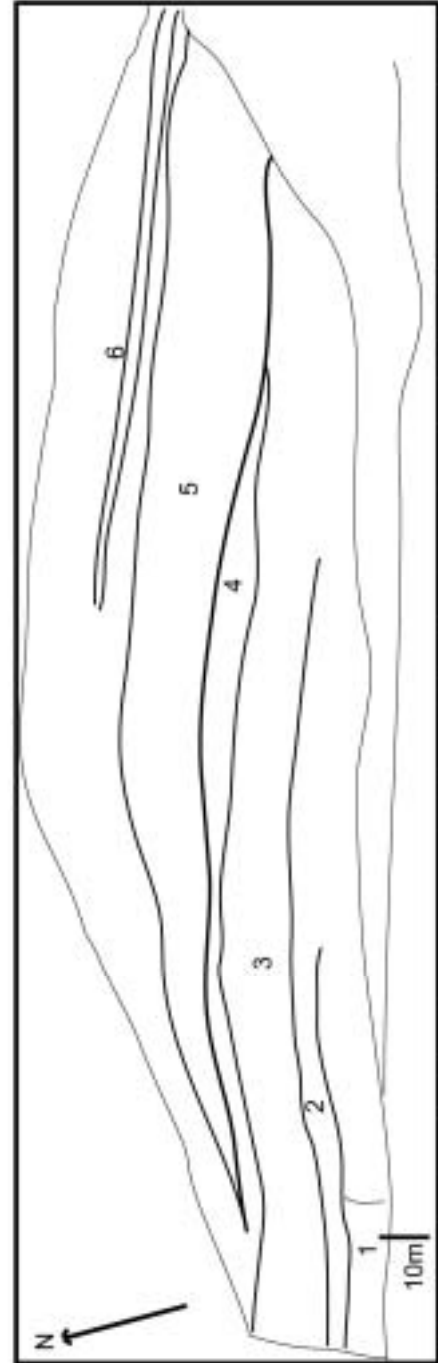
#### *Preliminary interpretation of Baer Bassit Middle Eocene Facies*

The Middle Eocene-age strata on the Baer Bassit are interpreted as sequences and parasequences (Emery et al. 1996) of chalk in a stacked channel system, with marl background sedimentation. Debris flows of chalk 'washed-down' shallow marine fauna. Faunal data for this hypothesis is two-fold: 1, Marcelle BouDagher-Fadel indicated a faunal province that was 'reefal' and shallow marine. 2, Dan Howard identified symbiotic algae, these require <80m water depth. 'Channels' within the chalk do not contain visible palaeocurrent data, only secondary evidence of 'flow' in thin section, but, from the outcrops the transport direction is suggested as E-W, shallow marine to deeper shelfal water depths.





**Figure 3.20** (continuation of previous figure)  
Eocene channelling and individual sequences visible at Nahr El Qandil.



1-6 Large-scale channelled limestone sequences: 1 - Planar chalk and chert, 2 - Channelled chalk, 3 - Distorted soft beds, 4 - Truncated sequence 5 - Unconformity (Mid-Eocene?) and NW margin of large channel?, 6 - Thin resistant bed of hard limestone

Therefore, syn-depositional instability is thought to have been common with slump folding of unlithified and partially sediments (see Chapters 4, 6 and Tucker et al. 1990).

Structuration, faulting and fracturing is not common in outcrops of this age (except near Latakia, Chapter 4), but shallow, large folds are and they are orientated approximately 50°-230° (see Chapter 4), which is similar to the orientation of channels.

Near Latakia City, the Middle Eocene strata were intensely deformed during and after deposition, with slumping, folding and faulting identified.

#### *Jebel An-Nassuriyeh*

Outcropping along the Jebel An-Nassuriyeh Mountains, Middle Eocene-age strata are predominantly composed of light orange, massive, nummulitic packstones and grainstones. A measured thickness of up to 90m was recorded in this study. Nummulites foraminifera constitute the majority of the rock (80-90%) in the uppermost exposures. Peloids, glauconite and rare bivalves are also found within the samples (Figure 3.18) and micrite appears to infill gaps between the foraminiferal tests. Intercalations of marl are rare. There is little sign of bedding, bedding disturbance or bedding architecture, perhaps because most outcrops are karstified.

At the southernmost exposures the Middle Eocene succession unconformably overlies the Early Eocene interval sub-horizontally and is typically less than 10m thick. White, nummulites-rich, bioclastic wackestone and coarse breccia are prominent.

At the north of the Nahr El-Kabir Valley a 15cm thick, red bed of caliche and angular clasts of chert is found between white, foraminiferal wackestone (Early Eocene?) and nummulitic grainstone (Middle Eocene).

#### *Central Syria*

Middle Eocene-age strata prominently outcrop in the vast desert plains between the Ghab Valley and Aleppo City (Ponikarov et al. 1963). They typically comprise micritic wackestones with patches of nummulitic packstones and grainstones.

#### *Preliminary interpretation of Middle Eocene nummulitic facies*

The Middle Eocene nummulitic facies is widespread in northwest Syria. Little mud is present and *Nummulites* thrived in shallow marine conditions (20-100m water depth, Saller et al. 1993). Glauconite and bivalves can also be indicative of shallow water. The

interpretation of these Middle Eocene facies is that water depth was less than 100m (inner shelf), but that water depth decreased to the east, where 'biostrome-like' accumulations of nummulites predominated, probably close to the shoreline in central Syria.

The facies distinction between the Baer Bassit Massif facies and those further south indicates that shallow-water conditions (*Nummulites*-rich) predominated to the southeast. Deeper-water conditions (redeposited *Nummulites* only), were close presumably to the current continental shelf edge that existed to the west and north (see Chapter 6).

The existence of a palaeosol (red, caliche bed) would indicate that the north of the Nahr El-Kabir Valley was sub-aerial for a time prior to Middle Eocene deposition. A major unconformity is not evident.

Aquitanian-age strata unconformably overlie the Eocene facies, although only within the Nahr El-Kabir Valley. Ponikarov et al. (1963, 1966) indicated that Upper Eocene sediments may have existed near Bdama Village, north of the Jebel An-Nassuriyeh Mountains. This could not be confirmed but samples collected from the region during this project and studied by Silvia Gardin, indicate reworking of Eocene to Oligocene age flora within Miocene age rocks.

### ***Time-slice 3, Aquitanian Transgressive Limestones***

Biostratigraphic evidence suggests that sedimentation in the region restarted in the Aquitanian, after a Middle-Late Eocene to Oligocene hiatus (see also Chapter 6). The Nahr El-Kabir Valley was the principle area of deposition within the project region and small outcrops are found only at the margins of the valley. No Aquitanian sediments have been found south of the village of Nqourou (the same latitude as Latakia City, on the Jebel An-Nassuriyeh Mountain foothills).

Very small Aquitanian- age outcrops exist on the Baer Bassit Massif, but only very close, if not on, the heavily wooded northern margin. North of the Nahr El-Kabir Valley, large outcrops of the Aquitanian succession are visible near the Nahr El-Abyad River, directly overlying nummulitic Eocene facies and are overlain unconformably by the Burdigalian succession. To the northeast, the Aquitanian succession terminates against the large faults of the Ghab Valley. Ponikarov et al. (1967) indicated that marine Aquitanian age deposits might exist near Aleppo (150km northeast). The Aquitanian succession is not therefore, particularly well exposed within the project area.



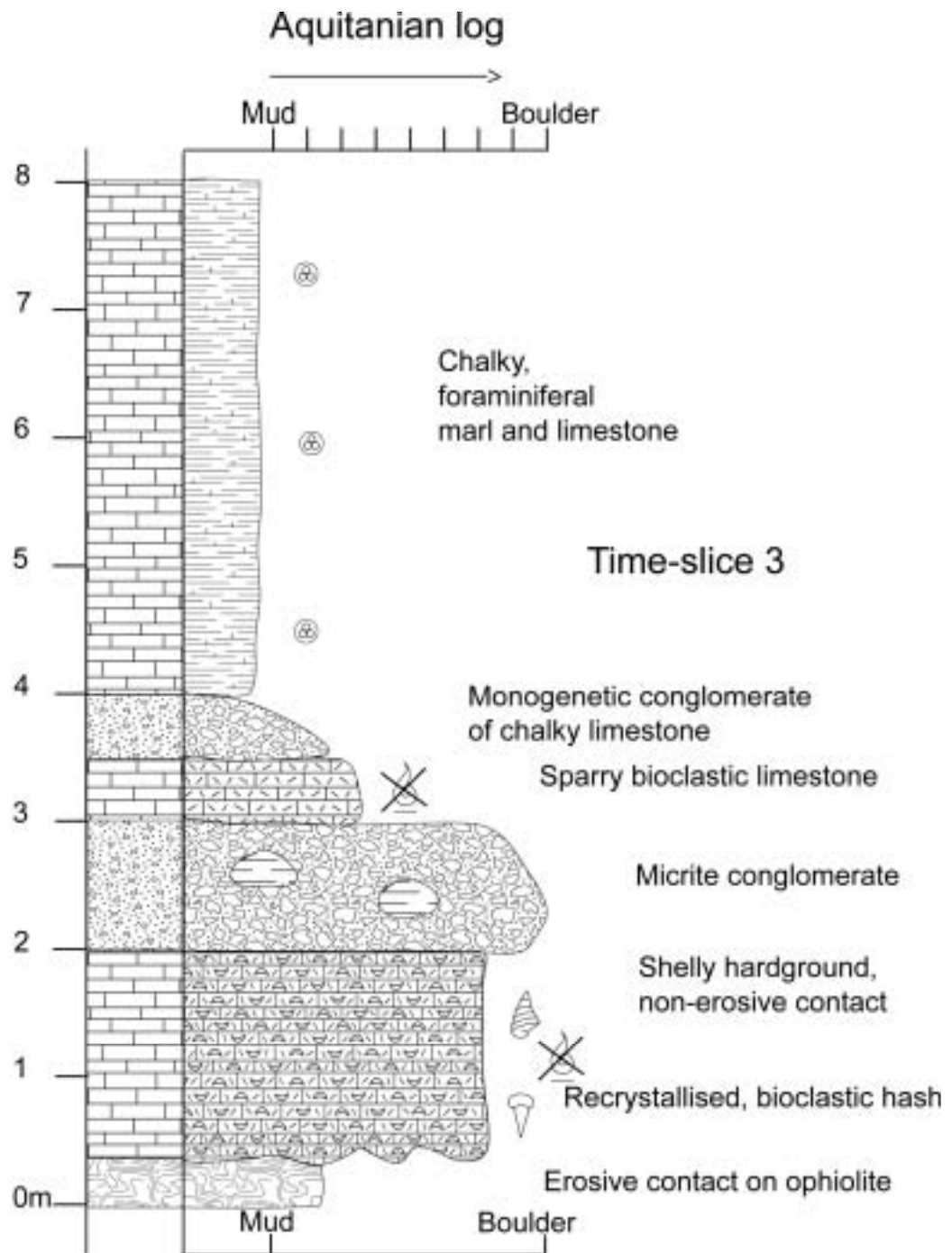
*Within the Nahr El-Kabir Valley*

The majority of the Aquitanian succession comprises bright white, chalky, foraminiferal limestones. This study supports the view that the maximum thickness ranges from 120-150m (Ponikarov et al. 1967), although it is normally much thinner. In this study, three distinct and important facies variations were seen across this unit, varying with locality. These areas are: 1. The northern margin of the Nahr El-Kabir Valley, 2. To the north of the Nahr El-Kabir valley, along the Abyad River and 3. Along the flanks of the Jebel An Nassuriyeh Mountains and the southern margin of the Nahr El-Kabir Valley (Figure 3.21).

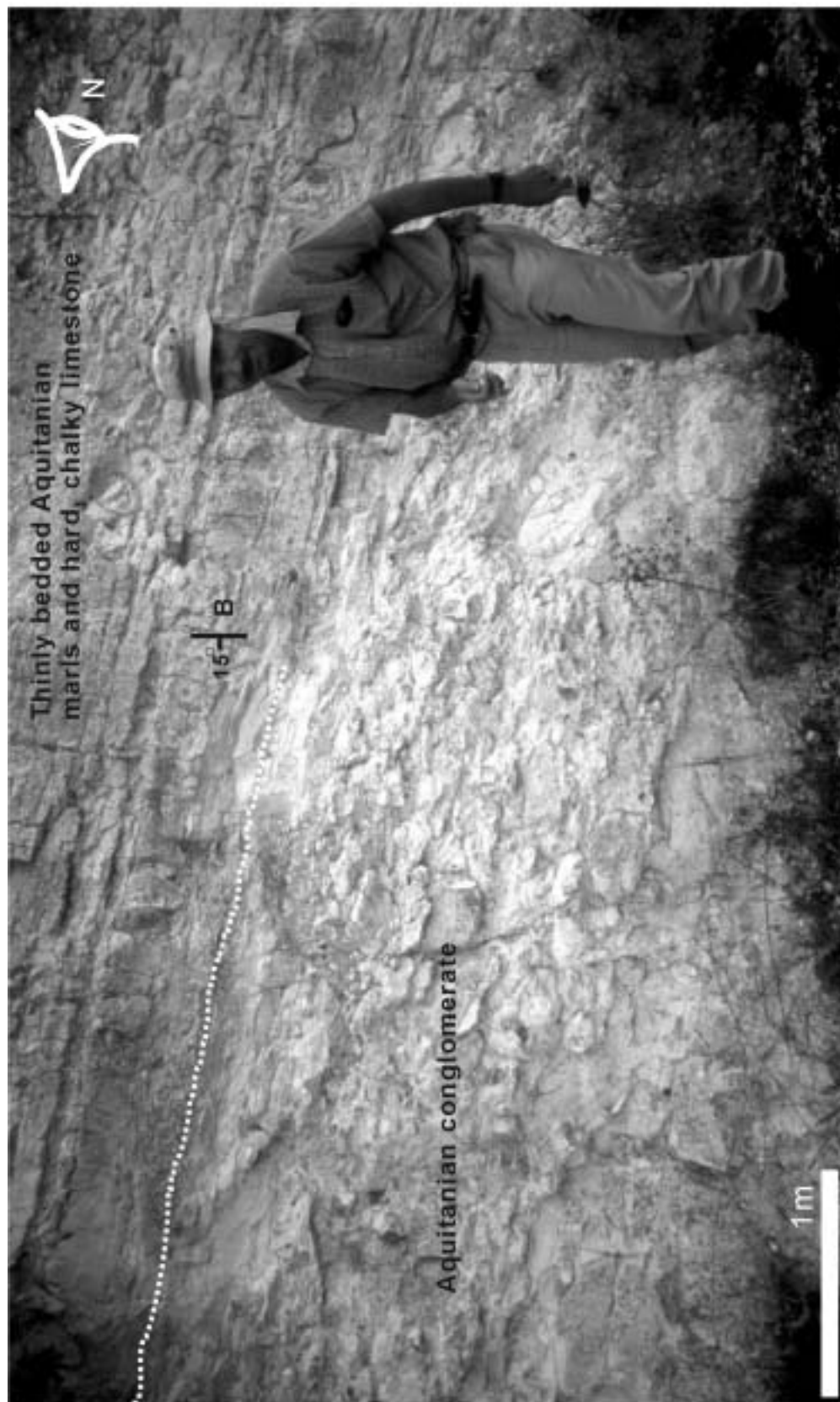
*1. Northern margin of the Nahr El-Kabir Valley*

The base of the Aquitanian time-slice is observed only along the flanks of the El-Kabir lineament (Chapter 6), which extends northwards from Latakia to beyond the Turkish border (see pull-out maps). These outcrops are usually small and of poor quality, especially where there is thick woodland. Often the sedimentary rocks appear disturbed and broken close to this fault. It can also difficult to observe the Aquitanian strata in the field as it is lithologically similar to the Eocene-age rocks. One obvious distinguishing feature though, is the absence of chert, where this exists in the Paleogene strata. The contact with underlying units is often an minor erosive angular unconformity, with sub-horizontal or slightly basinward dipping (southeast) Aquitanian overlying.

Although there is no evidence of deep erosion at the commencement of the time-slice, there is a series of facies changes before the typical shelfal, white foraminiferal marl and limestone that Ponikarov et al. (1966, 1967) described. The lowest of the Aquitanian facies is bioclastic conglomerate or a shell fragment bed (shell hash) (Figures 3.21 and 3.22). A 1.5m thick bed of recrystallised corals, gastropods, bivalves and pecten is found near the village of Qasmin (12km northeast of Latakia). It is overlain by a conglomerate of dark grey micritic clasts (1m) without erosion and then by a yellow sparry limestone with algal bioclastic debris (0.5m). At this locality, no Eocene-age rocks were present and the sediments lie directly on ophiolitic massif related facies. No clastic material from the ophiolitic massif was found within the sediments. The succession, therefore, commences with a mix of wackestones, packstones and grainstones.



**Figure 3.21** Sedimentary log of the Aquitanian facies seen on the northern margin of the Nahr El-Kabir Valley, 15km northeast of Latakia City.



**Figure 3.22** A rare view, from the northern valley margin, of intra-Aquitanean instability, with a monotypic conglomerate overlain by the more usual well-bedded, chalky, wackestone typically seen in the Nahr El-Kabir Valley. The conglomerate is truncated abruptly at a minor intra-succession unconformity. Initial dip was shallow, there has been some post-depositional tilting of the unit.

Overlying the coarse unit, there is a transition to marls and chalky foraminiferal limestones (wackestones) over a metre of sedimentation. The remaining 65m of exposure comprises entirely of foraminiferal wackestones. Bedding is typically medium thickness and planar, with occasional syn-depositional deformation and folding apparent (Figure 3.22).

Monogenetic, thinly bedded, conglomerates of white, chalky foraminiferal limestone are occasionally found within this unit.

Further north towards Qaballi Village, clasts of fresh ophiolitic material are found within the lowest part of the succession. These rocks contain a much higher proportion of grey-coloured mud and clastic sedimentary clasts than observed further south. Bedding, however, has been obscured as the rocks are intensely fractured. A later stage of bitumen commonly infills pore space, especially foraminifera tests, within the rock. Chert-rich samples often contain more than 10% grains (packstones) (Figure 3.23).

Close to the Turkish border, at the furthest north possible to visit in the Nahr El-Kabir Valley, the Aquitanian-age limestones are found to be sub-vertical (see Chapter 4). The marl content is much less than previously observed and the limestones are planar, silty, and thinly bedded (3-10cm thick). These wackestones and packstones are typically organic rich, often with hard, brown organic-rich beds intercalated with the white foraminiferal limestone. Large foraminifera (millioids), sponges spicules and fish debris present are not observed at other localities.

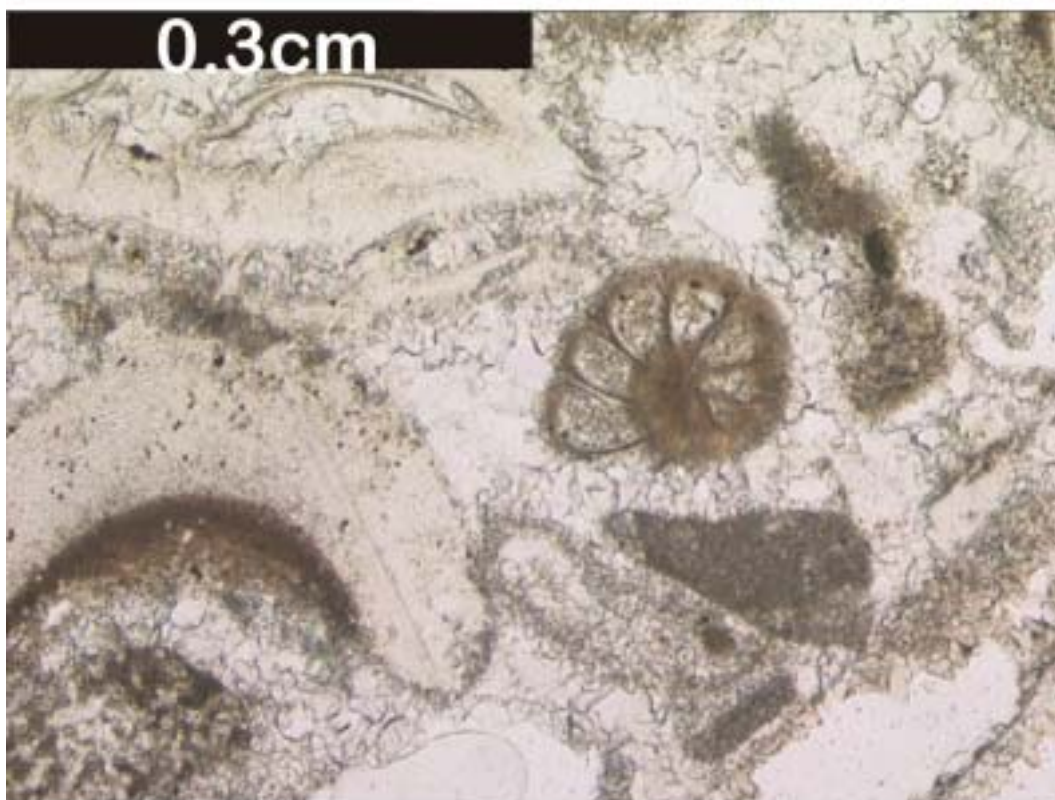
The contact with the Burdigalian succession is erosive and Aquitanian limestone clasts are reworked into many of the later time-slices.

## *2. Abyad River Valley, northeast of the Nahr El-Kabir Valley*

The Aquitanian is well exposed within the valley and observed to overlie directly on Eocene, Maastrichtian and Cretaceous-age rocks, north of the Nahr El-Kabir Valley, without obvious erosion. This time-slice is >120m thick (as seen in fault scarps, Chapter 4), typically comprising white, foraminiferal wackestones and occasional packstones, very similar to the rocks observed further south. There are, however, key differences; at the base of the unit, the (5m thick) limestone has a 'sugary texture' of sparry calcite and shell molds are visible. These grainstones are overlain by planar wackestones that grade to more marly limestone (wackestones) intercalated with buff coloured, thin, sand-rich (chert) and calcarenites beds for the remainder of the succession.



**Figure 3.23 A.** Aquitanian foraminiferal packstone. Moldic porosity infilled with bitumen. Sample from the northern margin of Nahr El-Kabir Valley. PPL.



**B.** Aquitanian sample from the southern margin of the Nahr El-Kabir Valley. Intraclasts and extraclasts of micrite and bioclasts (shell fragments) are present in a sparite matrix. PPL.



The Burdigalian succession overlies the Aquitanian succession with minor down-cutting and erosion.

### *3. Southern margin of the Nahr El-Kabir Valley*

Small limestone exposures of Aquitanian-age strata exist on the southern margin of the Nahr El-Kabir Valley, similar in character to those on the northern margin. Sparitic grainstones are common, as are bioclastic packstones in the lowermost part of the succession. Micrite clasts and shell fragments are a major constituent of the rock. No clastic material is present in the samples collected, but organic material is present. Less than a 30m thickness of Aquitanian succession is exposed along this margin, the majority of which is white, chalky foraminiferal wackestones.

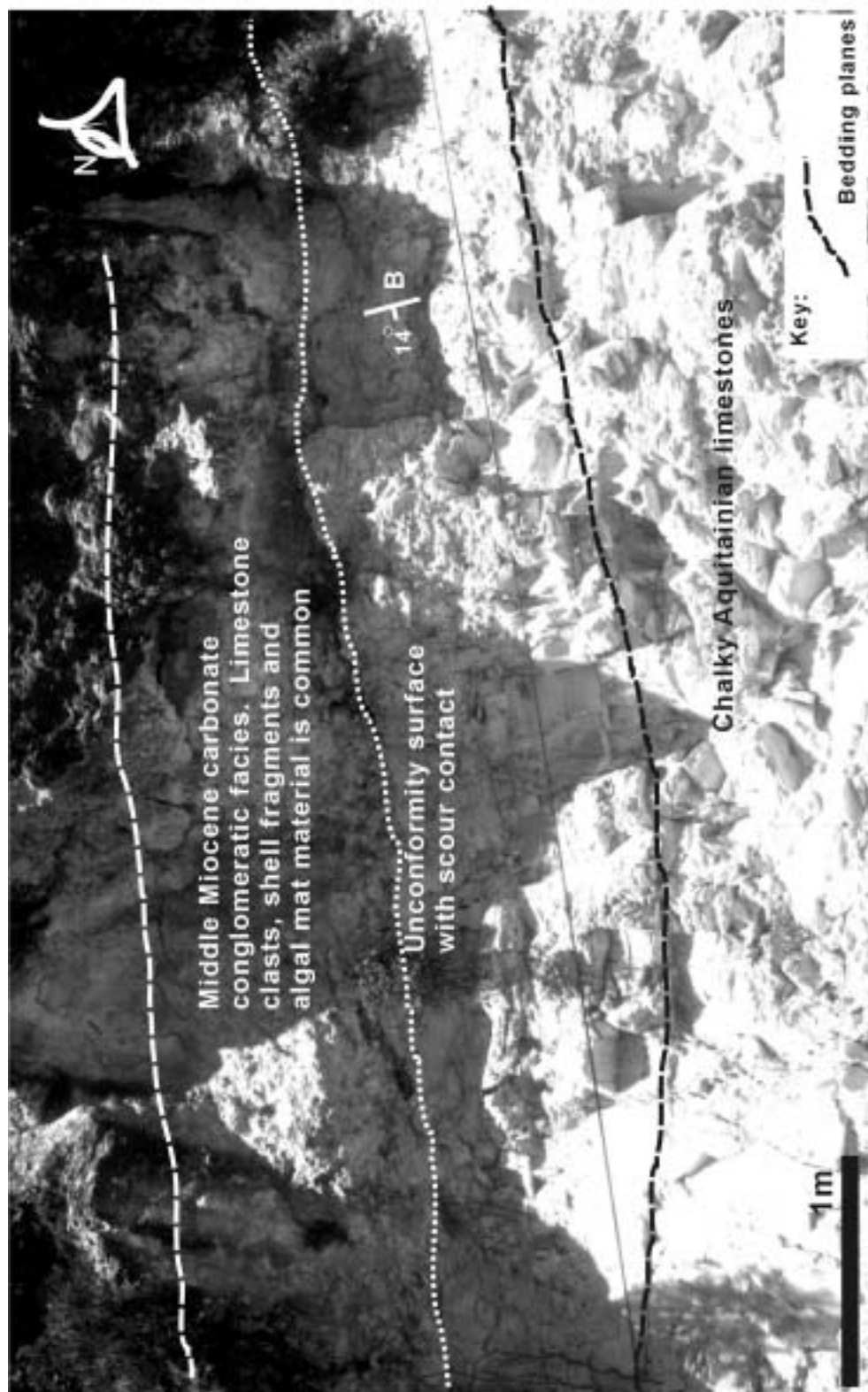
The base of the Aquitanian succession is indistinct in this area and was only identified by dating samples. Older rocks, clasts and fauna are often reworked into the lowermost beds of this unit, especially Middle Eocene-age rocks. Burdigalian and occasionally Langhian-Serravallian facies (Figures 3.23b and 3.24) erosively overlie the Aquitanian time-slice.

### *Preliminary interpretation of Aquitanian-age facies*

The Aquitanian is the first preserved rock unit deposited after the Eocene-Oligocene hiatus (see Chapter 6). On the northern margin of the Nahr El-Kabir Valley the initial facies and fauna are indicative of a very shallow marine setting. They are overlain by marly background sediment, probably of deeper water (mainly foraminifera). A reef setting is not preserved but faunal evidence indicates similar water depths. This initial stage of deposition changed rapidly to a deeper, probably shelfal water depth and marl-rich facies. This margin also shows evidence of fault movement of the El-Kabir Lineament (refer to Chapter 4), with both syn-depositional (conglomerate formation) and later episodes of fracturing.

Aquitanian successions of the southern margin of the Nahr El-Kabir and Abyad River valleys, also commence with bioclastic rich sediments. It is not immediately clear whether a carbonate shoreline or patch reefs could have supplied the bioclastic material found within the sediments as diagnostic faunal assemblage was not found.

The Aquitanian time-slice marks the return of sedimentation to the region after the end of the Palaeogene. Sedimentation is thought to be restricted to the Nahr El-Kabir Valley



**Figure 3.24** Middle Miocene (Langhian-Serravallian) southern valley margin deposits overlying and downcutting into the Aquitanian succession, 10km north of Al-Haffeh Town & 2km north of Kfeyeh Asphalt Pit. This region is mapped as Middle Miocene overlying Cretaceous platform sediments. The Aquitanian here is very thin (<10m), as is the Middle Miocene (<20m). Facies relationships on this margin of the Nahr El-Kabir Valley are strongly controlled by structuration in this region (see Chapter 4).

as a shelfal depth basin (see Chapter 6), whereas the margins of the valley contain sediments from shallow water environments.

### ***Time-slice 4, Burdigalian transgressive limestones***

Burdigalian-age rocks crop-out on the northern and southern margins of the Nahr El-Kabir Valley and in the Abyad River Valley. As with the Aquitanian, no outcrops were found south of Qerdaha Town. In general, the Burdigalian consists of much coarser sedimentary rocks than observed in earlier time-slices and is a distinct facies, although poorly exposed.

#### *Northern margin of the Nahr El-Kabir Valley*

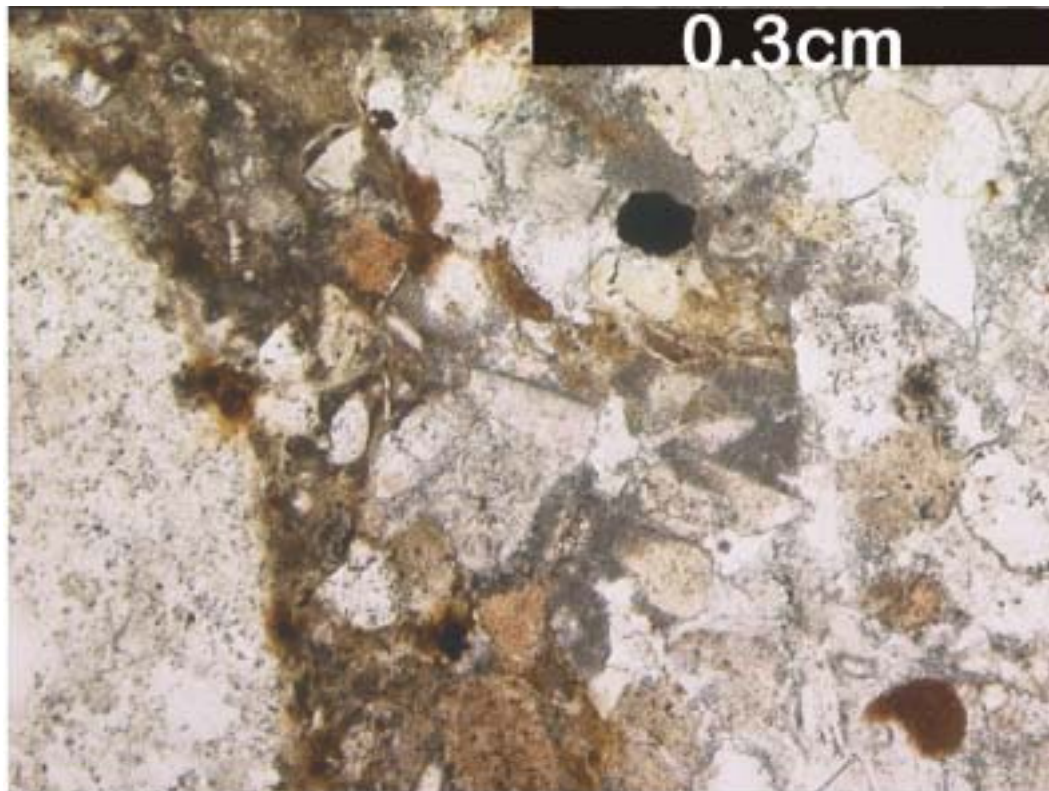
On the northern margin of the Nahr El-Kabir Valley, Burdigalian-age rocks are much coarser grained than any of the Palaeogene and Lower Miocene rocks previously described within the study area. The Burdigalian-age rocks are calcilithites, wackstones and conglomerates. Angular chert fragments, micrite and mafic minerals dominate most samples collected.

Adjacent to the Baer Bassit Massif (El-Kabir Lineament; Chapter 4 & 6), the Burdigalian time-slice commences with a siltstone containing organic matter. The siltstones (4m thickness) are overlain by 10m of graded, clastic-rich, medium thickness beds of conglomerate and sandstone. The grainsize varies from pebbles to fine sand in these clast supported beds. No limestone is entrained within the sediments nor are fossils evident. These clastic-rich, lens-shaped beds down cut into older beds of limestone (similar to well exposed Langhian-Serravallian-age sediments, Figure 3.39).

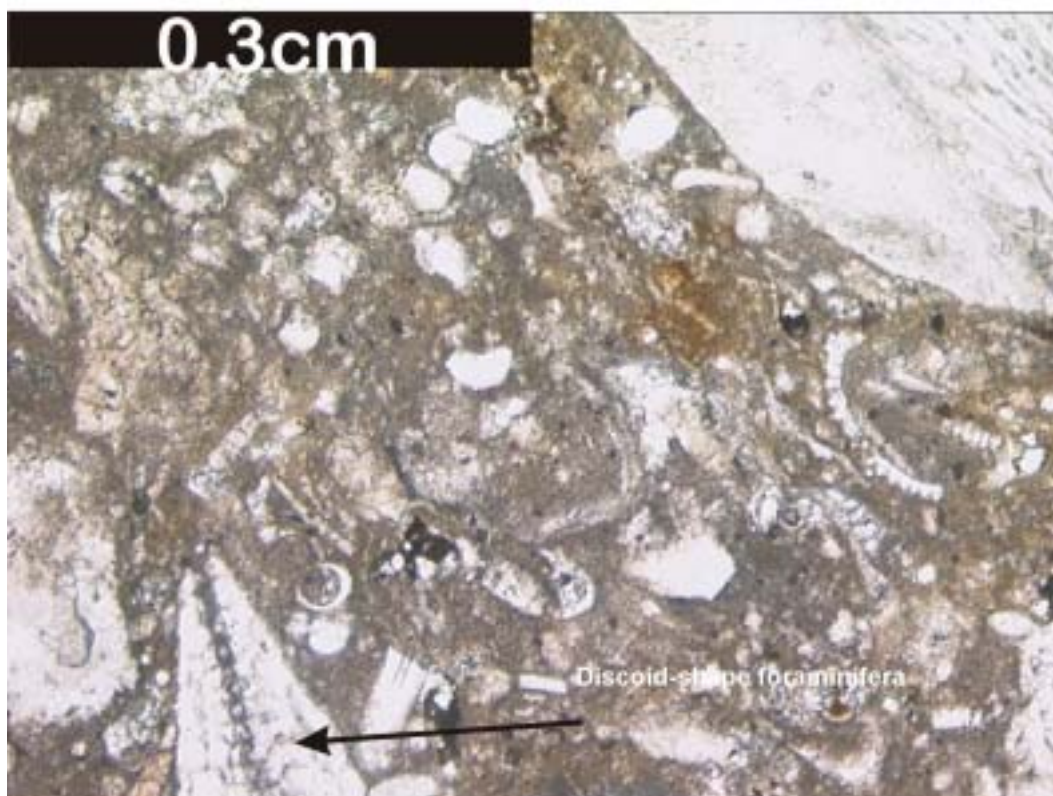
The siltstones are directly overlain by planar bedded limestone and chert clast-rich conglomerates. Dating of the limestone clasts shows that reworked Maastrichtian-age fauna are present (Marcel BouDagher-Fadel). The conglomerates (7m thick) terminate abruptly and are overlain, in turn, by wackstones (Figures 3.25 and 3.26). Bioclast-rich grainstones and calcarenites are intercalated with these background marls. Each fining-upward bed increases in grain-size until a thick boulder conglomerate scours into the succession.

Poorly developed clast imbrication within the conglomerate suggests a southeast palaeoflow direction. The detrital chert clasts within the conglomerate are red and grey coloured radiolarian cherts. They are similar to cherts deformed within the Baer Bassit Massif Melange. Mud clasts within the conglomerate may be derived from serpentinite and dark brown shale clasts appear to include organic matter.

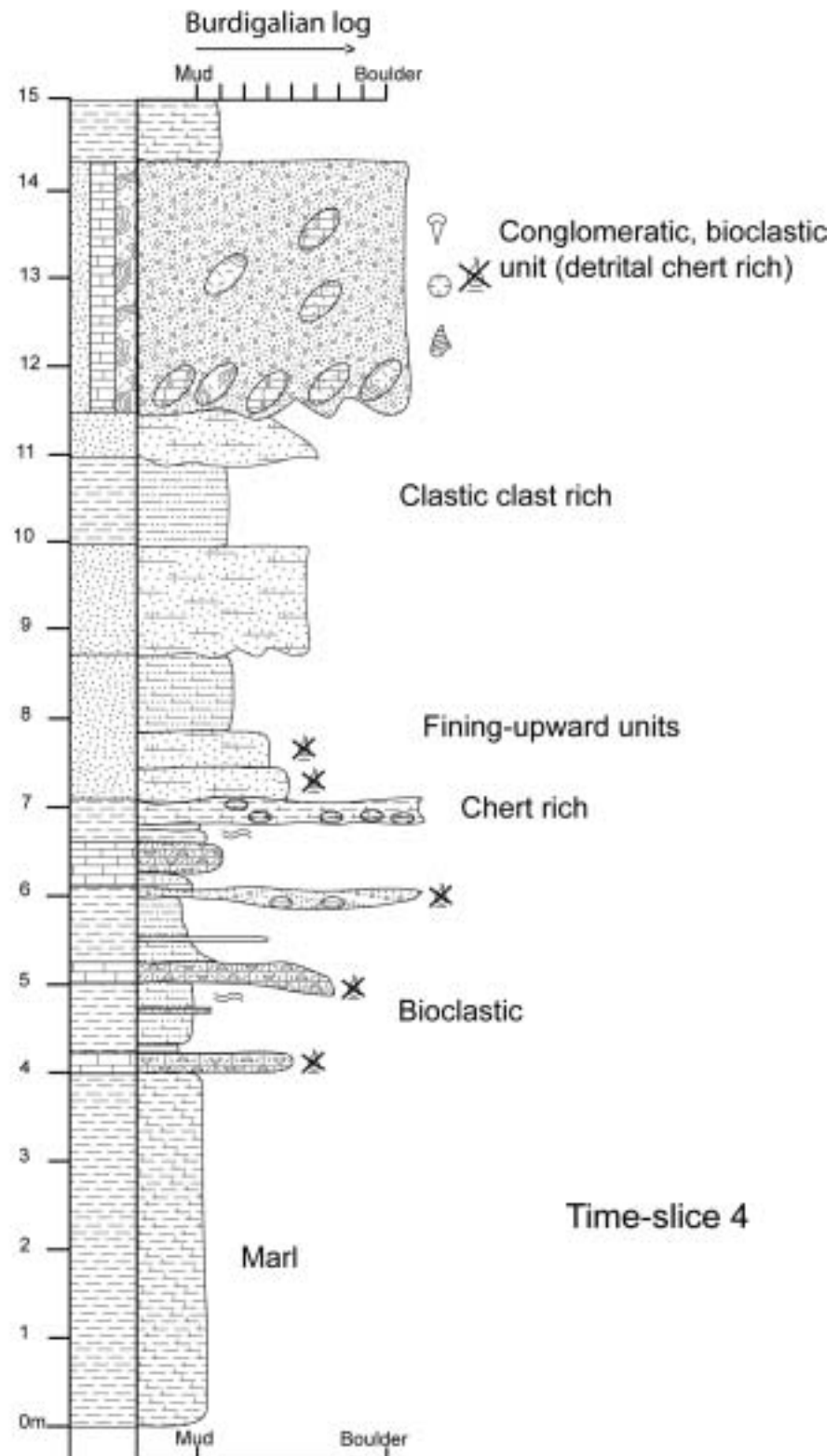




**Figure 3.25 A** Burdigalian age calcilithite, detrital chert fragments in a micritic matrix from the Baer Bassit margin of the Nahr El-Kabir Valley. PPL.



**B** Burdigalian packstone from the southern margin of the Nahr El-Kabir Valley. Shell fragments and large discoid foraminifera are common. Micrite matrix predominates. PPL.



**Figure 3.26** Sedimentary log of the Burdigalian facies seen on the northern margin of the Nahr El-Kabir Valley, 25km northeast of Latakia City.

The coarse clastic rocks are overlain by marl and limestone alternations containing minor quantities of detrital chert.

*Southern margin of the Nahr El-Kabir Valley*

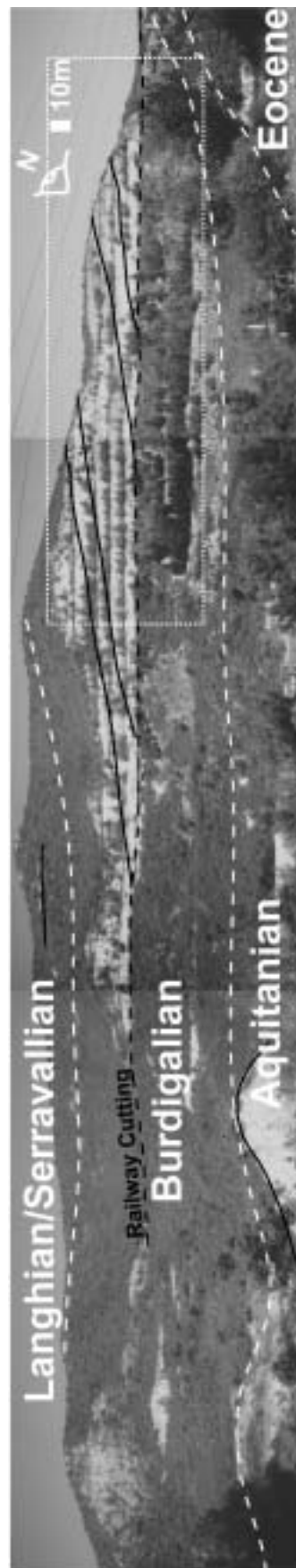
The southern margin of the Nahr El-Kabir Valley is dominated by bioclastic packstones, rich in shell fragments and discoid foraminifera (Figure 3.25). Some of these foraminifera appear to be of Eocene age. Chert is found in samples from this margin, but only in very small quantities. The chert is dark coloured, probably reworked from Cretaceous platform sediments.

Only one large (400m) outcrop of Burdigalian-age rocks was found within the Nahr El-Kabir Valley, near Khan El Jouz Village. It exposes the architecture of this time-slice in an oblique section from the Jebel An-Nassuriyeh Valley margin (Figure 3.27). Marl predominates and is intercalated with bioclastic debris in medium thickness, fining-upward beds. The beds dip into the valley and appear to build outwards, thickening towards the base (subtle prograding architecture, Emery et al. 1996, see below). Individual beds (1m) are grouped in 'packages' of beds (10-30m), observed across the entire outcrop.

One small exposure on the southern margin hints at both the sedimentary and structural processes affecting the Burdigalian succession (see Chapter 4). Coarse bioclastic conglomerates truncate underlying Aquitanian wackestones. These conglomerates are proximal (20m) to a large fault running sub-parallel to the valley margin (NE-SW). From the base of the exposure to the uppermost, bedding dips decrease (suggesting a growth fault, see Chapter 4). The outcrop is also cross-cut by another large fault, perpendicular to the valley margin. Faulting appears to be synchronous with deposition (see Chapter 4).

*Nahr El Abyad Valley, north of the Nahr El-Kabir Valley*

The contact between the Aquitanian and the overlying Burdigalian time-slices is unconformable. The Burdigalian commences either with a series of erosive clastic conglomerate beds (northern margin), or with a chalky clast conglomerate (southern margin), overlain by calcarenites and bioclast-rich beds. In both examples erosion occurred at this contact (i.e. scoured bed bases).



Inset picture.

White and black lines denote primary bedding planes, obscured slightly by railway terracing. Dashed lines mark succession boundaries.

**Figure 3.27** Downlapping of Burdigalian sediments onto horizontal Aquitanian strata near the southern margin of the Nahr El-Kabir Valley, 1 km north of Khan El-Jouz Village. These sediment packages appear to be subtly prograding into the basin; however, there are no other extensive outcrops to confirm this hypothesis or a continuous view of the basin margin. The overlying Langhian-Serravallian succession downcuts into the Burdigalian succession and is sub-horizontal. The railway line shown in these pictures was restricted from access.

The conglomerates with scour bases form lenticular beds up to 1m thick in a stack of cross-cutting beds 9m thick. These beds are orientated approximately east-west. Clast imbrication had not developed and a transport direction could not be accurately inferred.

The southern margin chalky conglomerates contain clasts of Aquitanian-age wackestone and 'sugary textured' sparitic grainstone (Eocene?) and were deposited in planar, medium thickness beds.

The majority of the remainder of the succession (approximately 120m) comprises white foraminiferal marls and limestones. Laminated wackestones are often impure with organic and fine-grained clastic detrital material. The top of the succession consists of similar sedimentary rocks, but pteropod gastropods are common.

#### *Preliminary interpretation of Burdigalian-age facies*

The Burdigalian succession is predominantly wackestones with derived clasts from both margins of the Nahr El-Kabir Valley (bioclastic and ophiolitic massif origin). The clastic pulses of sedimentation show that the unit was prograding from the margins as a sequence of stacked beds, although evidence for multiple point sources or a line-source of deposition is not immediately obvious (Chapter 4).

The valley centre shows marl background sedimentation as planktic foraminifera-rich wackestones were deposited, probably in shelfal water depths (perhaps shallower water to the east). These background sediments are intercalated with intraclasts derived from much shallower water (shell fragments and shell hash). These suggest possible shallow water maybe biostrome or patch reef settings on the southern margin of the valley, although this could not be confirmed. Eroded clastic-rich sediments were sourced from what must have been a sub-aerial Baer Bassit Massif on the northern margin.

#### ***Time-slice 5, Langhian bioclastic limestone***

Langhian-age bioclastic limestone is found on the western margin of the Baer Bassit Massif, near the villages of Borj Islam and Ras El-Bassit. Elsewhere, Langhian-age rocks could not be reliably distinguished by mapping from those of Langhian to Tortonian-age (i.e. the Nahr El-Kabir Valley).

Langhian-age rocks comprise bioclastic packstones and grainstones, as seen in a small outcrop unconformably overlying Middle Eocene-age limestones. The Middle Eocene-

age rocks are erosionally overlain by a thin conglomerate unit (15cm thick) consisting of Eocene-age chalk clasts (Borj Islam) or ophiolitic massif clasts (Ras El-Bassit). The conglomerate is overlain by massive, bioclastic, 'sugary texture' sparry limestone (Figure 3.28). Large, benthic foraminifera are common, as is algal material. No macrofossils were found but carbonate dissolution and bivalve molds are common, as is karstification. Quaternary-age neptunian dykes, filled with red silt are also prominent.

Planar cross stratification was visible at one karstified locality rich in foraminifera, but not macrofossils. The planar laminations were observed in 20cm thick beds, stacked into a 2m thick package; these laminations dipped shallowly ( $<10^\circ$ ) north and south. This limestone is exceptionally hard and quarried extensively for building stone.

#### *Preliminary interpretation*

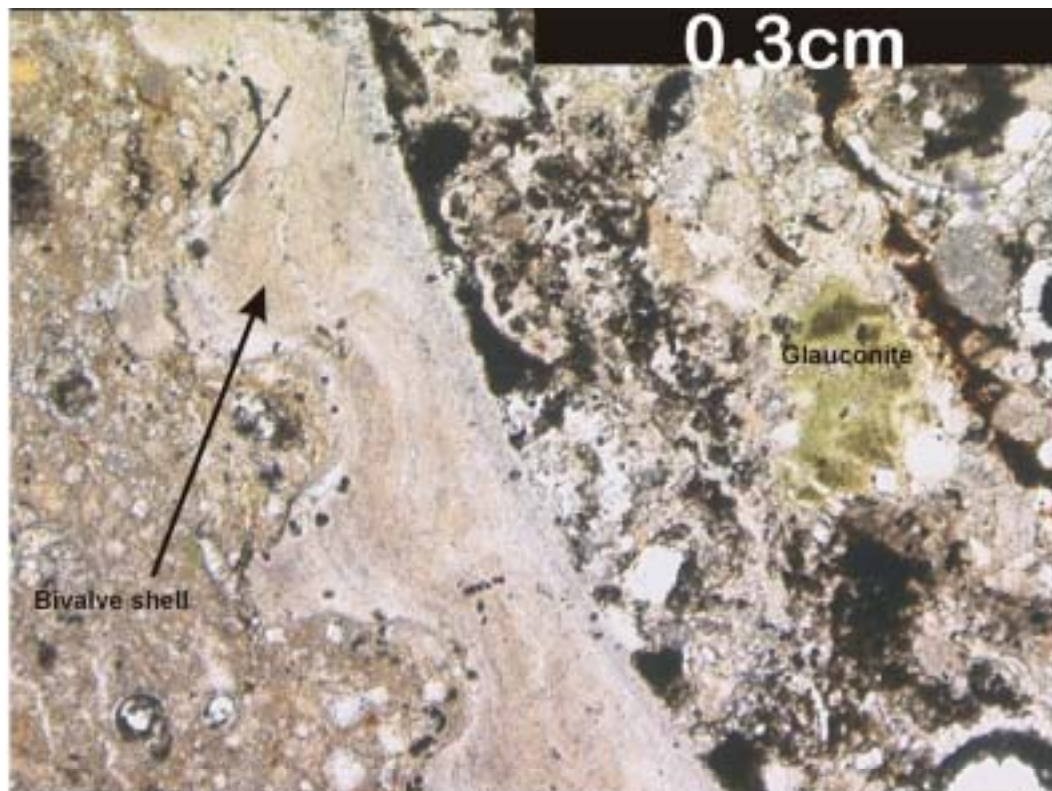
The faunal assemblage, planar cross stratification and massive bedding within the succession, indicates a very shallow marine environment (either shoreface or foreshore at both localities, Tucker et al. 1990, see Chapter 6, Figure 6.3). The bioclastic grainstone is laterally restricted and shows a transition to benthic foraminifera-rich limestone over a distance of 200m near Borj Islam Village. The interpretation of this unit is that a small biostrome or patch reef existed at both localities and a foreshore environment (planar stratified) existed to the west of Borj Islam.

### ***Time-slice 6, Langhian-Serravallian debris flows***

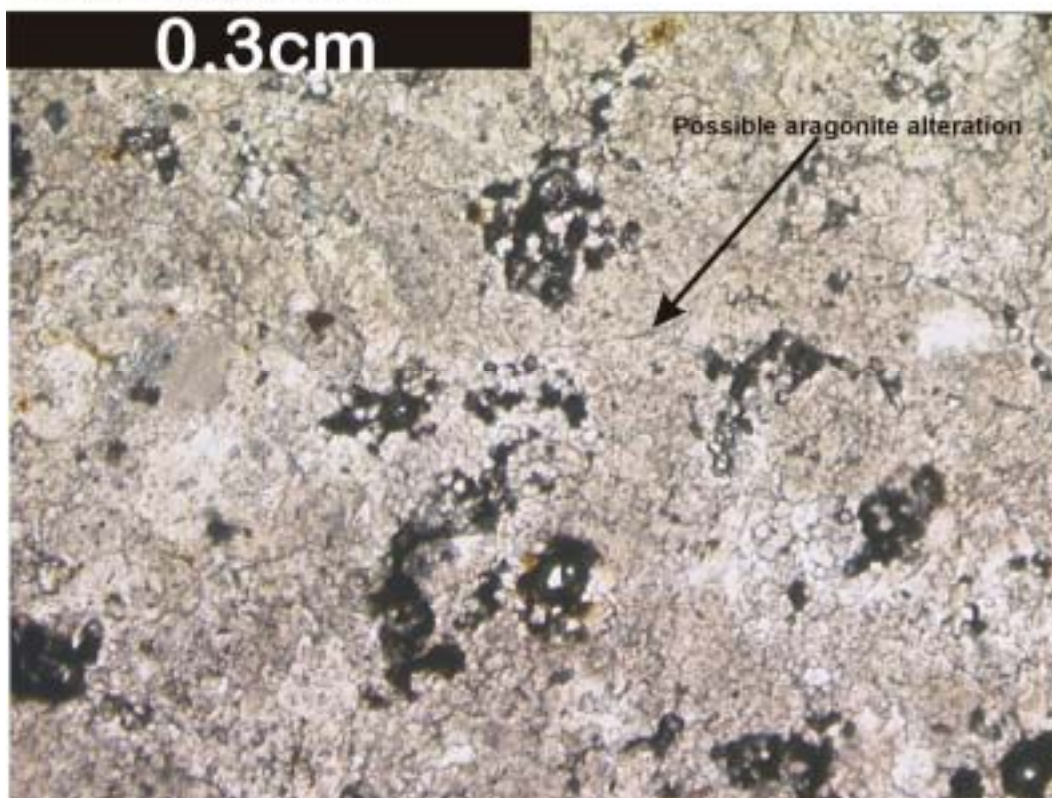
Langhian to Serravallian-age rocks are found within the Nahr El-Kabir Valley and further north. Ponikarov et al. (1963, 1966, 1967) and Krashenninnikov (1971, 1994) indicated that one undifferentiated Langhian to Tortonian-age unit of conglomerate or marl existed at that time but further work here has indicated that this unit can be subdivided.

The Langhian-Serravallian unit comprises the most dynamic and lithologically varied time-slice seen in the project area. It crops out in the north of the Nahr El-Kabir River Valley and further north in the Nahr El-Abyad River Valley, although there are very distinct facies changes between these two localities. At every known locality, it unconformably and erosively down-cuts into the succession below.





**Figure 3.28 A.** Middle Miocene-age bioclastic packstone from the small outcrop overlying the Baer Bassit Massif (near Borj Islam Village). Glaucinite is present, indicating deposition in shallow marine conditions. PPL.



**B.** Aragonite alteration to Mg Calcite and more stable forms of carbonate. Same locality and age as above. PPL.



### Middle Miocene biostratigraphy

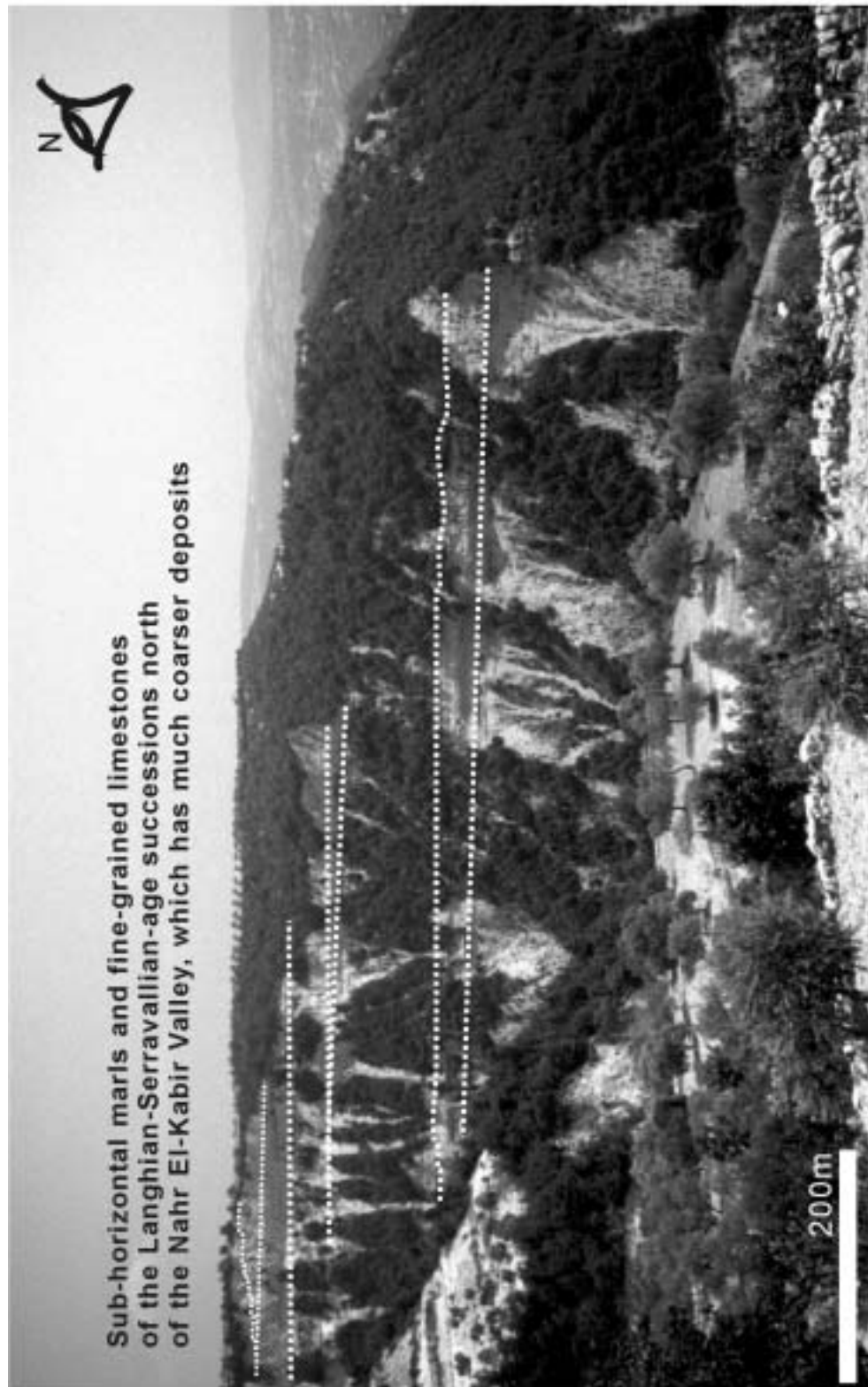
Extensive effort was directed at dividing this Middle Miocene mapped unit into several time-slices (from the undifferentiated Langhian-Tortonian succession by Ponikarov et al. 1963). This would enable differentiation of the timing of sedimentological events (therefore, relating to structural and tectonic events). Key samples were taken for foraminiferal dating and then these dates were used in the last field season to attempt to improve this mapping (see preliminary interpretation, this time-slice, time-slice 7 and Chapter 6).

### *Nahr El-Abyad River Valley*

This area is located between the Nahr El-Kabir Valley and the Ghab Valley. Middle Miocene-age facies crop out extensively there and across the Syrian-Turkish border to the Hatay Province.

The unit comprises alternating chalky limestone and marls, mainly wackestone, with occasional packstone containing pteropod fragments. Unit thickness in the east was measured as at least 200m (visible due to the steep topography). It overlies the Burdigalian-age rocks without a noticeable erosive unconformity, although the lithologies are very similar and the contact is poorly exposed. Figure 3.29, shows the typical sedimentary architecture of this unit in this region, which contrasts strongly with that seen further south (see Nahr El-Kabir Valley). Limestones are typically planar stratified, medium thickness bedded (10-30cm) and sub-horizontally. Packages of beds (5-10m) are observed to pinch-out to the north (parasequences, Emery et al. 1996), although the extent of these features or further indicators to assess if they are channels, could not be seen due to the lack of exposure. Intra-parasequence instability was also evident close to the top of the succession. The bedding pinch-outs suggest a northerly or easterly palaeocurrent direction but sediment imbrication was poor and do not indicate a predominant direction.

Ponikarov et al. (1963, 1966, 1967) and Krashenninnikov (1971, 1994) did not describe the lithologies in this region, except to say that conglomerates were absent. During this work, thin conglomerates were found towards the top of the succession. Lenses of calcarenites with redeposited chalk clasts are common and ophiolitic massif derived debris (e.g. angular detrital chert granules) is also present in these fining-upwards units. The uppermost beds are rich in bioclasts, which are typically fragments of bivalves and gastropods. The amount of redeposited material and clastic clasts increases towards the top



**Figure 3.29** A view north of the Langhian-Serravallian deposits north of the village of Baksariyeh. In marked contrast to the coarse, gravity driven sediments of the same age in the Nahr El-Kabir Valley, these sedimentary rocks are predominantly marls and chalky limestones. Clastic input occurs at the top of the succession, as do signs of instability. Bedding packages pinch out to the north. This region forms the catchment area for the Abyad and Orontes Rivers, hence the deep valley topography.

of the succession and laterally continuous conglomerate beds replace lenses of clastic material (beds averaging 40cm thickness are intercalated with 5cm thick chalky limestone beds). The clastic-rich beds abruptly terminate and are overlain by laminated chalky limestones within the uppermost 10m of exposure.

#### *Near Banyas*

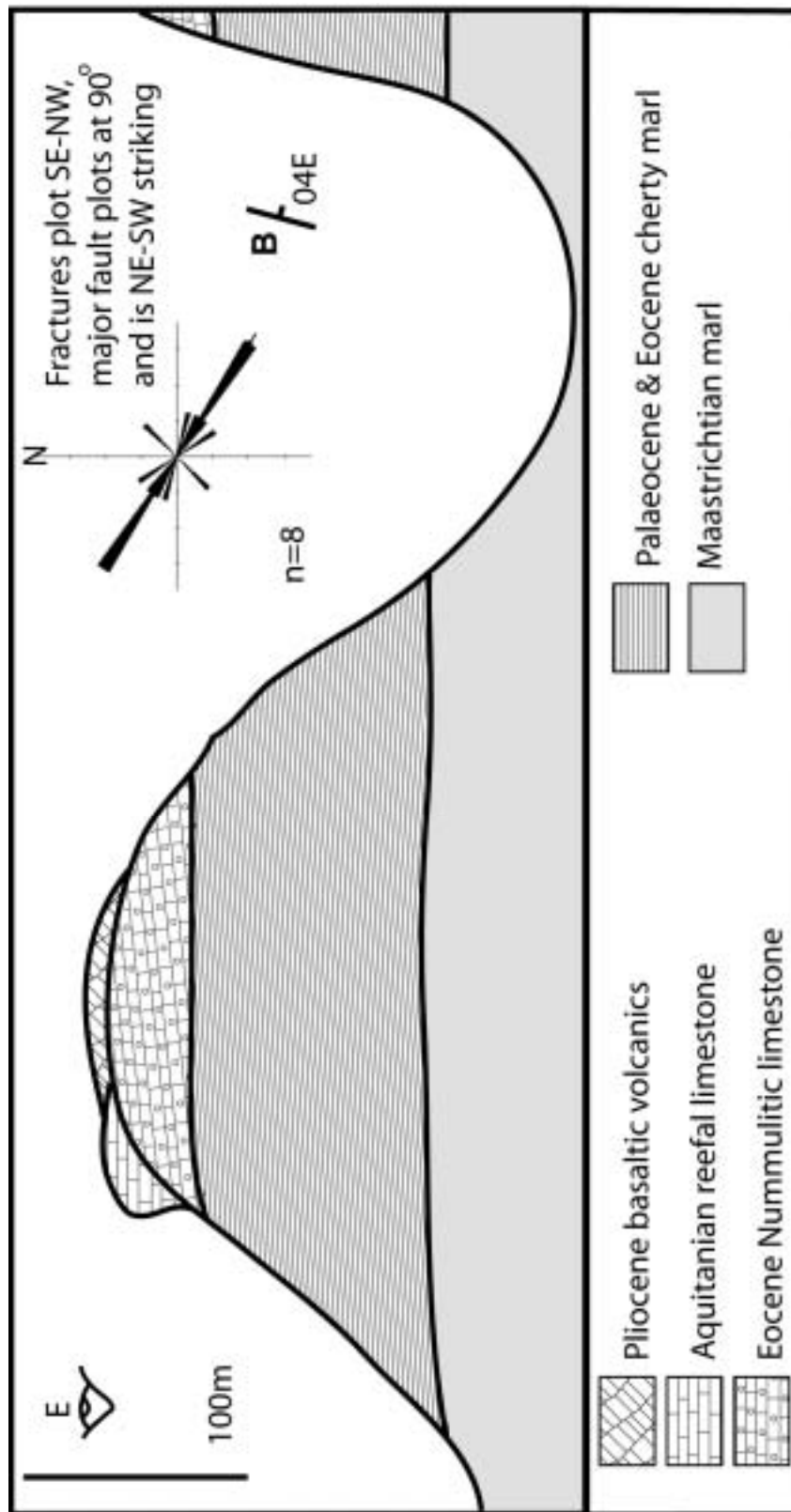
Although not mapped by Ponikarov et al. (1963, 1966), a small outcrop of inferred Middle Miocene-age bioclastic packstones overlies Eocene Nummulitic limestone and is overlain by Pliocene volcanics, 5km inland of Banyas Town (Figure 3.30). The outcrop could not be accurately dated as foraminifera were rare, but it contains fauna similar to that seen on the southern margin of the Nahr El-Kabir Valley (see below), such as calcareous algal material, miliolids, bryozoan, gastropods and shell fragments. The matrix is predominantly micritic with a later sparite cement and is very dissimilar to the surrounding Eocene Nummulitic grainstone.

#### Nahr El-Kabir Valley

The Langhian-Serravallian-age unit is exposed throughout the northern region of the Nahr El-Kabir Valley. Typically, it comprises dark grey marls, conglomerates and bioclast-rich limestones. Packstones, calcilithites, calcarenites and calcirudites comprise the Middle Miocene-age rocks of the northern margin and centre of the Nahr El-Kabir Valley. Packstones and bioclastic-rich calcilithites predominate on the southern margin of the valley. Intense lateral variation is common within this time-slice.

#### *Northern margin of the Nahr El-Kabir Valley*

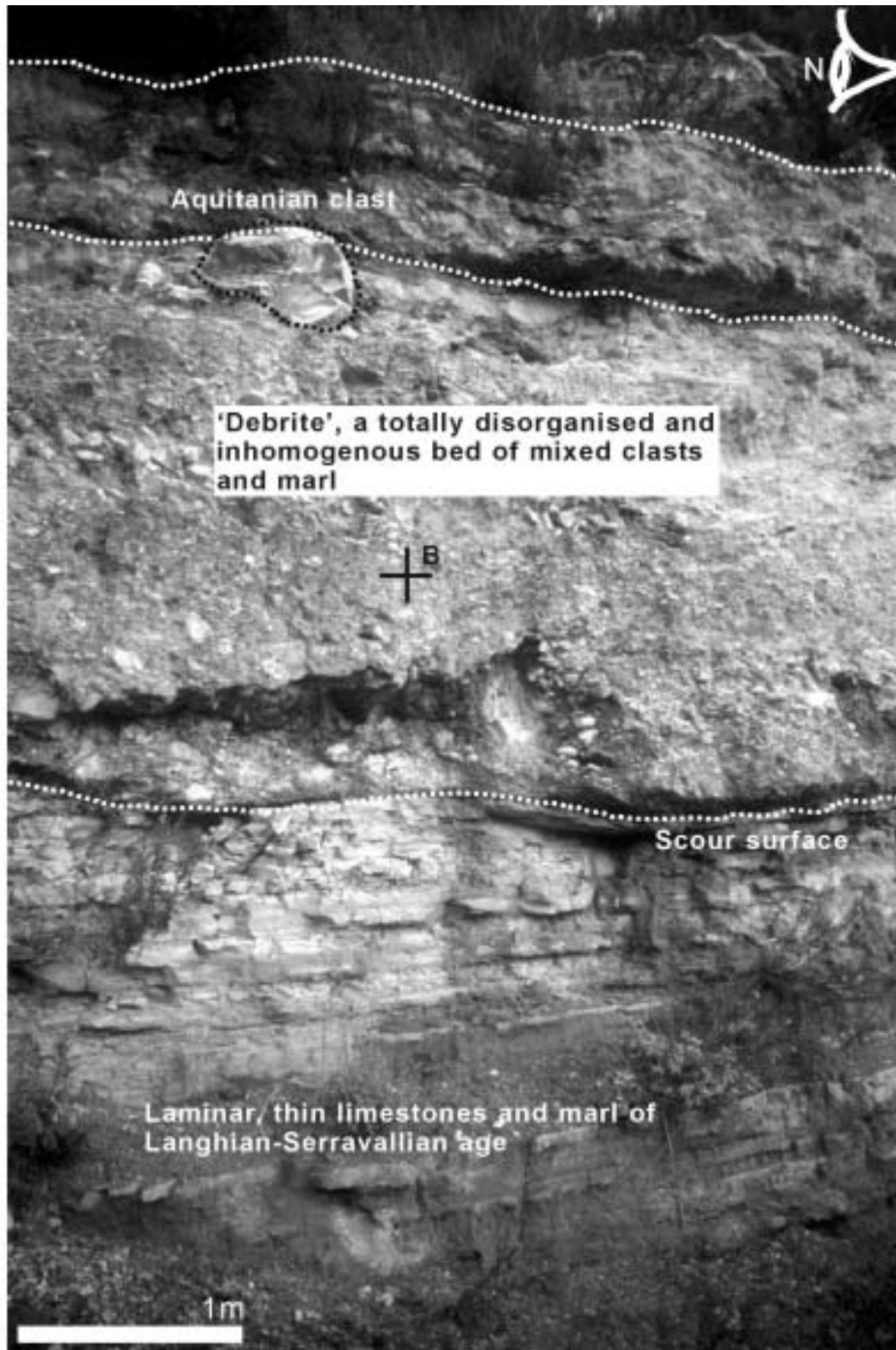
Foraminiferal wackestones are found throughout the succession but predominately towards the base of the unit and graduate into clastic-rich packstones. These rocks contain calcareous algal material and angular chert clasts. Further up the time-slice, the micritic rocks are intercalated with coarse calcilithites, chert and ophiolitic massif derived clast-rich sparitic grainstones. Reworked, soft clasts of micritic limestone are also very common within the coarse-grained units (Figures 3.31 and 3.32). Calcilithites from the northern margin contain clasts of limestone (grey micritic and white, chalky limestone), angular chert, bivalves, bryozoan, algal material and gastropods (Figures 3.33 and 3.34).



**Figure 3.30** Condensed Palaeocene sediments discordantly overlie the Maastrichtian succession and the Eocene overlies the Palaeocene with a minor angular unconformity, near Banyas Town. Small Miocene bioclastic outcrops are found perched on these Palaeocene hills and are possibly patch reefs. Pliocene haloclastite and lavas top the sequence.

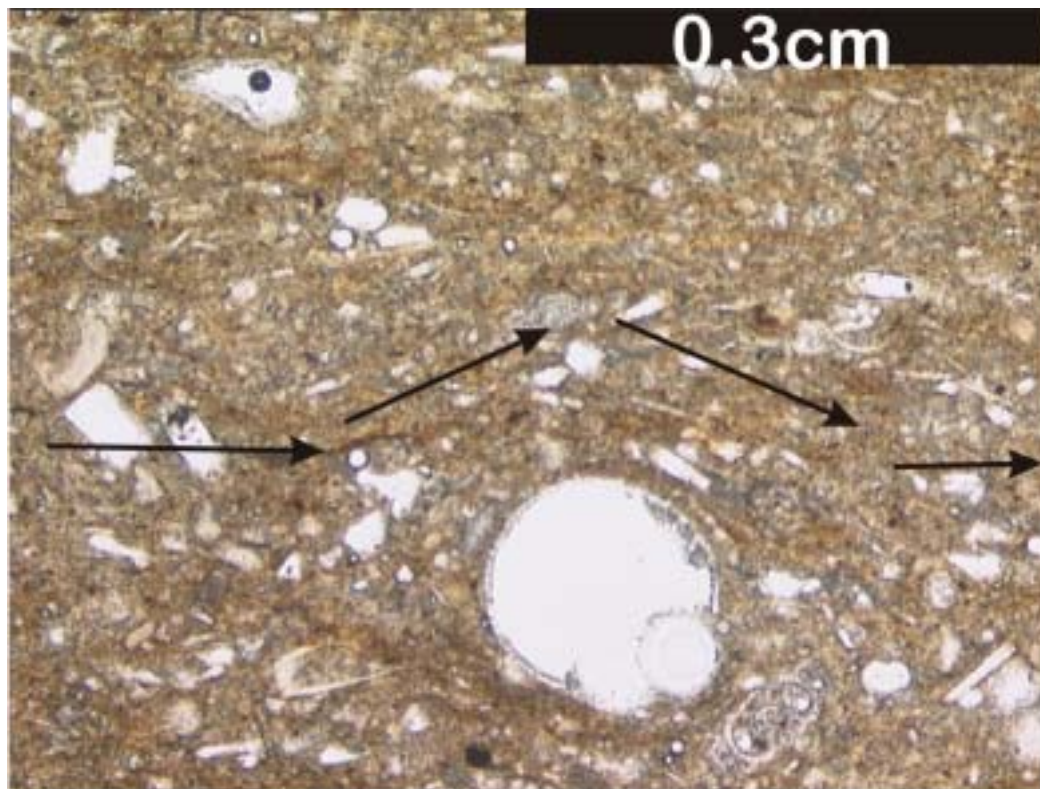


**Figure 3.31** Coarse, loose, clastic conglomeratic deposits are common on the ridges parallel to the margins of the Nahr El-Kabir Valley (near the Baer-Bassit Massif). They consist of well-rounded clasts of white limestone, ophiolitic fragments and bioclastic limestone supported in an angular sandy matrix. Numerous ages of foraminifera are found within the clasts and matrix, indicating either a Middle Miocene age or intensive Quaternary reworking of all previous deposits; although as the deposits are so widespread and at an altitude of 3-400m above sea level it is likely that they are Middle Miocene deposits. Imbrication is poor and fining cycles are poorly developed in what appear to be channelled beds.

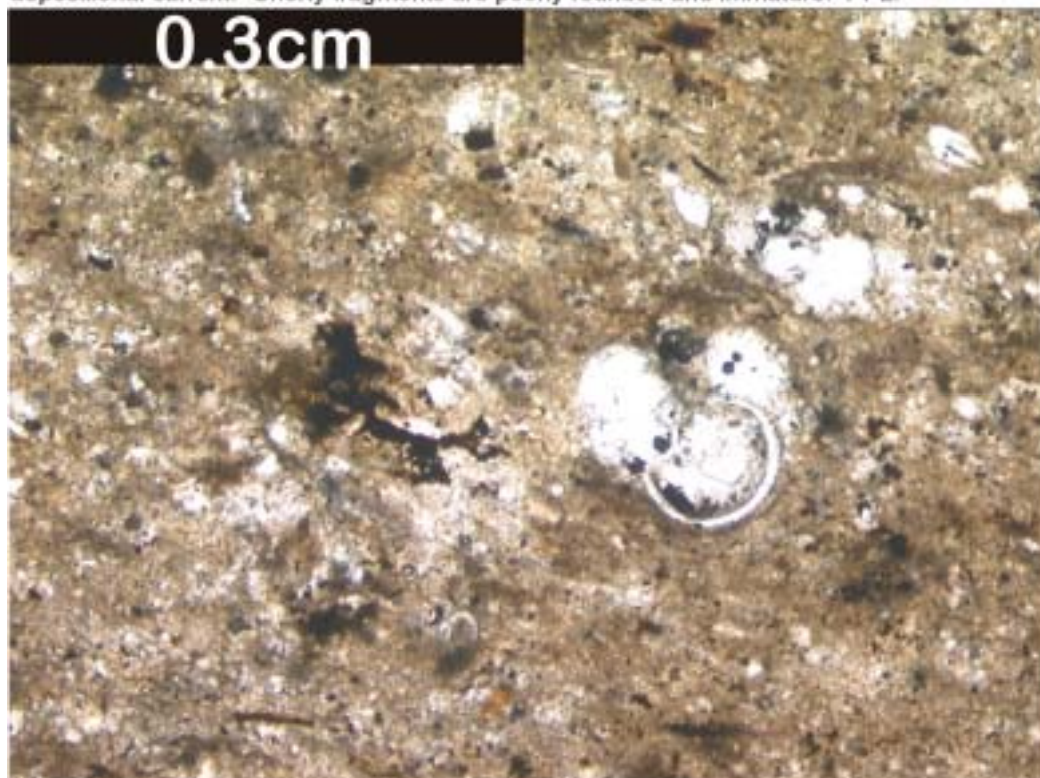


**Figure 3.32** Immature debris flows of Middle Miocene age, the typical deposit found within the Nahr El-Kabir Valley. Langhian-Serravallian succession deposits often contain large clasts of white limestone, thought to be Aquitanian in age. The main sedimentary rocks are thin chalky limestones and marl, with tectonic episodes supplying coarser material. This locality is 15km north of Khan El-Jouz Village, in the basin centre.





**Figure 3.33 A** Langhian-age wackestone with lithic fragments and *Globigerinoides* foraminifera. A 'flow' orientation is apparent, probably representing the direction of depositional current. Cherty fragments are poorly rounded and immature. PPL.



**B.** Both samples A & B are from the northern end of the Nahr El-Kabir Valley, near the Turkish border. They are representative of the subtle change in facies seen from north to south. This wackestone appears 'dirty' (impure), in hand specimen terrigenous material is apparent. PPL.





**Figure 3.34** Langhian-age sparitic grainstone from the faulted northern margin of the Nahr El-Kabir Valley. This sample shows reworking of numerous micritic foraminiferal wackestones and ophiolitic massif debris. (extraclasts predominate), PPL.

It was very difficult to estimate the thickness of Langhian-Serravallian succession as most units cut-down into the units below or are laterally restricted, but a working estimate is 2-300m. Continuous, thin, marl beds occasionally intercalate with coarser deposits and allow lateral comparisons of coarse facies, which typically form lenticular beds. Intra time-slice unconformities are common.

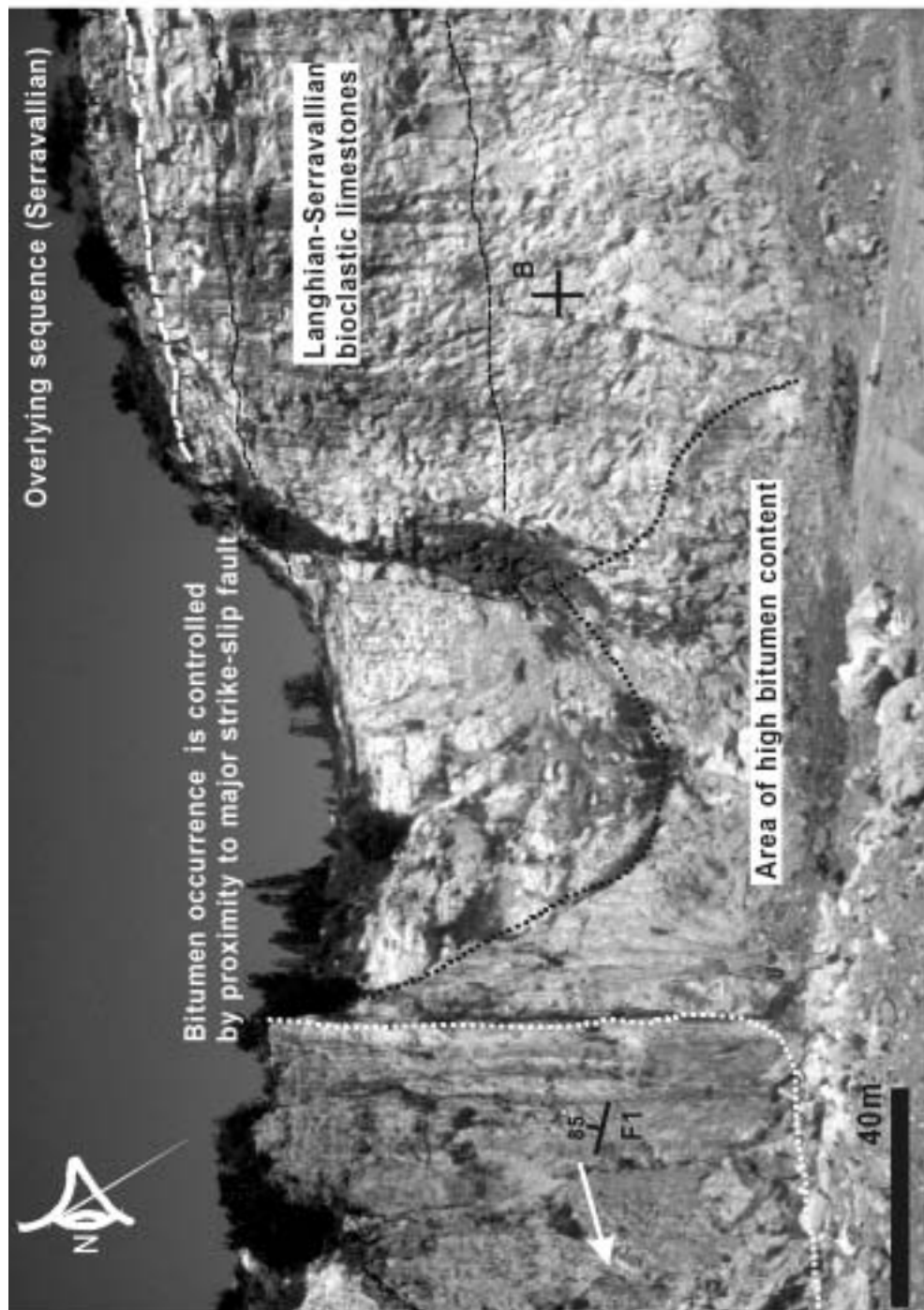
The uppermost part of the succession is exposed on the southern margins of the Baer Bassit Massif. Sub-horizontal conglomerates cap the hilltops and are overlain by 11m metres of thinly bedded, white, foraminiferal wackestones in the more northerly area of the valley. These facies are very similar to those found further north in the Nahr El-Abyad region and are believed to be Serravallian in age.

#### *Southern margin of the Nahr El-Kabir Valley*

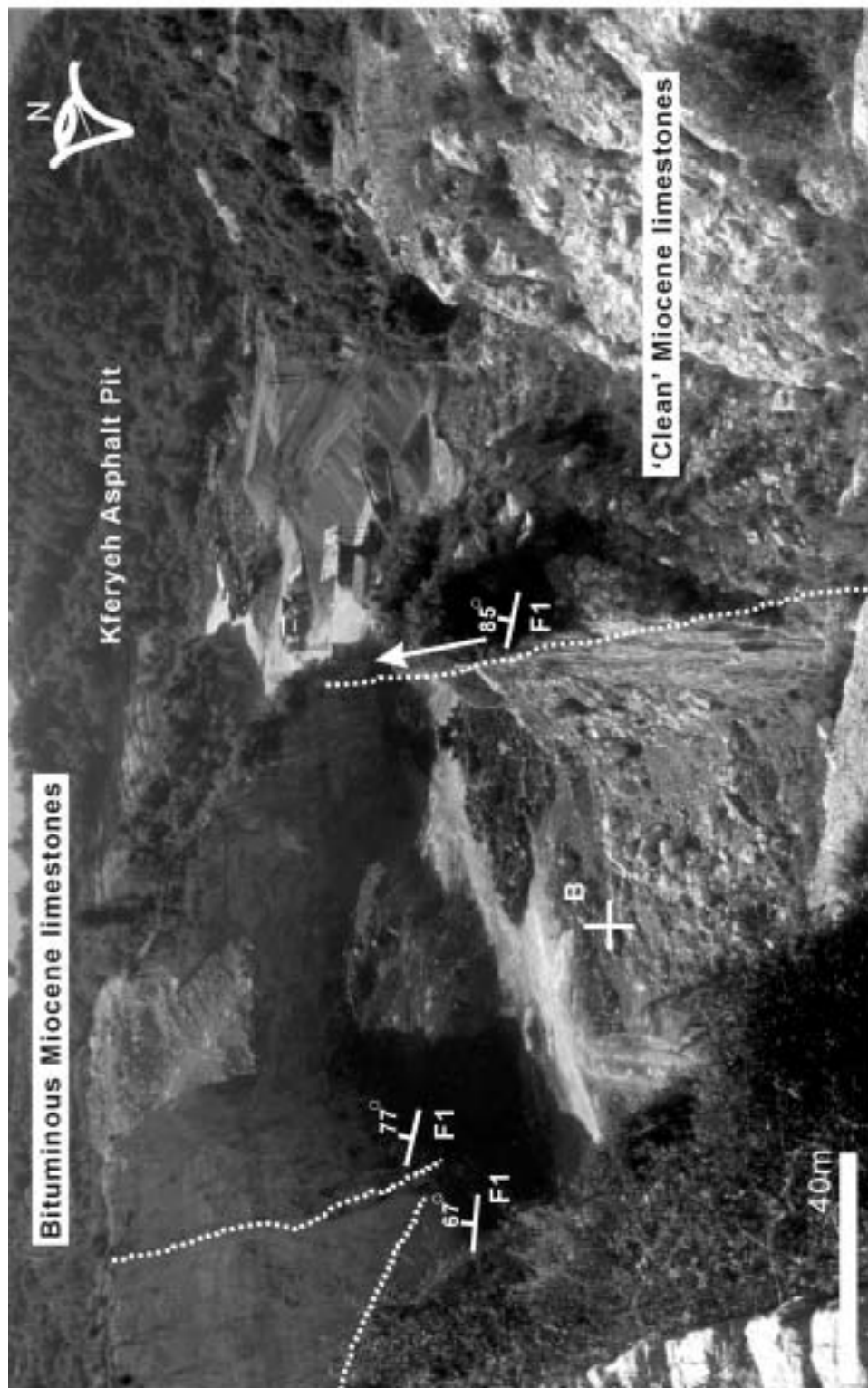
The time-slice typically consists of impersistent thick beds, which downcut (20cm to 1m) those beds below. Near Kferyeh Village, a large, working asphalt pit shows the most continuous exposure (Figures 3.35 and 3.36). The Middle Miocene is at least 250m thick and contains bitumen where close to faults. The succession abuts directly against the Cretaceous Platform limestones and is in faulted contact against it (striking northeast-southwest, see Chapter 4). The succession also covers this faulted margin and overlies the platform in the highest exposures (see Chapter 6).

Wackestones and packstones (Figure 3.37a) dominate the lowermost part of the time-slice. Much coarser packstones and grainstones overlie, partially cemented bioclastic conglomerates (Figure 3.37b). The uppermost part of the succession marks a return to finer grained, but still bioclast-rich packstones (Figure 3.38).

The bioclastic debris is the most varied observed within the region and contains: whole and fragmentary *Porites* coral, bivalve shells (including *Glycimeris*), gastropods, miliolids, algal material, foraminifera (both planktic and benthic) and scaphopods, within thick beds of packstones and grainstones. Bivalve shell fragments are also common and often have borings. Extraclasts of micritic (wackestones) and dark coloured chert are prominent. *Conus* gastropods, that are characteristic of the valley axis sedimentary rocks (see below) were not common on the margins.

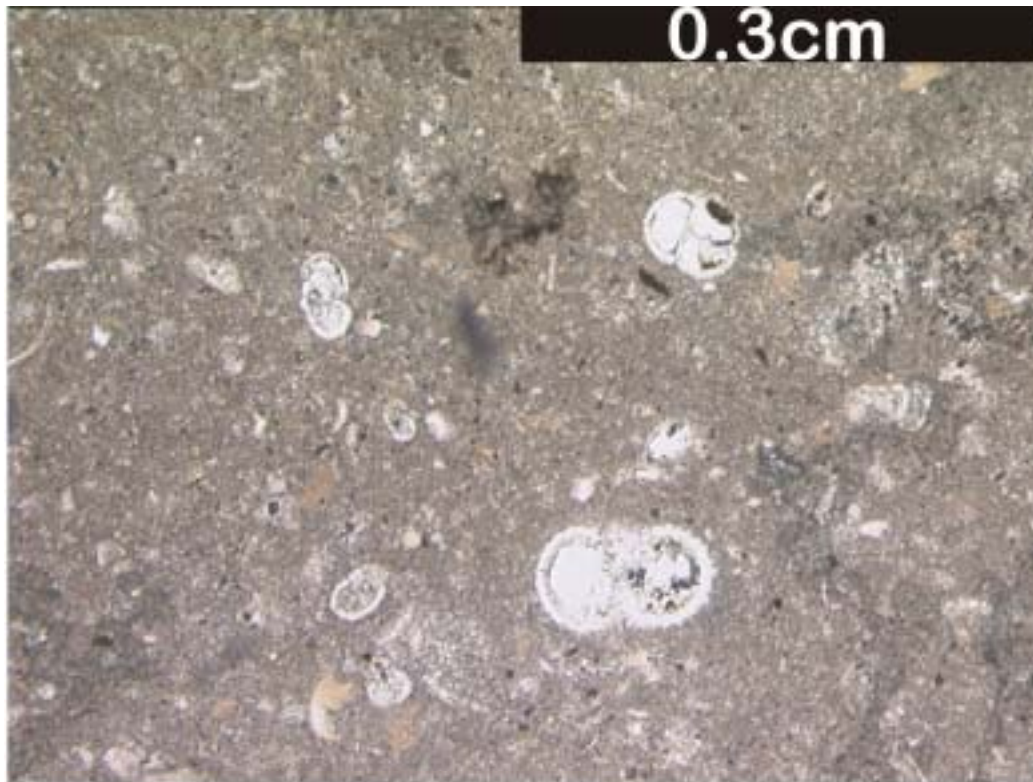


**Figure 3.35** A view into the Kferyeh Asphalt Pit and the main extraction wall. Two successions are visible, the lower Langhian-Serravallian bioclastic limestones and the overlying Serravallian thinly bedded limestones. Bitumen occurrences in the quarry are limited to within 100m of the major strike-slip fault. It is uncertain whether the producing horizon is within the Miocene, Palaeocene or Cretaceous strata as there are no published organic chemistry data.

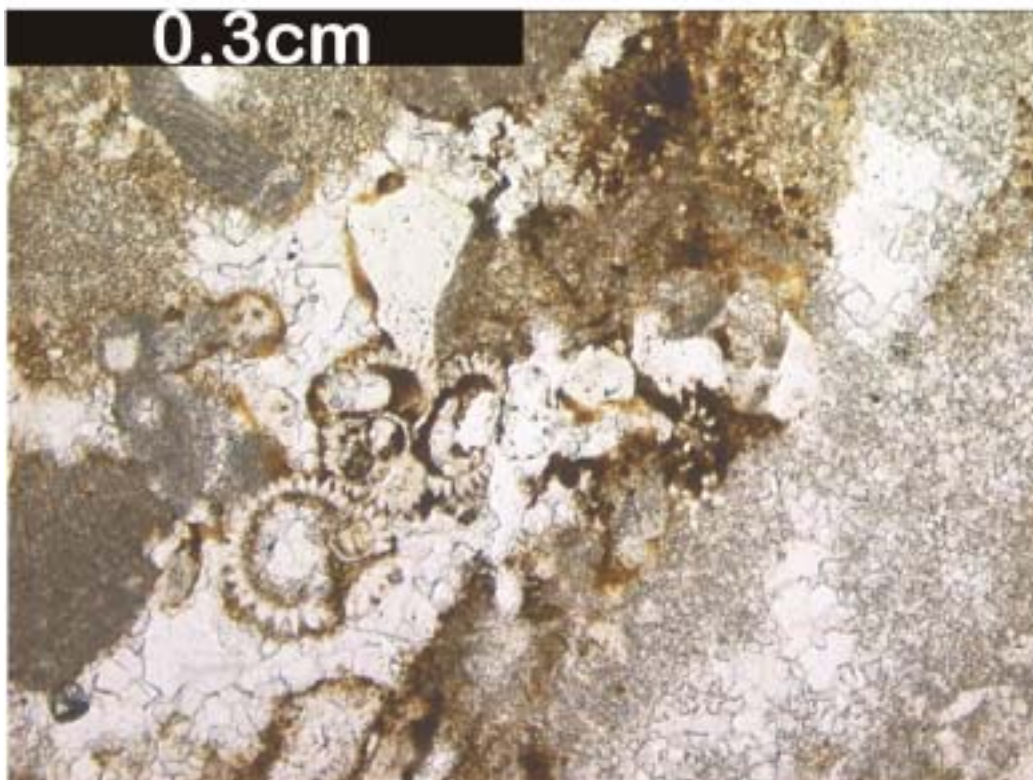


**Figure 3.36** The view looking into the Nahr El-Kabir Valley from the top of the Kferyeh Asphalt Pit (owned by the Establishment of Geology, Damascus). The major pit wall trends along the lower margin of the photograph and is parallel to the margins of the Nahr El-Kabir Valley. The marked faults appear strike-slip type and are associated with bitumen. However, no slickensides are preserved, so the exact sense of movement has to be inferred. The limestones within the pit are of Langhian to Serravallian age and are mostly bioclastic wackestones and packstones.

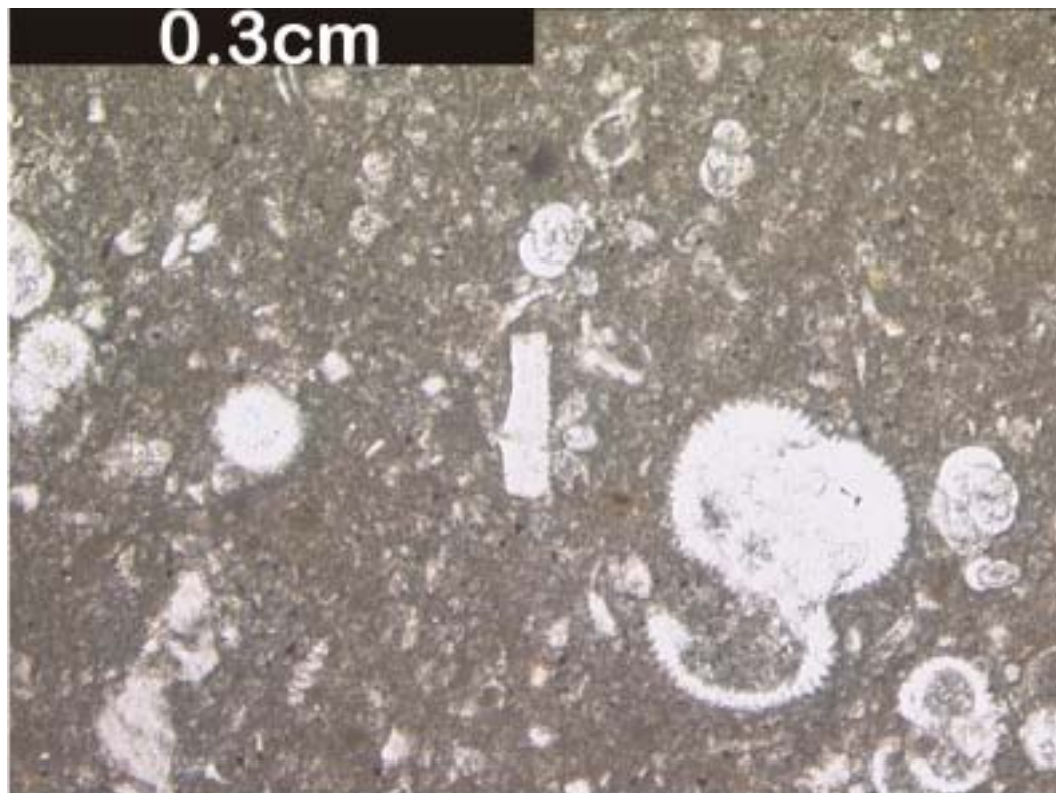




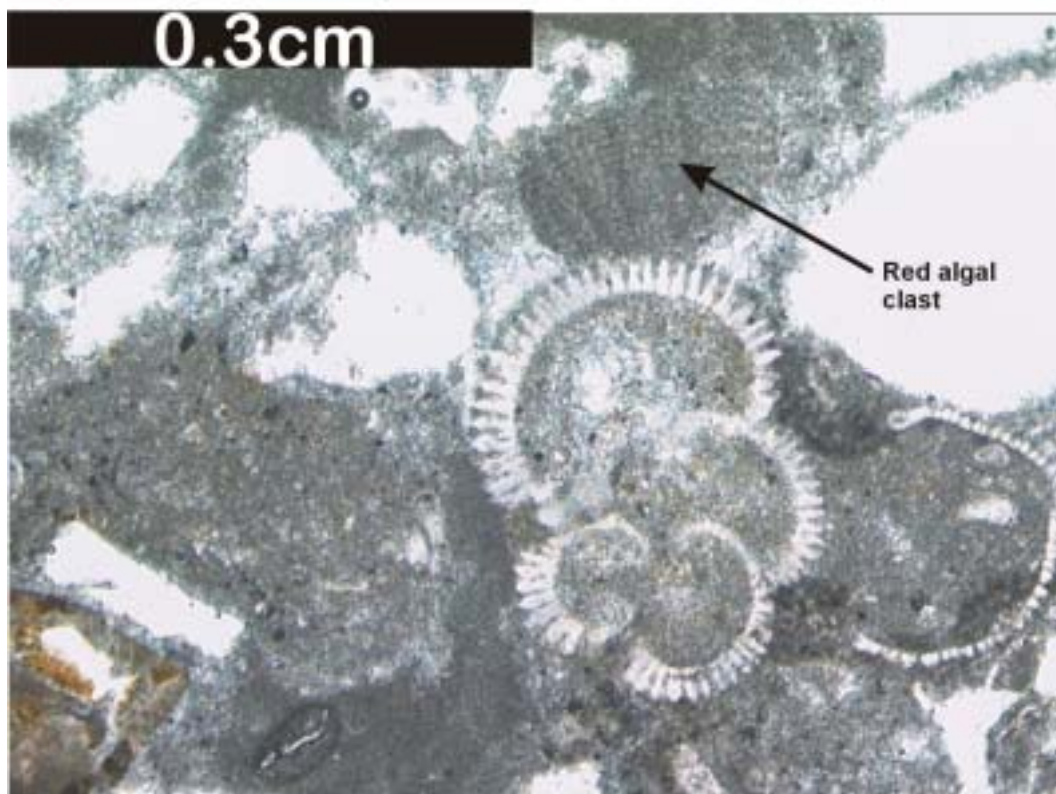
**Figure 3.37 A** Foraminiferal wackestone of Langhian-age, from the Jebel An-Nassuriyeh Mountain margins, PPL.



**B** sparry grainstone with clasts of redeposited limestone (micrite and foraminifera) and algal fragments. Sample B downcuts into the rocks of sample A. This sample was dated as Late Serravallian-age, by MBF. PPL.



**Figure 3.38 A.** Compacted foraminiferal wackestone, showing dissolution of planktonic foraminifera and very minor detrital clasts (chert). Serravallian-age, from the southeastern margin of the Nahr El-Kabir Valley. PPL.



**B.** Serravallian-age. Packstone contains foraminifera (with early infilling), red algal material and intraclasts. Dissolution porosity. XPL.



*Nahr El-Kabir Valley axis*

Within the axis of the valley, rocks of both margins are intercalated, although rarely mixed. Marl deposition is prevalent throughout the succession and is interspersed with thick beds of either ophiolitic massif derived clasts or bioclastic rich-beds. Debris flows, graded beds, scour unconformities and channeling is common (Figures 3.39 to 3.45).

Throughout the Middle Miocene deposits within the Nahr El-Kabir Valley fragments or occasionally whole, large *Conus* gastropods are found, although never in life positions. They are the most common macrofossils, although not age diagnostic.

*Preliminary interpretation of Langhian-Serravallian facies (further discussion Chapters 4 and 6)*

The Langhian-Serravallian time-slice exhibits a wide range of facies, most of which relate to shallow marine carbonates (patch reefs?) or sub-aerial erosion (Baer Bassit Massif)(see below, Tucker et al. 1990). These units were mass wasted due to faulting (debrisites, Leeder, 1999, see Chapter 6) and then the sediments transported to a deeper shelf-depth. All the debris flows appear proximal to the point of origin as there is little sorting, grading or imbrication of clasts. Bedding is also poorly defined and stratification is rare in the lowermost part of the time-slice. Graded turbidity current beds, channeling and cyclical deposition of limestones characterise the uppermost part of the time-slice.

The small outcrop of Miocene found near Banyas is the only indicator that Miocene deposition occurred south of the Nahr El-Kabir Valley (not mapped by Ponikarov et al. 1963). This result is used with caution as it could not be confirmed by independent dating, but has implications for the palaeogeography of the area (see Chapter 6).

*Confirmed Langhian-age facies*

Langhian-age sediments are some of the most varied in the project area and lateral variation is considerable. Outcrops on the northern margin of the Nahr El-Kabir Valley are a mix of limestones and clastic deposits (foraminiferal wackestones and packstones, with intercalated sparitic grainstones, calcilithites and clastic dominated conglomerates).

Further north, near the Syrian-Turkish border and along the southern margin of the Nahr El-Kabir Valley wackestones predominate, with occasional bioclastic conglomerates.

On the southern margin of the Nahr El-Kabir, wackestones and packstones predominate throughout the confirmed Langhian-age succession (Figures 3.46 to 3.49).



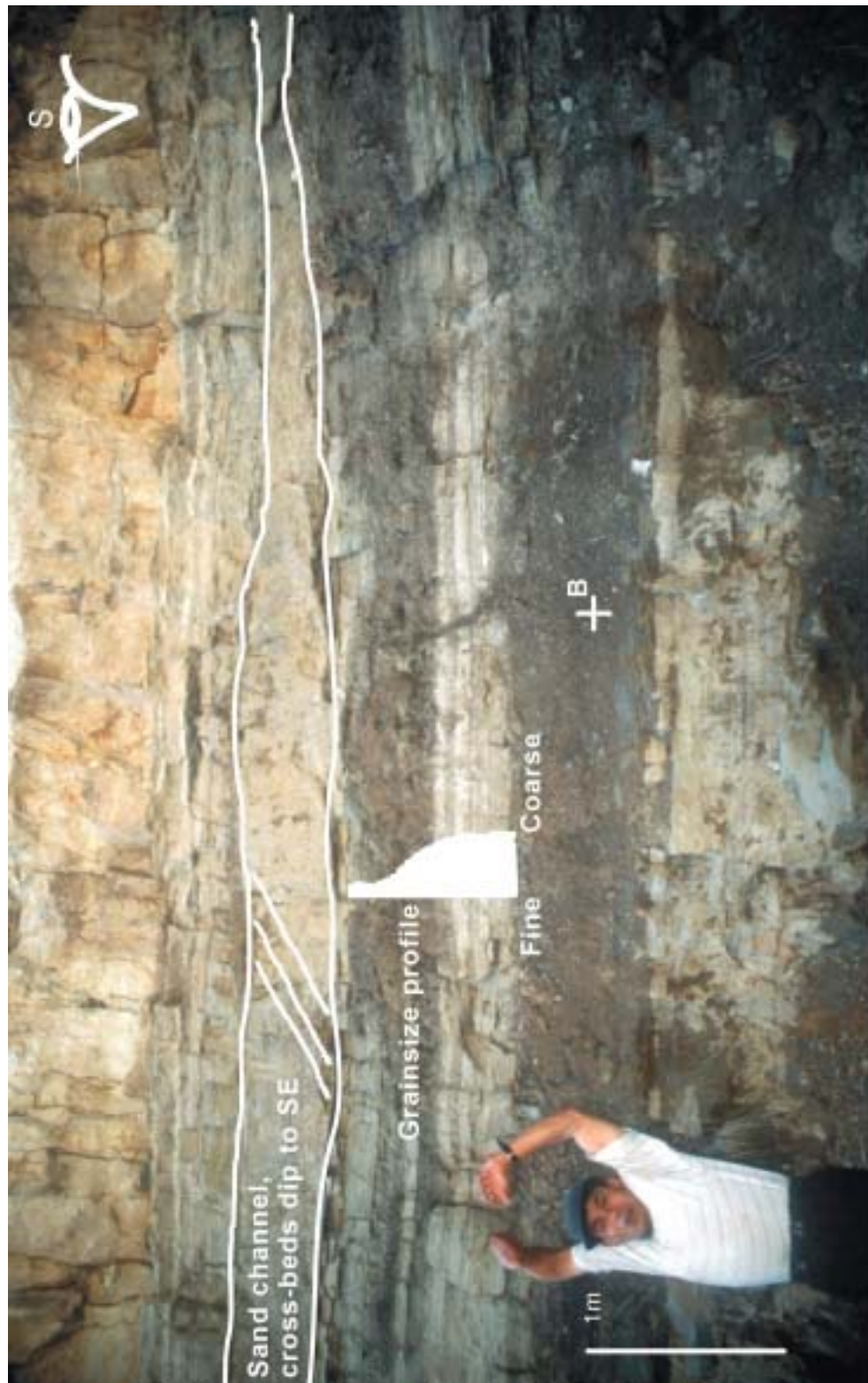


**Figure 3.39** A cross-sectional view perpendicular to the valley margins of the Langhian-Serravallian succession. The majority of the sediments appear to be either ophiolite derived clastic material with marl or fossiliferous marls and limestones. Very few of the beds are mixed, indicative of two source regions for the sediments. The majority of beds also appear truncated or scoured, probably due to mass wasting deposition, slumping of material and sediment bypass to the shelf margin.

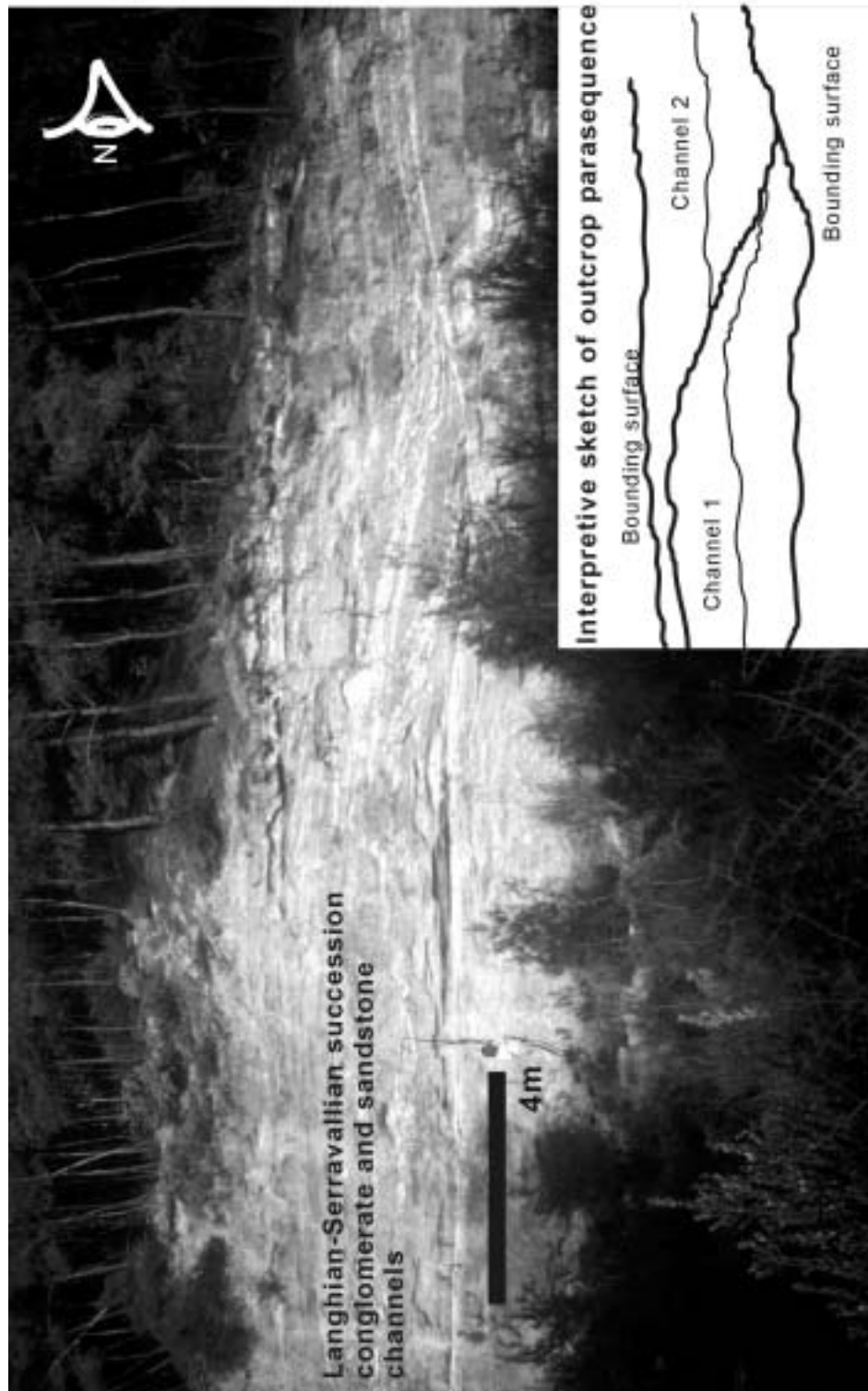


**Figure 3.40** Moving 200m west from the previous figure, the sand channel is replaced by poorly sorted 'debris' flow deposits with coarse blocks of limestone and sandstone in a marly matrix. Channeling is still apparent when looking at the whole outcrop. The thick sandstone bed still caps this part of the succession. Numerous blocks of sandstone contain reworked chert, thin shelled bivalve and plant debris.

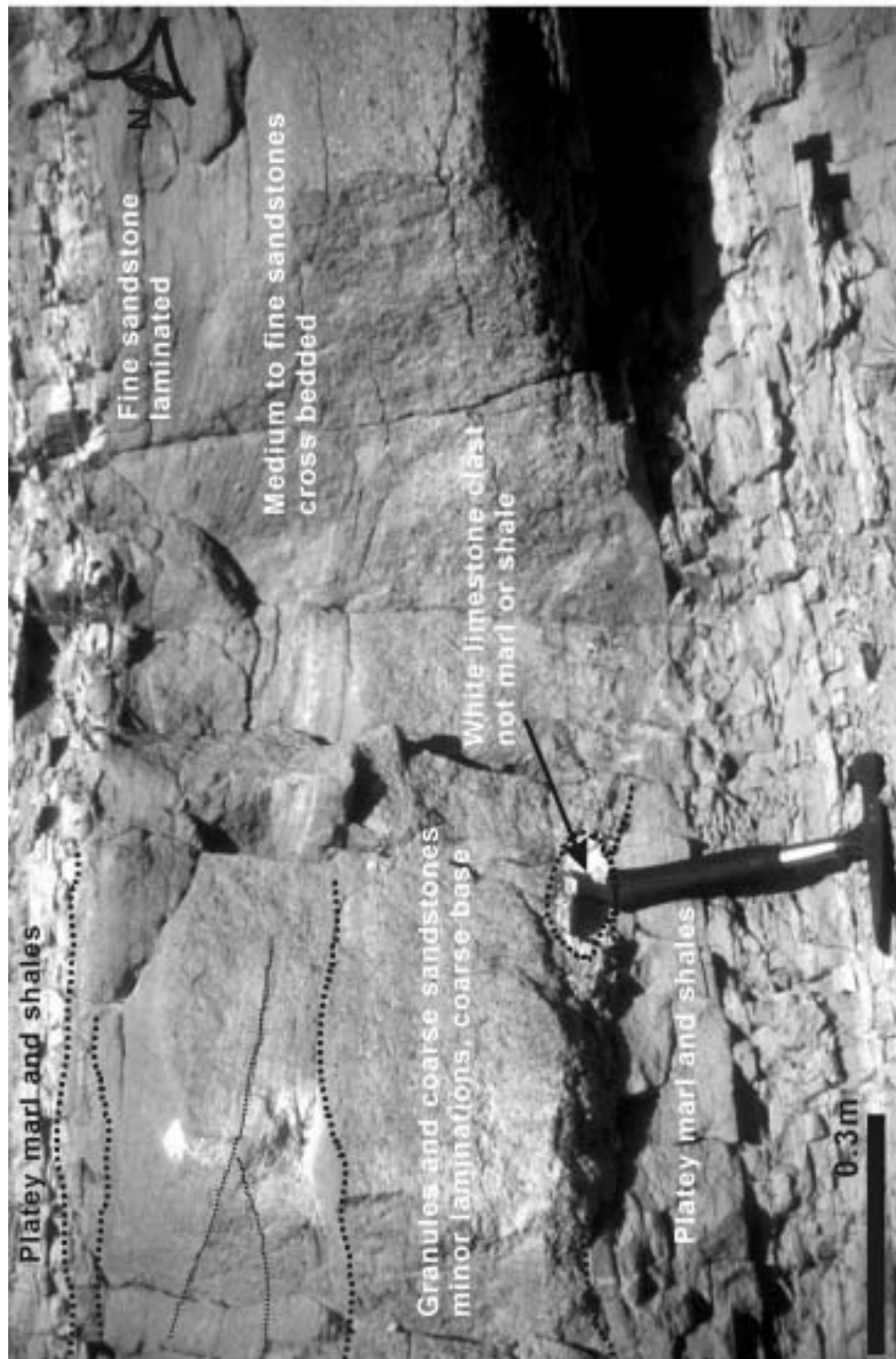




**Figure 3.41** Middle Miocene clastic deposition showing channelised beds with cross-bedding and bed pinch-outs and truncations. The majority of the succession is marl, shale and muds, with an increasing clastic component, before reverting to fine-grained sediments. The sandstone unit varies from fine sand to granule-size grains and is occasionally graded, fining upwards.



**Figure 3.42** A small parasequence of Langhain-Serravallian stacked sandstone (with conglomeratic lag) channels near Khan El-Jouz village. The clastic material is well sorted and relatively free of clays and marls, although the majority of clasts are ophiolite massifs derived. Palaeocurrent indicators are poor as the outcrop is curved, but a NE to SW direction following the current Nahr El-Kabir Valley is likely..

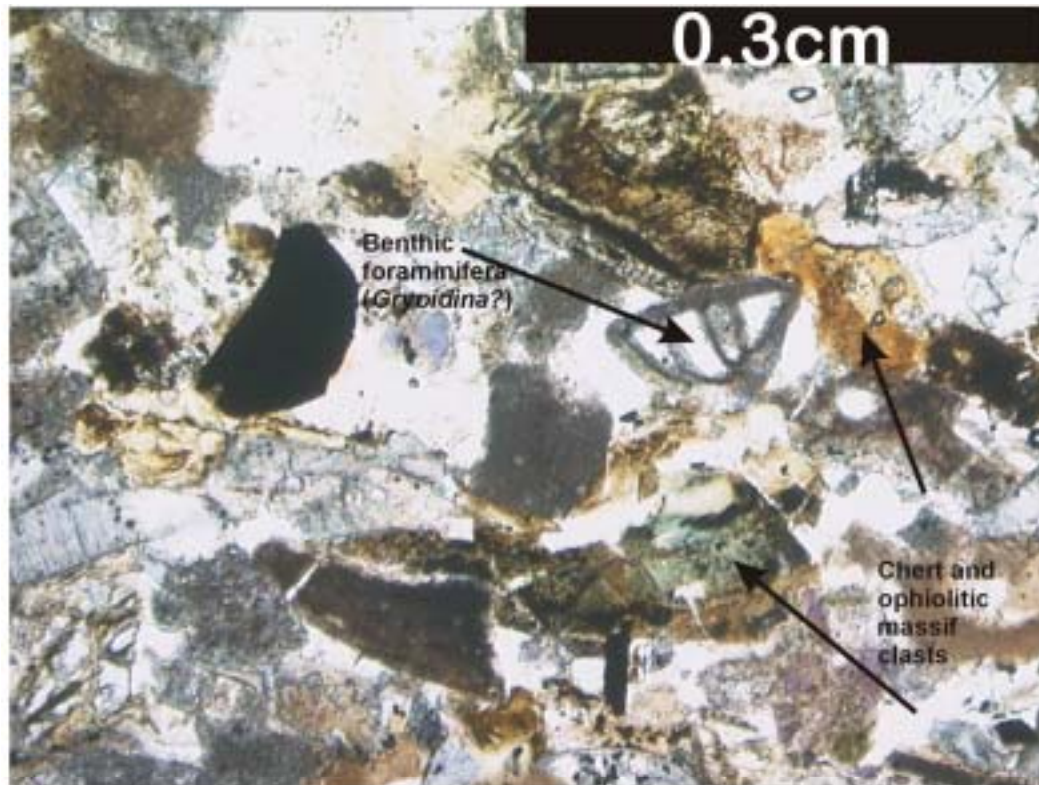


**Figure 3.43** A turbidite bed from the upper part of the Langhian-Serravallian succession. Clasts of Aquitanian chalky limestone are present at the base of beds, probably derived from the northern margin of the Nahr El-Kabir Valley. The sandstone unit is very well sorted and free of mud, clay and marl, showing a high degree of sediment maturity which is unusual. Photograph taken 10km north of Khan El Jouz, near the centre of the valley.

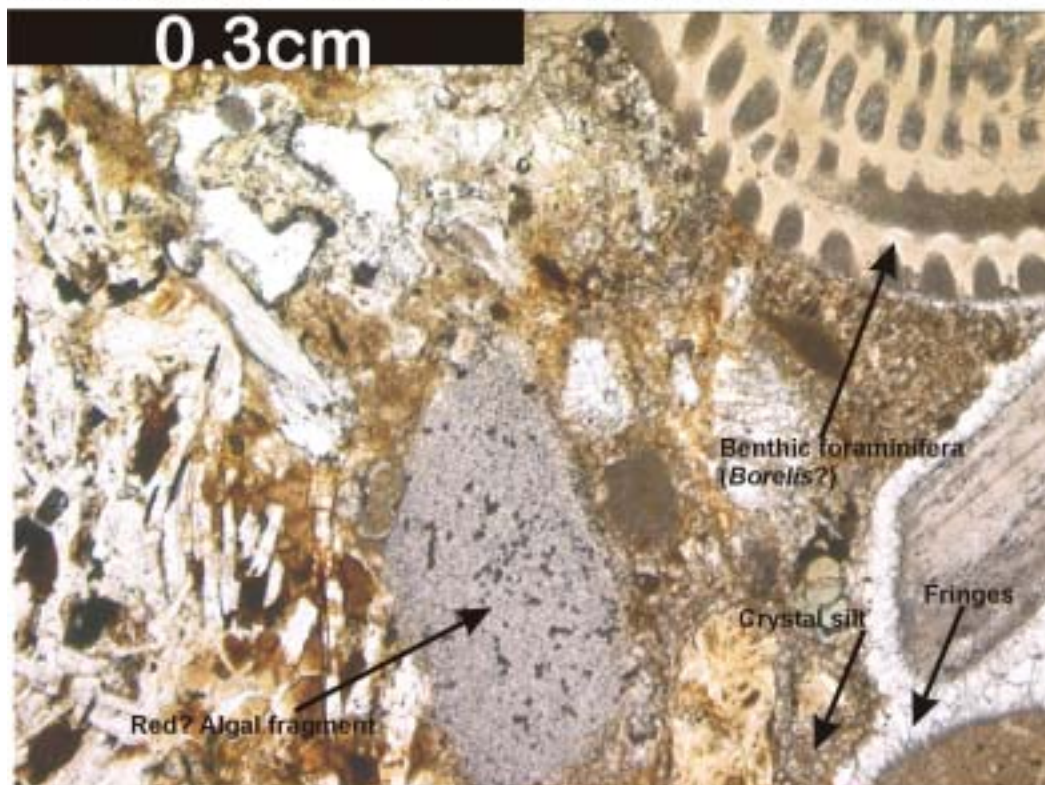


**Figure 3.44** Miocene sandstones and conglomerates close to the Turkish border, 5km east of Bdama Village. Conglomeratic clasts consist of well-rounded chert pebbles and ophiolitic massif material. Such a degree of pebble roundness is not found elsewhere in the Miocene deposits of the Nahr El-Kabir Valley.



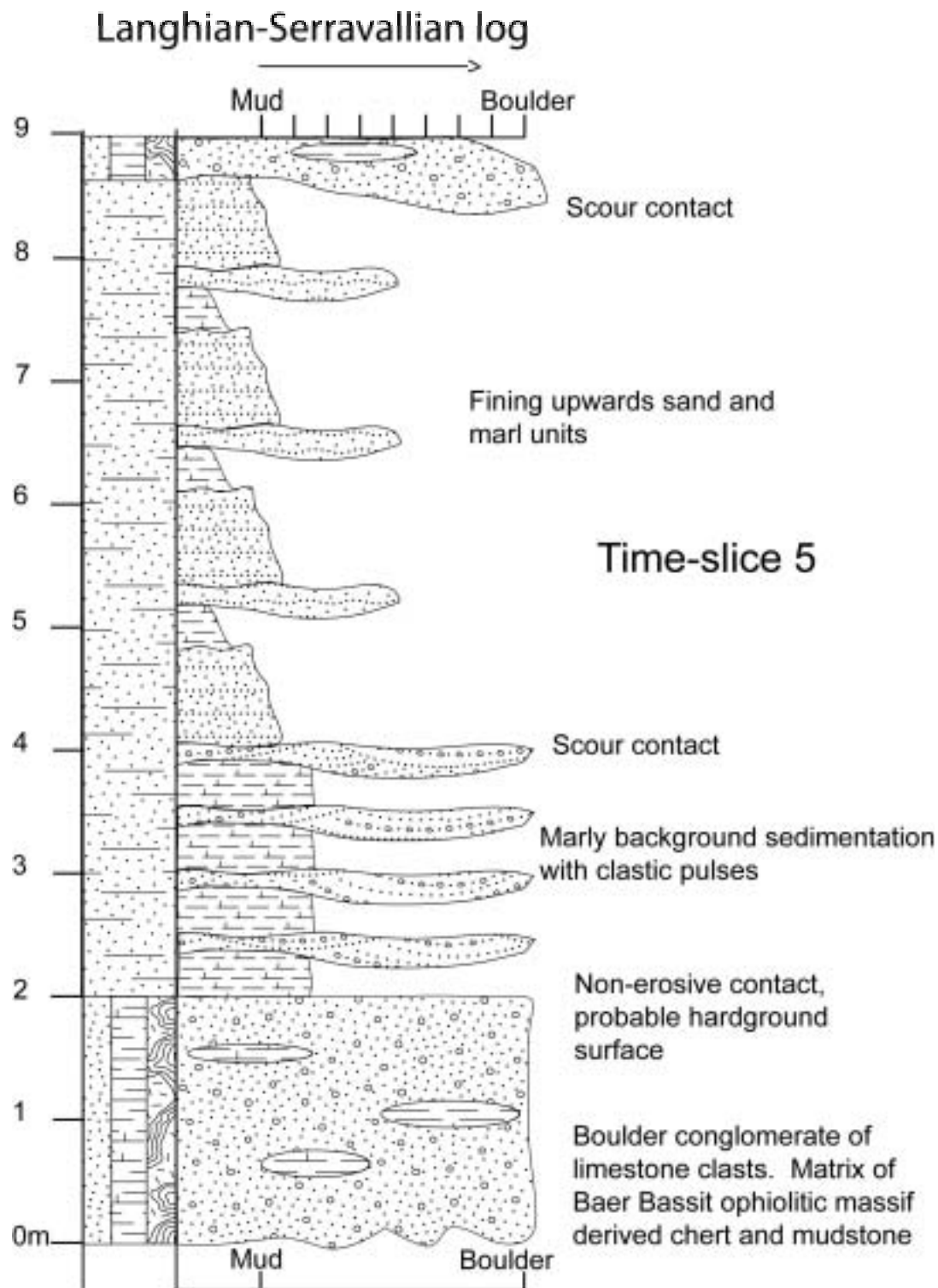


**Figure 3.45 A** Mixed lithic and bioclastic extraclasts of ophiolitic massif provenance (calcilithite). Chert and iron fragments are also common in the sparite matrix. Middle Miocene-age sample from debris-flow facies in the centre of the Nahr El-Kabir Valley. XPL



**B.** This sample was collected 1m above A. Algal fragments and bryozoa are common bioclasts. This packstone is probably recrystallised, from an initial micrite cement to a sparite cement. PPL.

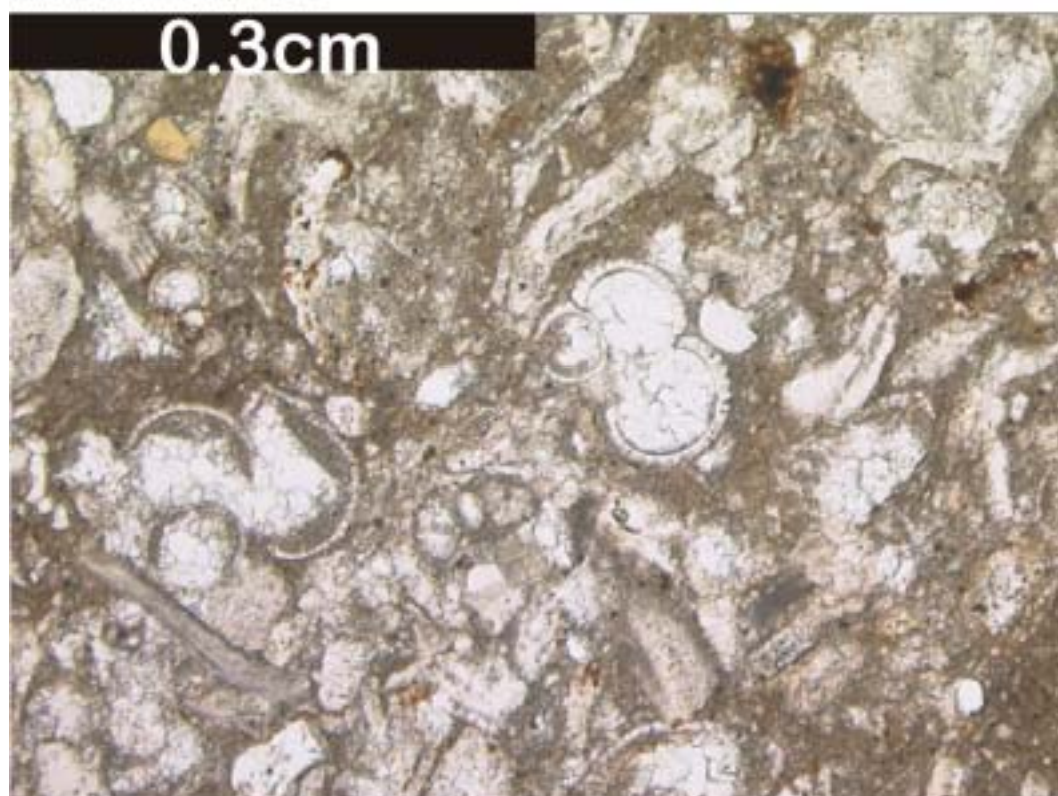




**Figure 3.46** Langhian-Serravallian log from the same locality as Fig 3.39, in the axis of the Nahr El-Kabir Valley, 5km south of Khan El-Jouz Village.



**Figure 3.47 A.** Langhian-age foraminiferal packstone with lithic fragments (mainly chert). Later sparitic infilling of void space. This sample is proximal to the northern margin of the Nahr El-Kabir Valley. XPL.

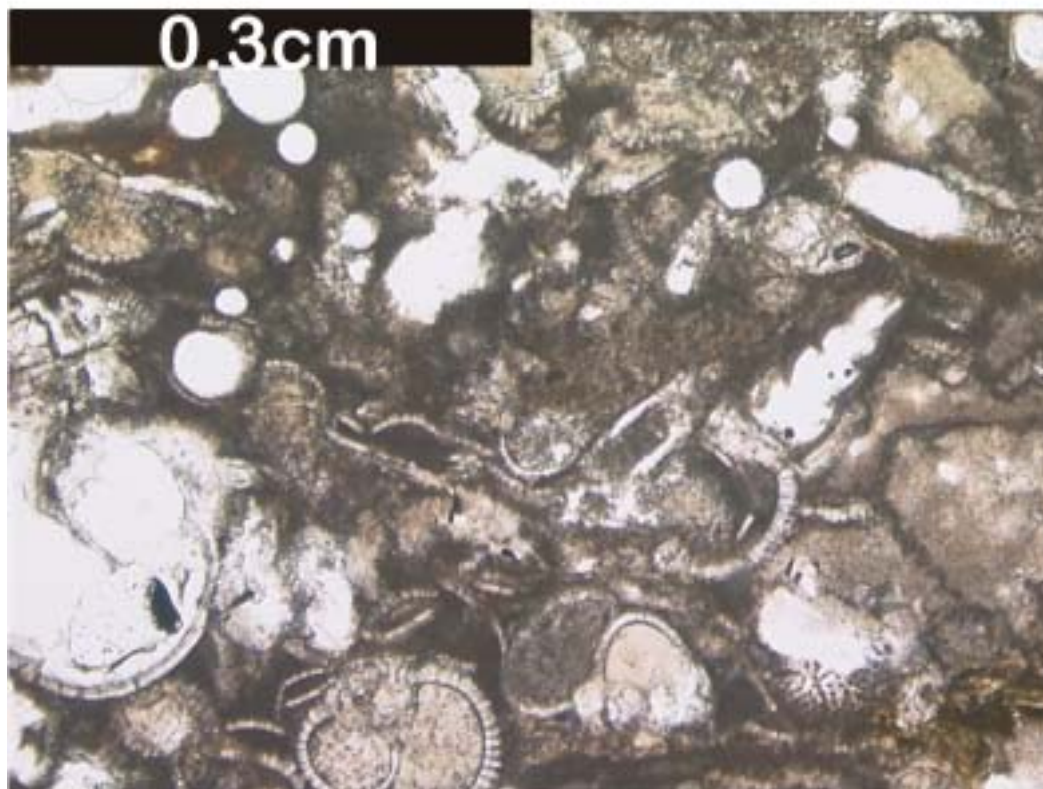


**B.** Similar age and location packstone to sample A. Chert is in much higher abundance in this sample, it is a calcilithite with micritic and bioclastic clasts. PPL.



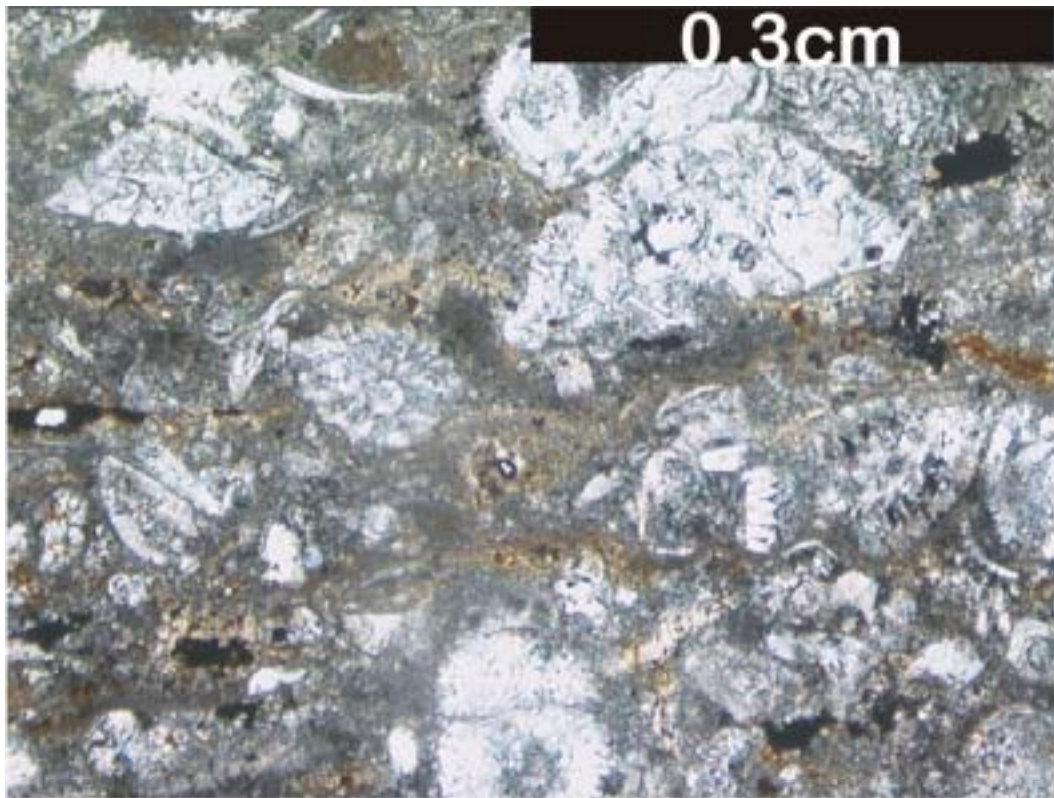


**Figure 3.48 A** Langhian-age foraminiferal wackestone from the northern margin of the Nahr El-Kabir Valley. Bitumen infilling of foraminifera. PPL.

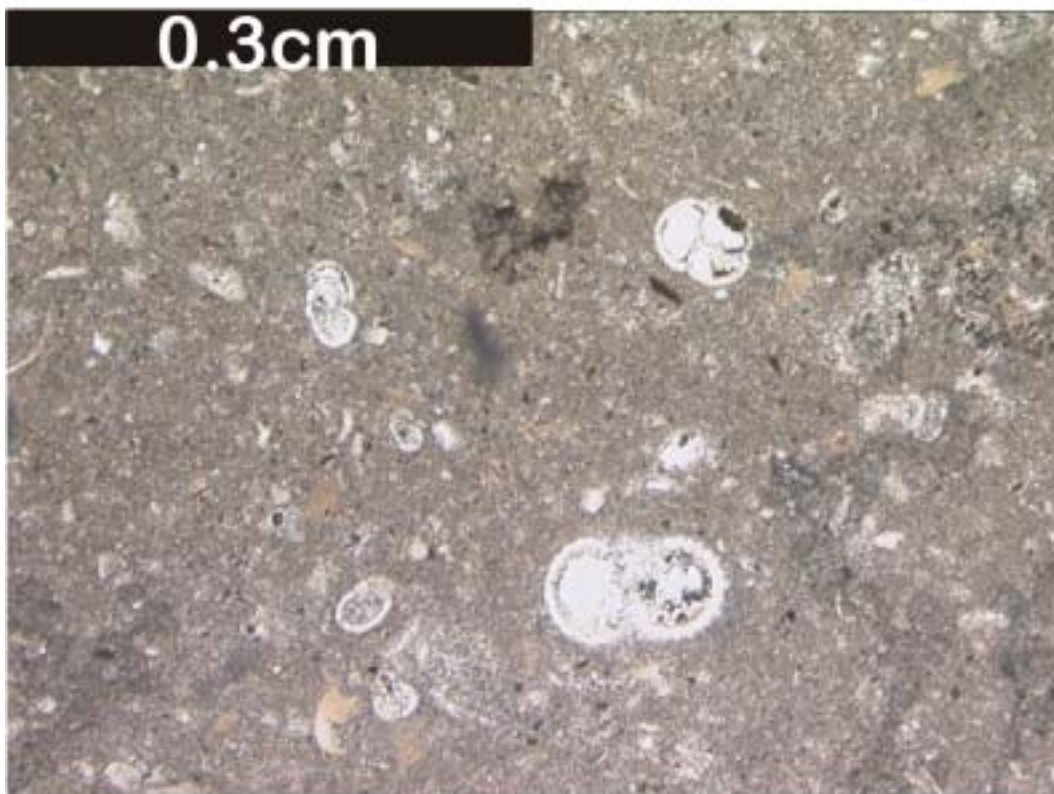


**B** Foraminiferal packstone sample from overlying bed to sample A. Foraminifera and algal material predominate. PPL.





**Figure 3.49 A** Langhian-age sparitic packstones from the center of the Nahr El-Kabir Valley. Recrystallised foraminifera and chert clasts are visible in the micrite matrix. XPL.



**B.** Langhian-age foraminiferal wackestone of contemporaneous age to the above sample, but from the southeastern margin of the Nahr El-Kabir Valley. PPL.

Coarser grained rocks could either not be differentiated or are Serravallian-age. In the centre of the Nahr El-Kabir Valley sparitic packstones are common although difficult to differentiate by age. Many beds appear to be reworked and contain Serravallian-age fauna (as well as Cretaceous, Maastrichtian, Eocene, Oligocene, Early and Middle Miocene, based on nannofossil flora identified by Sylvia Gardin, Table 3.4)

#### *Confirmed Serravallian-age facies*

Samples positively determined as Serravallian age were found on the northern and southern margins and in the centre of the Nahr El-Kabir Valley.

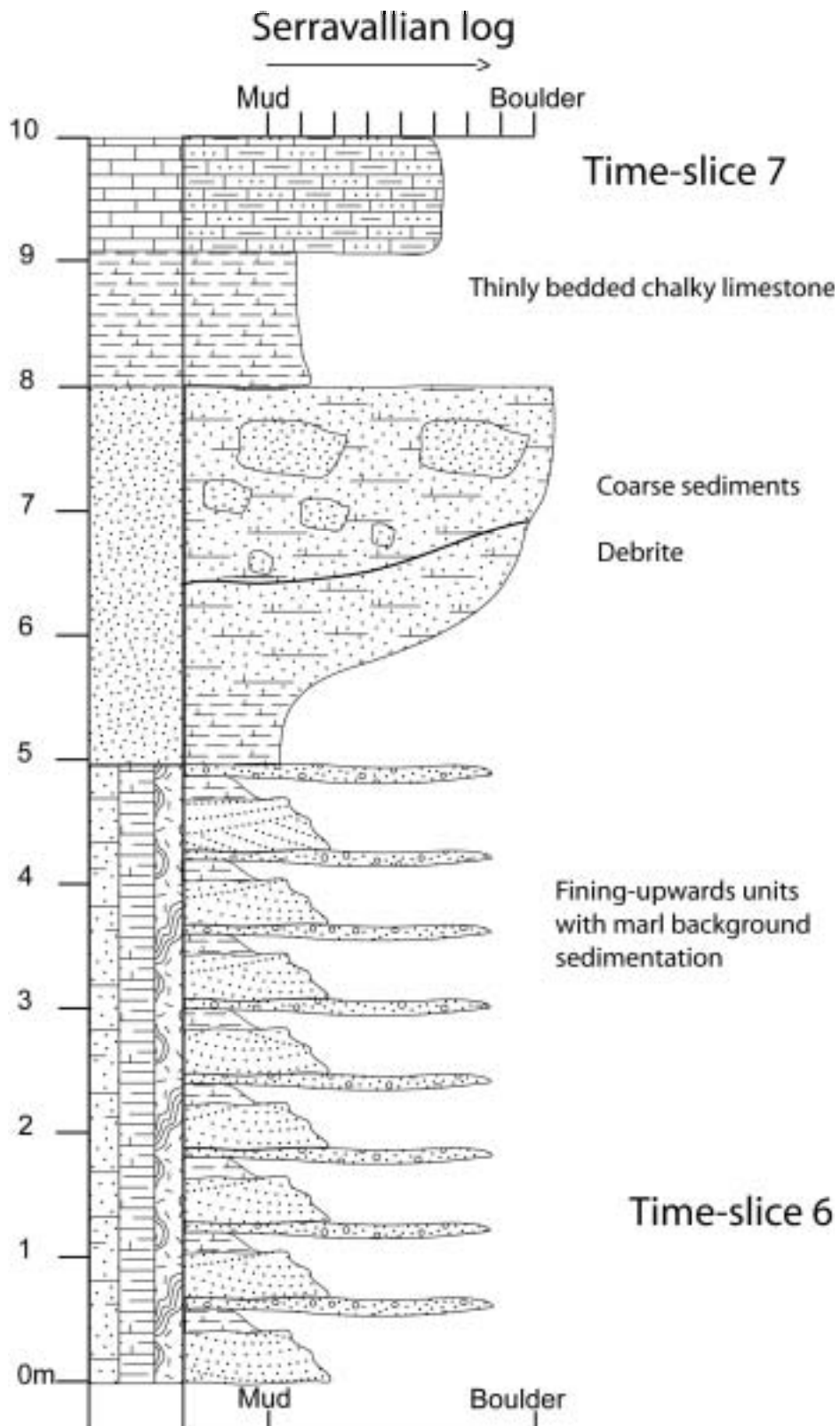
Serravallian-age samples were found in abundance on the southern margin of the valley and are a mix of wackestones, packstones and grainstones, many containing clasts of other limestones (Figures 3.50 and 3.51). Reef building bioclasts are common within these sedimentary rocks, but are rarely found as carbonate bound clasts. Conglomerates are common, inferring that mass wasting was the predominant mechanism of deposition.

In the centre of the Nahr El-Kabir Valley, Serravallian-age sediments consist of material from both the north and south margin. Limestones dominate the upper part of the succession as clastic input (Baer Bassit Massif-derived) was reduced from the amounts deposited throughout the Langhian. Individual beds show clear grading of coarse sediments (turbidite beds compared to debrites, Figures 3.32 and 3.43, Leeder, 1999) and poorly developed palaeocurrent indicators show transport direction out of the valley towards the current coastline.

On the northern margin of the valley, the localised conglomeratic beds near the top of the succession could not be dated. Only the thin, laterally persistent chalky limestones that cap the succession were dated as Serravallian.

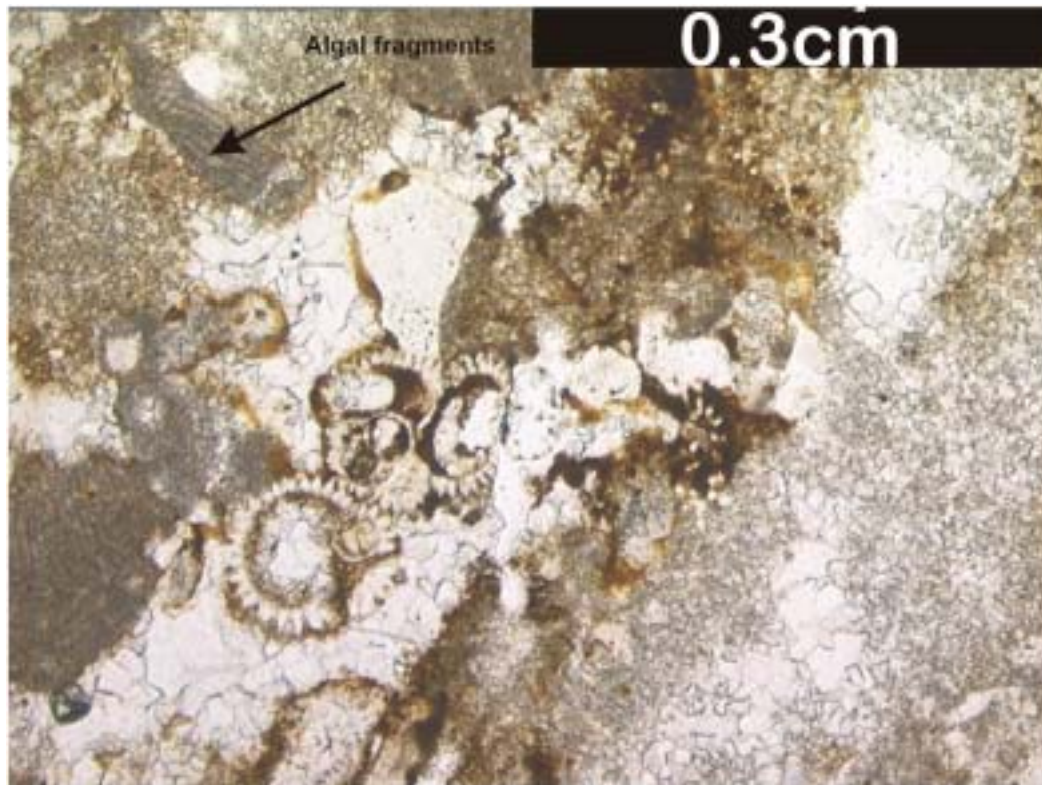
#### *Middle Miocene-age facies*

The majority of samples collected, could not be reliably differentiated between Langhian and Serravallian ages, especially within the centre of the Nahr El-Kabir Valley. This may simply be due to a lack of diagnostic fauna or poorly preserved samples, although care was taken to recover prime samples. Time-slice 7 is regressive (see below), and it is a possibility that some reworking of the sediments occurred at this time.

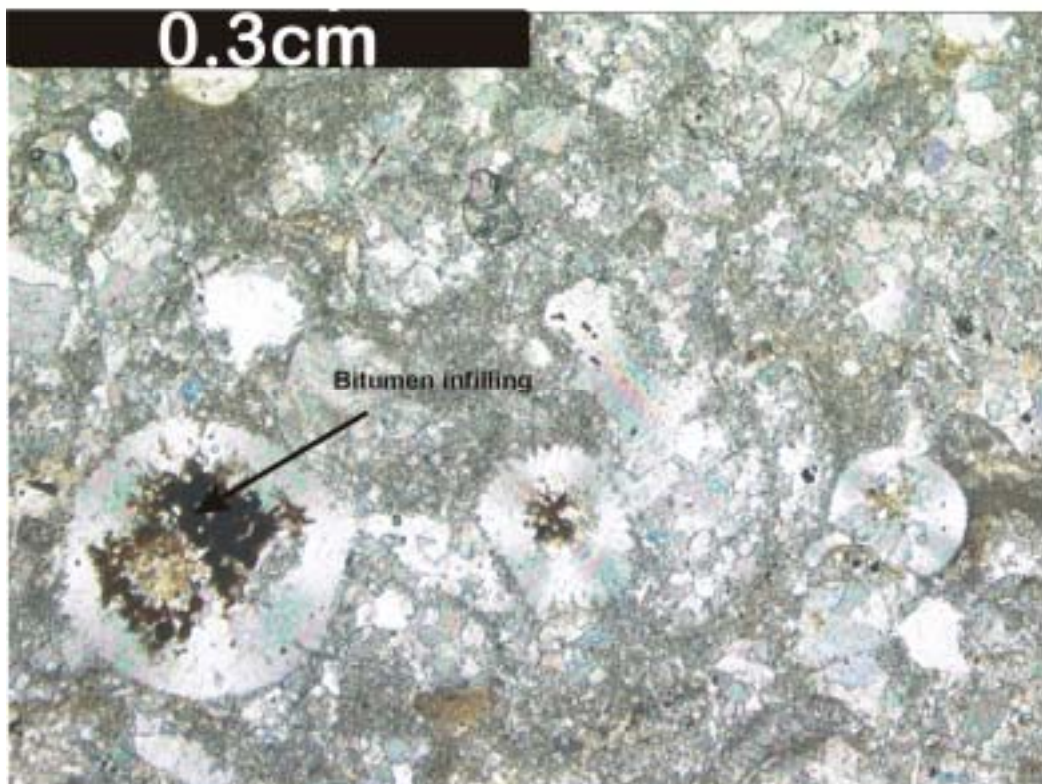


**Figure 3.50** Serravallian log, from 5km northeast of Bahlouiyeh Village. 150m stratigraphically higher than Fig 3.46.





**Figure 3.51 A.** Sparry grainstone with clasts of older limestone (micrite and foraminifera) and algal fragments. Southern margin of the Nahr El-Kabir Valley. Late Serravallian. PPL.



**B.** Late Serravallian-age packstone, located 5km north of the above sample. This sample shows bitumen infilling of moldic porosity and solution cavity fill recrystallisation of foraminifera XPL



## Summary of time-slice 6

As previously stated, the Langhian-Serravallian is the most heterogeneous of the time-slices observed within the project area. The key findings are that shelfal (inner?) depth water existed within the valley and much shallower water environments on the margins depositing coarse, proximal debris flows into the centre of the valley (see Chapters 4 and 6). The valley has faulting on both margins (a graben) and the northern margin was active throughout, but especially during the Langhian. The southern margin has numerous faults (not previously mapped, see Chapter 4), which were also active throughout, but especially during the Serravallian.

## ***Time-slice 7, Serravallian-Tortonian regressive limestones***

The uppermost exposures of Serravallian rocks were dated by Marcel BouDagher-Fadel as Late Serravallian-age. These rocks were found only in small outcrops in the centre of the Nahr El-Kabir Valley, near Bahlouliyah Village. They comprise white, thinly, planar bedded, foraminiferal wackestones with planktonic and fragments of benthic foraminifera.

In the fieldwork area, no confirmed samples of Tortonian age were recovered. Thinly bedded, chalky limestones were found directly below Messinian gypsiferous facies. However, Marcel BouDagher-Fadel dated a sample collected from 10m below this contact as Late Serravallian. Ponikarov et al. (1963, 1966, 1967) and Krasheninnikov (1971, 1994) indicated that Tortonian-age facies do exist in the Nahr El-Kabir Valley, but do not state where, only that Tortonian fauna exist in their undifferentiated Miocene unit. This could not be confirmed by the limited biostratigraphic studies undertaken during this work as no positive Tortonian biomarkers were found. The previous work (Jaquet, 1933), indicated that large *Conus* gastropods were the diagnostic marker fossils. Fragments of these gastropods were found throughout the Langhian-Serravallian strata during this study, but only with foraminiferal assemblages of older ages. If Tortonian-age rocks exist, then they can only be presumed to be the thinly bedded to laminated, marly limestones deposited above the sample location. This would restrict the unit solely to the Nahr El-Kabir Valley axis.

*Preliminary interpretation of Serravallian-Tortonian-age limestones*

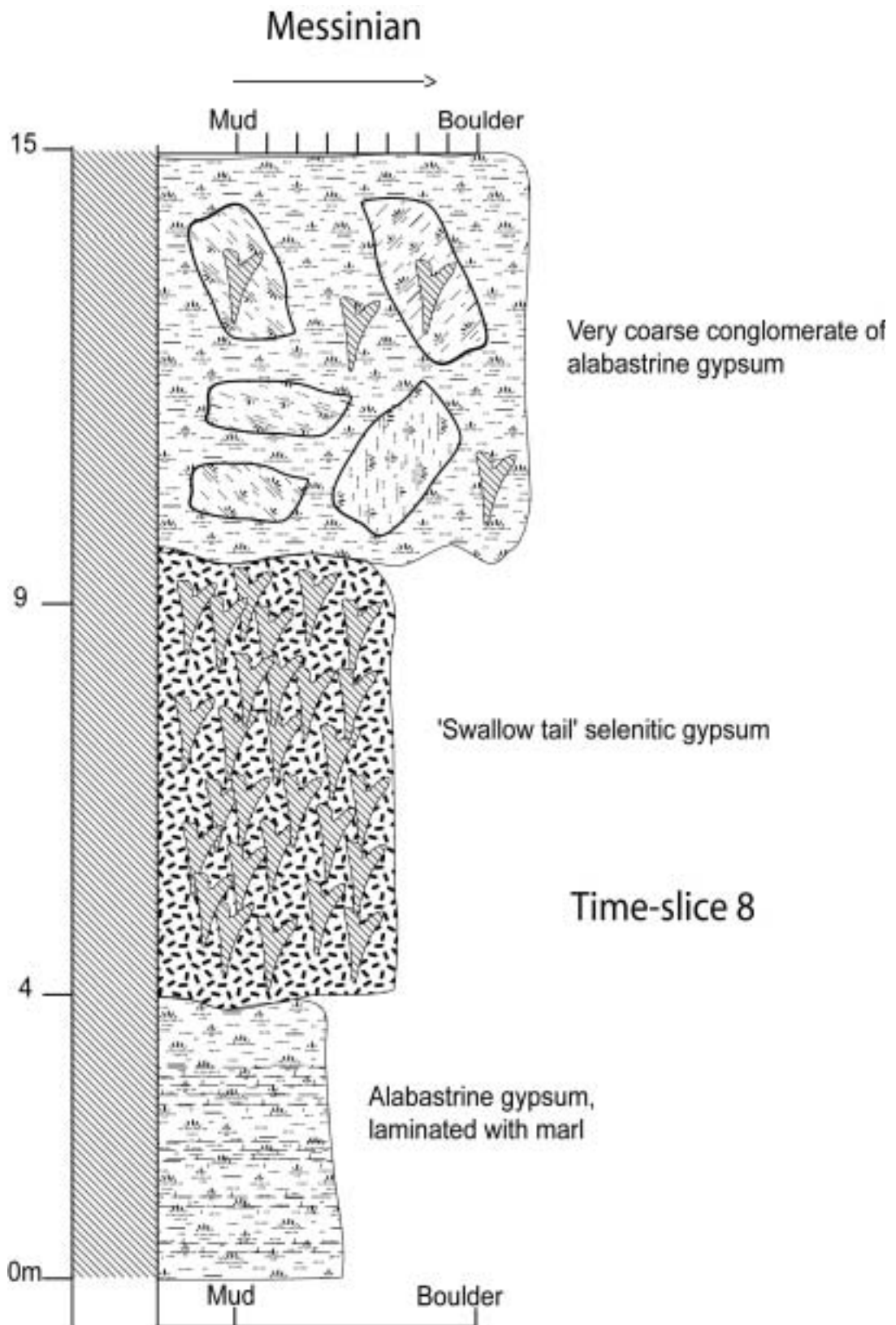
There is very little field evidence for substantial deposition in the area throughout Late Serravallian and Tortonian time. From the limited field and microfossil evidence, it is suggested here that this time-slice represents a change from neritic conditions to either sub-aerial (erosive) or lagoonal conditions found during the Messinian (regression, see Chapter 6).

***Time-slice 8, Messinian evaporites***

The Messinian-age evaporites crop out only locally within the axis of the Nahr El-Kabir Valley and the lithologies are consistent with Messinian-age sedimentary rocks in the Eastern Mediterranean (i.e. Cyprus and Turkey). They consist of gypsiferous facies and marls. The gypsum is found in two forms; fine-grained, bedded crystals and twinned crystals. Both crystal forms are intercalated with marl. The total thickness is variable but normally less than 100m and increases down-dip towards the current coastline.

The lower contact with the Middle Miocene succession is not well exposed and could not be accurately identified. As previously stated, the Late Serravallian is the last confirmed succession prior to Messinian deposition (see time-slice 7). The upper contact with the base of the Pliocene is obvious in the field and commences with light grey foraminiferal marl containing gypsum rip-up clasts. Messinian strata are poor in foraminifera, probably due to the high salinity present with evaporation. Gastropods however, were reported to have thrived and were successfully used for stratigraphic purposes by Jaquet (1933). This study could not confirm this and relied on the mapping by Ponikarov et al. (1963) and obvious sedimentary features to interpret Messinian-age outcrops.

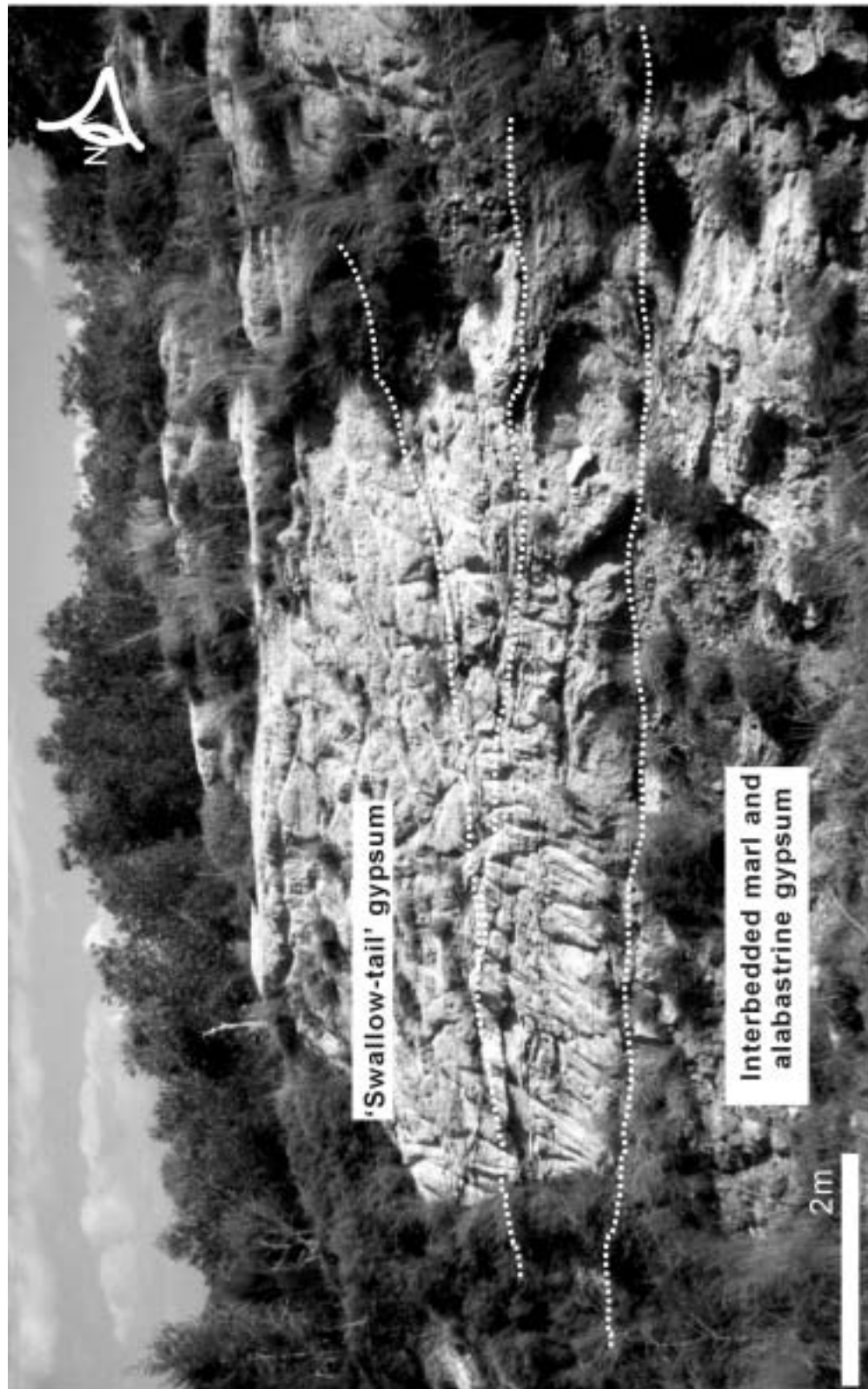
The two differing gypsum crystal types found within the succession are rarely found co-existing (although see below). The lowermost 30m of the Messinian succession is typically fine-grained alabastrine gypsum (Figure 3.52), intercalated with minor quantities of marl and mudstone (Figure 3.53). The alabastrine gypsum is locally laterally replaced and overlain by twinned 'swallow-tail', selenitic gypsum, precipitated displacively within background marly layers (Figure 3.54). Selenitic gypsum forms very thick beds (2-3m), that often cross-cut previous layers and are finally overlain by 5m of marl that caps the succession.



**Figure 3.52** Messinian log drawn from an outcrop near Bahloulieh Village, on the Aleppo-Latakia highway.



**Figure 3.53** Well laminated alabastrine gypsum from a disused quarry in the centre of the Nahr El-Kabir Valley (15km south of Khan El-Jouz Village). Very little argillaceous material is present within the gypsum and there is no sign of tectonic disturbance syn or post-deposition, in contrast to areas to the west.



**Figure 3.54** 'Swallow-tail' gypsum outcrop in a railway cutting 5km east of Bahloulieh village. The crystals appear to have grown in clumps, about a small nuclei, with minor infilling by muddy sediments. Uneven bedding appears draped rather than disturbed by structural movements.



**Figure 3.55** Intra or post -Messinian deformation was only observed at this one locality 25km north of Latakia on the Latakia-Aleppo highway. Horizontally bedded selenite ('swallow-tail' gypsum) is overlain by massive blocks of selenite, interbedded and overlain by yellow clays (Messinian or even possibly Pliocene-age). Messinian debris flows appear elsewhere in the Mediterranean region e.g. Polis Graben, Cyprus, but are not seen elsewhere in the Nahr El-Kabir Valley.

Throughout most of the succession, there is little sign of any syn-depositional disturbance during the Messinian; although there is a later stage of pervasive fracturing and faulting seen at outcrop. At one locality, however, there is evidence of slumped beds and a mega-conglomerate of selenitic and alabastrine gypsum blocks (Figure 3.55). These coarse clasts are often 'welded' together, perhaps due to groundwater solution. Fragments of selenitic gypsum are intercalated in the overlying, planar, thinly bedded wackestones.

#### *Preliminary interpretation of Messinian facies*

The Messinian-age gypsum in the Mediterranean reflects the closed nature of the basin at this time and intense evaporation ("Messinian salinity crisis", Hsü et al. 1973, 1977). Therefore, this region of Syria is likely to have been linked to the repeated episodes of Mediterranean Sea desiccation rather than being in a lacustrine setting as suggested by Ponikarov et al. (1966).

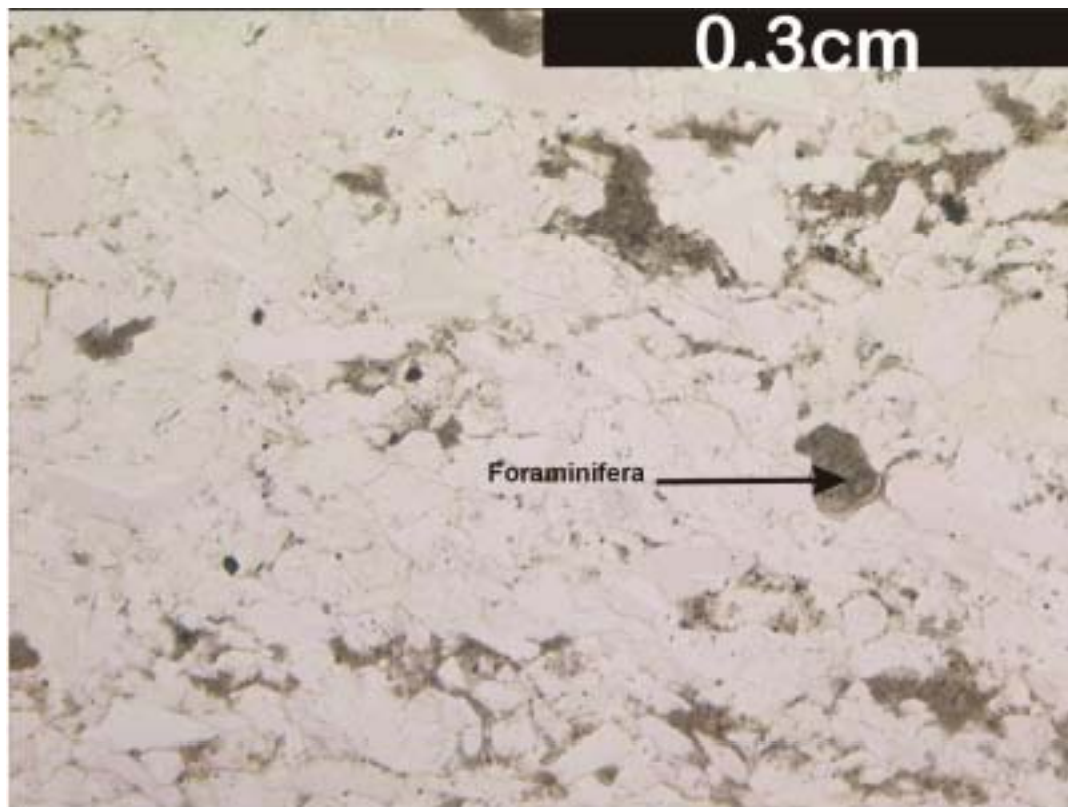
The initial Messinian facies deposited was alabastrine gypsum and marl, with rapidly precipitating small crystals (Figure 3.56). Alabastrine gypsum typically requires high concentrations of brine (300-325 g/L, Leeder, 1999) and these concentrations could be found in evaporitic settings. A lagoon or small barred basin is suggested as the depositional setting. The overlying selenitic crystals typically need lower concentrations of brine to precipitate (230-300 g/L, Leeder, 1999) and so may be closer to the margin of such a small barred basin or formed when water influx increased.

The uppermost sections of Messinian show tectonic instability with conglomerates and debris flows. Syn-depositional down cutting of earlier selenitic beds may indicate the start of this instability. The top of the succession appears to return to more normal salinity and a more stable tectonic regime, with the deposition of planar bedded, foraminiferal wackestones, although these could represent the lowermost Pliocene.

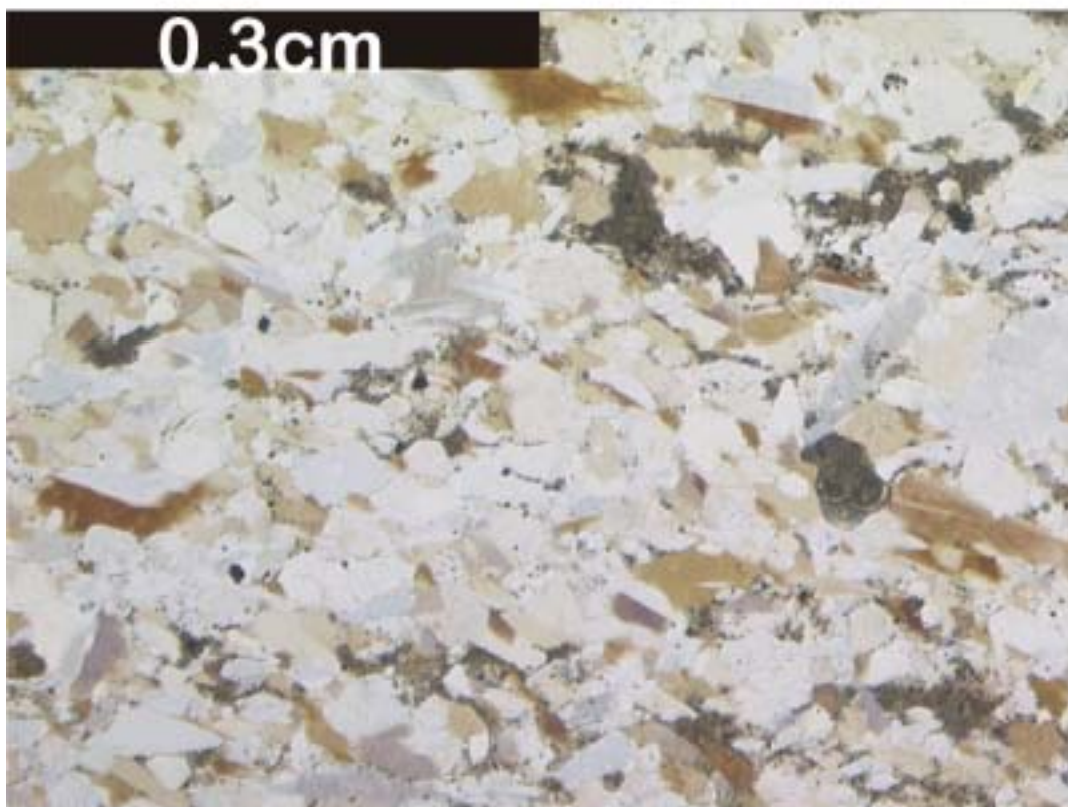
#### ***Time-slice 9, Pliocene transgressive marls***

The Early to Middle Pliocene succession forms the low-lying, undulating hills near the mouth of the Nahr El-Kabir Valley (Figure 3.57). The time-slice consists of greater than 200m thickness of grey marls and occasional thin sandstones (Figure 3.58). Pliocene-age facies are also found further south near Banyas town, intercalated with basaltic rocks (see time-slice 10), on the Baer Bassit Massif and in the Ghab Valley.

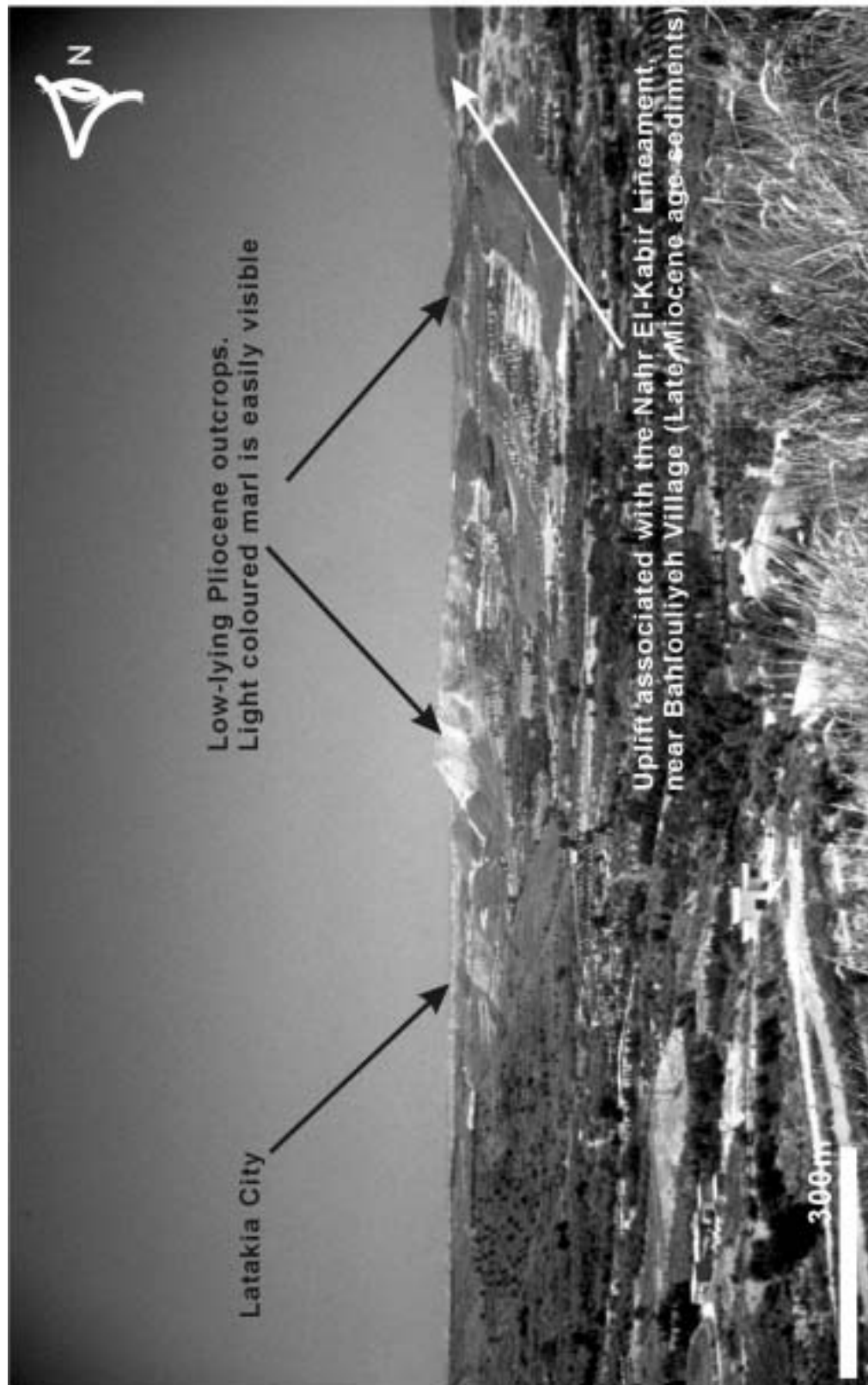




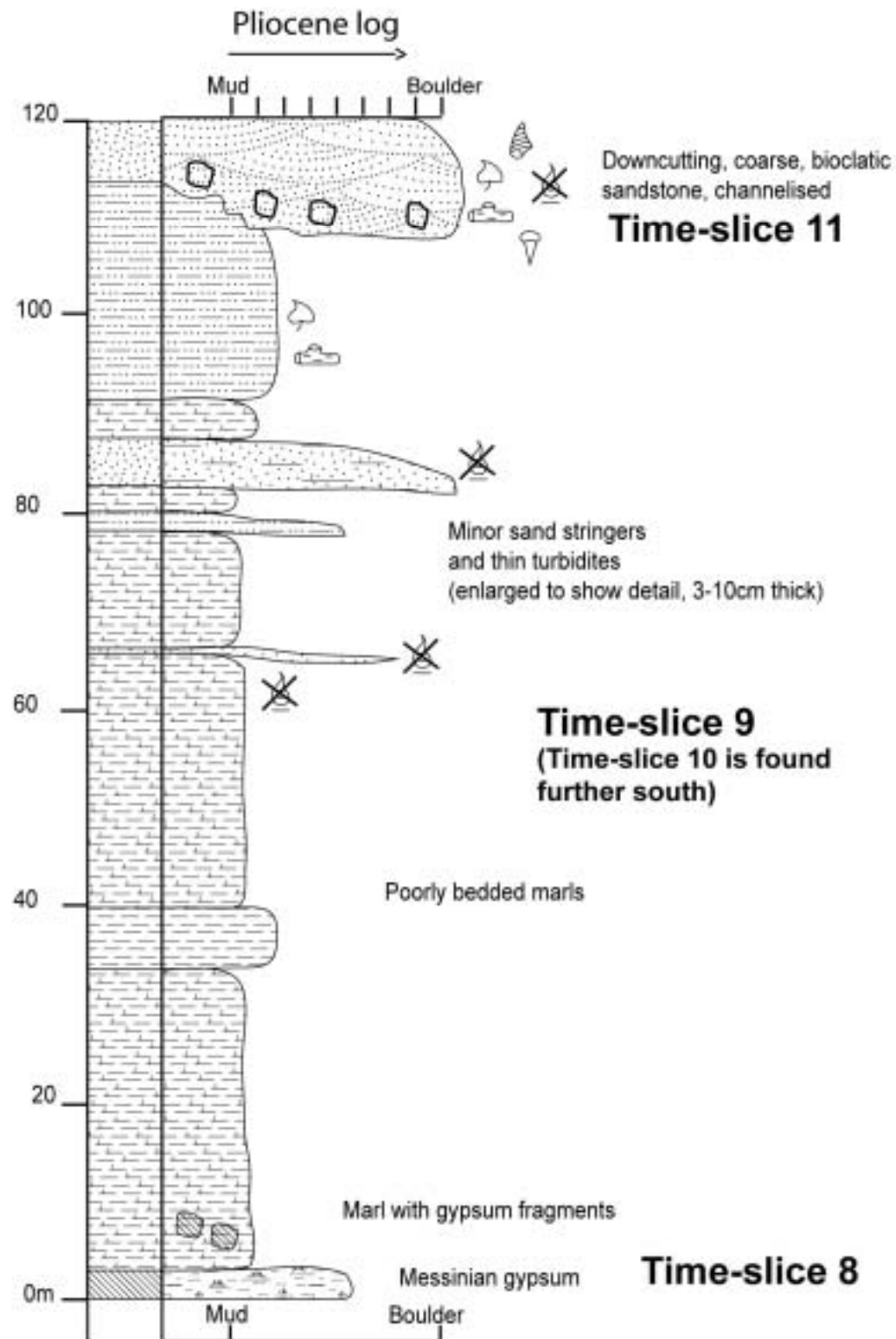
**Figure 3.56 A** Messinian-age alabastrine gypsum, intercalated with mud. This sample is from Al-Haffeh Town, in the centre of the Nahr El-Kabir Valley. PPL.



**B.** The same sample in XPL. The very fine gypsum crystals are visible in layers.



**Figure 3.57** A view west towards the coastline from 25km due east of Latakia City, emphasising the low topography associated with the Pliocene succession. The foreground is Lower Pliocene, with uppermost Lower Pliocene at the highest hilltops. Uplifted areas to the north show the margin of the Baer-Bassit Ophiolitic Massif and the Nahr El-Kabir lineament (see Chapter 5).



**Figure 3.58** Sedimentary log of the Pliocene facies seen near Fadreh, 15km NE of Latakia.

*Nahr El-Kabir Valley*

The main Pliocene facies is planar laminated, intercalated marl and shales with thin sandstone beds. The marls are foraminiferal and gastropod-rich wackestones and packstones. Micrite intraclasts are common throughout the succession and sparite cement infilling of pore space is common.

Near the base of the succession, gypsum clasts of alabastrine and selenite are common, from the underlying Messinian succession. Bioclastic material increases towards the top of the succession and is characterised by *Dentalium* scaphopods, *Turritella* and *Nerinea* gastropods, *Orbulina universa* planktonic foraminifera, fish teeth and fish scales (Figures 3.59 and 3.60). Laminations of carbonate sands and bioclastic debris commenced from the middle of the succession, increasing towards the upper part of the succession. These coarser beds are commonly graded (fining-upwards).

At the southern margin of the Nahr El-Kabir Valley, steep topography exposes the middle section of the Pliocene time-slice. Marls and limestones predominate (wackestones) and the thin beds appear to be lenticular, truncating against adjacent channeled beds (Figure 3.61). Very little carbonate sand is present.

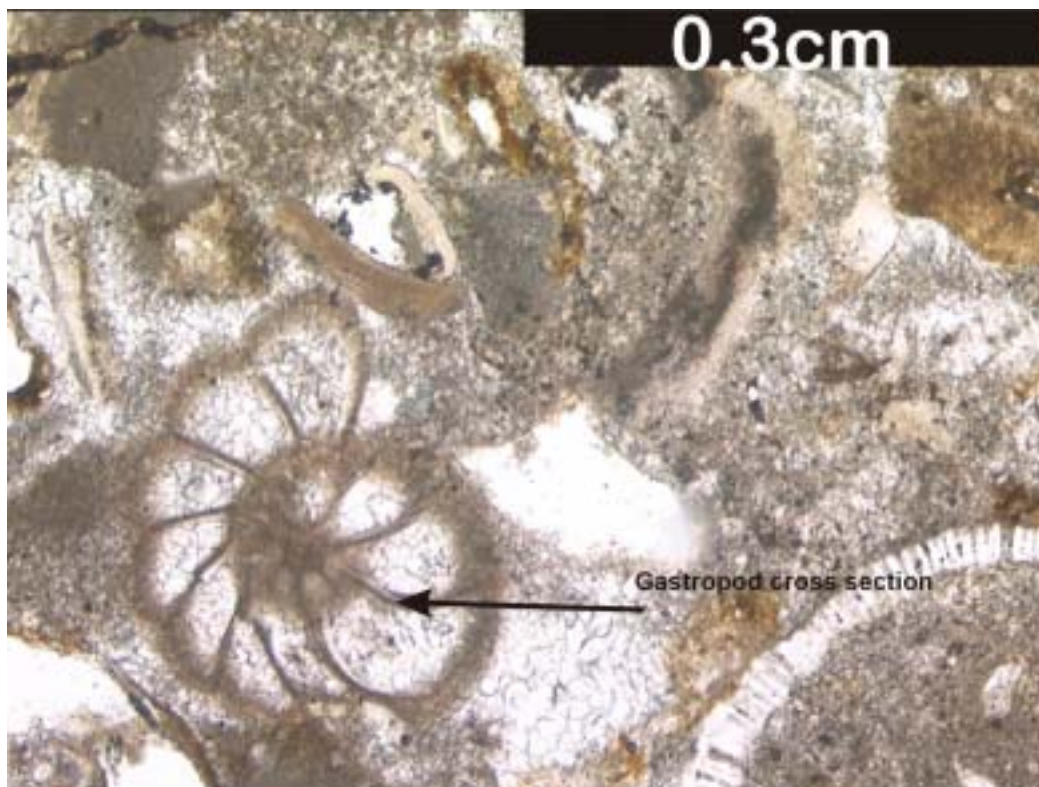
*Ghab Valley*

To the north of the Ghab valley, the most of the marine Pliocene-age facies are planar laminated, foraminiferal packstones (Figures 3.60). These rocks also contain a high proportion of detrital chert (unknown provenance) and bioclastic material. The provenance of the chert is unclear, although it may be from the Baer Bassit or Kizil Dağ Ophiolite in Turkey (see Chapter 5).

*Preliminary interpretation of Pliocene-age marls*

The Pliocene time-slice indicates a return to fully marine conditions after the Messinian and an increase to outer shelf depth. The increase in bioclastic material, macrofossils and algae throughout the succession indicates a shallowing of water depth and minor clastic beds may indicate turbidity currents. Bedding truncation in limestones on the southern margin is indicative of a shallower carbonate setting and downslope channeling of material into the basin. Marcel BouDagher-Fadel inferred an inner shelf water depth for the uppermost samples and an Early Pliocene age for the fauna.

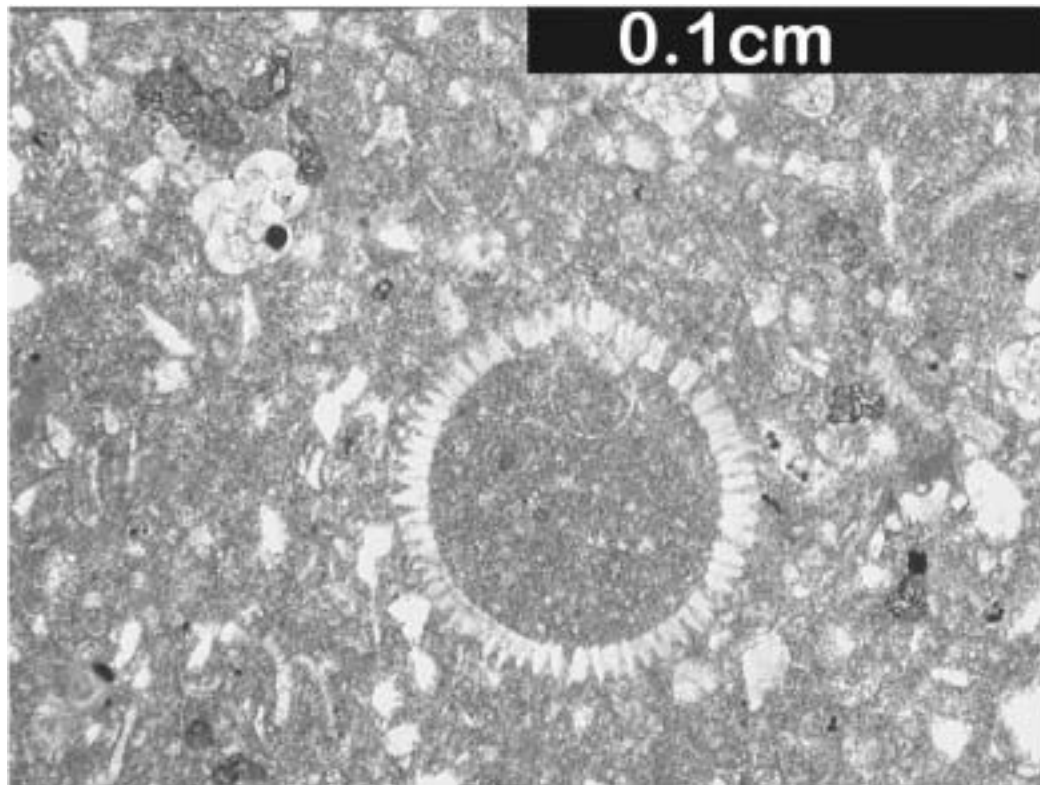




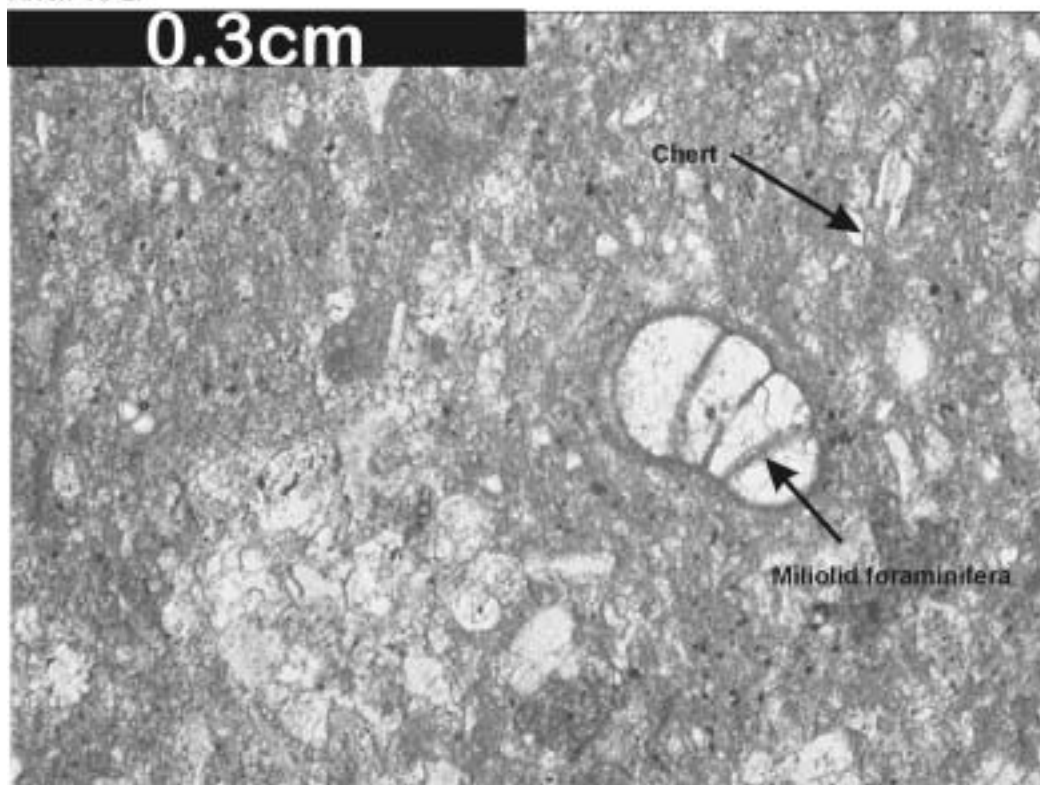
**Figure 3.59 A.** Gastropod shells and foraminiferal fragments in a micrite and sparite matrix. Numerous intraclasts. Packstone from Nahr El-Kabir Valley. Early Pliocene age. XPL.



**B.** Prominent gastropod and recrystallised intraclasts forming grainstone facies. Early Pliocene age. Uppermost unit of Pliocene-age found near Al-Haffeh town. PPL.

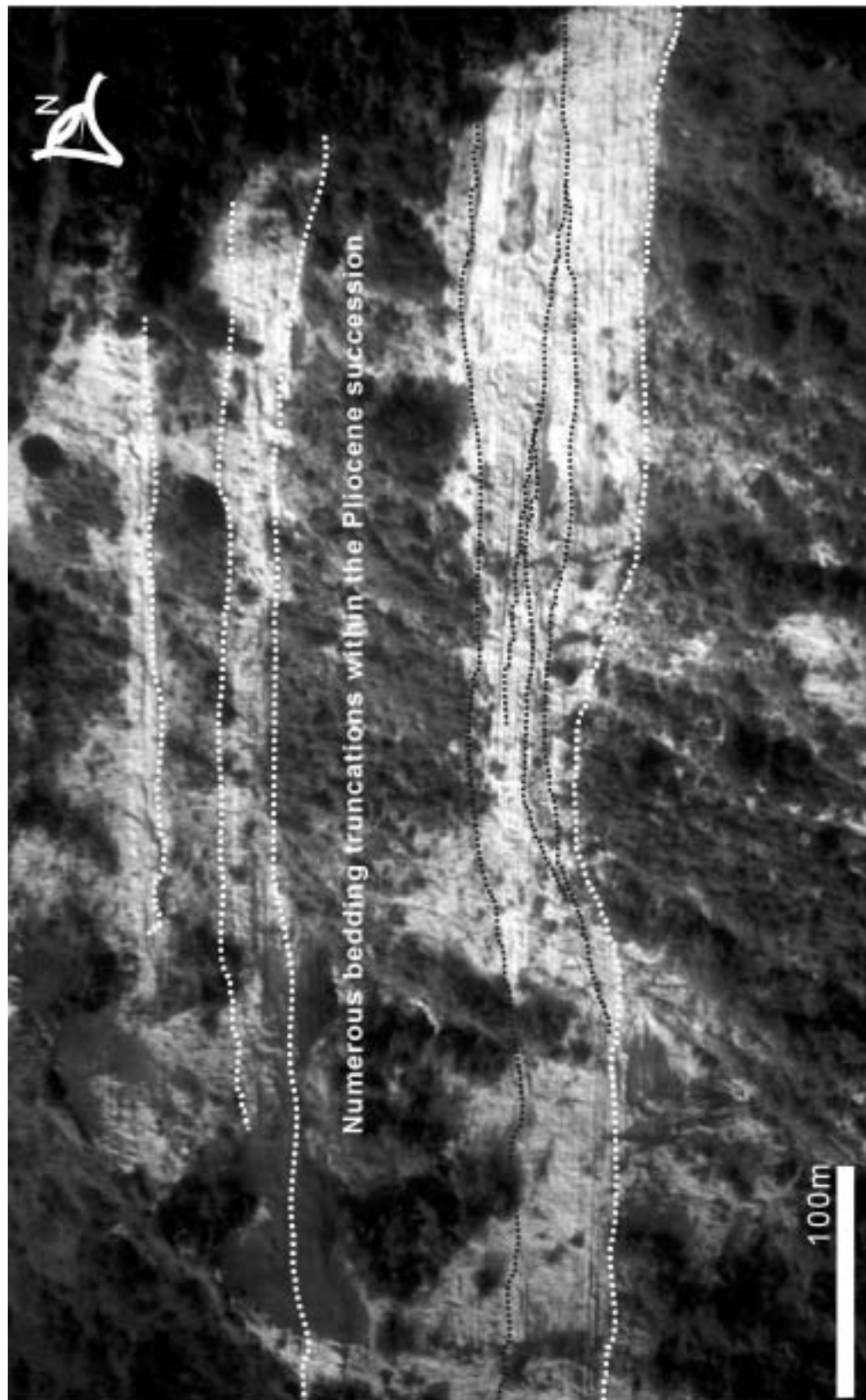


**Figure 3.60 A.** Early Pliocene age packstone, containing *Orbulina universa*. Angular clastic grains of chert and bioclastic detritus with a micrite matrix. Ghab graben, northeast of Abyad River. XPL.



**B.** Also from the Ghab Graben Pliocene-age facies. A packstone of miliolid foraminifera with bioclastic debris and chert. Chert provenance is probably from the Jebel An-Nassuriyeh Mountains. PPL





**Figure 3.61** A well exposed view of the middle of the Pliocene succession. Alternating hard and soft, limestones and marls appear channelled, with bedding truncations and pinch outs easily seen. Unfortunately, access to this site was not possible, but a palaeoflow was orientated approximately NE-SW. Bedding is sub-horizontal. Locality is 5km south of Al-Haffeh Town.

A thin section sample suggests that Pliocene-age facies existed in the far north of the Nahr El-Kabir Valley, but this cannot be substantiated from field evidence alone. It is, therefore, likely that the Pliocene seas never completely drowned the Nahr El-Kabir Valley (see time-slice 11) and the Ghab Valley marine deposits are from a marine incursion through the Hatay Graben (see Chapter 5).

### ***Time-slice 10, Pliocene transgressive marls and Pliocene eruptives***

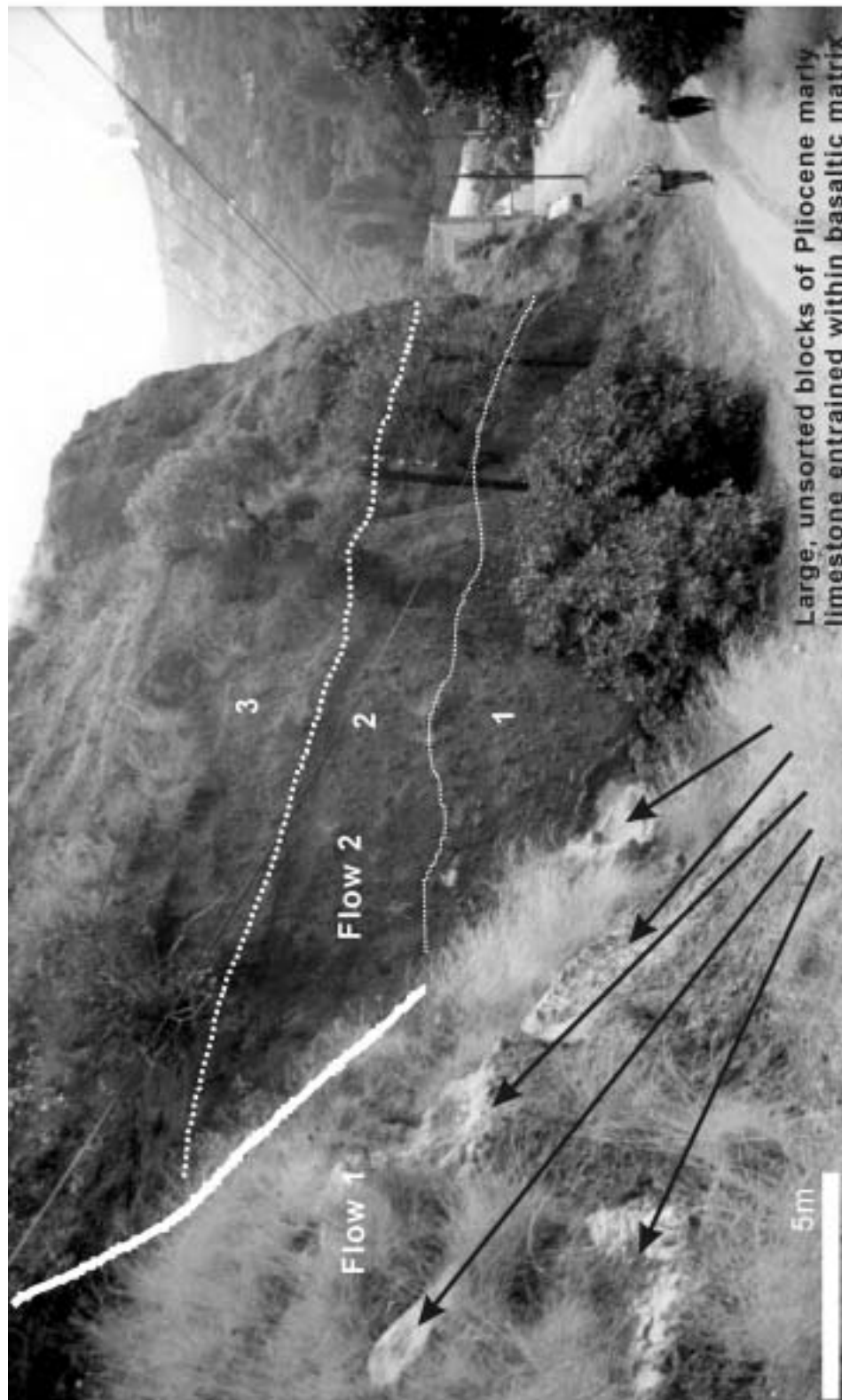
#### ***Banyas Town***

Near Banyas Town the character of the Pliocene-age sediments is considerably different to from further north. Two lithologies (time-slices) co-exist in the same region, marine marls and basaltic volcanic rocks.

The Pliocene-age sedimentary rocks in this southern region are also marly, but contain much more detrital material than in the Nahr El-Kabir Valley. These carbonate sandy marls are also rich in bivalves and *Turrolites* gastropods as bioclasts. The sandy, bioclastic marls total more than 50m and are overlain by basalts.

Deposition of the marly sediments is thought to have occurred in palaeovalleys as the deposits are spatially restricted to narrow outcrops, flanked by topographically steep Cretaceous and Maastrichtian-age rocks. The bedding laminations drape against the valley margins rather than being in fault contact (see pull-out maps).

The overlying basalts are heavily altered, most are breccias or simply layers of fist-sized clasts. Each clast typically shows alteration rims where broken, a dark brown colour for the outer centimeter, and a grey or black colour internally. Marl surrounding these clasts are often altered and friable, with a glassy appearance. Two prominent layers of clasts were found during fieldwork (each some 20m thick). White limestone and marl is often entrained within these basaltic layers and large clasts (>1m) are common (Figure 3.62). The clasts layers are overlain by pillow lavas, also showing alteration rims and internal brecciation and then by three complete, thin lava layers. The 'lava-flow' layers have red, rubbly bases and 1-2m thick, grey, lava beds. Five metre-high cones of dark grey to black coloured, fragmented and friable basalt overlies the 'lava-flow' layers. The rock is intensely altered in fractures (blue to orange colours) and extremely friable. These 'cones' of lavas are approximately 200m above modern sea level. Marl deposition to the west appears to have been



**Figure 3.62** 12km south of Banyas town, a view of basaltic lavas, tuffs and entrained Pliocene limestones. There are 2 'flows' and 3 sequences in 'flow 2'. Flow 1 is basalt and coarse limestone clasts. Flow 2, sequence 1 is coarse lava breccia with large (>1m) blocks of Pliocene limestone. 2 is tuff with limestone pebbles. 3 is haloclastite; the lavas appear to have erupted or been rapidly deposited in water, exhibiting intense red-brown colour, blocky texture, intercalated marl and friability. Devyatkin et al. (1997) reported an age of  $4.35 \pm 0.22$  Ma for the basalts in this area, from isotope dating.

synchronous with these eruptive rocks as the marls contain angular fragments of volcanic debris, dark grey ash layers and rounded clasts of basalt.

*Preliminary interpretation of Pliocene-age eruptives*

The marls and carbonate sandstones with bioclastic material are inferred as being deposited in very shallow marine conditions. Planar cross stratification throughout the unit suggests deposition in shoreface or shallower water depths (no faunal evidence), in comparison to the shelfal facies observed to the north. Minor landslips or slumps occurred in the restricted paleovalleys.

The basalts illustrate two major alteration features; that of rapid cooling (fracturing) and interaction with marl. The basalt erupted either on the sea-floor (pillow basalts) or as ejecta-clasts (hyaloclastite). In thin section the hyaloclastites from the Banyas region show altered, bladed crystals of plagioclase and olivine phenocrysts set in a glassy matrix.

The hyaloclastites were erupted into a shallow marine environment during the Early Pliocene. A 'delta' of debris (refer to geological pull-out map), built out and then collapsed, entraining blocks of limestone and marl in debris flows. Pillow basalt eruptions continued sub-aqueously, overlain by lava sheets. The final eruptive stage was mostly scoria cone eruptions, which gave rise to cones of basaltic material. The 'cross-beds' noted by Ponikarov et al. (1966), relate to the growth of these scoria cones; each layer is steeper than the last. There is no evidence of a final regressive phase in the local sedimentary record.

Devyatkin et al. (1997) dated the basalt flows as  $4.35 \pm 0.22$  Ma, using the K/Ar whole-rock dating method and stated that the geochemical signature was that of intra-plate basalts.

Basalts from 10km east of Banyas (approximately 500m above sea level) were dated by Devyatkin et al. (1997) as  $5.42 \pm 0.16$  Ma (Messinian/Pliocene) and were described by Ponikarov et al. (1963, 1966) as hypabyssal. These basalts include hyaloclastites with well preserved olivine phenocrysts. Basalt evolution appears more basic than the later ejecta-clasts, so may have intruded directly into water (pers. comm. Lass-Evans, Edinburgh, 2003). In outcrop, they are either rubble, with no indication of pillow lavas or thinly bedded lavas.

### ***Time-slice 11, Pliocene regressive sandstones***

Prominently capping the Pliocene-age marls in the Nahr El-Kabir Valley near Al-Haffeh Town is a 10m thick yellow, bioclastic grainstone and carbonate sandstone. This unit erosively overlies the uppermost section of the marl (Figure 3.57). At the base of the succession a 50cm-thick conglomerate comprising marl and grainstone deposited, this is overlain by 5-10m of medium thickness, trough cross-bedded carbonate sands and shell fragments. Gastropods, bivalves, scaphopods and organic material comprise the majority of this carbonate sand unit. Sparite cement dominates and micrite clasts are often recrystallised. The trough-cross beds are typically truncated by overlying beds. Two kilometres west of Al-Haffeh Town, the carbonate sandstone is missing and the Pliocene successions consist solely of marl with numerous gastropods.

#### ***Preliminary interpretation***

The carbonate sands and bioclastic grainstones are typical of shallow marine deposits (Tucker et al. 1990) and as such, represent a much shallower water facies than previously represented by the Pliocene-age marls. Trough cross-bedding, shell fragments and organic material indicate an upper shoreface or possibly even a foreshore setting. The trough-cross beds are laterally continuous over 50-100m before pinching out, characteristics of channeling (Figure 3.58). The disappearance of shallow marine facies to the west was due to transition downslope to deeper water conditions and probably a shoreface marine environment.

The complete Pliocene-age succession lithologies show a cycle of transgression to regression. Marine incursion occurred after the Messinian succession and reached open shelf marine depths. Throughout the Early Pliocene marine conditions then shallowed to foreshore depth before sub-aerial exposure.

### ***Time-slice 12, Quaternary (and Late Pliocene)***

Quaternary-age exposures and geomorphological features are widely developed across the region. Ponikarov et al. (1963) mapped four distinct, time-related facies (see pull-out geological map), starting with 'marine' rocks. Different facies are observed along the coastline from north to south and rarely are all four facies seen in any one area.

On the Baer Bassit Massif, the most obvious Quaternary features are the prominent beachrock terraces that cut into the ophiolite and further south into Tertiary cover rocks (Figure 3.63). These terraces are interspersed with large flat-lying sandy beaches at the mouths of river valleys. Moving inland, the Quaternary facies were seen in a sinkhole, allowing some 12m of succession to be presented (Figure 3.64). This commences with red caliche containing dark organic matter and rootlets. This is unconformably overlain 7m of thick bedded, planar cross-stratified, red, poorly lithified, bioclastic sands. Very large blocks of material are entrained in the uppermost exposures.

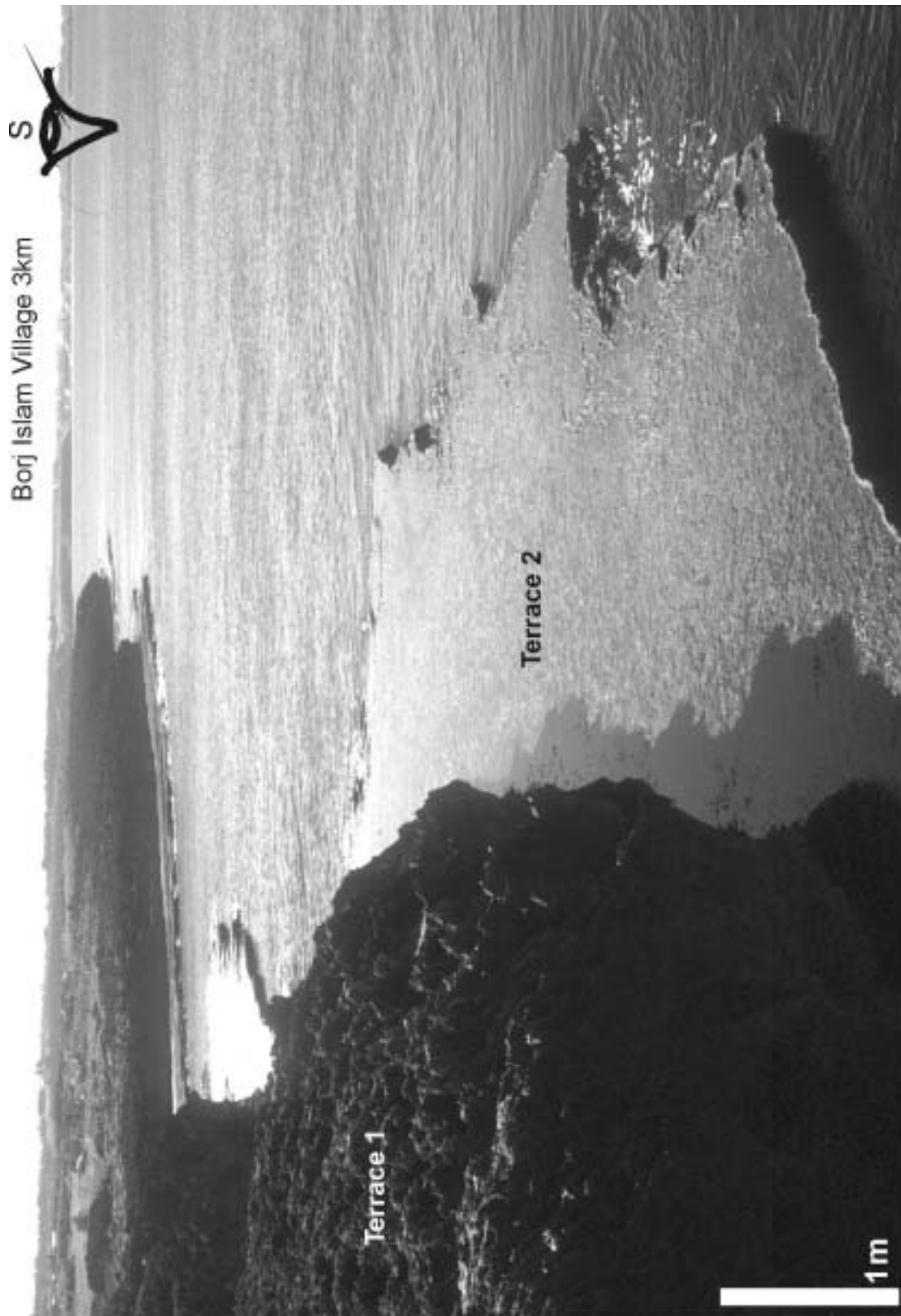
At the beachfront of Latakia City, the succession commences with coarse, bioclastic-rich conglomerates, overlain by shell-rich sands (Figure 3.65). These sands are unconformably overlain and truncated by overstepping, planar cross-stratified, laminated, carbonate sands. Very shallow marine fauna (e.g. serpulid worms and solitary corals) dominates the overlying carbonate masses, which comprise numerous large blocks.

In the area south of Latakia City, the majority of the Late Quaternary deposits are grainstones comprising clasts from all the siliceous rocks units seen in the study area, set in a sparite matrix (Figure 3.66). Gastropod and foraminiferal bioclasts are also common. A recent motorway cutting (c. 2km inland) exposes a succession in which four units were logged (Figures 3.67 and 3.68). They illustrate the extent and heterogeneity of marine to fluvial deposition.

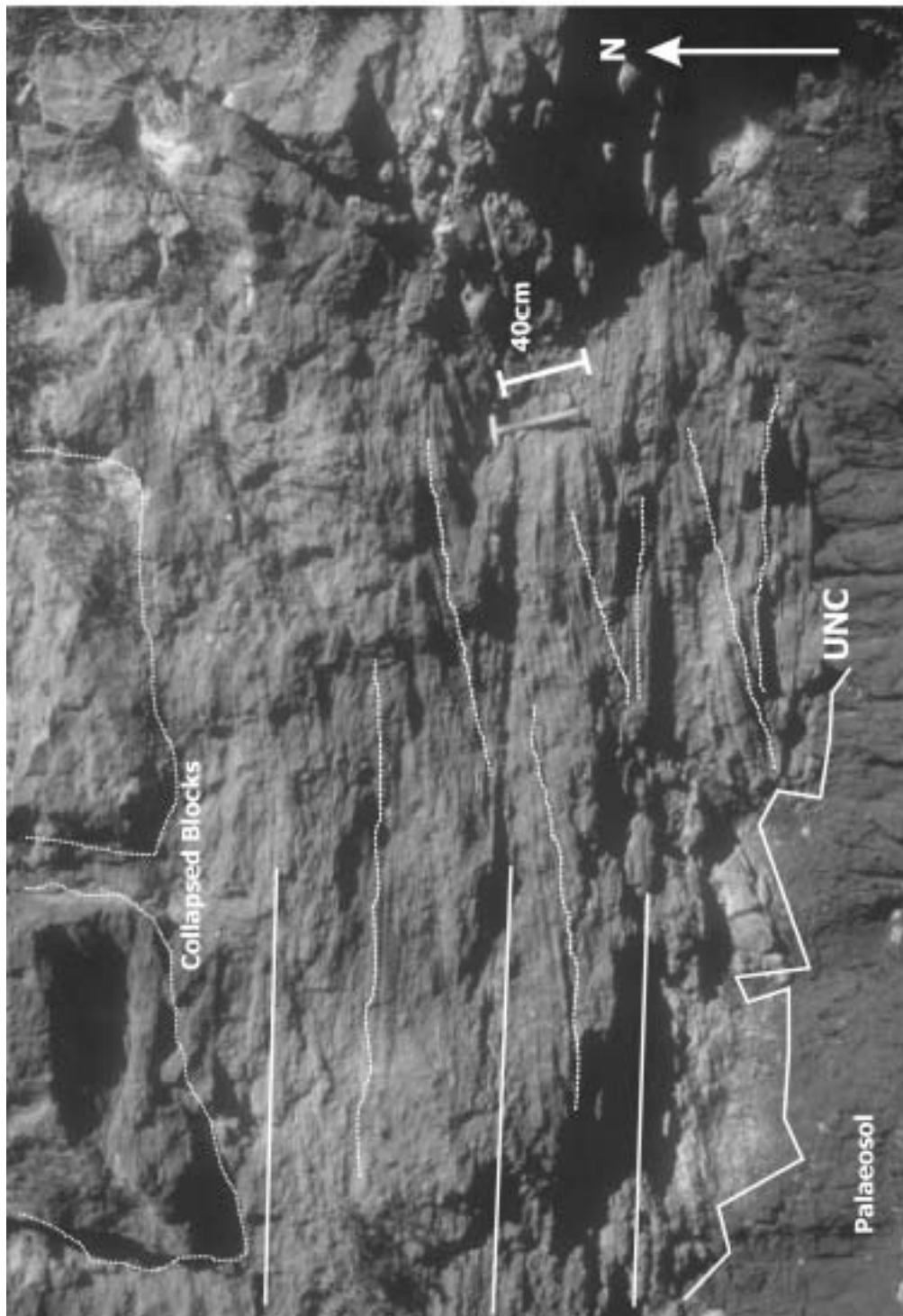
Further south, towards Jebleh Town, bioclastic packstones are usual (the inclusion of micrite within the samples is common). Shell fragments, gastropods and foraminifera are the main bioclasts (Figure 3.66). Two flat-lying terraces are prominent along this coastline and, in general, this whole area is only 10-15m above sea level (extending 5km inland)(Figure 3.69).

Although not mapped by Ponikarov et al. (1963), very large exposures of coarse gravel exist on the flanks of the Nahr El-Kabir Valley. These deposits cross-cut the older Miocene conglomerates and are typically form thick lenticular beds, steeply dipping (20-30°) into the valley. They consist of large clasts (<20cm) of every rock type seen within the Nahr El-Kabir Valley, are clast supported and have a sandy matrix. These rocks are the only exposures seen in the region exhibiting strong clast imbrication (also into the valley, northwest and southwest).

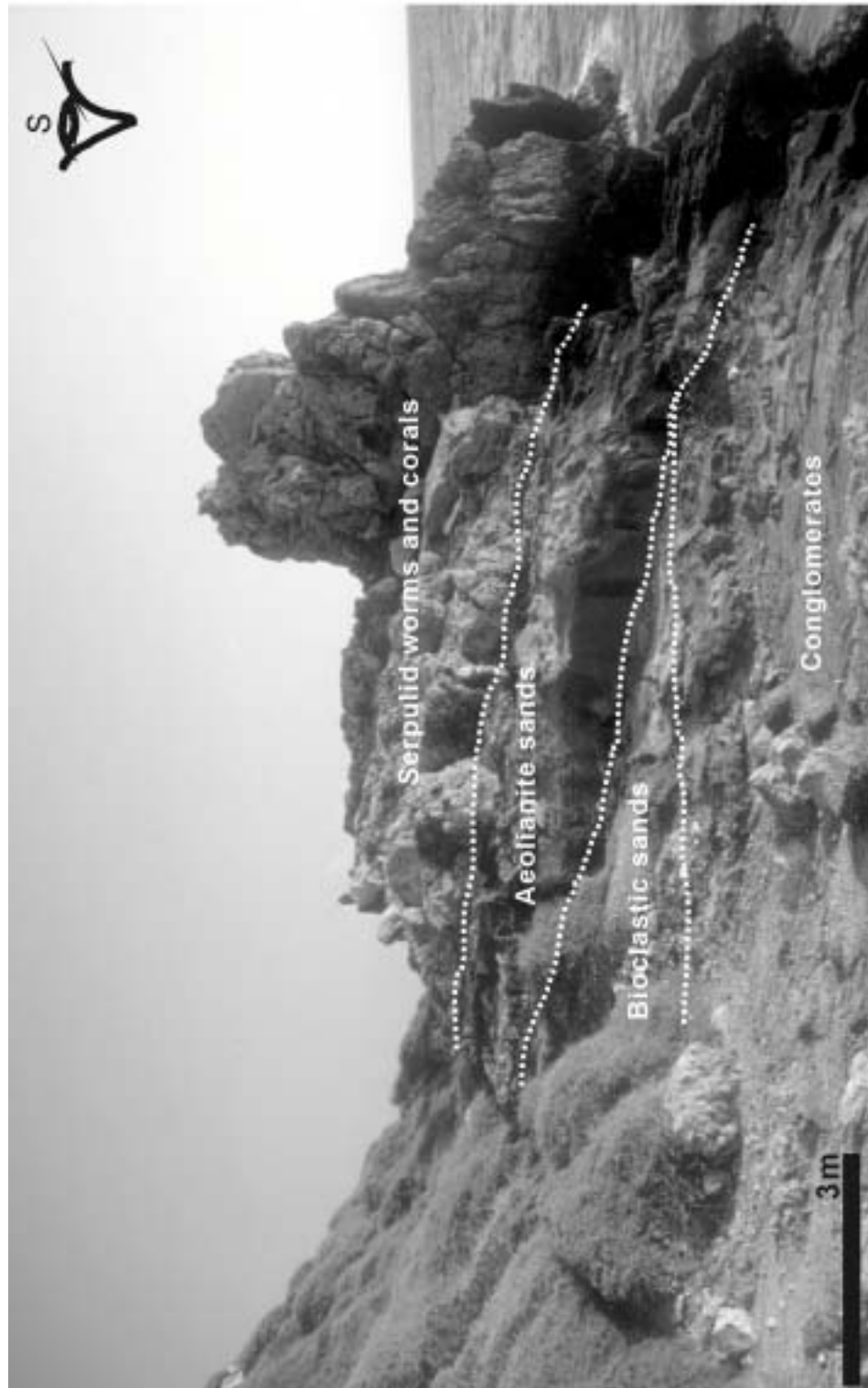




**Figure 3.63** Shoreline terraces north of Borj Islam Village on the Baer Bassit Massif. The terraces consist of aeolianite facies.



**Figure 3.64** Quaternary aeolianite deposits from a small sinkhole outcrop 10km south of Borj Islam Village. Wind blown bioclastic sandstone overlies a palaeosol horizon. The palaeosol horizon is at present sea-level and close by the aeolianite forms a wave cut platform along the coast. An upper unit of collapsed blocks is common along the coast north of Latakia City.

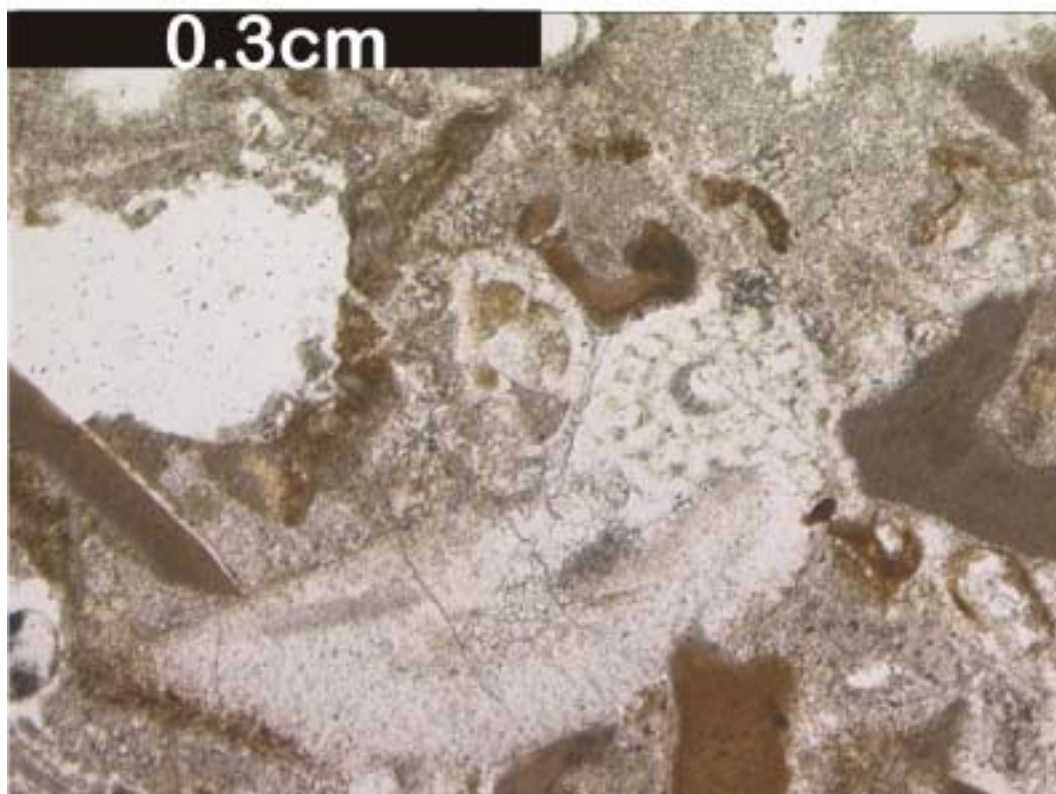


**Figure 3.65** A view of slumped Quaternary coastal deposits near Latakia Port. Horizontal conglomerates pass upwards to shelly bioclast sands which in turn are overlain by sub-horizontal aeolianite sandstone. Capping the sequence are slumped blocks containing bioclastic limestone consisting of serpulid worm tubes and corals. Much of the limestone clasts were derived from the adjacent Eocene limestones, with chert pebbles also being common clasts. Tertiary and Neotertiary ages are likely for these deposits based on the wave-cut platform heights seen elsewhere in the region e.g. Cyprus (Poole and Robertson, 1990).

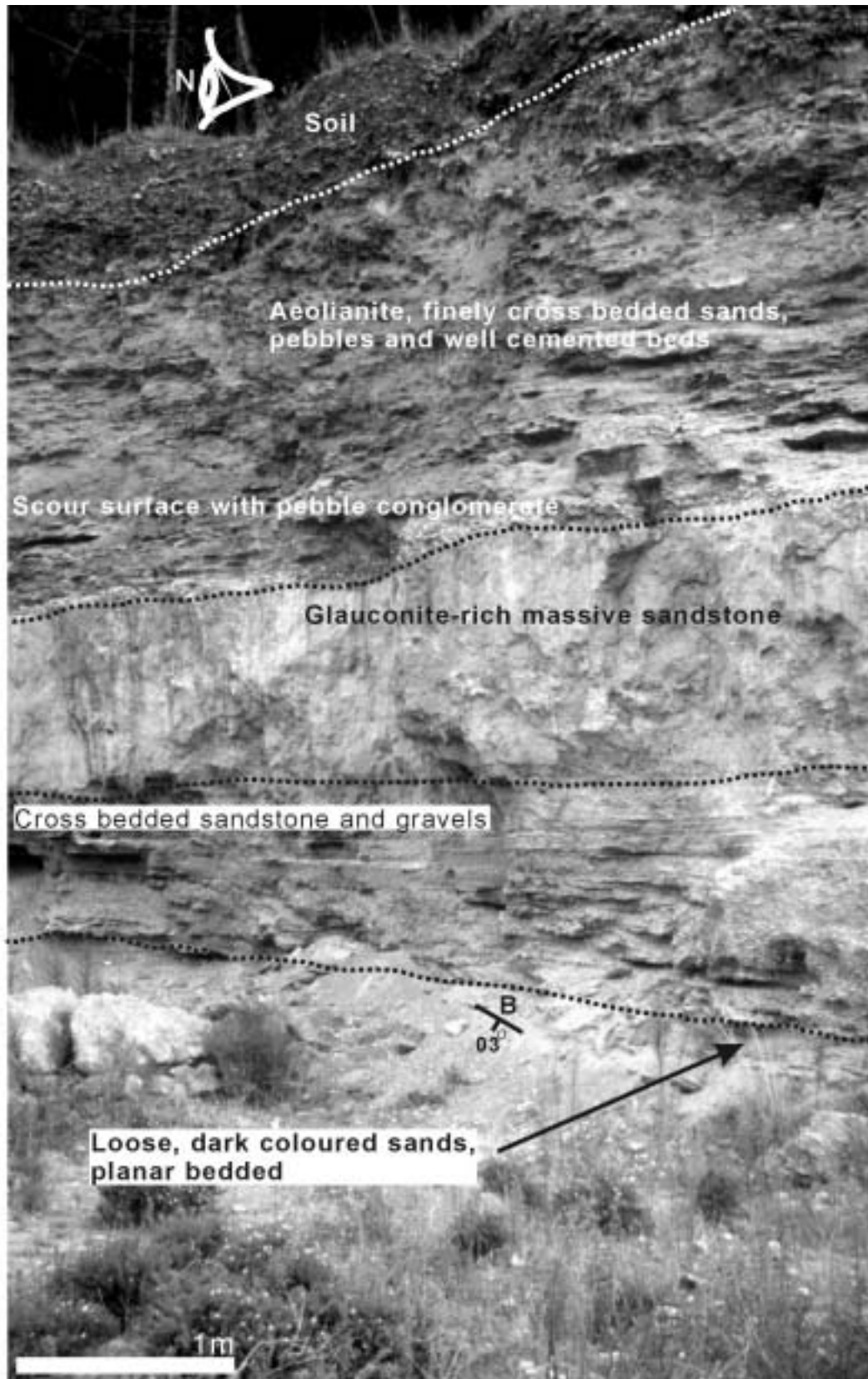




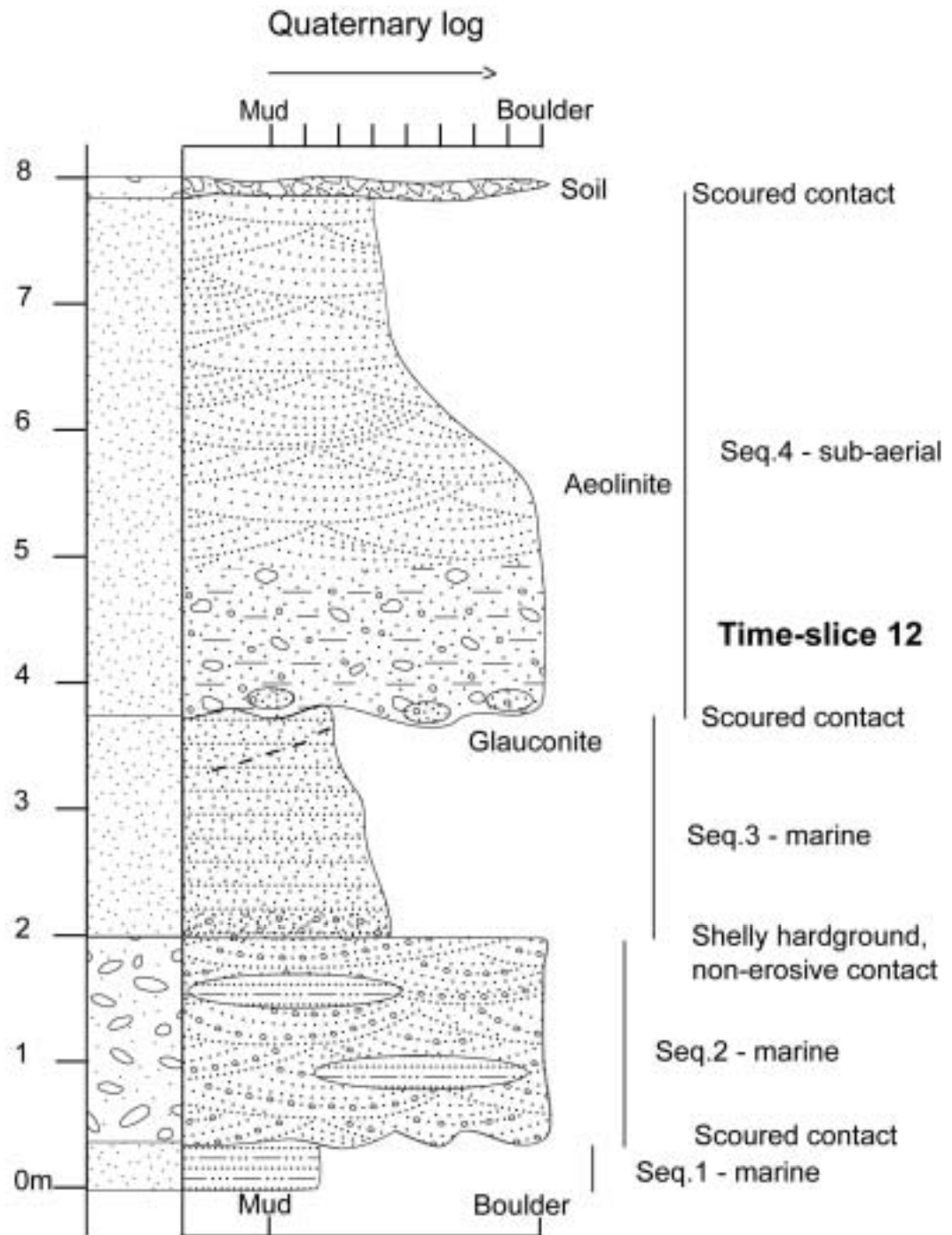
**Figure 3.66 A.** Grainstone of Quaternary age, from beachrock 10km south of Latakia City. Extraclasts of older rock (micrite and chert) and bioclastic intraclasts cemented by sparite. XPL



**B.** Partially recrystallised shell fragments, foraminifera and intraclasts from the beach terraces at Jebleh Town. Quaternary age packstone. PPL.



**Figure 3.67** The full Quaternary succession seen 25km south of Latakia City on the Latakia-Banyas highway, 5km east of the current coastline. Four major units are exposed chronicling the transition from marine to non-marine deposition.



**Figure 3.68** Sedimentary log of Quaternary facies on the Banyas-Latakia highway, 10km south of Latakia.





**Figure 3.69** Quaternary exposures at Jebbleh Town. The prominent lithology is bioclastic sandstone, forming an aeolianite facies at many locations, with cross-bedding and caliche surfaces. The wave-cut platforms are prominent and indicate uplift/sea-level drop of about 1.5m.

*Preliminary interpretation of Quaternary-age facies*

The extent and facies of the Quaternary-age rocks were used to assess neotectonic movements of the region (see Chapter 4 and 6). One section, south of Latakia City illustrates the four sequences described by Ponikarov et al. (1963) (Figures 3.67 and 3.68). Elsewhere, only specific sequences are apparent.

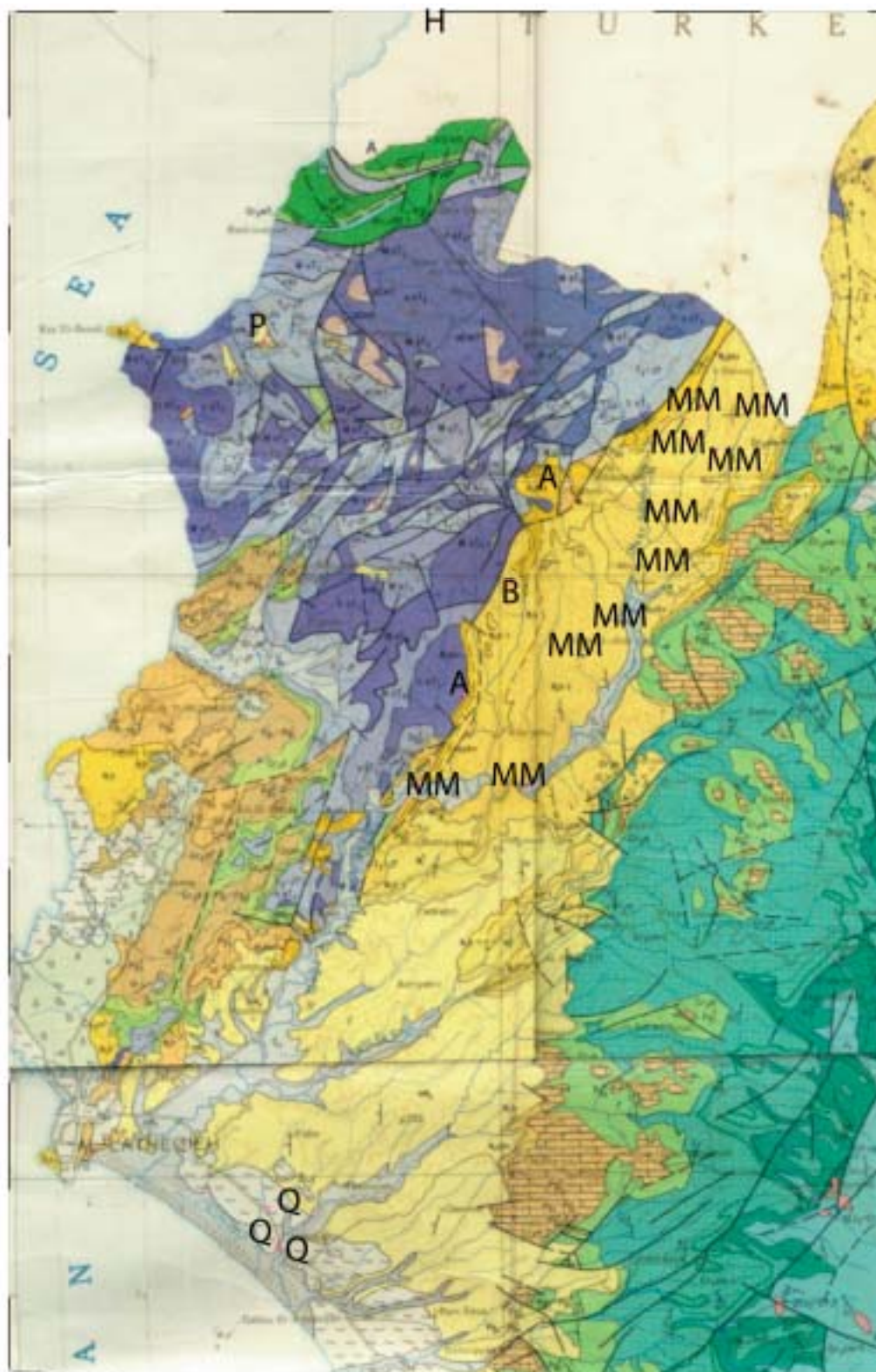
Of the four distinct mini-sequences that are present within the Quaternary, the first two are marine dominated and represent the shoreline moving westwards and then overlain by a mix of marine and fluvial deposits. Aeolianite deposits of near shoreline wind-blown carbonate sands and bioclastic material form lithified terraces, which were later down-cut and wave reworked. The fact that these platforms are visible above the shoreline in some areas points to uplift of these regions at a later date rather than eustatic change. In general, the terraces north of the El-Kabir lineament comprise multiple platforms with sharp relief and elevations between 2-4m (Figure 3.63). In contrast, terraces further south typically exhibit one platform 1-1.5m above sea level (see Chapter 6). Broad eustatic changes or uplift of the area are discussed fully in Chapter 6 (neotectonics).

From the low hills east of Latakia, Devyatkin et al. (1996) reported that Pleistocene-age mammalian fauna of large continental herbivores existed (although none were seen in this study).

The large, unmapped exposures of coarse gravel within the Nahr El-Kabir Valley are interpreted as fluvial in origin. Simakova (1994) indicated that the Late Pliocene to Quaternary climate in Syria was marked by a considerable increase in precipitation and this may have resulted in the gravel deposition. It is, therefore, possible that the Late Pliocene marks beginning of the phase of sub-aerial erosion, which then continued throughout Pleistocene and Holocene time.

***Point counting of coarse sediments***

From the 350 or samples taken, some 100 were thin sectioned for dating and petrological examination. Of these, 17 were well-cemented coarse samples that survived the sectioning process and could be point counted. They represent, therefore, the sediments with a strong, usually carbonate matrix and a fine to granular grainsize (Figures 3.70 and 3.71).



**Figure 3.70** Point counting localities of Miocene to Quaternary arenites. A - Aquitanian, B - Burdigalian, MM - Middle Miocene, Q - Quaternary. See text and appendix for details. Base map by Ponikarov et al. (1966).

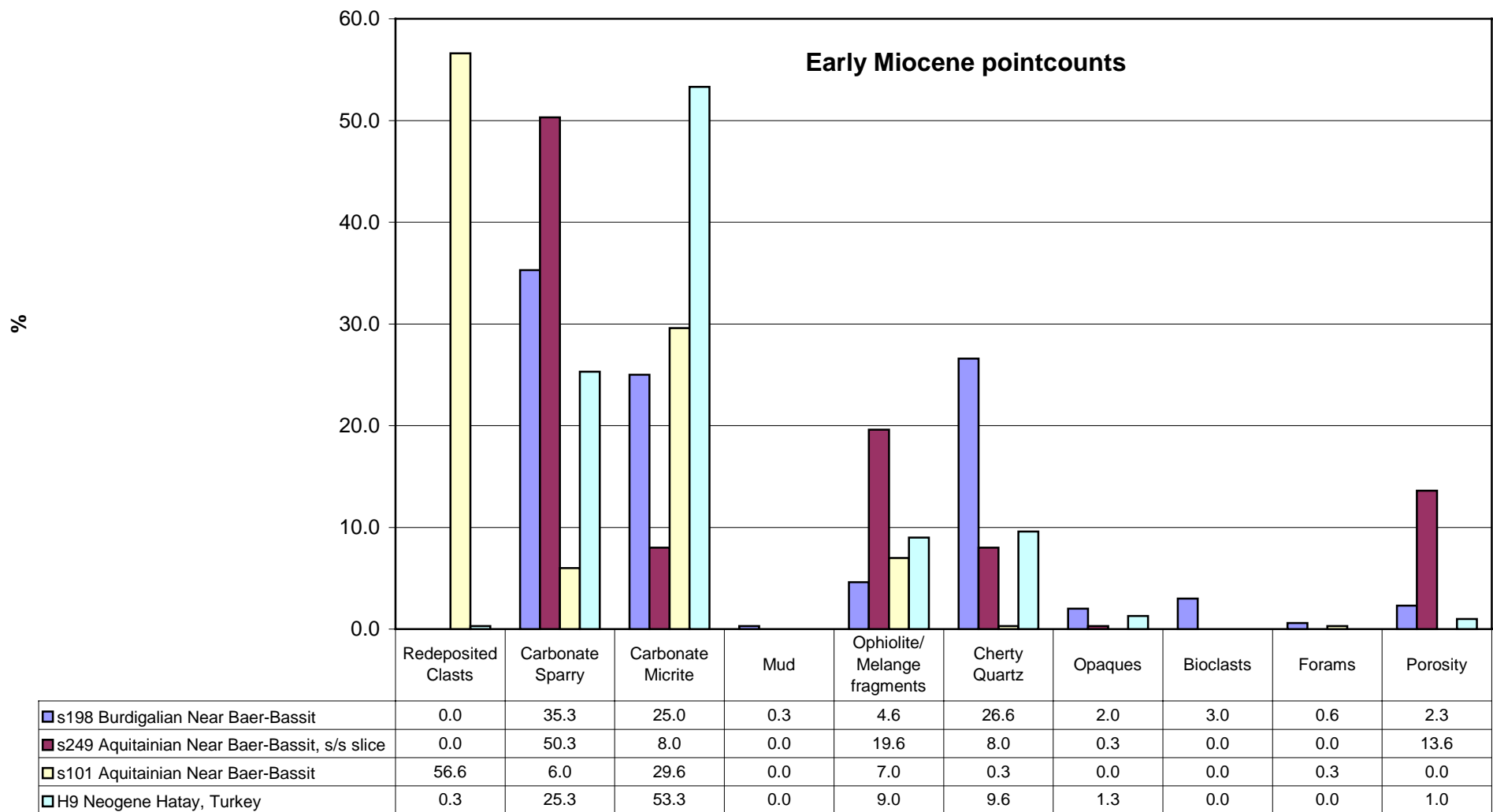
### Sample dating

The original sample dating by Ponikarov et al. (1963, 1966) rarely indicates which sediments were used for extract foraminiferal dates. These coarse sediment samples show that, the percentage of foraminifera (benthic and planktic) in the matrix of the samples is extremely low to non-existent. Foraminifera are, however, very prominent in the redeposited clasts from within the samples, which would result in erroneous dating. Therefore, in this project, attempts were made to obtain dates from the youngest nannofossils present in coarse samples or from foraminifera within marls and the dating results were used together.

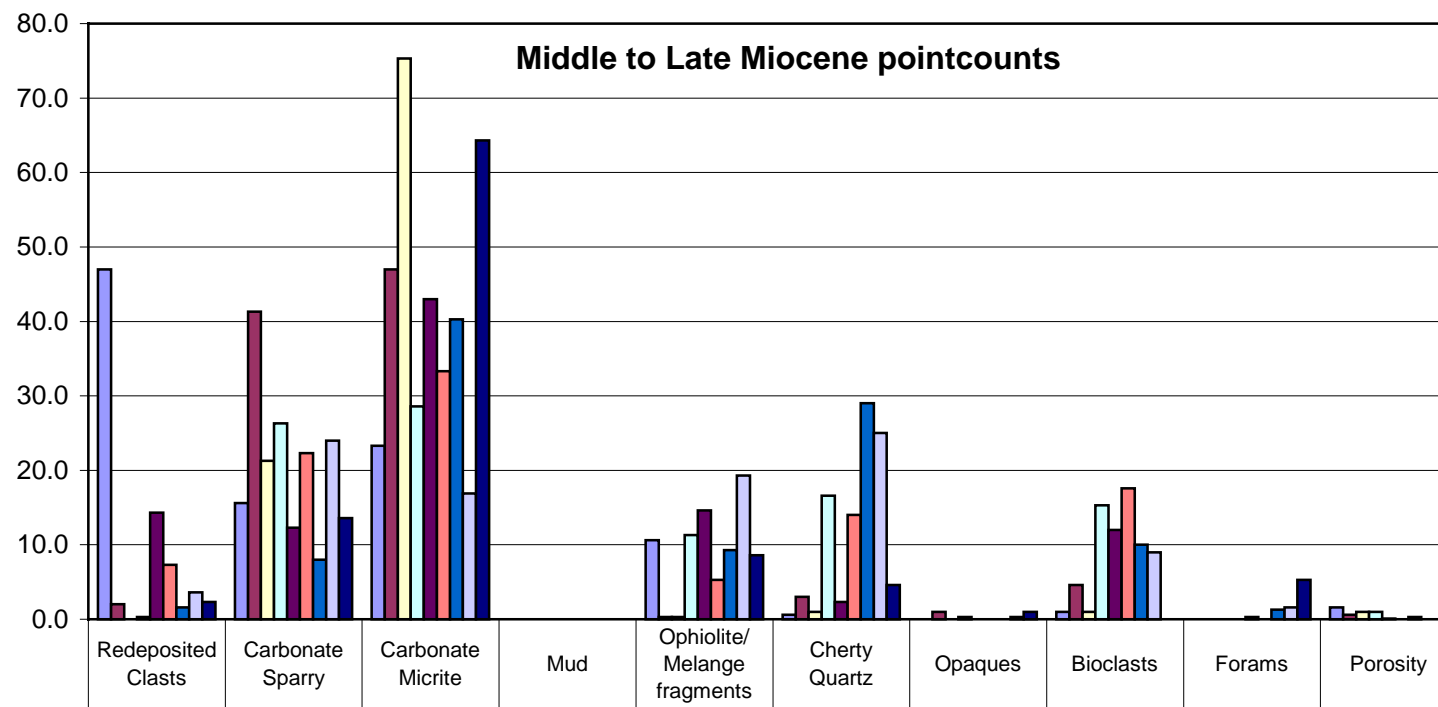
### ***Diagenesis of the Nahr El-Kabir sedimentary rocks***

Very little diagenesis of any of the sediments can be seen in hand specimen or thin section apart from minor dissolution and sparite re-cementation (and rare bitumen). This is most common in rocks that have been fractured or faulted, as would be expected, although is also common in the bioclastic limestones. The timing of this dissolution and re-cementation is very hard to pinpoint as it is often most prevalent in surface exposures, with no overlying sequences. None of the exposed rocks show indicators of having been deeply buried as compaction appears minimal and most rocks are poorly lithified.

Much of the carbonate dissolution may have occurred as late as Quaternary exposure. In the one core section viewed (drilled Miocene facies, abandoned near a roadside at Khan El-Jouz), there was no obvious diagenesis. Oxidation and reduction of the carbonate sediments is fairly common, however, probably due to groundwater fluid flow through the rocks. This is evident by the quantity of ferric and ferrous iron staining present, especially in the Paleogene-age succession.

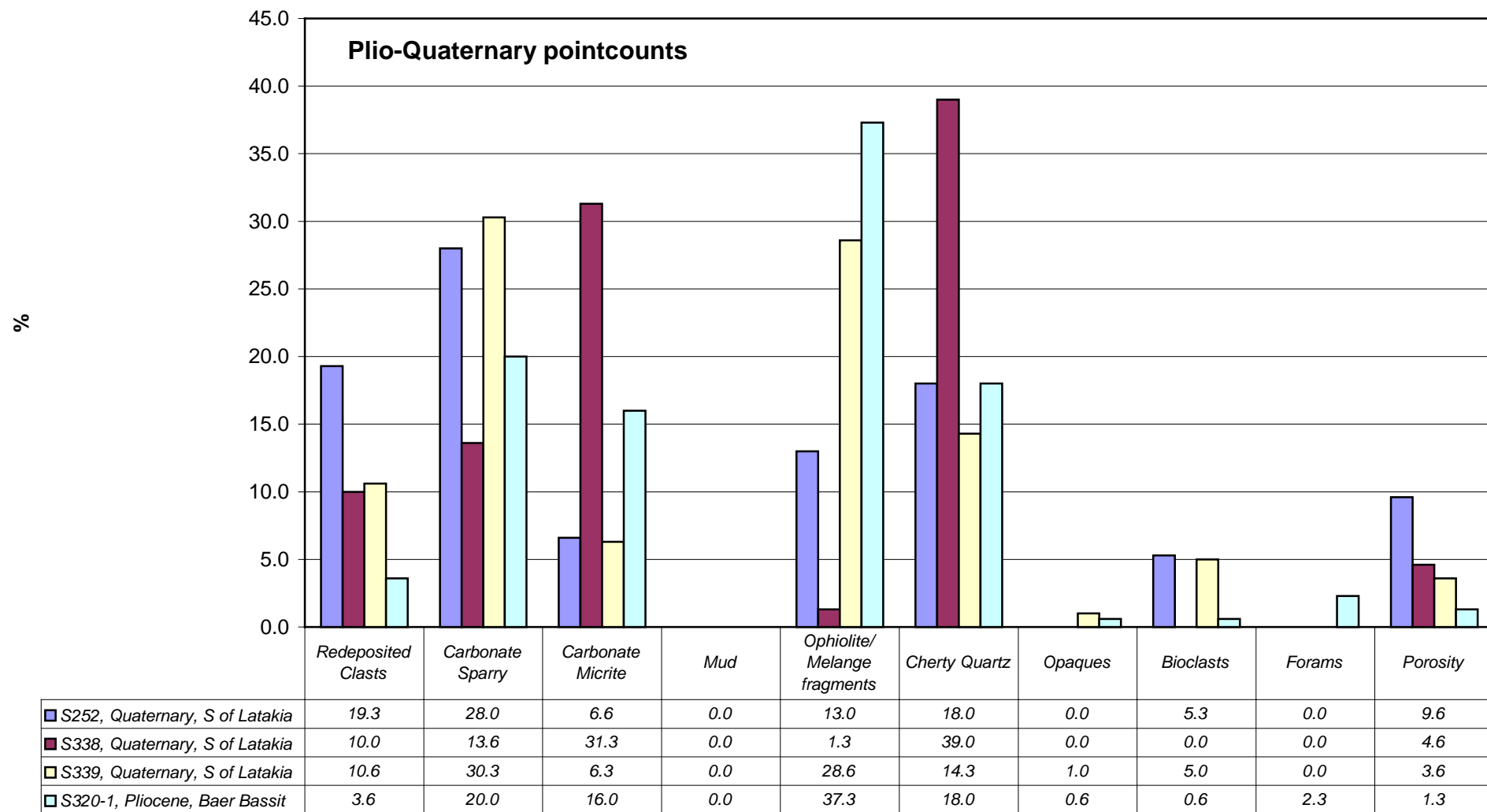


%



s120 Mid-Late Miocene Mid-graben, to north	47.0	15.6	23.3	0.0	10.6	0.6	0.0	1.0	0.0	1.6
s130 Mid-Late Miocene Mid-graben, to north	2.0	41.3	47.0	0.0	0.3	3.0	1.0	4.6	0.0	0.6
s130-2 Mid-Late Miocene Mid-graben, to north	0.0	21.3	75.3	0.0	0.3	1.0	0.0	1.0	0.0	1.0
s206 Mid-Late Miocene Mid-graben	0.3	26.3	28.6	0.0	11.3	16.6	0.3	15.3	0.0	1.0
s208 Mid-Late Miocene Mid-graben, South	14.3	12.3	43.0	0.0	14.6	2.3	0.0	12.0	0.3	0.1
s323 Mid-Late Miocene Near Turkish border	7.3	22.3	33.3	0.0	5.3	14.0	0.0	17.6	0.0	0.0
s324 Mid-Late Miocene Mid-graben, to north	1.6	8.0	40.3	0.0	9.3	29.0	0.0	10.0	1.3	0.3
s331-1 Mid-Late Miocene Mid-graben	3.6	24.0	16.9	0.0	19.3	25.0	0.3	9.0	1.6	0.0
s332-1 Mid-Late Miocene Mid-graben, to north	2.3	13.6	64.3	0.0	8.6	4.6	1.0	0.0	5.3	0.0





## Structural Data - introduction

This chapter discusses structural studies undertaken during this project, especially faulting and stress regimes. Al-Riyami (2000) and Al-Riyami et al. (2001) previously investigated the structure of the Baer Bassit Massif (see Chapters 2 and 6). Chapter 6 assimilates the sedimentological and structural interpretations to provide a tectonic framework.

Structural data were acquired from three sources: 1, field-based data from measurements within the project region. 2, ancillary seismic reflection data of the Eastern Mediterranean, offshore from Latakia City. 3, a simple seismology survey. This chapter is split into two sections, first, the field and remote sensing data acquisition and methodology, then a synthesis of the interpretations by area.

Previous structural work in the region on the structure was published by Ponikarov et al. (1963). Their map shows numerous large faults, but does not include any kinematic data for the region. Ponikarov et al. (1966 & 1967) in their later review papers, refers to the 'Lattakia-Killis Fault' (see El-Kabir Lineament, below) as Cretaceous, but do not infer any other movements. Their work was primarily concerned with the Ghab Graben (see Chapter 5). Field-based kinematic studies in the Plio-Quaternary Ghab Graben (relating to the Dead Sea Transform Fault) are limited to the eastern margin (Zanchi et al. 2002). No data are published for the western margin, which borders the project area.

### *Structural data from fieldwork*

Structural data were recorded from every possible locality visited. Strikes and dips of bedding and faulting, sense of fault movement, fold plunges and fracturing were all recorded and over a thousand measurements were taken in the course of fieldwork. One major shortcoming in the dataset that I acquired however, is the rarity of kinematic data (i.e. showing sense of movement). The soft lithologies in the region and the vegetated nature of most outcrops do not preserve much in the way of slickensides or striations on fault planes. The only successions that preserve these data are the Cretaceous Platform limestone rocks of Jebel An-Nassuriyeh and the Eocene Nummulitic limestone in the same region. In virtually every other case, faults could be identified only by observing fault gouge or zones of fractured or broken bedding planes. For these reasons, fault data are presented as stereonet and rose diagrams of fault strike. However, the sense of fault movement often had to be

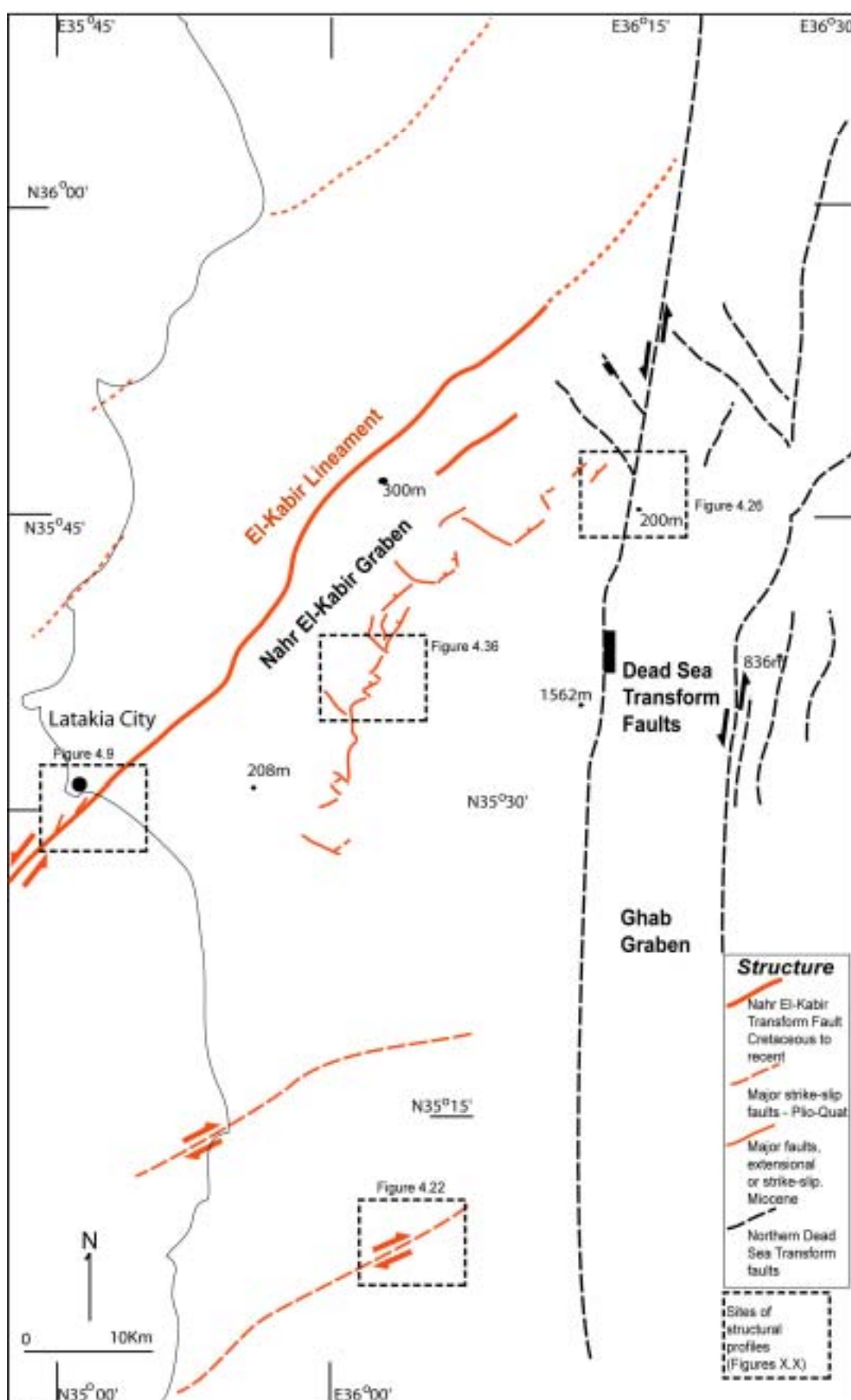
inferred e.g. using map relations, fractures and stratigraphic or sedimentological discordance.

### Dataset

Six major areas with good structural data were found, that demonstrate a relative chronology of fault movement. These are (Figure 4.1):

1. The sea front, Latakia City,
2. Outcrops at the western margin of the Bahlouliyah Reservoir,
3. The northeastern margin of the Nahr El-Kabir Valley (abutting the Turkish border),  
 € {the above 3 outcrops refer to the El-Kabir Lineament, described later in this chapter; offshore Latakia City is also related to this lineament, but is known from seismic data only},
4. On the Jebel An-Nassuriyah Mountains directly east of Banyas town.
5. The western margin of the Ghab Valley near Jus-Ash Shaghour,
6. The eastern margin of the Nahr El-Kabir Valley between the towns of Kansaba in the north and Qerdaha in the south.

Away from the above areas, faulting is poorly exposed, absent, or difficult to differentiate and no major lineaments were observed. The map of Ponikarov et al. (1963) indicates numerous fault lineaments throughout the mapped area, but does not assign orientations or fault throws except by stratigraphical juxtaposition. Geologists at the Establishment of Geology, Damascus, suggested that much of their dataset was interpreted from aerial photography, however, their numerous mapped faults were difficult to find in the field even with the help of GPS positioning. In the thesis of Al-Riyami (2001), much effort went into identifying and re-mapping fault movements in the Baer Bassit Massif as field interpretations did not agree with the original mapping (Ponikarov et al. 1963, 1966, 1967). During the course of this work, the Establishment of Geology kindly allowed me to see some of the original aerial photo survey data from 1947. However, many features originally mapped could not be identified. Many of the lineaments of Ponikarov et al. (1963 & 1966) are also difficult or impossible to identify on the SPOT satellite images used in this project, which has a maximum resolution of 10m (Figure 4.2). The maps prepared in this thesis show only the major fault lineaments that it was possible to confirm in the field by a combination of mapping, stratigraphical juxtaposition and the use of SPOT images (see pull-out geological map).



**Figure 4.1** Sites of structural data within the project region.

## Fault Hierarchy

For this project a hierarchical scheme of fault analysis is used, based on the amount of inferred slip (normal, reverse and strike-slip) observed to have taken place on any particular lineament. A hierarchy of faults was needed as large faults were rarely observed, but fractures were common, near the large faults. This scheme applies to faults seen on seismic images (which appear to approach full crustal thickness), down to fractures with little or no movement. The scheme ranks faults into one of five categories from  $F_0$  (the largest) to  $F_4$  (the smallest):

$F_0$  - transform or transverse faults (mainly interpreted from seismic data)

$F_1$  - 10-100's m of throw (observed or field interpreted)

$F_2$  - <10's m of throw (observed in the field)

$F_3$  - <1's m of throw (observed in the field)

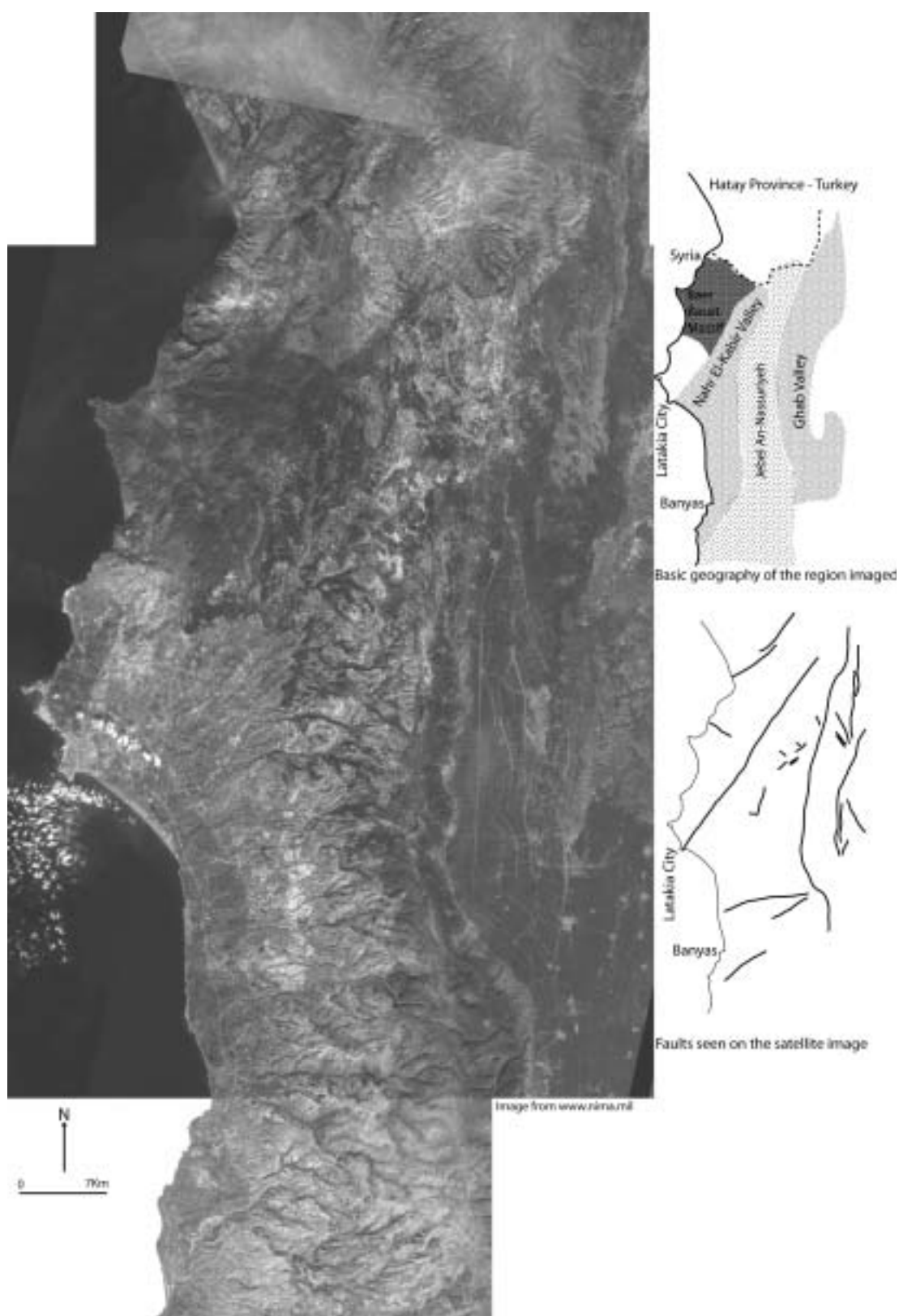
$F_4$  - fracture scale (observed in the field)

As would be expected with a power-law hierarchical scheme, the majority of data observed are in the  $F_4$  category. Where pervasive fracture orientations and pressure solution cleavage exist at outcrop, these data were recorded as such. They were separated from the larger fault data on plotted stereonet, so that the dataset was not biased and the prominent fault orientations could be identified (i.e.  $F_1$ - $F_3$  faults are separate from  $F_4$ ).

## ***Structural data from remote sensing***

SPOT image interpretation and bathymetry data

SPOT images were acquired from the US Defense Department website (see Southern and eastern margin of the Nahr El-Kabir Graben, this chapter; Chapter 1; <http://www.nima.mil>) (Figure 4.2). These data are free to download and monochromatic images with a resolution of 10m for the project area were available (original data are panchromatic, visible light spectra). After acquisition of the data, the digital images were sepia tinted to show maximum contrast and plotted at A0 scale to enable their analysis. Key topographic reference points and geological features were interpreted and traced (Figure 4.2).



**Figure 4.2** SPOT Satellite image of northwest Syria and the Hatay region of Turkey



Dark colours on the images represent areas of water or woodland. Habitation and agricultural land is represented by the shades of grey. Bright white is indicative of marl-rich soils (the underlying Maastrichtian and Palaeogene sediments are recognisable).

Overview-scale bathymetric image data of the Eastern Mediterranean were obtained from the United States National Oceanic and Atmospheric Association website (<http://www.noaa.gov>, 5' dataset)(Figure 1.1). More detailed bathymetric block models (Hall and Krasheninnikov, 1994), were computer manipulated and combined with the seismic and field interpretations derived from this study (see Chapter 6). Sea-floor depths derived from the seismic reflection data were also used.

### Seismic reflection data

Spectrum Energy and Information Technology Ltd. kindly made available 5 lines of data from their 1975 2D survey of the Eastern Mediterranean (Figure 4.3). Four lines run approximately N-S between the Syrian coast and Cyprus and one line is orientated E-W to tie the seismic data together. Seismic line spacing is approximately 10km between the N-S lines and the closest profile to the shore is approximately 15km offshore (see Chapter 1).

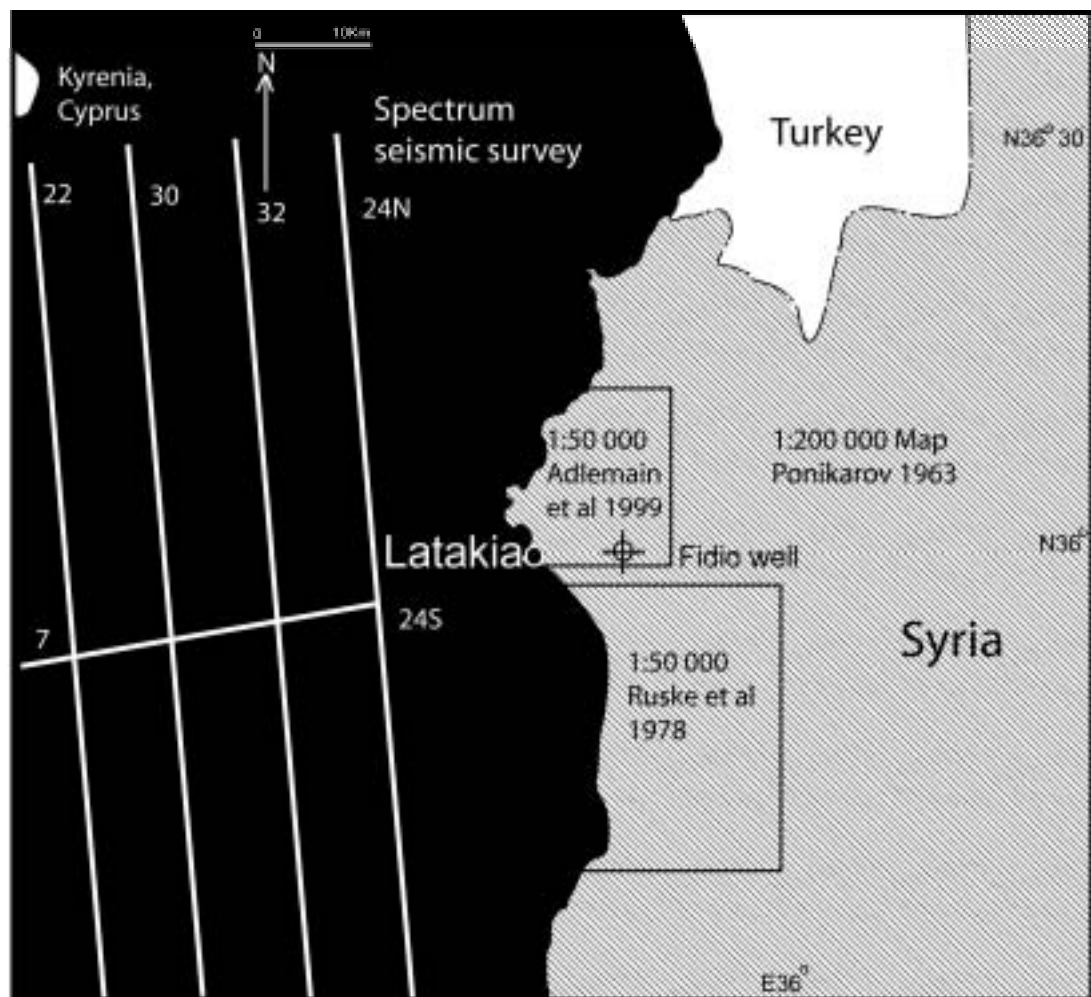
No well data (greater than 100m deep) are available for the offshore region bordering Syria (shallow coring described by Hall & Krasheninnikov, 1994). Three wells exist onshore in the mouth of the Nahr El-Kabir valley, but no data are released for them. Dzhabur (1985) published uncorroborated results (see Chapter 1 & 2 and see Offshore Latakia section, below). Wells offshore the Hatay Graben exist (40km north of Latakia, see Chapter 5), but the data are again not released.

The seismic data are interpreted, but only without reference to drilled horizons. A broad overview of features can be inferred from the data, focussing on prominent aspects of the data; i.e. faulting, folding and prominent reflectors. Two main assumptions were made, similar to those used by Vidal et al. (2000 A & B). Vidal et al. (2000 A & B), reinterprets data used by Kempler (1993), Kempler et al. (1994), Ben-Avarham et al. (1995) and Garfunkel (1998)(see also *Previous seismic interpretations*, the project area was not interpreted by previous work) (Figure 4.17):

- ∉ The first major reflector below the sea-bed (a double reflector) is the Messinian or 'M' reflector. Onshore it comprises evaporites (see Chapter 3), which have been found within the Mediterranean Basin (Hs<sup>c</sup> et al. 1973; Ryan et al. 1973). They form a

prominent reflector due to the high velocity of anhydrite ( $5\text{--}7000\text{ ms}^{-1}$ , Sheriff et al. 1995), contrasting with the overlying Pliocene marl ( $2500\text{--}4000\text{ ms}^{-1}$ , Sheriff et al. 1995).

- € There is a layer of angular discordance at 3-5 seconds TWT. This is possibly the K reflector, representing the base Tertiary.
- € The seismic sections are not depth converted; interpretations are presented in time. Depth conversion is ongoing work and is not presented here due to the uncertainties of interval velocities (see below) and problems converting large paper sections (digital data maybe forthcoming).



**Figure 4.3** Geological map and seismic dataset localities, showing the extent and coverage

### *Problems with the Spectrum Energy seismic data*

It is uncertain whether the initial survey or reprocessing of the paper data in 2000 by Spectrum Energy allowed for the high velocity of the Messinian evaporite strata.  $V_{INT}$  (velocity of interval) figures record a steady velocity increase in the seismic section with depth, there is no high velocity spike at the Messinian horizon. The concept of a Messinian Salinity Crisis was initially established by Hsü et al. (1973), and the key review paper of the extent of the desiccation was not published until 1977 (Hsü et al. 1977, after 2<sup>nd</sup> DSDP leg took place). The Spectrum Energy data were collected in 1975.

The thickness of the Messinian succession is uncertain within the Mediterranean Basin in this area. Vidal et al. (2000 a and b), suggests 1500m. Such a contrast in velocity in the reflection profile would distort every horizon deeper on a seismic section. Spectrum Energy have recently shot a 3D survey over this area, which highlights the Messinian evaporites, however, these data were unavailable.

### Seismology

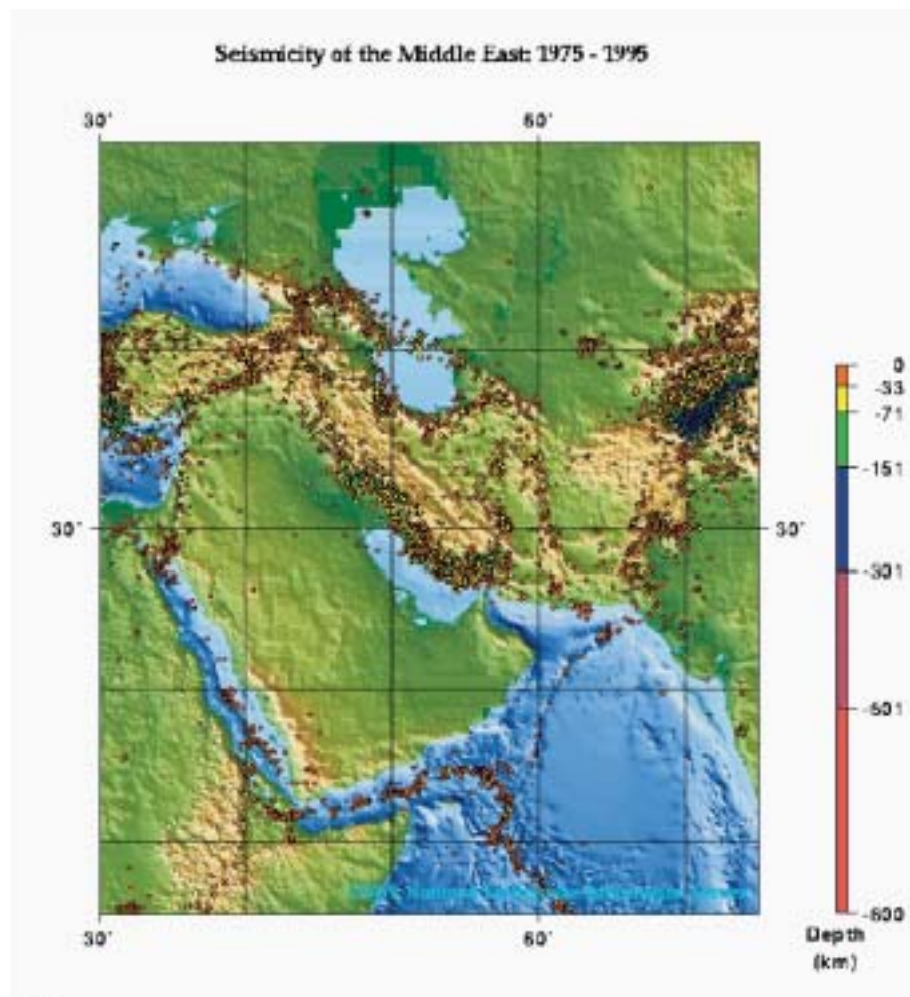
In conjunction with the Establishment of Geology (Syria), three analogue, bi-pole seismometers were set up by the during the second field season (2000) to assess microfaulting of the El-Kabir Lineament. The sites used for the survey were at the villages of Qaastal Maaf, Bahlouliyah and Qaballi police station (see pull-out location map). These three sites triangulated the lineament and in theory should have received data from any seismic event along a 20km segment of the lineament. Events within the Nahr El-Kabir Valley and Baer Bassit Massif would also would have been recorded.

Worldwide, large events were recorded during the survey (teleseismic), showing that the network was fully functioning, but no seismic events could be positively attributed to the El-Kabir Lineament during the two months of continuous recording. The Syrian National Seismology Center did record minor earthquakes (<magnitude 4) offshore from the Hatay region of Turkey and to the east of the Ghab Graben during that time. The United States Geological Survey and Israeli surveys, which record seismological data from much greater distances, do not record any onshore activity in the Latakia region since records started in 1963 (Figure 4.4). However, earthquakes offshore between Syria and Cyprus are common (see Figure 4.5).

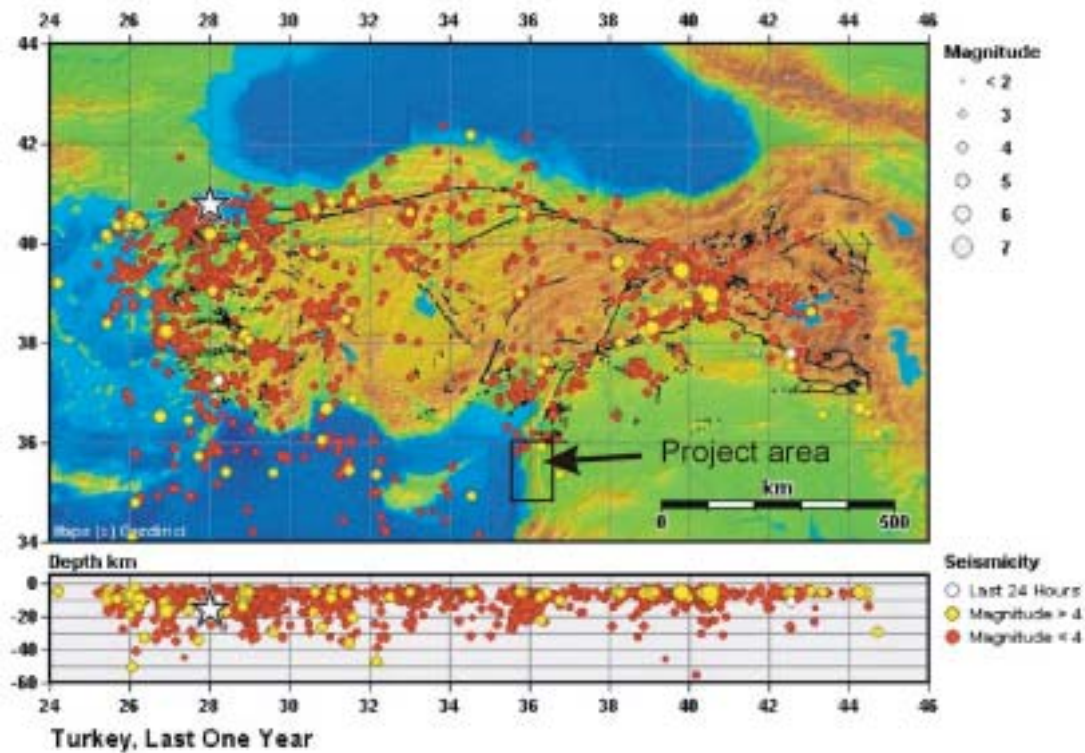
### *Syrian Earthquakes*

The lack of recent earthquake evidence is not conclusive for faulting quiescence in the project area. Latakia City was almost destroyed twice, in 494AD and 555AD by massive earthquakes (probably greater than magnitude 7, from historical literature) and prominent fault scarps can be seen onshore i.e. the 10m high cliff trending northeast from the beach at Latakia City. Meghraoui et al. (2003), notes that almost 900 years of quiescence might be observed from examining Recent-age terraces and walls in historical buildings, but that evidence of fault movement can be seen. Their hypothesis is that strain is building in the region and a large earthquake is due.

As of early 2003, one earthquake has been recorded to the north of the Nahr El-Kabir Valley, on trend with the inferred extension of the El-Kabir Lineament (near Zeiniye village, see Chapter 6 & pull-out geological map). On the 26<sup>th</sup> February 2003, a 4.2 magnitude, 21.8km deep, earthquake originated on, or very close, to the predicted extension of the fault as mapped in this work from field and SPOT data analysis (Figure 4.6). Movement tensors are not known for this event. Garfunkel (1998), indicated that the thickness of the crust is 25-30km in this region (see Offshore Latakia section, this chapter & Figure 4.7).



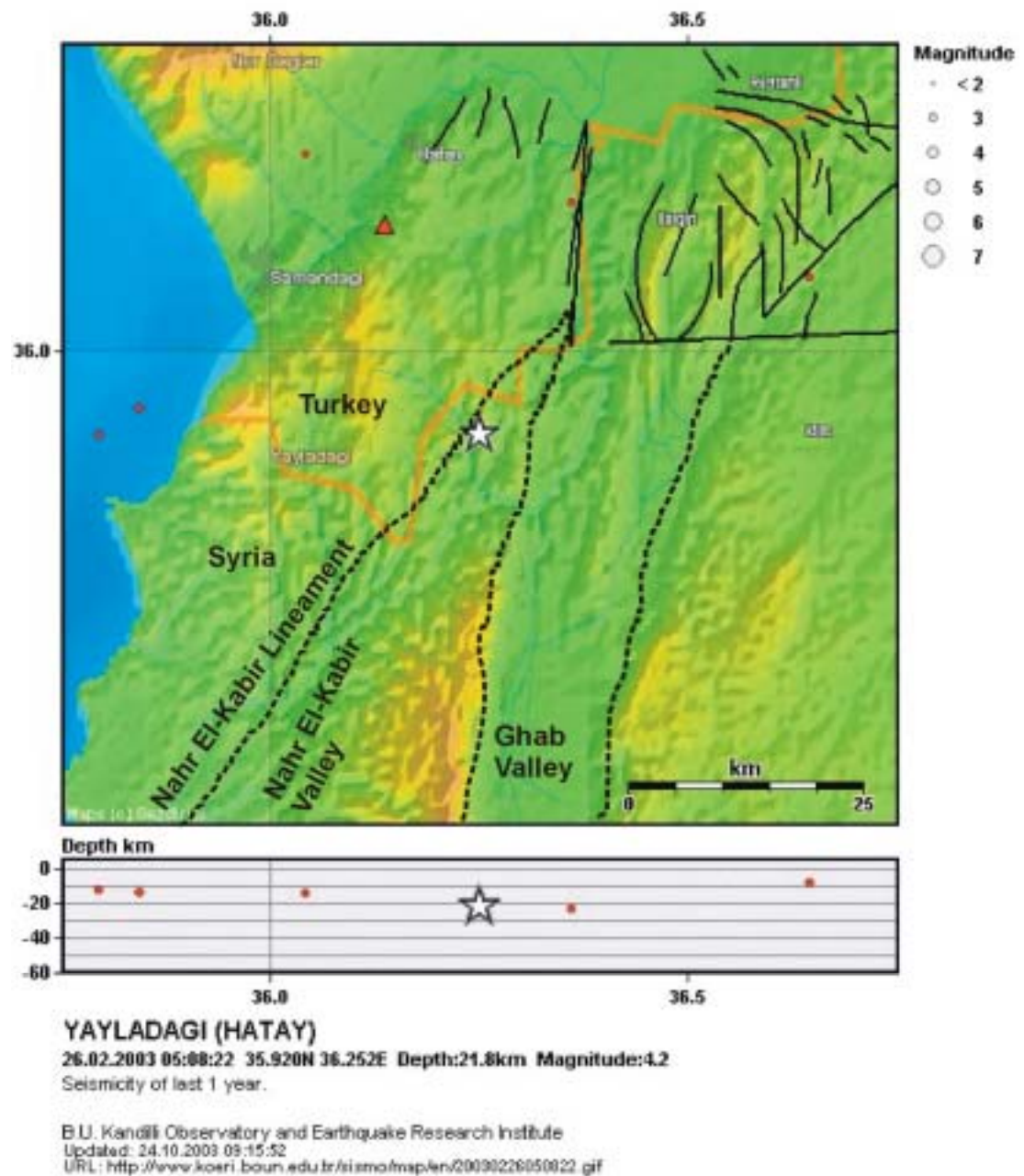
**Figure 4.4** Middle East seismicity recorded by the United States Geological Survey between 1975 and 1995. Events greater than magnitude 4 are detailed according to depth. [Http://www.usgs.gov](http://www.usgs.gov)



B.U. Kandilli Observatory and Earthquake Research Institute  
 Updated: 27.10.2003 12:53:48  
 URL: <http://www.koeri.boun.edu.tr/sismolojisi/oneyear.gif>

**Figure 4.5** Turkish seismology data for 2002/2003, as collected by the Kandilli Observatory. The project area is marked (see above) and one earthquake was recorded within the area (yellow spot). Offshore lineaments appear active in the Eastern Mediterranean

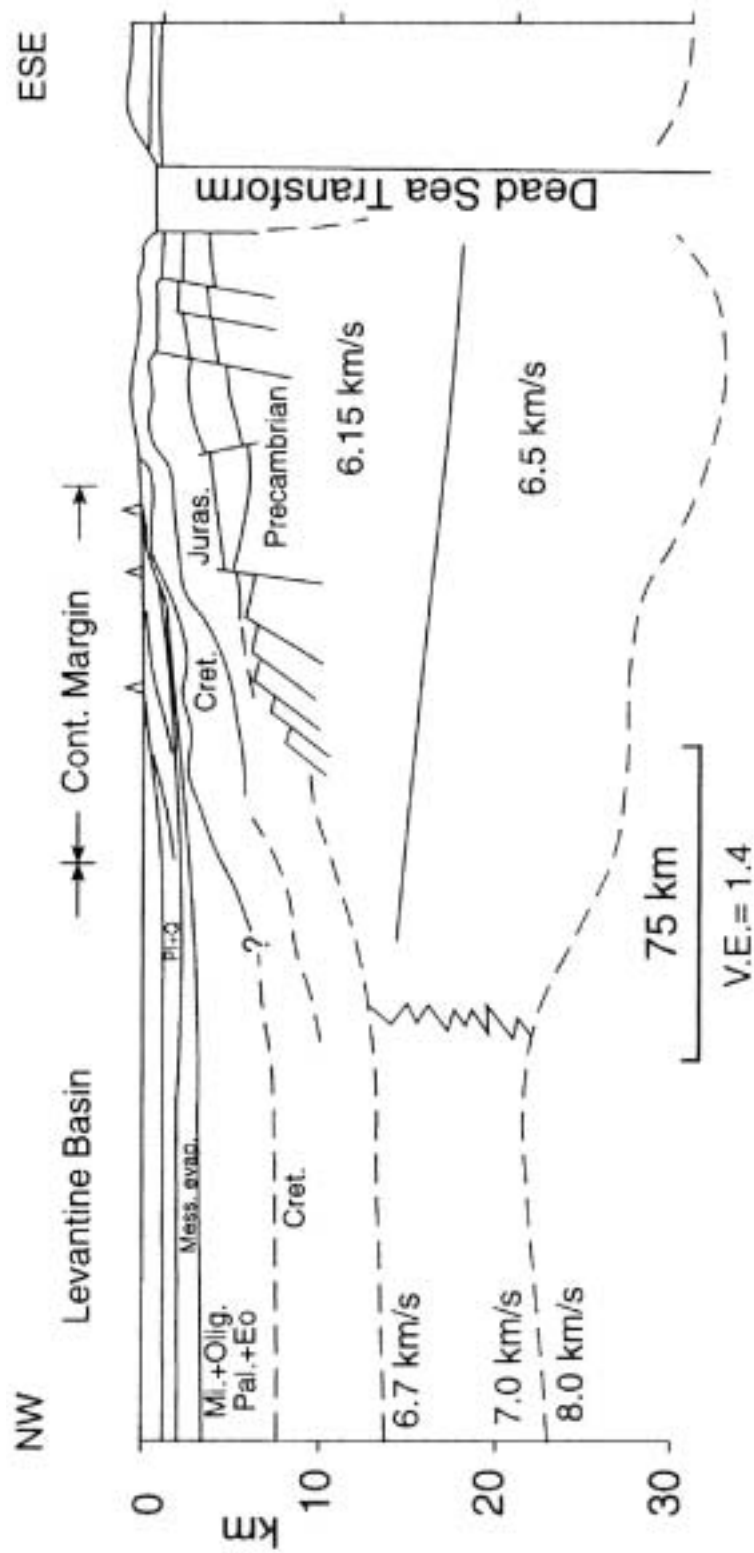




**Figure 4.6** Active seismic events over the period 26/2/02 - 26/2/03, as recorded by the Kandilli Observatory, Turkey. Note the major seismic event on trend with the projection of the Nahr El-Kabir lineament. No faults have been mapped in the earthquake area prior to this study.

..... Projection of major lineaments from the study area superimposed on earthquake map.





**Figure 4.7** From Vidal et al. (2000A). Velocity profile and crust thickness beneath the Levant Basin and Levant continental margin. Data from Garfunkel (1998).

## ***Regions of structural detail***

### **El-Kabir Lineament**

#### ***Introduction***

The El-Kabir Lineament separates the Baer-Bassit Ophiolitic Massif from the Nahr El-Kabir Valley, trending ENE from the city of Latakia. It was previously named the 'Latakia-Killis Fault' (or 'Latakia Geosuture') by Ponikarov et al. (1963, 1966) in their mapping. They proposed that this fault was a thrust, responsible for the emplacement of the Baer-Bassit Massif. This fault was reported to link Latakia City with the town of Killis in southern Turkey (north of Aleppo, 150km northeast of the project area)(Figure 1.4). Since their work, the Kizildag ophiolite has been identified as matching their location in Turkey, so their idea would imply that the Kizildag and Baer-Bassit ophiolites were emplaced and associated with the same fault. The 'Latakia-Killis Fault' in their mapping is cross-cut and offset by the northern extent of the Dead Sea Transform Fault. More recent work (Domas, 1989; Trifinov et al., 1991; Devyatkin et al., 1997; Brew et al., 2001; Zanchi et al., 2002) speculates that the faults mapped to the east of the Ghab Graben are related solely to the Plio-Quaternary graben (see Chapter 5).

In this work, I was able to study the El-Kabir Lineament both in the field and in offshore seismic data, west of the Ghab Graben. In this chapter, I will argue that the El-Kabir Lineament has a long-lived movement history with definite movement episodes during the Eocene and Plio-Quaternary to the present day. Miocene movements are inferred (see Chapter 3). Chapter 6 synthesises all of the evidence of faulting with the sedimentology and puts forward a combined hypothesis that this lineament marks the Anatolian-African plate boundary.

#### ***Fieldwork - summary***

In the field, the El-Kabir Lineament is identified mainly through the juxtaposition of stratigraphic units. There are, however, no piercing points along the fault. The Miocene fill of the Nahr El-Kabir Valley terminates abruptly against the Baer-Bassit Ophiolitic Massif, with only Eocene and Aquitanian successions overlying this contact to any extent and even then, never by more than a few hundreds of metres. Proximal deposits are always found close to the fault, mainly consisting of conglomerates with ophiolitic clasts (see Chapter 3). Where finer-grained sediments exist they appear as 'broken formations', intensively fractured and smeared, or with pervasive pressure solution cleavage. This intense

disruption has resulted in kinematic data being very scarce along the lineament. Figure 4.8, shows some of the fault and bedding data associated with the fault, which provides evidence of sinistral strike-slip as the most recent movement episode (see below). Figures 4.9, documents in detail well exposed faulting along the coast. This locality is one of the best preserved sites in the region for recording structural data.

#### *Field evidence*

Ponikarov et al. (1963) mapped a discontinuous fault trending sub-parallel to the northern extent of the northern margin of the Nahr El-Kabir Valley. In their summary of the mapping region (Ponikarov et al. 1966 & 1967), this fault was stated as being latest Cretaceous in age and responsible for the emplacement of the Baer Bassit Massif. Later work in this region has either ignored this feature completely or restated this hypothesis (Krashennnikov, 1994; Brew et al. 2001).

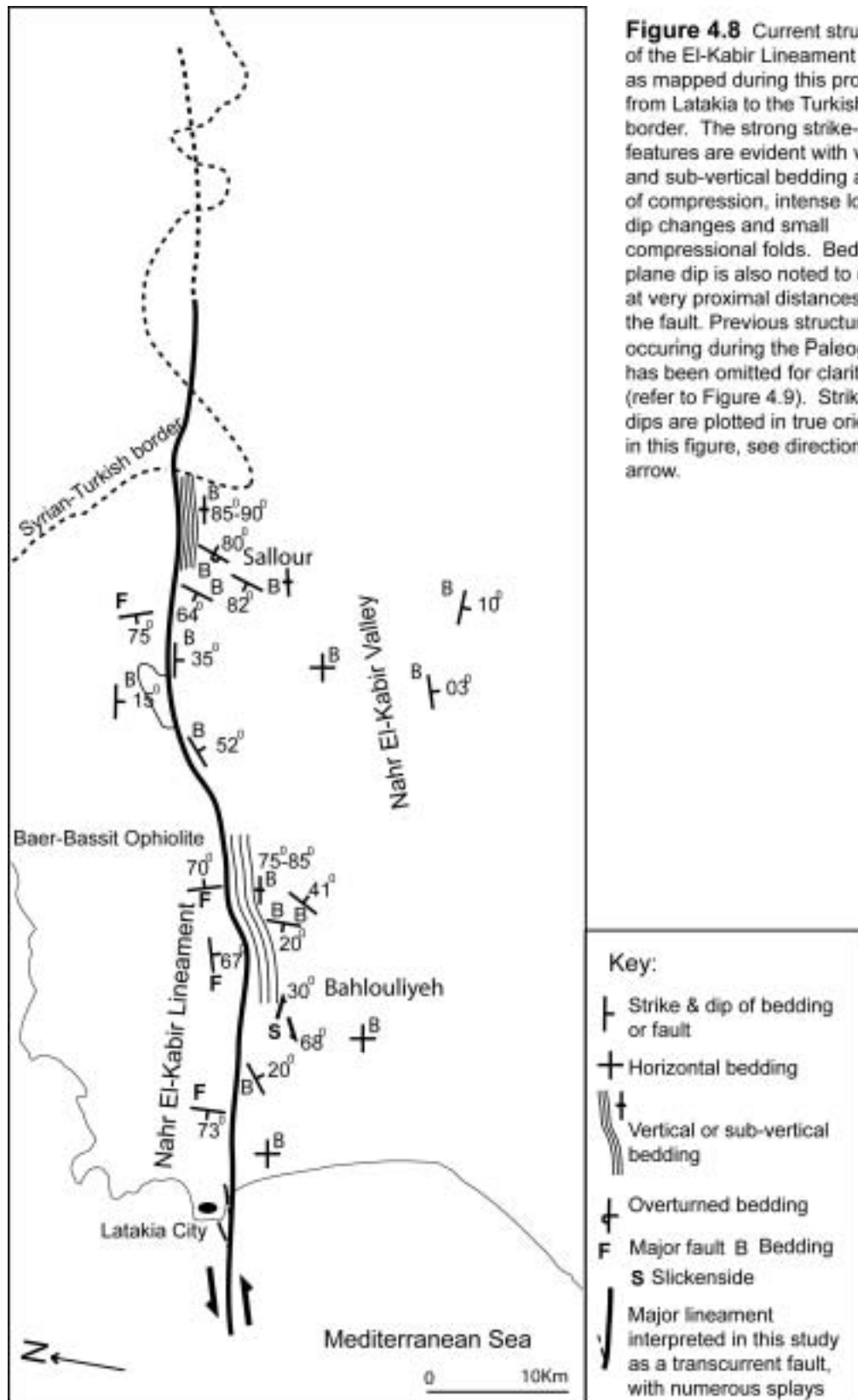
In the field the northern margin of the valley is typically delineated by a steeply rising ridge in the south (near Latakia City) or by broken formations of sedimentary rocks abutting ophiolitic massif rocks further north. Miocene-age strata are locally sub-vertical in these northern localities. Slickensides are very rare, as are visible fault planes.

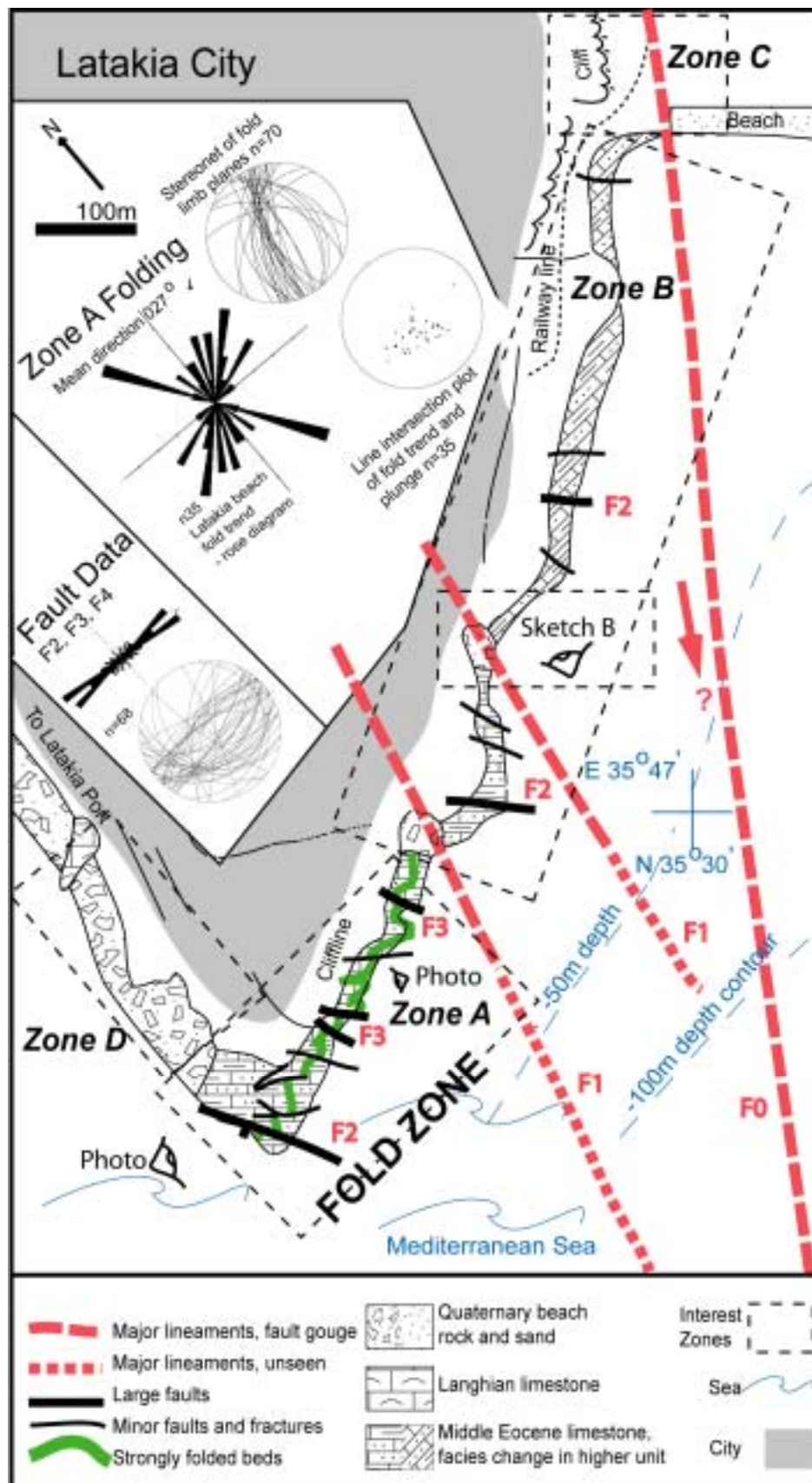
In this study, the lineament and associated features are described from south to north (Latakia City to Sallour Village), as follows:

#### *Latakia City beachfront*

If the northern margin of the Nahr El-Kabir Valley is projected as a line south to the sea, then this projection is directly to the south of Latakia City (not mapped by Ponikarov et al. 1963). Latakia City is built on a raised platform (10-20m high) of Middle Eocene-age limestone overlain by localised Miocene bioclastic limestones and Quaternary beach-rock. Directly south of Latakia City, the coastline is a flat Quaternary beach overlying Pliocene-age marls. The beachfront is a 500m long outcrop, shaped in a right-angle, north to south, west to east (Figure 4.9). It is described from north to south, which is the inferred younging direction.

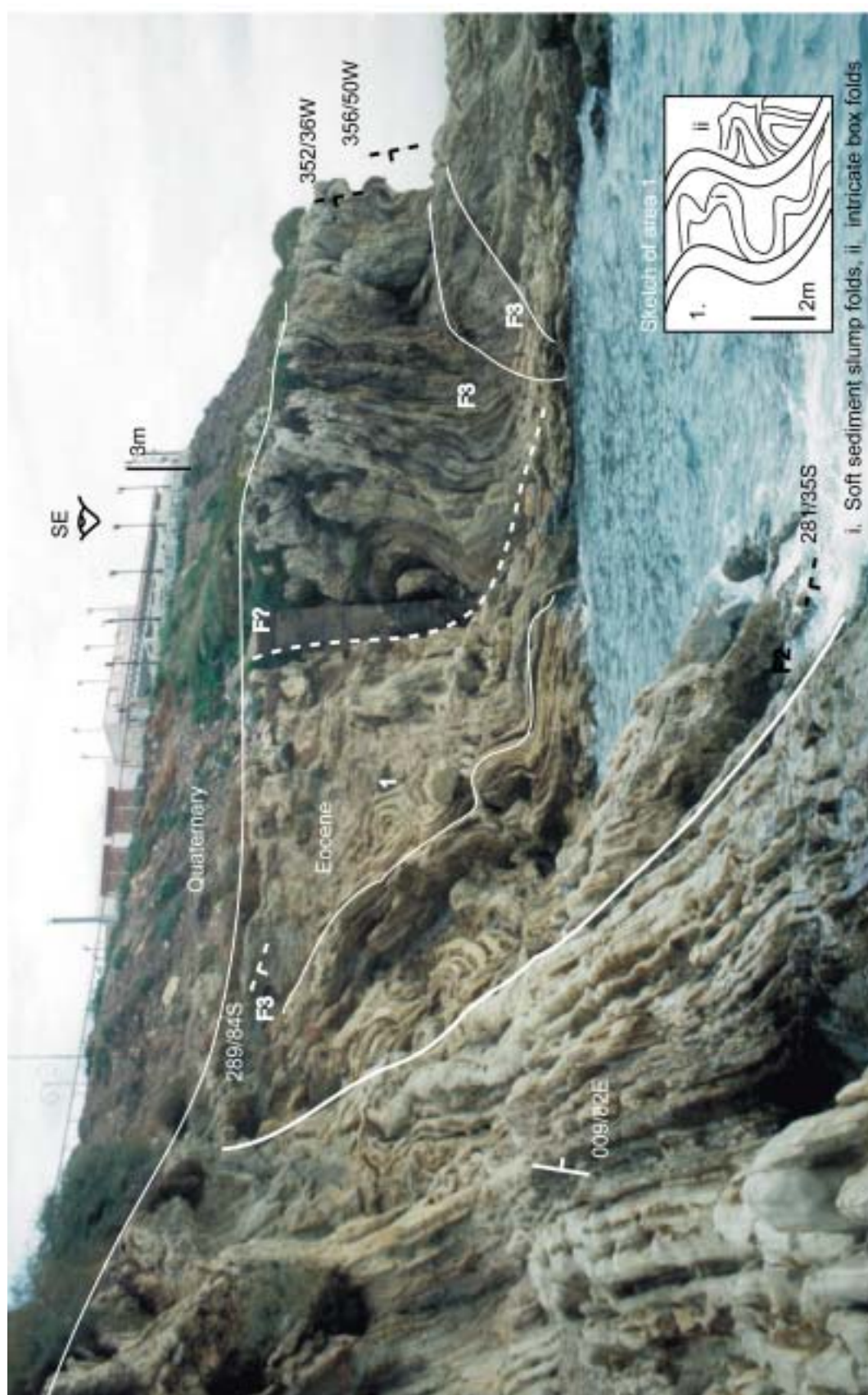
The raised beachfront at Latakia City exhibits intense folding and faulting of Eocene-age strata (Figure 4.10). These intensely disturbed rocks are overlain by Quaternary-age deposits which exhibit neotectonic disruption. Evidence gathered in the field shows that folding occurred prior to faulting (all folds are cut by faults) and there is more than one fault orientation and episode of fault movement (Figure 4.10 and 4.11).





**Figure 4.9** Description of the Middle Eocene outcrop at the Latakia seafront. Major faults, slump folding and fracturing is present. Faulting offsets folding.





**Figure 4.10** A view of the main folded section, parallel to the El-Kabir Lineament. Complex box folds and plastic deformation is apparent, cut by later faulting.





**Figure 4.11** A view of post-slump faulting of the Eocene limestones at the main Latakia beach locality. The Eocene succession is overlain by Quaternary deposits. The fault is not visible in the Quaternary strata and offsets similar intensively folded Eocene slumped limestones in both hanging and footwall blocks. Fault gouge is prominent in a zone approximately 5cm thick, but no kinematic data are preserved in what appears to be a normal fault. Oblique view to Fig 4.10.

*Latakia City beachfront folding*

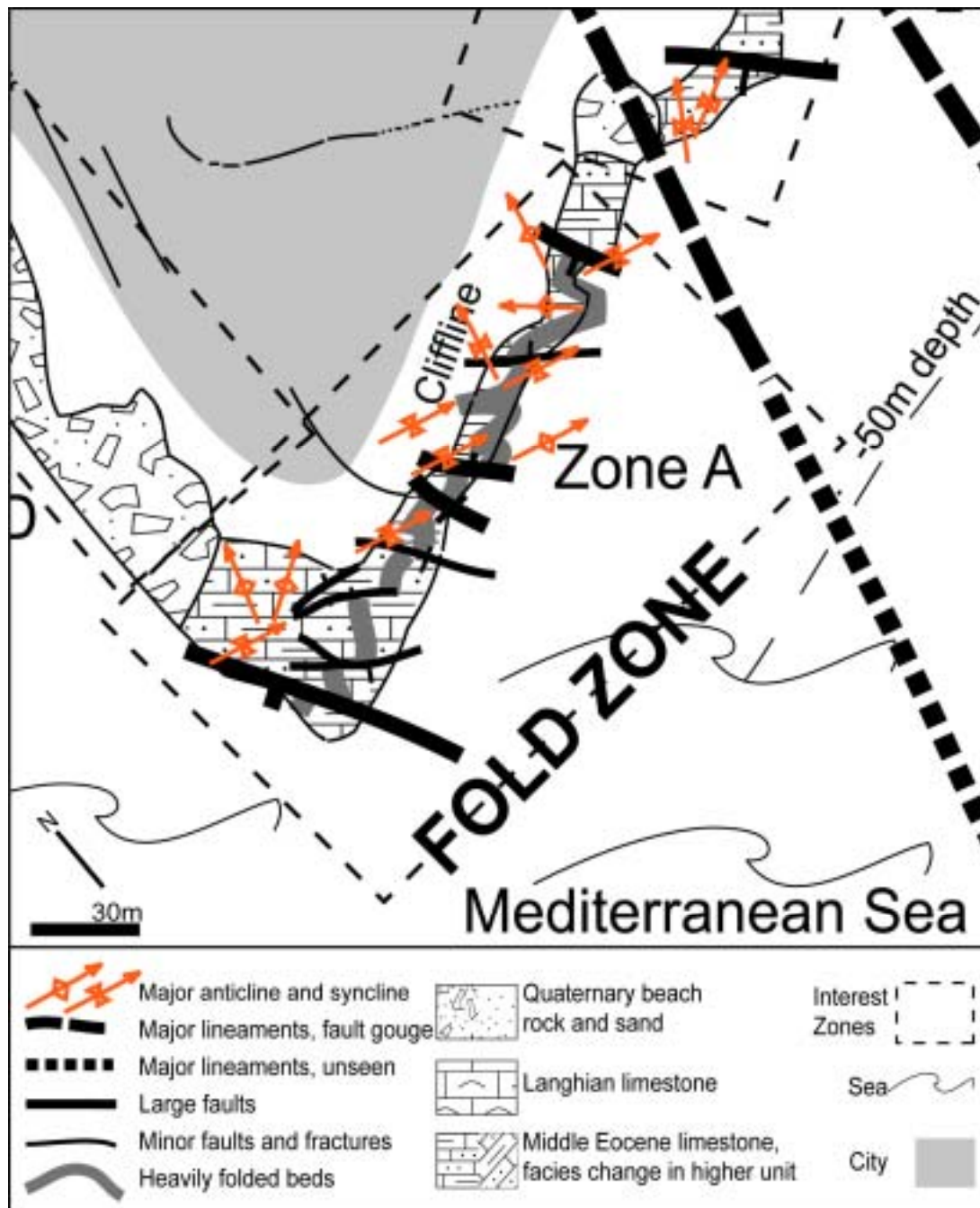
Folding is not limited to one particular orientation. Folds plunge in all directions from north-northwest to south-southeast (Figure 4.12), in alternate limestone and marl lithologies (see Chapter 3). Fold orientation and plunge varies dramatically from fold to fold, even where adjacent. Large folds contain smaller folds, often as intricate box (conjugate) folds (Figure 4.10). When plotted on a stereonet, no preferred orientation is apparent, except that NW-W to E-SE orientations are absent. However, the majority of fault strike orientations plot west-northwest to east-southeast (see below). Individual folds pinch and swell, with highly variable bed thicknesses and fold amplitudes.

Folding varies considerably from north to south. It is not observed in the outcrops directly north of Latakia City. At the northern extent of Eocene-age beach-front exposure, sub-vertical beds with intercalated debris flows are common. Moving south (over a distance of 150m), the beds become progressively more disrupted, and folds become tight or isoclinal. Parasitic folding becomes progressively more common. This extensive folding abruptly ceases at the first major fault to cut the succession (most northerly inferred F<sub>1</sub> fault, Figure 4.9). Beds further south and east dip steeply to the south, with minor folding. These folds are poorly developed by comparison to those described previously. Faulting is often associated with the folds closest to Latakia Beach.

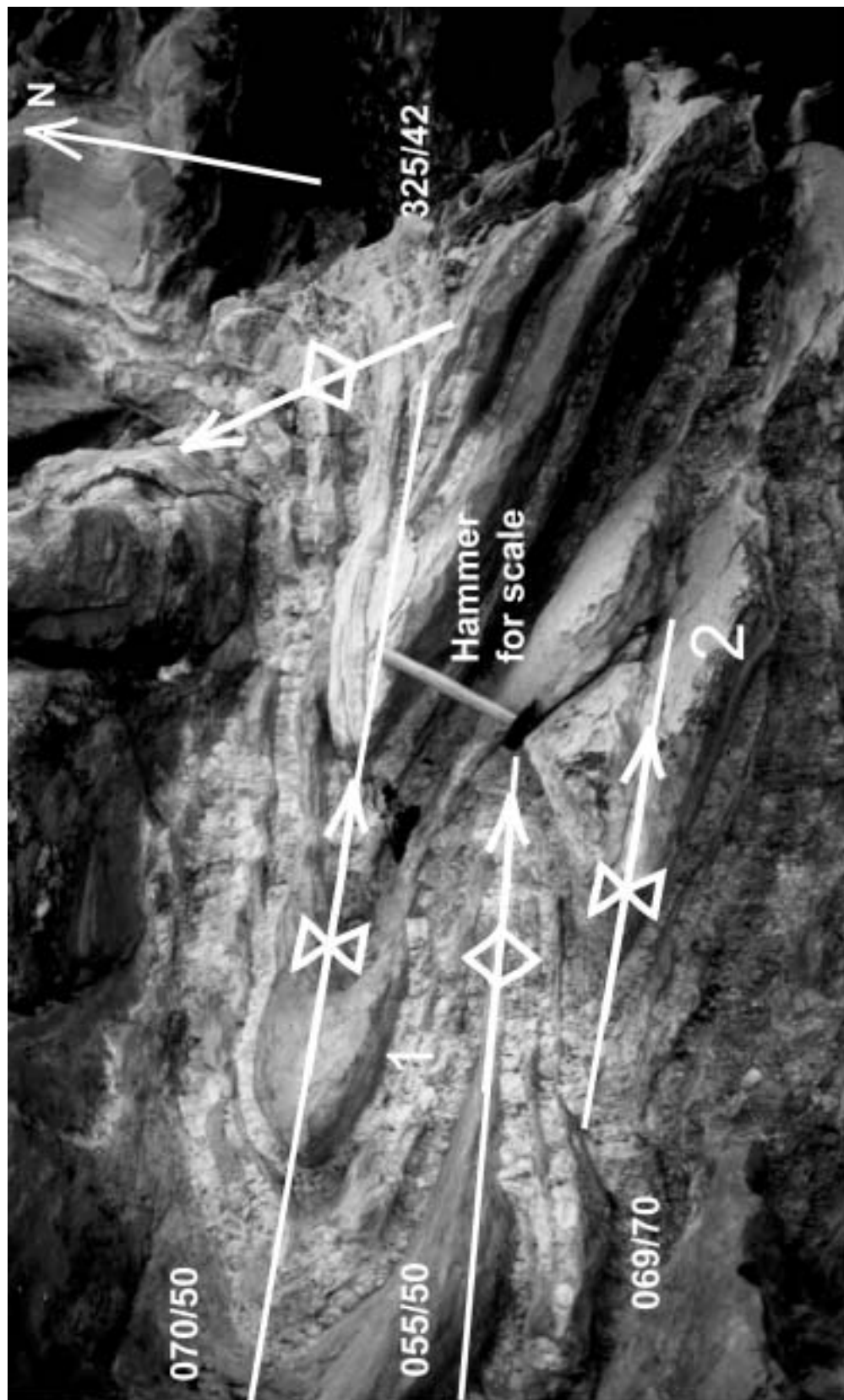
Here the folds are interpreted not as true tectonic folds but instead as soft-sediment slumps (see Chapter 6). The lack of predominant orientations and intensifying convolution near a major inferred fault could indicate that soft-sediment deformation (shear and slumping, Figure 4.13) is the main process (Tucker et al. 1990). Parasitic, conjugate folds are thought to be indicative of slumps rather than tectonic folding. Liquefaction of the sediments is not evident, perhaps due to partial lithification and shallow burial rather than disturbance on the sea-floor (Maltman, 1994). A 'stick through treacle' analogy might be appropriate. Partial lithification would probably indicate a Middle to Late Eocene-age of deformation.

*Latakia City beachfront faulting*

Faulting at Latakia Beach is complex. The faults cut the folds. Stereonet plots of all the fault strikes (Figure 4.9), show a predominant E-W trend in fault orientation. However, the main orientation from the major faults is less clear; every orientation is apparent. The F<sub>2</sub> and F<sub>3</sub> faults shown on Figure 4.9, are clearly NW-SE to N-S orientated, although few in number.



**Figure 4.12** A close-up view of the previous figure showing ZONE A and emphasising the orientations of the major folds seen throughout the Eocene strata. The structural data are plotted on the stereonet with the previous figure and shows that the orientations of plunge vary from NW to SE. Plunge angle also varies from sub-horizontal to sub-vertical, often in adjacent folds.



**Figure 4.13** Detailed structure of the Eocene slumped marls and limestones on Latakia beach (see Figure 4.9, for location). Such fold orientations are unlikely to have been produced by close proximity to active faulting before lithification.



F<sub>1</sub> and F<sub>0</sub> (i.e. extremely large faults) are inferred, based on geomorphological evidence but are not directly observed. Intense fault gouge is present within the cliff-face at the points indicated (?Quaternary age movement, Figure 4.14).

F<sub>4</sub>, fractures are orientated predominantly E-W. These fractures are often calcite filled and also contain bitumen. The only indicator of fault timing is that beachrock (?Middle to Late Quaternary) is cut or included to the fracture. This is not observed in the NW-SE faults; therefore, their timing cannot be constrained between the Late Eocene to Pliocene.

Fault throw is a combination of normal throw and strike-slip (commonly oblique and both sinistral and dextral). The larger (F<sub>2</sub> and F<sub>3</sub>) faults are essentially normal, extensional faults, with some transpressional faults (i.e. positive flower structures). Fractures (F<sub>4</sub>) are typically small strike-slip faults, mainly sinistral, but many show more than one sense of movement or multiple small movements. The inferred F<sub>1</sub> and F<sub>0</sub> faults are likely to be strike-slip faults due to offset sections of the same stratigraphical unit. Sinistral movement is implied as the Latakia outcrop appears to be displaced sinistrally from the shoreline (see Chapter 6).

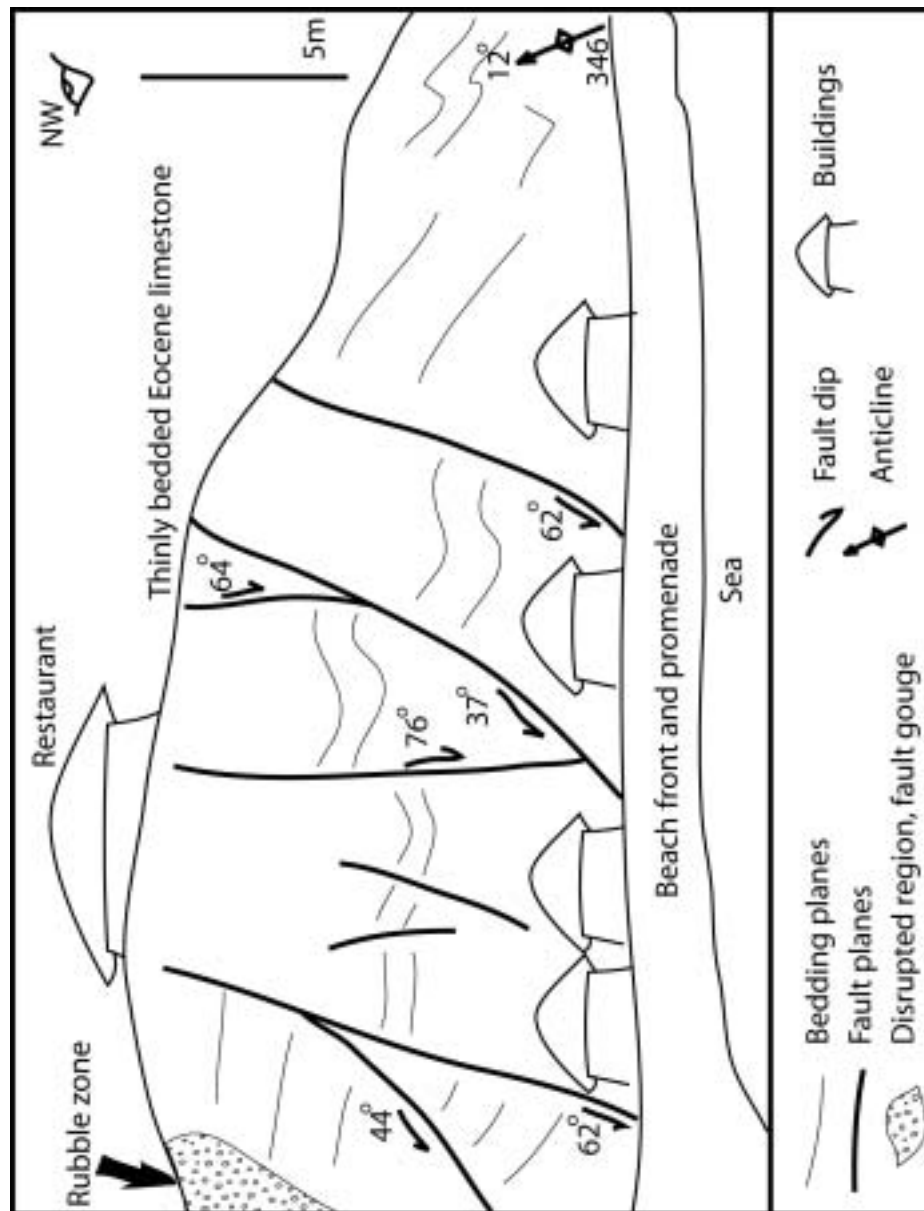
#### *Latakia Beach summary*

There is no definitive evidence of large faults and fault motion at this locality. Too little information is preserved, and there are no well defined contacts to establish timing of events. However, the fact that folding and faulting, is of an intensity not observed at any other locality within the region, is indicative of large structural events.

If the interpretation above is correct, then large fault movements have occurred in the Middle to Late Eocene (i.e. inducing slump folding). Minor faulting occurred in the Neogene (i.e. extensional and transpressional, large faults) and most recently in the Quaternary (i.e. intensive E-W fracturing). Two other sites on the El-Kabir Lineament were also investigated to test these inferences.

#### *Near Bahlouliyah Reservoir*

At the time of the Russian mapping, the large Bahlouliyah Reservoir had not been built (see Figure 4.8 and pull-out maps). Ponikarov et al. (1963) mapped a repeated series of fault-bounded slices containing Maastrichtian, Middle Eocene and Early Miocene-age strata, younging east. During this work, this area was re-investigated, since their map implies



**Figure 4.14** ZONE B faulting in close proximity to a major splay (synthetic) fault of the El-Kabir Lineament. In outcrop, this major fault is identified only as a zone of intensive fracturing and rubble (to the left of the diagram), which can be traced onshore from the cliff-line. These proximal faults cross-cut the Eocene folded beds and are normal or strike-slip in throw sense.



Middle Miocene-age or later faulting. Description of this region in the Russian mapping report is absent (Ponikarov et al. 1966).

In the field, the mapped units are not readily discernable. Intensive fracturing has occurred. Careful observations, sample collection and subsequent dating (by Marcelle BouDagher-Fadel) were employed. The mapped successions of Ponikarov et al. (1963), could not be replicated at this locality (immediately south of the reservoir or up to 5km further north), where fault slices of Miocene-only strata were mapped.

Along the north bank of the reservoir, the contact with the Baer Bassit Ophiolitic Massif is visible. This is the only locality along the entire Baer Bassit Ophiolitic Massif, that the contact can be observed directly. Pervasively fractured Upper Langhian-age limestones, dipping steeply east (almost sub-vertically), overlie fractured ophiolitic rocks. Rare, widely distributed, slickensides indicate oblique sinistral and dextral motion, in an east to west orientation or sub-horizontal sinistral north-south strike-slip motion (Figure 4.8). The ages of these motions could not be determined.

Moving east into the mapped 'slice' zones, the succession returns to Burdigalian strata, progressing upwards to Langhian-age detrital limestones. Little sign of disturbance is seen within these rocks and they dip gently east.

From this study the mapping of 'slices' of strata by Ponikarov et al. (1963) could not be confirmed. A fault contact (with strike-slip episodes) between the ophiolitic massif and Miocene age strata can be observed, in a zone approximately 50-100m wide. At the southern extent of the reservoir, similar features are less well exposed and the disrupted strata are thought to be of Palaeogene or Aquitanian-age. Directly to the east of this area, shallow dipping, unfaulted successions are again observed.

Two kilometres north of the Bahlouliyah Reservoir, a small outcrop of Miocene age strata, thought to be in close contact with the Baer Bassit Ophiolitic Massif, is sub-vertically bedded. Structurally it is accompanied (300m northeast) by a poorly exposed, north-south trending anticline. The El-Kabir Lineament trends northeast (see Figure 4.8 and pull-out geological map) and bends north (20-30°) at this point. This is perhaps indicative of compression on a bend in a strike-slip fault, which would indicate sinistral motion.

#### *Interpretation of Bahlouliyah*

The interpretation of this area is based on the evidence of small outcrops of intensely faulted and fractured rocks. 'Slices' of strata are not apparent. It is inferred that this region was

structured due to rotation of small fault blocks of Palaeogene and Early to Middle Neogene-age rocks within a strike-slip fault zone. Exposure is too poor to accurately re-map this area.

#### *Sallour Village*

Sallour Village is close to the Syrian/Turkish border, north of the Nahr El-Kabir Valley (Figure 4.8 and pull-out maps). Ponikarov et al. (1963) mapped vertical Aquitanian-age strata, forming a 5km long, sub-parallel contact with the Baer Bassit Massif.

During this study, this heavily-wooded area was revisited. The contact with the ophiolitic massif is not seen, but consists of very broken Aquitanian-age chalky limestones. Two hundred metres south, sub-vertical beds, running sub-parallel with the contact crop-out (100m thick, rather than the 1km mapped by Ponikarov et al. 1963). The Aquitanian-age sediments are 'dirty' (see Chapter 3), containing more organic material than observed elsewhere and are also occasionally overturned (dipping 80° to the south). A further 200m south, Aquitanian strata are not directly observed until they crop-out again as sub-horizontal beds, unconformably overlain by clastic-rich Burdigalian limestones. To summarise, the base Aquitanian contact is not seen, but over a distance of half a kilometre, the strata commence as a 'broken formation', are tilted vertically and then return to a more usual sub-horizontal bedding dip.

The only locality that Langhian-Serravallian-age strata (undifferentiated) can be observed as fault rotated is 4km south of Sallour Village. The outcrop bedding rotations are similar to those closer to Sallour Village, with vertical bedding, interspersed with horizontal strata. Bedding dip changes are for the most part not observable. The section was studied however, at four localities, over a 1km section, moving northwards towards the fault. Sub-vertically bedded Langhian-Serravallian-age rocks are transitioned to sub-horizontal, then directly adjacent to sub-vertical Aquitanian-age rocks. This would date this episode of faulting as post-Langhian-Serravallian-age.

#### *Interpretation of Sallour Village*

The sub-vertical bedding at Sallour Village occurs where the El-Kabir Lineament bends subtly to the east (10-15°)(see Figure 4.8). If the system is strike-slip dominated; sinistral movement near this Sallour Village area would create an area of compression, if dextral this would be in extension. Either motion could produce sub-vertical strata. No slickensides data were recoverable from the soft, chalky limestones, nor were any faults observed. Sub-

vertical bedding is not observed elsewhere within the Nahr El-Kabir Valley; almost all dips are sub-horizontal. The data from the Sallour region identifies an area of intense local deformation and hints that this could be strike-slip related, perhaps due to a series of faults or fault splay.

#### *North of the Nahr El-Kabir Valley*

The El-Kabir Lineament crosses the border into Turkey, north of Sallour village (Figure 4.8). It appears that the lineament could extend back into Syria some 15km further north, where the border meanders further to the north (see pull-out maps), but this region is not readily accessible to field-studies. Careful examination of the SPOT images reveals a possibility to link to the El-Kabir Lineament with the Ghab Graben, but this could not be confirmed by field-studies (see seismology, this Chapter)(Figure 4.2).

#### *Overview of the onshore El-Kabir Lineament*

The El-Kabir Lineament is poorly exposed within the Nahr El-Kabir Valley. Sallour Village to Latakia City is a direct distance of 50km and the ophiolitic massif fault contact is only exposed for approximately 5m, at Bahlouliyah Reservoir.

Direct structural measurements are distinctly lacking. The majority of the contact is a zone of pervasive, un-orientated, tectonised marl breccia, now severely eroded. From the three noted fieldwork localities, a sense of strike-slip motion, or series of strike-slip motions is apparent. Sinistral motion may be the overriding sense of the most recent motion, although this is far from clear. From field evidence, fault movement occurred in the Middle to Late Eocene and probably post-Langhian-Serravallian time (and/or Quaternary). These initial results need to be correlated with the timing of clastic deposition within the valley, especially of ophiolitic derived clast-rich facies. Chapter 6 summarises both sedimentological and structural events, to produce a combined geological setting.

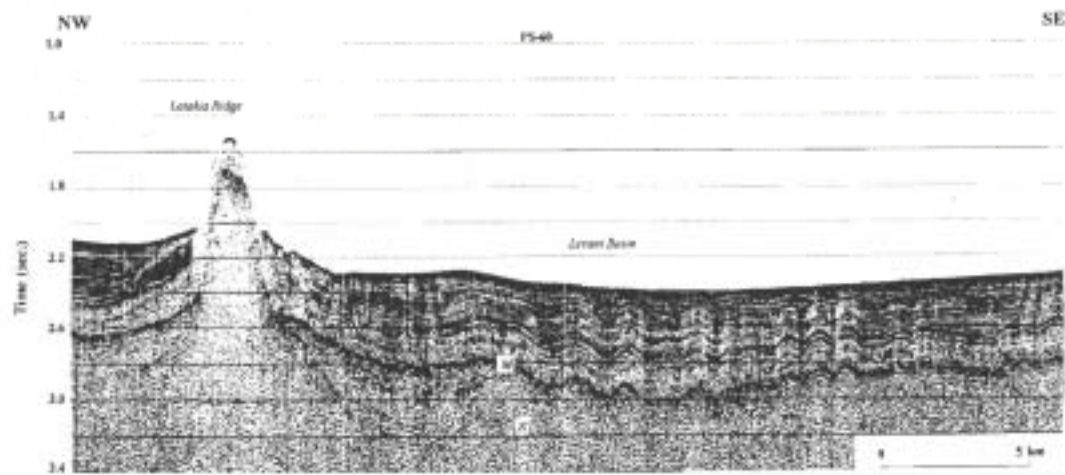
## Offshore Latakia City, the northern margin of the Levant Basin

### *Previous seismic interpretations of the Eastern Mediterranean*

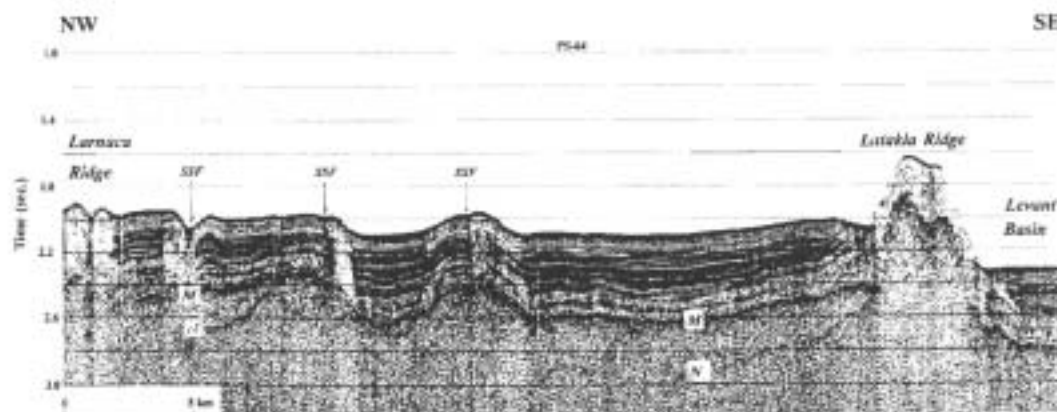
Limited seismic data have been acquired in the Eastern Mediterranean, mainly by Israeli research cruises and by the Russian 'Training Through Research' program. Initial studies (Ben-Avarham et al., 1976; Ivanov et al., 1992; Kempler, 1993; Kempler et al., (1994); Ben-Avarham et al., 1995; Garfunkel, 1998), inferred as to the nature of the crust, interpreted the main basins in the Levant region (Figures 4.15 and 4.16) and made shallow-depth interpretations of the main structural features using high-frequency datasets. Vidal et al. (2000a and b) published the first depth converted study of the main lineaments, which delineate the northern margin of the Levant ('Levantine') basin and infers a connection between the south of Cyprus subduction zone and the Syrian coastline. A synopsis of their work is given below. In this study, access was gained to non-released commercial seismic data and the possibility of tying onshore and offshore datasets together is detailed below. Chapter 6, summarises the key tectonic features and findings of this work.

Vidal et al. (2000a and b) reprocessed and reinterpreted seismic data from the Cruise 5 of the 'R/V Akademik Nikolaj Strakhov' (Hall & Krasheninnikov, 1994). The survey shot six NW-SE orientated lines between Cyprus and 10km offshore from the Syrian coastline at Latakia City (Figure 4.17).

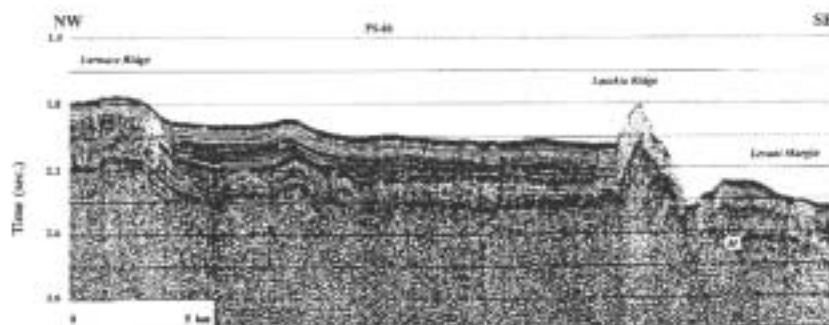
Their seismic profiles are based on two calculations of the crust: 1, Garfunkel (1998) calculated the crustal thickness as increasing from 20km under the Levant Basin to 30km onshore from the African/Arabian continental margin (Figure 4.7). 2, Vidal et al. (2000a and b), indicated that from their velocity profiling of the data, the moho exists at 25km depth beneath the Levant Basin, overlain by 10km of crust. The sedimentary cover above the crust was calculated as being 12-14km thick. The nature of the crust is unknown. Velocity surveys ( $8\text{km/s}^{-1}$ ) initially suggest oceanic crust, but both Robertson (1998) and Vidal (2000a and b) argue that stretched continental crust is likely, probably related to Permian-Triassic rifting. Velocity modeling of the basin sedimentary fill was based on the sedimentary log of southern Cyprus (Figure 4.17).



Part of seismic reflection profile No. 60; M = top Messinian evaporites; and N = base Messinian evaporites. location of profile

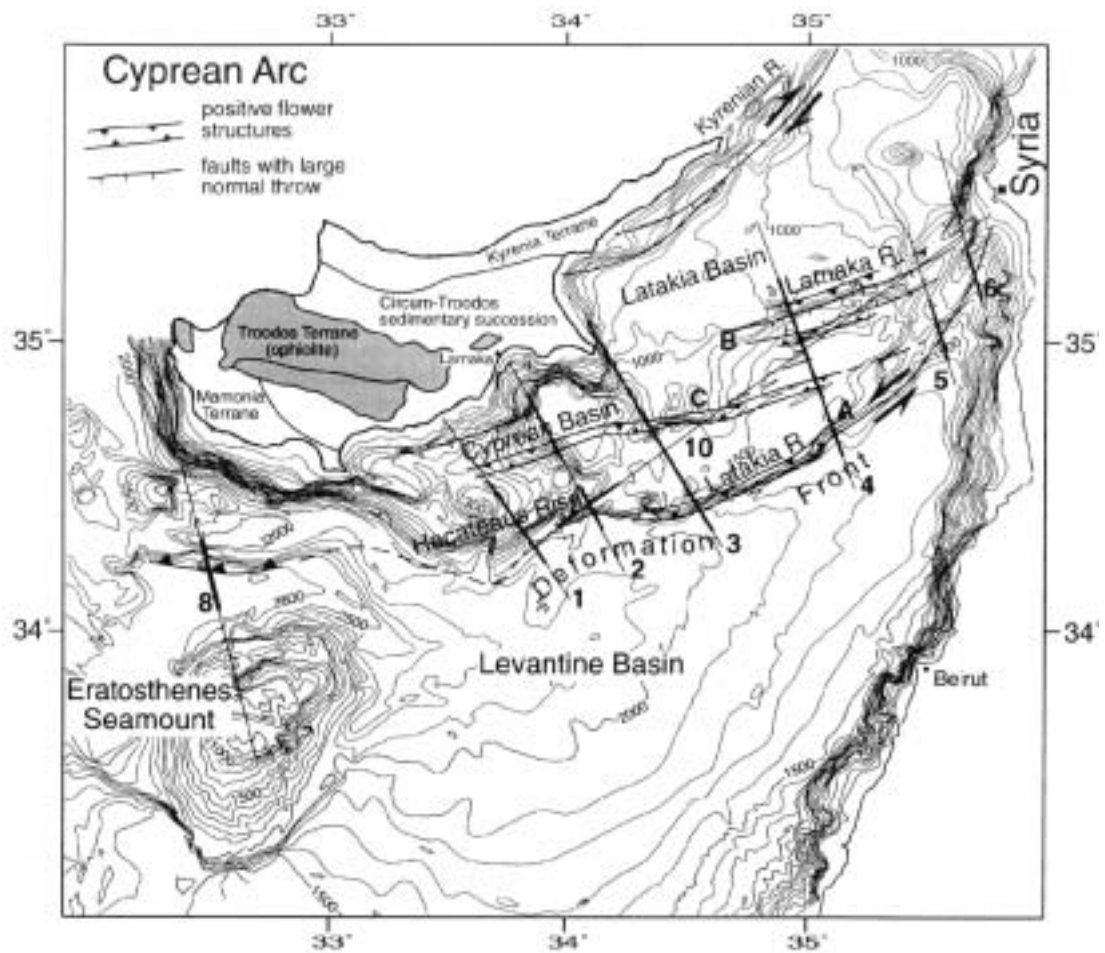


Seismic reflection profile No. 64; M = top Messinian evaporites; N = base Messinian evaporites; and SSF = strike-slip fault.



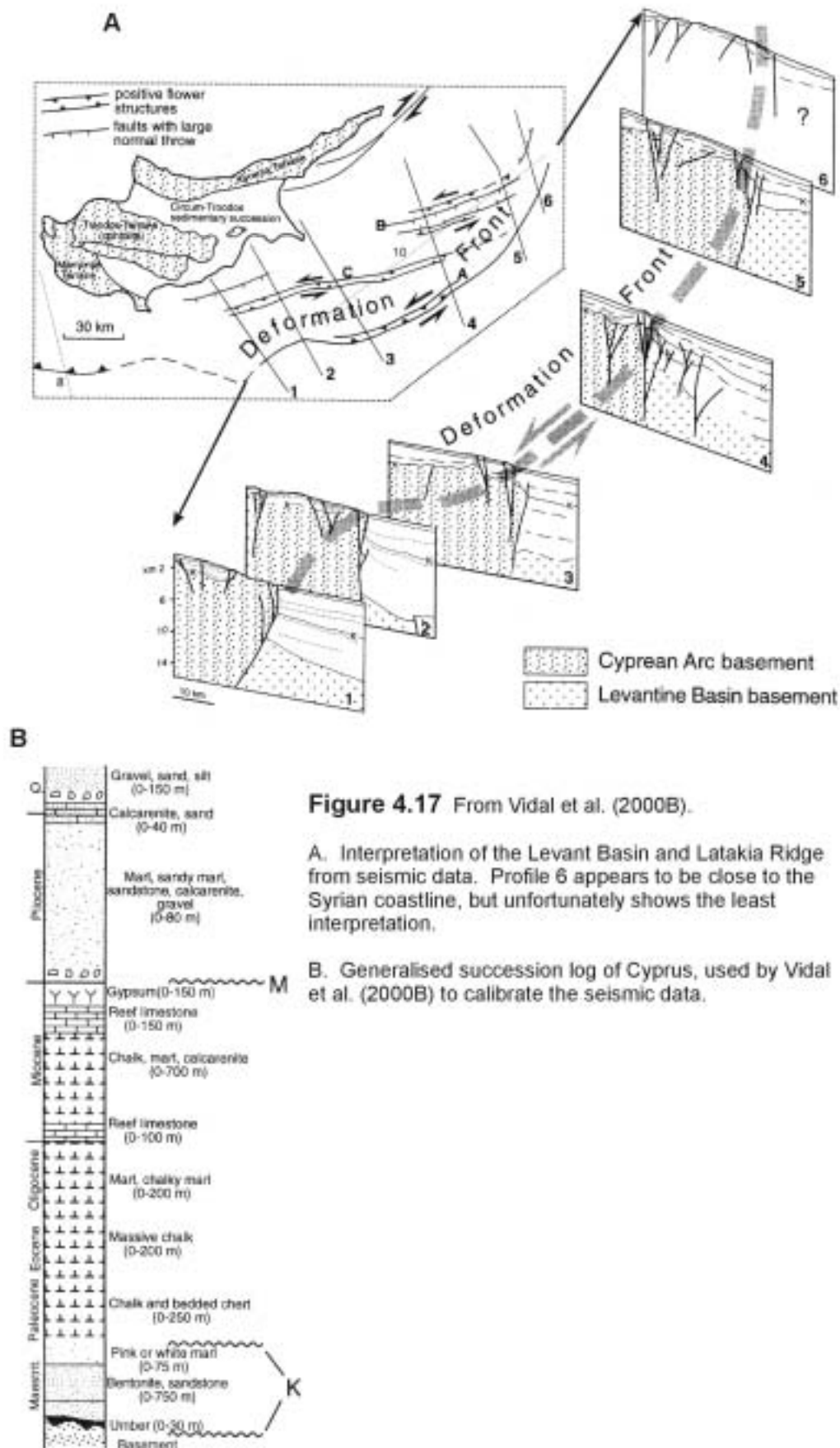
Seismic reflection profile No. 68; M = top Messinian evaporites.

**Figure 4.15** From Ben-Avram et al. (1995). Shallow seismic profiles of the Latakia Ridge on the Eastern Mediterranean. From top to bottom, the profiles are taken progressively west, from approximately 50km offshore Syria. Sinistral movement is inferred on this plate boundary fault and active faulting is evident.



**Figure 4.16.** From Vidal et al. (2000B). Bathymetry of the Eastern Mediterranean from Hall et al. (1994), showing locations of interpreted seismic data and proximity to Syrian coastline at Latakia City (•).

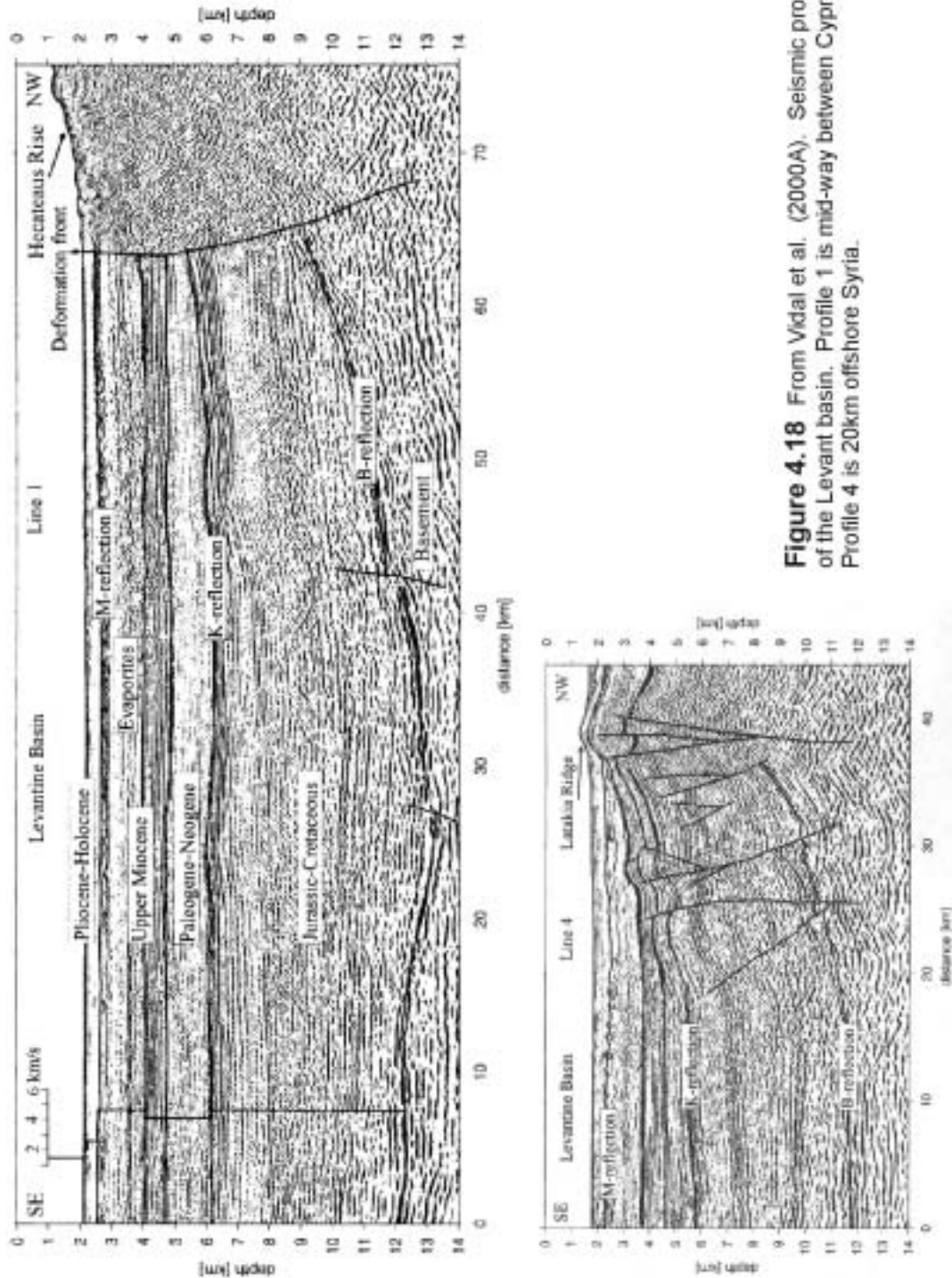




The Vidal et al.s (2000a and b) interpretations are based on three reflectors (M, K & B; Figure 4.18), none of which has been drilled (or data released) in this region of the Levant Basin (refer also to Seismic reflection data, this chapter):

- ∄ The M reflector represents the Messinian Salinity Crisis (Hsü et al. 1973; Ryan et al. 1973) evaporites. Vidal et al. (2000a and b) calculates that 500m of Plio-Quaternary sediments overlie 1500m of evaporites (probably anhydrite and halite), that form a prominent high-velocity, high amplitude reflector. This reflector is seen on every section and covers most fault structures.
- ∄ The K reflector marks the base Tertiary and is less distinct, but often discordant with the underlying Cretaceous (5-6km beneath sea-level). The thickness between M and K reflectors is highly variable.
- ∄ The B reflector is the deepest and hardest to define as noise is prevalent in the sections (11-12km beneath sea-level). This basement reflector is usually subtly dipping or sub-horizontal. Vidal et al. (2000a and b) state that up to 4km of pre-Cretaceous-age fill is likely to be present in the Levant Basin.

The seismic interpretations by Vidal et al. (2000 A & B) are shown by Figures 4.17 and 4.18. They detail the northern margin of the Levant Basin and the Latakia and Larnaca Ridges. Their work reinterprets these ridges (after Kempler, 1993; Kempler et al., (1994); Ben-Avraham et al., 1995) as having a sinistral strike-slip motion and implies that the ridges coalesce near the Syrian coastline at Latakia City, on topographic features which correspond to the bathymetry mapped by Hall & Krasheninnikov (1994). The Latakia Ridge is interpreted to mark the southernmost extent of the deformation front and is inferred to represent the continuation of the plate boundary running south of Cyprus (Robertson, 1998). It is described as a 'sharp tectonic boundary' and as a 'few kilometers wide sub-vertical fault zone' (Vidal et al. 2000a and b). These authors go on further to state east of Cyprus (towards the Syrian coastline), the faults can be interpreted as a linked strike-slip system with positive flower structures (an easily identifiable ridge on the sea-floor). The reflectors they mapped, thin towards the ridge, especially those of Messinian to Recent-age. However, the published profiles closest to the coastline give the least detail (Figure 4.17).



**Figure 4.18** From Vidal et al. (2000A). Seismic profiles of the northern margin of the Levant basin. Profile 1 is mid-way between Cyprus and Syria (50km offshore), Profile 4 is 20km offshore Syria.

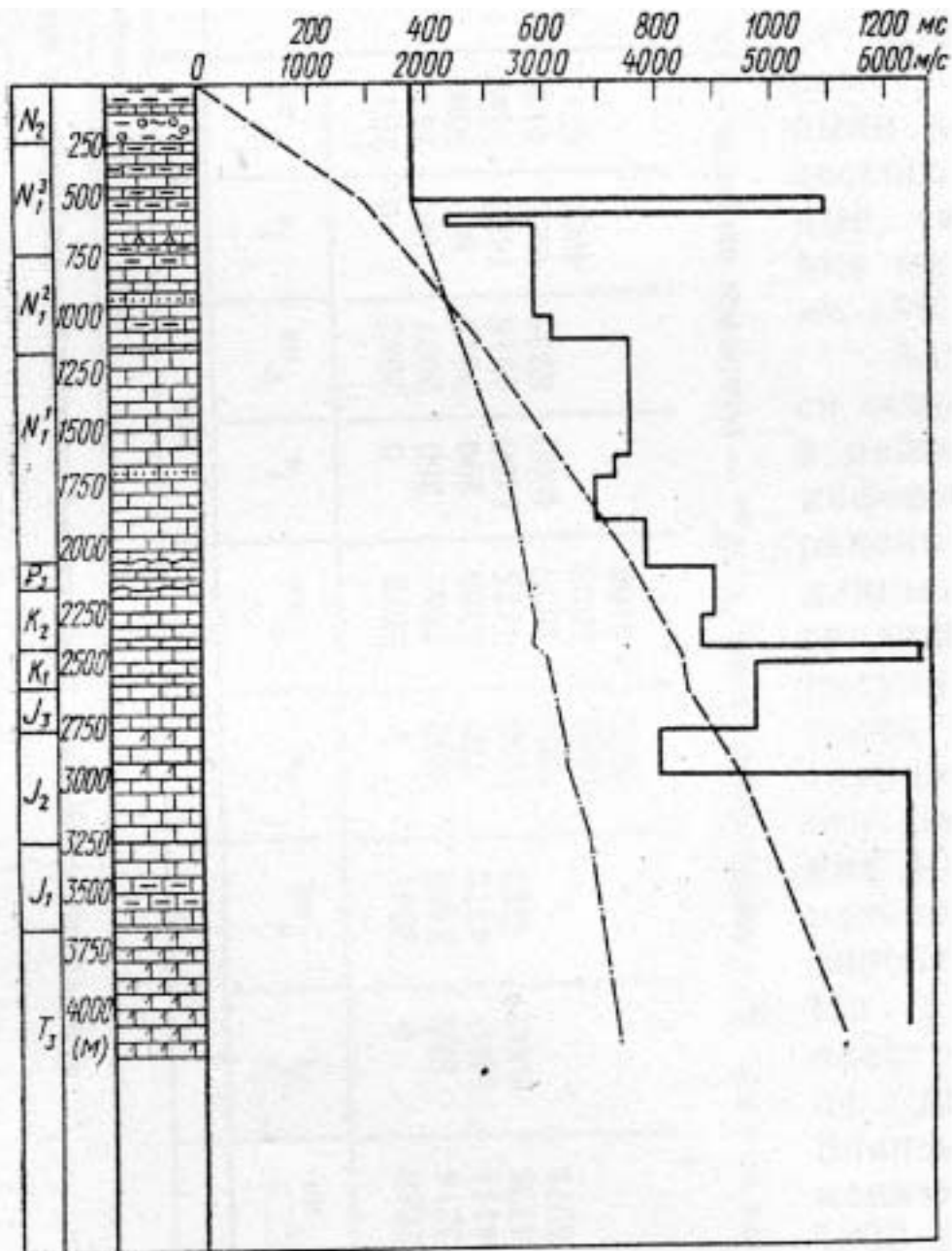
*Syrian well data*

Figure 4.19 shows the well log interpreted by Dzhabur (1985). As previously stated (Chapters 2 and 3), the author published a well log of Nahr El-Kabir Valley stratigraphy from the Fidjo 1 well, near Latakia City. The well is situated within the Quaternary plateau, south of the city and is the closest well data to the offshore sections. Dzhabur (1985) presented a sonic log which infers a gradual increase in velocity. His velocities for the Plio-Quaternary are:  $1800 \text{ ms}^{-1}$ , Messinian evaporites  $5400 \text{ ms}^{-1}$  (65m), with the remainder of the Tertiary section increasing from  $2000\text{--}4000 \text{ ms}^{-1}$ , 2147m total. The Cretaceous is marked by increases to  $6000 \text{ ms}^{-1}$ .

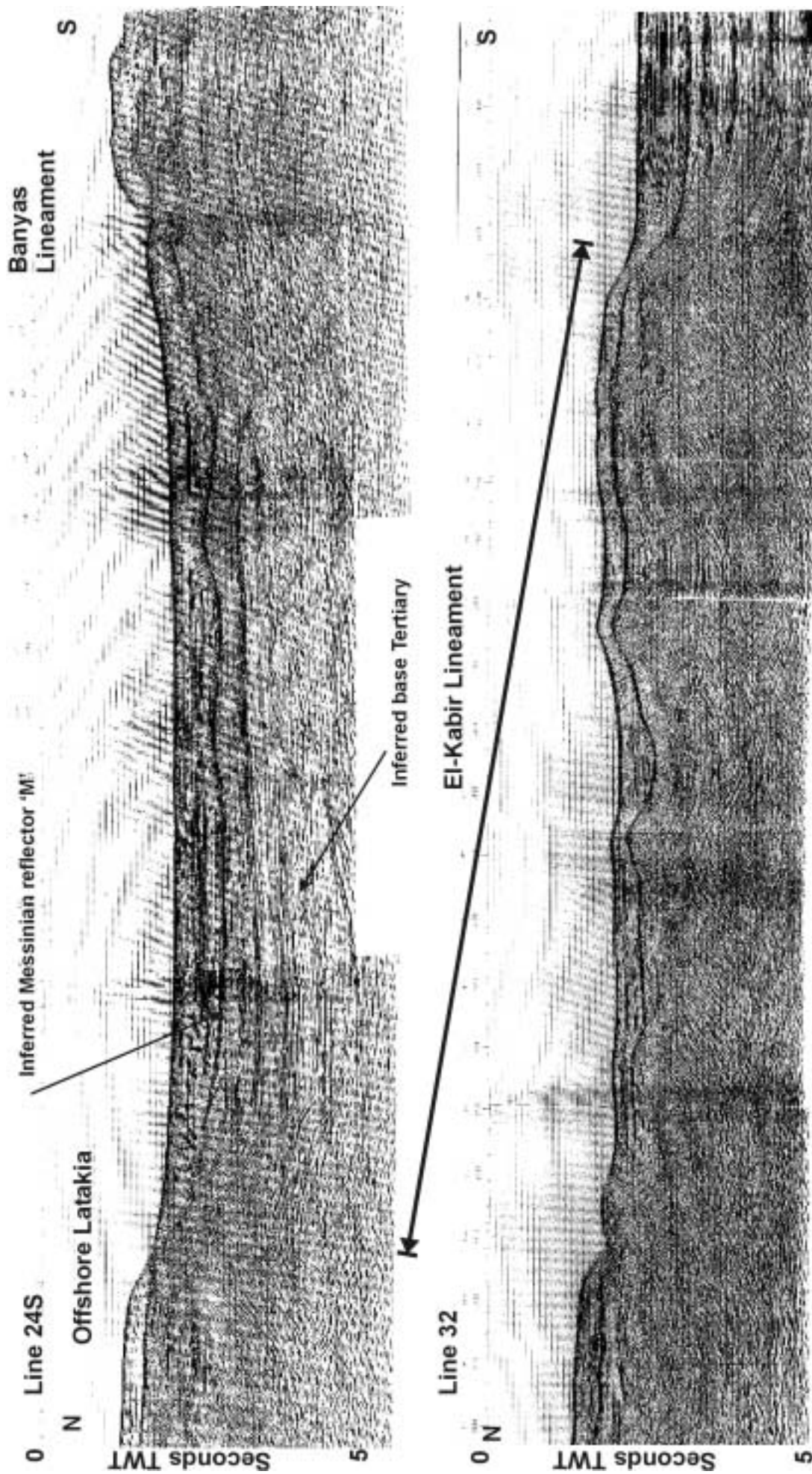
It is unclear how Dzhabur (1985) correlated his well data, as there is no biostratigraphy presented with the data. If his velocities are correct for the Nahr El-Kabir Valley, then quite possibly they cannot be applied to the Levant Basin, simply due to the fact that overburden is much greater offshore than on. For these reasons and the differing stratigraphy given in his work (see Chapter 3), reliance was not placed on these data.

*Basic observations and interpretations during this study*

Seismic line '24 south', runs north-south, 10km west of Latakia City to south of Banyas Town and was the most thoroughly studied (Figure 4.20). The Spectrum Energy seismic lines have much higher resolution than previous research cruise data (i.e. Hall and Krashennnikov, 1994), but are oblique to the predominant structural trend. Figure 4.21, gives a basic interpretation (based on the assumptions detailed in the 'seismic reflection data' section; this Chapter). The most prominent reflector in the seismic section is the 'M' reflector (thought to be Messinian evaporites). Vidal et al. (2000a and b) estimated the thickness of this succession as 1500m in the Levant Basin. In section 24S, the maximum thickness of this 'M' unit is 0.8 seconds TWT (approximately 2000-2800m, dependant on lithology and velocity,  $5000\text{--}7000 \text{ ms}^{-1}$ ; Sheriff et al. (1995), see seismic reflection data section, this chapter). The Messinian is identified by the strong reflector (see above), which undulates or domes (possible salt swell). The lower contact, at the base of the succession, is on a continuous, sub-horizontal, un-deformed reflector (possible Top Middle Miocene or Tortonian). To the north this reflector thins over a large fault with a demonstrable vertical sea-floor throw of approximately 290m (0.4 seconds TWT,  $1450 \text{ ms}^{-1}$  velocity of sea water) (Figure 4.21). This fault is on trend with the mapped El-Kabir Lineament and follows a bathymetric ridge.

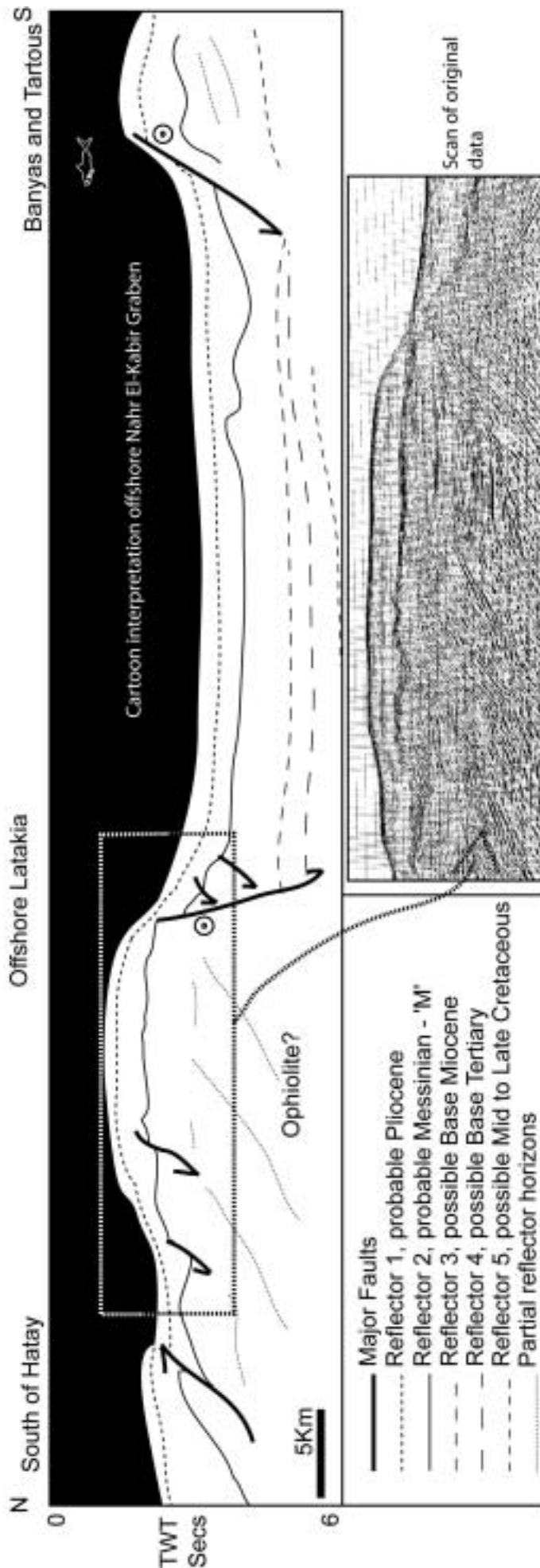


**Figure 4.19** From Dzhabour (1985). Sonic log and stratigraphy from the Fidjo 1 well, 10km southeast of Latakia City. The terminology for the stratigraphy is that used by Ponikarov et al. (1963). P3 is Oligocene.



**Figure 4.20** Spectrum Energy seismic data offshore Latakia, Syria. Location of major lineaments is marked, see Chapter 4 for details and interpretations..





**Figure 4.21** A composite interpretation of lines 245 and the southern end of line 24N from the Spectrum Energy seismic survey, offshore the Eastern Mediterranean (see Figure 4.3 for locality). No wells are known to have been drilled in this offshore section and so the depth of reflectors and their assigned ages are interpreted from estimates and land derived data. The Messinian reflector (evaporite) is known throughout the Mediterranean as a strong reflector ('M' reflector, Ryan et al. 1973; Vidal et al. 2000) and so forms the basis of this interpretation. The onshore well data at Fidjo (Dzhabbour, 1985, chapters 1, 3, 5 and 6) do not correlate with the seismic profile, although there is less than 15km distance between them.

The seismic profile shows that a graben exists offshore south of Latakia, which correlates closely with the observations made onshore in this study. If the Messinian reflector is correct then the major faults in the region show continuous movement throughout the Tertiary, but with the largest movements in the Plio-Quaternary. Sea floor topography shows that faulting is still active and has been extensive in the Quaternary.

The 'M' reflector shallows towards the fault and, therefore, the Plio-Quaternary-age fill also thins. Fault disturbance of this reflector takes the form of a deformation zone 6.5km wide, with most reflector disturbance to the south of the fault. The offset of the Messinian reflector is 1.2 seconds in TWT (for metres, one-way time  $\times$  water velocity,  $0.6 \times 1450\text{ms}^{-1}$ ); therefore, a vertical throw 870m is implied. The Plio-Quaternary-age strata reduce in thickness (velocity estimates  $2500\text{-}2800\text{ms}^{-1}$ ; Sheriff et al. 1995) to 1000-1120m south of the fault and 500-560m, north of the fault.

This large fault, which appears to be the extension of the El-Kabir Lineament (see bathymetric model and Chapter 6), appears to cut every reflector on the section. The seismic character to the north of this fault is distinctly different to the south and there are few reflector horizons (?possible ophiolite)(Figures 4.20 and 4.21). The fault is unclear on the seismic sections. Vidal et al. (2000a and b), interpreted it as a vertical strike-slip fault (profile 6, Figure 4.18). The interpretation in this study is that it is a major vertical fault with a series of smaller splaying faults in a flower structure, although this is far from clear. As such it is likely to be of strike-slip origin, but does not conform to either a 'tulip' or 'palm tree' configurations of transtension or transpression (Woodcock et al. 1994). The Messinian reflector deformation hints that transpression or a 'palm tree' configuration may have existed, but this is in direct contrast to the current throw shown by sea-floor relief. This fault is also observed on seismic line 32 (Figure 4.20). However, the flower structures are very poorly developed there and there is little deformation to the south of the fault. One, maybe two strands of a fault can be observed.

At the southernmost extent of Line 24S, another large fault cuts the section. This is the only seismic section in which this fault can be observed, as it is too far south to be included on the next line west (Line 32, Figure 4.20). The orientation of the southerly fault is uncertain; it maybe related to faulting at Banyas (see below and Chapter 6), or it could be a fault propagating from Lebanon (i.e. the Roum Fault, Butler et al. 1999). On the assumption that it is related to faulting near Banyas, it is named and described here.

The southernmost fault, the 'Banyas Lineament', has a ramp-flat geometry (Figures 4.20 and 4.21). Sea-floor relief is extensive, with more than 500m of vertical throw and possibly up to 1km of south-north heave. All reflector packages thin towards the fault, the footwall of which appears to be a horst block and is undeformed. The 'M' reflector demonstrates considerable undulation near the fault, affecting the overlying Plio-Quaternary strata, which pinches out against the flanks of the swells. This salt disturbance appears to

have ceased midway through the deposition of the Plio-Quaternary succession as the upper sequence is undeformed.

#### *Summary of interpretation*

Two major fault zones are observable on the seismic lines (Line 24S). The northern fault is probably the western extension of the El-Kabir strike-slip lineament, whereas the southern fault, 40km south, is most likely represent faulting associated with the Banyas structure. A graben almost 9km deep lies between these two faults (i.e.  $3500\text{ms}^{-1}$  average velocity, 5 seconds TWT deep, 8750m depth). Horst blocks with only latest Tertiary-age strata are discernable and abut this graben. The deep seismic character is very different to the north of the El-Kabir Lineament, where only a few steeply north dipping reflectors are visible. To the south, in contrast, beneath the onlapping graben fill, well defined, shallow north-dipping reflectors hint at a conformable sequence. An interpretation could be that the northern reflectors are thrust planes associated with the emplacement of the ophiolite, whereas the southern reflectors show the pre-existing Cretaceous carbonate platform. Vidal et al. (2000a and b) interprets the K reflector to the south of the Latakia Ridge at a similar depth, approximately 30km to the west. This would imply massive uplift of the ophiolite (outcrops onshore, dipping west), or approximately 9km of subsidence of the graben floor to the south.

Most of the sedimentary fill of the graben is sub-horizontal and appears to onlap the basement reflectors to the south. No structuration within the succession is observable, but the reflectors are terminated by the northern fault. The Messinian reflector is deformed by faulting and domed by salt flow. The upper part of the Plio-Quaternary is not deformed, except by truncation or drape on the faults. A considerable amount of active faulting is present on both faults and the graben is presently underfilled.

### Banyas structures

#### *Introduction*

To the east of the town of Banyas (see pull-out maps), the southern extension of the Jebel An-Nassuriyeh Mountains extends westwards to the coastline. The southernmost margin of the Nahr El-Kabir Valley is abruptly terminated there. Small exposures of Maastrichtian and Palaeogene rocks are present, but the usual stratigraphy is Plio-Quaternary successions resting directly on eroded sedimentary rocks of the Cretaceous Platform sequence. The Plio-

Quaternary rocks in this area are predominately characterised by the presence of eruptive lavas and pyroclastic rocks (see Chapter 3), rather than marls as seen elsewhere in the Nahr El-Kabir Valley.

Ponikarov et al. (1966) mapped lineaments in this area, trending NE-SW and showed a stratigraphical juxtaposition suggestive of dextral strike-slip. They did not give any further information and these faults do not appear on their structural maps. Devyatkin et al. (2000), in their summary of Syrian geology (in Russian), show one of these major Banyas faults as having a dextral sense and imply pre-Quaternary faulting throughout the Jebel An-Nassuriyeh Mountains (i.e. Quaternary deposits overlie fault trace).

In this study, these lineaments were reassessed for movement sense, age and their importance, if any, for the history of the region. It seems likely that these lineaments trend offshore. Ridges are indeed observed on bathymetric profiles (Hall and Krashennnikov, 1994) and it is inferred that these lineaments are present on seismic Line 24S (see Offshore Latakia section). Were they important for the formation and uplift of the Nahr El-Kabir Valley or to the Ghab Valley/Dead Sea Transform fault or to both?

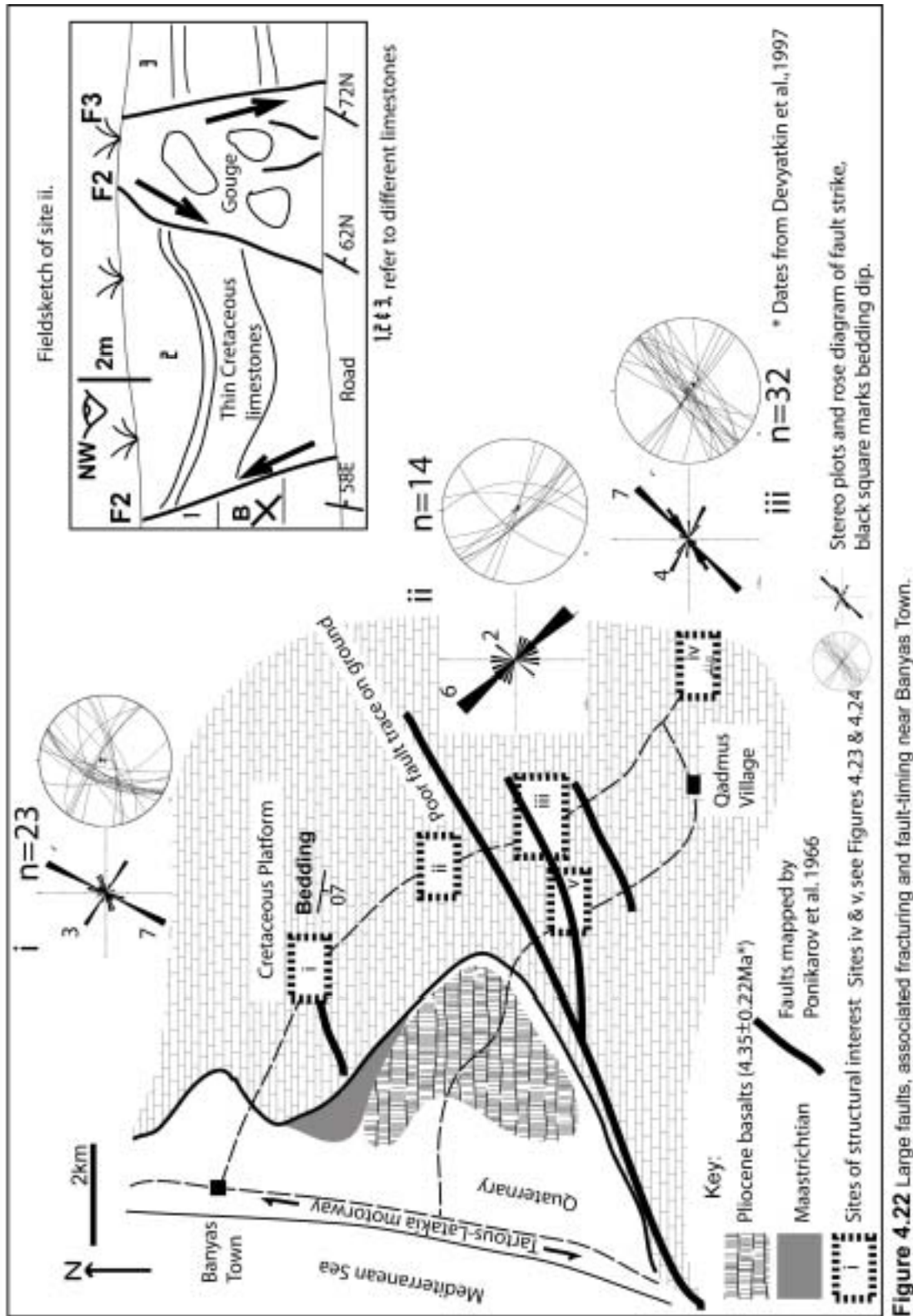
#### *Banyas field studies*

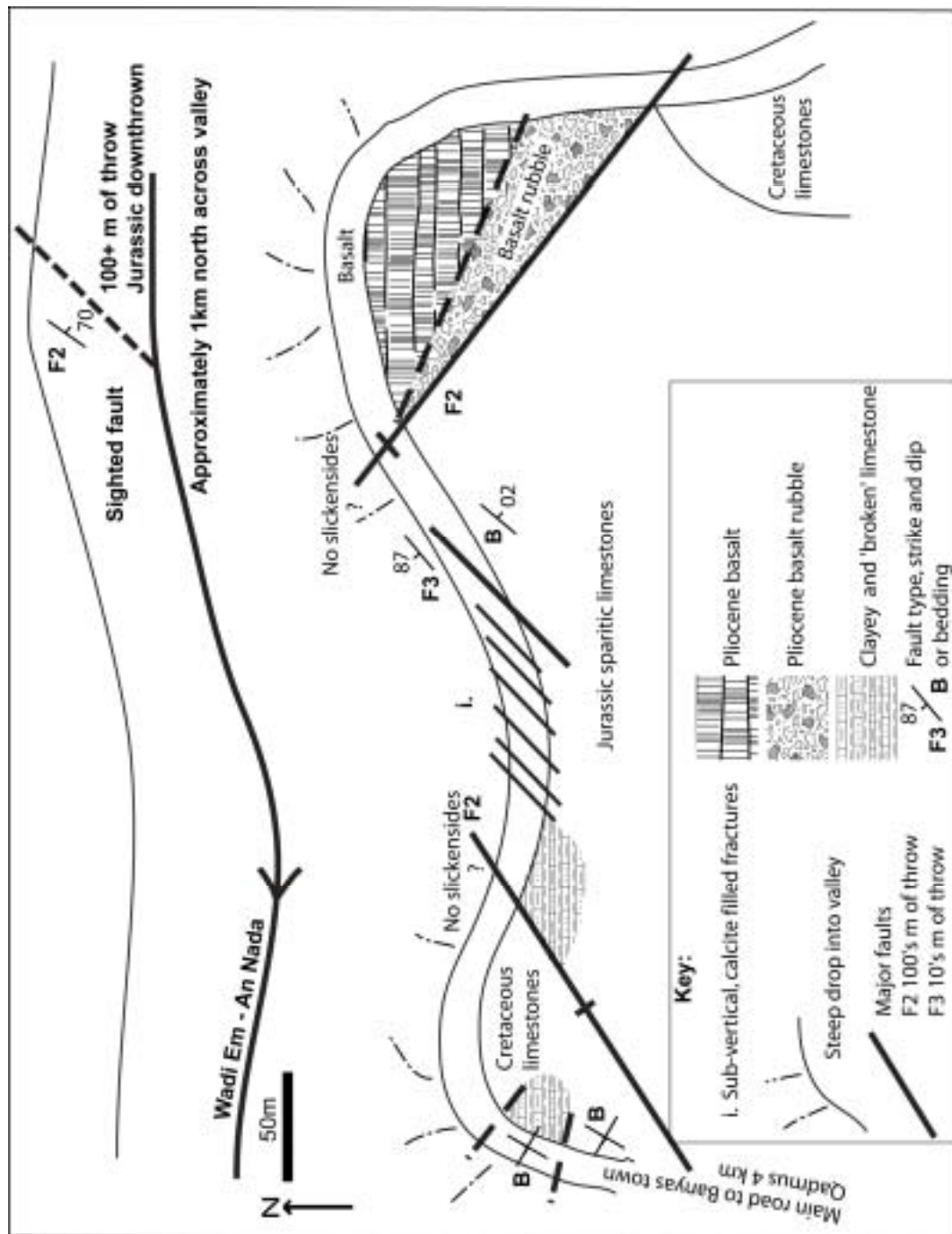
This region was investigated at five key localities on the Jebel An-Nassuriyeh Mountains (Cretaceous Platform) (Figure 4.22) and also near the seafront (see Chapter 3). Steep topography and a lack of vegetation in this region allowed better ground tracing of faults than at localities within the Nahr El-Kabir Valley. As stated in Chapter 3, unconformities exist within Palaeogene and Neogene stratigraphy. Two episodes of volcanic eruptions occurred during the Pliocene at  $4.35 \pm 0.22$  Ma and  $5.42 \pm 0.16$  Ma (Devyatkin et al. 1997). Both eruptive sites are proximal to the faulting observed (within 500m).

Figure 4.22, shows the localities of the field studies and measurements of fault strike and dips. Bedding within the Cretaceous Platform limestones is sub-horizontal. Intense fracturing of the whole region is a common feature, with the predominant orientations being NW-SE and NE-SW.

#### *Summary of Banyas area*

Figures 4.22 to 4.24, show faulting in the Banyas area to be predominantly strike-slip. This strike-slip could not be confirmed by kinematic data, but only by the current outcrop offset, indicating dextral movement. Two major strike orientations are recorded when all the faults

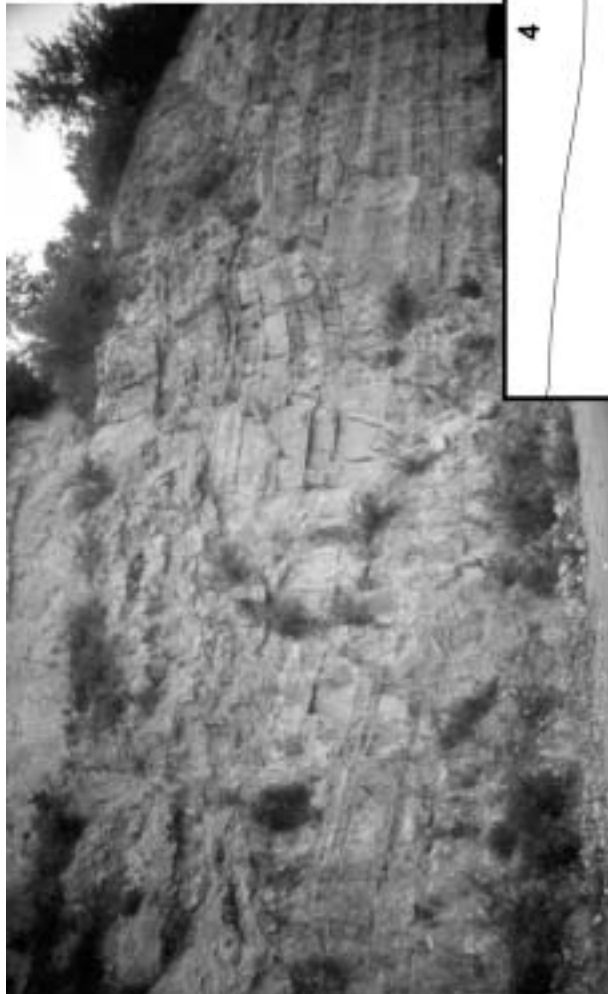




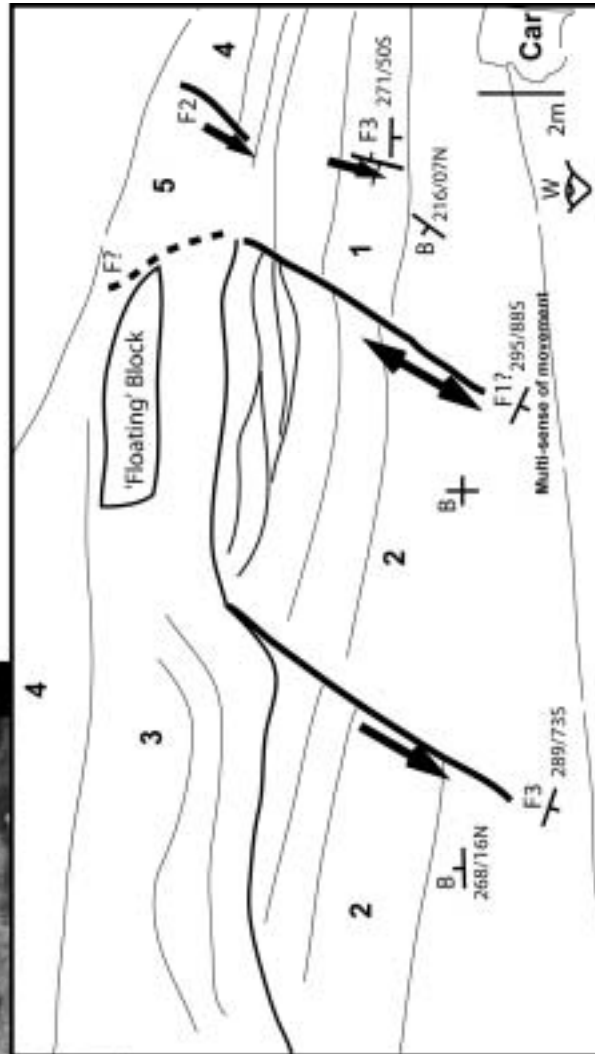
**Figure 4.23** Site Iv, Banyas Town structural profiles. Two stages of faulting; second is post-Pliocene in age.



**Figure 4.24** Site V, major NW-SE faulting on the Baryas lineaments (post Early Pliocene age).



- 1 - Alternating limestone (50%) and marl (50%)  
- Cretaceous age (Cenomanian - Turonian)
- 2 - Limestone, no marl
- 3 - Broken limestone formation
- 4 - White limestone
- 5 - Rubble zone, probable Quaternary fluvial deposits



(F2 & F3) are plotted (Figure 4.22). These two directions are: NW-SE and NE-SW. Close to the mapped faults (NE-SW) the majority of subsidiary faults are orientated NW-SE i.e. at 80°-90° to the mapped lineaments. Away from the large mapped lineaments (NE-SW), the faults are orientated approximately NE-SW, with a minor, but significant component trending NW-SE. A large outcrop of Pliocene basalt ( $5.42 \pm 0.16\text{Ma}$ ; Devyatkin et al. 1997), seems to be associated with the largest of the Banyas lineaments (NE-SW) (Figure 4.23). This strongly suggests that this feature was active at that time and perhaps reached a deep crustal depth, influencing magmatism.

In contrast, the NW-SE faults are post-Pliocene in age (Figure 4.23). At localities near Qadmus Village (Figure 4.24), the NE-SW faults cut Jurassic and Cretaceous successions. These faults are cross-cut by a later stage of faulting in a NW-SE orientation which offsets a Pliocene basalt outcrop. This episode of faulting seems to be less strongly developed than the original NE-SW orientation. The earliest age of movement along the original NE-SW fault orientation is difficult to constrain.

## Jus Ash-Shaghour Town, western margin of the Ghab Graben

### *Introduction*

The Aquitanian and Eocene successions at the northern extent of the Nahr El-Kabir and Nahr El-Abyad Valleys are exposed on the western margin of the Ghab Graben (see pull-out maps and Chapter 5). The topography is dissected by a vertical scarp slope, interpreted as the western Dead Sea Transform Fault (Dubertret, 1932, 1933, 1953; Ponikarov et al., 1963, 1966, 1967; Krasheninnikov, 1971, 1994; Domas, 1989; Trifinov et al., 1991; Devyatkin et al., 1997; Brew et al., 2001; Zanchi et al., 2002). This fault was assigned a sinistral sense of motion and a Pliocene age (see Chapter 5) by most previous workers (Figure 4.25). The fault plane cannot be observed in the field, it is covered by Quaternary alluvium. Fieldwork measurements were taken in this study to assess the primary directions of fracturing and faulting, and to facilitate comparison with the structural regime within the Nahr El-Kabir Valley, which is not constrained accurately with respect to timing of fault movements.

### *Field studies*

Two main sites were used to obtain structural data in this area. The first, on the Latakia-Aleppo Highway, near Jus Ash-Shaghour and the second, 15km north, east of Zeiniye

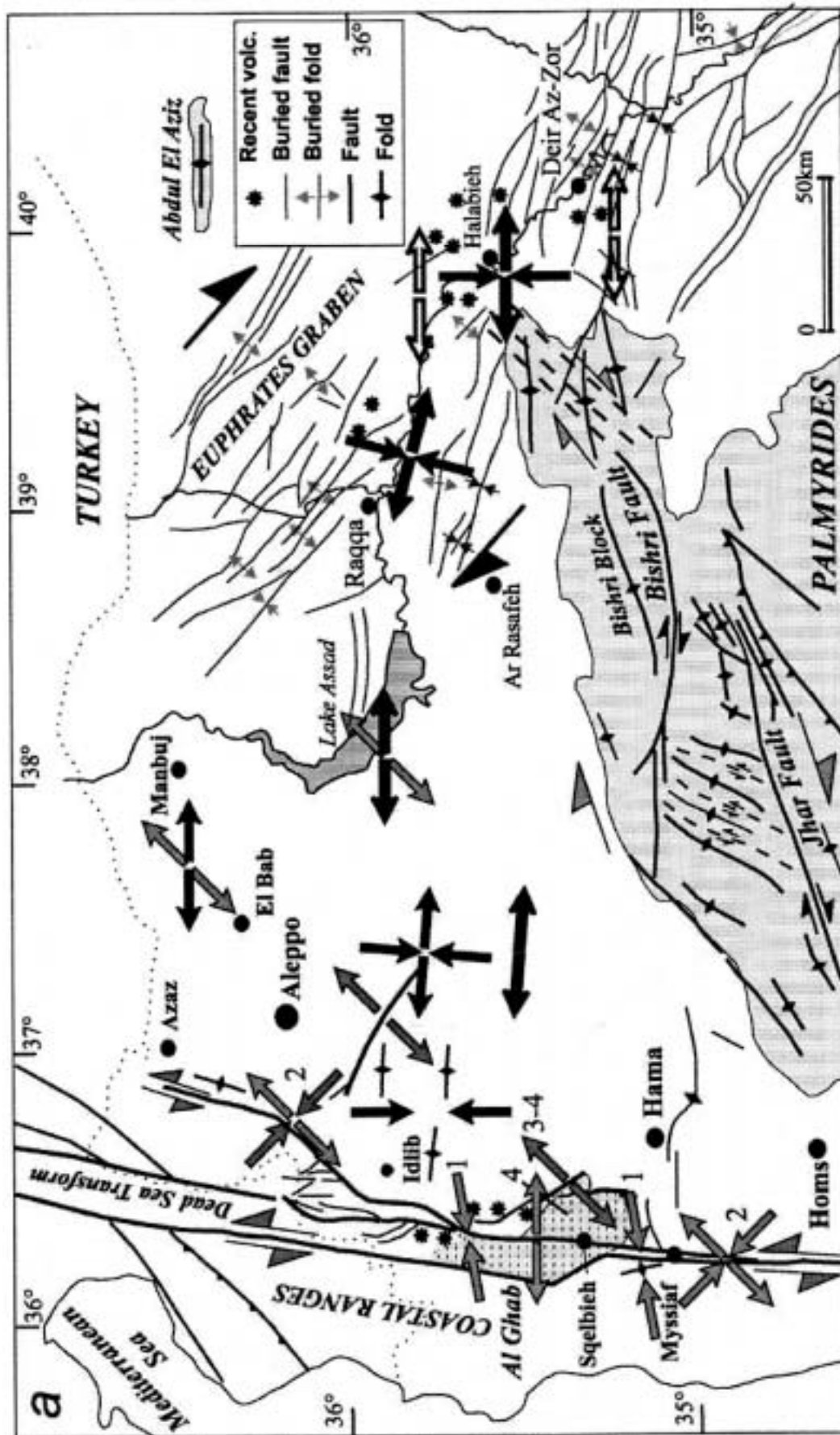


Figure 4.25 From Zanchi et al. (2002). Main stress directions during the Miocene and Quaternary, affecting the northwestern margin of the Arabian Plate.

Village (see pull-out maps). The Jus Ash-Shaghour locality is very near to the Dead Sea Transform fault (50m); further north a possible synthetic fault was studied.

The approach road to Jus Ash-Shaghour Town is relatively new and a well exposed, steep road cutting could be used to obtain structural data (Figure 4.26). Regionally, the bedding is sub-horizontal, although local dip variation is common near faults. Many of the outcrops (approximately 90%) are pervasively fractured (Figure 4.27), in a northwest-southeast orientation, with very little data spread (NE-SW is also a minor trend). Large faults ( $F_2$  and  $F_3$ ), plot in numerous orientations (Figure 4.26), but the predominant orientation is northwest-southeast. This is the same orientation as the large inferred  $F_1$  synthetic fault. No Plio-Quaternary strata overlie these successions to constrain timing of the fault and all the rock units have similar fault orientations.

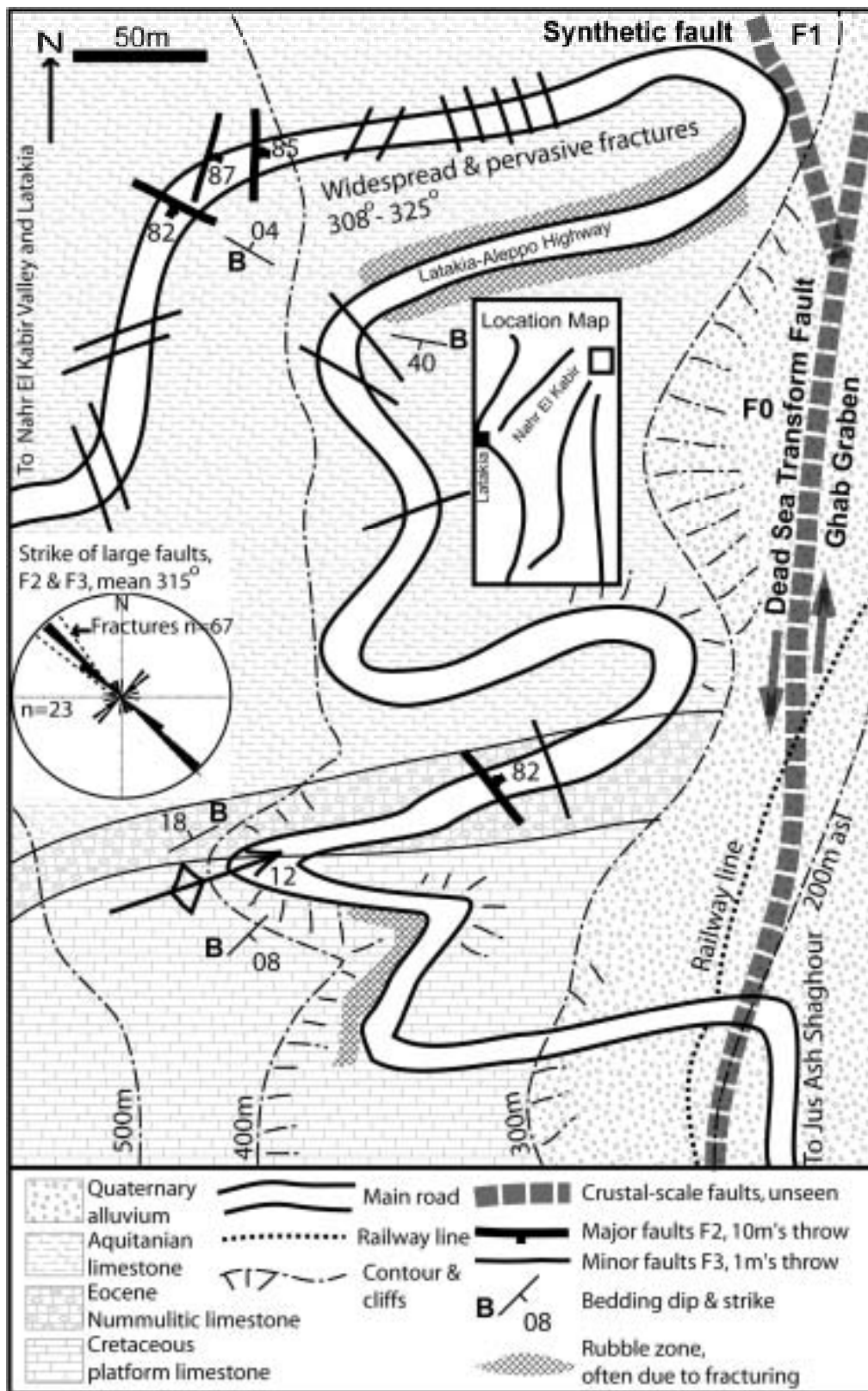
Slickensides could not be observed on fault and fracture planes. In a few faults, offset could be estimated. Both sinistral and dextral senses of movement were observed, especially in northwest-southeast fractures and faults. Occasional NE-SW trending fractures are offset by NW-SE fractures. One anticline is observed in Eocene and Cretaceous-age strata and plunges towards ENE.

Near Zeiniye Village, to the north of Jus Ash-Shaghour, a large normal, NW-SE trending fault is observed (Figure 4.28). The fault juxtaposes Aquitanian marl in the hanging wall against Middle Eocene-age nummulitic limestone in the footwall, inferring 100m+ fault throw. Striations on the fault plane indicate almost pure dip-slip and extension. Ponikarov et al. (1963) mapped faults in this region, but did not infer a sense of movement.

#### *Summary of Jus Ash-Shaghour region*

The large fault, north of Jus Ash-Shaghour is interpreted as a synthetic fault to the Ghab Graben, Dead Sea Transform faults. The last sense of motion is normal and it is unclear if this fault had any previous movements. The fault is orientated NW-SE which is a direction common to faults in the Nahr El-Kabir region.

At the Jus Ash-Shaghour localities, two senses of fracture and faulting orientations are apparent i.e. a minor sense of NE-SW fracturing, cross-cut by the predominant NW-SE orientations. Strike-slip motion is inferred. The NE-SW orientation is sub-parallel to the Dead Sea Transform Fault, whereas the NW-SE orientation is synthetic (almost antithetic, see Riedal shears, this chapter).

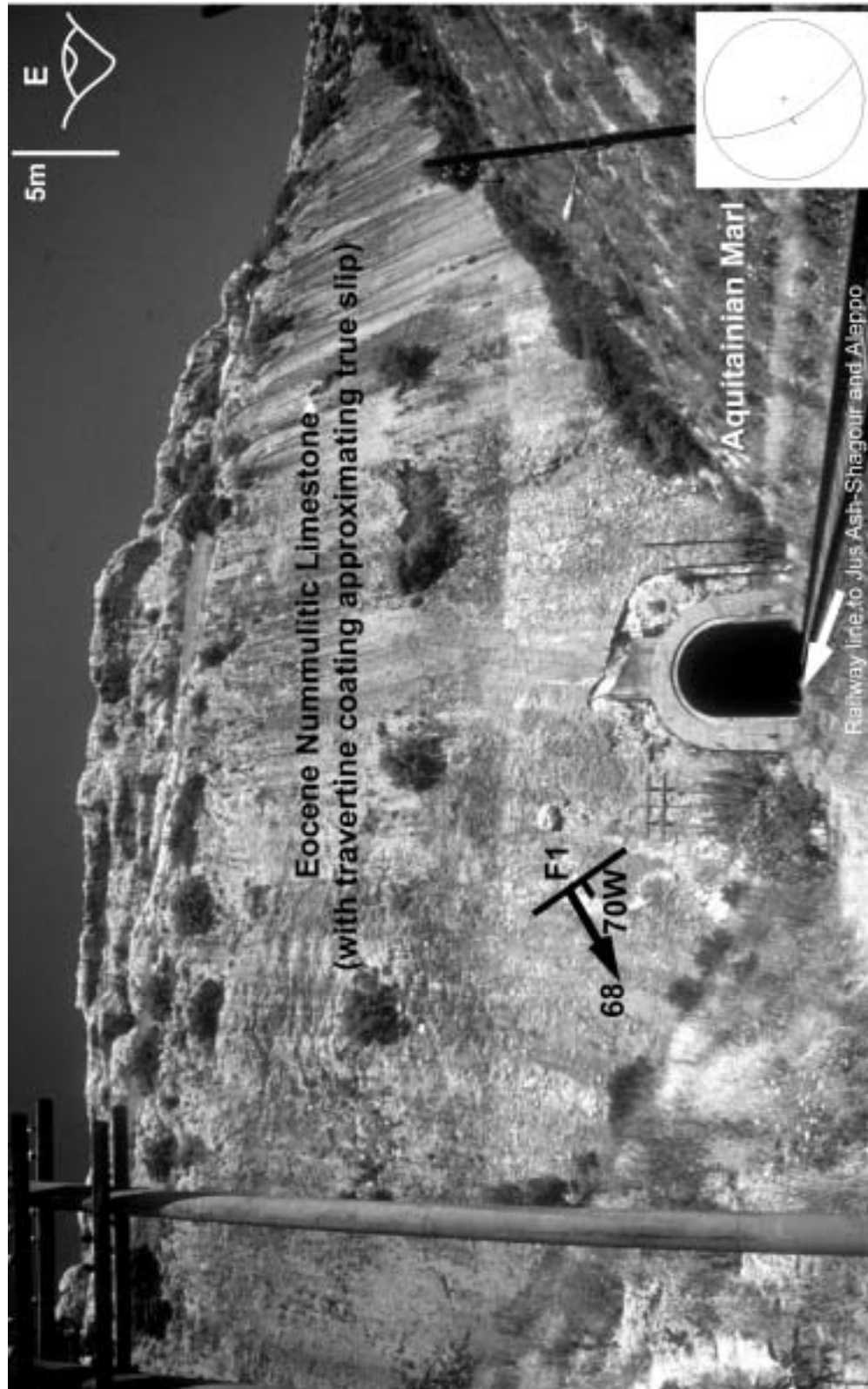


**Figure 4.26** The structure of Aquitanian and Eocene successions near the town of Jus Ash-Shaghour and on the western margin of the Ghab Valley. NW-SE faulting and fracturing predominates and may be synthetic to the Dead Sea Transform Fault.



**Figure 4.27** A heavily fractured Aquitanian outcrop near to the Ghab Valley, part of the 'pervasively fractured zone' seen in figure 4.26 on the approach road to Jus Ash-Shaghour. Bedding is approximately horizontal.





**Figure 4.28** 15km northwest of the town of Jus Ash-Shaghour, this major synthetic fault to the Dead Sea Transform fault is exposed and Eocene and Aquitainian sediments are juxtaposed. The fault is normal with an almost pure dip-slip throw which could be greater than 100m.

## Southern and eastern margin of the Nahr El-Kabir Graben

### *Introduction*

Throughout this chapter and those preceding, the Nahr El-Kabir region has been referred to as a valley. The field data from the El-Kabir Lineament indicates that the valley might be a half-graben (see above and Chapter 6). During the Early to Middle Miocene, the Nahr El-Kabir valley developed as a graben, with both the north (see Chapter 3 and 6) and the south (southeastern) margins being affected by active faulting. The field data for the previously unobserved southern margin are discussed below and in Chapter 6.

The eastern and southern margins of the Nahr El-Kabir valley are characterised by an abrupt termination of Miocene successions against scattered hilltop outcrops of Palaeogene strata on the gradually ascending Cretaceous platform sediments of the Jebel An-Nassuriyeh Mountains. Ponikarov et al. (1966) indicates that this is an unconformity, due to the valley being a shallow, geo-synclinal depression. Further examination of the margin during this study infers that the margin is primarily a series of extensional growth faults offset by small strike-slip transfer faults. These faults were only found at the narrowest points of the Nahr El-Kabir Valley. There is no evidence of them being associated with the large offshore faults or faulting near Banyas.

### *Nahr El-Kabir southern margin field studies*

The area 10km south of Al-Haffeh town, extending 25km northeast to the village of Bdama, best exposes the southern margin of the Nahr El-Kabir Valley (see pull-out map). Maastrichtian marly sediments (see Chapter 3) unconformably overlie the Cretaceous Platform. These in turn, are commonly overlain by Eocene Nummulitic Limestones and also occasionally by Palaeocene strata. The Middle Eocene nummulitic limestones define the margin of the valley. Miocene sediments abut and only occasionally overlie this margin. In the field, this area is heavily cultivated, with little exposure (Figure 4.29)

Three localities were found which expose the nature of this margin: 1. The eastern margin of the valley north of Khan El Jouz Village (see pull-out maps), 2. The Kyfereh Asphalt Pit. 3. Nqourou Village, near Qerdaha Town.

### *Khan El Jouz Village*

Khan El Jouz Village marks the narrowest part of the Nahr El-Kabir Valley. Tertiary successions there are thin and the Neogene is poorly exposed or absent except to the west



**Figure 4.29** View towards the town of Al-Haffeh Town, showing the southern margin of the El-Kabir Valley. In the foreground the horizontally bedded and heavily terraced Pliocene sediments fill the basin centre. The basin margins are also visible as the topography rises. In the middle distance the Miocene succession rests on Paleogene strata, whilst the Cretaceous Platform strata form the mountains in the distance

(Figure 4.30). Large faults running sub-parallel to the valley margins are visible in the Cretaceous Platform strata, faults that appear active to this day (i.e. active scarps, Figure 4.30). These faults are cut by obvious cross-cutting lineaments, that offset the normal faults (see Figure 4.31 and pull-out geological map). Eocene nummulitic limestone blocks are entrained within Aquitanian and Burdigalian-age rocks on this margin. This region is well defined on SPOT images (see Figure 4.2)

#### *Kferyeh Asphalt Pit*

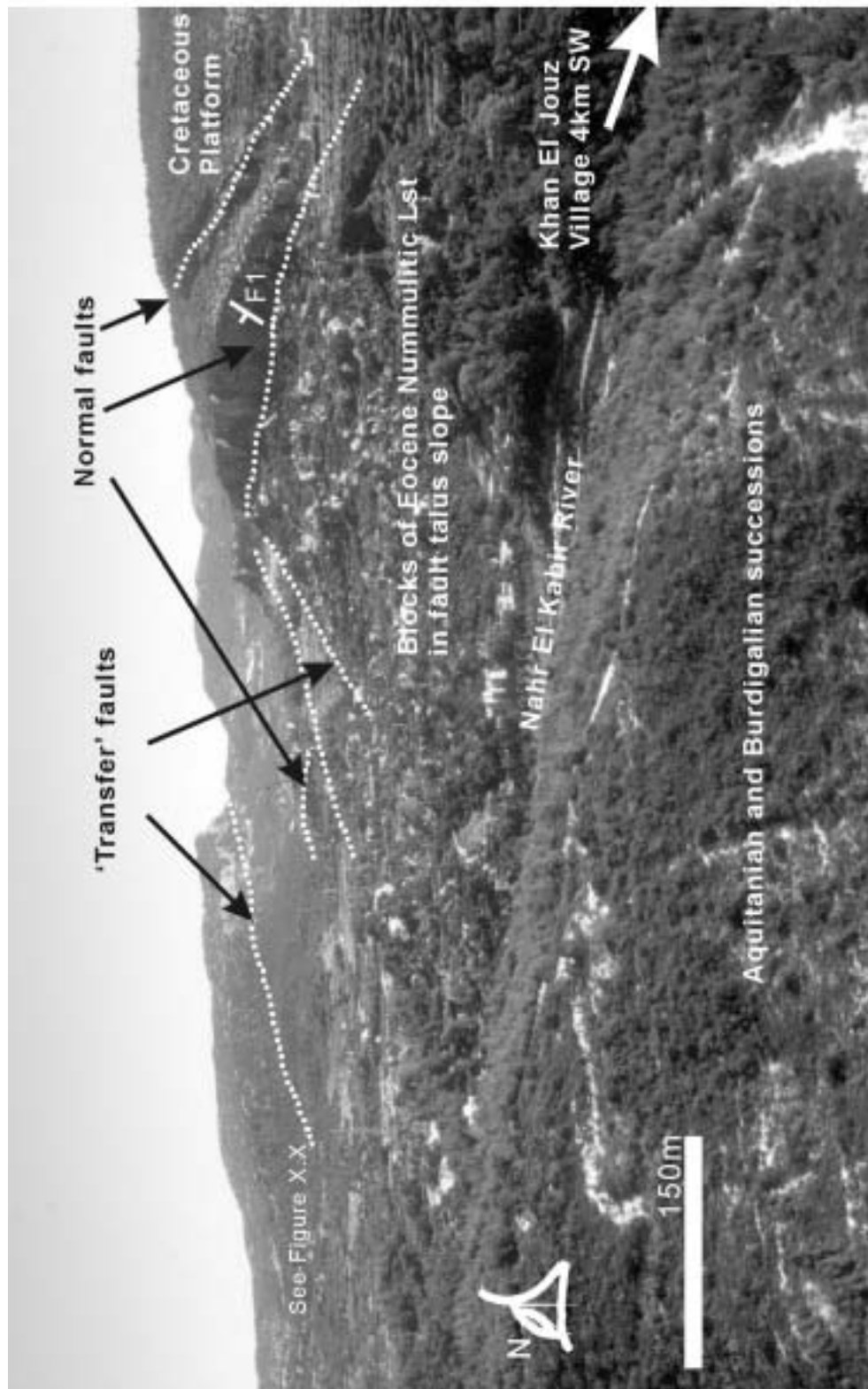
Kyferreh Asphalt Pit is a working open-cast mine. The main bitumen bearing rocks are Langhian-age bioclastic limestones (see Time-slice 5, Chapter 3 & Figures 3.35 and 3.36). These are overlain by thin, sub-horizontal Serravallian-age limestones that also overlie the Cretaceous Platform, 100m to the east. The main feature of the pit is that large, valley-perpendicular faults define the northern and southern extent of bitumen.

Figures 4.32 and 4.33 indicate the structure of the region. The Miocene strata forms the footwall of a large normal fault. At least 250m of throw is visible (Figure 4.32), but probably much more occurred. The strike-slip faults may have formed synchronously to these normal faults but there is no direct evidence of this. The uppermost Langhian-Serravallian-age succession (Time-slice 6, Chapter 3), covers the normal faults.

#### *Nqourou Village*

Nqourou Village is at the southernmost margin of extensive Miocene outcrops in the Nahr El-Kabir Valley (see Time-slice 6; near Banyas). Large sections of the area were remapped during this work as the mapped stratigraphy of Ponikarov et al. (1963, 1966) did not support the evidence on the ground. The nature of the structuration and timing of events also became clearer during this work.

Figures 4.34 and 4.35, show the stratigraphy near the village. Eocene Nummulitic limestone abuts directly against small exposures of Aquitanian and Burdigalian-age rocks (Time-slices 3 & 4), seen in local fault contact. These successions are overlain by erosive, down-cutting Langhian-Serravallian (Time-slices 5 & 6), which also overlies the Eocene but only at the uppermost part of the succession. The complete Miocene stratigraphy is less than 50m thick at these localities (100's m thick further north). The Miocene facies coarsen upwards and dip progressively less steeply into the valley. Aquitanian chalky marls are found at the base of the outcrop and overlie the Eocene succession directly. This unit is



**Figure 4.30** Southeastern margin of the Nahr El-Kabir Valley, near Khan El Jouz Village. The basin margin is primarily extensional with strike-slip transfer faults allowing offset of individual faults (i.e. transtensional). The normal faults appear to be long-lived, as Eocene Nummulitic limestone blocks are entrained within the Aquitanian and Burdigalian successions, whilst also forming an active scree talus at the present day.

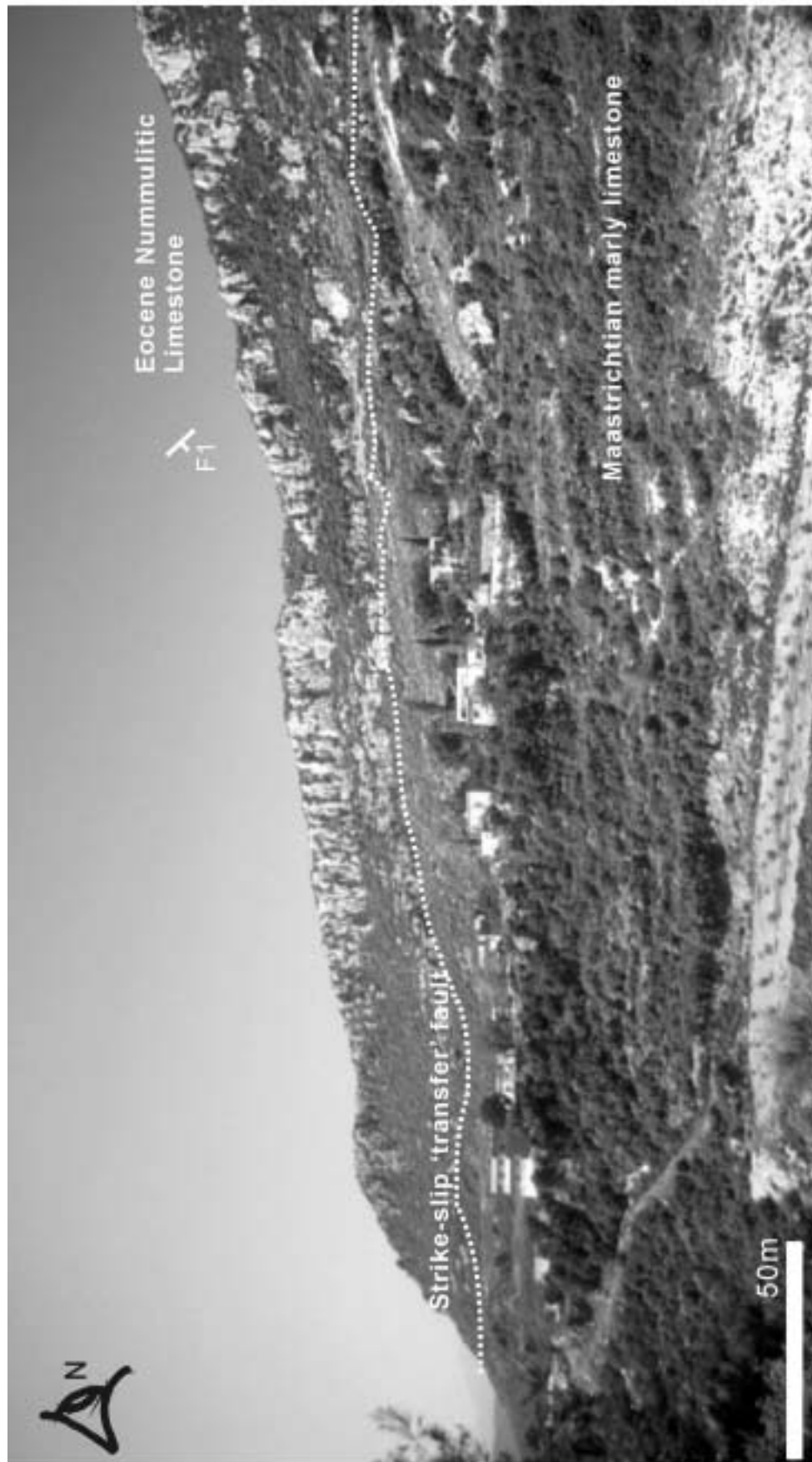
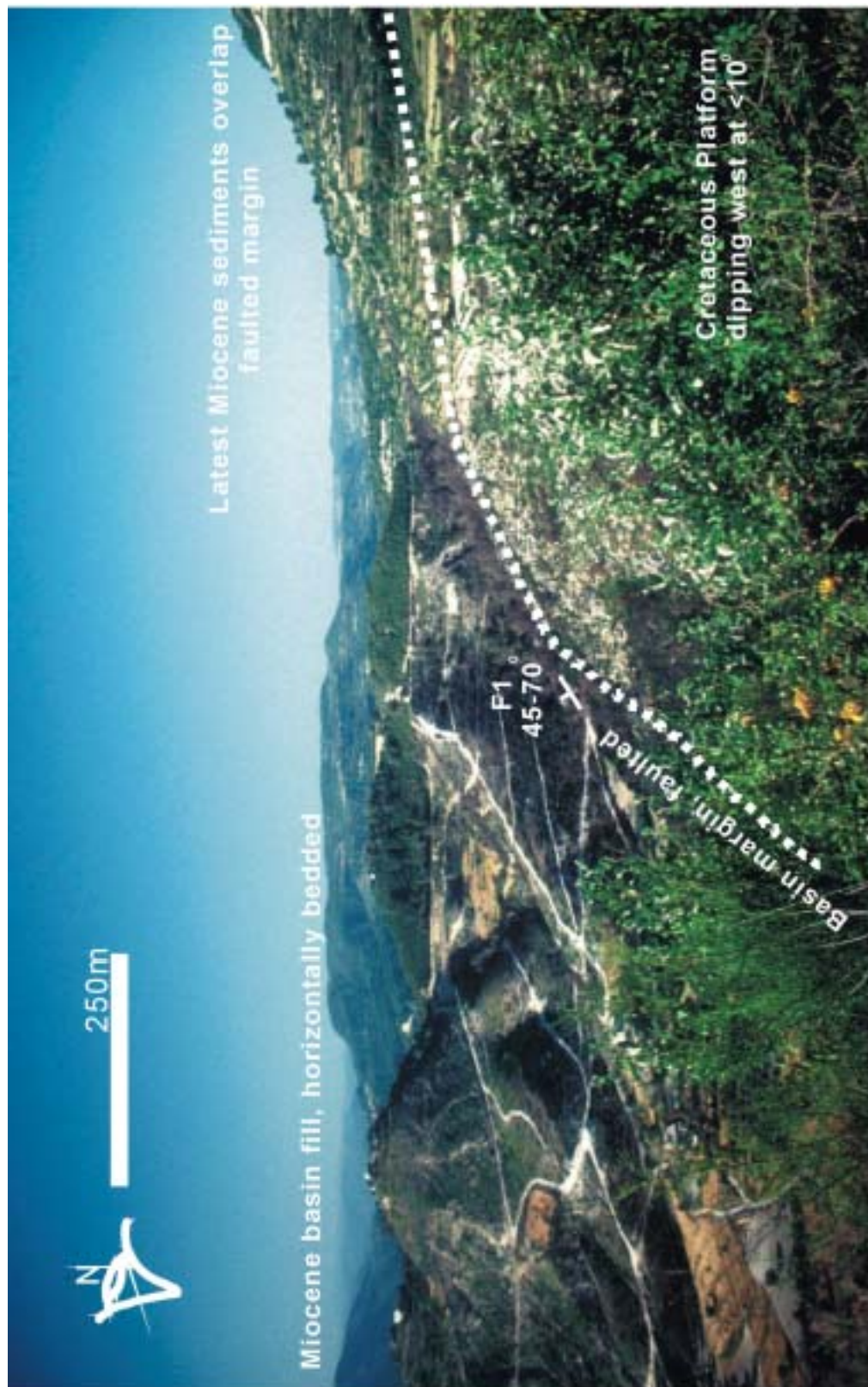
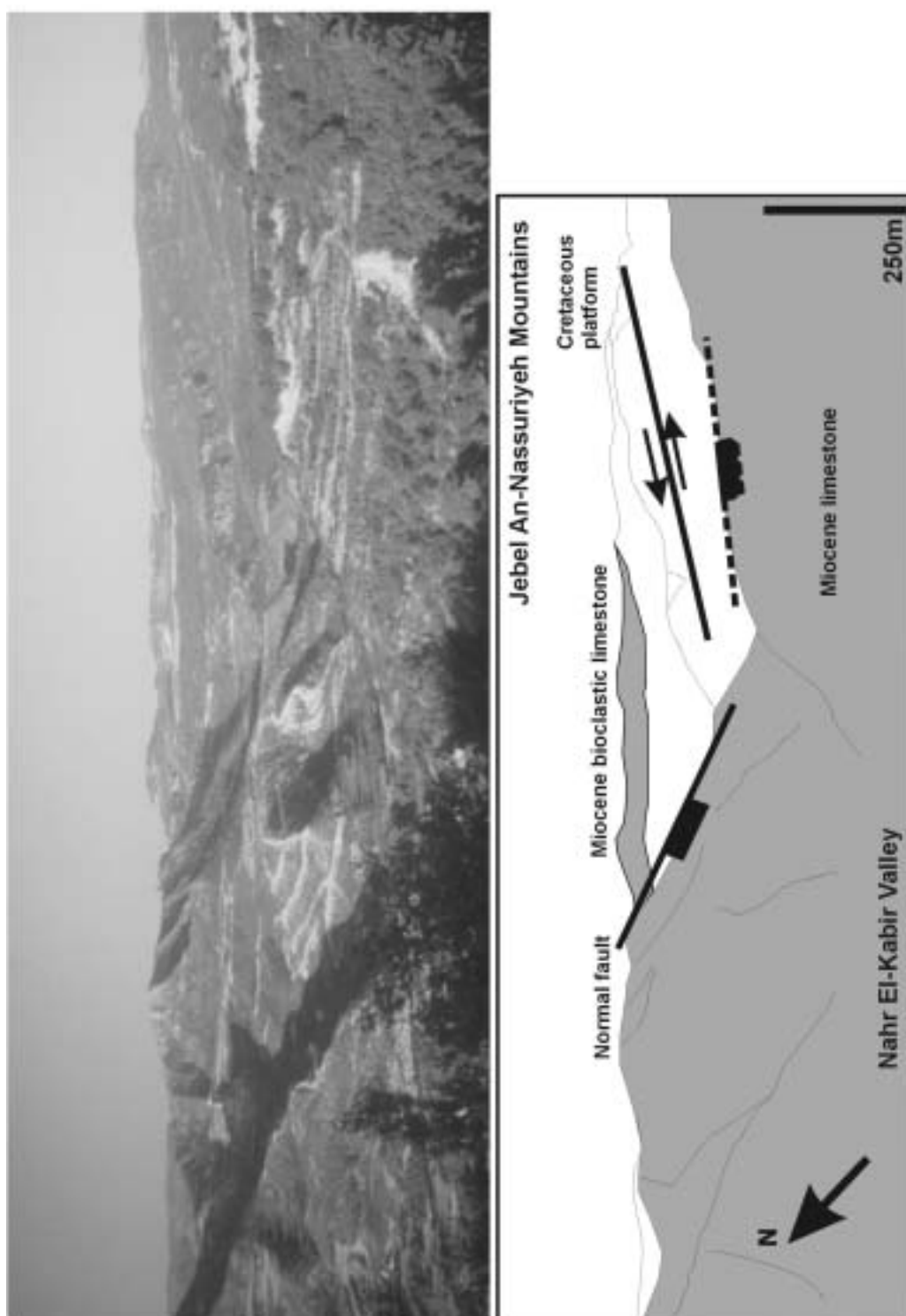


Figure 4.31 From previous figure (4.30), a close-up view of a 'transfer' fault on the southern, transpressive margin of the Nahr El-Kabir Valley (graben). Throw is difficult to assess, but does not appear to be more than a few hundred metres and the fault is sub-vertical.



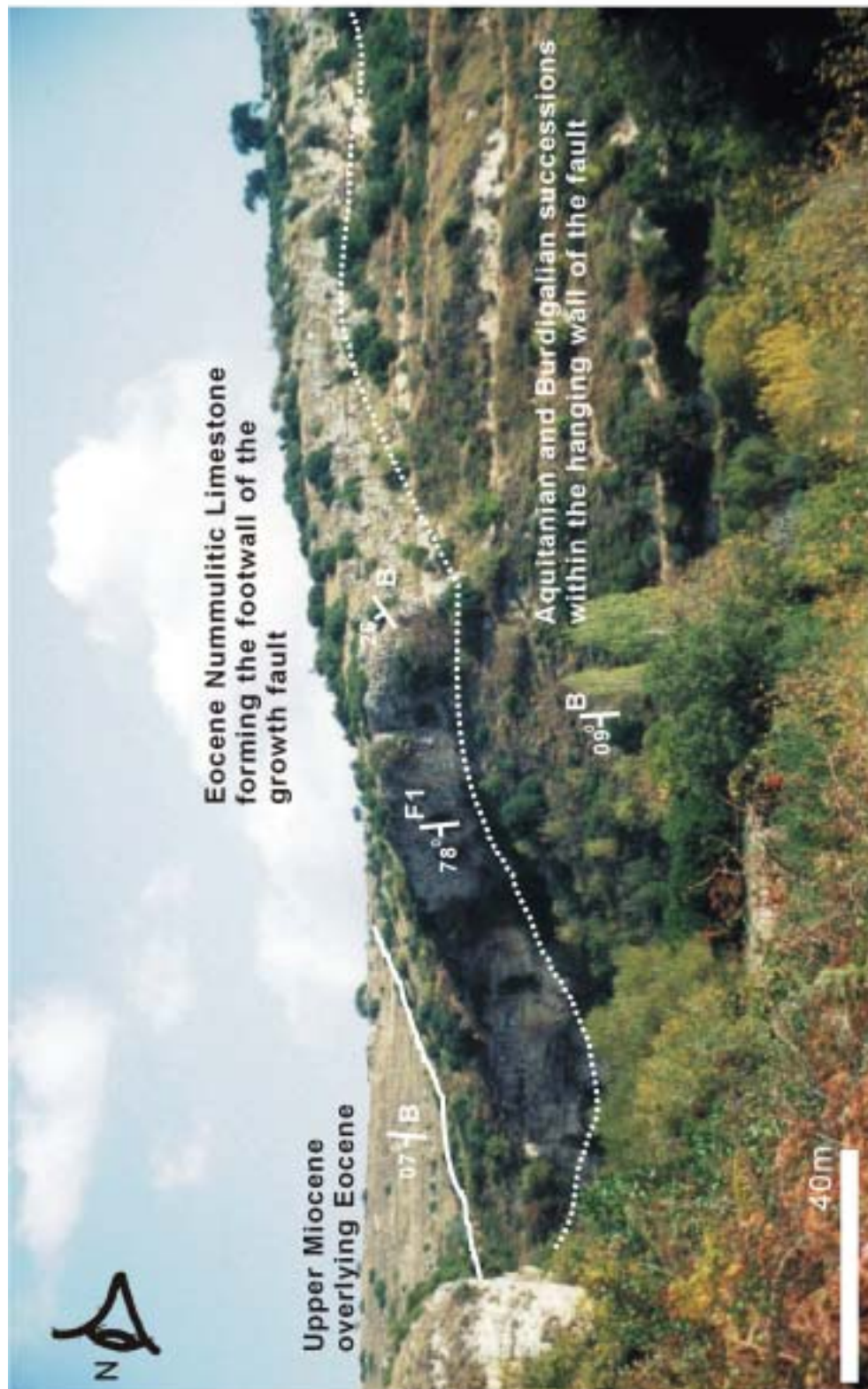


**Figure 4.32** View from 4km southeast of Khan E Jouz Village, of the eastern margin of the Nahr El-Kabir Valley, showing Miocene sediments abutting against and overlapping the Cretaceous Platform. In this view the faulted nature of the contact can be recognised through the colour change of the rocks exposed.

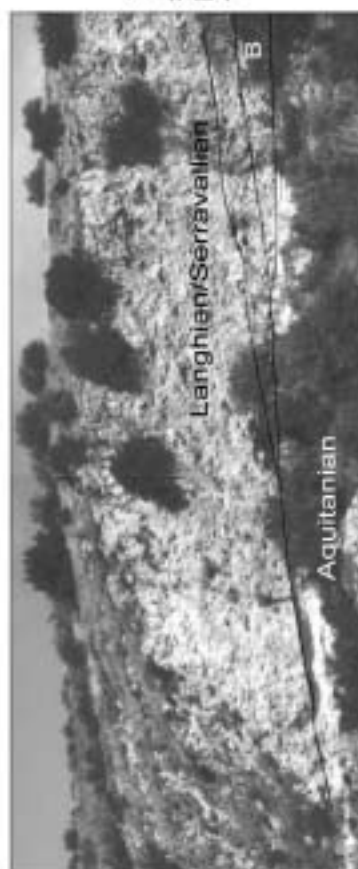
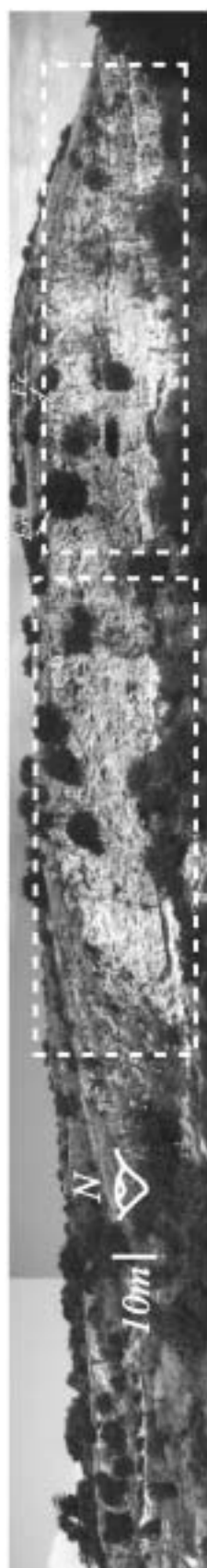


**Figure 4.33** View of the eastern margin of the Nahr El-Kabir Valley (graben). Large normal faults are cross-cut by transverse lineaments. The Miocene-age graben fill abuts the Cretaceous-age platform. The topmost Miocene overlies the faults and platform. 3km north of Kferyeh Village.

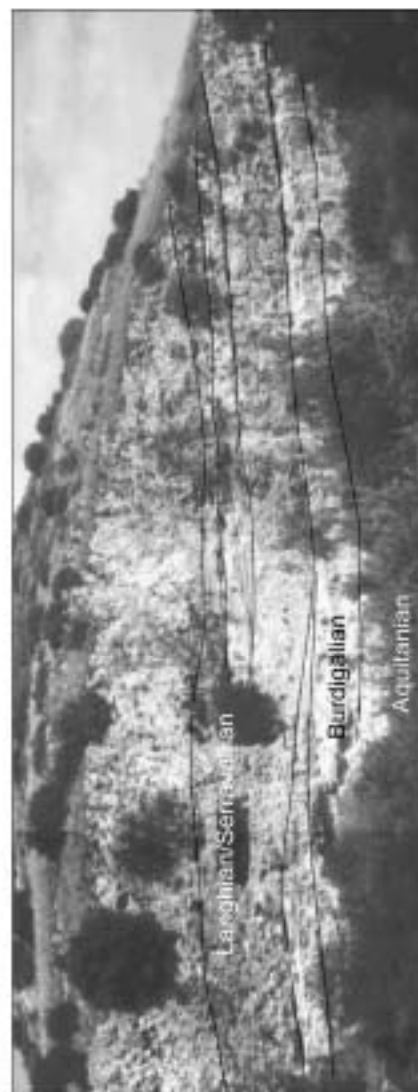




**Figure 4.34** View looking east, at the eastern margin of the Nahr El-Kabir Valley, 5km north of Nqourou Village. The Eocene succession is easily recognizable as the footwall of the fault with the softer Miocene successions forming the hanging wall and overlapping the entire fault system at the latest Miocene. This fault is inferred to be an extensional growth fault, split into segments, hundreds of metres, or a few km's long by series of strike-slip transfer faults.



**Figure 4.35** 1km north of Nquorou Village, Aquitanian and Burdigalian strata dip away from a normal fault to the south. These units are down-cut by sub-horizontal Langhian-Serravallian-age bioclastic conglomerates. The bedding architecture could suggest growth fault deposition.



eroded by a much coarser Burdigalian succession forming a series of down-cutting 'pinched-out' sequences. These are, in turn, down-cut by Langhian-Serravallian-age coarse sediments, which dip progressively less steeply into the Nahr El-Kabir Valley. This locality exhibits deposition against a growth-fault, with the down-thrown block representing the valley.

North of Nqourou (Figures 4.36 to 4.38), this inferred growth-fault could be tested at a larger scale. The map produced (Figure 4.36), shows numerous small faults, cut by a transverse fault. The normal faults appear to be associated with subtle dip changes and forward dip increases into the valley (forward collapse of blocks). A low factor of extension could provide this kind of structure (see Chapter 5 & 6 and Payne et al. 1995).

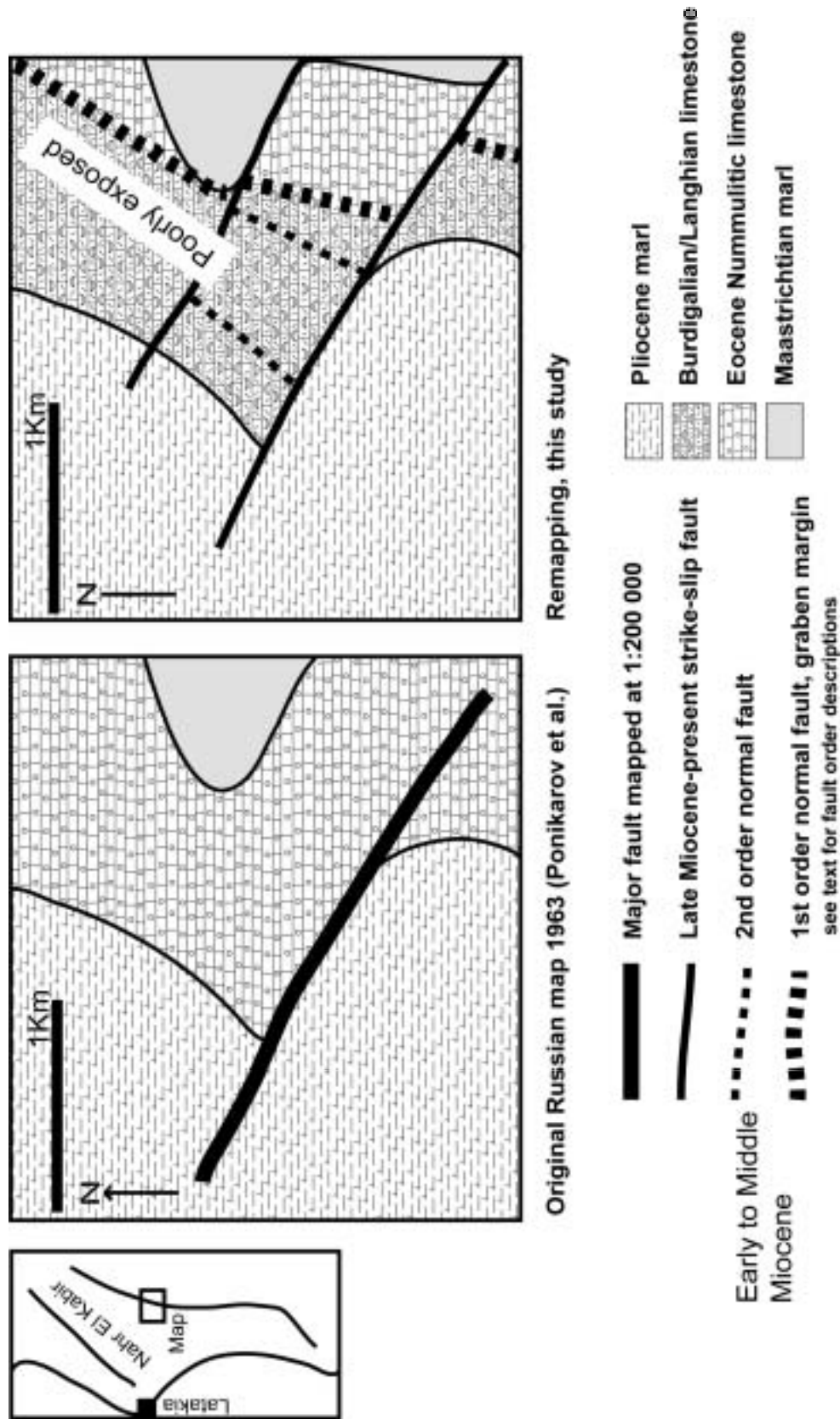
#### *Summary of Eastern Margin*

The eastern margin of the Nahr El-Kabir Half-Graben commenced with extensional, normal faulting during the Early Miocene (Late Aquitanian or Early Burdigalian), although the majority of accommodation space did not form until the Langhian. Normal faulting appears to have ceased in the latest part of the Langhian-Serravallian time-slice (6). Normal faulting (striking NE) was often accompanied by forward rotation of blocks, perhaps indicating only a small amount of extension (Payne et al. 1995) within the graben as a whole. Perpendicular strike-slip faults (transfers, NW striking) are associated with the normal faults and offset them. Indications from most other normal faulted regions implies that transfer faults form at the same time as normal faulting (McKenzie, 1978). This could not be confirmed, only inferred as the fault ground trace is poor. Strike-slip movement does seem to be active or recent as the faults scarps are well exposed, whereas active normal faulting could only be seen at Khan El-Jouz.

Therefore, the eastern margin of the Nahr El-Kabir Graben was active during the Miocene and the basin was fault bounded on both margins, as a subsiding linear graben.

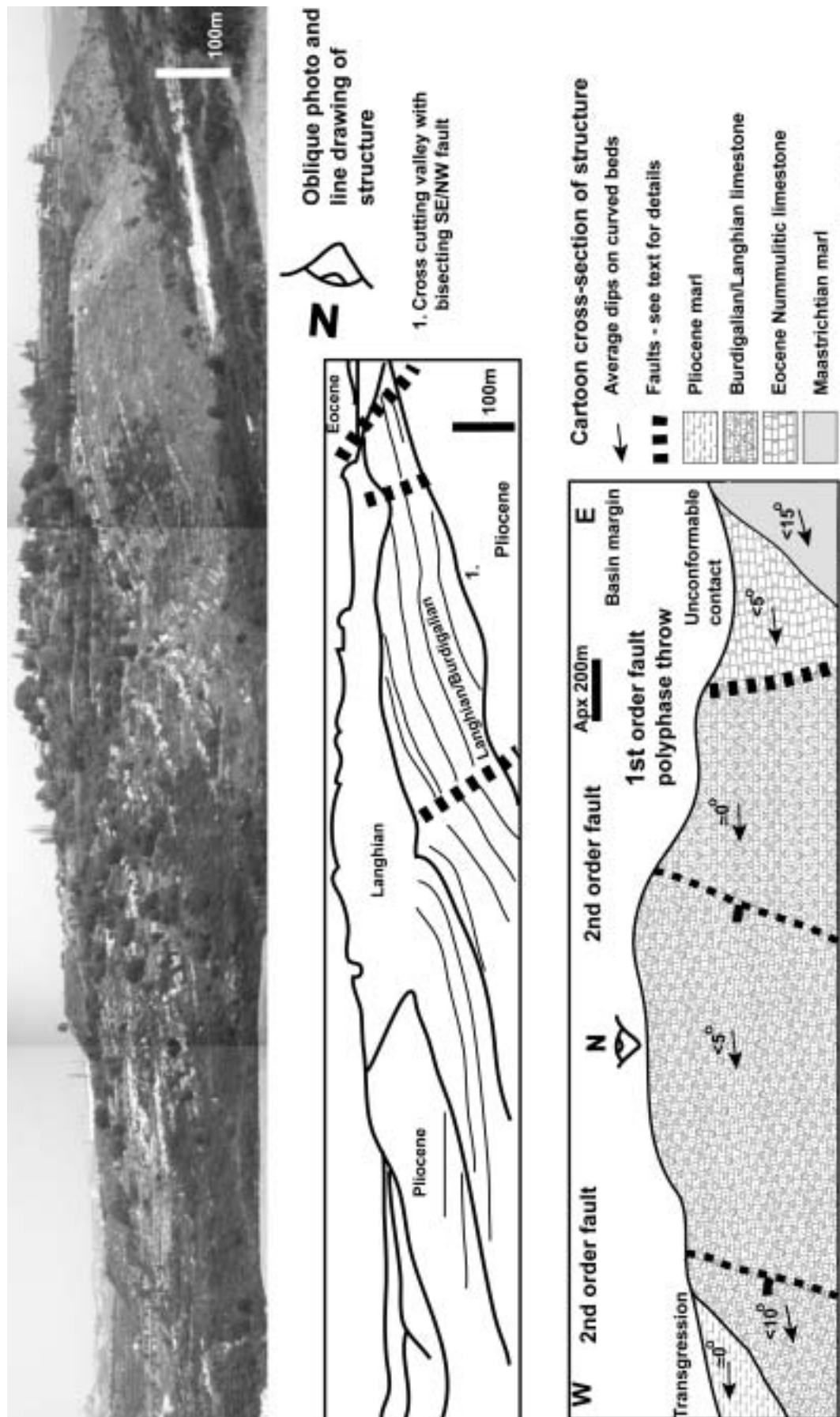
#### Faulting within the Nahr El-Kabir Graben

Faulting within the Nahr El-Kabir Graben where present, is usually very poorly exposed within the mainly marl-rich sedimentary rocks. Three fault localities were found in Langhian-Serravallian-age strata in the north of the graben, north of Khan El-Jouz Village (Figures 4.39 to 4.41). In each outcrop, the fault orientations are predominantly north to

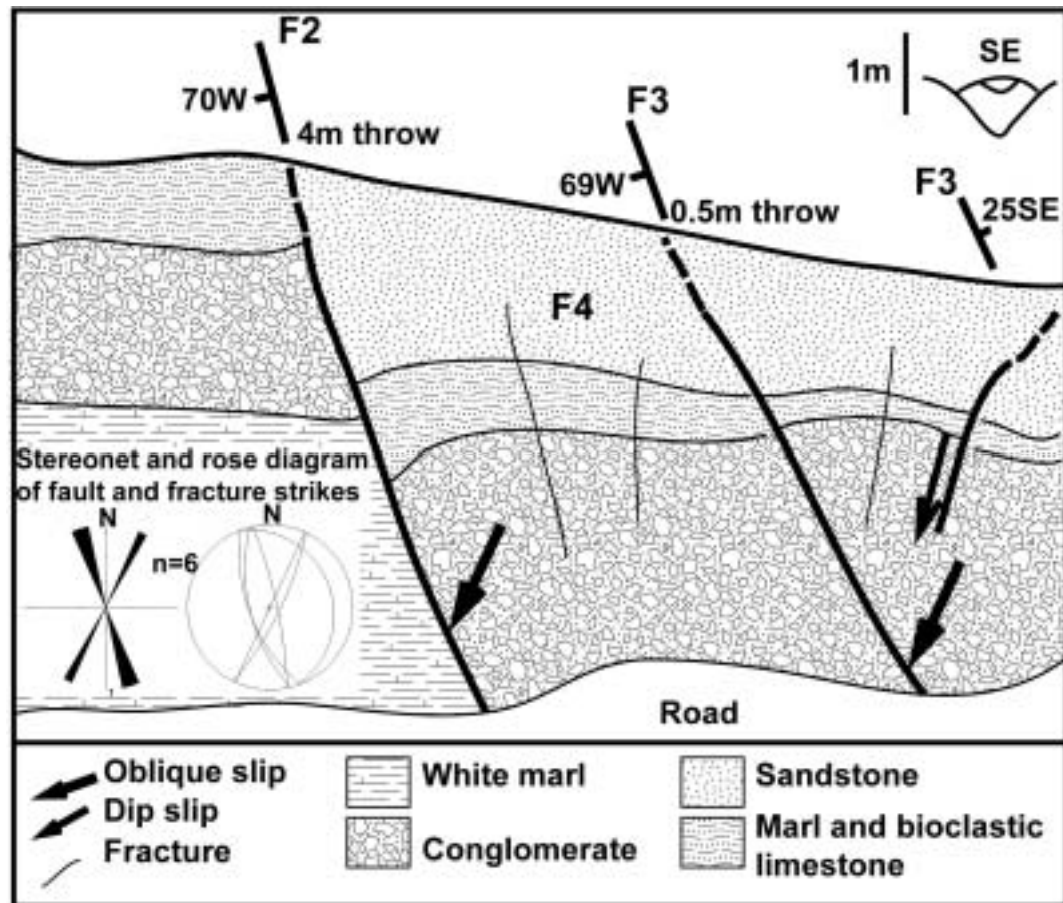


**Figure 4.36** Remapping of the southern and eastern margin of Nahr El-Kabir Valley to assess the structuration and tectonic stratigraphy revealing that the margin is much more complex than had previously been observed. The relation between the Eocene succession and the Miocene strata is shown by the mapped extensional faults with strike-slip 'transfer' or linking faults.

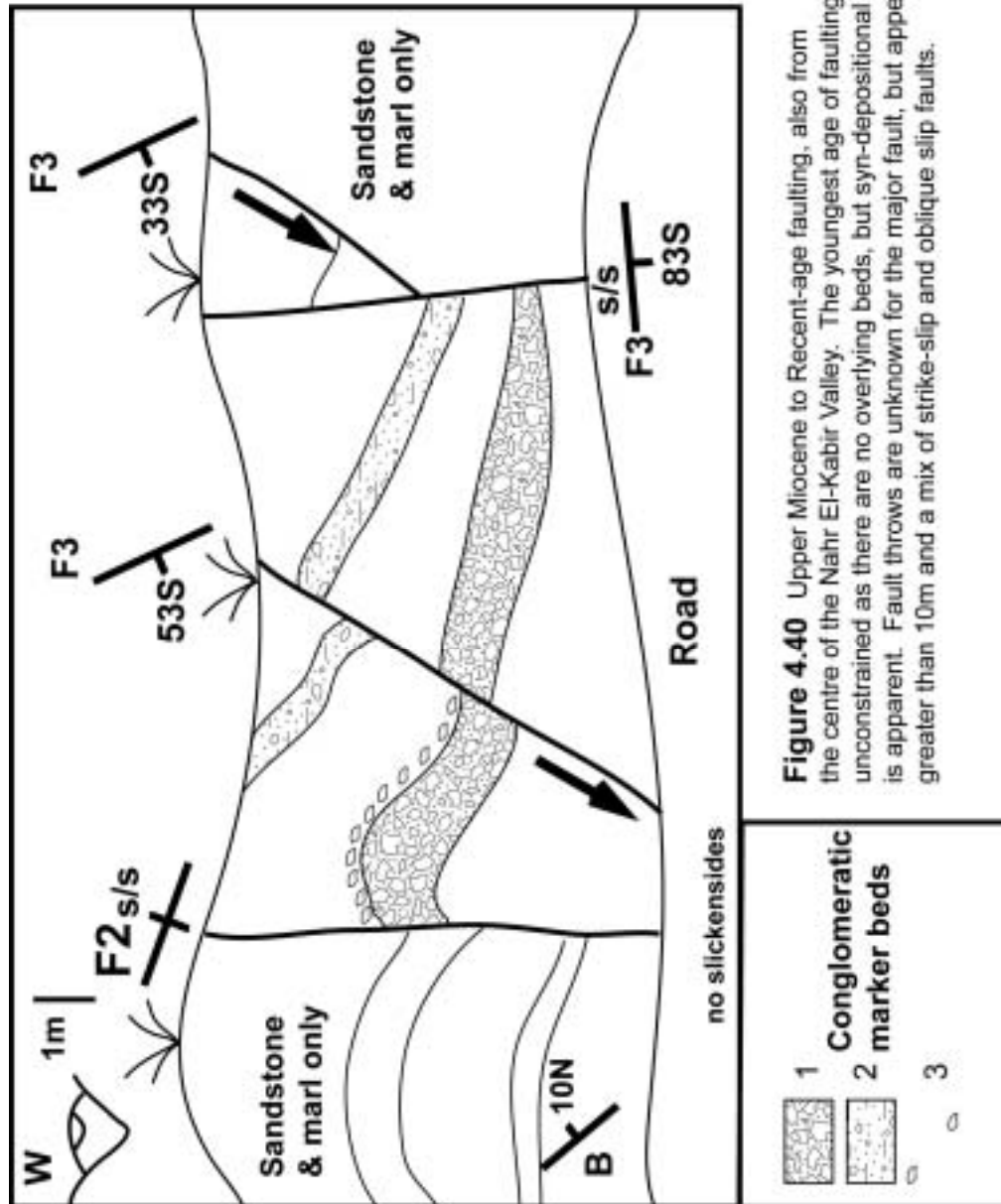




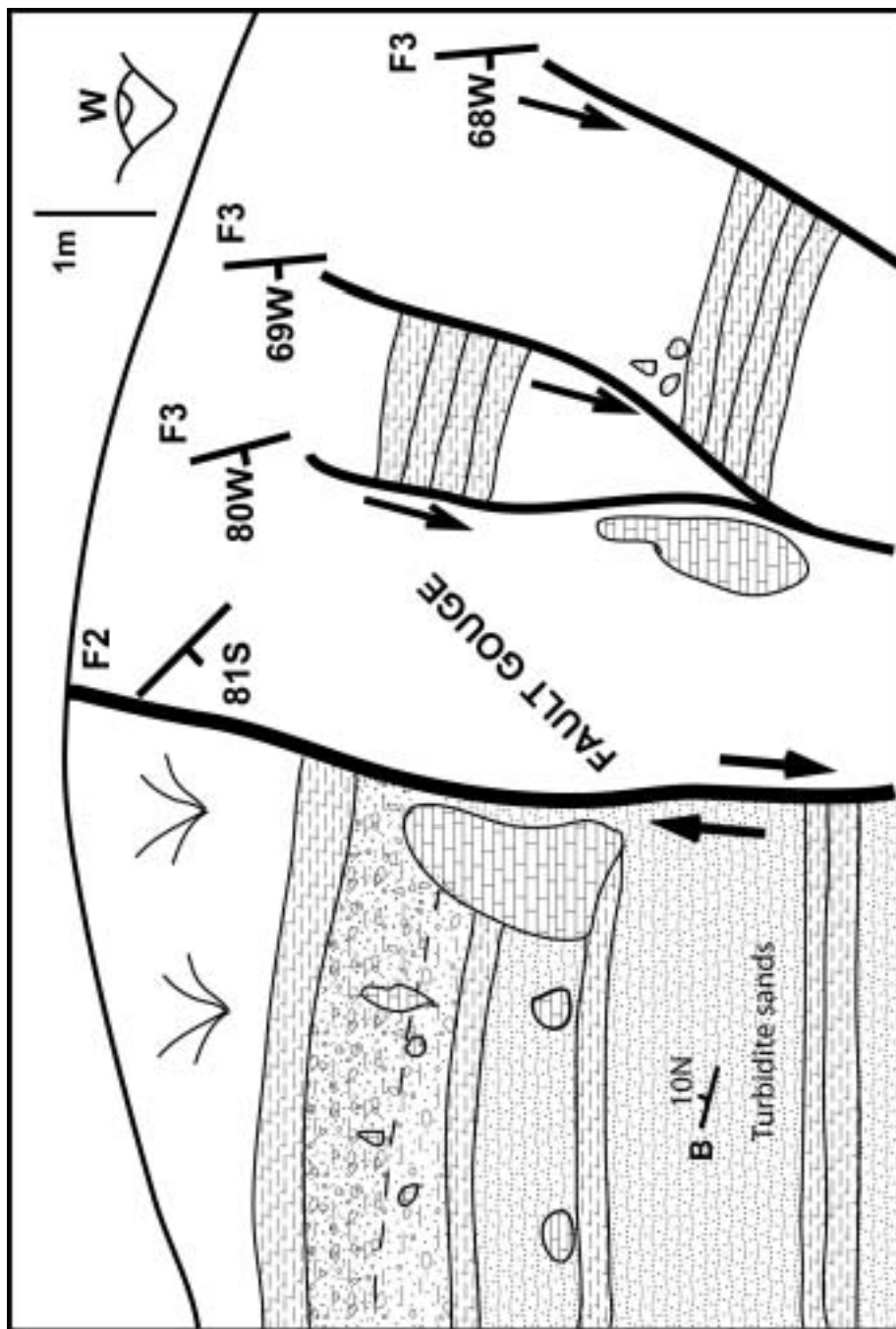
**Figure 4.37** A cross-section view of the structure of the southern margin of the Nahr El-Kabir Valley. Low  $\beta$  extension is inferred (see text and Fig. 4.36).



**Figure 4.39** Transtensional faulting within the Middle Miocene succession 5km north of Khan El Jouz Village.



**Figure 4.40** Upper Miocene to Recent-age faulting, also from the centre of the Nahr El-Kabir Valley. The youngest age of faulting is unconstrained as there are no overlying beds, but syn-depositional faulting is apparent. Fault throws are unknown for the major fault, but appear to be greater than 10m and a mix of strike-slip and oblique slip faults.



**Figure 4.41** Strike-slip faulting observed in Serravallian to Quaternary-age sediments, from the centre of the Nahr El-Kabir Valley. Vertical fault throw is uncertain but is greater in some cases than the visible outcrop. Faulting appears to have started in the Serravallian as some of these deposits show syn-sedimentary disturbance, but the majority of movement was probably Plio-Quaternary to Recent.

northwest – southeast. The faults cut both the Miocene-age strata and the overlying Plio-Quaternary alluvium. The faulted Miocene sedimentary rocks show some evidence of earlier and occasional syn-depositional disturbance. Thickness variations are common close to fault planes, as is evidence of syn-depositional clasts. Juxtaposition of unrelated units is also a common feature. A later stage of subsidiary, extensional, normal faulting is present.

These outcrops suggest a Langhian-Serravallian-age of extensional (minor) faulting. These faults were then reactivated during the Plio-Quaternary as strike-slip (oblique) lineaments ( $F_2$  faults) with subsidiary oblique ( $F_3$ ) and extensional faults. The large strike-slip faults ( $F_2$ ) often displace the footwall facies completely, indicating considerable movement (Figure 4.40 and 4.41 and pull-out geological map). The subsidiary and oblique faults could represent negative ‘flower’ structures.

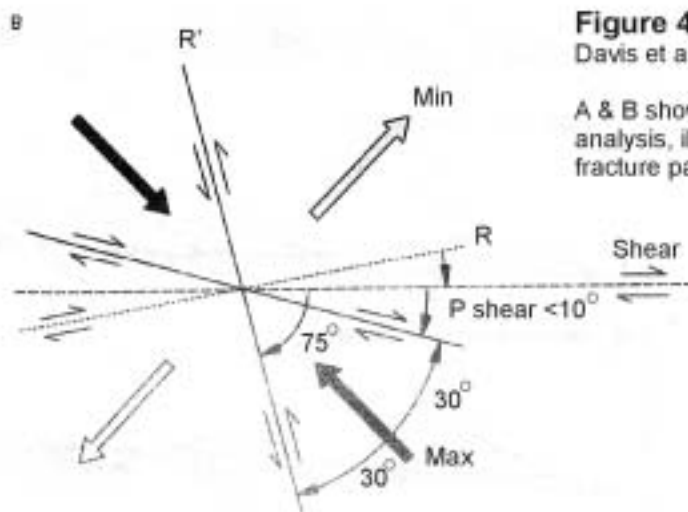
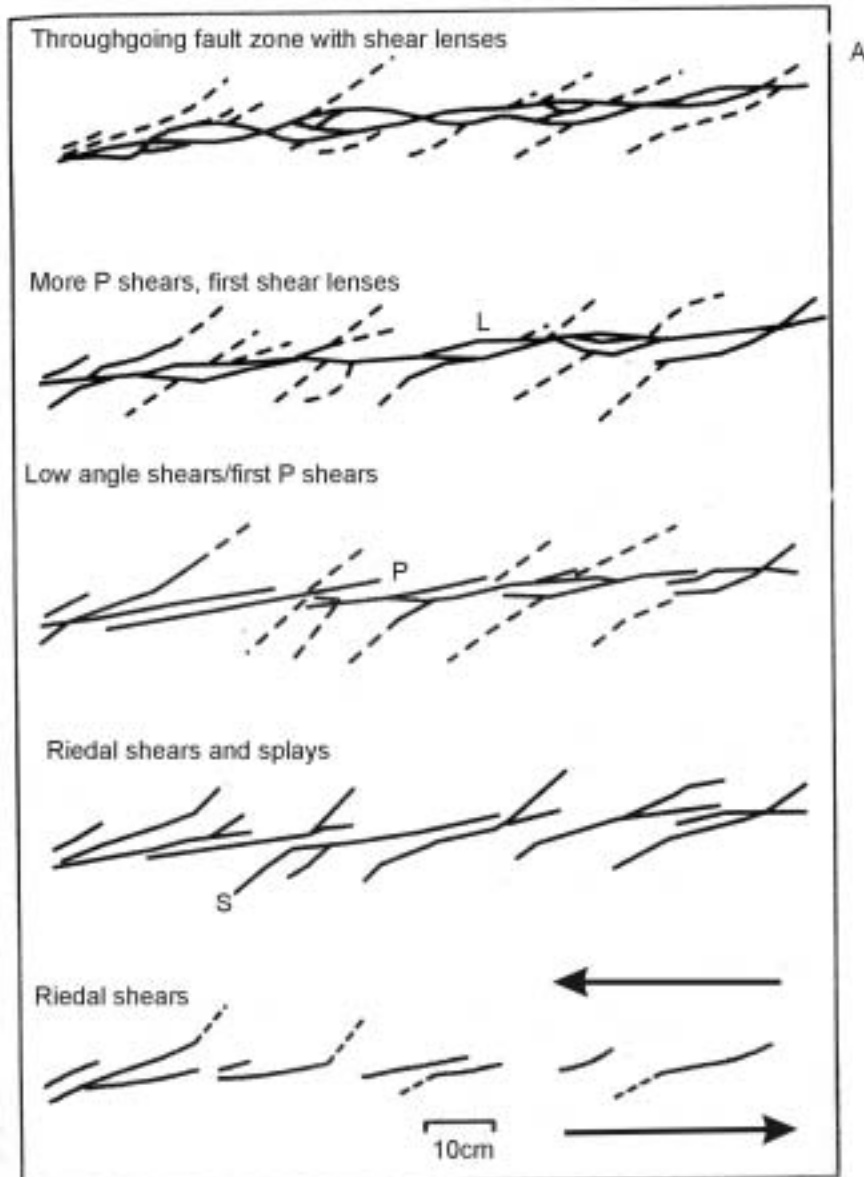
### Strike-slip faulting and Riedal shears

Once a dataset of strike-slip faults and accompanying shears, with sense of movement, had been obtained, then the following comparisons are useful to assess the inferred strike-slip faults.

Both the El-Kabir Lineament and Dead Sea Transform are interpreted as having a sinistral throw and both strike in a north to northeast direction. Riedal shear arrays, in theory (sinistral, Figures 4.42 and 4.43), should support that the main fault would have synthetic shears forming approximately  $15^\circ$  anticlockwise to it. These synthetic shears should have the same sense of motion (i.e. sinistral, north striking). Antithetic shears will be dextral in motion sense and form  $75^\circ$  anticlockwise to the main fault (i.e. northwest striking). P shears form last and propagate a few degrees clockwise of the main fault, in the same sense (i.e. northeast striking).

If the dataset acquired during this study is not interpreted with respect to time, fault relations, or sedimentological events, then the above hypothesis suggests that all the faulting (NE-SW and NW-SE) originates from one episode of northeast striking strike-slip faulting (i.e. relates to the the Dead Sea Transform Fault).

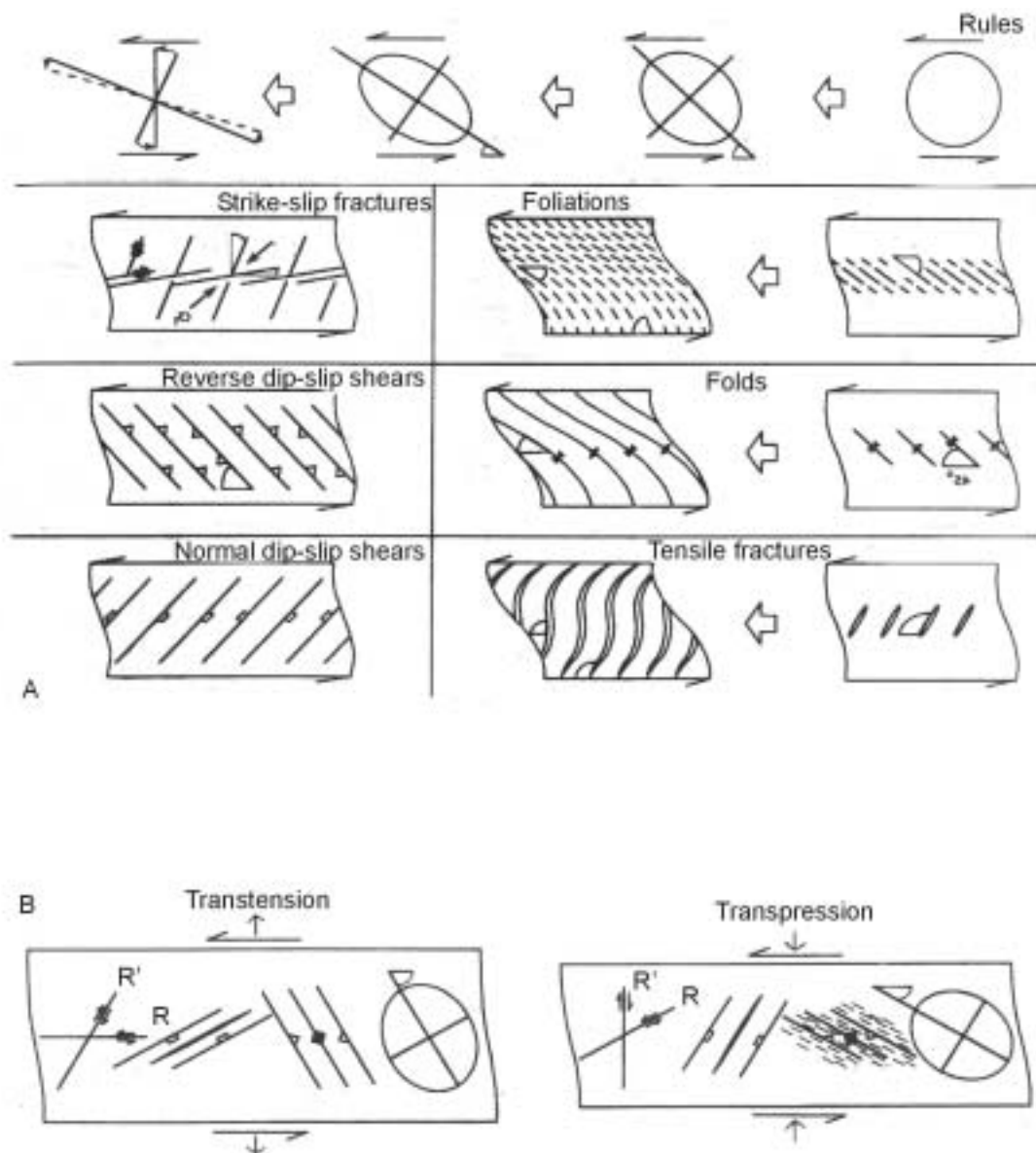
However, the northeast orientation is interpreted here as older, multi-episodic and dominant within the Nahr El-Kabir Valley. By contrast the northwest orientation is limited to a secondary phase (predominant in the Ghab region) of Late Neogene to Plio-Quaternary-age (Domas, 1989; Brew et al. 2001; Zanchi, 2002).



**Figure 4.42** Modified after (reversed) Davis et al. (1996).

A & B show the theory of Riedal shear analysis, illustrating development of fracture patterns and direction of strain.





**Figure 6.43** Modified (reversed) and simplified from Woodcock et al. (1994). A & B show horizontal sections through vertical strike-slip zones and predicted geometric patterns for structures.

Summary of faulting within the Nahr El-Kabir Valley, a possible graben NW-SE and NE-SW orientated faults are common throughout the Nahr El-Kabir region. From field data, it is inferred that the NE-SW faulting gives rise to the largest faults ( $F_0$  and  $F_1$ ). The timing of the fault movement is inferred to be Middle-Late Eocene and Plio-Quaternary, with possible fault movement during the Miocene. This fault orientation is cut by later fractures with a NW-SE orientation and with timings identified as Middle to Late Pliocene and possibly Middle Miocene. The NW-SE fault orientation as the prominent direction of Pliocene-age fracturing close to the Ghab Graben, perhaps indicating that this orientation is due to propagation of the Dead Sea Transform Fault (?synthetic fracturing, Figure 4.43).

The El-Kabir Lineament defines the northern margin of the Nahr El-Kabir Graben (in reality a half-graben). Faulting commenced in the Late Palaeogene, if not before (see Chapters 3 and 6), providing the accommodation space for Miocene-age sediments to accumulate (see Chapter 3 and 6). Miocene-age faulting on the southern margin of the valley, provides evidence that during this time the Nahr El-Kabir region was a fault bound graben (both the northern and southern margins). Faulting on the southern margin is not apparent from the Late Miocene onwards, perhaps indicating that graben subsidence had reverted to a half-graben.

Chapter 6 combines the sedimentological and structural data to provide a geological history.

## Regional analogues

The Nahr El-Kabir Graben is poorly exposed, due to heavy cultivation. Very little published literature exist about this area, except that done by Russian researchers (see Chapter 2).

Therefore, to aid interpreting the geological history, sedimentology and tectonics, it was useful to study basins with analogous features and settings.

The Tertiary was a time of closure of the Tethys Ocean, followed by continental collision (see Chapter 6). Once initial continental collision occurred, intense faulting and reorganisation of the tectonic plates began (i.e. accretion of Anatolian Plate and the splitting of the Arabian and African Plates). Numerous small basins formed. Figure 5.1 illustrates the occurrence of Neogene depocentres, both continental and marine in the Eastern Mediterranean.

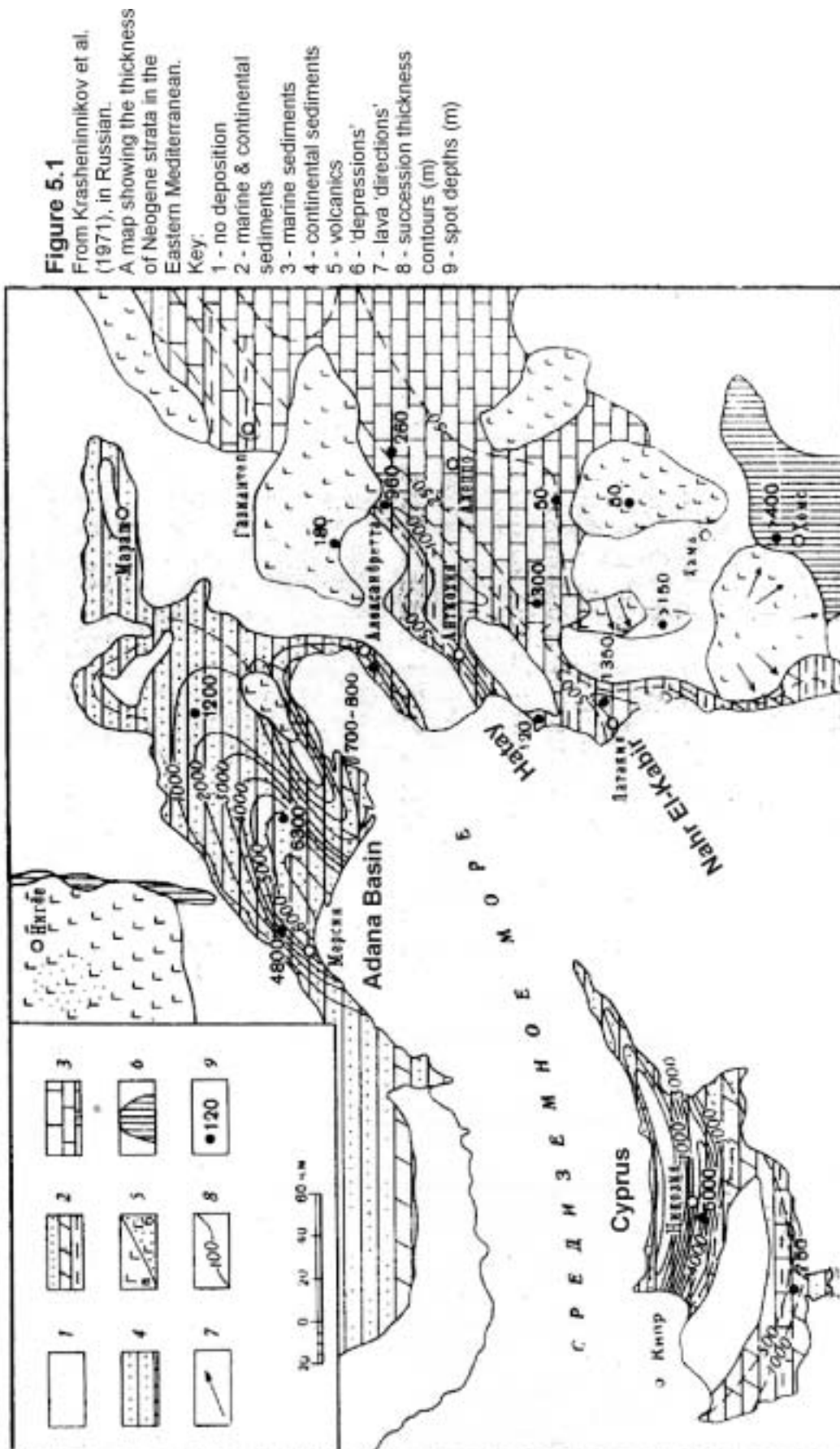
Four basins with similarities to the Nahr El-Kabir Graben were chosen for comparative fieldwork, in Cyprus, Turkey and Syria (Figure 5.2). These were, the Polis Graben (Cyprus), Hatay Graben (Turkey), Adana Basin (Turkey) and the Ghab Graben (Syria). This chapter sets out to compare aspects of geological similarity between basins to enable better understanding of the graben forming processes in Syria.

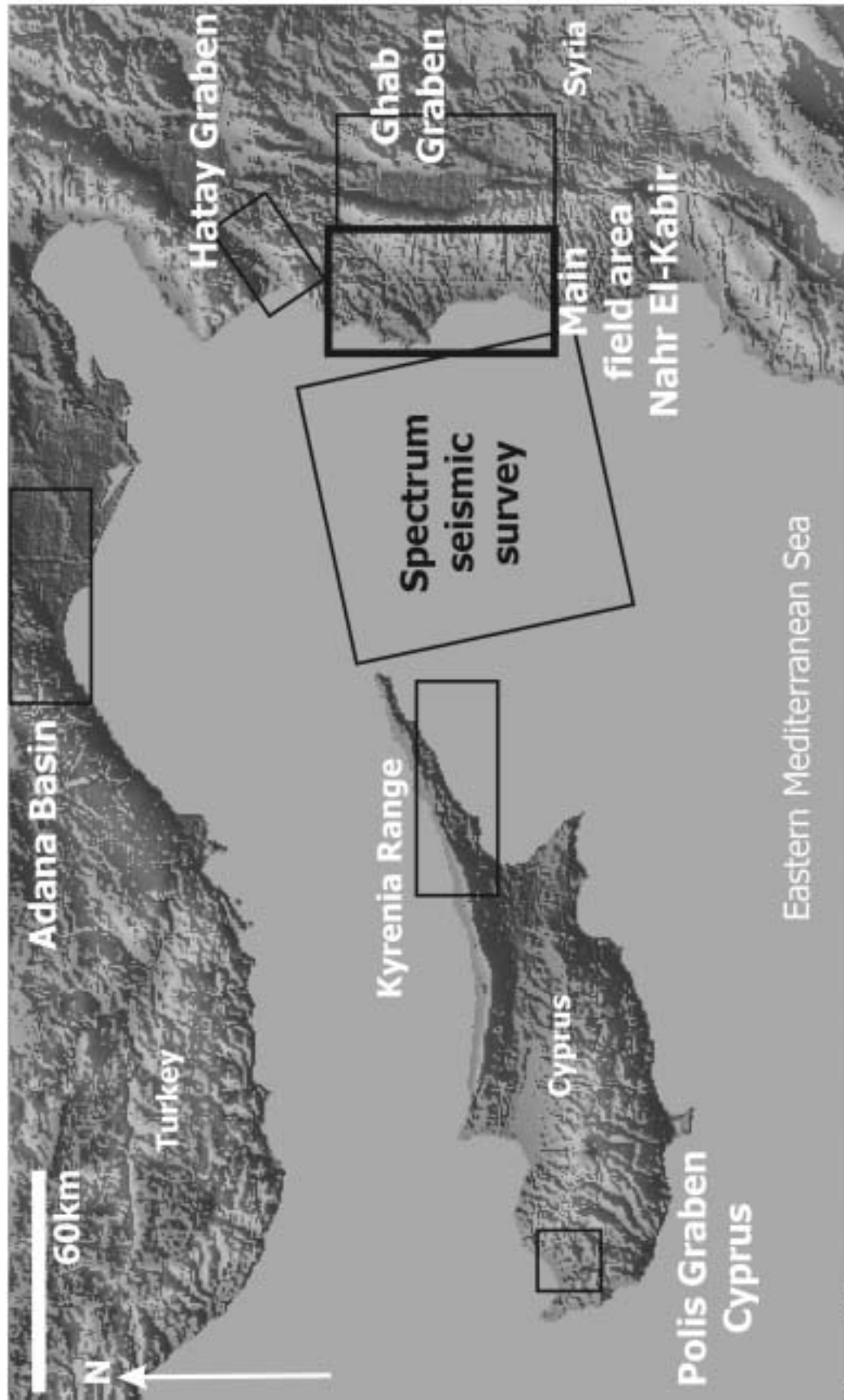
### *Polis Graben, Cyprus*

The Polis Graben is a Late Miocene basin situated in the west of Cyprus. A day of reconnaissance field-studies were carried out in 2000 with Professor Alastair Robertson to re-examine some of the localities used by Payne et al. (1995, 2000). She studied the region in detail for her Ph.D. at Edinburgh University as part of the Tethyan Research Project.

Previous studies have also been undertaken by Follows et al. (1990), relating the structure of western Cyprus, Eaton et al. (1993, Miocene reef facies and Poole et al. (1991, 1998 & 2000), examining the Plio-Quaternary.

The Polis Graben is situated to the north of the Eastern Mediterranean subduction zone, on the uplifted Cyprus block (Figure 5.2 & 1.5). It is located to the southwest of the Troodos Ophiolite in a region of inferred supra-subduction zone extension (Payne et al. 1995); drag on the over-riding plate, extends to the surface of the crust above, creating a zone in extension.





**Figure 5.2** Location map of the regional, comparative studies undertaken in the Eastern Mediterranean area for this thesis. Basemap of topographic data is from [www.nima.mil](http://www.nima.mil)

The Polis Graben is an extensional rift basin, with perpendicular transfer faults linking the extensional faults. The extensional faults form a series of “steps” within the graben. Payne et al. (1995) calculated that 7% (1.01) extension occurred perpendicular to the basin margins; this low amount was due to basin formation in an area of incipient extension Cyprus. The location of faults within the graben was thought to have been heavily controlled by the underlying basement morphology.

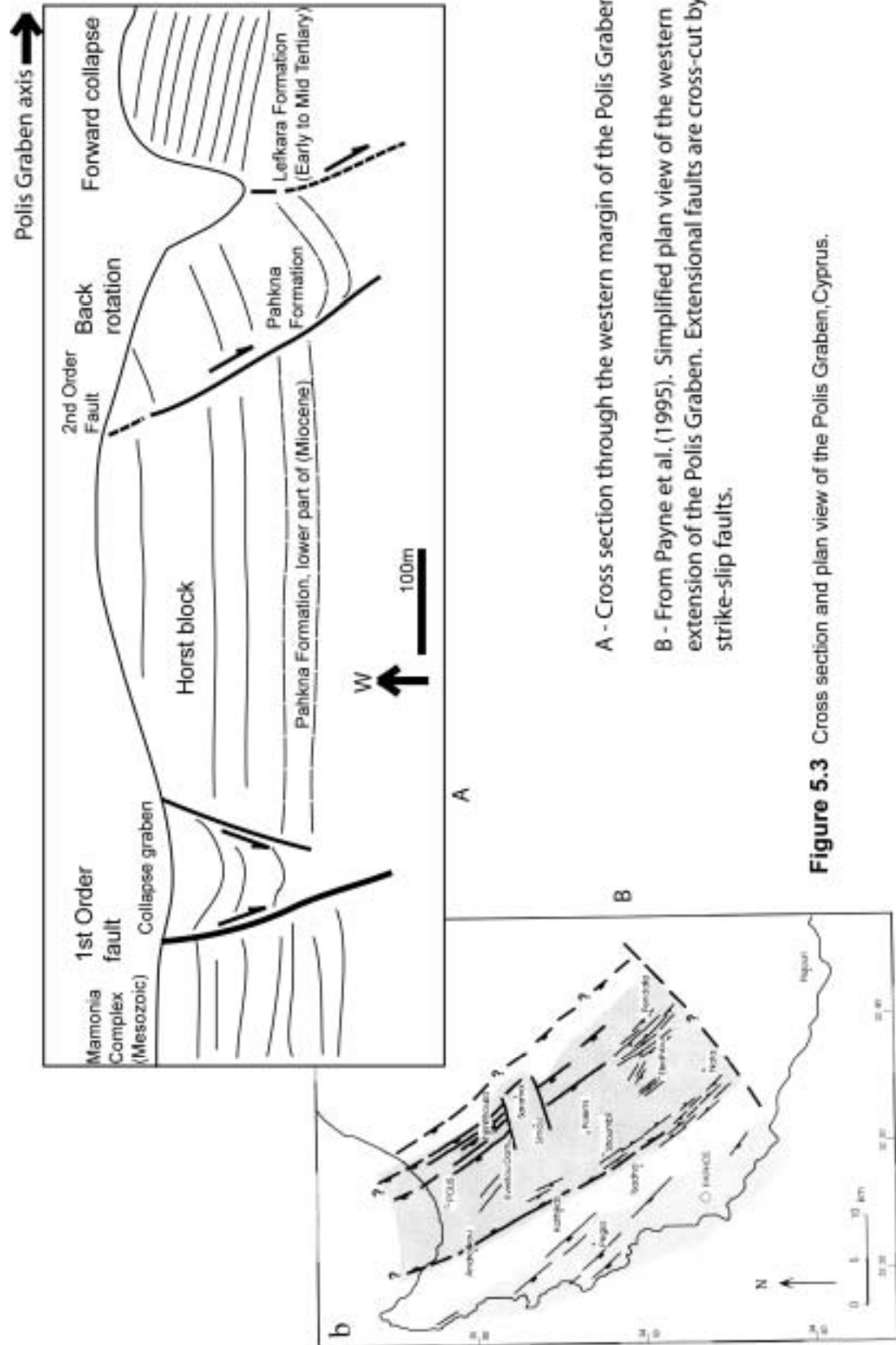
The basement rocks are Mesozoic to Early Tertiary-age, part of the Mamonia Complex and form the graben margins. The graben fill comprises the Tertiary formations Lefkara (Lower to Middle Tertiary – pre-rift) and Pahkna Formation (Miocene, syn-rift). Both formations are primarily chalk with redeposited bioclastic sediments. The Terra Member of the Pahkna Formation (Early Miocene), then the Koronia Member (Late Miocene), were ‘reefal’ limestones on the basin margins (Follows et al., 1990; Franseen et al., 1996). The overlying Messinian strata (syn-rift), marked a eustatic fall and shallowing of water depths (Robertson et al. 1985). This led to gypsum deposition and then to erosion and faulting derived debris flows. Plio-Quaternary formations record fan-delta and conglomerate deposits as was Cyprus uplifted (Poole et al. 1991).

In the field, the primary investigative sites for comparison were those which showed the basin margins and the related faulting (Figure 5.3). Possible similarities were observed with the southern margin of the Nahr El-Kabir Graben. The largest extensional faults bound the margin of the Polis Graben. These large normal faults controlled development of horst and back-rotated blocks of pre-rift sediments. Later, smaller, synthetic normal faults within the graben, resulted in forward rotation (forward collapse) of the syn-rift sediments. The interpretation is that back-rotation of blocks required more extension than forward collapse and therefore, differing rates and amounts of extension occurred at different times.

Transfer faults linked strands of the major extensional faults and provided pathways for redeposited sediment transport. The genesis of the transfer faults was thought to have to have been contemporaneous with initial extension.

The Polis Graben sedimentary rocks are similar in some ways to those observed in Syria. Shallow-marine (reefal in Cyprus) carbonate sediments on the margins were actively faulted (with both normal and transfer faults) and these sediments redeposited as debris flows by fault controlled pathways into deeper water conditions.





A - Cross section through the western margin of the Polis Graben.  
 B - From Payne et al. (1995). Simplified plan view of the western extension of the Polis Graben. Extensional faults are cross-cut by strike-slip faults.

*Preliminary comparisons with the Nahr El-Kabir Graben*

The Polis Graben is in a different tectonic setting to the Nahr El-Kabir Graben as it is on the overriding Anatolian Plate, in a region of subduction “roll-back” leading to extension in the upper crust. The Nahr El-Kabir Graben is in a continental collision zone of a promontory. However, both grabens have similarities in architecture and both formed due to small amounts of extension, although this could not be quantified for the Nahr El-Kabir Graben:

- € The structure of the southern margin of the Nahr El-Kabir Graben is very similar to that of the southern margin of the Polis Graben.
- € Both graben margins were controlled by large extensional faults (see Chapter 4), linked with strike-slip ‘transfer’ faults.
- € Internally, both grabens show forward collapse of large fault blocks, thought to be due to low factor extension.
- € Shallow marine carbonate sedimentation is similar on the graben margins (perhaps an escarpment setting), with redeposition and debris flow into the grabens utilising the transfer faults.

There are also distinct differences:

- € The Nahr El-Kabir Graben is asymmetrical and the northern margin is strike-slip fault controlled.
- € The Polis Graben is underfilled with respect to the basin fill, whereas in the Nahr El-Kabir Graben there are signs of overfilling the graben margins.
- € The Polis Graben was continuously in extension (in Miocene to Recent), in an uplifted extensional plate tectonic setting. This is in direct contrast to the Nahr El-Kabir Graben which is in a compressional, continental plate setting.

From the comparisons in the geology, some common features are observed between the two grabens. The most important are those relating to graben formation. The southern margin of the Nahr El-Kabir Graben has very similar features to those seen in Cyprus. Specifically, the large extensional faults and transfer linking faults. These compare closely with features observed in the Burdigalian to Serravallian-ages in Syria.

### ***Hatay Graben, Southern Turkey***

Two days field-studies were carried out in 2001 on the western edge of the Hatay Graben (Pisken, 1985) (Figure 5.2). The graben is situated 45km due north of the Latakia region and is filled with Tertiary-age sediments. Numerous strike-slip faults and 'reefs' are mapped on the graben margins (Pisken, 1985). It was expected that there would be similarities with the Latakia region due to its proximity and the mapped similarities of rock ages and structure.

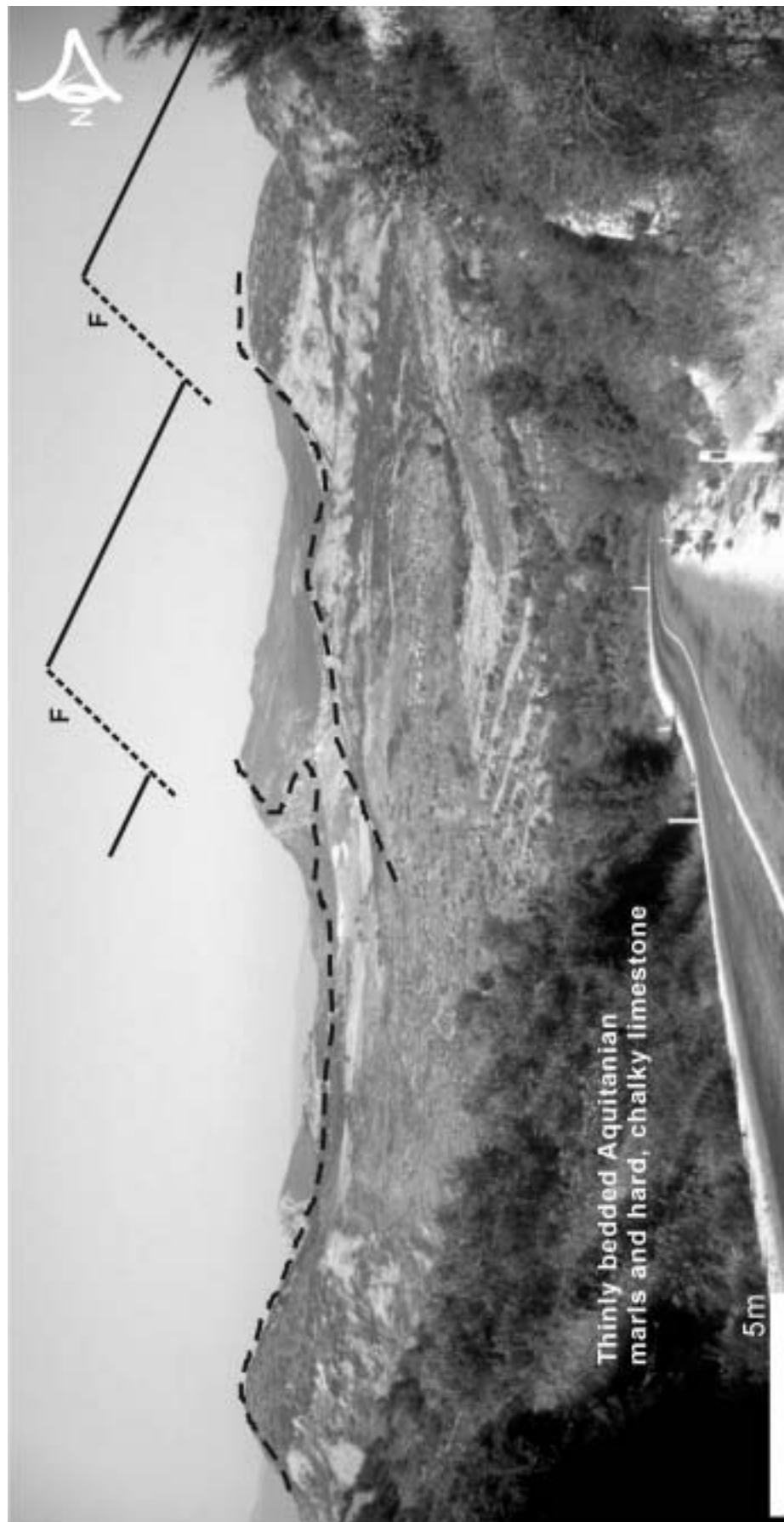
The Hatay Graben is a Tertiary graben, situated on the southern margin of the Anatolian Plate. The Baer Bassit Ophiolitic Massif is directly to the south and the northern margin of the graben is delineated by the Kizil Dağ Ophiolite. The graben is narrow (<20km wide), trends SW-NE and opens into a broad Quaternary plateau north of the town of Hatay (Antioch), north of the Ghab Graben. Outcrops of Palaeogene and Neogene strata are found on both the north and south margins, whereas the graben axis is dominated by Messinian to Plio-Quaternary successions and no older rocks crop-out.

#### *Southern margin and graben center*

Palaeogene and Neogene sedimentary rocks crop-out high up on the southern flank of the graben, usually in well-defined, back-rotated extensional blocks (see Figure 5.4). To the south of these fault blocks, Pisken (1985), mapped faults which bound the southern margin of the graben. These faults were identified during fieldwork and show oblique-slip, in numerous orientations.

Lower Miocene and Palaeogene facies are similar to those found in the Nahr El-Kabir Graben i.e. chalky, foraminiferal wackestones. Middle Miocene facies are very bioclast-rich and do not contain ophiolitic massif-derived fragments, in contrast to facies seen in the Nahr El-Kabir Graben. The facies contain fragments of bivalves, algae and gastropods. The Upper Miocene (Messinian) occurs only very locally and is dominated by gypsum in the form of selenitic crystals (swallow-tail), which crop-out at a height of 250m above sea level, roughly the same height as in the Nahr El-Kabir Graben.

Plio-Quaternary marls are found at, or just above sea-level in the axis of the graben; none are found on the graben margins. Roman-age harbor ruins are apparent on the beach at Samandāgi Town, indicating that approximately 2m of uplift has occurred in the last 2000 years in this area.



**Figure 5.4** A series of backrotated, extensional fault blocks on the southern margin of the Hatay Graben, Turkey. This locality is 25km due north of the Baer Bassit Ophiolitic Massif and the Nahr El-Kabir Graben, where extension is limited to low-beta, forward slumping blocks and transtensional features

*Northern margin*

The northern margin of the graben is dominated by Lower and Middle Miocene-age facies, that crop-out at sea-level. The Lower Miocene is a chalky, white foraminiferal wackestone, often redeposited as carbonate cemented conglomerate. It is overlain by Middle Miocene-age bioclastic packstones and grainstones in small debris flow units (Figure 5.5). This unit typically comprises thinly bedded, upwards fining, carbonate conglomerates, in a prograding architecture. The suggestion from this study is that reefs existed on this margin, probably higher up on the Kizil DaŪ Ophiolite and reef talus slope debris was transported into the graben.

*Preliminary comparisons to the Latakia region*

This project carried out only a reconnaissance study of the Hatay region, but puts forward some basic comparisons between it and the Latakia region:

- ≠ The Palaeogene and Lower Miocene strata are widely developed and contain similar facies to those seen in northwest Syria.
- ≠ Middle Miocene facies consist of purely carbonate facies, with no clastic input from either the Baer Bassit Ophiolitic Massif or the Kizil DaŪ Ophiolite. The facies show more bioclastic material and less marl than those seen in Syria. This maybe due to deposition in a shallower-water marine environment than those studied in Syria.
- ≠ Messinian-age sediments were found as selenitic gypsum crystals, with no accompanying marl on the graben margins. Alabastrine gypsum with marl, exists in small outcrops in the graben axis. Alabastrine gypsum and marl is most common in Syria, perhaps indicating a lesser influx of seawater.
- ≠ Pliocene facies appear similar to those in Syria, but no bioclastic sands are found at the top of the succession.
- ≠ Latest Quaternary beach terrace uplift is similar or slightly greater than that seen 50km south at Latakia (Pirazzoli et al., 1991; Dalongeville et al., 1993).
- ≠ Summary of events: A wide basin probably existed in the Palaeogene and earliest Miocene. No evidence of Oligocene facies is seen. The formation of the Hatay graben seems to have commenced in the Miocene (Burdigalian? Figure 5.5) with a high beta factor (unknown) of extension leading to back-rotation of fault blocks. The overlying Messinian strata are found both perched high above the graben (250m above, selenitic gypsum) and in the basin axis (alabastrine gypsum), perhaps indicating syn and

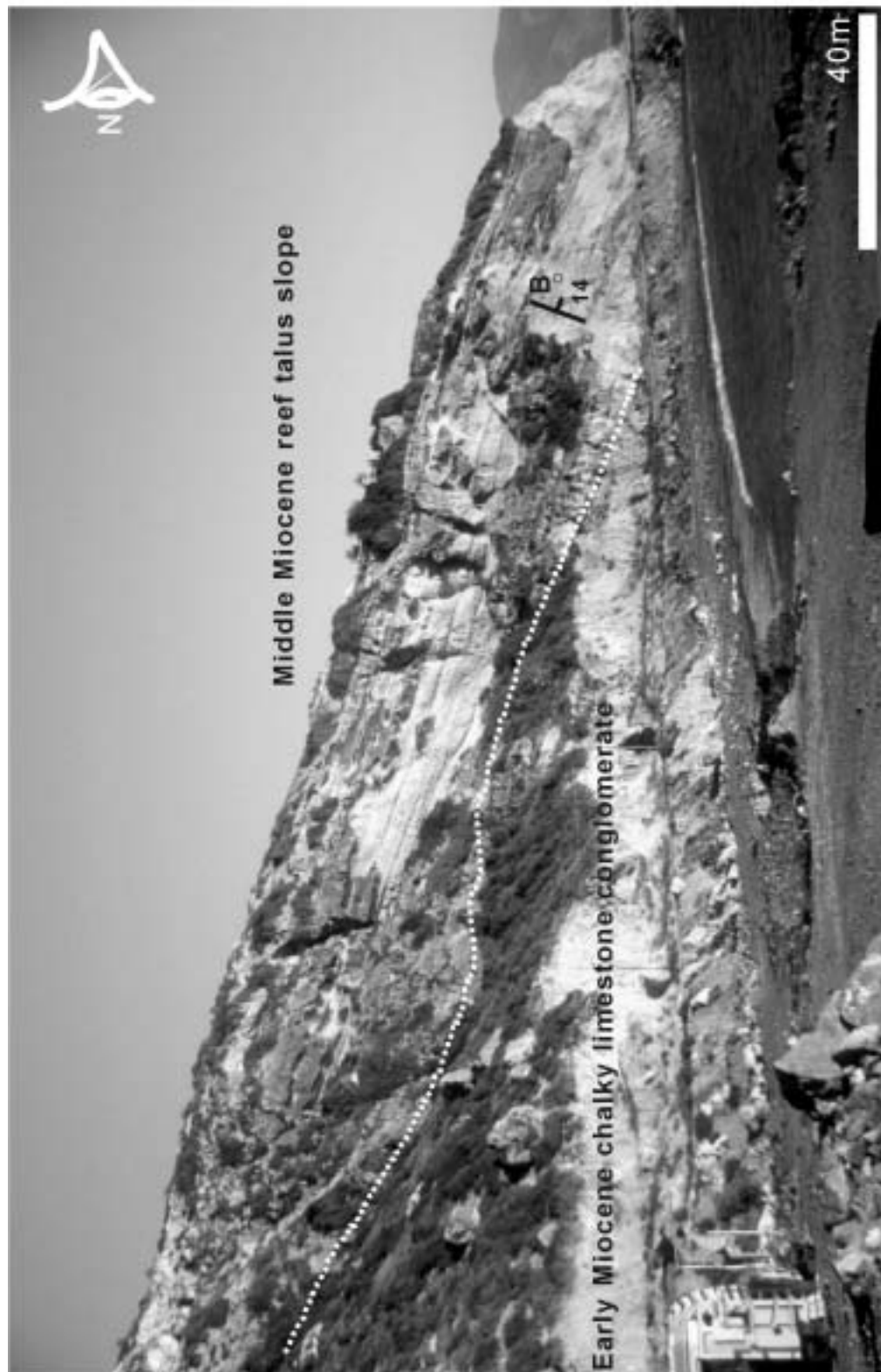


Figure 5.5 View of the northern margin of the Hatay Graben, Turkey, at the northernmost point of Samandagi Bay (40km north of Latakia). The Early Miocene succession is white, chalky, sandy limestone, overlain by an unconformable Middle Miocene unit, consisting of large quantities of bioclastic debris and shell fragments in a sparitic matrix.



definitely indicating post-Messinian uplift of the graben margins. Very little uplift at the basin axis occurred during, or since, the Plio-Quaternary successions, as they are at sea level. In the Nahr El-Kabir Graben, these sediments are over 200m above sea level.

This brief summary shows that far from the expected similarities between the areas, there are some important differences. Events which feature prominently in the Nahr El-Kabir Graben are not evident at the same time within the Hatay Graben. Therefore, despite the proximity of the regions to one another and initial mapped similarities, each area must be regarded as distinct.

Since this preliminary study was undertaken, Sarah Boulton, Edinburgh University, has commenced studying this area further for her PhD.

### ***Adana Basin, Turkey***

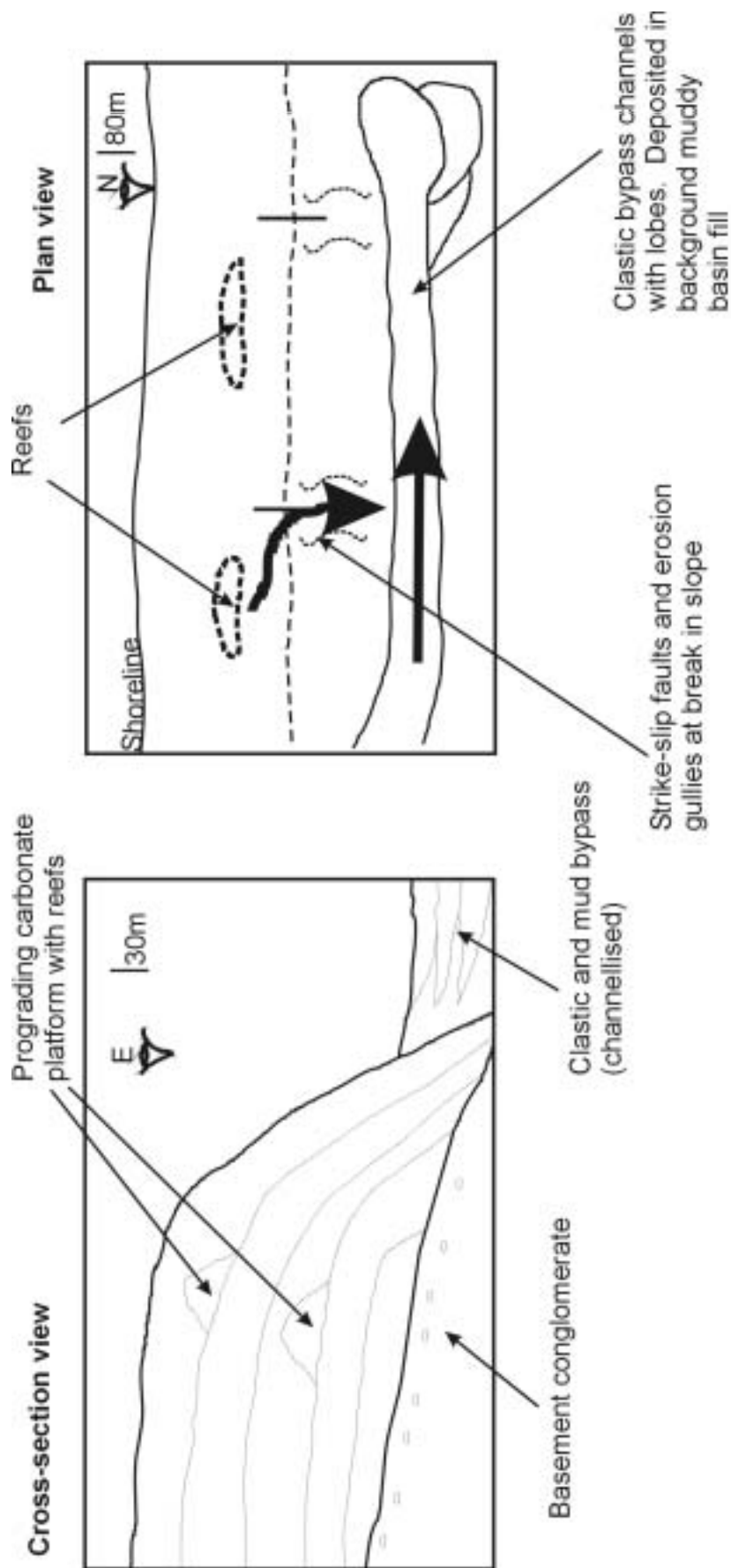
Professor Gilbert Kelling organised a short fieldtrip (2 days) to the Adana Basin in 2001, for representatives of the Turkish Petroleum Company, which I was very kindly allowed to join.

The Adana Basin (Figure 5.2) is a large (10000sq km), Neogene basin sited within the Tauride Orogenic Belt (Kelling, 2001, personal communication). To the north it is bounded by the Ecemi Fault Zone (strike-slip transform fault) and the basin fill is Miocene to Quaternary-age (c.9000m). The basin fill overlies a deformed Palaeozoic and Mesozoic basement. The majority of the sedimentary rocks are Early to Middle Miocene-age, as rapid subsidence occurred at this time. Very variable facies are observed within the basin, ranging from submarine fan turbidites to fluvio-deltaic clastics and Messinian evaporites. Eight formations with significant regional unconformities are present.

During the fieldtrip we visited numerous localities throughout the basin and were able to assess the structure and facies. Many of these features seem analogous to those seen in the Nahr El-Kabir Graben. The essential comparisons are:

- ≠ The Adana Basin is cut by and deposition was controlled by a major strike-slip fault (Ecemi Fault, Jaffey et al. 2001). Burdigalian-age rocks are the first clastic sediments in the Adana Basin and accumulated along a series of backstepping faults, running in parallel to the Tauride Mountains to the north. The timing and setting is very similar in Syria, except there is no evidence of the major lineament backstepping there.
- ≠ They both contain similar age and types sedimentary rocks, is this related to regional events and collision?

- € Shallow-marine carbonate sediments were transported downslope, associated with transfer faults in the Adana Basin. In the Nahr El-Kabir Graben, both extensional growth faults and transecting strike-slip faults are apparent and similarly control deposition.
- € The Adana Basin sedimentary fill is much better exposed than in the Nahr El-Kabir. Clastic debris flow sediments are observed to bypass the basin margin and were transported out of it (Figure 5.6). The field evidence from Syria points to a sequence of down-cutting, proximal debris flows. The hypothesis suggested is that these debris flows also transported large quantities of material into the Mediterranean Basin (Levant Basin) (see Chapters 3 and 6). The scale difference between the Adana Basin (100's km across) and the Nahr El-Kabir Graben (10-15km across) is considerable.



**Figure 5.6** Field sketches of the northern margins of the Adana Basin, Turkey. Basin fill is Early to Middle Miocene-age.

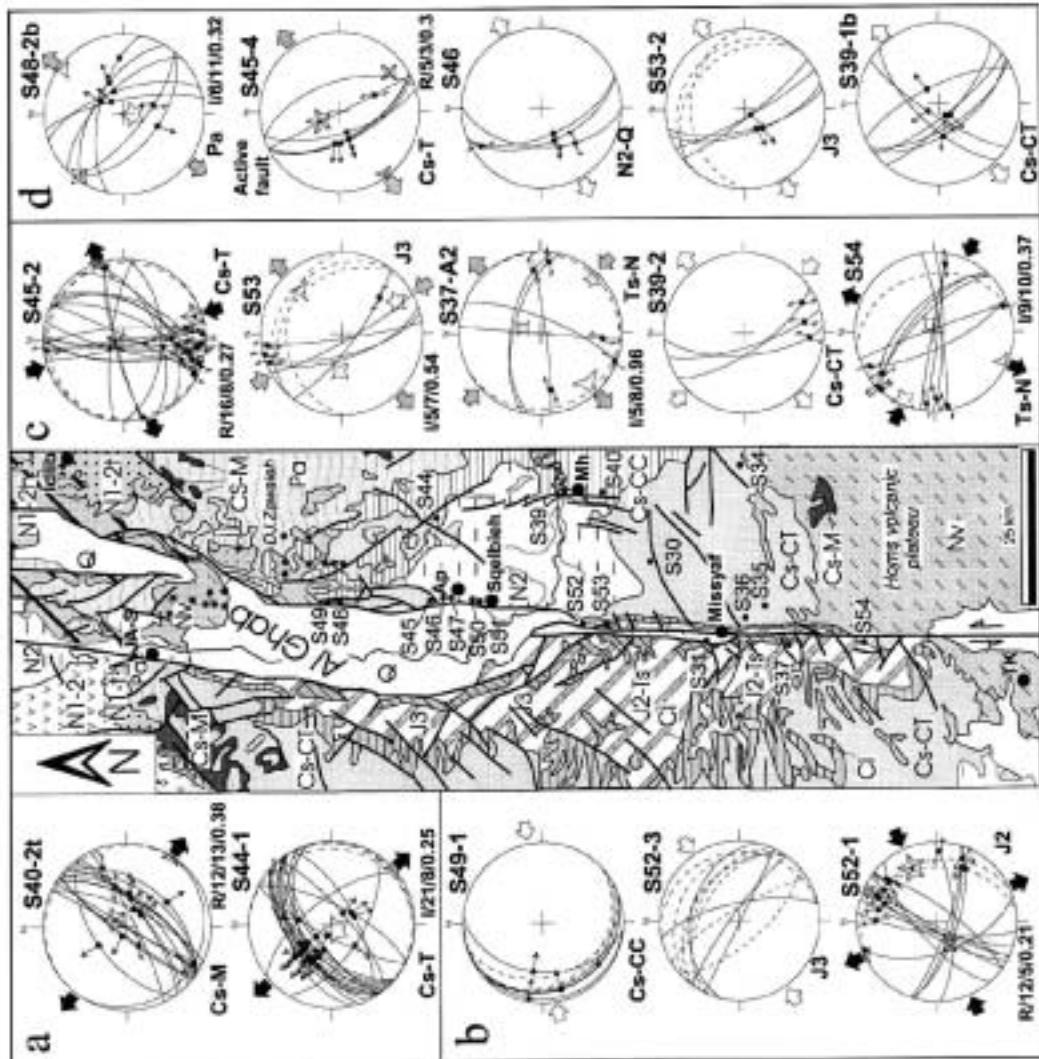
### ***Ghab Graben, Syria***

The Ghab Graben in Syria (Dubertret, 1932, 1933, 1953; Ponikarov et al., 1963, 1966, 1967; Krashennnikov, 1971, 1994; Domas, 1989; Trifinov et al., 1991; Devyatkin et al., 1997; Brew et al., 2001; Zanchi et al., 2002) abuts the northern end of the Nahr El-Kabir Graben, where the two coalesce, in the Nahr El Abyad region (Figure 5.7 & pull-out maps). The graben formed due to pull-apart mechanisms related to the sinistral motion of the northernmost extension of the Dead Sea Transform Fault (Quennell, 1956; Garfunkel, 1981; Hempton, 1987; Walley, 1998; Matar et al. 1993). This section discusses only the northernmost extent of the Dead Sea Transform Fault, where it is of most relevance to the project area.

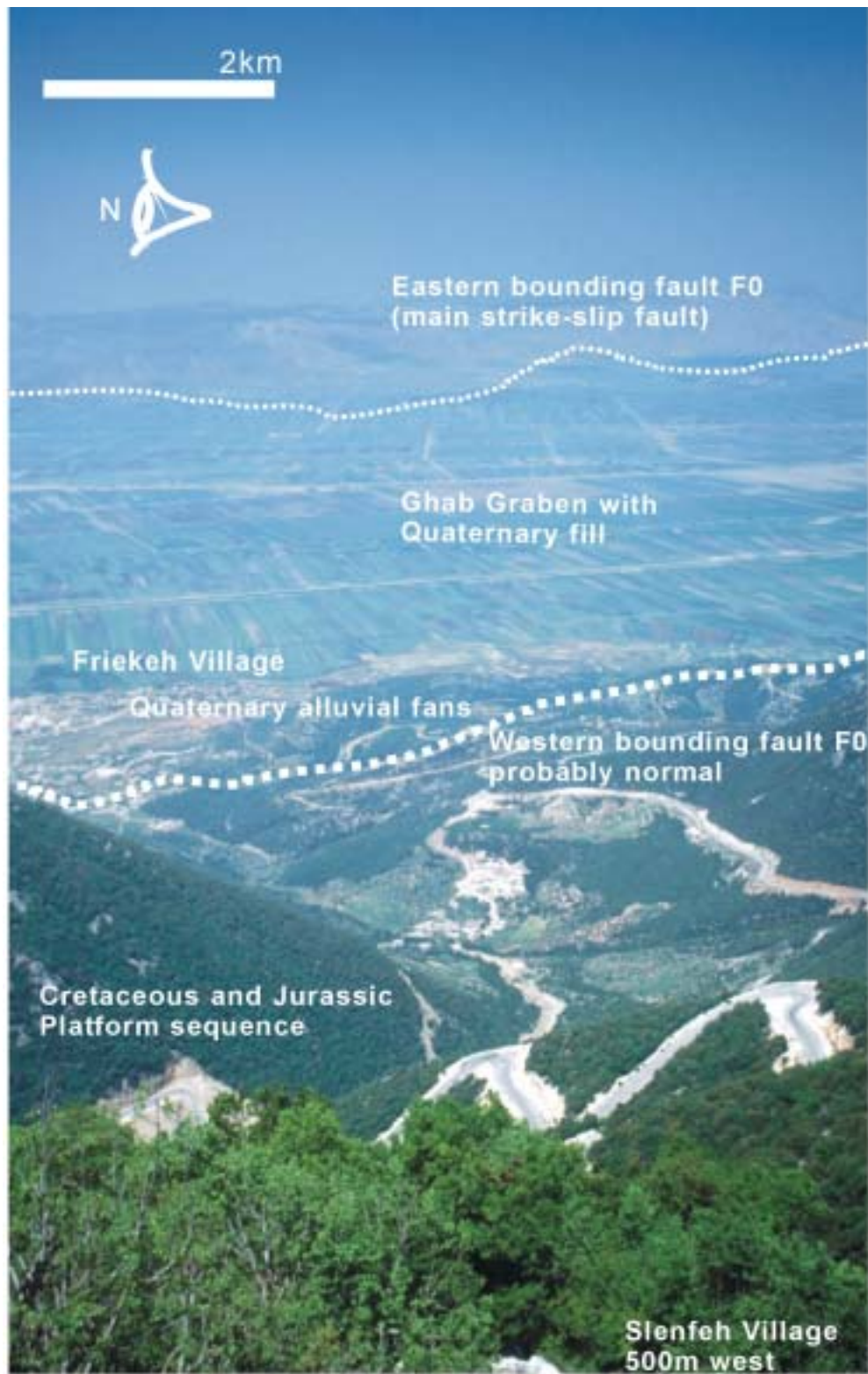
The graben forms an elongate valley, 15km and 80km long, which extends due north-south. To the west it is flanked by the Jebel An-Nassuriyeh Mountains, with a steep scarp slope over 1000m high from the graben floor (Figure 5.8); to the east the margin also forms a steep scarp 500m high, bordering the Syrian Desert (Figure 5.9). Debate is ongoing in the literature about the age of formation and the amount of strike-slip displacement necessary for the graben to have formed. Late Miocene to Pliocene-age formation was suggested by Ponikarov et al. (1963, 1966, 1967); Domas (1989) and Devyatkin et al. (1997). Whereas a Plio-Quaternary-age is favoured by Trifinov (1991) and Brew et al. (2001). The displacement of the Dead Sea Transform Fault is cited as 105-110km in Israel and Lebanon (Quennell, 1956; Freund et al., 1970; Garfunkel, 1981, Chaimov et al., 1990); however, in the Ghab Graben region it is thought to be much less (20-27km, Domas, 1989; Trifinov et al., 1991; Brew et al., 2001; Zanchi et al., 2002). This discrepancy is due in part to shortening of the Palmyride Fold Belt (20km, Chaimov et al. 1990), but may also be due to the existence of branching faults that propagate into the Mediterranean (Walley, 1998; Butler et al. 1999). No offshore data exists to corroborate this. Piercing points are rare in the Ghab Graben region of the fault.

Regionally, the Dead Sea Transform Fault is critically important as it forms the plate boundary between the African and Arabian plates. The junction between the Dead Sea Transform Fault, the East Anatolian Fault and the Anatolian/African plate boundary (see Chapter 6 & 7) is of regional tectonic importance. If it exists, then this juncture could possibly be a triple point junction; existing just to the north of the Ghab Graben.

During this project, four days of fieldwork were undertaken with the Syrian Establishment of Geology (and Professor Alastair Robertson), who are currently mapping the area at 1:50 000 scale. Together we reviewed the surface outcrops and further

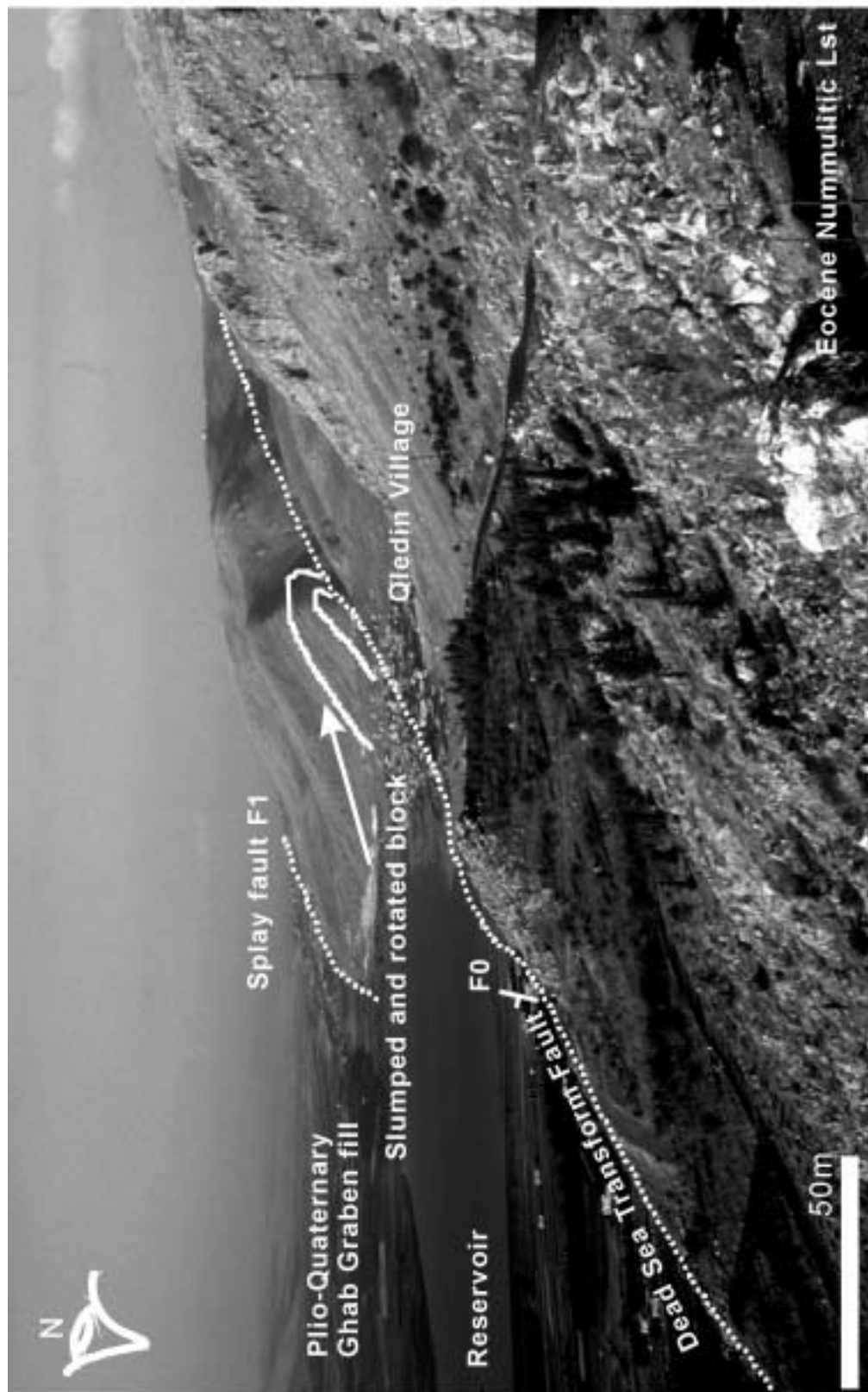


**Figure 5.7** From Zanchi et al. (2002). Structural interpretations from the eastern margin of the Ghab Graben (refer to pull-out geological map for comparison). Localities are given on the map. Northeast and northwest striking faults are common.



**Figure 5.8** View into the Ghab Graben, the major pull-apart basin at the northern extension of the Dead Sea Transform Fault. This graben is regionally important to the tectonics of the area, it forms the juncture between the African and Arabian plates.





**Figure 5.9** View looking north along the eastern margin of the Ghab Graben. The fault trace of the Dead Sea Transform Fault follows the break in slope. Small splay faults are also present. The main Eocene Limestone block in the centre of the picture is strongly rotated and slumped forward due to a minor amount of extension (transtension).

complementary individual study was also carried out. The aim of the following section is to give an overview to the Ghab Graben and note any similarities or important events with may also be relevant to the Nahr El-Kabir region.

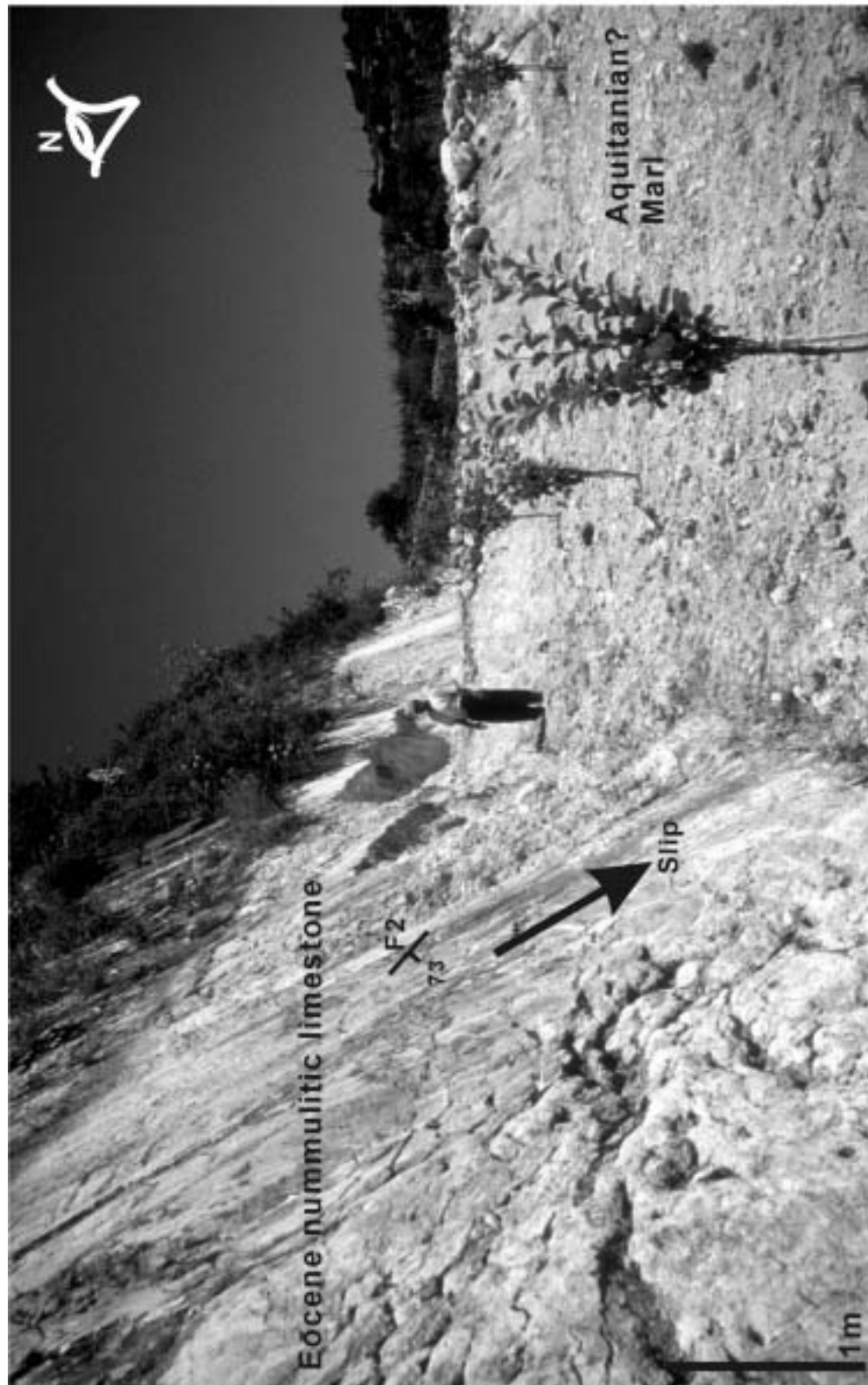
### *Sedimentology*

Within the graben, the oldest rocks to crop-out are continental and marine Pliocene-age limestones and basalts. Drilling of the graben by the Establishment of Geology (and Ponikarov et al. 1963) did not find any older rocks prior to reaching the latest Cretaceous-age basement. The division between the continental-derived (within graben) and marine Pliocene-age rocks lies at the north of the graben, north of Jus Ash-Shaghour Town. No direct facies transition is observed. However, Marcel BouDagher-Fadel dated one sample collected during this study, mapped as Oligocene-age strata. It contained Early Pliocene-age foraminifera, which may indicate a transition. The marine Pliocene rocks outcrop as far north as the Hatay region of Turkey and up to 2km further west than the westernmost Ghab Graben faults. There is no indication that the Pliocene marine environment in the Ghab Graben was connected to that of the Nahr El-Kabir Graben.

On the margins and northern extension of the graben, Cretaceous-age rocks are overlain by Eocene Nummulitic limestones, Oligocene-age limestones and Middle Miocene-age limestones. Maastrichtian, Palaeocene, Lower Eocene, Early Miocene and latest Miocene-age strata are very poorly exposed, if present. The sedimentary rocks are almost uniformly wackestones and bioclastic packstones, often-showing early karstification surfaces (sub-aerial erosion) and shallow-water marine fauna (i.e. numerous benthic foraminifera and bivalves). No evidence of clastic material was found within the pre-Pliocene-age Ghab Graben sediments.

### *Graben structure*

The Ghab Graben has been analysed by drilling (Ponikarov et al. 1963; Kopp, 2000), seismic and gravity data (Brew et al. 2001) and by Plio-Quaternary environmental studies (Trifinov, 1991). No field based kinematic work has been published for the western margin of the graben, only the work of Zanchi et al. (2002) (see below & Figure 5.7), exists for the eastern margin. Numerous remote sensing studies were carried on the region (Trifinov, unknown; Golovina, 1996) but none so far supported by field data. Chapter 4, details field-based



**Figure 5.10** Normal, synthetic faulting on the western strand of the Dead Sea Fault, 5km north of the Ghab Graben. Poorly preserved kinematic indicators show dip-slip movement. The amount of throw is unknown, but Eocene strata are juxtaposed, next to Aquitanian strata.

kinematic studies, undertaken in this project, on the northern section of the western margin of the graben.

The western margin of the Ghab graben forms a steep scarp slope covered in Quaternary-age alluvial deposits (Figure 5.8). The fault is poorly defined within the graben, but it outcrops clearly just north of Jus Ash-Shaghour Town (see Chapter 4). Here it is observed as a sinistral strike-slip fault from this point north to the Turkish border. Branching normal faults at this margin are discussed in Chapter 4 (Figure 5.10). Domas (1989) and Brew et al. (2001), both noted that the western margin of the Ghab Graben exhibits a 'normal fault' topography, that of a horst block.

The eastern margin is very well exposed. The main fault plane is visible, as are large subsidiary, sinistral, strike-slip faults (Figure 5.9). The main fault and the eastern margin of the graben change trend from N-S to NE-SW (renamed as the Sheik Barakat Fault; Ponikarov et al. 1967), 5km south of Jus Ash-Shaghour Village. At the point where the fault changes orientation, kilometre-scale blocks of Eocene Nummulitic limestone are observed to have rotated (forward collapsed) into the graben. Evidence of a N-S strand of the fault is also apparent further north. It is unclear why the Dead Sea Transform Fault splays, but the NE-SW trend is very similar to that of the El-Kabir Fault within the project region (see Chapters 4, 6 & 7).

Within the graben, Eocene and Pliocene-age strata are observed at the northern margin, before the graben splits into two prominent forks. The Eocene Nummulitic limestones are faulted in a NW-SE orientation and the faults are large, south-dipping, normal faults (similar to those described in Chapter 4). These faults continue on trend and propagate through the Pliocene-age limestones, but are poorly exposed. Plio-Quaternary-age lavas (1-2 Ma) infill depressions on the Eocene-age limestones; faulting was not observed within them.

#### *Synthesis of the most recent Ghab Graben literature*

Brew et al. (2001) and Brew (2001) studied the Ghab Graben using remote sensing (limited seismic data and gravity profiles). They put forward the hypothesis that numerous Plio-Quaternary extensional faults cross-cut the graben (E-W, NE-SW and NW-SE striking) and that the main depocentre was originally in the south. The depocentre was asymmetrical and propagated north during the Late Pliocene.

Zanchi et al. (2002) proposed that a NW-SE compressional setting related to movement of the Dead Sea Transform Fault in the western region of the Ghab, although the time-relations were not specific. Prior to this, in the Syrian Desert to the east, E-W trending folds were seen as due to N-S compression (Figure 5.7). This orientation of folding is also seen in the Jebel An-Nassuriyeh Mountains (Ponikarov et al. 1963, 1966, 1967). The main N-S sinistral faults and accompanying WNW-ESE dextral faults that developed with continuing compression, were pre-dated by early folds and thrusts. The most recent stage of faulting is NW-SE extension within the strike-slip zone.

Devyatkin et al. (1997) dated (K/Ar) the numerous Tertiary basaltic lavas exposed near the Ghab Graben. The oldest basalts are those southeast of the graben near the town of Homs ( $17.3 \pm 0.6$  Ma to  $9.7 \pm 0.6$  Ma). There was then a quiescent period until approximately 6 Ma. Large lava flows directly south of the Ghab Graben are dated as between 4-6 Ma and these lava flows extend towards the coast at Banyas Town (see Chapter 3). Devyatkin et al. (1997) inferred that these lavas were due to the propagation of the Dead Sea Fault. The third and final stages of eruption were observed at the north of the Ghab Graben, after it had formed and are much younger ( $1.95 \pm 0.05$  to  $1.1 \pm 0.2$  Ma). Devyatkin et al. (1997) suggested that reorganisation of the deep structure was responsible for the relocation of eruptions, which could be inferred as a shift in fault motion.

### *Key points*

The Ghab Graben and the Dead Sea Transform Fault are large tectonic features, brought about by both the collision of Africa and Eurasia and the splitting of the African and Arabian Plates. These features have had an impact on the project area of the study, especially during Plio-Quaternary time. It is important to isolate which features are related to different tectonic episodes. A summary of the essential features and timings seen in the Ghab Graben is given below. They are compared, and contrasted in Chapter 6, which synthesises the processes and tectonics; relating the following conclusions.

- € Early N-S compression led to the doming of the Jebel An-Nassuriyeh Mountains. A later shift to NW-SE compression was followed by the onset of graben formation. The timing of these two features is not constrained within the Ghab Graben. Local evidence is inferred to relate to the Syrian Arc structures (Cretaceous and younger) and Palmyrides uplift and folding (Cretaceous to Miocene)(Chaimov et al. 1990; Guiraud et al. 1997) for the initial tectonic setting.

- € The Early Pliocene (5-6Ma) was the timing of initial volcanism and fault propagation in the region (Devyatkin et al. 1997). A second stage of faulting occurred in the latest Pliocene-Quaternary and was associated with extensional NW-SE faulting and faults splay of the Dead Sea Transform Fault.
- € This latest stage of strike-slip pull-apart and internal graben extension led to extensive uplift of Jebel An-Nassuriyeh Mountains. The amount of uplift could not be modelled by pure transtension (Brew et al. 2001). The Jebel An-Nassuriyeh Mountains are inferred as having some extension and are therefore, a horst block (Domas, 1989; Brew et al. 2001).



## Discussion of results and tectonic implications

Chapters 3 & 4 have provided the field data for the sedimentary successions situated in northwest Syria. Whilst the work undertaken during this project has characterised the facies and re-examined the lithologies discussed by the previous workers (Ponikarov et al. 1963, 1966 & 1967), questions relating to the sedimentary and structural processes still have to be answered. It is the aim of this chapter to integrate all the existing data on the region with a view to formulating hypotheses for the environments of deposition and the tectonic development of the region.

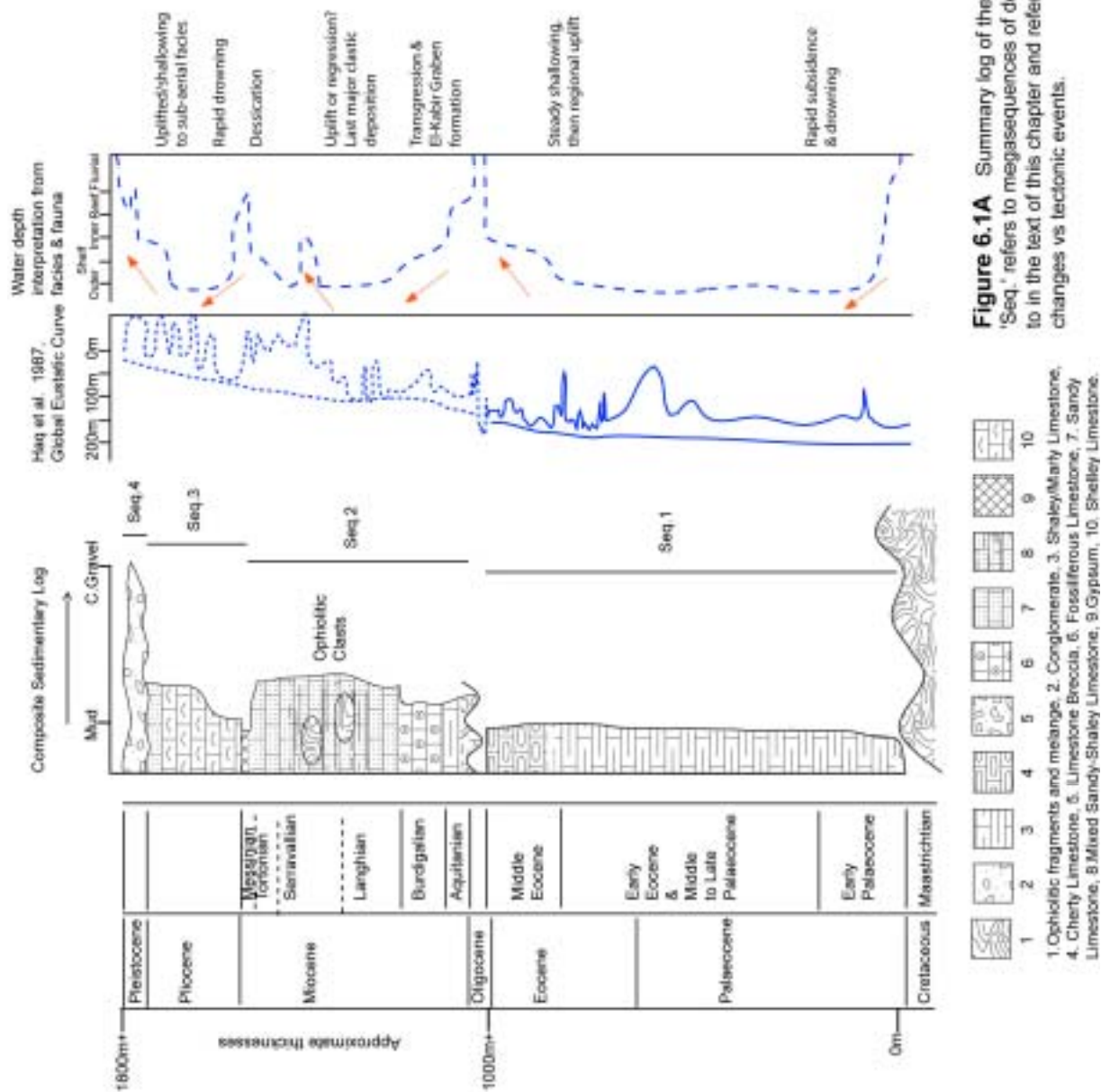
### *Sedimentary processes and environments*

Chapters 2 & 3 (and 4) have supplied the main field data for understanding the environmental settings and provided brief summaries of the possible processes involved (Figure 6.1a & 6.1b). This section applies the field data to determine the settings involved.

Most of the post-ophiolitic succession was deposited under marine conditions (except parts of the Maastrichtian and Plio-Quaternary successions, see Chapter 3). The Haq et al. (1987) eustatic curve can be applied to the Paleogene and the majority of the Miocene, but the Mediterranean Basin closed at the Messinian. No published relative curve exists for this part of the Mediterranean Sea, for the Neogene. Most of the structuration of the region occurred during the Neogene, when a relative sea-level curve would be most useful.

Although the study region is spatially restricted, there are strong variations between facies in close proximity to one another. The north and south margins of the Nahr El-Kabir Graben is one example. Differences are also noticeable between Paleogene successions on the Baer Bassit Massif and the Jebel An-Nassuriyeh Mountains.

This section applies all the available data to infer environments for each time-slice (Chapter 3). The time-slices are grouped when the sedimentary environment is related or appears continuous. This discussion is limited to the area bordering the Nahr El-Kabir Graben. The region to the northeast of the graben has been shown (Chapter 3) to have differing environments and does not appear to be as closely linked to the El-Kabir Lineament.



A3 diagram

## Carbonate and clastic environments

The following criteria have been used to help determine the sedimentary environments from the facies observed. Carbonate settings are inferred based on reference texts by: Tucker (1990), Tucker et al. (1990)(Figure 6.2), Reading (1996)(Figure 6.3) and Demicco et al. (1994)(Figure 6.4), clastic settings from Reading (1996), Leeder (1999)(Figure 6.5) and Stow and Piper (1984)(Figure 6.6). Comparative and regional analogues are utilised where available. Stratigraphic terms are based on Emery et al. (1996)(Figure 6.7).

### *Biofacies*

Marcelle BouDagher-Fadel and Sylvia Gardin supplied anecdotal evidence of environment in their results (Appendix 1). Sartorio et al. (1988) utilised generic biofacies depths in their atlas of the southern Tethys biofacies:




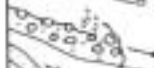



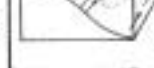
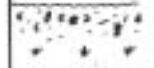

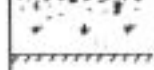
1. Maastrichtian limestones – planktic and benthic foraminifera together are indicative of a carbonate slope.
2. Eocene-age limestones – with mainly planktic foraminifera – imply a basinal setting.
3. Middle Eocene Nummulitic limestone – deposited at the edge of the slope, seawards from the inner shallow platform. Large *Nummulites* became extinct at end of Middle Eocene.
4. Limestone with mixed planktic and benthic foraminiferal limestones are indicative of carbonate slope deposition.

### ***Time-slice analysis***

#### Maastrichtian and Paleogene (time-slices 1 & 2)

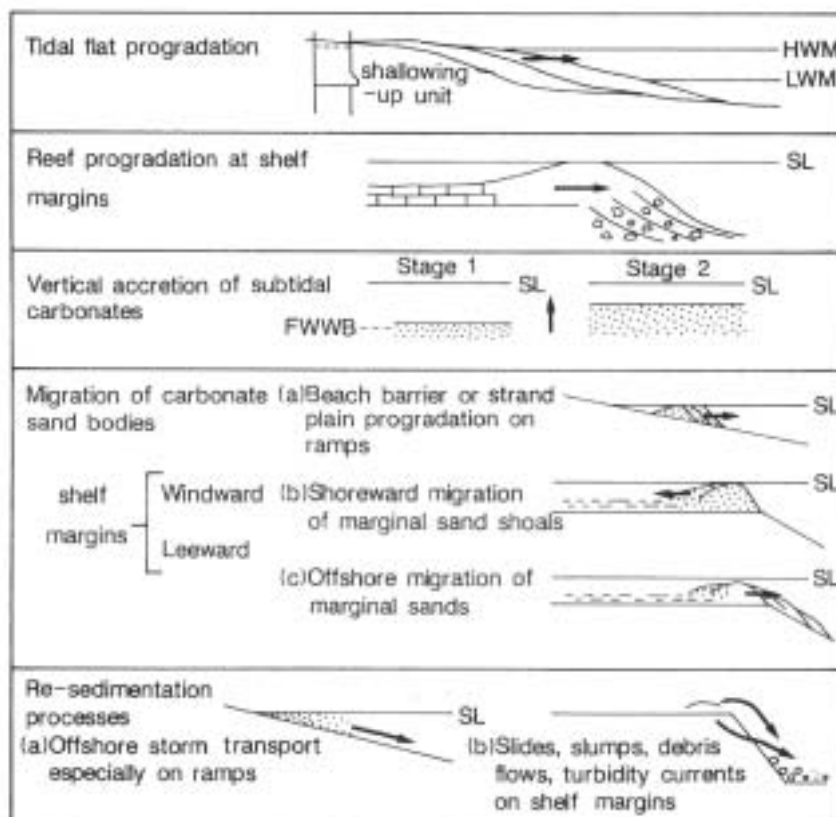
Maastrichtian and Paleogene sedimentary rocks (time-slices 1 & 2), represent deposition under neritic conditions. Water depth is hard to establish as it was variable across the region. Fauna typical of upper shelf to foreshore settings are found in pelagic rocks and accurate benthic to planktic foraminiferal ratios are not available. Marcelle BouDagher-Fadel suggested water depths for some of the thin sections she dated.

The majority of facies are foraminiferal wackestones, transitioning to packstones. Time-slice 2 (Middle Eocene)(see palaeogeographic maps, Figure 6.20) is characterised by packstones and grainstones in the east.

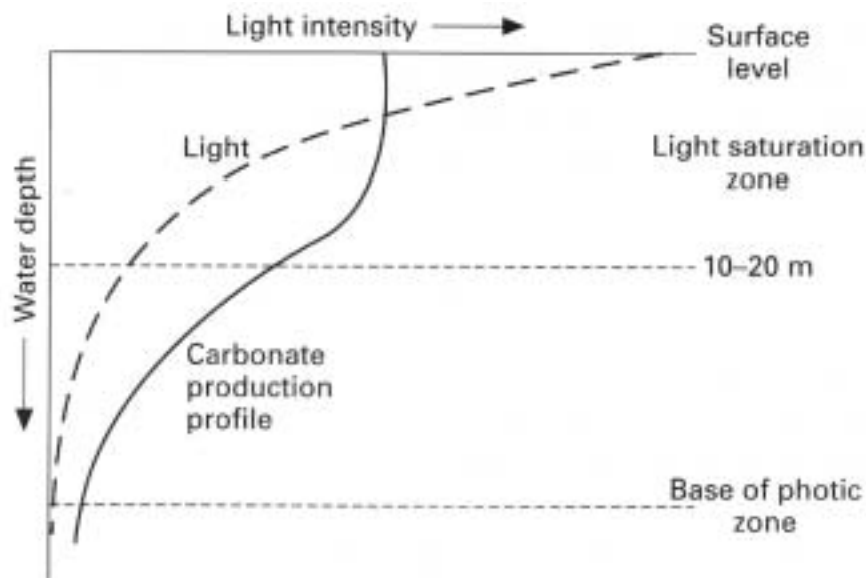
Processes	Characteristics	Deposits
<u>Resedimentation</u>		
Rock fall		Isolated blocks and breccias
Creep		Creep lobes
Slide		Slides
Slump		Slumps
Debris flow		Debris
Grain flow		Grain flow
Fluidized flow		Fluidized flow
Liquified flow		Liquified flow
Turbidity current (high/low density)		Turbidites coarse-medium / fine grained
<u>Normal bottom currents</u>		
Internal tides and waves		Current deposits, lags, hardgrounds
Canyon currents		Contourites
Upwelling currents		
Bottom (contour) currents		
<u>Surface currents and pelagic settling</u>		
Flocculation		Pelagic and hemipelagic oozes
Pelletization		

A

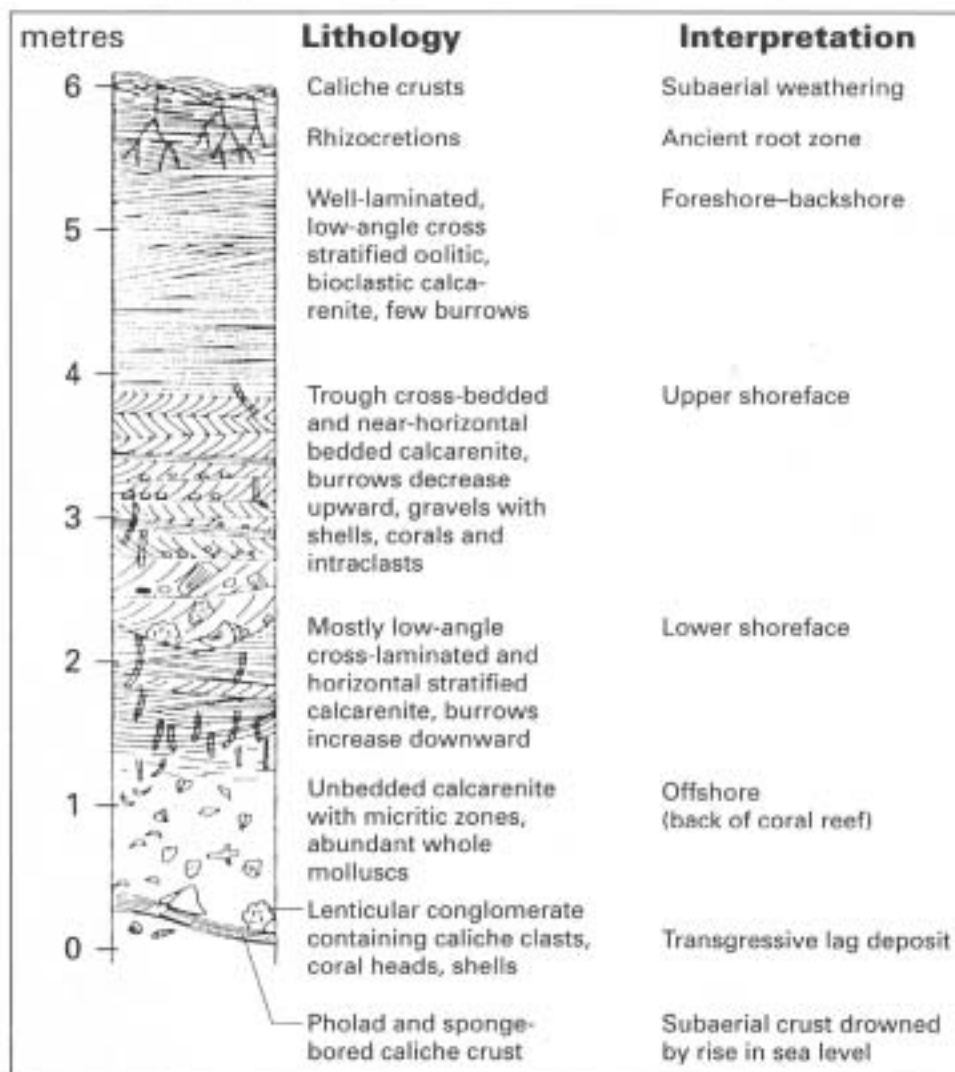
B



**Figure 6.2.** From Tucker et al. (1990). A- schematic illustrations of main marine transport and depositional processes. B - Principle carbonate depositional environments.



From Reading (1996). Carbonate production variation with water depth.



**Figure 6.3** From Reading (1996). Shallowing-upwards, regressive marine system, Yucatan, Mexico.



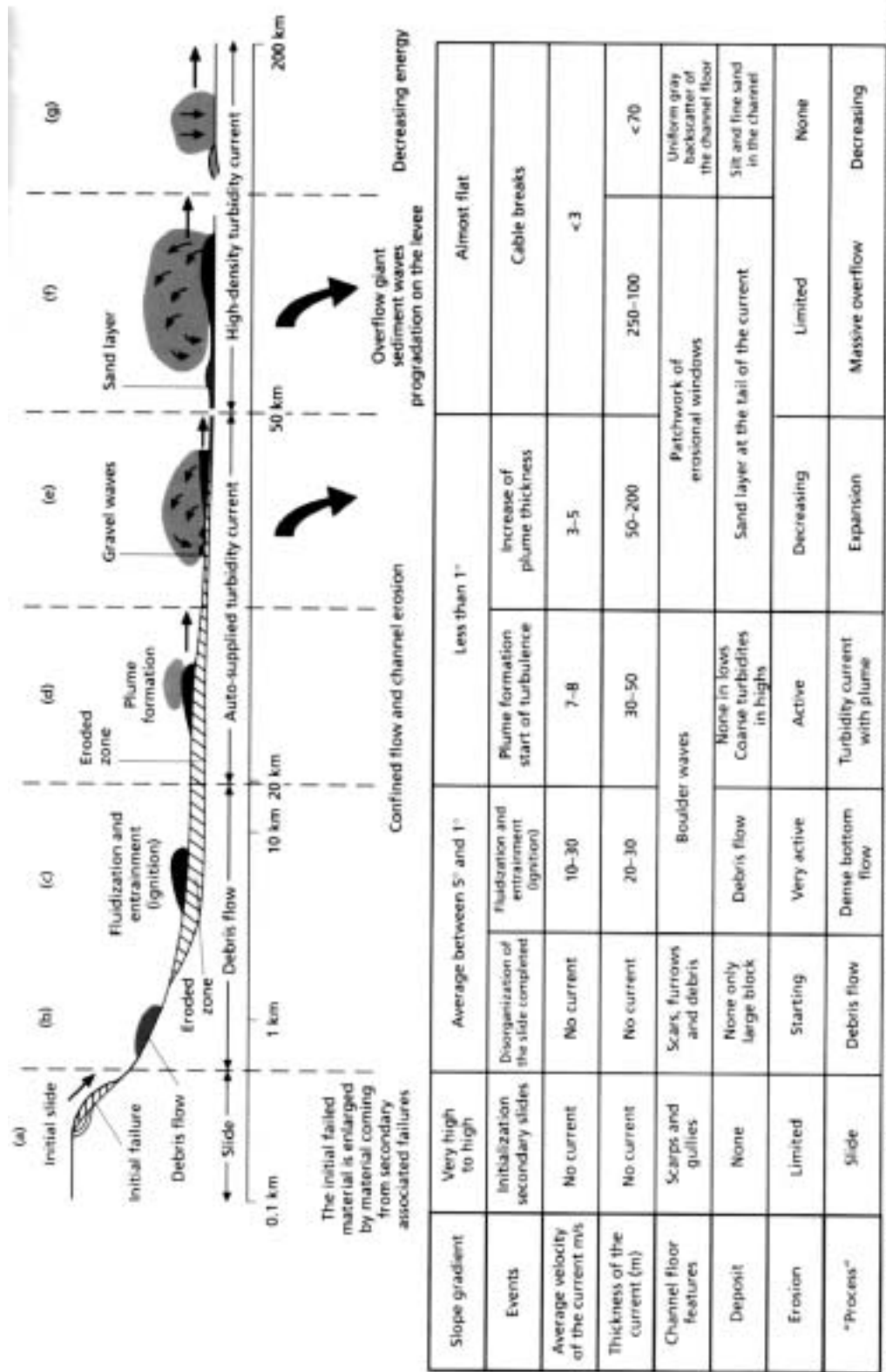
# Important Associations of Sedimentary Structures of Shallow Marine Carbonate Deposits

	FLATS	TIDAL	FLATS
Rainy Supratidal Flats			
Evaporitic Supratidal Flats			
Low Tidal-Range (<1m) Intertidal Flats			
High Tidal-Range (>1m) Intertidal Flats			
Subtidal Ponds			
Tidal Channels			
Beach Ridges			
MUDDY INNER SHELF			
SANDY INNER SHELF			
OUTER SHELF			
MARGINAL SHOALS			

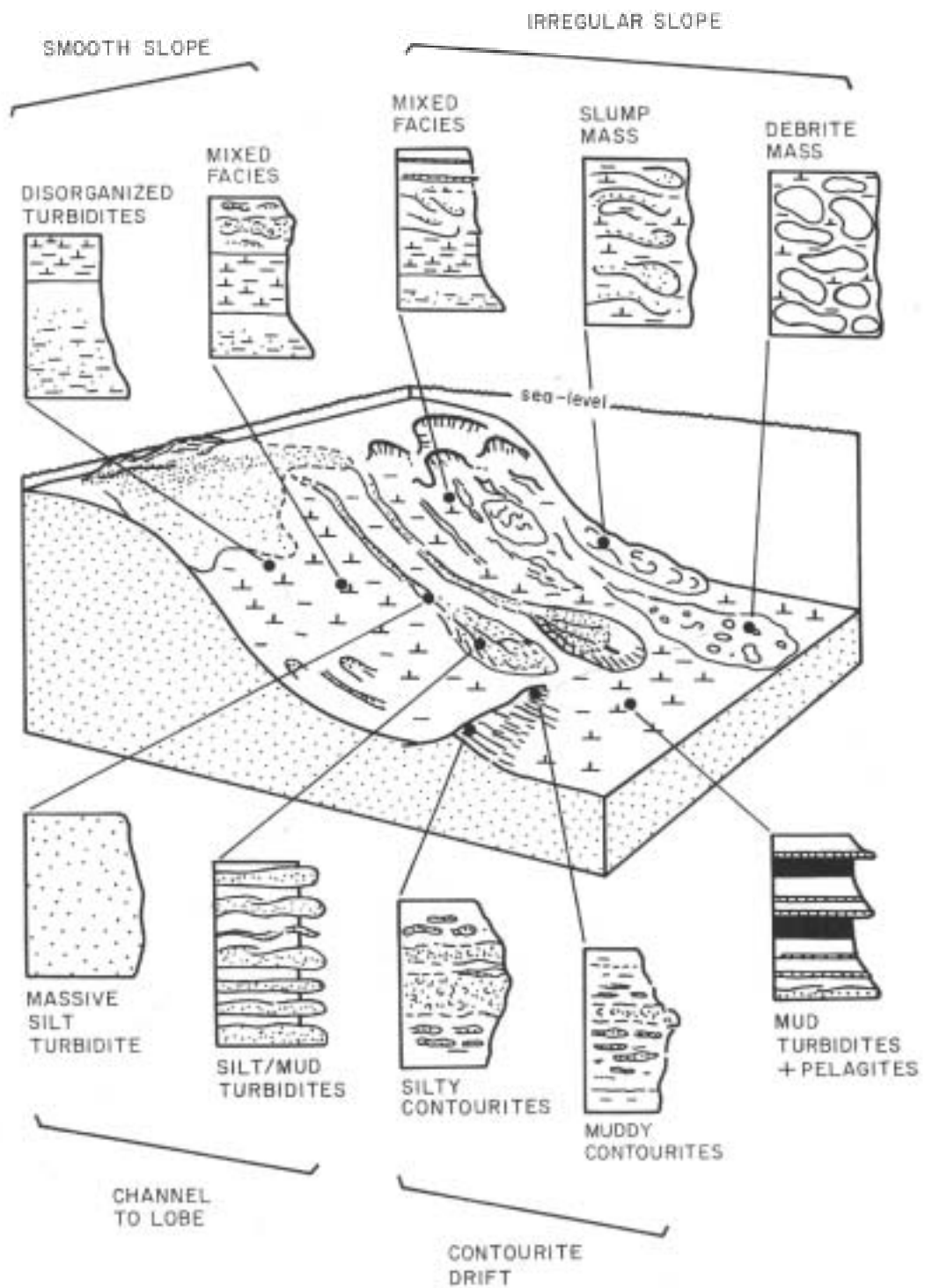
  

	FLATS	TIDAL	FLATS
Neptunian Dikes			
Hummocky Cross-Stratification			
Storm-Lag Lithoclast Gravels & Conglomerates			
Channel-Lag Gravels & Conglomerates			
Large-Scale Cross-Stratification			
Submarine Hardgrounds			
Thrombolites			
Wave Ripple Cross-Stratification			
Small-Scale Cross-Stratification			
Biurbation Structures			
Erosional Scour Marks			
Scalloped & Planar Erosion Surfaces			
Planar Laminæ			
Mechanical Compaction Structures			
Fenestrae			
Stromatolites			
Heterolithic Cross-Stratification			
Planar Thick Beds			
Wavy-Crinkled Thick Beds			
Planar Thin Beds			
Wavy Thin Beds			
Wavy Laminæ			
Edgewise Gravels & Conglomerates			
Imbricate, etc., Gravels & Conglomerates			
Crinkled Laminæ			
Crinkled Thin Beds			
Biurbation Pseudobreccias			
Mudcracks			
Prism Cracks			
Sheet Cracks			
Molar Tooth Structure			
Cryptomicrobial Laminites			
Jellyroll Structures			
Tulas & Travertines			
Caliches & Associated Soil Features			
Supratidal Crusts			
Teppe Structures			
Solution Pores, Cavities, etc.			
Evaporite Minerals, Casts, & Molds			
Nodular & "Chicken Wire" Sulfates			
Bedded Evaporites			
Deformed Sulfate Layers			

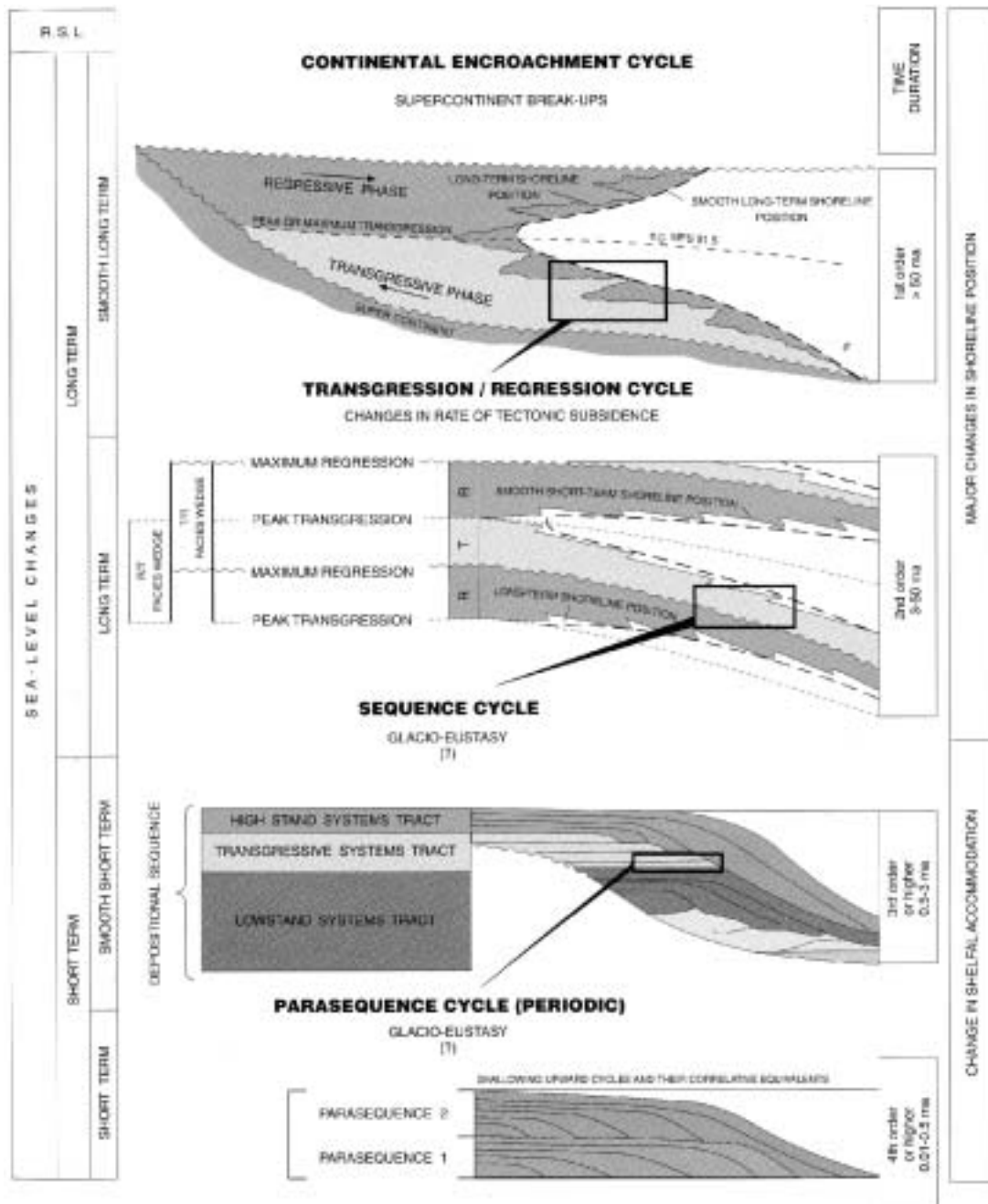
**Figure 6.4** From Demicco et al. (1994). Classification of carbonate environments.



**Figure 6.5** From Leeder (1999). The chart shows the sequence of events that occurred near Nice Airport in 1979, immediately following a landslide. It is presented here as an analogue to sedimentary rock features seen within the Nahr El-Kabir Valley. Coarse facies observed within the graben are comparable to a-c in the chart.



**Figure 6.6** From Stow et al. (1984). Fine-grained sediments across a 'typical slope' and rise. Irregular distribution of facies is noted.



**Figure 6.7** From Emery & Myers (1996), data from Duval et al. (1992). Hierarchy of stratigraphic cycles. The terminology 'parasequence' is used in this work, to describe minor facies changes due to eustatic changes (may have structural control).

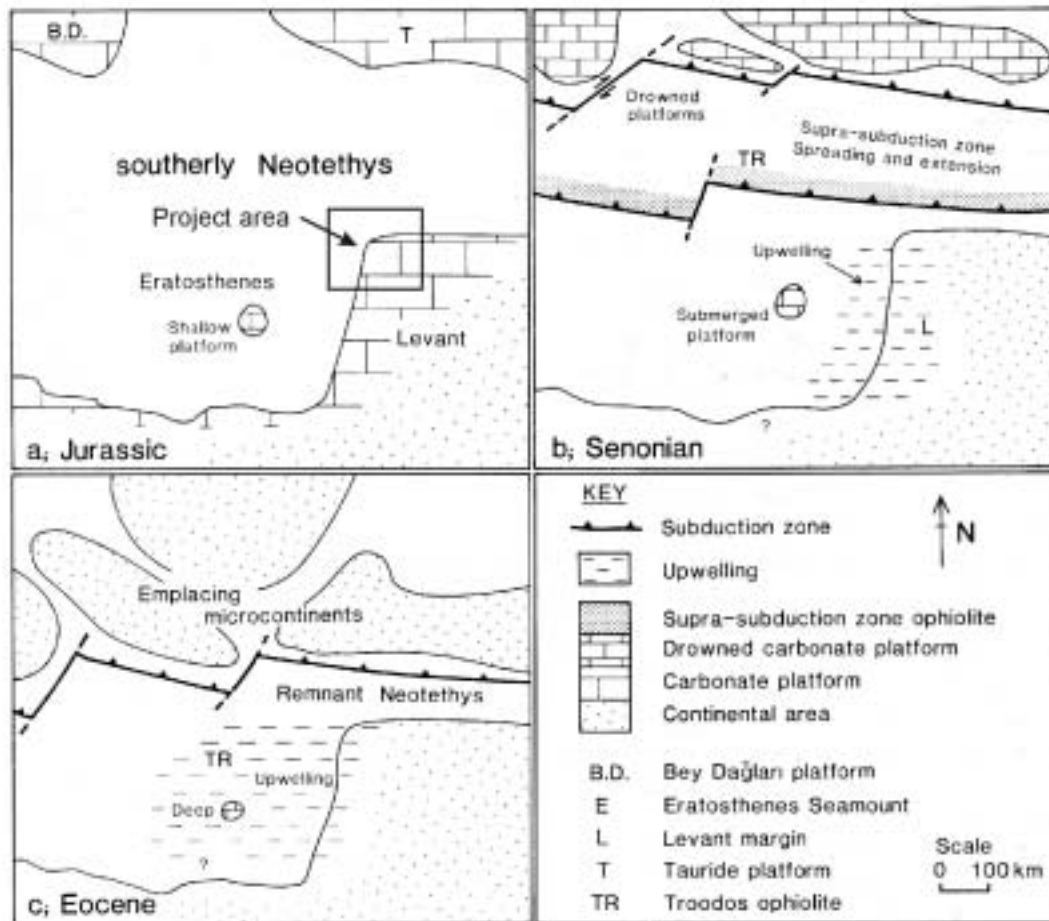
Chert is common throughout time-slices 1 & 2 and the earlier Cretaceous platform sediments of the Jebel An-Nassuriyeh Mountains (see below).

*High productivity marine environments*

Diagenetic chert, intercalated in the Paleocene and Eocene-age rocks, is common in bathyal to abyssal depth water, although it is also prevalent in shelf-depth waters in high productivity oceanic conditions (i.e. Cretaceous chalks of southern England). Robertson (1998) infers that upwelling of deep marine waters occurred from the Late Cretaceous to Eocene on the flanks of the Eratosthenes Seamount (Figure 6.8). Perhaps this was part of a return current to the remainder of the Tethys Ocean to the east ( similar to the current Straits of Gibraltar)? It is, therefore, possible that upwelling also occurred along the continental shelf in Syria at this time, leading to high-productivity marine conditions. Porcellenite is common in the Eocene outcrops near Banyas, whereas flinty chert is predominant on the Baer Bassit Massif. Similar chert-rich facies are observed in Eocene-age strata in Cyprus and Israel (Robertson, 1978).

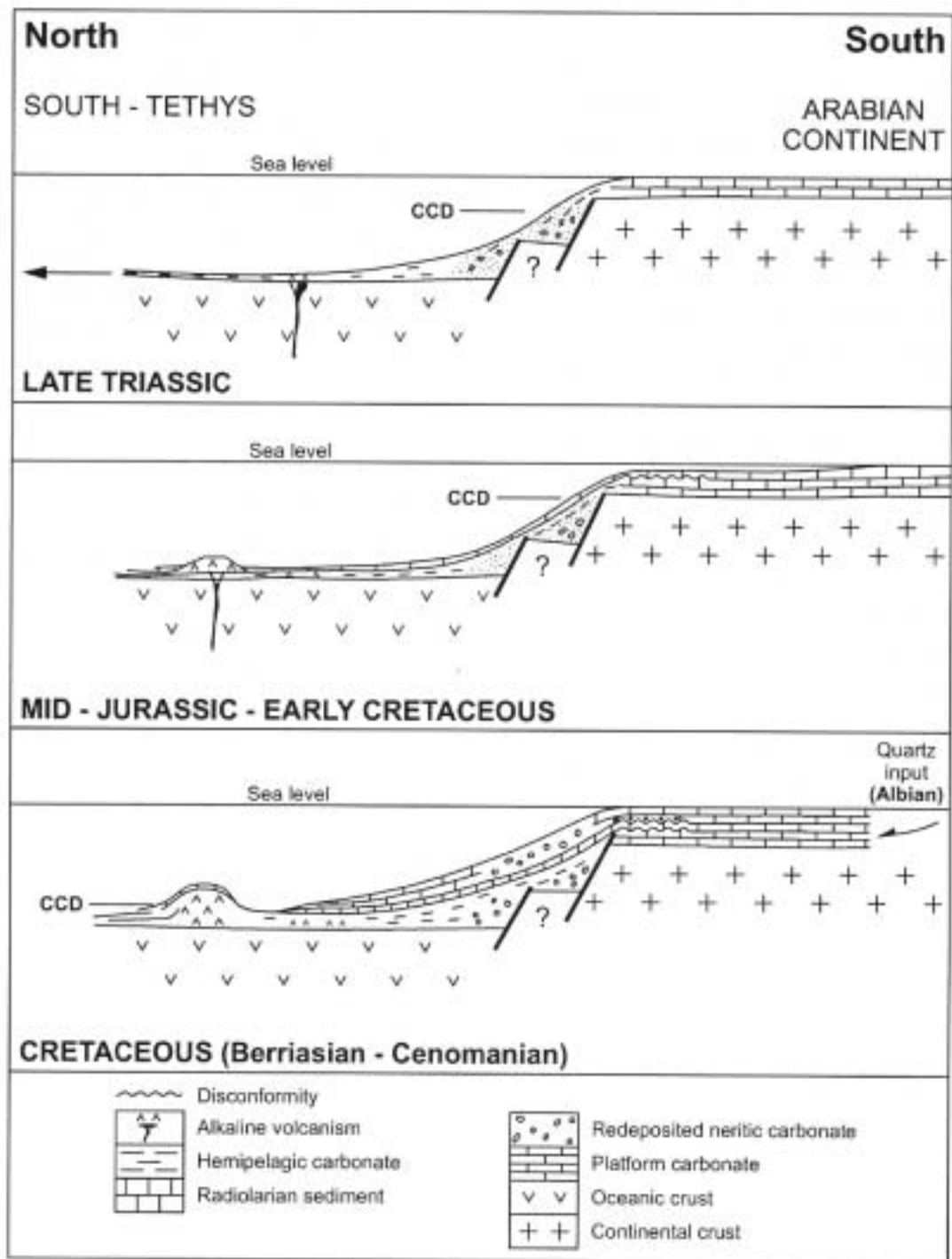
Of importance to this work are also the chert found within the older melange deposits of the Baer Bassit Ophiolitic Massif and the Cretaceous of the Jebel An-Nassuriyeh Mountains. They are redeposited in Miocene-age facies as detrital chert. The Baer Bassit Massif cherts are commonly red and grey, Al-Riyami et al. (2001) interpreted these as radiolarian cherts that deposited below the carbonate compensation depth (Figure 6.9). Carbonate production was controlled by a fluctuating Carbonate Compensation Depth (CCD), leading to silica-rich sediments in the Baer Bassit Massif. Jebel An-Nassuriyeh cherts are typically black or dark grey and associated with neritic carbonates. Eastern Mediterranean upwelling could be responsible for their formation, as it is inferred at the time of deposition (Robertson, 1998).

Redeposition of sediments is also common throughout the uppermost beds of time-slices 1 & 2, as is folding and slumping. Tucker et al. (1990)(Figure 6.10), demonstrates similar processes occurring in the Cretaceous chalks of the North Sea, especially close to faults (Maltman, 1994). The mechanisms for deposition of the differing types of chalky limestones and marls is also summarised (Figure 6.10b).

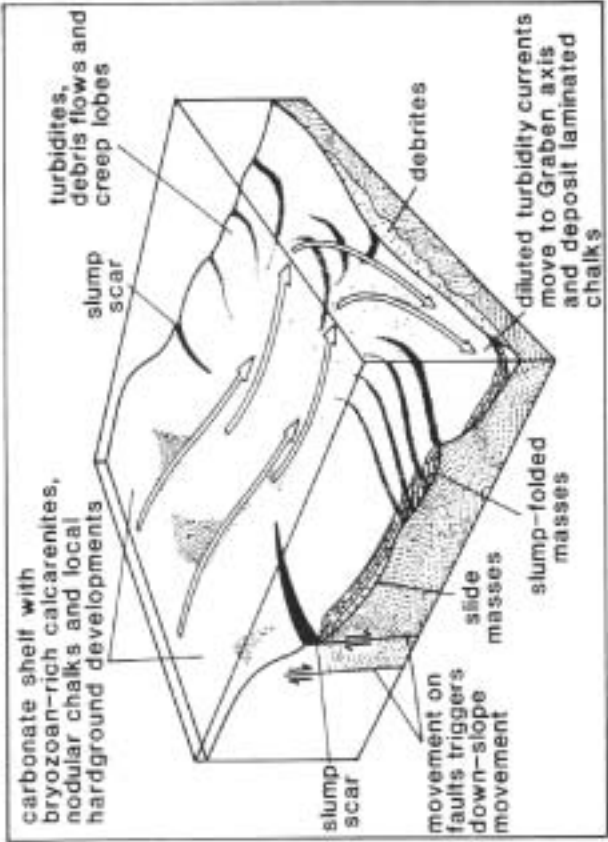


**Figure 6.8.** From Robertson (1998). Palaeogeographical setting of the Eratosthenes Seamount. Note the occurrence of upwelling in the Eastern Mediterranean during the Late Cretaceous and Early Tertiary.





**Figure 6.9** From Al-Riyami et al. (2001). Triassic to Late Cretaceous tectonic setting of the northern margin of the Arabian Platform, pre-ophiolite obduction.



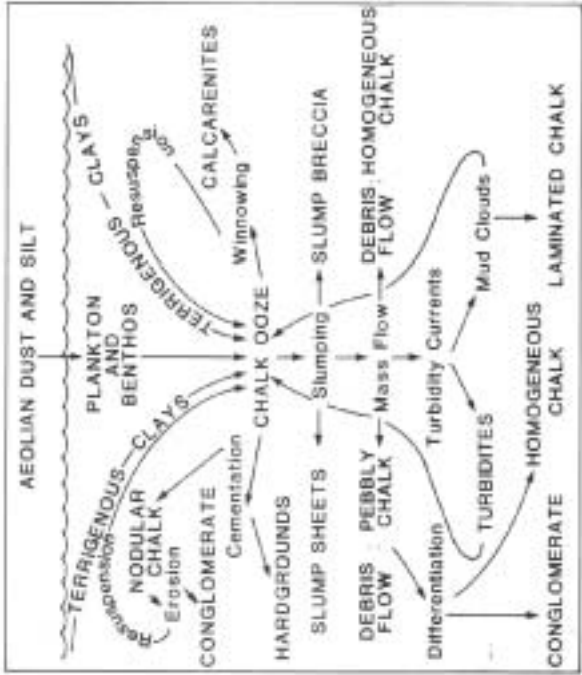
A

**Figure 6.10.** From Tucker et al. (1990). Chalky limestone deposition.

A - Chalk slumping and folding close to fault movements, example from North Sea. Compare to Latakia City beachfront; this project (Chapter 3 & 6).

B - Flow diagram of chalk deposition in the North Sea, showing processes and chalk types produced.

B



*Interpretation of depositional environment*

Time-slices 1 & 2 are inferred to have been deposited on a carbonate ramp or shallow slope. Exact water depths cannot be deduced for time-slice 1, except that inner and outer shelf depths are likely, moving from south to north (from limited biostratigraphical data; see Chapter 3). An unconformity prior to the Middle Eocene led to minor sub-aerial exposure (see Chapter 3) in the extreme southeast of the area. The Middle Eocene Nummulitic limestones are restricted to the photic zone for Nummulites foraminifera to thrive. Nummulites are redeposited in the north of the region suggesting deeper water there. Planktic to benthic foraminiferal ratios are needed to justify accurate water depth inferences, but these would be questionable in any case if the sediments are redeposited.

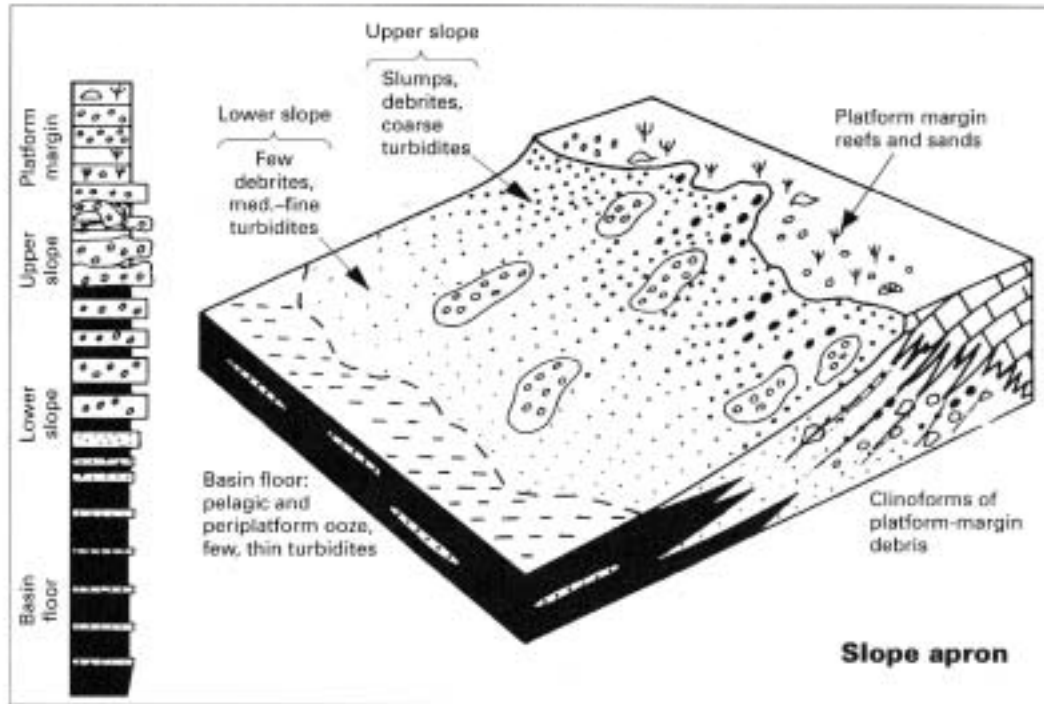
## Early to Middle Miocene (time-slices 3 &amp; 4)

The Early Miocene (Aquitanian) commences with chalky facies, similar to those observed throughout the Paleogene successions. At the northern and southern margins of the Nahr El-Kabir Graben, differing facies are exposed which highlight a different environmental setting to that of the Paleogene. Macrofossils (gastropods and bivalves), presumably from the photic zone (as indicated by foraminiferal evidence) are found within redeposited beds.

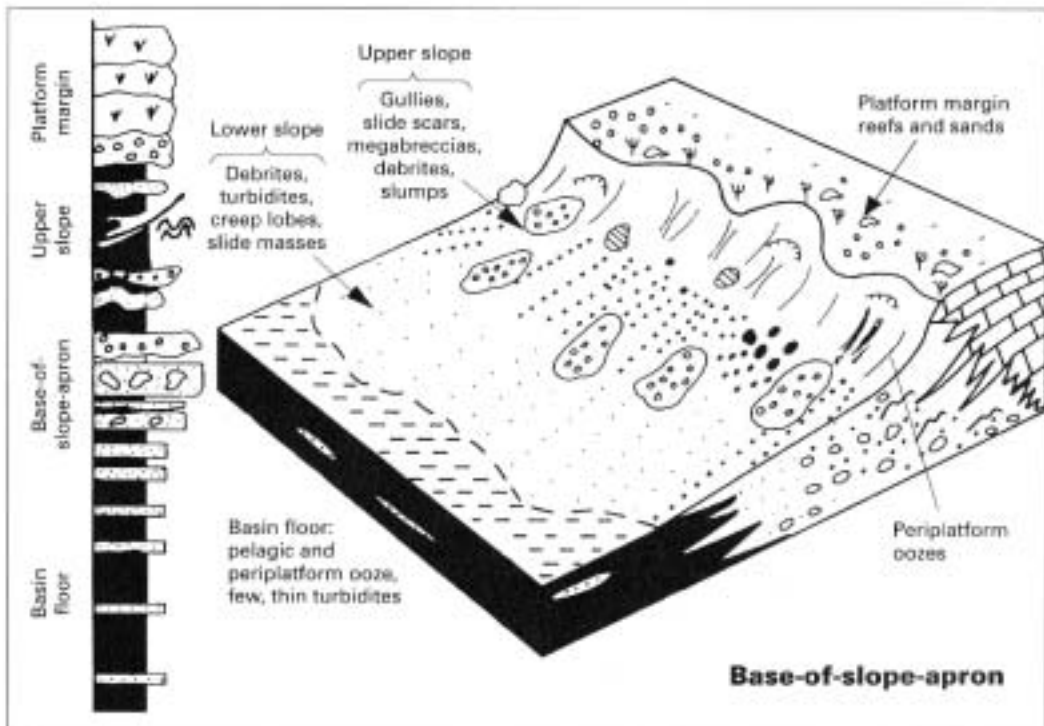
These limited exposures suggest that a shallow marine environment existed near the margins of the graben or depression. There is no indication of a reef, or reef mound, just shallow-marine fauna (no evidence was found of binding skeletal material or preserved microbial layering). The sediments are redeposited, suggesting down-slope deposition, but there is little clastic deposition to indicate active faulting. Organic material is present in the north of the graben suggesting a sub-aerial region or anoxic conditions.

Time-slice 4 (Burdigalian) commences with an unconformity, down-cutting into time-slice 3. Bioclastic detritus is common throughout the sedimentary succession suggesting a similar setting as for the Aquitanian. Fault activity did occur on the northern margin of the graben as angular detrital chert fragments from the Baer Bassit Massif are common. One locality shows progradation of sediments from the southern margin of the graben.

Water depth indicators are poor for time-slices 3 & 4. Shallow or even foreshore faunas are found within shelf water depth marls and basin floor facies predominate (Figure 6.11 & 6.12).



(a)



(b)

**Figure 6.11** From Reading (1996). Carbonate apron facies models.

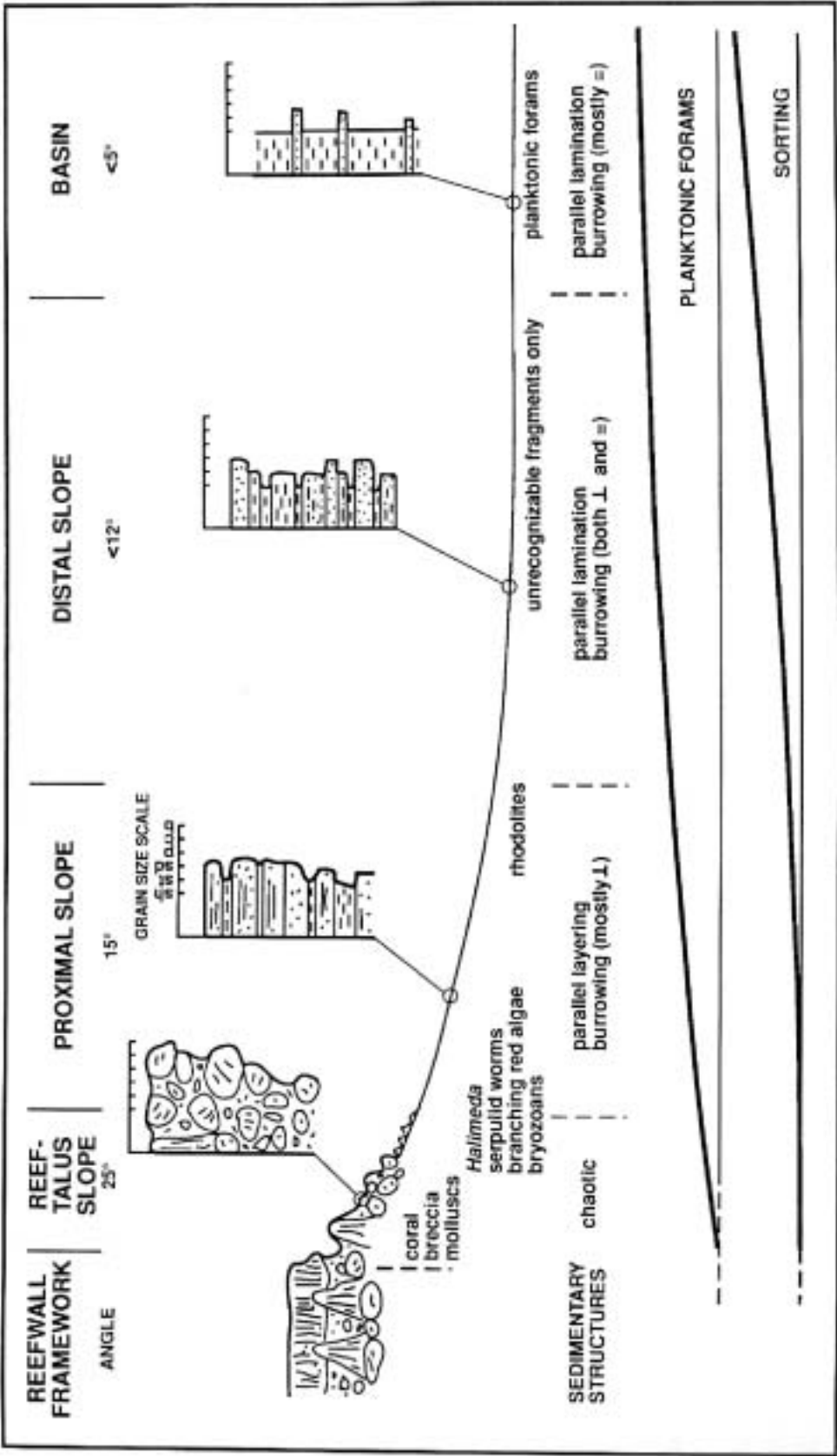


Figure 6.12 From Estaban (1996). Facies model of reef slopes at Nijar (southeastern Spain), showing distribution of organisms and sedimentary structures.

### Middle to Late Miocene (time-slices 5&6)

Although the original mapping description of the Middle to Late Miocene in the Nahr El Kabir Valley was “....monotonous clayey, mostly unclearly bedded limestone alternating with marl...with occasional polymict sandstones” (Ponikarov et al. 1967), the area was found to be one of the most interesting with regard to the range of sedimentary rocks encountered, their bedding relationships and the inferred sedimentary facies and environments.

The Miocene is an important time as it immediately postdates (Eocene-Oligocene), the initial continental collision in the area (Yilmaz et al., 1997; Robertson, 1998, 2000). During the Miocene, there are three major sites of sediment production, which were deposited at differing rates and at varying times. These are: 1. clastic input from the Baer-Bassit; a mix of ophiolitic and melange clasts, muds, Triassic to Cretaceous siliceous oozes and chert fragments, 2. Jebel An-Nassuriyeh mountains, comprising Jurassic and Cretaceous well-lithified platform carbonates with abundant black chert, and 3. pelagic and shallow marine carbonates in tropical seas.

#### *Sedimentary environments- Miocene*

Almost all the clastic and bioclastic sedimentary rocks within the Nahr El-Kabir Valley accumulated close to the margins of the graben (<1km). Most models in the literature concentrate on large marine basins hundreds of kilometres across, which allows sorting of sediments and the full, zoned development of individual facies. The Nahr El-Kabir Graben was at most 15km across and there are no indications of it ever having been any wider throughout the Miocene. Sediments were sourced from both margins of the graben, associated with faulting (see later this chapter), so facies in the centre of the graben were transported less than 10km. Leeder (1999; Figure 6.5) shows the range of facies derived from a landslide (<1km from failure) to 200km or more downslope. In comparison with his model, all the facies seen within the Nahr El-Kabir Graben would be confined solely to the debris flow zone, if deposition rather than scour, occurred at all, with turbidites being deposited further away from the margins. At outcrop, many Middle Miocene-age sections show signs of sediment bypassing by coarser facies (see Chapter 3), down-cutting, mass wasting and slumping of successive beds (see escarpment models below). These features are also predicted in the Leeder (1999) model as erosion would be ‘very active’. The palaeocurrent data (although poor in the field area, almost anecdotal) suggest that the transport direction was to the west. As such, these deposits would have flowed downslope



through the Nahr El-Kabir Graben, west across the narrow continental shelf and into the Levant Basin at the edge of the Mediterranean Sea. Unfortunately, no Miocene-age cores exist from the Levant basin to extend the facies models seen from onshore exposures, but by extrapolation the Miocene basin fill could include turbidity currents interbedded with hemipelagic and pelagic sediments.

#### *Sub-aerial Baer Bassit?*

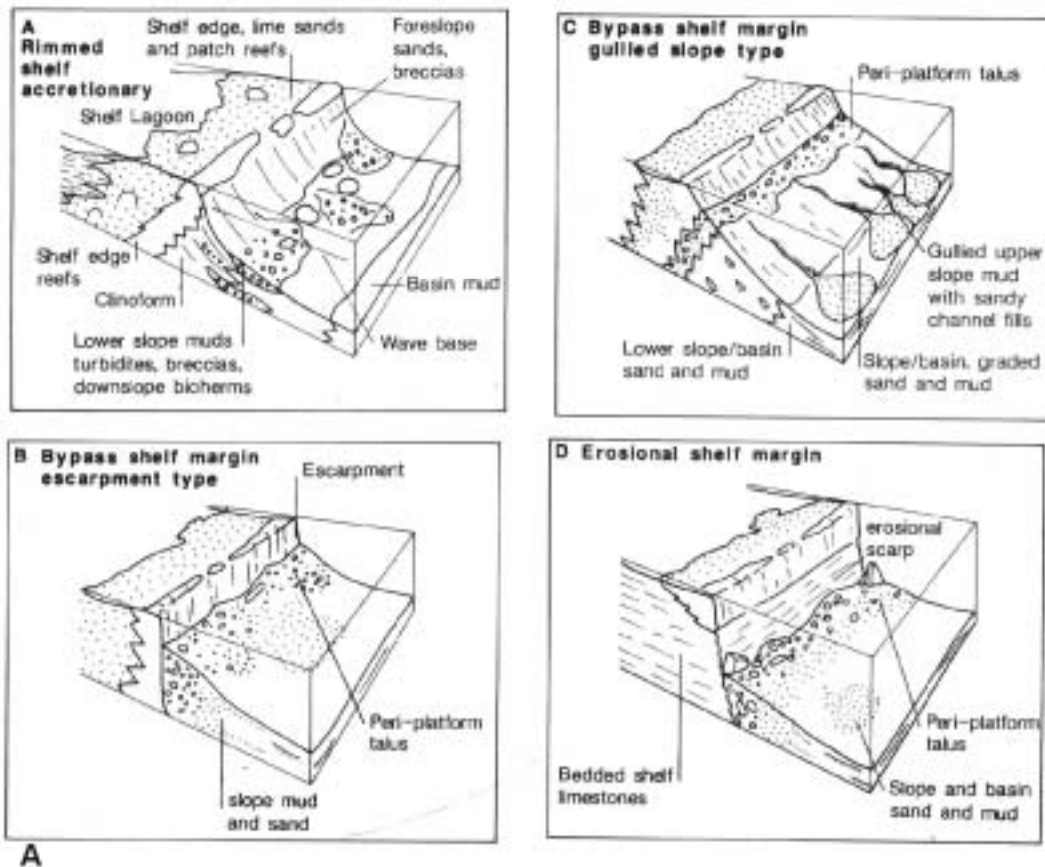
A high proportion of the Miocene-age facies in the Nahr El-Kabir Graben contain sediments inferred to have been sourced from the Baer Bassit Massif. Chert, mud and rock clasts are all common clastic components within sediments derived from the northern margin of the graben. Similar sedimentary-rocks are also seen in the farthest northern exposures of the Hatay Graben (not seen in southern Hatay, Chapter 5, personal communication, S Boulton, Edinburgh, 2003). The quantity of clastic sediments is considerable and is found in rocks of Burdigalian, Langhian, Serravallian and Quaternary-ages.

The majority of these sediments are very poorly sorted and contain clast sizes from boulder to sand grainsize within the same bed. Roundness of grains is also highly variable. Angular and rounded grains often co-exist. Only in the Burdigalian and earliest Langhian are angular grains predominant and then only proximal to the El-Kabir Fault.

It is suggested that Baer Bassit Massif was sub-aerial for much of the Miocene. During the Aquitanian organic matter is found within the limestones at the far north of the graben (although this could be due to anoxic sea conditions). Clast material increases throughout the remainder of Middle Miocene times. Thin, chalky, clastic-free limestones were deposited on the flanks of the El-Kabir Lineament and the Baer Bassit Massif in the Late Serravallian.

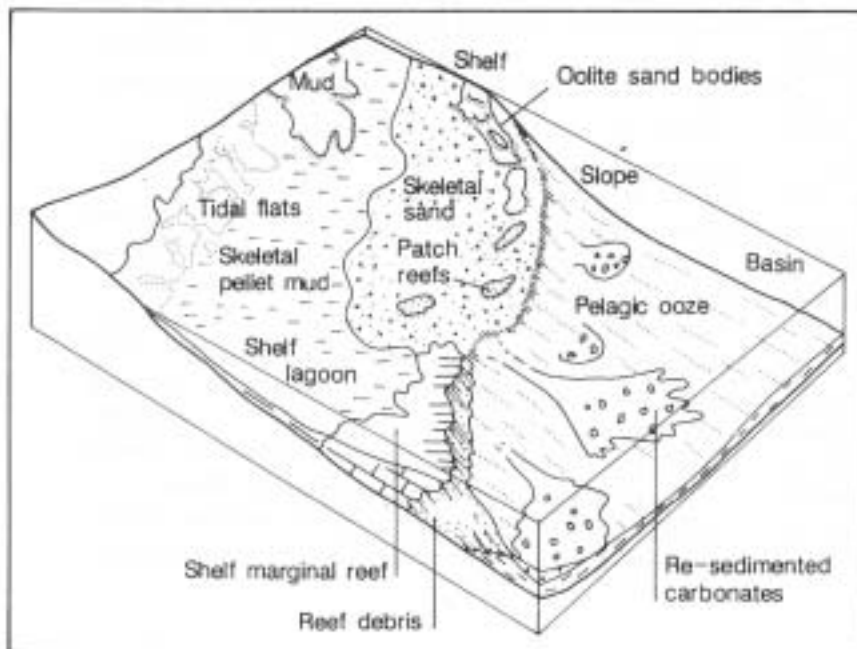
#### *Escarpment criteria*

Figure 6.13 illustrates the models developed for escarpment carbonate margins (Tucker et al. 1990). Shelves can be rimmed with carbonate accretion regions or consist of abrupt escarpments, but all have an abrupt break in slope to deeper-water settings. Such settings are suggested for the Middle Miocene by the sedimentary record, as faulting is also inferred (Figure 6.14). During the uppermost Langhian and Serravallian large quantities of clastic material and redeposited carbonate material were being deposited or bypassing the graben.

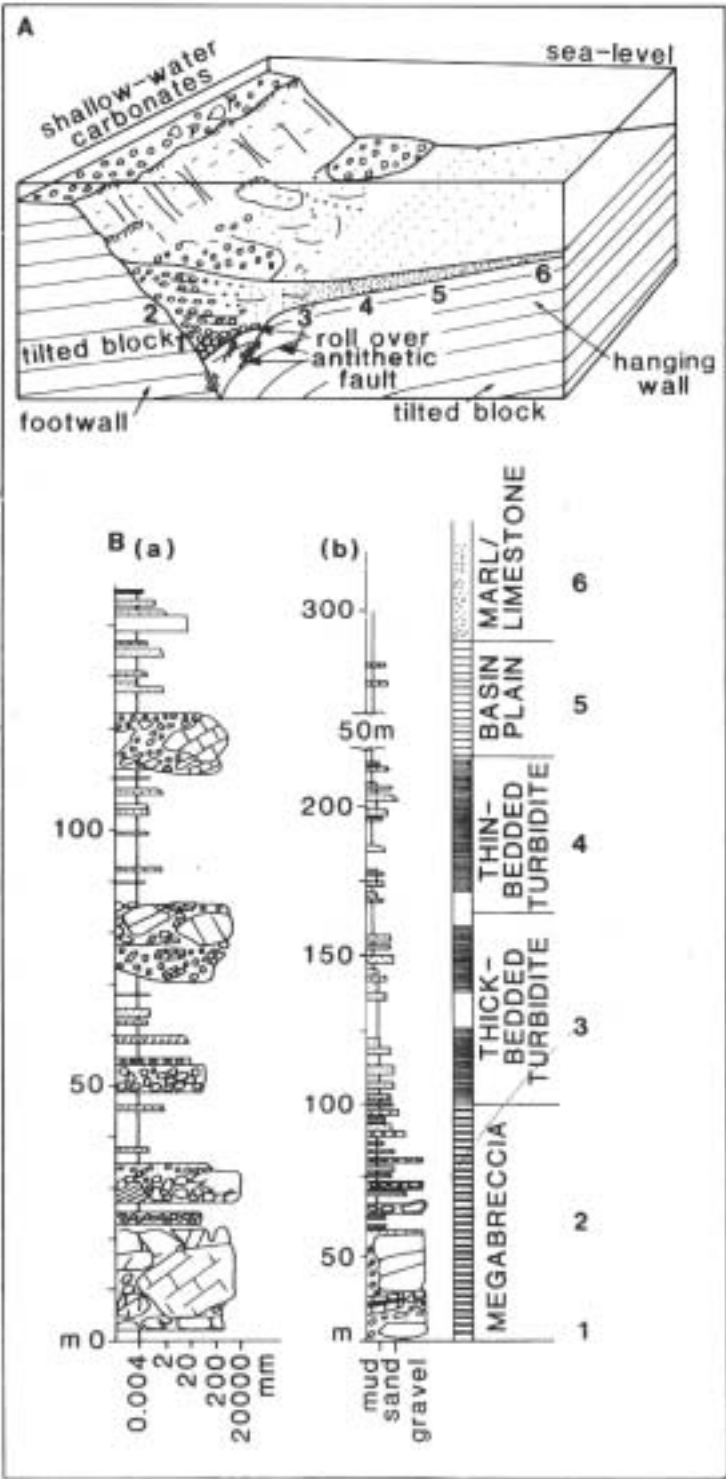


A

B



**Figure 6.13.** From Tucker et al. (1990). A - Rimmed carbonate shelf types - type B & C bypass the shelf margin and could be inferred for the Nahr El-Kabir margin.  
 B - Carbonate rimmed shelf depositional model and facies.



**Figure 6.14.** From Tucker et al. (1990). An example of fault-related, resedimented carbonates from the Lias rift basins of the western Alps.

Scouring of the beds near the graben axis implies that energy levels were very high. Emery et al. (1996)(Figure 6.15) illustrates modes of gravel rich deposition into marine environments. From the limited exposure in the Nahr El-Kabir Graben, similar processes are inferred (see Figure 3.31).

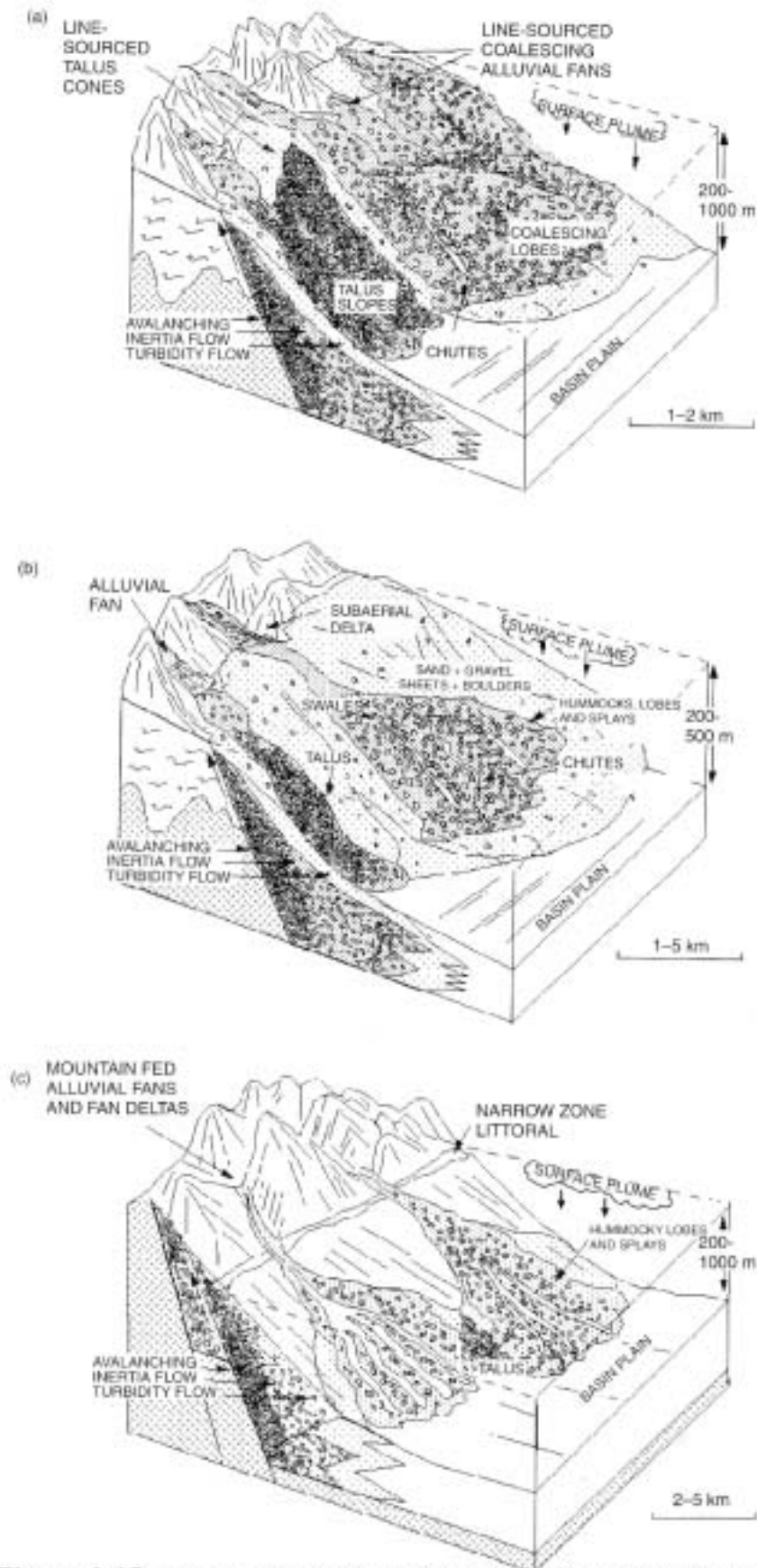
#### *Sedimentary environments and settings*

The Miocene sediments and sedimentary architecture found within the Nahr El-Kabir Graben are very different to those found elsewhere in Syria (similar sediments were found in the Polis and Hatay Graben, Chapter 5). Basin margin sediments are absent or poorly preserved. In areas where shallow water marine settings occurred, only small patches of 'reefal-like' material are present; no actual reefs were observed (ie near Banyas town and the southern margin of the Nahr El-Kabir Graben). Reefs did exist within the Mediterranean region at varying times during the Miocene (Esteban et al, 1996)(Figures 6.16 & 6.17), but their existence bordering the Nahr El-Kabir Graben was not confirmed by this study (c.f. Ponikarov et al. (1966).

At the northern margin of the Nahr El-Kabir Graben, material was been deposited in an active fault setting, with large quantities of mud and clay derived from the breakdown of serpentinite within the ophiolitic rocks in the footwall. This material mixed with chert from the ophiolitic melange led to coarse, proximal, gravity driven, clastic deposits, probably retaining enough energy to bypass west, out of the graben onto the shelf. Re-deposition of sedimentary rocks is very common, as is mixing of clastic and carbonate sediments from opposing margins of the graben and it is almost impossible to follow individual beds for more than a few hundred metres.

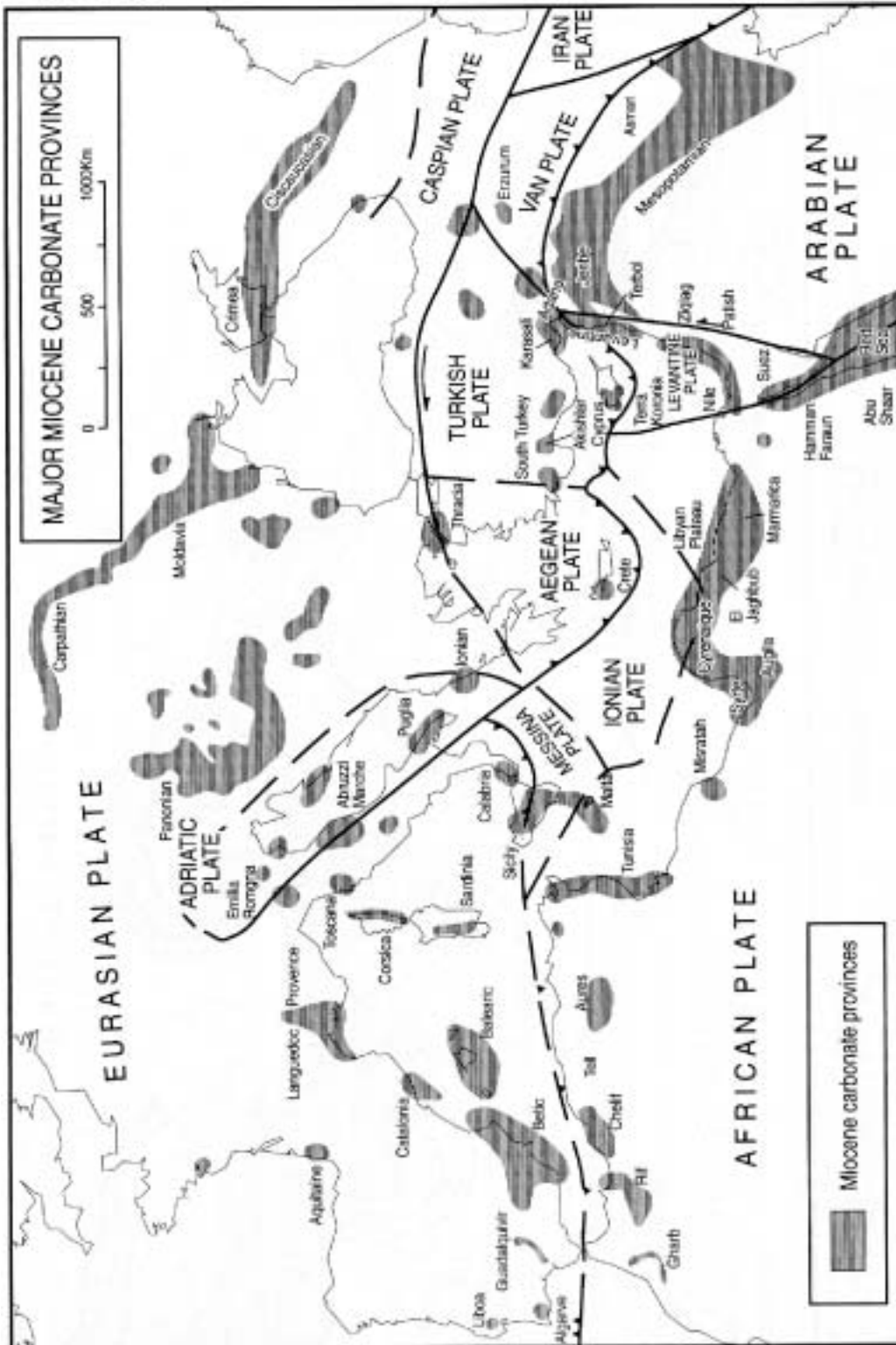
#### *Carbonate facies and water depths*

Water depths cannot be inferred from the clastic or resedimented mixed clastic carbonate deposits found within the graben axis. To enable this, the fauna and flora of the succession was also examined by Marcelle BouDagher-Fadel and Sylvia Gardin. Sylvia Gardin stated that Ascidian spicules (see Appendix 1) are common in the Late Miocene facies (uppermost Langhian-Serravallian time-slice samples) and Early Pliocene-age rocks. Ascidiaceans (sea-squirts) are only found in specific marine conditions at the present day. They normally inhabit normal marine salinity, littoral water depths (50m, more commonly 25m), often on rocky substrates. Tide or wave action, must normally be at a minimum.

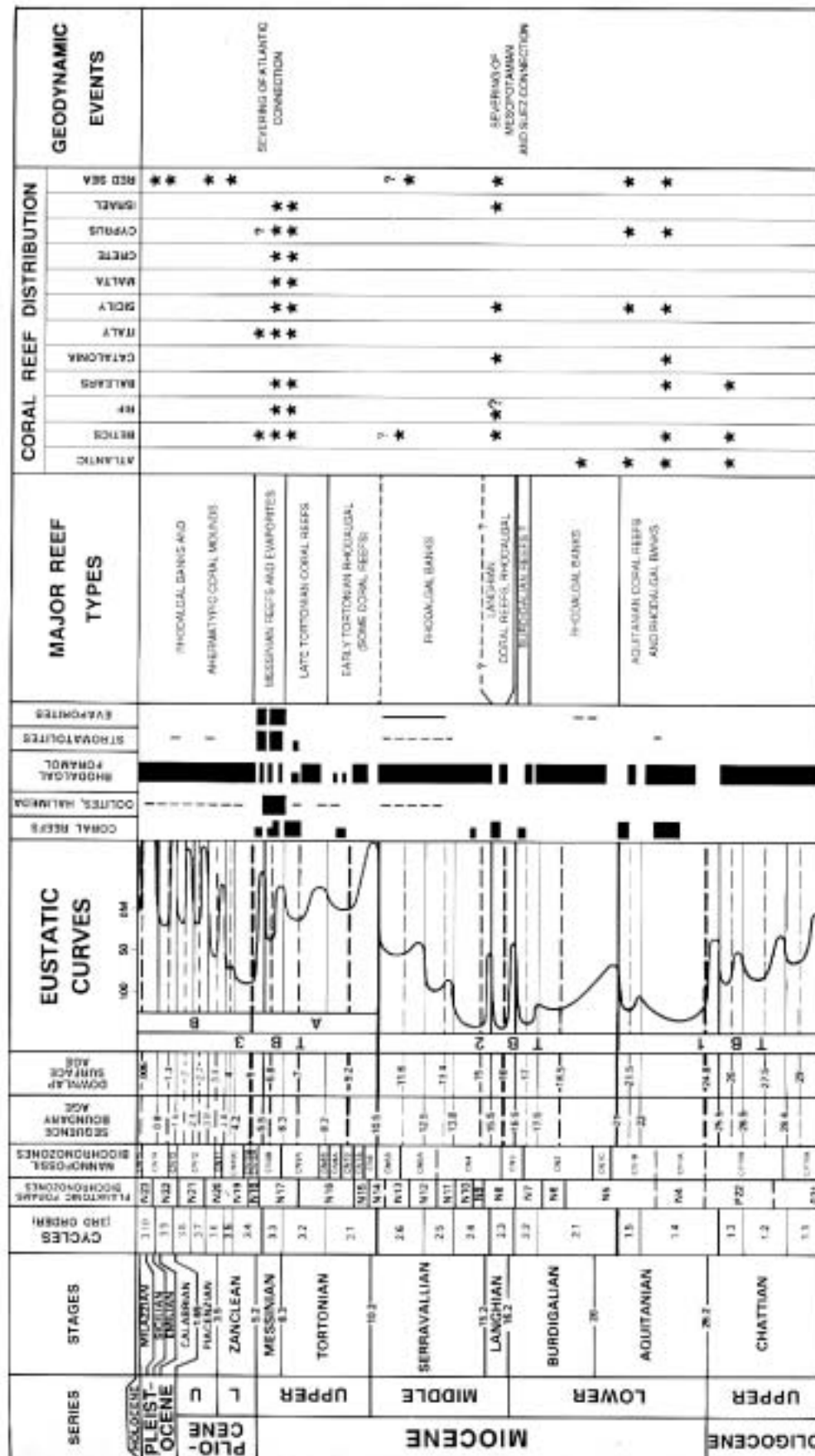


**Figure 6.15** From Emery & Myers (1996). Gravel-rich deep-marine clastic system models.

**Figure 6.16**  
From Estabab (1996).  
Main onshore  
Miocene carbonate  
provinces of the  
Mediterranean.







**Figure 6.17** From Estaban (1996). Stratigraphy of major reef types in the Mediterranean region during the Miocene.

Diagnostic fauna and flora for shallow marine conditions are not otherwise obvious within the sediments. There is little evidence of skeletal reefs in the Langhian-Serravallian

or Pliocene, as most bioclastic debris is loose. Peloids and rhodoliths are common, indicating shallow marine to shoreface conditions existed, but these components are not found in-situ, but as redeposited clasts. Very occasional *Porites* coral fragments are found within the Middle Miocene sediments. These encrusting corals would indicate near-shore environments, but none were found in-situ. *Porites* may have survived due to its tolerance to changing salinity and water turbidity.

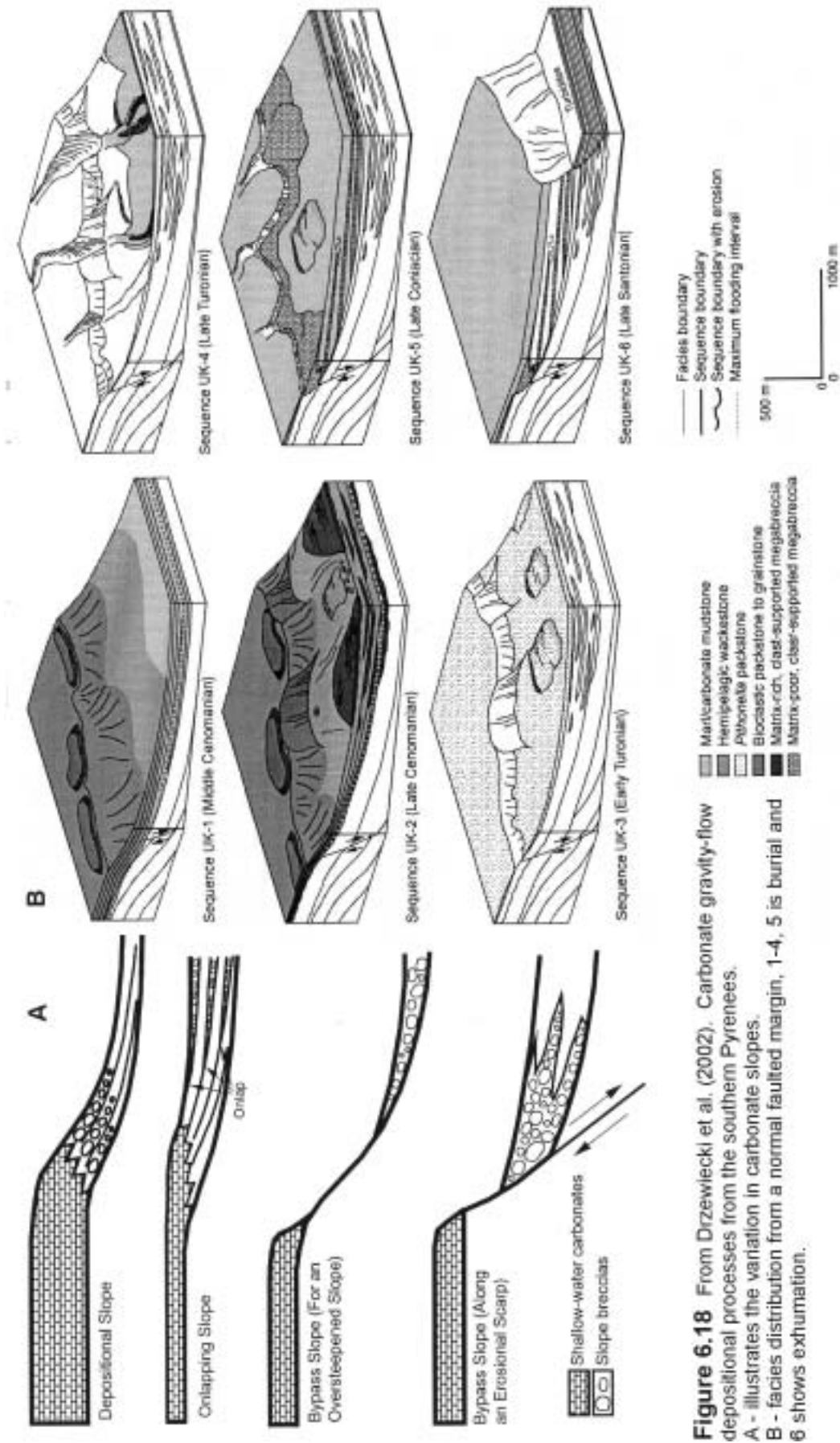
Therefore a shallow marine setting is suggested with shallow marine fauna, occasional coral and algal material (possibly 'reef mounds'), abutting a fault-controlled escarpment. Shelf depth waters are inferred within the graben.

An analogue of this setting is described by Drzewiecki et al. (2002) They cite a well exposed carbonate slope and margin example from the southern Pyrenees. A faulted margin controlled megabreccia deposition into hemipelagic background marls (Figures 6.18). They also cite numerous examples relating to active faulting, eustatic low-stands and sediment bypass (i.e. modern Bahamas; Miocene, Las Negras, southern Spain; Late Cretaceous, Pyrenean Basin, northern Spain). Avalanching (debris flows) of sediments was common in the Cretaceous-age, fault-bound lineament (narrow basin), studied.

#### Late Miocene (time-slices 7 & 8)

Late Miocene facies are restricted to the axis of the Nahr El-Kabir Graben, implying a regression from the Middle Miocene. Little evidence for the environment is evident for the Late Serravallian to Tortonian-age limestones (see Chapter 3). They are inferred to be mainly laminated, chalky limestones, with small foraminifera, and as such, they are not diagnostic of any particular setting (Figure 6.4). Further study, (especially biostratigraphy) is needed to add to these results.

The Messinian marks a major cycle of regression throughout the Mediterranean basin (Hsü et al. 1973 & 1977). Very shallow hyper-saline marine conditions and sub-aerial conditions would have prevailed at this time within the Nahr El-Kabir Graben (see Chapter 3).



**Figure 6.18** From Drzewiecki et al. (2002). Carbonate gravity-flow depositional processes from the southern Pyrenees.  
A - illustrates the variation in carbonate slopes.  
B - facies distribution from a normal faulted margin, 1-4, 5 is burial and 6 shows exhumation.

### Early Pliocene (time-slices 9-11)

Early Pliocene marls are developed in the axis of the Nahr El-Kabir Graben, indicating marine transgression after the Messinian. Foraminiferal evidence from the middle part of the succession provided by Marcelle DouDagher-Fadel, suggests outer shelf depth deposition. The sediments are mainly laminated marls with occasional clastic input so her interpretation is in accord with the field evidence. This sequence is unconformably down-cut by bioclastic sands, indicating a rapid shallowing event to foreshore depth water, before the succession terminates.

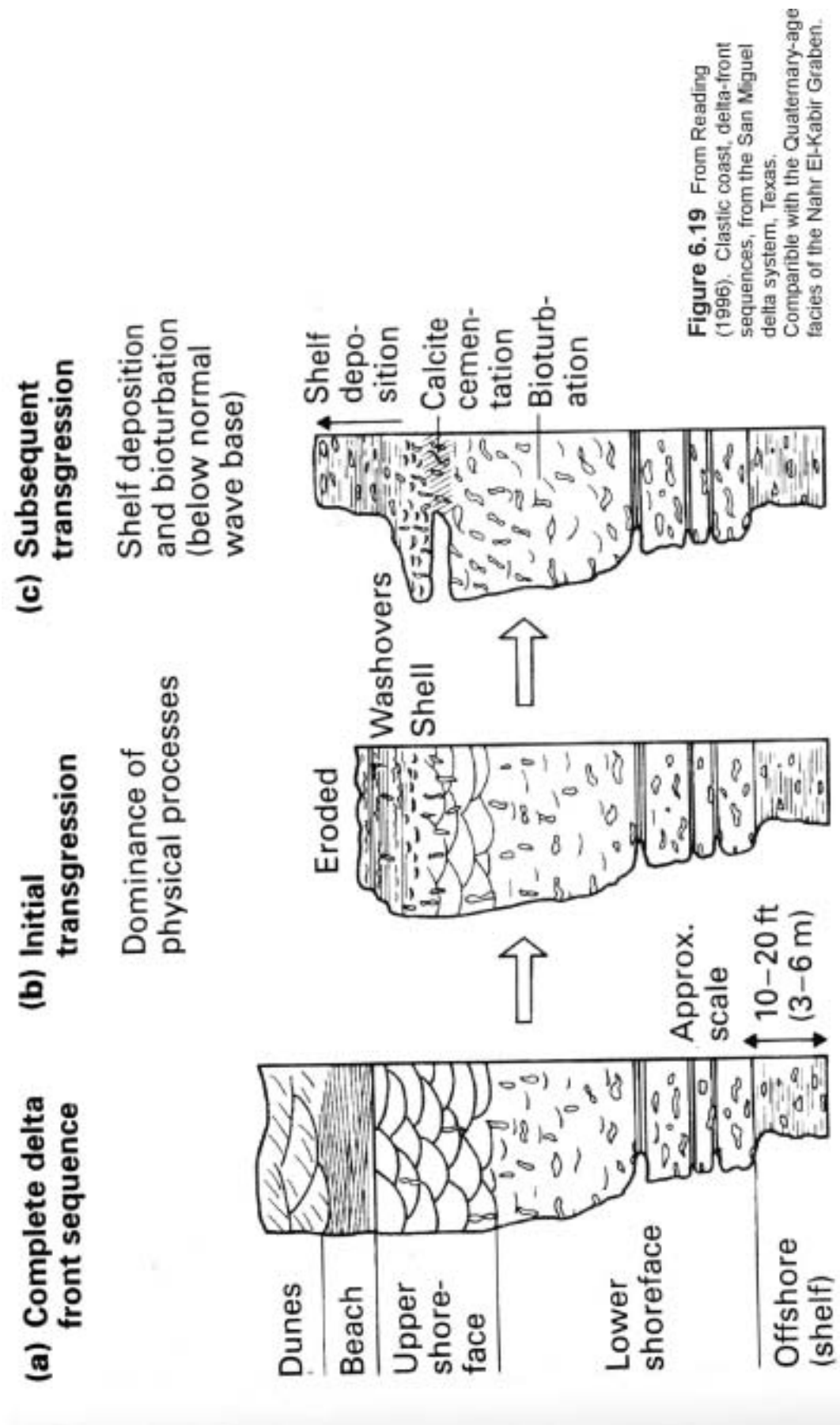
Near Banyas, the oldest lavas exposed (latest Messinian to Early Pliocene-age)(see Chapters 2 & 3) are sub-aqueous, indicating that uplift in this region occurred prior to the main eruptive episode, during the Early Pliocene when deposition occurred at or near the shoreline.

### Quaternary (time-slice 12)

The Late Pliocene to Quaternary-time interval marked the final regression and uplift of the Nahr El-Kabir Graben and its surrounds. Very shallow, shoreface deposition occurred during the Late Pliocene to earliest Quaternary and was overlain by beach and fluvial deposits, similar to those described by Reading (1996) (Figure 6.19). Terracing of Quaternary beach facies is common on the Latakia coast and relates to neotectonics (see neotectonics and Figure 6.24).

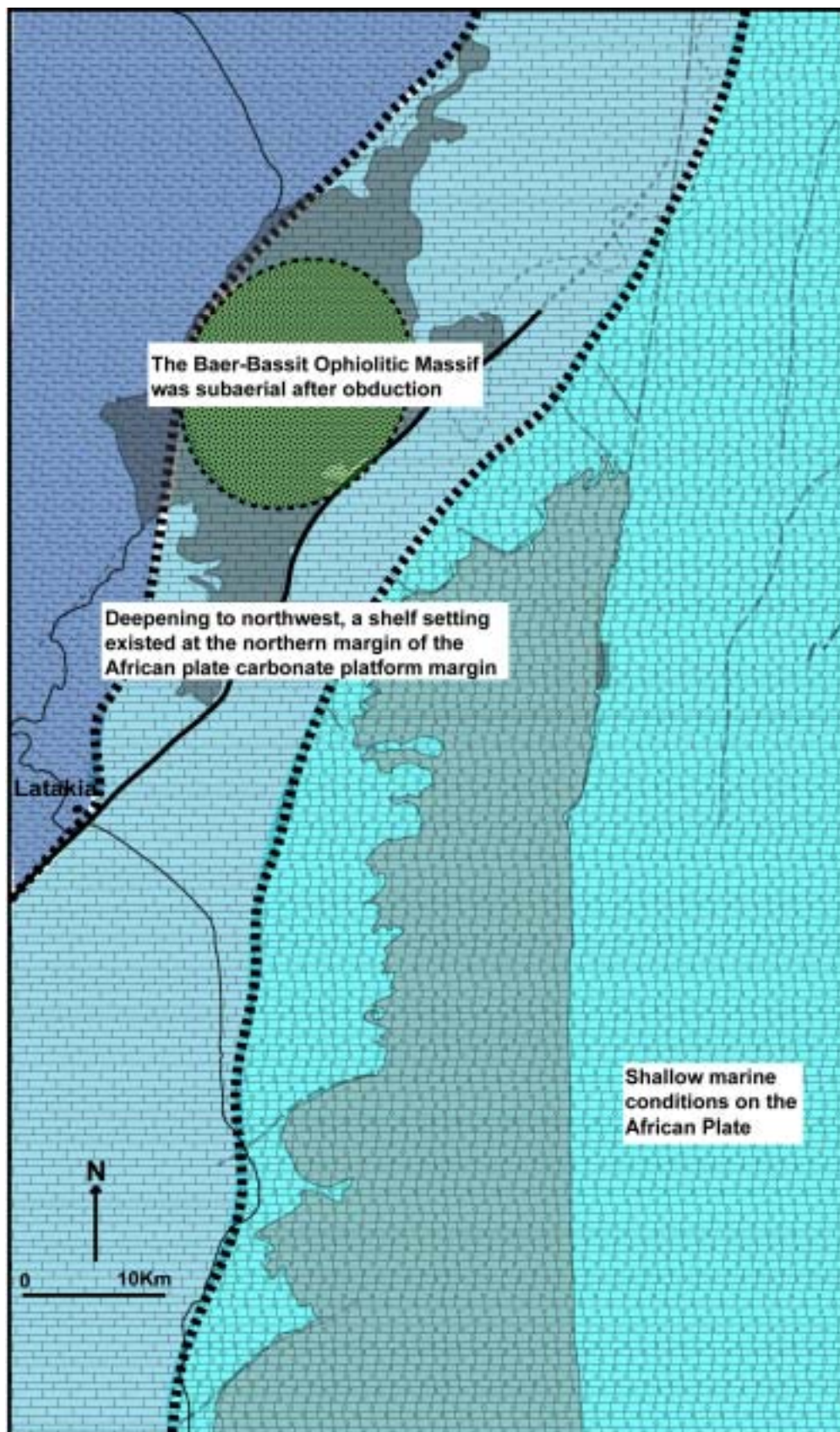
## ***Palaeogeography***

Figures 6.20 a-e illustrates the inferred palaeogeographies of the project region during the Paleogene, Early Miocene, Middle Miocene, Late Miocene and Pliocene. Evidence for the reconstructions is given in Chapters 2, 3, 4 and 6.



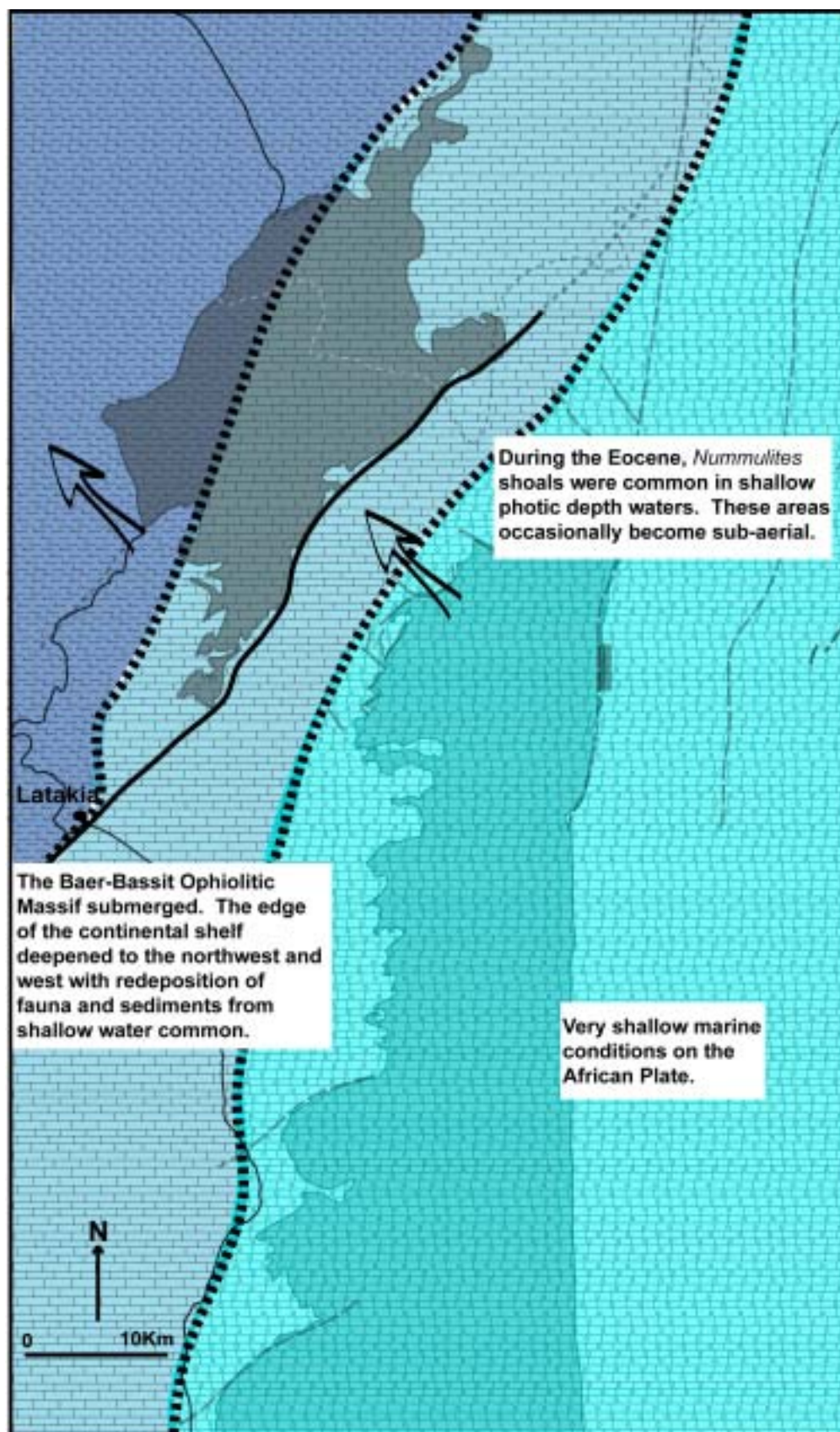
**Figure 6.19** From Reading (1996). Clastic coast, delta-front sequences, from the San Miguel delta system, Texas. Comparable with the Quaternary-age facies of the Nahr El-Kabir Graben.





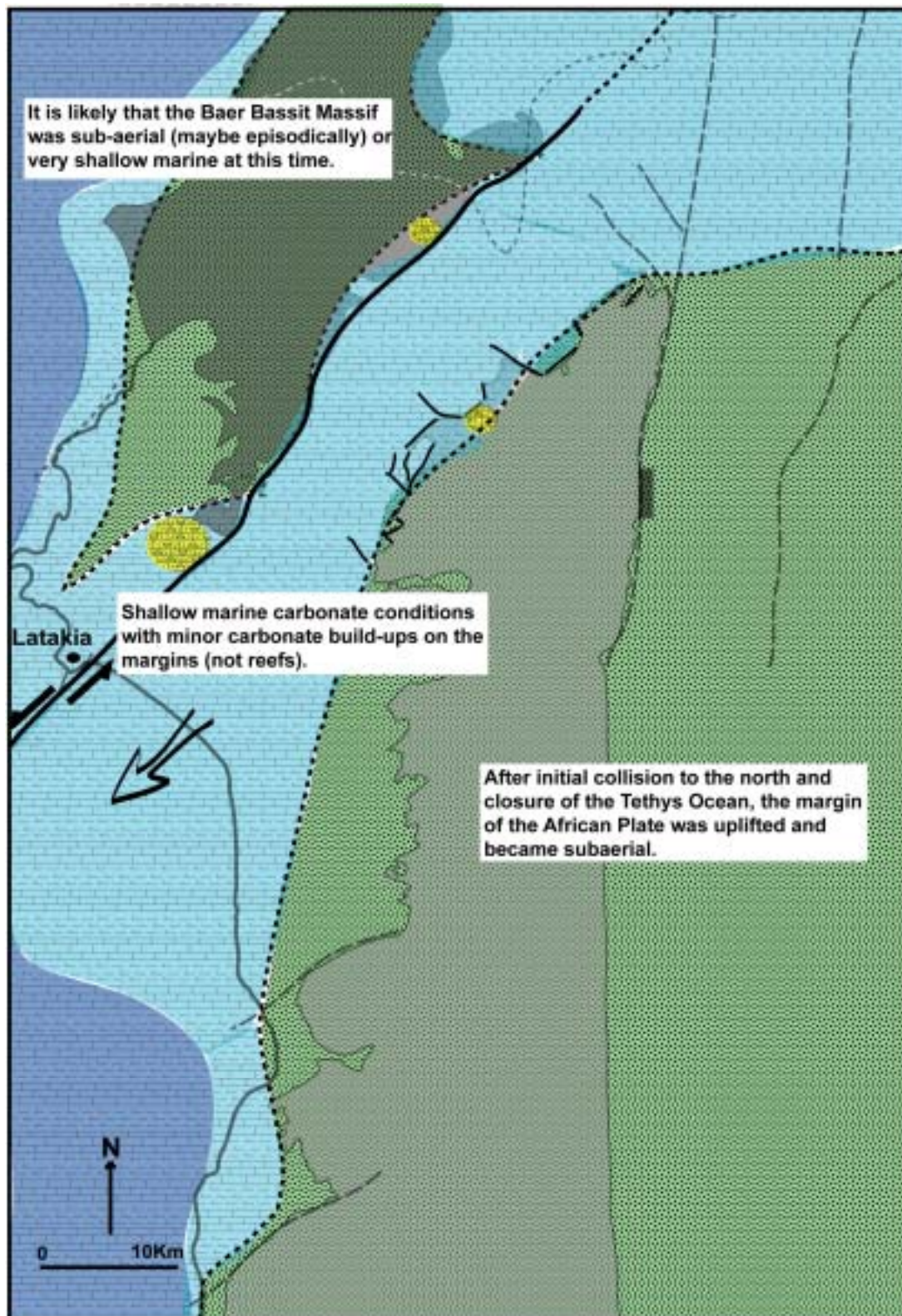
**Figure 6.20A** Palaeogeographic map of the project area at latest Maastrichtian-Early Palaeocene time. Continental deposits exist on the base Late Maastrichtian, whereas marl is common throughout the remainder of the Early Paleogene succession.





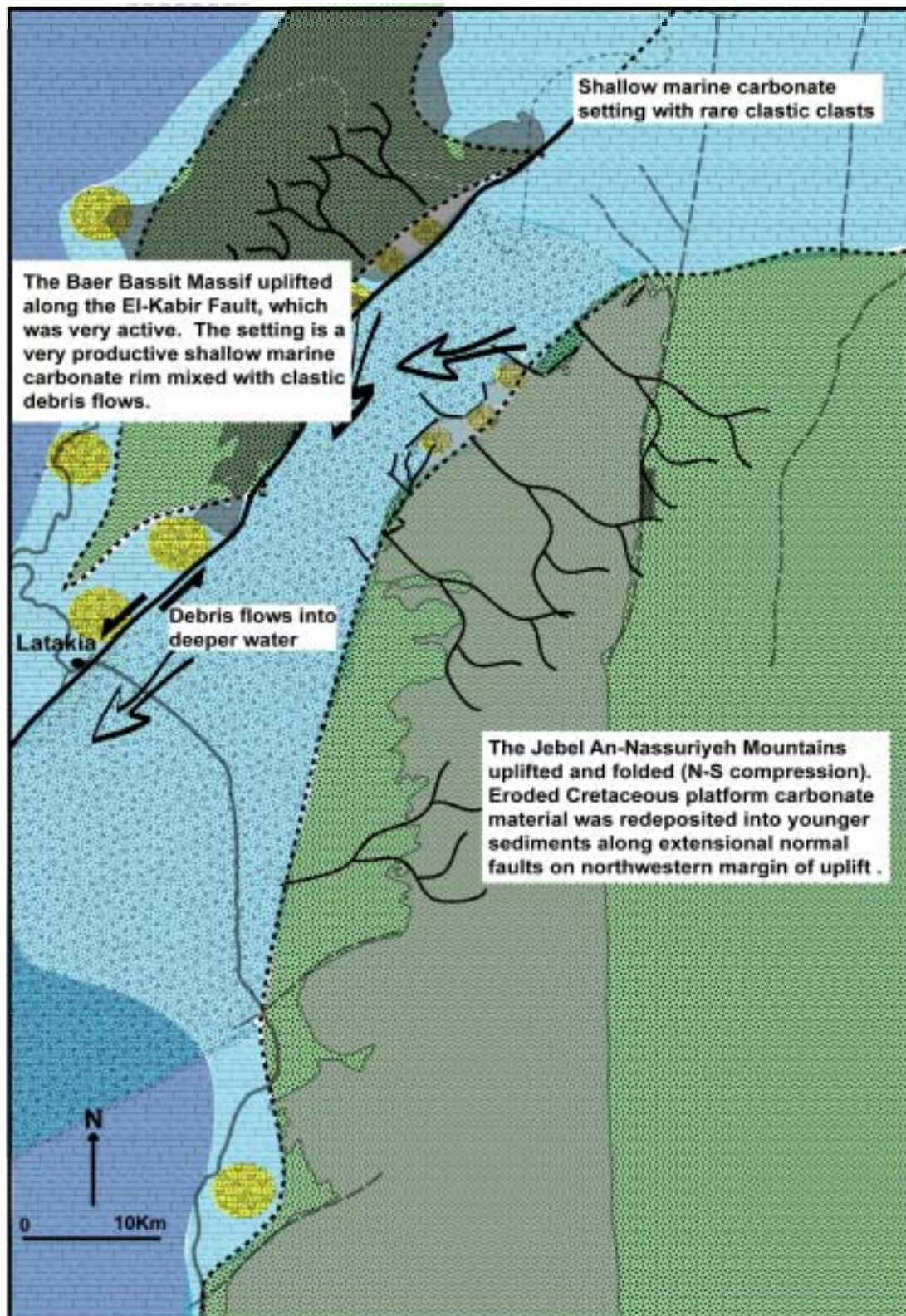
**Figure 6.20B** Palaeogeographic map of project area at late Palaeocene to Middle Eocene (and potentially to the earliest Oligocene). Shallow marine carbonate sedimentation dominated the region. Strong faulting occurred on the El-Kabir fault, especially near Latakia.





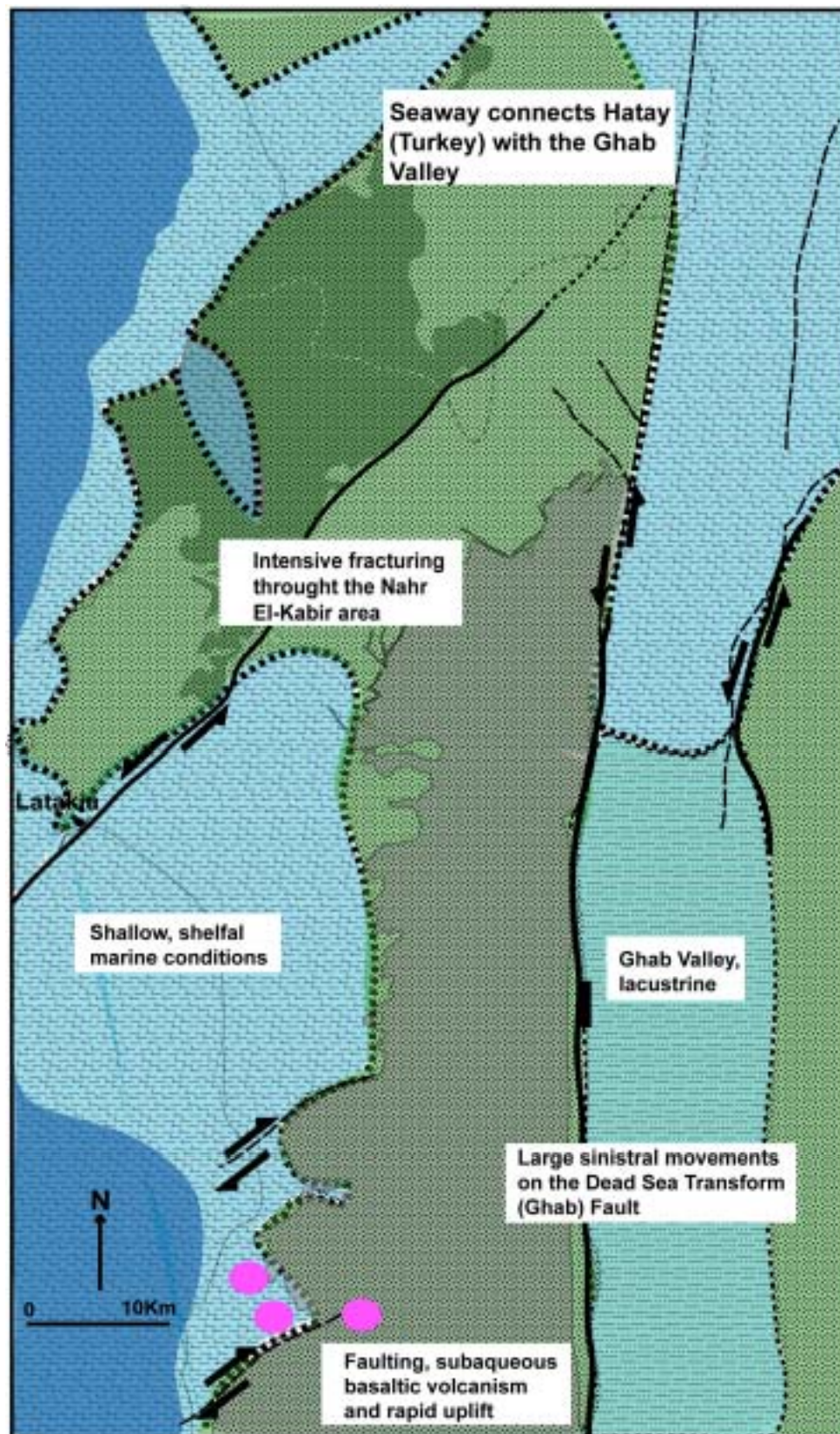
**Figure 6.20C** Palaeogeographic map of project area immediately after the Oligocene hiatus and unconformity due to collision of the Misis Mountains to the north (now Northern Cyprus - Hatay, Turkey). The Nahr El-Kabir valley was drowned and white, marly carbonate production occurred with minor bioclastic input. Limited faulting.





**Figure 6.20D** Palaeogeographic map of the project area during the Langhian-Serravallian. Regional compression led to localised uplift controlled by large movements on the El-Kabir Transform Fault. Localised extensional faulting also controlled sedimentation in the area. Mixed clastic-carbonate deposition, bypassing into deeper water is distinctive of this period.





**Figure 6.20E** Palaeogeographic map of the project area during the Pliocene. The Late Pliocene-Quaternary led to continued uplift. Major faulting occurred along the Dead Sea Transform Fault, with intensive, small scale, movement observable along the El-Kabir Fault from this time and large movements offshore.

### ***Structural history with relation to sedimentology***

Most of the sedimentary successions within the area studied are marls and fine-grained limestones that accumulated in shelf-depth environments. Pulses of coarser sediments with shallow water (shoreface or shallower) fauna are suggestive of structural events. In the Miocene, the coarse sediments originate from the margins of the Nahr El-Kabir Graben and were due to movement on the graben margin faults. Fault movement and major structural events are summarised below in relation to deposition (see also Chapter 4). Table 6.21:

<b>Time period/Time-slice</b>	<b>Baer Bassit Ophiolitic Massif and northern margin of the Nahr El-Kabir Graben</b>	<b>Jebel An-Nassuriyeh Mountains and southern margin of the Nahr El-Kabir Graben</b>
<b>Cretaceous to Maastrichtian</b> <b>1</b>	Sub-aerial exposure then transgression, Baer Bassit Massif dips to west	Continuous? sedimentation, minor disturbances to bedding in upper section and at base of Maastrichtian.
<b>Palaeocene</b> <b>1</b>	Continuous sedimentation with calci-turbidites	Unconformably overlies Maastrichtian
<b>Lower Eocene</b> <b>1</b>	Shallowing water conditions, occasional chert-rich beds	Unconformably overlies Palaeocene, erosive and transgressive
<b>Middle Eocene</b> <b>2</b>  <b>(Figure 6.20a)</b>	Erosive unconformity onto Lower Eocene Intense slump folding and faulting on the El-Kabir Lineament and on the Baer-Bassit Massif	Erosively and unconformably overlies all Paleogene and Cretaceous successions
<b>Oligocene</b>	Not observed. Uplift.	Not observed but fauna present in younger rocks
<b>Aquitanian</b> <b>3</b>	Restricted to Nahr El-Kabir Valley (start of graben?) and margins	Also restricted, but contains clast of older rocks, especially Middle Eocene and Oligocene
<b>Burdigalian</b> <b>4</b>	Coarse, chert-rich, shallow water facies. Fault related or sub-aerial uplift of Baer Bassit Massif?	Coarse, bioclast-rich facies, prograde into graben from normal-faulted margin

<b>Middle Miocene</b> <b>5,6</b>  <b>(Figure 6.20b)</b>	Very coarse, fault-related, chert-rich, debrite facies. Sub-aerial uplift of Baer Bassit Massif?	Very coarse, bioclast-rich facies, prograde into graben from normal-faulted margin. Uplift of Jebel An-Nassuriyeh Mountains?
<b>Serravallian-Tortonian</b> <b>7</b>	Thin, chalky limestones observed at one locality only. Uplift?	Chalky limestone in graben axis. Uplift of Jebel An-Nassuriyeh Mountains?
<b>Messinian</b> <b>8</b>	None observed. El-Kabir lineament faulting?	Gypsiferous facies in graben axis and later debris flows.
<b>Pliocene</b> <b>9, 10, 11</b>  <b>(Figure 6.20c)</b>	Marl-rich facies overlie northern margin in the south of area.	Marl-rich facies in the graben axis only, overlain by shallow marine bioclastic sands. Volcanic eruptions in the south, related to Dead Sea Transform Fault.
<b>Late Plio-Quaternary</b> <b>12</b>	Raised terraces of bioclastic grainstone common. Numerous fractures and strike-slip faulting.	Occasional terraces, mostly beaches, marine to fluvial coarse sediments

**Table 6.21.** Examination of structural history in relation to sedimentology.

## Megasequences

The sedimentary record in northwest Syria comprises three cycles of deposition at an overview scale, prior to the Late Plio-Quaternary (Figure 6.1). Three cycles of transgression to neritic conditions and then uplift are inferred. These cycles are: 1. The Maastrichtian to Middle Eocene (time-slices 1 & 2), 2. Aquitanian to Tortonian (time-slices 3 to 7), 3. Messinian to Pliocene (time-slices 8 to 11). Each of these cycles is referred to as a megasequence in this study. Individual time-slices exhibit distinct diachronism, expressed as irregular disconformities, due to the fact that transgressions and uplifts are often very localised initially. The megasequence however, represents the regional scale event. These megasequences form the tectonostratigraphy, as they highlight the timing of the key tectonic events.



## ***Supplementary data***

### Subsidence curve

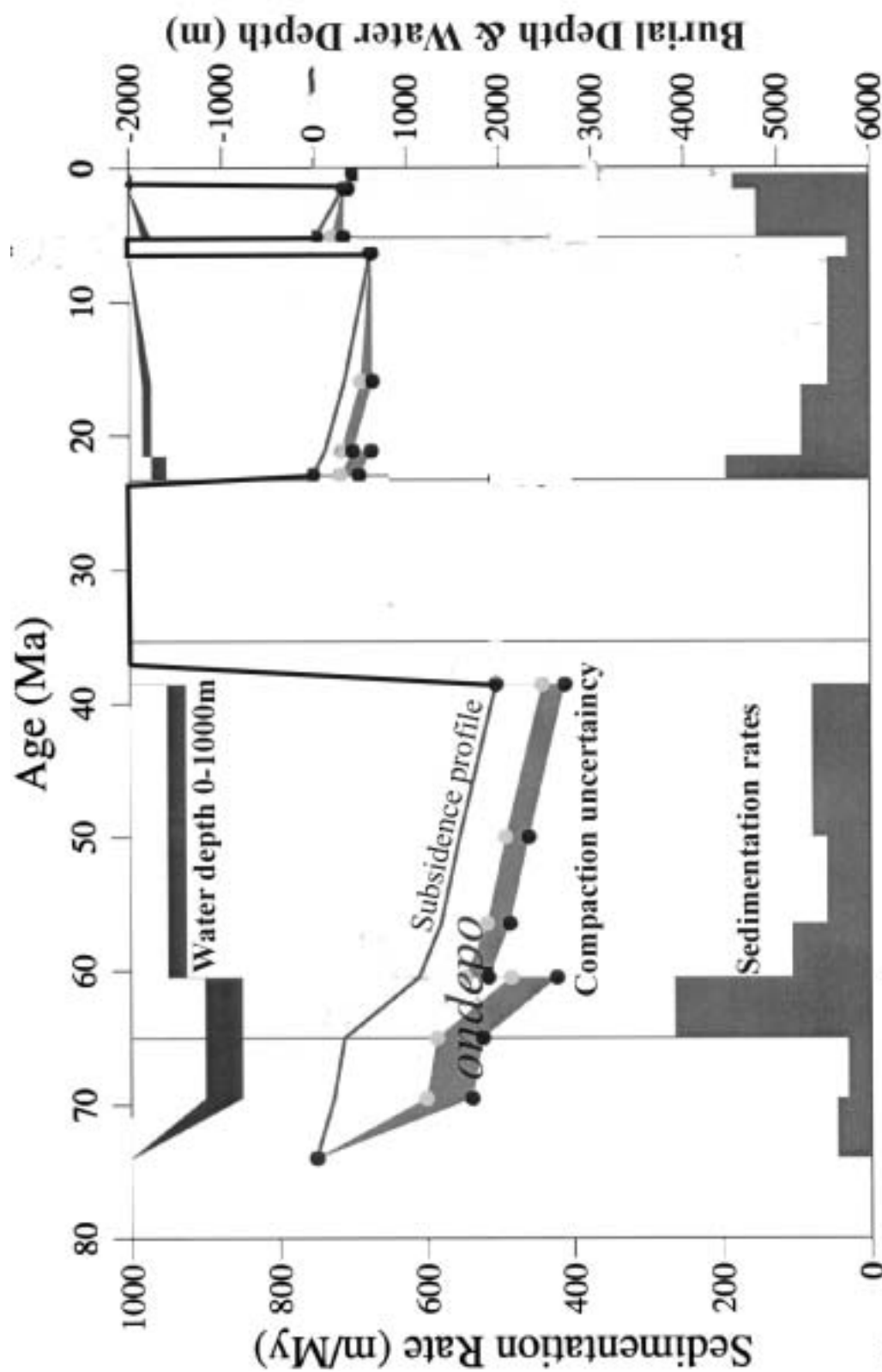
The Nahr El Kabir Graben was modelled for its subsidence profile using UNIX software developed by Dr Jon Turner (Edinburgh University). Sediment lithology (clay, sand, etc), logged maximum sediment thickness, water depth and age were input for each succession and a graph of sedimentation rate, compaction and subsidence was produced. The software cannot account for uplift (Figure 6.22). The input data primarily utilised the sediment thicknesses based on this study and those given by Ponikarov et al. (1966).

The graph produced was then adjusted to take account of periods of uplift and to determine if trends in sedimentation could be seen. The three major 'megasequences' previously identified (Chapter 3 & this chapter) are easily identified and the graph also shows that the maximum sedimentation occurred at the start of each of these 'megasequences'. After the initial sediment pulse, sedimentation gradually decreased until the next period of uplift occurred. The subsidence profile for each 'megasequence' is closest to those produced in extensional basin settings, having too shallow a profile for strike-slip or foreland settings (personal communication with J Turner, 2001)(Figure 6.23).

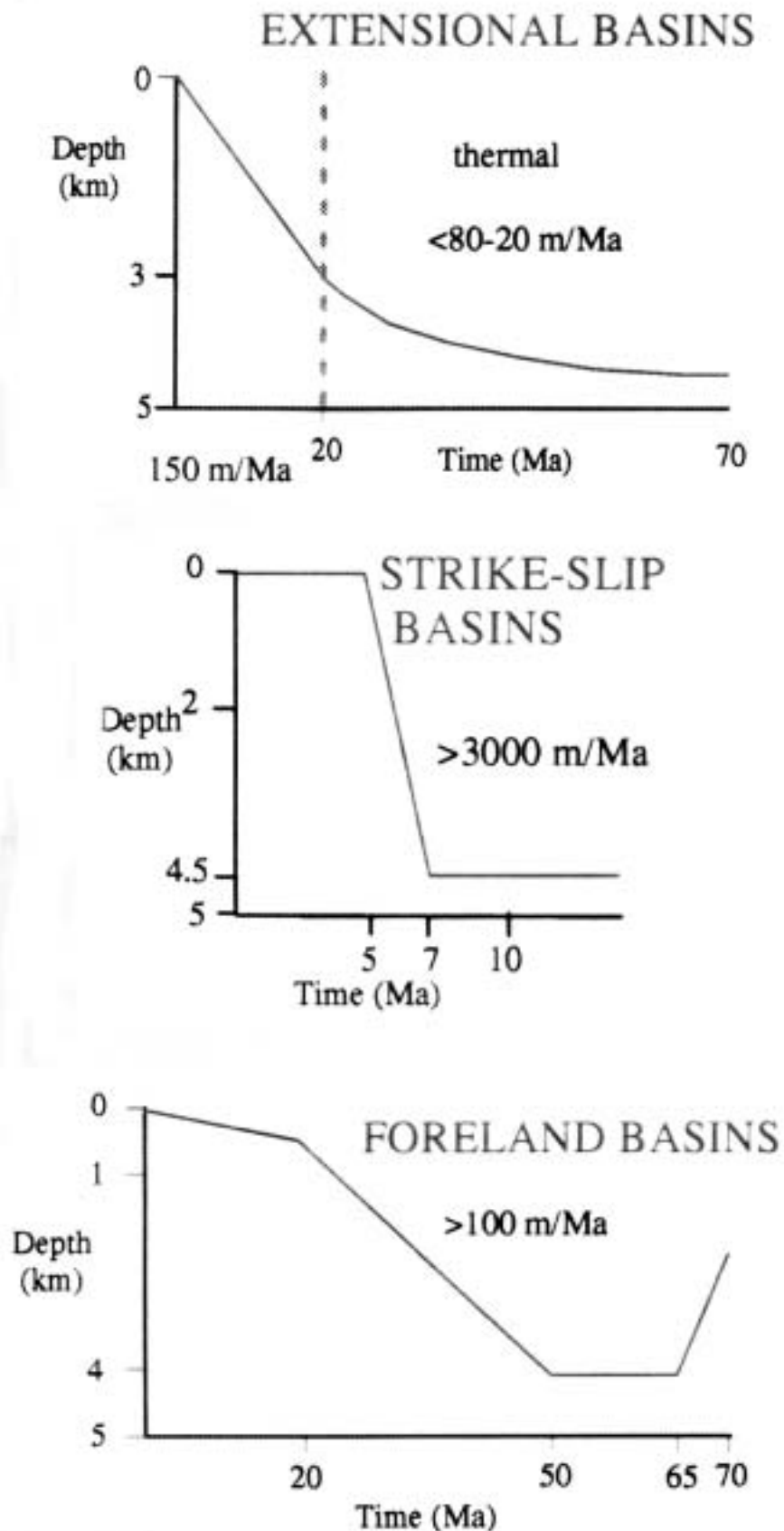
If the graph is compared to the actual geology of the Nahr El-Kabir Graben then the model appears not to hold up too well in the Miocene successions but appears accurate for those of Paleogene age. This is probably due to data missing in the model rather than the modelling software itself. The Miocene 'megasequence' is a prime example of an increasingly clastic, shallowing-water depth succession. Coarse sedimentation increased throughout the succession and bypassed into deeper water settings, a feature that cannot be modelled. Structural events such as uplift, unfortunately also upset the compaction, burial depth and sedimentation rates inferred later in the graph. It would, therefore, be prudent to suggest that the graph presented is only taken to represent the Paleogene successions and not the remainder of the Tertiary.

### Palaeo-rotation and palaeo-magnetism

Tony Morris (Plymouth University) is currently studying orientated samples of the Paleogene and Miocene successions from the Latakia region to assess remnant magnetism and possible palaeo-rotation of the region, following their earlier work on the Baer-Bassit



**Figure 6.22** Subsidence curve of the Nahr El Kabir Graben, using sediment thicknesses from Ponikarov et al. (1966) and water depths from this study. Software by Jon Turner (Edinburgh). The graph has been edited as uplift cannot be modelled and the subsidence/uplift profile has been superimposed.



**Figure 6.23.** Data from J Turner (pers.comm, 2001, Edinburgh University). Typical subsidence profiles in differing basin forming processes.

Ophiolite (Morris et al. 2002). The Palaeocene successions have been mildly re-magnetised since deposition and gently, tectonically folded, showing only moderate clockwise or anti-clockwise rotations (the Baer Bassit Massif studies showed rotations in discrete blocks of  $>200^\circ$ ). This indicates that the majority of rotation occurred prior to post-emplacement deposition.

The Miocene successions have also been re-magnetised, but, the palaeomagnetism is statistically indistinguishable from the current field direction or Miocene reference direction. This magnetic overprinting could be due to a number of factors: i.e. fluid flow during faulting or later groundwater leaching.

Therefore, it is possible to say from these results that only minor rotation occurred during the Palaeocene, but not within the Miocene, when the major faulting occurred.

### Hydrocarbon geology

Bitumen was found at three localities within the Nahr El-Kabir Graben and as a minor show in the Baer Bassit Massif. At each locality, bitumen shows are located near faulting, especially northwest striking strike-slip (transfer) faults.

On the Baer Bassit Massif, minor quantities of crystalline bitumen and organic material were found in faulted Paleogene marl-rich rocks bordering the Nahr El-Qandil. The timing of faulting is unconstrained and bitumen is a very minor component of the rock.

In the Nahr El-Kabir Graben, bitumen was found at two localities on the El-Kabir Lineament and at Kferyeh Asphalt Pit. In the pit, (a commercial mine, see Chapters 3 and 4), bitumen is found in Langhian to Serravallian-age bioclastic limestones. The bitumen is spatially restricted to proximal deposits on or near strike-slip transfer faults. Chapter 4, examined this area in detail. Faulting cannot be constrained to only the Miocene and was probably active in Pliocene to Recent times. Similar settings are found at Jeqourjaq Village on the El-Kabir Lineament. At the beachfront in Latakia City, minor shows of bitumen are found in northwest striking fractures. These fractures are almost certainly constrained to Late Plio-Quaternary to Recent-ages (see Chapter 4), but the source rock is unknown.

Onshore hydrocarbon exploration is limited to wells drilled by the Syrian Petroleum Company in the 1970's, data which are unreleased. Dzhabur's (1985) unconfirmed interpretation of one of these wells, has been discussed previously (Chapter 1, 2, 3 and 4). Onshore petroleum potential seems to be restricted to small asphalt deposits.

Offshore, seismic line 24S shows the potential for trap formation beneath the domed Messinian evaporite layer (a potentially excellent seal) and above the inferred extension of the El-Kabir Lineament (flower structures; Chapter 4). The Messinian evaporite layer has been estimated to be thicker than the 300m of Recent offset on this fault (2000m +; Chapter 4). Burial depth would also be considerably deeper, almost certainly entering the oil or even gas generation windows (depends on geothermal gradient, which is unknown; Selly, 1998). Exploration drilling would be expensive due to the 1500m water depth.

This summary identifies the sites of hydrocarbon production; mature hydrocarbons are present onshore and infers that bitumen occurrences are related to the later stage of faulting (northwest striking). This faulting is time constrained as Late Pliocene to Recent. Exploration awaits the brave!

### ***Neotectonics (Late Plio-Quaternary structures)***

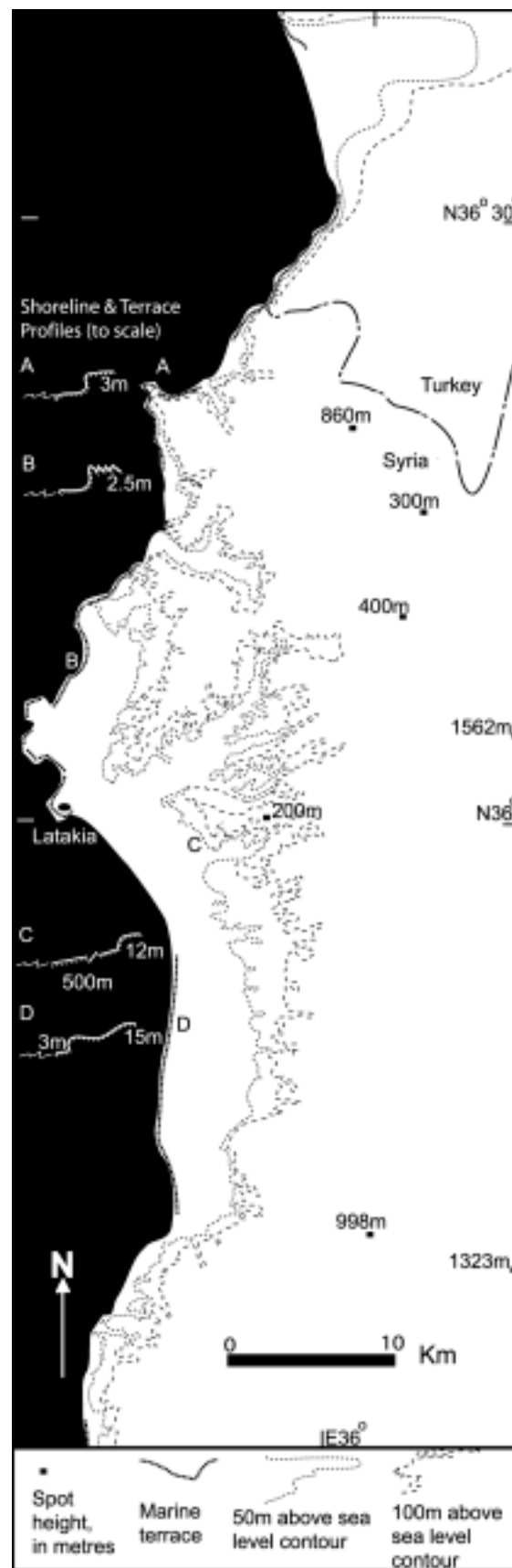
#### *Quaternary terracing*

Quaternary terracing is prominent north of Latakia and on the Baer-Bassit Massif coastline, where two major marine terraces are present (Figure 6.24). Uplift in these areas is 2.5-3m, implying this amount of uplift since the Tyrrhenian (100Ka) (Poole & Robertson, 1990). Borj Islam Village also appears to be located on the margin of a higher and more widespread terrace, this could indicate a Neotyrrenian terrace (200Ka), 10-15m above sea-level. South of Latakia, terraces are only found at Jebleh (1-2m). Most of the coastline consists of dunes and is very flat.

Terracing of Quaternary-age deposits is linked to uplift variations across the El-Kabir Lineament. This variation is most apparent at the beachfront of Latakia City, where sea-level beach sands abut a 10-15m high platform of Eocene and Quaternary-age rocks, in exactly the location inferred for the fault (see pull-out maps). Similar Plio-Quaternary features are seen in Cyprus (Poole et al. 2000), suggesting regional sea-level fall.

#### *“Straight Coastline Theory” of neotectonic movements*

The southeastern margin of the Mediterranean follows a fairly smooth linear south to north profile from the Sinai to southern Lebanon. North of Lebanon (Syria and Turkey), the coastline becomes uneven with numerous bays and promontories. Ivanov et al. (1992) put forward the idea that the “step-like” profile of the coast of the Eastern Mediterranean Sea



**Figure 6.24** Present day topography with Quaternary terrace locations.



was due to neotectonic movement of wrench faults and shear zones they observed between Cyprus, Syria and Turkey. The West Tartus Ridge they inferred as sinistral (named 'Latakia Ridge by Vidal et al. 2000 A & B) and extrapolated it as the likely southernmost boundary fault between the Anatolian and African/Arabian plates. This fault was interpreted as reaching the Syrian coast (named El-Kabir Lineament; this study, see Chapter 4). Three (possibly four) shear belts were inferred to the north, reaching Iskenderun Bay in Turkey (Figure 6.25A). Each shear belt was interpreted as having small Plio-Quaternary pull-apart basins within them.

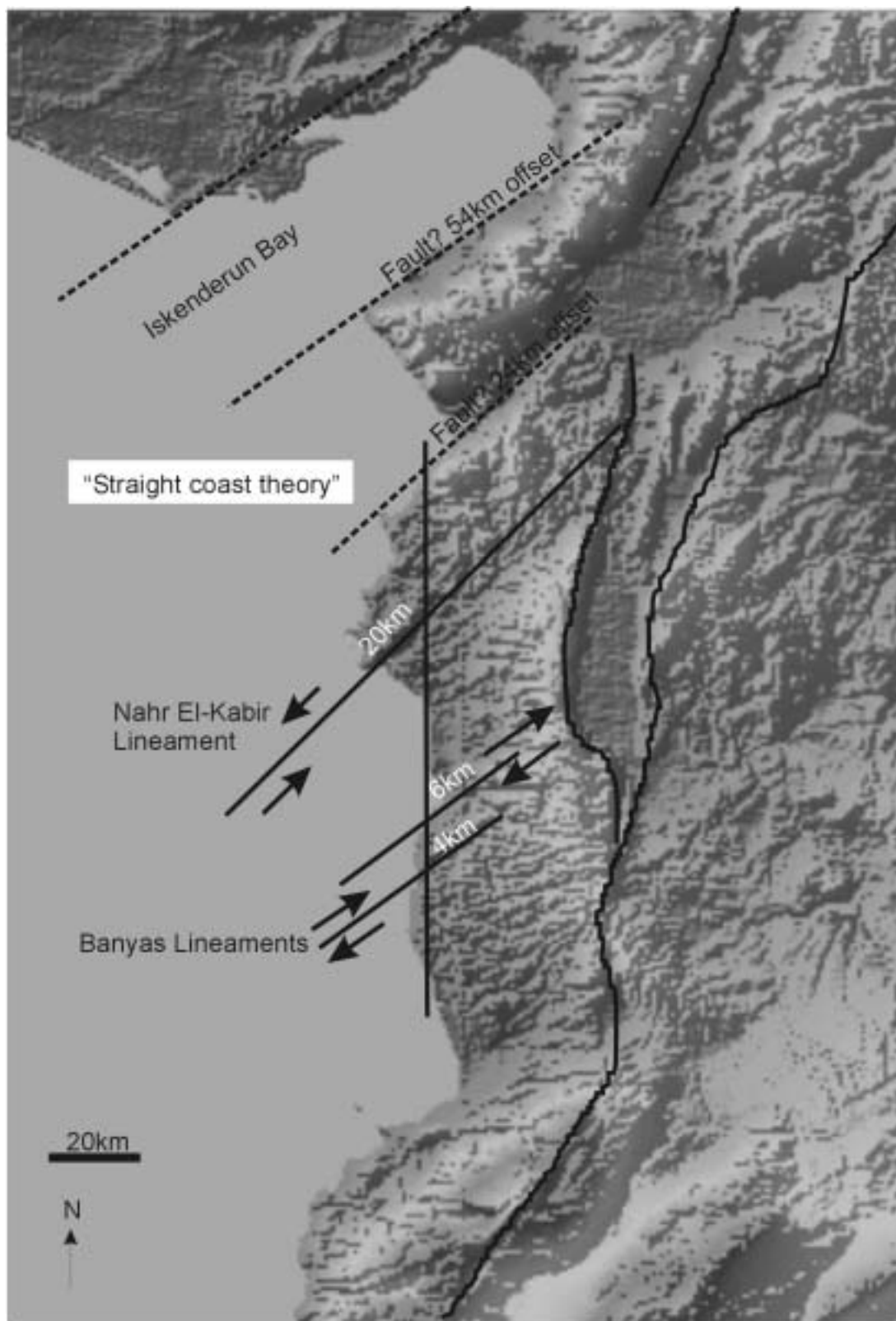
If Ivanov et al.'s (1992) concept of a stepped coastline being directly related to neotectonic shear belts is applied, a sinistral throw of 20km for El-Kabir Lineament would have occurred since the Plio-Quaternary (Figure 4.25B). The large faults found near Banyas Town would have dextral throws of 6km and 4km (i.e. northern, then southern fault).

The Ghab Graben, which also formed at this time (Trifinov, 1991; Brew et al., 2001) is on average 10-12km wide with an inferred large, normal, extensional fault on the western margin (Domas, 1989; Brew et al., 2001).

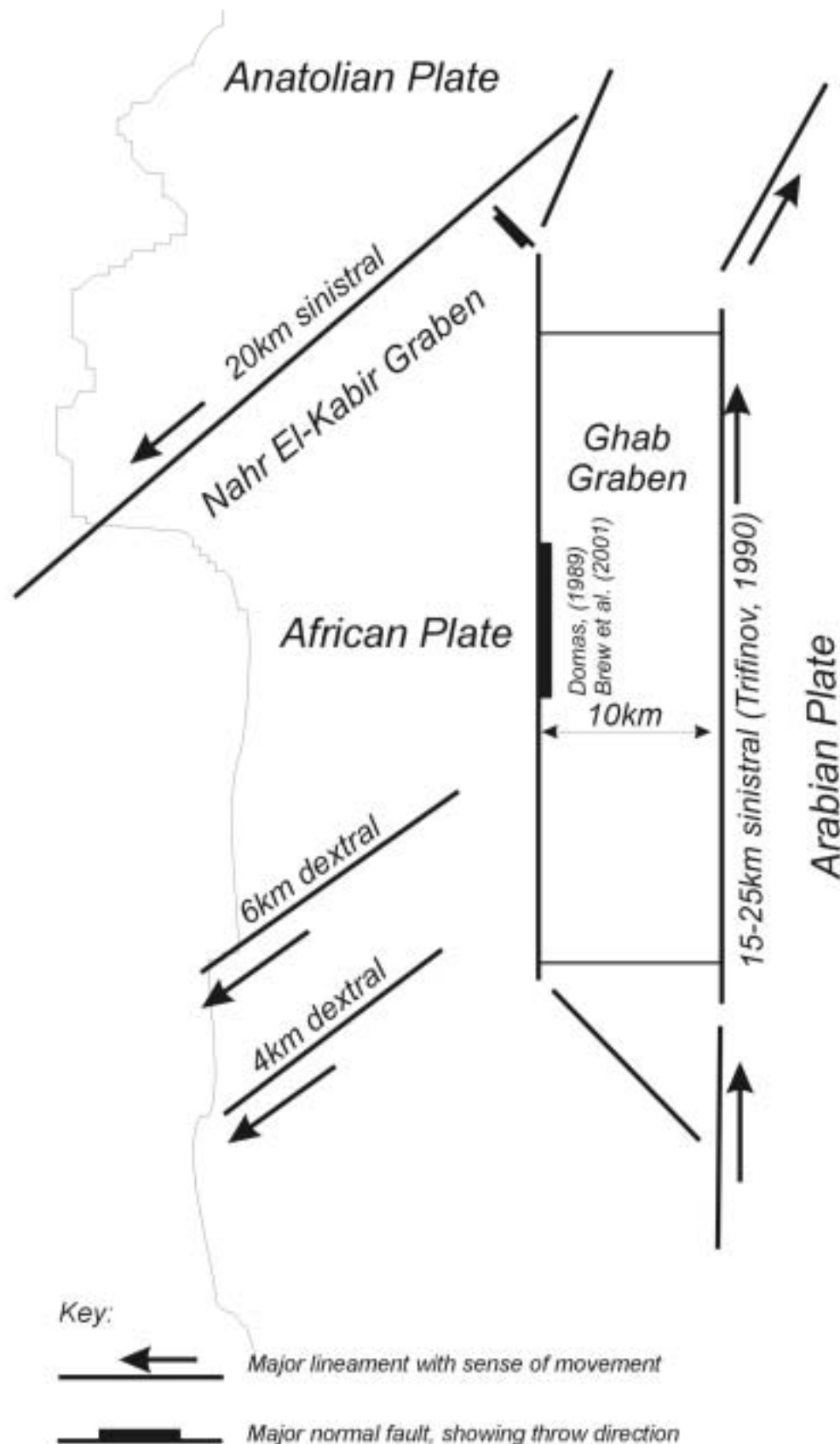
These figures and this technique are hypothetical based on a straightforward notion; however, in the case of the Latakia region and particularly the El-Kabir Lineament, this movement is hard to substantiate from field observations. Some movement has definitely taken place but 20km seems to be an exaggeration. During the Plio-Quaternary a rate of motion  $>4\text{km Ma}$  is implied using their hypothesis. The Baer Bassit Massif is inferred in this study (see Chapter 4) to trend offshore. Differential erosion of the Baer Bassit Massif and the Nahr El-Kabir Graben could create an irregular coastline.

#### *Offshore slope instability*

Recent work by Martinez et al. (2003) shows that offshore slope instability is common near the Israeli and Lebanese coastline (Figure 6.26). The Latakia coastline has a similar bathymetric profile. Further study is required in this region especially as the region south of Latakia City is a major depositional zone and has a recorded history of earthquakes.



**Figure 6.25.** The "straight coast" idea is basically a simple measurement against a projected coastline; based on current fault movements the Nahr El-Kabir fault would have moved at least 20km sinistrally, whilst the two Banyas faults would have dextral throws of 6km and 4km (north to south). This approach could be applied to the Iskenderun Bay region further north in Turkey or to Lebanese faults.





**Figure 6.26.** From Martinez et al. (2003). An image interpreted from seismic reflection data of post-Messinian/Recent reflectors showing slumping along the Israeli coastline into the Levant Basin. This setting is approximately 100km south of the project area, but has a similar bathymetric profile.

## ***Geological history of northwest Syria***

### *Fieldwork results*

The earlier sections of this chapter demonstrate the additional data and interpretations provided by this study. One major feature of this work was the mapping of features observed during fieldwork.

The *pull-out geological map* represents extensive re-mapping and re-drafting of key aspects of the geology. Faults, age of faulting and fault throws are updated (in red and black) from the original mapping of Ponikarov et al. (1963) and Piskin (1985) (Figure 1.3). Sedimentary facies, especially Miocene-age facies, have been revised to illustrate facies variability by locality. The map demonstrates the existence of essential features of the Nahr El-Kabir Graben and its surrounds. Through the combination of Syrian and Turkish basemaps, a better visualization of the regional geology was achieved.

### *Oligocene hiatus*

Previous work (Ponikarov et al. 1963, 1966, 1967; Krasheninnikov, 1971 & 1994) indicated that Oligocene-age facies were absent within the Latakia region. Late Eocene and probably the earliest Aquitanian-age rocks were also inferred to be absent. Oligocene-age rocks were, however, mapped by these authors within the Ghab Graben. The Oligocene was interpreted as a hiatus, probably due to regional uplift (Chaimov et al., 1990; Yilmaz et al., 1997).

In this study, no rocks were found with a confirmed Oligocene-age. A sample taken from the Ghab Graben was dated as Pliocene from foraminifera (Marcelle BouDagher-Fadel, Chapter 3 and Appendix 1). However, two lines of evidence support the existence of Oligocene-age strata. The first, discussed already (Chapters 2, 3 and 4), is the work of Dzhabur (1985) from the Latakia wells. Very recent results from Silvia Gardin (Chapter 3 and Appendix 1), indicate that Oligocene nannofossils are present within a considerable proportion of the Miocene samples collected during fieldwork, mainly those near to the Jebel An-Nassuriyeh Mountains. Some samples contain more 'Oligo-specific fauna' than fauna of the rock. Oligocene rocks must therefore, have been deposited within the Latakia region and were later eroded and redeposited into younger rocks, much in the same way as Cretaceous and Eocene fauna were extensively reworked (see sedimentary environments; this chapter). The majority of the Miocene-age samples are proximal deposits (see sedimentary processes,

this chapter), so it is unlikely that they were transported a great distance. Silvia Gardin has identified Late Oligocene-age nannofossils, so the timing of a hiatus is limited to the Late Oligocene to Early Aquitanian (the Misis Mountains, in southern Turkey are of similar age; Yilmaz et al., 1997; Robertson, 1998, 2000).

### Geological history

The three megasequences highlight the tectonostratigraphy of the northwest of Syria. Three cycles of subsidence/transgression were followed by uplift and regression (Figures 6.20a, b and c). Chronostratigraphically, the northwest of Syria has the following geological history since the Latest Cretaceous:

**Maastrichtian** – emplacement of the Baer Bassit Ophiolitic Massif. Marine transgression of the whole region to neritic water depth.

**Palaeocene** – carbonate slope deposition; the northwest was under deeper water than the southeast.

**Eocene** – instability in the Middle Eocene, minor folding and slumping, major faulting. *Nummulites* foraminifera thrived in foreshore water-depth to the southeast and were redeposited in deeper shelf-depth water in the northwest.

**Oligocene** – marine deposition in northwest Syria until Late Oligocene? Uplift at a regional hiatus.

**Aquitanian** – marine transgression in the Nahr El-Kabir half-graben (newly forming). Reef-mound deposition on the margins of the graben and chalks in shelf depth water.

**Burdigalian** – active faulting on both the northern and newly formed southern margin of the Nahr El-Kabir Graben. Prograding carbonate sediments from both faulted margins. The linear Nahr El-Kabir Graben was transtensional.



**Langhian** – uplift and active faulting on the southern margin of the Baer Bassit Massif led to catastrophic slope failure (fault influenced) debris flow deposition into the Nahr El-Kabir Graben and bypass of sediments. The Baer Bassit Massif was probably sub-aerial.

**Serravallian** – uplift and normal faulting (with transfer strike-slip faults) of the southern margin of the Nahr El-Kabir Graben led to continuing catastrophic slope failure related deposition on both margins. Alternating, redeposited carbonates with clastic debris flow deposits and turbidites. Faulting ceased in the Late Serravallian, regression commenced. Uplift of the Jebel An-Nassuriyeh Mountains possibly took place? Was this then the initial compressive pulse of Dead Sea Transform faulting further south? Later deposition was restricted solely to the Nahr El-Kabir Graben.

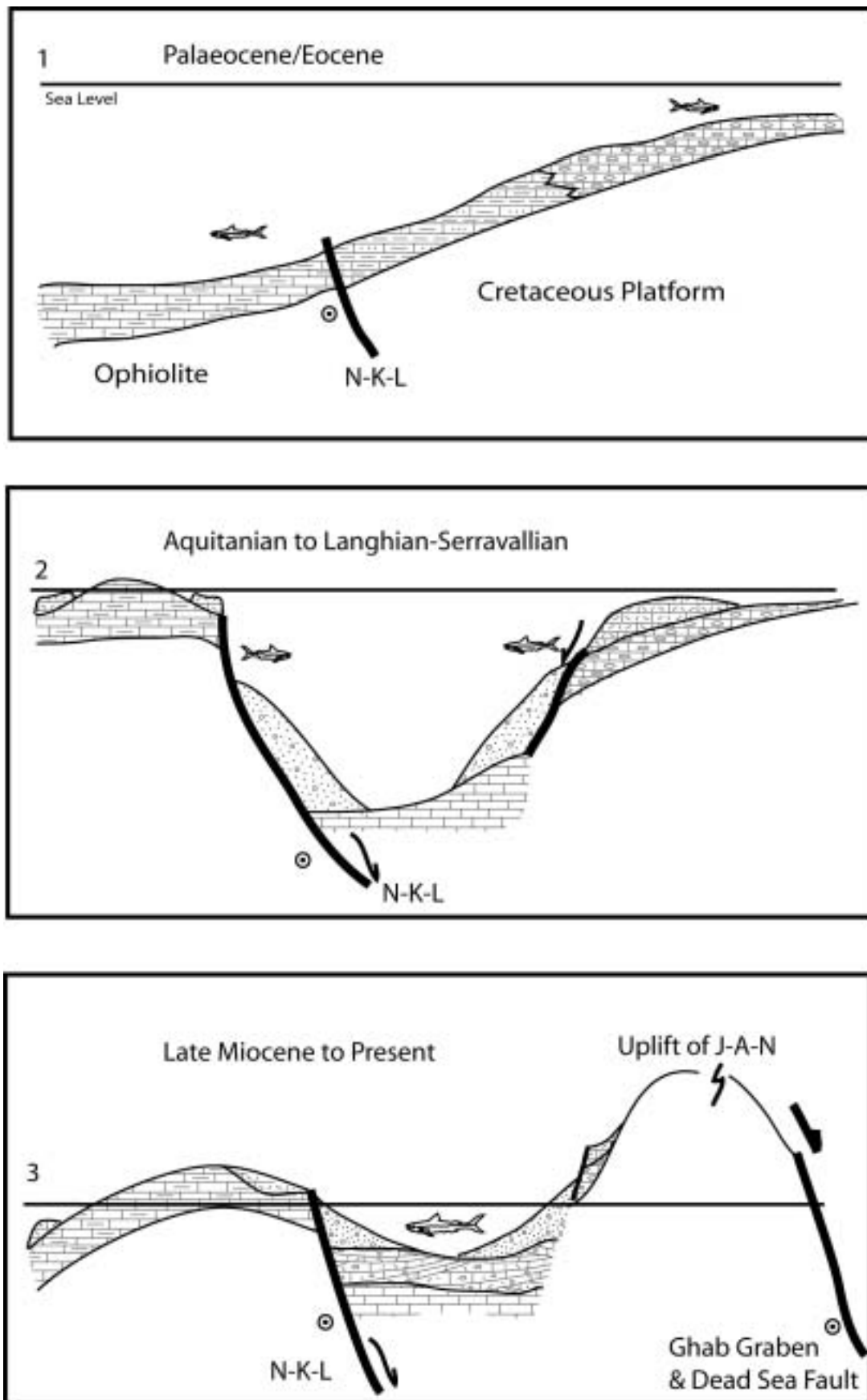
**Tortonian** – continued regression; marine conditions prevailed in the graben axis.

**Messinian** – regional regression. Salinity crisis with gypsum and marl deposition. Minor faulting and debris flow deposits in the Late Messinian.

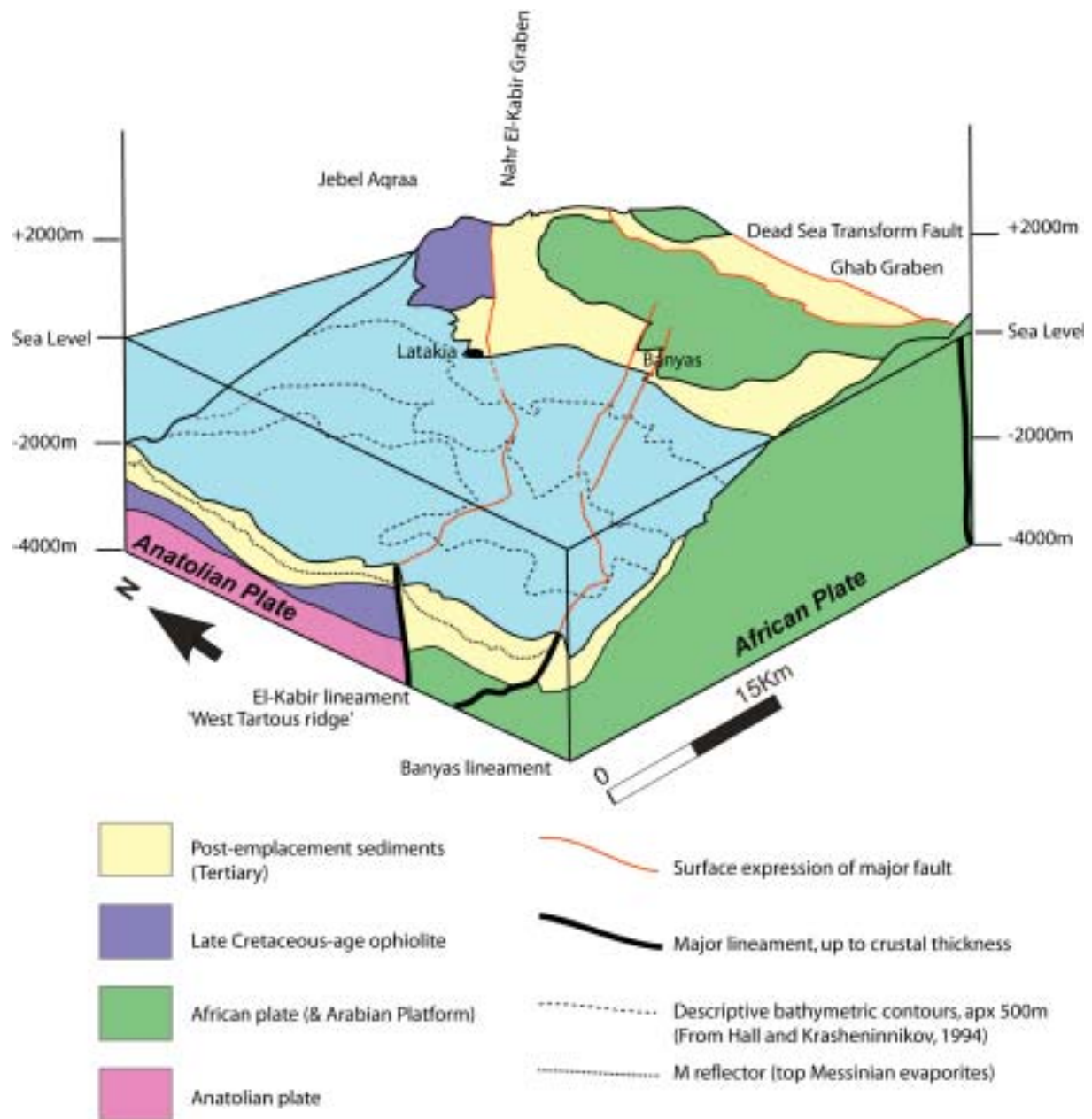
**Pliocene** – marine transgression to outer shelf water depths, followed by regression/uplift to sub-aerial conditions in the Late Pliocene. Active faulting in the Ghab Graben; volcanism and strike-slip faulting in the south near Banyas. Intense fracturing throughout the field area. Fluvial and alluvial deposition.

**Quaternary** - continued sub-aerial uplift. Uplift was greater in the north than the south, due to offset on the El-Kabir Lineament. The lineament was active to the present day and shows sinistral strike-slip movement.

Figures 6.27 & 6.28, summarise the evolution of the Latakia region and the current three dimensional extent of major tectonic features.



**Figure 6.27** Cartoon reconstructions of the formation of the Nahr El-Kabir Graben. Representative of graben perpendicular cross-sections near Khan El-Jouz Village. J-A-N, Jebel An-Nassuriyah Mountains, E-K-L, El-Kabir Lineament. See text for further details. Considerable vertical exaggeration.



**Figure 6.28** Block diagram of the transition between onshore and offshore faulting. The El-Kabir fault follows the prominent ridge (Latakia/West Tartous Ridge).

## ***Tectonic implications***

### *Previous work*

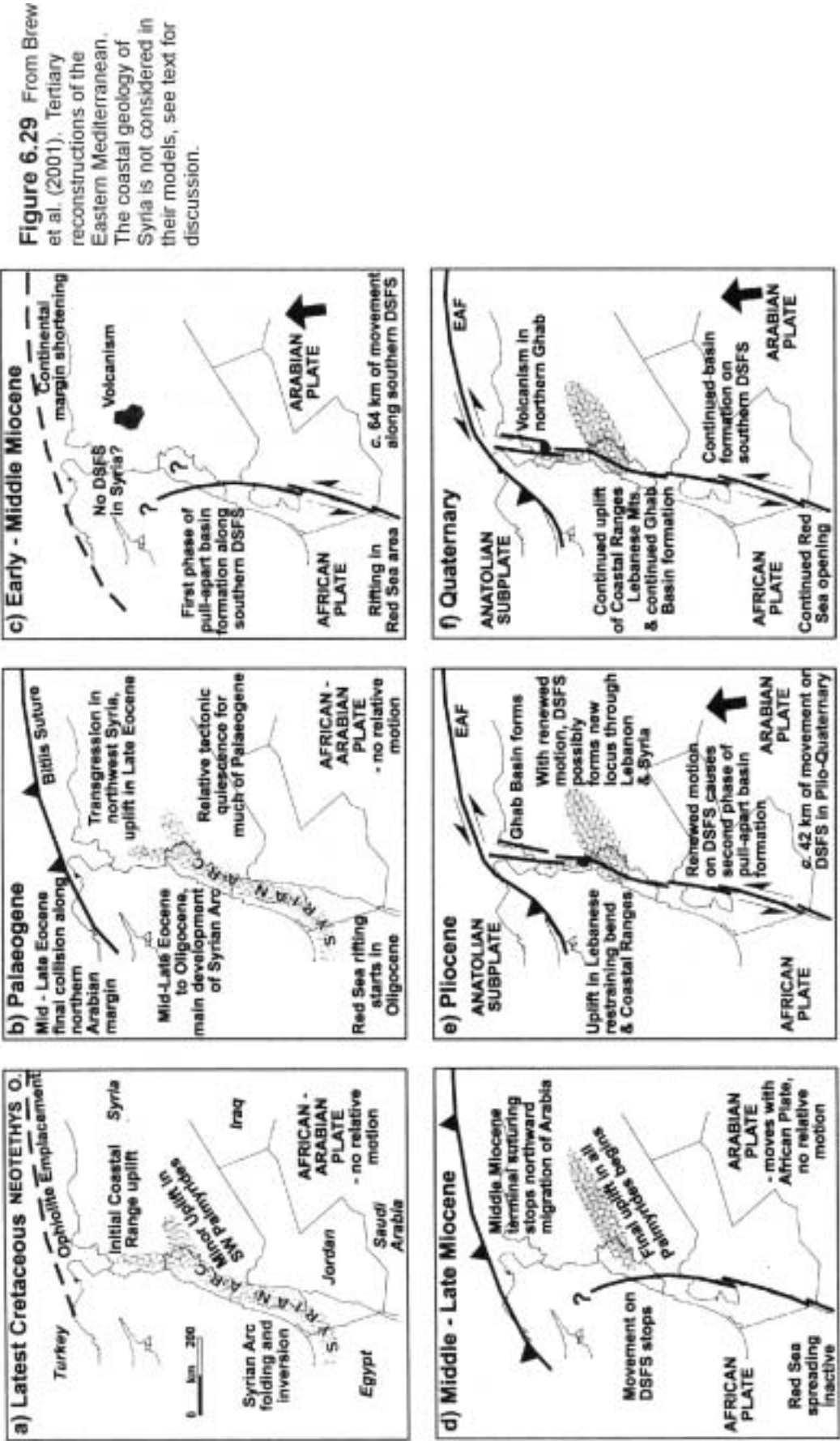
Previous work on the Tertiary tectonic setting of the northwest of Syria is limited. Almost all previous authors concentrated on the Dead Sea Transform Fault (except an introduction to the area by Al-Riyami et al. 2002; see Chapter 1 and tectonic evolution of Latakia, below).

The three most recent authors to have worked in or close to northern Syria and their implied geological settings were:

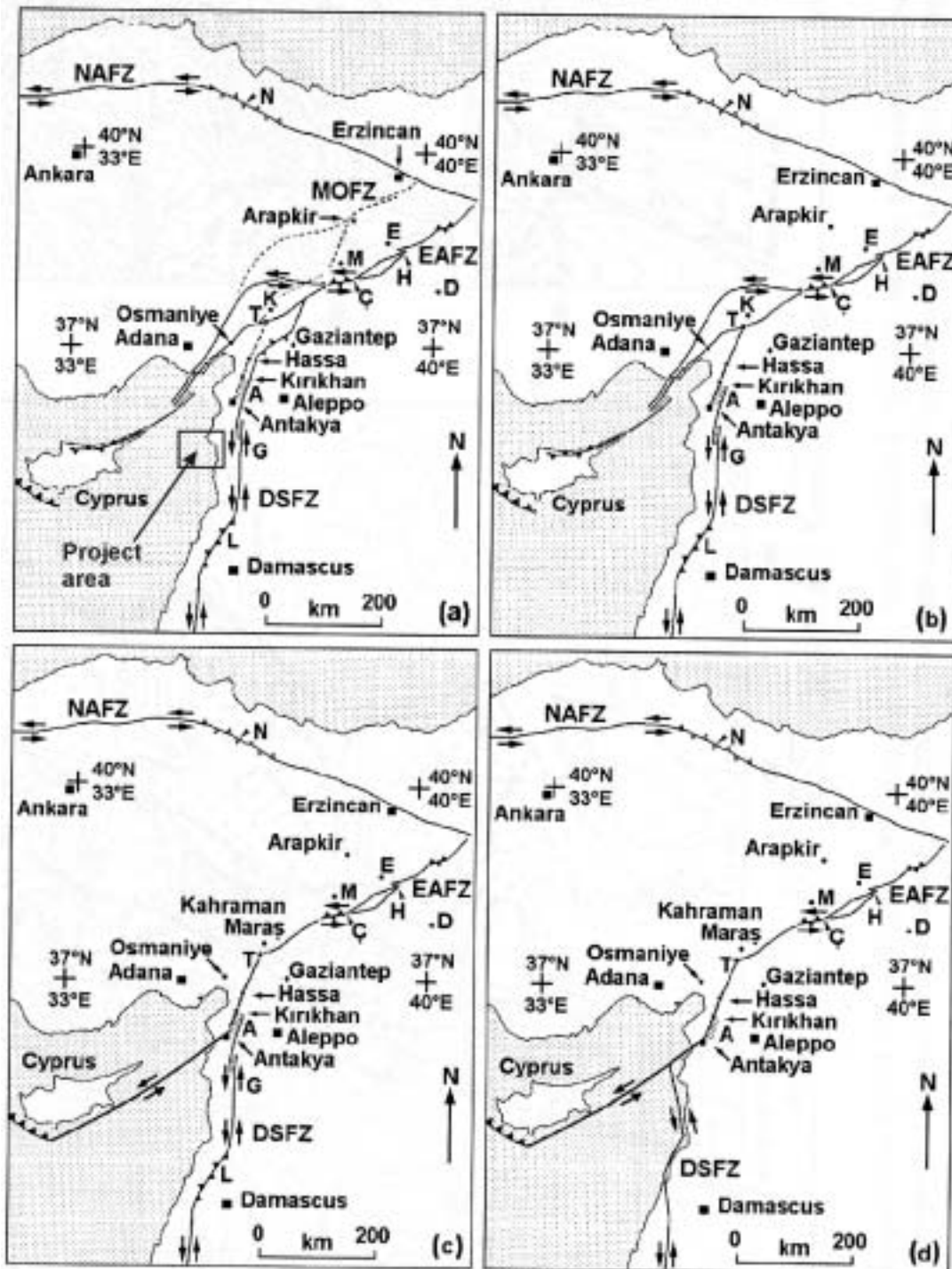
1. Brew et al. (2001) published reconstructions of the Tertiary of the Eastern Mediterranean, with regard to the structuration of the Ghab Graben and Dead Sea Fault System (Figure 6.29). Their reconstructions do not include the geology of the Latakia region. They infer the earliest motions of the Dead Sea Fault System in the Early to Middle Tertiary, with a lineament trending northwest towards Cyprus, from Lebanon (following the ideas of Butler et al. 1997; Walley 1998). This faulting was implied to have continued until the Late Miocene. In the Plio-Quaternary, the Ghab Graben formed and the Dead Sea Fault coalesced with the East Anatolian Fault in southern Turkey. The plate boundary between the Anatolian and African plates was not discussed.
2. The tectonic reconstructions presented by Yurtman et al. (2002), (Figure 6.30), demonstrates the present-day regional kinematic setting inferred by numerous authors from work in southern Turkey. The geology of this project area is not included. The plate boundary is inferred to extend from (or even across) Cyprus to Iskenderun Bay and/or the Misis Lineament.
3. Mascle et al. (2000) hypothesised a modern 'Sinai-sub-plate', linking Sinai, the Florence Rise and the Dead Sea Transform Fault in northern Syria or Southern Turkey (Figure 6.31). This work agrees that the southern Cyprus to Dead Sea Transform connection does exist near the El-Kabir Lineament (see below).

### ***The Tertiary tectonic evolution of the Latakia area, especially the Nahr El-Kabir Lineament***

Guiraud et al. (1997), suggested a chronostratigraphy of Cretaceous and Tertiary events in Africa-Arabia (Figure 6.32). Their figures show two regional stages of inversion; during the late Maastrichtian and the Late Eocene, principally at times of change in plate motion. The two stages of inversion are similar to those seen within the project area. Rifting is noted to

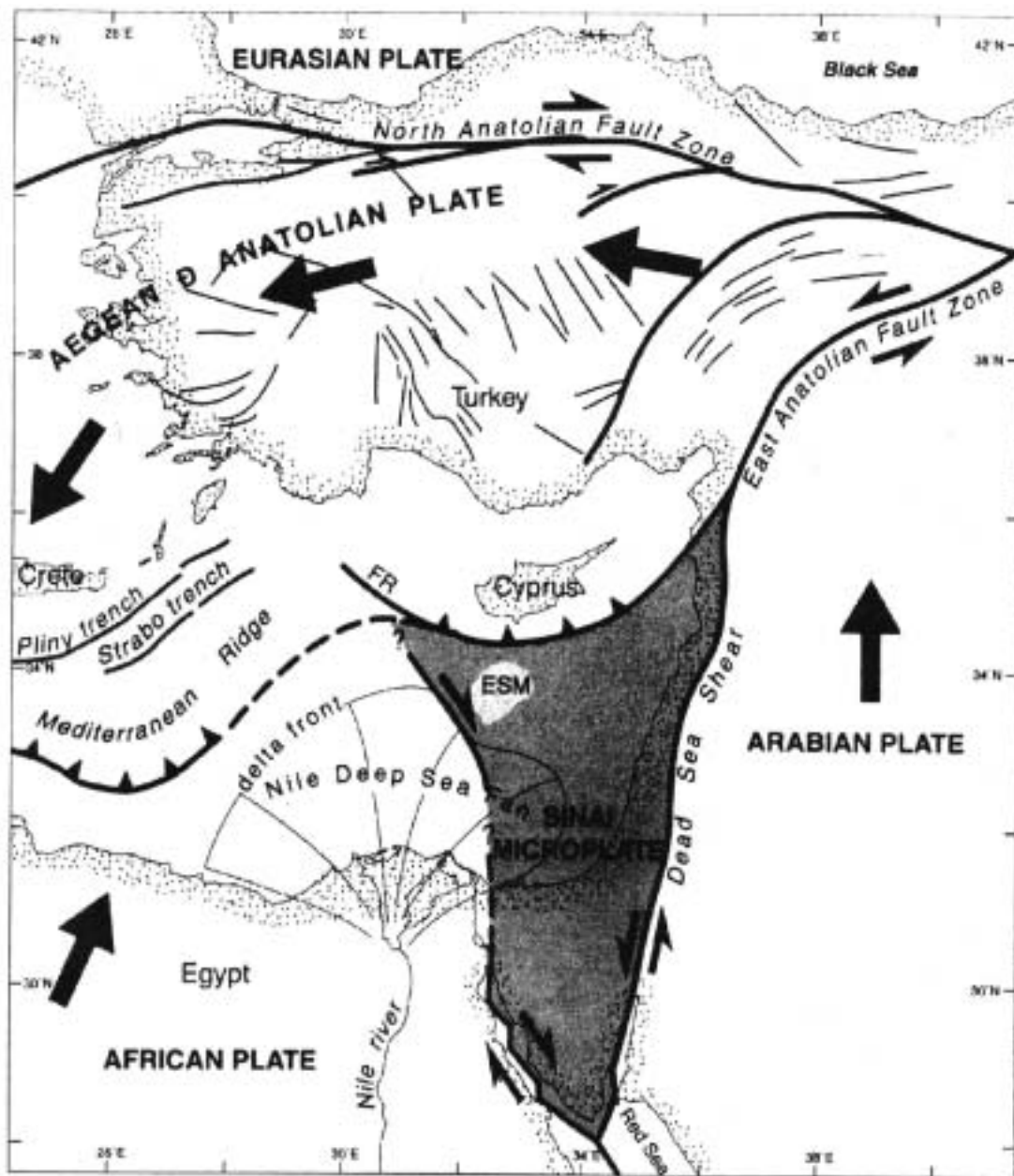


**Figure 6.29** From Brew et al. (2001). Tertiary reconstructions of the Eastern Mediterranean. The coastal geology of Syria is not considered in their models, see text for discussion.



**Figure 6.30.** From Yurtmen et al. (2002). Regional kinematic interpretations from work in southern Turkey. A - Westaway & Arder (1996), B - Karig & Kozlu (1990), C - Yurur & Chorowicz (1998) and D - Girdler (1990); Butler et al., (1997). The geology of northwest Syria is absent in these reconstructions (project area marked), see text for details.





**Figure 6.31** From Mascle et al. (2000). The Levantine-Sinai sub-plate hypothesis. Notice the northeastern margin of the plate is inferred to be close to the project area. ESM - Eratosthenes Seamount, FR - Florence Rise.



occur during the Miocene, at a time when plate motion (Figure 6.33) changed from northwest, reverting to the prominent northeasterly direction of closure. Therefore, the following section puts forward ideas for the tectonics of the project region.

Robertson (1994), summarised basin formation settings, with regard to the tectonics, especially of the Mediterranean region (Figure 6.34 & 6.35). The criteria for 'Post collisional extensional basins' or 'strike-slip basins (in collisional settings)', would at first appear to be the closest ideas to the setting observed in northwestern Syria. However, neither matches exactly the geology observed in the Nahr El-Kabir Graben. This is perhaps due to the early stage of collision inferred within this work. The setting is on the promontory of the African Plate and a major lineament (El-Kabir Lineament) is the most distinct feature, rather than a zone of uplift (the Kyrenia-Misis overthrust belt from the orogenic front, Yilmaz et al. 1997).

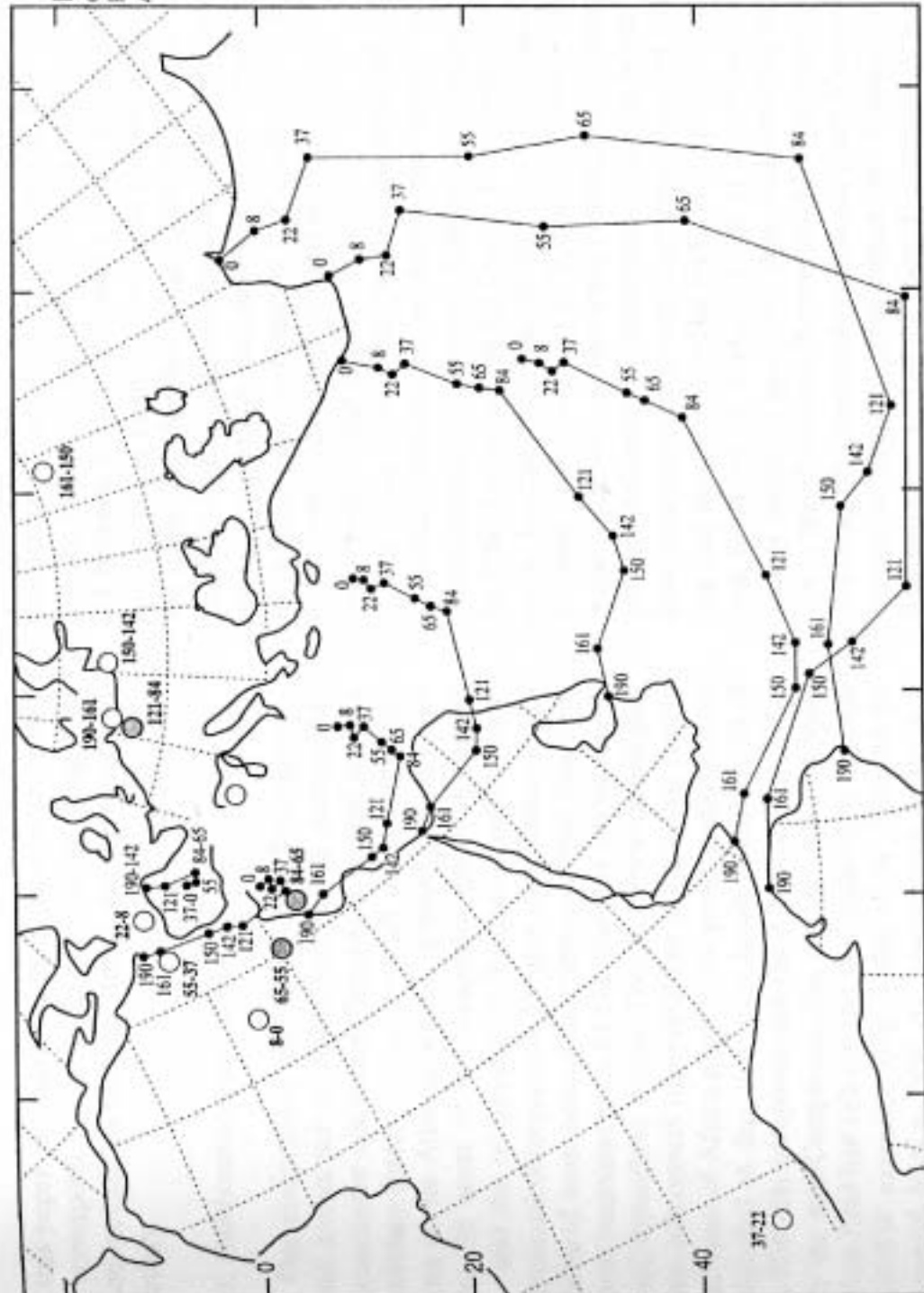
### Inherited structure?

Early studies by Ponikarov et al. (1966 & 1967), did not recognise the processes involved in emplacement of ophiolites (see Chapters 1, 2, 3 & 4). The main lineament mapped in the region was inferred as quiescent and only to relate to the ophiolite. The Baer Bassit Ophiolite was emplaced but probably by a series of thrust faults as it is very broken. Thrusts young to the north, as demonstrated by the uplift of Jebel Aqraa on the Syrian-Turkish border. As such, the mapped 'Lattakia-Killis' fault of Ponikarov et al. (1963, 1966 & 1967), probably marks the inferred arc of ophiolitic thrust material, part of the 'peri-arabic crescent' (Ricou, 1971). This might explain their connection to the town of Killis in Turkey and the Kurd Dagh Ophiolite.

Figure 6.9, suggests the Late Triassic to Cretaceous setting of the northern Arabian Platform (Al-Riyami et al. 2001), prior to emplacement. Extensional faulting is implied from their work and that of Delaune Meyère (1984), although cannot be seen in the field. The El-Kabir Lineament studied in this work, is sited at the southern edge of a thin wedge of ophiolitic material which Al-Riyami et al. (2001) interpreted as a 'feather edge'. Did the ophiolite stop at this margin as one of the extensional faults reactivated?

Chaimov et al. (1990) and Robertson (1998) respectively infer that Syrian-Arc structures in the Palmyrides (central Syria) and Israel, did extensively reactivate older faults to accommodate compression. The timings of these events are synchronous to the Latakia region.

**Figure 6.33** From Guiraud et al. (1997).  
Relative motion history of  
Africa and Arabia.



Convergent margin settings, with examples from the Eastern Mediterranean Tethys

Tectonic facies	Characteristics	Examples
Supra-subduction zone ophiolite	Complete ophiolite, with harzburgitic depleted mantle, sheeted dykes and IAT-type/boninitic extrusives; locally includes acidic calcalkaline extrusives and volcanics.	Eastern-type ophiolites, Albania; Pindos and Vourinos ophiolites, Greece; Troodos ophiolite, Cyprus; Hatay, Biser-Bassit and Guleman ophiolites, south and southeastern Turkey.
Oceanic arc	Thick piles of basalts and basaltic andesites; subordinate more fractionated extrusives and volcanics; tuffaceous, where shallow-water and/or subaerial.	Palaeotethyan Çangalıdağ, Central Pontides, northern Turkey; Neotethyan units in central and southeastern Turkey (not well documented).
Subduction/accretion complex	Thick units of structurally repeated deep-sea sediments, often with slivers of scraped-off oceanic crust; successions ideally thicken and coarsen-upwards in individual thrust slices and show downward younging in age of accreted units; many structural complications; often melange units are present.	Palaeotethyan Karakaya Complex, western and central Turkey; Neotethyan Pindos–Olympos nappes, western Greece; Avdella Melange, northwestern Greece; Ermioni Complex, south-eastern Greece; Cetmi and Ankara melanges, northwestern and central Turkey.
Fore-arc basin	Structurally overlies subduction/accretion units, comprises thick, variable sequences of moderately deep- to shallow-marine or sub-aerial deposits including carbonates, siliciclastics and/or volcanics; often relatively structurally intact, with only low-grade metamorphism	Neotethyan Kastamonu–Baybat basin, Central Pontides; Tüz–Golü basin, central Turkey (in part); Bilecik Lst. and underlying clastics, north-western Turkey.
Back-arc basin (intra-continental)	MORB- and/or IAT-type ophiolite overlain by terrigenous and/or volcanogenic sediment shed from both active arc and continental basement; locally siliceous and/or organic-rich sediments.	Palaeotethyan Kire Complex, Central Pontides; modern Black Sea basins.
Back-arc basin (intra-oceanic)	MOR- and/or IAT-type ophiolite, overlain by mainly volcanogenic sediments, including tuffs. Little or no coarse clastic sediment input; volcanoclastic turbidites and debris flows in areas proximal to active arcs.	Not specifically recognised, but may include some ophiolite-related units in Neotethys of southeastern Turkey.

**Figure 6.34.** From Robertson (1994). Criteria of convergence-related settings.

Strike-slip related tectonic settings, with examples from the Eastern Mediterranean Tethys		
Tectonic facies	Characteristics	Examples
Transform rifts and passive margins	Passive margin bordered by subsiding basin, with outer ridge composed of sediments and/or continental basement blocks; structural evidence of shear, especially near continent-ocean boundary; reduced subsidence and relaxation relative to "normal" margins.	Late Palaeocene-Early Miocene (non orophylous) rifted Levant, western margin of Mesopotamia; Early Tertiary (orophylous) rifted Levant, eastern margin of Mesopotamia; more local margin rifts, including Suez-Pot, Albania.
Oceanic transform basins	Ophiolites (or by major fault zones) showing pervasive strike-slip, fragmentation of ophiolite crust; local initiation, fault-controlled sedimentary basins with intercalations of extrusives and coarse tuffs; ophiolite where submarine exposure of ultramafics.	South Troodos Transform Fault Zone, Cyprus and Tektonik Zone, southwestern Turkey (both intra subduction zone ophiolites); no well documented examples within MOR-type ophiolite in E. Mediterranean region.
Oceanic crust in pull-apart basins	MORB-type ophiolite overlain by relatively proximal terrigenous sediments; possible evidence of strike-slip within ophiolites; bordering margins may show thermal extension-phen related to extension/spreading.	Neotethyan Gopiad ophiolite, and related ophiolitic units, e.g. Meglenia ophiolite, Vardar Zone, northeastern Greece.
Convergence-related (pre-collisional)	Sedimentary basins in forearc/backarc locations that were influenced by oblique subduction and/or strike-slip. Hard to recognise as tectonic basins.	Palaioethyas marginal basins (e.g. Kırşehir, Söğütözü) forearc basins (e.g. Kastamonu-Bayındır, Central Pontides and Hozat), southwestern Turkey; modern eastern Hellenic active margin, Cyprus active margin between Cyprus and Antalya.
Strike-slip and rotation (pre-collisional)	Complex and variable settings marked by compression, strike-slip and/or tectonic rotation (about vertical axis); also transextensional pull-apart basins related to oblique collision.	Southeastern segment of the Antalya Complex, southwestern Turkey; Palaeotethyan of the Troodos microplate and related deformation of the Marmara Complex and Kyzas Range, Cyprus; and Tertiary Late "pull-apart" basin, southeastern Turkey.
Strike-slip and rotation (post-collisional)	Regions of pervasive strike-slip and distributed shear, including zones of compression, transpression, localised volcanism and deep-level (granitic) intrusion; block rotations; localised mélange gneiss; strike-slip pull-apart basins.	Neotethyan evolution of Vardar Zone, Greece; Macedonia and Serbia; Tertiary escape of Anatolia westwards, with compression, localised uplift, block rotation and pull-apart basin development.

Figure 6.35. From Robertson (1994). Criteria of strike-slip and collision-related settings in the Eastern Mediterranean.



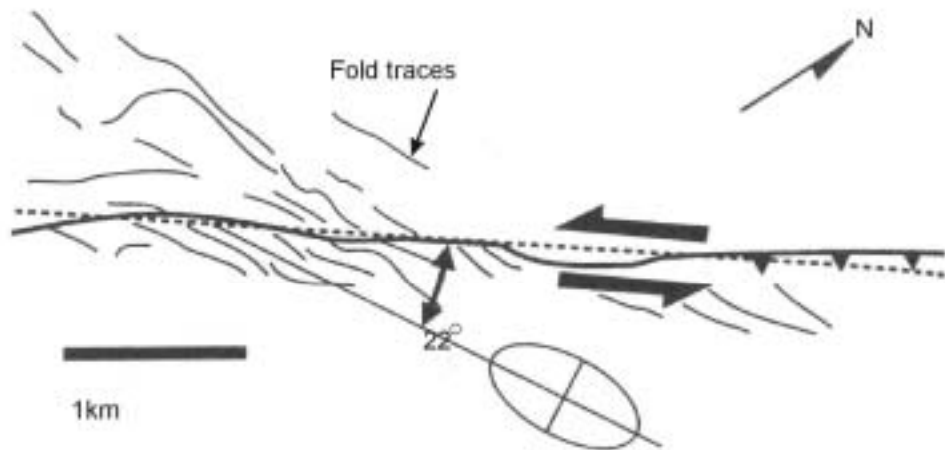
Tertiary movements on the El-Kabir Lineament indicate that in the Nahr El-Kabir region a linear feature existed, it was not just the edge of the ophiolite. It is proposed in this work that the El-Kabir Lineament could be a re-activated lineament from the break-up of Pangea (rifted margin, Delaune-Meyère, 1984). This study cannot support this idea with field evidence but has two lines of anecdotal evidence for this hypothesis. The first is the depth of faulting observed on seismic data (almost through the crust, Chapter 4), the second the depth of a recent on-trend earthquake (22km, Chapter 4). Robertson (1998) and Vidal et al. (2000 A & B) infer that the crust beneath the adjoining Levant Basin is stretched continental crust. Whereas, to the north of the Latakia City latitude in the Mediterranean it is presumed to be oceanic (Makris, 1984).

Large strike-slip faults (commonly transform faults) are often the associated with graben formation by 'pull-apart' (i.e. Ghab Graben, Quennell, 1956; Garfunkel, 1981; Hempton, 1987; Walley, 1998; Matar et al. 1993; Brew 2001). These basins are characterised by both graben bounding faults being active and rapid subsidence. The Nahr El-Kabir Graben does not share these characteristics. Woodcock et al. (1994) summarises the major classes of strike-slip faults at plate tectonic scales (Figure 6.35) none of which are immediately applicable to the project region. Large strike-slip faults in the Mediterranean region (i.e. Eçmiş Fault, Jaffey et al. 2001), show extensive slip (approximately 80km), and tectonic escape. Sengor et al. (1985) implies that strike-slip zones in the Mediterranean can have a wide range of scales, from minor (perhaps the El-Kabir Lineament) to 10's km (i.e. Eçmiş and North Anatolian Faults).

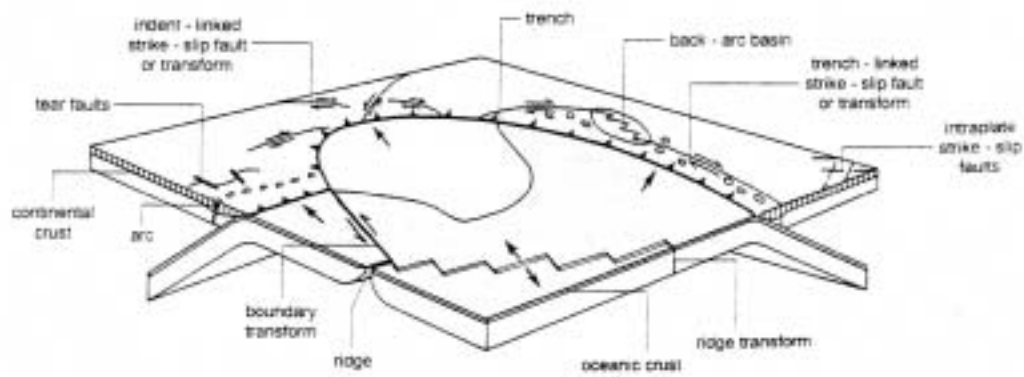
The northern margin of the graben, the El-Kabir Lineament, was evidently active from Maastrichtian to the Recent times. No such faulting was observed on the southern margin, at Banyas Town or along the southern margin of the graben. At these localities either the faulting is Plio-Quaternary or Miocene.

Is the El-Kabir Lineament also the plate boundary fault between the African and Anatolian Plates?

Ivanov et al. (1992); Kempler (1994); Krashenninnikov (1994); Ben-Avraham et al. (1995); Vidal et al. (2000A&B) and Al-Riyami et al. (2001) have all inferred the connection between the south of Cyprus subduction to the African-Anatolian Plate boundary. None of the above authors presented factual evidence to prove this point. This project has demonstrated through extended fieldwork and onshore-offshore correlation that the El-Kabir



Modified from Krantz (1995), (reversed for sinistral motion). Transpressional strain modelling. Surface fold traces at Eagle Canyon Fault, Mecca Hills, southern California.



**Figure 6.35** From Woodcock et al. (1994). Tectonic settings and major classes of strike-slip faults.

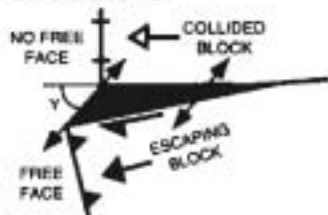
A. PULL-APART BASIN RESULTING FROM STEPOVER FAULT GEOMETRY



B. BASIN RESULTING FROM TRANSFORM-NORMAL EXTENSION



C. BASIN RESULTING FROM TECTONIC ESCAPE



From Mann 1997. Models of Pull-apart basin formation (poor original).

Lineament does connect to the Latakia Ridge offshore and to the Dead Sea Transform onshore (Chapter 4), thus, forming the plate boundary in this region.

### ***Comparison to regional geology of the Eastern Mediterranean***

Krasheninnikov's map (Krasheninnikov, 1971) of Neogene deposition in the Eastern Mediterranean (Figure 6.36), highlights the extent of small marine basins during this period, in Cyprus, Turkey and Syria. Chapter 5 has discussed features of similar age basins within the Eastern Mediterranean (Polis, Hatay and Adana basins).

The northwest of Syria shares many similarities with other parts of the Eastern Mediterranean region, especially with regard to the timing of large tectonic events (i.e. uplift). It also has striking differences in sedimentology and structure to similar-age basins in the region (i.e. Hatay Graben). Although these two grabens are essentially the same age, there are important differences in basin setting. The Polis Graben is in a 'supra-subduction zone', the Adana basin is dissected by the Eċ̇nis Fault and the Hatay Graben is situated between two ophiolitic provinces, the plate margin (Latakia Ridge – El-Kabir Lineament) and the orogenic front (Kyrenia-Misis)(Figure 6.37).

The essential feature of the Nahr El-Kabir Graben and El-Kabir Fault is that they formed a continuously reactivated lineament throughout the Tertiary.

### ***Diachronous collision?***

This work has shown that extension and strike-slip faulting have occurred throughout the Tertiary in northwest Syria. Pulses of uplift have occurred, but most of the geological record reflects deposition in a linear, reactivated fault controlled zone.

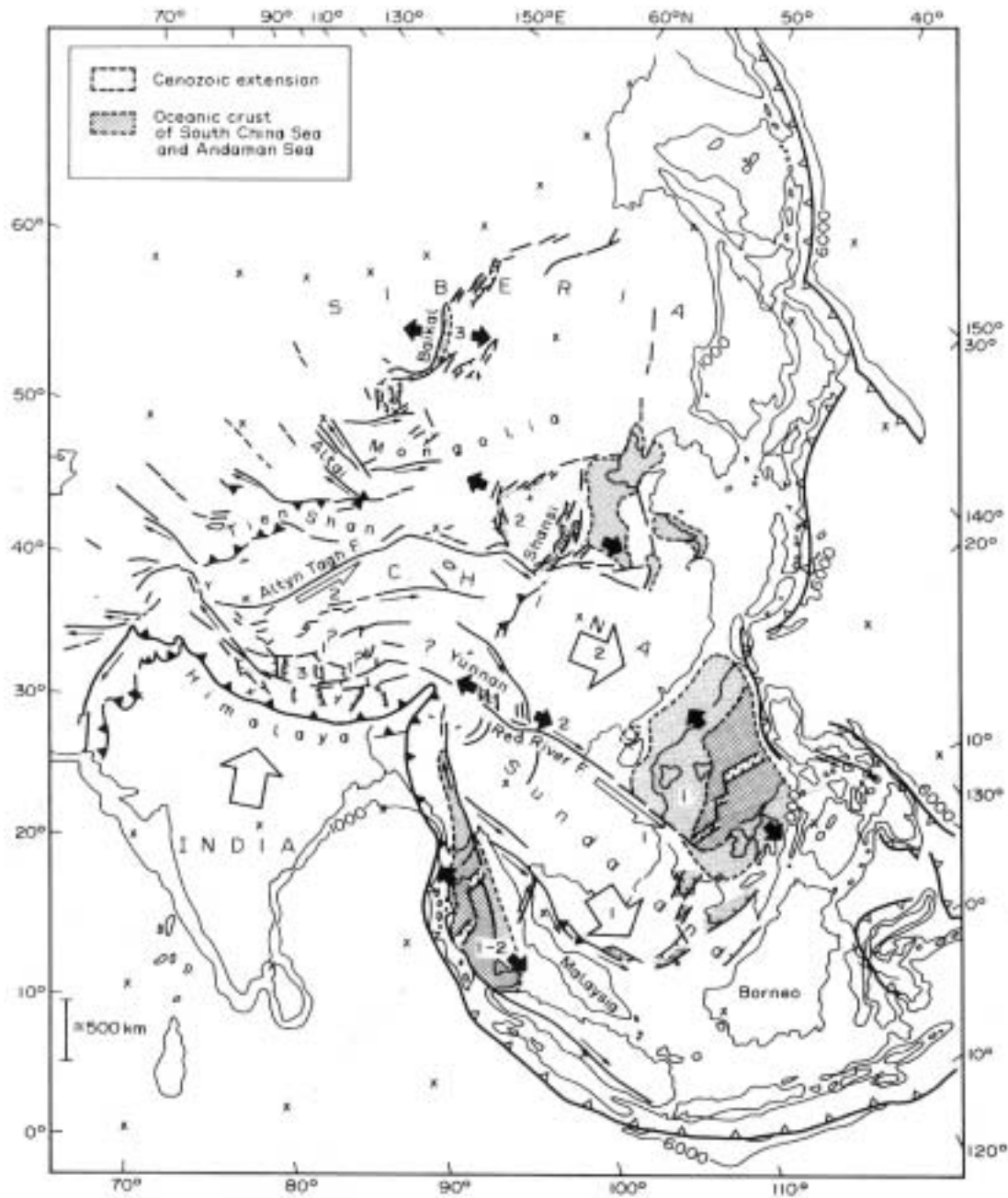
This region reflects the initial stages of continental collision. If regions with much greater collisional effects are examined then similar strike-slip features can be observed at the margins of the collision zone (i.e. Himalayas, Coward, 1994)(Figure 6.38).

Holdsworth et al. (1997) states that "old structures form long-lived zones of weakness that tend to repeatedly accommodate successive crustal strains, often in preference to the formation of new zone of weakness".

Collision mechanisms have evolved throughout the Tertiary of northwest Syria, but basement weaknesses seem to have exerted the strongest influence on surface geology.

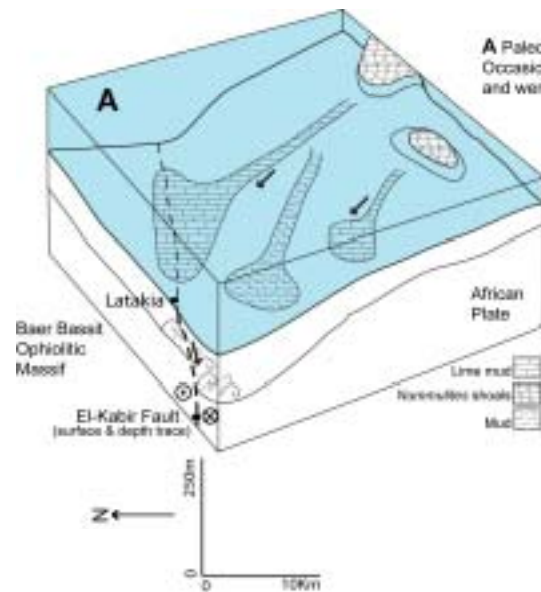


**Figure 6.37** From Robertson et al. (1995). Reconstructions of the Mediterranean, from Aquitanian to Recent. Plate promontories and embayments are detailed.



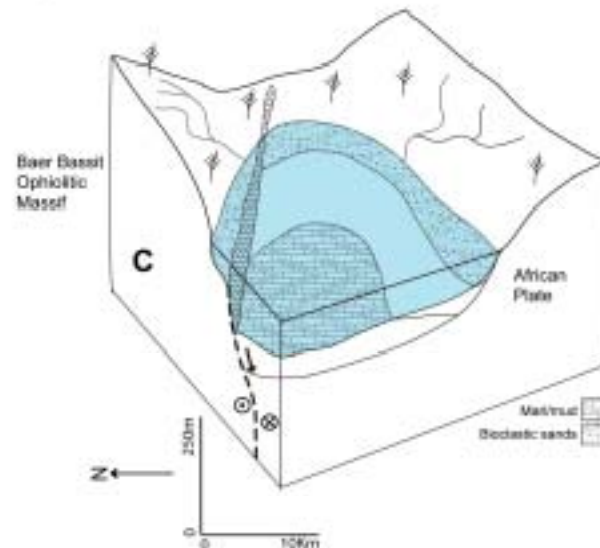
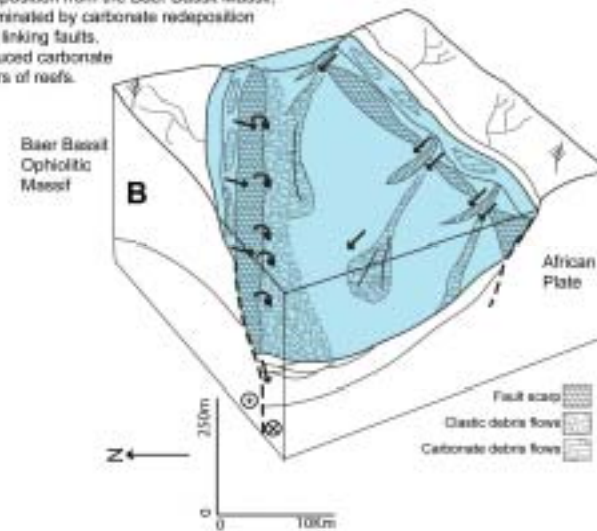
**Figure 6.38** From Coward (1994) after Tapponier. Map of SE Asia and the Himalayas, showing Tertiary extrusion of terranes and large faults, due to the continental collision of the Indian Plate.





**A** Paleogene setting. Shallow neritic conditions on an open shelf. Occasional shoals of *Mammillites* were sub-aerial during the Eocene and were often redeposited by mass flow to deeper water settings.

**B** Fault controlled setting during the Langhian-Serravalian. The El-Kabir fault controlled clastic deposition from the Baer Basalt Massif, whereas the southern margin was dominated by carbonate redeposition from minor extensional and strike-slip linking faults. Narrow regions of shallow water produced carbonate material. There are no direct indicators of reefs.



**C** Pliocene setting (similar to pre-Messinian). A neritic marine setting constrained to the Nahr El-Kabir Valley. The carbonate facies were controlled by depth (ponded) rather than by redeposition due to structuration. Uplift progressed rapidly at this time due to movement of the Dead Sea Transform Fault immediately to the east, but fault activity was probably limited in this region.

**Figure 6.1B** Sediment and facies settings inferred within this work, from the Nahr El-Kabir Valley from combining structural (Chapter 4) and sedimentological (Chapter 3) evidence. Analogues from the literature are presented throughout this chapter. The paleogeographies interpreted within this work are explained in more detail within **Figures 6.20A-E**.

## Conclusions

Numerous conclusions have resulted from this study of the northwest of Syria, mainly from the fieldwork presented within this thesis. The following is a summary of the essential factual and interpretive points. The Nahr El-Kabir region also has implications for the tectonic evolution of the Eastern Mediterranean and this is also summarised.

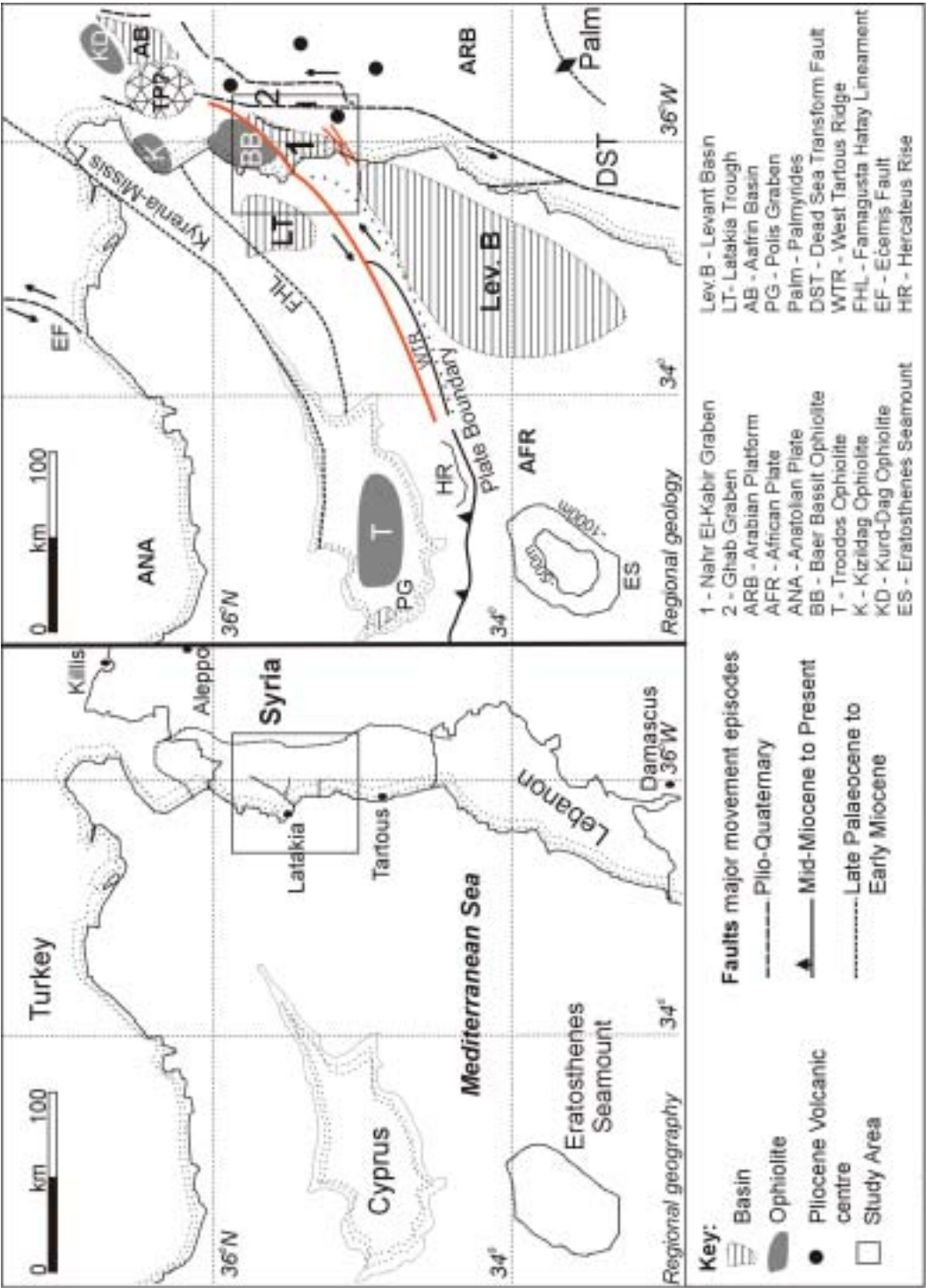
Much work has been carried out to update the sedimentology of the region, by inferring sedimentary environments and processes in the rock-record and by re-mapping key elements of the region (with the aid of remote sensing data). This has led to the following main conclusions:

- ≠ The Nahr El-Kabir region represents the northernmost extent of the African-Arabian Platform in the Eastern Mediterranean. It is a region in the early stages of continental collision. It is bordered to the east by the Dead Sea Transform Fault, dividing the African and Arabian Plates.
- ≠ The El-Kabir Lineament is a strike-slip fault (a transcurrent fault, probable transform fault). Evidence of fault activity has been demonstrated in the Paleogene, Neogene, Pliocene-Quaternary and Recent.
- ≠ The Recent El-Kabir Lineament movement is considered to be sinistral and it is seismically and geomorphologically active.
- ≠ The El-Kabir Lineament joins the Latakia Ridge offshore at the northern margin of the Levant Basin (i.e. it is the onshore continuation) and is inferred to coalesce with the Dead Sea Transform Fault. Therefore, it is suggested to delineate the Anatolian/African Plate boundary in the Eastern Mediterranean.
- ≠ The NW Syria basin Tertiary sediments record initial carbonate passive margin subsidence and then slow uplift, following Maastrichtian ophiolite obduction. The El-Kabir graben formed, then subsided and uplifted twice during the Late Tertiary. It is a spatially restricted, asymmetrical graben, characterised by mixed clastic-carbonate sediments. Transtensional graben extension and subsidence was followed by regional uplift.
- ≠ Three megasequences of deposition developed during the Maastrichtian-Paleogene, Miocene and Pliocene. Uplift has been continuous since the Late Pliocene.

- € The well-known regional hiatus giving rise to an unconformity between Late Middle Eocene to Aquitanian-age strata can now be confined to the Late Oligocene – Early Aquitanian, through examination of key samples during this work. Sylvia Gardin (Paris) examined the nannofossils and has shown that Oligocene age fauna are present in the majority of Miocene-age rocks.
- € The present-day Nahr El-Kabir Valley delineates the Miocene-age Nahr El-Kabir Graben. This graben existed as a half-graben during the Early and Late Miocene, developing as a graben (with minor extension on the southern margin) during Burdigalian to Serravallian time.
- € The Nahr El-Kabir Lineament and the Dead Sea Transform faults have an intricate Late Tertiary interaction. Regional uplift and folding of the Jebel An-Nassuriyeh Mountain range (previously unaccountable amounts of uplift; i.e. Brew et al. (2001), was due to motions on both of these faults. This uplift is recognised as a possible mechanism for relieving compressional stress generated by incipient tectonic escape as the African, Anatolian and Arabian plates shorten.
- € The potential for block escape in this region is inferred, due to the strike-slip nature of faulting.
- € Diachronism during collision? Yes, over the entire region as the tectonic settings have changed constantly and the system is unstable (see below). However within the project area this is not demonstrated

### ***Diachronism and tectonics***

The original title of this thesis inferred diachronous collision; changing tectonic and depositional settings during continental collision. This thesis has demonstrated that these changes are not seen as diachronous within such a small area, but would be with regard to the setting of the western margin of the African promontory during collision. From initial oblique collision to progressive continental collision, tectonic settings have been demonstrated to be far removed from the continuous uplift and shortening expected in a simple collision zone. Collision was instead highly episodic. Extension occurred, leading to graben formation and this is more prominent at the present day than uplift. Strike-slip is the primary fault mechanism and reactivation of basement weaknesses is likely. The tectonic and sedimentary settings are shown to have been very dynamic (Figure 7.1).



**Figure 7.1** Location map of the northeastern Mediterranean Sea, showing the project area and interpreted tectonic features (Benarharham et al., 1995; Robertson, 1998; Vidal et al., 2000; this study)

### ***Wider applicability of results***

Worldwide, this study is applicable to the study of other regions of continental collision. The plate collision of India with Eurasia has progressed to full continental collision (the Himalayas). Workers on the earliest stages of that collision should find interest in the ideas put forward here, as full-collision settings have largely destroyed earlier evidence. Indeed the study of early continental-collision is restricted to a few examples in the current world, simply because these settings are transient. The large strike-slip provinces to the east of the main collision (i.e. Red River Fault area, see Figure 6.38), may be related to structures that formed at the onset of collision.

Indonesia, Taiwan and Northern Australia are also currently undergoing early collision (arc passive), as small continental blocks are colliding; active strike-slip faulting is the dominate fault mechanism and affects millions of people. The western USA is undergoing oceanic to continental oblique collision, leading to large, transform faults and transtensional graben formation (i.e. Death Valley).

Closer to home, the Mediterranean is continually closing. The Anatolia region to the east, and the Pelagian shelf region and Libyan promontory in the central Mediterranean (Grasso, 1995; Argnani, 2001), may be undergoing the earliest stages of continent-continent collision and are characterised by linear grabens.

## Reference list

- AKSU, A.E., CALON, T.J., PIPER, D.J.W., TURGUT, S. & IZDAR, E. 1992. Architecture of late orogenic Quaternary basins in northeastern Mediterranean Sea. *Tectonophysics*, **V210**, pp. 191-213.
- AL-RIYAMI, K. 2000. *Mesozoic-Tertiary sedimentary and tectonic evolution of the South-Tethyan continental margin and Late Cretaceous ophiolite in Baer-Bassit Region (NW Syria)*. PhD Thesis, Edinburgh University.
- AL-RIYAMI, K., ROBERTSON, A.H.F., XENOPHONTOS, C., DANELIAN, T. & DIXON, J.E. 2000. Tectonic evolution of the Mesozoic Arabian passive continental margin and related ophiolite in Baer-Bassit region (NW Syria). In: PANAYIDES, I., XENOPHONTOS, C., & MALPAS, J. (Eds). *Proceedings of the third international conference on the geology of the Eastern Mediterranean*. pp 61-81.
- AL-RIYAMI, K., ROBERTSON, A., DIXON, J. & XENOPHONTOS, C. 2002. Origin and emplacement of the Late Cretaceous Baer-Bassit ophiolite and its metamorphic sole in NW Syria. *Lithos*, **V65**, pp. 225-260.
- AL-RIYAMI, K. & ROBERTSON, A. 2002. Mesozoic sedimentary and magmatic evolution of the Arabian continental margin, northern Syria: evidence from the Baer-Bassit Melange. *Geol. Mag.*, **V139** (4), pp.395-420.
- ALSDORF, D., BARAZANGI, M., LITAK, R., SEBER, D., SAWAF, T. & AL-SAAD, D. 1995. The intraplate Euphrates fault system-Palmyrides mountain belt junction and relationship to Arabian plate boundary tectonics. *Annali Di Geofisica*, **V38**, N3-4, pp. 385-397.
- ARGNANI, A. & TORELLI, L. 2001. The Pelagian Shelf and its graben system (Italy/Tunisia). In: ZIEGLER, P. A., CAVAZZA, W., ROBERTSON, A. H. F. & CRASQUIN-SOLEAU. 2001. *Peri-Tethys Memoir 6, Peri-Tethyan rift/wrench basins and passive margins*. Mémoires de Muséum National D'Histoire Naturelle, Tome 186, p529-544.
- BANNER, F.T., LORD, A.R. & BOUDAGHER-FADEL. 1999. The Terra Limestone Member (Miocene) of western Cyprus. *Greifswalder Geowissenschaftliche Beitrage*, **V6**, pp. 489-501.
- BENAVRAHAM, Z., TIBOR, G., LINONOV, A.F., LEYBOV, M.B., IVANOV, M.K., TOKAREV, M.Y. & WOODSIDE, J.M. 1995. Structure and tectonics of the eastern Cyprean arc. *Marine and Petroleum Geology*, **V12**, N3, pp. 263-271.
- BouDAGHER-FADEL, M.K. & BANNER, F.T. 1999. Revision of the stratigraphic significance of the Oligocene-Miocene "Letter-Stages". *Revue de Micropaleontologie*, **V42**, N2, pp. 93-97.
- BouDAGHER-FADEL, M.K., BANNER, F.T., GORBACHIK, T.N., SIMMONS, M.D. & WHITTAKER, J.E. 1998. On the evolution of the Hedbergellidae from the Praehedbergellidae. *Journal of Micropalaeontology*, **V17**, pp. 97-103.
- BouDAGHER-FADEL, M.K. & LORD, A.R. 2000. The evolution of *Lepidocyclina* (L.) *Isolepidinoides*, L. (*Nephrolepidina*) *Nephrolepidinoides* Sp. Nov., L. (*N.*) *Broweri* and L. (*N.*) *Ferreroi* in the Late Oligocene-Miocene of the Far East. *Journal of Foraminiferal Research*, **V30**, N1, pp. 71-76.



- BouDAGHER-FADEL, M.K., LORD, A.R. & BANNER, F.T. 2000. Some Miogypsinidae (foraminifera) in the Miocene of Borneo and nearby countries. *Revue Paleobiology*, **V19**, N1, pp. 137-156.
- BREW, G. 2001. Tectonic evolution of Syria interpreted from integrated geophysical and geological analysis. *PhD Thesis*, Cornell University, USA. Online copy: <http://atlas.geo.cornell.edu/people/brew/gbthesisintro.htm>
- BREW, G., LITAK, R., BARAZANGI, M. & SAWAF, T. 1999. Tectonic evolution of Northeast Syria: Regional implications and hydrocarbon prospects. *GeoArabia*, **V4**, N3, pp. 289-318.
- BREW, G., LUPA, J., BARAZANGI, M., SAWAF, T., AL-IMAM, A. & ZAZA, T. 2000. Tectonic development of the Dead Sea Fault system in Syria: The Ghab basin and surroundings. *Submitted to Tectonics*, 2000. Online edition, <http://atlas.geo.cornell.edu/syria/Brew2000.html>
- BREW, G., LUPA, J., BARAZANGI, M., SAWAF, T., AL-IMAM, A. & ZAZA, T. 2001. Structure and tectonic development of the Ghab basin and the Dead Sea fault system, Syria. 2001. *Journal of the Geological Society*, **V158**, pp. 665-674.
- BUTLER, R. W. H., SPENCER, S. & GRIFFITHS, H. M. 1997. Transcurrent fault activity on the Dead Sea transform in Lebanon and its implications for plate tectonics and seismic hazard. *Journal of the Geological Society of London*, 154, 5, p.757-760.
- BUTLER, R. W. H. & SPENCER, S. 1999. Landscape evolution and the preservation of tectonic landforms along the north Yammouneh Fault, Lebanon. In: *Uplift, erosion and stability: geological and geomorphological perspectives on landscape evolution*. (Ed. B. J. Smith, W.B. Walley & P. A. Warke) Spec. Publ. Geol. Soc. Lond. 162, 143-156.
- CLARK, J. D. & PICKERING, K. T. 1996. Submarine channels, processes and architecture. Vallis Press, London.
- COWARD, M. 1994. Continental collision. In: Hancock, P. L. 1994. *Continental deformation*. Pergamon press, p264-288.
- CRAMPTON, S.L. & ALLEN, P.A. 1995. Recognition of forebulge unconformities associated with early stage foreland basin development: Example from the North Alpine foreland basin. *AAPG Bulletin*, **V79**, N10, pp. 1495-1514.
- CHAIMOV, T., BARAZANGI, D., AL-SAAD, D., SAWAF, T., GEBREN, A. 1990. Crustal shortening in the Palmyride Fold Belt, Syria, and implications for movement along the Dead sea Fault System. *Tectonics*, **V9**, N6, p1369-1386.
- DALATI, M. ?? Applications of remote sensing for tectonic purposes in El-Rouge depression, North-West of the Syria Arab Republic. *Internal Report*, General Organisation for Remote Sensing, Damascus, Syria, pp. 859-866.
- DALONGEVILLE, R., LABORAL, J., PIRAZZOLI, P., SANLAVILLE, P., ARNOLD, M., BERNIER, P., EVIN, J. & MONTAGGIONI, L-T. 1993. Les variations recentes de la ligne de rivage sur le littoral syrien. *Quaternaire*, **V4**, N1, pp. 45-53.
- DAVIS G. H. & REYNOLDS, S. J. 1996. *Structural geology : of rocks and regions*, 2<sup>nd</sup> Ed. Wiley & Sons, Chichester.
- DELALOYE, M. & WAGNER, J.J. 1984. Ophiolites and volcanic activity near the western edge of the Arabian plate. In: DIXON, J.E. & ROBERTSON, A.H.F.

- (Eds). 1984. *The Geological Evolution of the Eastern Mediterranean*. Geological Society Special Publication No. **17**, 225-233.
- DELAUNE-MEYERE, M. 1984. Evolution of a Mesozoic passive continental margin: Baer-Bassit (NW Syria). In: DIXON, J.E. & ROBERTSON, A.H.F. (Eds). 1984. *The Geological Evolution of the Eastern Mediterranean*. Geological Society Special Publication No. **17**, pp. 151-161.
- DEMICO, R. V. & HARDIE, L. A. 1994. *Sedimentary structures and early diagenetic features of shallow marine carbonates deposits*. SEPM Atlas series 1.
- DEVYATKIN, E.V., DODONOV, A.E., GABLINA, S.S., GOLOVINA, L.A., KURENKOVA, V.G., SIMAKOVA, A.N., TRUBIKHIN, V.M., YASAMANOV, N.A., KHATIB, K. & NSEIR, H. 1996. Upper Pliocene-Lower Pleistocene marine deposits of Western Syria: stratigraphy and paleogeography. *Stratigraphy and Geological Correlation (translation from Russian)*, **V4**, N1, pp67-77.
- DEVYATKIN, E.V., DODONOV, A.E., KHATIB, K. & NSEIR, H. 1991. Preliminary report on the project "Continental Neogene-Quaternary deposits of Syria" 1990-1991. *The General Establishment of Geology & Mineral Resources, Damascus, Syria*. Internal report.
- DEVYATKIN, E.V., DODONOV, A.E., KHATIB, K. & NSEIR, H. 1991. Preliminary report on the project "Continental Neogene-Quaternary deposits of Syria" 1992-1993. *The General Establishment of Geology & Mineral Resources, Damascus, Syria*. Internal report.
- DEVYATKIN, E.V., DODONOV, A.E., KHATIB, K. & NSEIR, H. 1991. The annual report of the studies of Neogene and Quaternary protocol in Syria 1992-1993. *The General Establishment of Geology & Mineral Resources, Damascus, Syria*. Internal report.
- DEVYATKIN, E.V., DODONOV, A.E., SHARKOV, E.V., ZYKIN, V.S., SIMAKOVA, A.N., KHATIB, K. & NSEIR, H. 1997. The El-Ghab Rift depression in Syria: Its structure, stratigraphy and history of development. *Stratigraphy and Geological Correlation (translated from Russian journal)*, **V5**, N4, pp. 362-374.
- DILEK, Y. & DELALOYE, M. 1992. Structure of the Kizildag ophiolite, a slow-spread Cretaceous ridge segment north of the Arabian promontory. *Geology*, **V.20**, pp. 19-22.
- DILEK, Y. & WHITNEY, D.L. 2000. Cenozoic crustal evolution in Central Anatolia: extension, magmatism and landscape development. In: PANAYIDES, I., XENOPHONTOS, C., & MALPAS, J. (Eds). *Proceedings of the third international conference on the geology of the Eastern Mediterranean*. pp 183-191..
- DIXON, J.E. & ROBERTSON, A.H.F. (Eds). 1984. *The Geological Evolution of the Eastern Mediterranean*. Geological Society Special Publication **17**, London.
- DOMAS, J. 1994. The Late Cenozoic of the Al Ghab rift, NW Syria. *Sbornik Geologich'ych Antropozoihum (translated copy)*, **V21**, pp. 57-73.
- DRZEWIECKI, P. A. & SIMO, J. A. 2002. Depositional processes, triggering mechanisms and sediment composition of carbonate gravity flow deposits:

- examples from the Late Cretaceous of the south-central Pyrenees, Spain. *Sedimentary Geology*, **V146**, p155-189.
- DUBERTRET, L. 1932. Les formes structurales de la Syrie et de la Palestine. *Comptes Rendus L'academie Scientifc*, **V195**, pp.66-68.
- DUBERTRET, L. 1933. La tectonique de la Syrie septentrionale á la fin du Cretace et du debut du Tertiaire. *Notes et Memoires du á Beyrouth, Paris*.
- DUBERTRET, L. 1943-1953. Carte géologique au 1/50 000 de la Syrien et du Liban. 21 sheets with notes. Damas et Beyreuth: Ministeres des Trav. Pub.
- DUVAL, B. C., CRAMEZ, C. & JACKSON, M. P. A. 1992. Raft tectonics in the Kwanza Basin, Angola. *Marine and Petroleum Geology*, **V9**, 4, p. 389-404.
- DZHABUR, I. 1985. Seismological description of Latakia region of Syria according to borehole evidence. *Geoloiya, Vestnik Moskovskogo University (In Russian)*, **V40**, pp. 90-93.
- EATON, S. & ROBERTSON, A.H.F. 1993. The Miocene Pakhna formation, southern Cyprus and its relationship to the Neogene tectonic evolution of the Eastern Mediterranean. *Sedimentary Geology*, **V86**, pp. 273-296.
- EMERY, E. & MYERS, K.J. (Eds). 1996. Sequence Stratigraphy. Blackwell Science, London.
- ESTEBAN, M. 1996. An overview of Miocene reefs from the Mediterranean area: general trends and facies models. In: FRANSEEN, E. K., ESTEBAN, M., WARD, W.C. & ROUCHY, J.M. (Eds) *Models for carbonate stratigraphy from Miocene reef complexes of Mediterranean regions*. Society of Economic Palaeontologists & Mineralogists; Concepts in Sedimentology & Palaeontology, 5, p3-53.
- FLECKER, R., ELLAM, R.M., MULLER, C., POISSON, A., ROBERTSON, A.H.F. & TURNER, J. 1998. Application of Sr isotope stratigraphy and sedimentary analysis to the origin and evolution of the Neogene basins in the Isparta Angle, Southern Turkey. *Tectonophysics*, **V298**, N1-3, pp. 83-101.
- FOLLOWS, E.J. & ROBERTSON, A.H.F. 1990. Sedimentology and structural setting of Miocene reefal limestones in Cyprus. In: MALPAS, J., MOORES, E.M., PANAYIOTOU, A. & XENOPHONTOS, C. (Eds), *Ophiolites: Oceanic crustal analogues*. Nicosia, Cyprus (Geol. Surv. Dep., Minist. Agric. Nat. Resour.), pp.207-216.
- GARFUNKEL, Z. 1998. Constrains on the origin and history of the Eastern Mediterranean basin. *Tectonophysics*, **V298**, pp. 5-35.
- GARZANTI, E., ANDO, S. & SCUTELLA, M. 2000. Actualistic ophiolite provenance: the Cyprus case. *The Journal of Geology*, **V108**, pp 199-218.
- GIRDLER, R. W. 1990. The Dead Sea Transform fault System. *Tectonophysics*, **V180**, 1, p.1-13.
- GOLOVINA, L.A. 1996. Palaeogeographic interpretation ? Stratigraphica Geologie Korrelyatsiya (In Russian), **V4**, N2, pp. 102-105.
- GOUDANT, J., BARKER, M.J., COURME, M.D., DI STEFANO, A., MARTILL, D.M., VENEC-PEYRE, M.T., ZORN, I., & PANAYIDES, I. 2000. Alassa: a new fish fossil fauna from the Middle Miocene (Serravallian) of Cyprus. In: PANAYIDES, I., XENOPHONTOS, C., & MALPAS, J. (Eds). *Proceedings of the third international conference on the geology of the Eastern Mediterranean*. pp 327-337.

- GRASSO, M., MIUCCIO, G., MANISCALCO, R., GAROFALO, P., LA MANNA, F. & STAMILLA, R. 1995. Plio-Pleistocene structural evolution of the western margin of the Hyblean Plateau and the Maghrebian Foredeep, SE Sicily; implications for the deformational history of the Gela Nappe. *Annales Tectonicae*, **V9**, 1-2, p7-21.
- GUIRAUD, R. & BOSWORTH, W. 1997. Senonian basin inversion and rejuvenation of rifting in Africa and Arabia: synthesis and implications to plate-scale tectonics. *Tectonophysics*, 282, pp.39-82.
- HALL, J.K. 1994. Eastern Mediterranean regional biography: Geology, geophysics, oceanology and related subjects. From: KRASHENNINKOV, V.A. & HALL, J.K. (Eds) 1994. *Geological structure of the northeastern Mediterranean – Cruise 5 of the research vessel 'Akademik Nikolaj Strakhov'*. Historical Productions-Hall Ltd, Jerusalem.
- HARDENBERG, M. F., ARAB, N. & LECHNER, M. 2001. Field visit report, Latakia Graben, NW Syria, October 2001. Syria Shell internal report.
- HEIMANN, A. 1993. Geometric changes of plate boundaries along part of the Northern Dead Sea Transform: Geochronologic and palaeomagnetic evidence. *Tectonics*, **V12**, N2, pp. 477-491.
- HEIMANN, A. & STEINITZ, G. 1989.  $^{40}\text{Ar}/^{39}\text{Ar}$  total gas ages of basalts from Notera #3 well, Hula Valley, Dead Sea Rift: Stratigraphic and tectonic implications. *Israel Journal of Earth Science*, **V38**, pp. 173-184.
- HEMPTON, M.R. 1985. Structure and deformation history of the Bitlis suture near Lake Hazar, southeastern Turkey. *GSA Bulletin*, **V96**, pp. 233-243.
- HEMPTON, M.R. 1987. Constraints on Arabian plate motion and extensional history of the Red Sea. *Tectonics*, **V6**, N6, pp. 687-705.
- HOLDSWORTH, R. E., BUTLER, C. A. & ROBERTS, A. M. 1997. The recognition of reactivation during continental deformation. *Journal of the Geological Society of London*. **Vol 154**, pp. 73-78.
- HOWARD, D. 2000. Unravelling ophiolite emplacement history using microfossils. *University College London, internal report*.
- HS , K.J., RYAN, W.B.F & CITA, M.B. 1973. Late Miocene desiccation of the Mediterranean. *Nature*, **V242**, pp. 240-244.
- Hs , K.J., GARRISON, R.E., MONTADERT, L., KIDD, R.B., BERNOULLI, D., MÈLIERÉS, F., CITA, M.B, MILLER, C., ERICKSON, A. & WRIGHT, R. 1977. History of the Mediterranean salinity crisis. *Nature*, **V267**, pp. 399-403.
- HUSEIN, K.M. 1973. Results of microplaeobotanical studies, NW Syria. *Ser Geol, Vestn. Mos. Gos. Univ. (In Russian)*, Part 3, pp. 108-112.
- ISSA, S. 1995. The stratigraphy of the Neogene in Syria. *The General Establishment of Geology & Mineral Resources, Damascus, Syria*. Internal report.
- ILANI, A., ROSENFELD, A. & FLEXER, A. 2000. Manganese within the Maastrichtian to Eocene “Chalk Sea” in Cyprus and Israel – a guide to tectono-volcanic and erosional events. In: PANAYIDES, I., XENOPHONTOS, C., & MALPAS, J. (Eds). *Proceedings of the third international conference on the geology of the Eastern Mediterranean*. pp 249-253.

- IVANOV, M.K., LIMONOV, A.F. & WOODSIDE, J.M. (Eds). 1992. *Geological investigations in the Mediterranean & Black Seas*. UNESCO, 1992, UNESCO Report of Marine Science No.56.
- JAFFEY, N. & ROBERTSON, A. H. F. 2001. New sedimentological and structural data from the Eceemis Fault Zone, southern Turkey: implications for its timing and offset and the Cenozoic tectonic escape in Anatolia. *J. Geol. Soc. Lon*, V158, p367-378.
- JAQUET, T. 1933. Une faune du Miocene moyen dans la vallee du Nahr el Kebir (Nord de Lattaquie, Syrie). *C. r. Soc. Geol., Fr.*, (5e) t.3, p67
- KARIG, D. E. & KOZLU, H. 1990. Late Palaeogene-Neogene evolution of the triple junction region near Maras, south-central Turkey. *Journal of the Geological Society of London*, V147, 6, p1023-1034.
- KEMPLER, D. & GARFUNKEL, Z. 1994. Structures and kinematics in the NE Mediterranean – A study of an irregular plate boundary. *Tectonophysics*, V234, N1-2, pp. 19-32.
- KEMPLER, D. 1993. Tectonic patterns in the easternmost Mediterranean. *PhD Thesis*. Hebrew University of Jerusalem.
- KEMPLER, D. 1994. An outline of Northeastern Mediterranean tectonics in view of cruise 5 of the Akademik Nikolaj Stakhov. In: KRASHENNINKOV, V.A. & HALL, J.K. (Eds) 1994. *Geological structure of the northeastern Mediterranean – Cruise 5 of the research vessel 'Akademik Nikolaj Strakhov'*. Historical Productions-Hall Ltd, Jerusalem.
- KERANS, C. & TINKER, S.W. 1991. *Sequence stratigraphy and characterisation of carbonate reservoirs*. SEPM Short Course No.40.
- KHAIR, K. & TSOKAS, G.N. 1999. The nature of Levantine (E Med) crust from multiple-source Werner deconvolution of Bouger gravity anomalies. *Journal of Geophysical Research – Solid Earth*, V104, B11, pp. 25469-25478. Ab only.
- KNIPPER, A.L. & SHARASKIN, A.Y. 1994. Tectonic evolution of the Western part of the Peri-Arabian Ophiolite arc. In: KRASHENNINKOV, V.A. & HALL, J.K. (Eds) 1994. *Geological structure of the northeastern Mediterranean – Cruise 5 of the research vessel 'Akademik Nikolaj Strakhov'*. Historical Productions-Hall Ltd, Jerusalem.
- KOPP, M.L. 2000. Geology of Latakia region. In: LEONOV, 2000. *Outline of the geology of Syria*. Moscow, 200pp. Extracts only, in Russian.
- KOURAMPAS, N. & ROBERTSON, A.H.F. 2000. Controls on Plio-Quaternary sedimentation within an active fore-arc region: Messenia peninsula (SW Peloponnese), S. Greece. In: PANAYIDES, I., XENOPHONTOS, C., & MALPAS, J. (Eds). *Proceedings of the third international conference on the geology of the Eastern Mediterranean*. pp 255-285.
- KRASHENNINKOV, V.A. 1994. Stratigraphy of the Maastrichtian and Cenozoic deposits of the coastal part of Northwestern Syria (Neoautochthon of the Bassit Ophiolite Massif). From: KRASHENNINKOV, V.A. & HALL, J.K. (Eds) 1994. *Geological structure of the northeastern Mediterranean – Cruise 5 of the research vessel 'Akademik Nikolaj Strakhov'*. Historical Productions-Hall Ltd, Jerusalem.

- KRASHENNINKOV, V.A., GOLOVIN, D. I. & MOURAVYOV, V. I. 1996. The Paleogene of Syria – stratigraphy, lithology, geochronology. *Geologisches Jahrbuch Reihe B*.
- KRASHENNINKOV, V.A. & KALEDA, K.G. 1994. Stratigraphy and lithology of Upper Cretaceous and Cenozoic deposits of the key Peripedi section (Neoautochthon of Southern Cyprus). From: KRASHENNINKOV, V.A. & HALL, J.K. (Eds) 1994. *Geological structure of the northeastern Mediterranean – Cruise 5 of the research vessel 'Akademik Nikolaj Strakhov'*. Historical Productions-Hall Ltd, Jerusalem.
- LEEDER, M. 1999. Sedimentology and sedimentary basins; from turbulence to tectonics. Blackwell Science, Oxford.
- LOUCHS, R.G. & SARG, J.F. (Eds). 1993. Carbonate Sequence Stratigraphy. AAPG Memoir **57**, Tulsa.
- LORD, A.R., PANAYIDES, I., URQUHART, E., & XENOPHONTOS, C. 2000. A biostratigraphical framework for the Late Cretaceous-Recent circum-Troodos sedimentary sequence, Cyprus. In: PANAYIDES, I., XENOPHONTOS, C., & MALPAS, J. (Eds). *Proceedings of the third international conference on the geology of the Eastern Mediterranean*. pp 289-297.
- MAKRIS, J., STACKER, J. & KRAMVIS, S. 2000. Microseismic studies and tectonic implications of Cyprus. In: PANAYIDES, I., XENOPHONTOS, C., & MALPAS, J. (Eds). *Proceedings of the third international conference on the geology of the Eastern Mediterranean*. pp 137-145.
- MALPAS, J. 2000. An earth system approach to the geology of the Eastern Mediterranean. In: PANAYIDES, I., XENOPHONTOS, C., & MALPAS, J. (Eds). *Proceedings of the third international conference on the geology of the Eastern Mediterranean*. pp 1-8.
- MALTMAN, A. 1994. Prelithification deformation. . In: HANCOCK, P. L. (ed), *Continental deformation*, Pergamon Press, Oxford.
- MANIGHETTI, I., TAPPONNIER, P., COURTILLOT, V., GRUSZOW, S. & GILLOT, P-Y. 1997. Propagation of rifting along the Arabia-Somalia plate boundary: The Gulfs of Aden and Tadjoura. *Journal of Geophysical Research*, **V102**, N B2, pp 2681-2710.
- MANN, P. 1997. Model for the formation of large, transtensional basins in zones of tectonic escape. *Geology*, **V25**, pp. 211-214.
- MARTINEZ, J. M. F, CARTWRIGHT, J. & HALL, B. 2003. 3D seismic analysis of slump systems, Eastern Mediterranean Sea. *AAPG, student seminar abstract, AAPG conference 2003*.
- MASCLE, J., BENKHELIL, J., BELLAICHE, G., ZITTER, T., WOODSIDE, J. & LONCKE, L. 2000. Marine geologic evidence for a Levantine-Sinai plate, a new piece of the Mediterranean puzzle. *Geology*, **V28**, N9, pp 779-782.
- MAY, P.R. 1991. The Eastern Mediterranean Mesozoic basin: evolution and oil habitat. *AAPG Bulletin*, **V75**, N7, pp. 1215-1232.
- McCALLUM, J.E. 1995. Sedimentology of two fan-delta systems in the Pliocene-Pleistocene of the Mesoria Basin, Cyprus. *Sedimentary Geology*, **V98**, pp. 215-244.
- MCCLUSKY, S., BALASSANIAN, S., BARKA, A., DEMIR, C., ERGINTAV, S., GEORGIEV, I., GURKAN, O., HAMBURGER, M., HURST, K., KAHLE, H.,



- KASTENS, K., KEKELIDZE, G., KING, R., KOTZEV, V., LENK, MAHMOUD, S., MISHIN, A., NADARIYA, M., OUZOUNIS, A., PARADISSIS, D., PETER, Y., PRILEPIN, M., REILINGER, R., SANLI, I., SEEGAR, H., TEALEB, A., TOKSOZ, M.N. & VEIS, G. 2000. Global Positioning System constraints on plate kinematics and dynamics in the Eastern Mediterranean and Caucasus. *Journal of Geophysical Research*, **V105**, N B3, pp. 5695-5719.
- MCKENZIE, D.P. 1978. Some remarks on the development of sedimentary basins. *Earth and Planetary Science Letter*, **V40**, pp25-32.
- MEGHRAOUI, M. 2003. Evidence for 830 years of seismic quiescence from palaeoseismicity, archaeoseismology and historical seismicity along the Dead Sea fault in Syria. *Earth Science and Planetary Letters*, **V210**, pp 35-52.
- MORRIS, A., ANDERSON, M.W., ROBERTSON, A.H.F. & AL-RIYAMI, K. 2002. Extreme tectonic rotations within an Eastern Mediterranean ophiolite (Baer-Bassit, Syria). *Earth and Planetary Science Letters*, **V202**, pp. 247-261.
- O'CONNOR, J.M., STOFFERS, P., VAN DEN BOGAARD, P. & MCWILLIAMS, M. 1999. First seamount age evidence for significantly slower African plate motion since 19 to 30Ma. *Earth and Planetary Science Letters*, **V171**, pp 575-589.
- ORSZAG-SPERBER, F. & ROUCHY, J-M. 2000. The Messinian-Zanclean transition in the Pissouri area (Cyprus): a well documented section in the Eastern Mediterranean. In: PANAYIDES, I., XENOPHONTOS, C., & MALPAS, J. (Eds). *Proceedings of the third international conference on the geology of the Eastern Mediterranean*. pp 243-247.
- PAYNE, A.S. & ROBERTSON, A.H.F. 1995. Neogene supra-subduction zone extension in the Polis graben system, west Cyprus. *Journal of the Geological Society, London*, **V152**, pp. 613-628.
- PAYNE, A.S. & ROBERTSON, A.H.F. 2000. Structural evolution and regional significance of the Polis graben system, western Cyprus. In: PANAYIDES, I., XENOPHONTOS, C., & MALPAS, J. (Eds). *Proceedings of the third international conference on the geology of the Eastern Mediterranean*. pp 45-59.
- PIRAZZOLI, P.A., LABOREL, J., SALIEGE, J.F., EROL, O., KAYAN, I. & PERSON, A. 1991. Holocene raised shorelines on the Hatay coasts (Turkey): Palaeoecological and tectonic implications. *Marine Geology*, **V96**, pp. 295-311.
- PISKEN, O. 1985. Carte geologique du Hatay et du NW-Syrien. *Universite de Geneve*, 1985.
- PONIKAROV, V., SHATSKY, V., KAZMIN, V., MIKAILOV, I., AISTOV, L., KULAKOV, V., SHATSKAYA, M., SHIROKOV, V. 1963. *Geological map of Syria, 1:200 000, I-36-XXIV; I-37-XIX*. V.O.Technoexport, Moscow, USSR.
- PONIKAROV, V. (ed) 1966. The geological map of Syria, explanatory notes, 1:200 000, sheet I-37-XIX, I-36-XXIV. V.O.Technoexport, Moscow, USSR.
- PONIKAROV, V. (ed) 1967. The geological maps of Syria, explanatory notes. V.O.Technoexport, Moscow, USSR.

- POOLE, A.J. & ROBERTSON, A.H.F. 1991. Quaternary uplift and sea-level change at an active boundary, Cyprus. *Journal of the Geological Society, London*, **V148**, pp. 909-921.
- POOLE, A.J. & ROBERTSON, A.H.F. 1998. Pleistocene fanglomerate deposition relative to uplift of the Troodos ophiolite, Cyprus. In: ROBERTSON, A.H.F., EMEIS, K., RICHTER, C. & CAMERLENGHI, A. (Eds). 1998. *Proceedings of the Ocean Drilling Program, Scientific Results, Vol. 160*, pp 545-566.
- POOLE, A.J. & ROBERTSON, A.H.F. 2000. Quaternary marine terraces and aeolinites in coastal south and west Cyprus: implications for regional uplift and sea-level change. In: PANAYIDES, I., XENOPHONTOS, C., & MALPAS, J. (Eds). *Proceedings of the third international conference on the geology of the Eastern Mediterranean*. pp 105-123.
- QUENNELL, A.M. 1956. Tectonics of the Dead Sea Rift. *Proc. 20<sup>th</sup> Int. Geol. Congr. (Ass. De. Serv. Geol. Africanos), Mexico, 1956*. pp. 385-403.
- QUENNELL, A.M. 1984. The western Arabia rift system. In: DIXON, J.E. & ROBERTSON, A.H.F. (Eds). 1984. *The Geological Evolution of the Eastern Mediterranean*. Geological Society Special Publication No. **17**, pp. 775-763.
- READING, H.G. 1996. *Sedimentary Environments: Processes, Facies and Stratigraphy*. Blackwell Science, London.
- REILINGER, R.E., MCCLUSKY, S.C., ORAL, M.B., KING, R.W. & TOKSOZ, M.N. 1997. Global Positioning System measurements of present-day crustal movements in the Arabia-Africa-Eurasia plate collision zone. *Journal of Geophysical Research*, **V102**, N B5, pp. 9983-9999.
- RICOU, L.E. 1971. Le croissant ophiolitique peri-arabe, une ceinture de nappes mises en place au Crétacé supérieur. *Rev. Géogr. Phys. Géol. Dyn.*, **N13**, pp.327-350.
- ROBERTSON, A.H.F. 1978. The origin and diagenesis of cherts from Cyprus. *Sedimentology*, **V24**, p11-30.
- ROBERTSON, A.H.F., 1994. Role of the tectonic facies concept in orogenic analysis and its application to Tethys in the Eastern Mediterranean region. *Earth Science Reviews*, **V37**, pp 139-213.
- ROBERTSON, A.H.F., 1998. Mesozoic-Tertiary evolution of the easternmost mediterranean area: Integration of marine and land evidence. In: ROBERTSON, A.H.F., EMEIS, K.C., RICHTER, C. & CAMERLENGHI, A. (Eds). 1998. *Proceedings of the Ocean Drilling Program, Scientific Results, Vol.160*.
- ROBERTSON, A.H.F., 1998. Significance of Lower Pliocene mass-flow deposits for the timing and process of collision of the Eratosthenes seamount with the Cyprus active margin. In: ROBERTSON, A.H.F., EMEIS, K.C., RICHTER, C. & CAMERLENGHI, A. (Eds). 1998. *Proceedings of the Ocean Drilling Program, Scientific Results, Vol.160*, pp 465-461.
- ROBERTSON, A.H.F., 1998. Miocene shallow-water carbonates on the Eratosthenes Seamount, Easternmost Mediterranean Sea. In: ROBERTSON, A.H.F., EMEIS, K.C., RICHTER, C. & CAMERLENGHI, A. (Eds). 1998. *Proceedings of the Ocean Drilling Program, Scientific Results, Vol.160*, pp 419-436.

- ROBERTSON, A.H.F., 1998. Late Miocene palaeoenvironments and tectonic setting of the Southern margin of Cyprus and the Eratosthenes Seamount. In: ROBERTSON, A.H.F., EMEIS, K.C., RICHTER, C. & CAMERLENGHI, A. (Eds). 1998. *Proceedings of the Ocean Drilling Program, Scientific Results, Vol.160*, pp 453-463.
- ROBERTSON, A.H.F., 1998. Tectonic significance of the Eratosthenes Seamount: a continental fragment in the process of collision with a subduction zone in the E Mediterranean (ODP Leg 160). *Tectonophysics*, **V298**, N1-3, pp. 63-82.
- ROBERTSON, A.H.F., 2000. Mesozoic-Tertiary tectonic-sedimentary evolution of a south Tethyan oceanic basin and its margins in southern Turkey. In: BOZKURT, E., WINCHESTER, J.A. & PIPER, J.D. (Eds). *Tectonics and magmatism in Turkey and the surrounding area*. Geological Society Special Publication No. **173**, pp. 97-138.
- ROBERTSON, A.H.F. 2000. Tectonic evolution of Cyprus in its Easternmost Mediterranean setting. In: PANAYIDES, I., XENOPHONTOS, C., & MALPAS, J. (Eds). *Proceedings of the third international conference on the geology of the Eastern Mediterranean*. pp 11-44.
- ROBERTSON, A.H.F. 2002. Overview of the genesis and emplacement of Mesozoic ophiolites in the Eastern Mediterranean Tethyan region. *Lithos*, **V65**, pp.1-67.
- ROBERTSON, A.H.F., DIXON, J.E., BROWN, S., COLLINS, A., MORRIS, A., PICKETT, E., SHARP, I. & USTAÖMER, T. 1996. Alternative tectonic models for the Late Palaeozoic – Early Tertiary development of Tethys in the Eastern Mediterranean region. In: MORRIS, A. & TARLING, D.H. (Eds), 1996, *Palaeomagnetism and Tectonics of the Mediterranean region*. Geological Society Special Publication No. **105**, pp.239-263.
- ROBERTSON AND SHIP. 1995. *Initial ODP Leg 160 Results*, Tectonic introduction. P5-19.
- ROBERTSON, A.H.F, UNLUGENC, U, NORDAN I, TASLI, K. in press. The Misis-Andirin Complex: Mid-Tertiary subduction/accretion and melange formation related to closure and collision of the South Tethys in Southern Turkey.
- RODD, D. 1988. Latakia graben. *Syria Shell PDBV*, internal report.
- RUSKE, R. (ED). 1978. *Qerdaha sheet, NI-37-S-1-c, 1:50 000*, Geological Map of Syria. VEB Hermann Haack, German Democratic Republic.
- RUSKE, R. (ED). 1978. *Jebleh sheet, NI-36-X-2-d, 1:50 000*, Geological Map of Syria. VEB Hermann Haack, German Democratic Republic.
- SALLER, A., ARMIN, R., ICHRAM, L.O. & GLENN-SULLIVEN, C. 1993. Sequence stratigraphy of aggrading and backstepping carbonate shelves, Oligocene, Central Kalimantan, Indonesia. In: Loucks, R.G. & Sarg, J.F. (Eds). *Carbonate sequence stratigraphy, recent developments and applications*. American Association of Petroleum Geology Memoir No. **57**, pp.267-290.
- SARTORIO, D. & VENTURINI, S. 1988. *Southern Tethys biofacies*. AGIP Archives, Italy.
- SCHIRMER, W. 1998. Havara on Cyprus – a surficial calcareous deposit. *Eiszeitalter u. Gegenwart*, **V48**, pp. 110-117.

- SCHIRMER, W. 2000. Neogene submarine relief and Troodos uplift in southeastern Cyprus. In: PANAYIDES, I., XENOPHONTOS, C., & MALPAS, J. (Eds). *Proceedings of the third international conference on the geology of the Eastern Mediterranean*. pp 125-134.
- SEELY, R. C. 1998. Elements of petroleum geology. 2<sup>nd</sup> Edition. Academic Press, London.
- SENGOR, A. M.C, GOR, R. N. & SAROGLU, F. 1985. Strike-slip faulting and related basin formation in zones of tectonic escape: Turkey as a case study. In: Biddle, K.T. & Christie-Blick, N (Eds). *Strike-slip deformation, basin formation and sedimentation*. Soc. Econ. Paleont. Mineral. Spec. Publ. 37, 227-264.
- SHIMAZAKI, K. & ZHAO, Y. 2000. Dislocation model for strain accumulation in a plate collision zone. *Earth Planets Space*, **V52**, pp. 1091-1094.
- SHERIFF, R. E. & GELDART, L. P. 1995. *Exploration seismology*. Cambridge University Press.
- SIMAKOVA, A. N. 1994. Palynology of the marine Upper Pliocene in Syria and a paleogeographical analysis. *Stratigraphy and Geological Correlation, translated from Russian*, **V2**, N2, pp. 188-193.
- SINCLAIR, H.D. 1997. Tectonostratigraphic model for underfilled peripheral foreland basins: an Alpine perspective. *GSA Bulletin*, **V109**, N3, pp.324-346.
- STEININGER, F.F. & RÖGL, F. 1984. Paleogeography and palinspastic reconstruction of the Neogene of the Mediterranean and Paratethys. In: DIXON, J.E. & ROBERTSON, A.H.F. (Eds). 1984. *The Geological Evolution of the Eastern Mediterranean*. Geological Society Special Publication No. **17**, pp. 659-669.
- STOKER, M. S., EVANS, D. & CRAMP, A. 1998. *Geological processes on continental margins: sedimentation, mass-wasting and stability*. Geological Society Special Publication No. **129**.
- STOW, D. A. V. & PIPER, D. J. W. 1984. Deep-water fine-grained sediments: facies models. In: STOW, D. A. V. & PIPER, D. J. W. (Eds) 1984. *Fine-grained sediments: Deep water processes and facies*. Geological Society Special Publication No. **15**, pp.611-646.
- TINKLER, C., WAGNER, J.J., DELALOYE, M. & SELÇUK, H. 1981. Tectonic history of the Hatay ophiolites (South Turkey) and their relation with the Dead Sea Rift. *Tectonophysics*, **V.72**, Issue 1-2, pp.23-41.
- TRIFONOV, V.G. ???. neotectonic studies of Syria with using of space images. ?? (in Arabic).
- TRIFONOV, V. G. 1991. Levant fault zone in northwest Syria. *Geotectonics* 25, p145-154.
- TUCKER, M. E. & WRIGHT, V. P. 1990. *Carbonate sedimentology*. Blackwell Science, Oxford.
- TUCKER, M. E. 1991. *Sedimentary petrology, an introduction to the origin of sedimentary rocks*, 2<sup>nd</sup> Ed. Blackwell Science, Oxford.

- VIDAL, N., ALVAREZ-MARRON, J. & KLAESCHEN, D. 2000A. Internal configuration of the Levantine Basin from seismic reflection data (Eastern Mediterranean). *Earth and Planetary Science Letters*, **V180**, pp. 77-89.
- VIDAL, N., ALVAREZ-MARRON, J. & KLAESCHEN, D. 2000B. The structure of the Africa-Anatolia plate boundary in the Eastern Mediterranean. *Tectonics*, **V19**, N4, pp. 723-739.
- WESTAWAY, R. & ARGER, J. 1996. The Golbasi Basin, southeastern Turkey; a complex discontinuity in a major strike-slip fault zone. *Journal of the Geological Society of London*, **V153**, 5, p729-743.
- WILGUS, C.K., HASTINGS, B.S., KENDALL, C.G., POSAMENTIER, H.W., ROSS, C.A. & VAN WAGONER, J.C.V. (Eds). 1988. *Sea-Level Changes – An integrated Approach*. SEPM Special Publication **42**. Tulsa, USA.
- WOODCOCK, N. H. & SCHUBERT, C. 1994. Continental strike-slip tectonics. In: HANCOCK, P. L. (ed), *Continental deformation*, Pergamon Press, Oxford.
- YILMAZ, Y. 1993. New evidence and model on the evolution of southeast Anatolian orogen. *Geol. Soc. Am. Bull.* **V105**, p251-271.
- YURTMEN, S., GUILLOU, H., WESTAWAY, R., ROWBOTHAM, G. & TATAR, O. 2002. Rate of strike-slip motion on the Amanos Fault (Karasu Valley, southern Turkey) constrained by K-Ar dating and geochemical analysis of Quaternary basalts. *Tectonophysics*, **V344**, 3-4, p.207-246.
- YURUR, M. T. & CHOROWICZ, J. 1998. Recent volcanism, tectonics and plate kinematics near the junction of the African, Arabian and Anatolian plates in the eastern Mediterranean. *Journal of Volcanology and Geothermal Research*, **V85**, 1-4, p.1-15.
- ZANCHI, A., CROSTA, G. B. & DARKAL, A. N. 2002. Paleostress analyses in NW Syria: constraints on the Cenozoic evolution of the northwestern margin of the Arabian plate. *Tectonophysics*, **V357**, P255-278.
- ZIEGLER, P. A., CAVAZZA, W., ROBERTSON, A. H. F. & CRASQUIN-SOLEAU. 2001. *Peri-Tethys Memoir 6, Peri-Tethyan rift/wrench basins and passive margins*. Mémoires de Muséum National D'Histoire Naturelle, Tome 186, 2001.

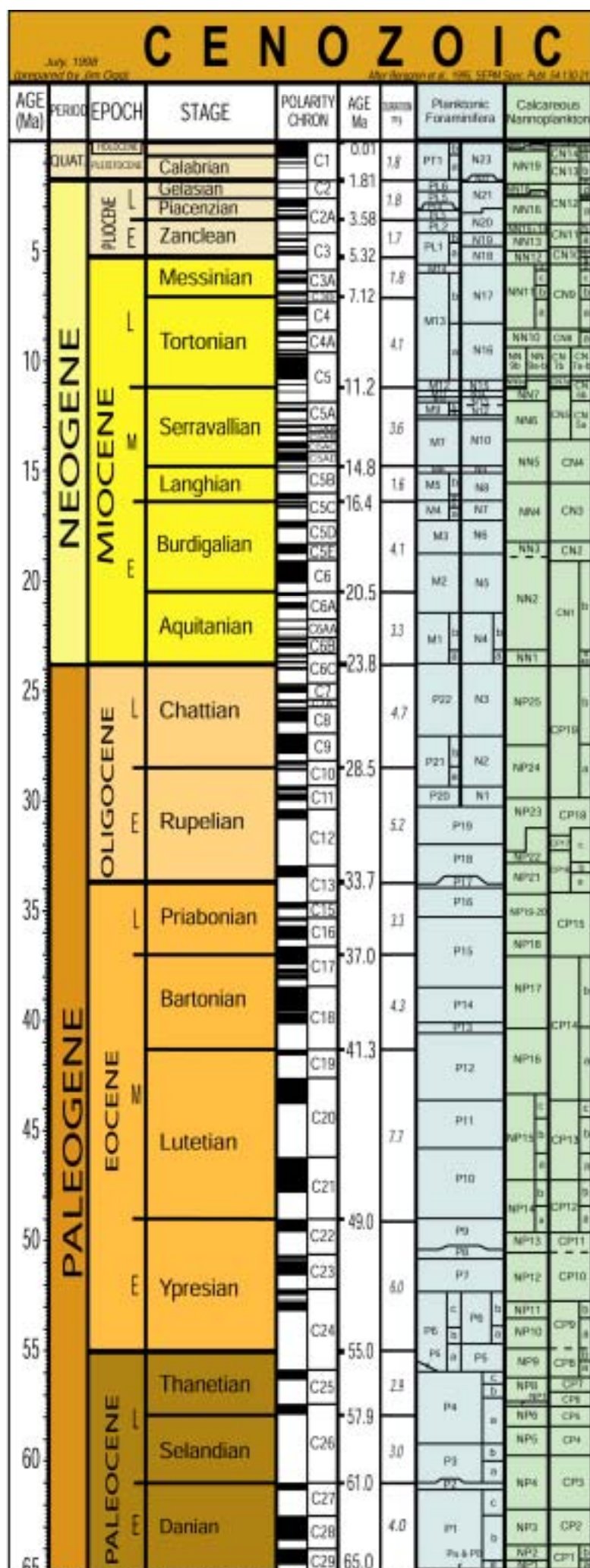
# **Appendix 1**

## ***Project biostratigraphy***



## **Project Biostratigraphy**

The biostratigraphy used throughout this project is detailed in this appendix. The Berggren et al. (1995), chronostratigraphic table is presented here as a guide (Figure 1) to the planktic foraminiferal biochronozones presented by Krasheninnikov (1994) (Figure 2) and Marcelle BouDagher-Fadel (Figures 3, 4 & 5), working on samples in this project. Nannofossil listings completed by Silvia Gardin are also presented (Figure 6). Chapters 3 and 6, contain the details of sample collection and the usage of the data supplied.



Appendix 1. Figure 1. Berggren et al. (1995) stratigraphy.

Krasheninnikov (1994), worked on the biostratigraphy of Ponikarov et al. (1963, 1966 & 1967) used in the original geological map. Krasheninnikov revised the biostratigraphy in 1971 (Krasheninnikov, 1971) and again in 1994. The table presented below (Figure 2) represents the latest edition of his work.

## Appendix 1. Figure 2.

Planktonic Foraminifera Zone: <b><i>Abathomphalus mayaroensis</i></b> Zone (Upper Maastrichtian)	<i>Abathomphalus mayaroensis</i> , <i>Globotruncana aepyptiaca</i> , <i>G. falsostuarti</i> , <i>Rosita contusa</i> , <i>Globotruncanita conica</i> , <i>G. stuarti</i> , <i>Globotruncanella havensis</i> , <i>G. citae</i> , <i>G. petaloidea</i> , <i>Rugoglobigerina rugosa</i> , <i>R. hexacamerata</i> , <i>R. macrocephala</i> , <i>Hedbergella holmdelensis</i> , <i>Globigerinelloides subcarinata</i> , <i>Pseudoguembelina costulata</i> , <i>P. excolata</i> , <i>Pseudotextularia elegans</i> , <i>Racemiguembelina fructicosa</i> , <i>Heterohelix striata</i>
Planktonic Foraminifera Zone: <b><i>Turborotalia pseudobulloides</i></b> Zone (Danian P1B)	<i>Eoglobigerina fringa</i> , <i>E. pentagona</i> , <i>E. tetragona</i> , <i>Globoconusa daubjergensis</i> , <i>Subbotina triloculinoides</i> , <i>Guembelitria irregularis</i> , <i>Chiloguembelina midwayensis</i>
Planktonic Foraminifera Zone: <b><i>Turborotalia trinidadensis</i></b> Zone (Danian P1C)	<i>T. pseudobulloides</i> , <i>T. varianta</i> , <i>T. quadrata</i> , <i>Planorotalites compressa</i> , <i>Globoconusa daubjergensis</i> , <i>Subbotina triloculinoides</i> , <i>S. trivialis</i> , <i>Chiloguembelina midwayensis</i>
Planktonic Foraminifera Zone: <b><i>Acarinata uncinata</i></b> Zone (Danian P2)	<i>A. uncinata</i> , <i>A. inconstans</i> , <i>A. schachdagica</i> , <i>A. indolensis</i> , <i>A. praecursoria</i> , <i>Turborotalia pseudobulloides</i> , <i>T. varinata</i> , <i>T. quadrata</i> , <i>Planorotalites compressa</i> , <i>Subbotina triloculinoides</i> , <i>S. trivialis</i> , <i>S. edita</i> , <i>Chiloguembelina midwayensis</i> , <i>Ch. morsey</i>
Planktonic Foraminifera Zone: <b><i>Morozovella angulata</i></b> Zone (Thanetian P3A)	<i>Planorotalites ehrenbergi</i> , <i>P. compressa</i> , <i>Acarinina multioculata</i> , <i>Turborotalia pseudobulloides</i> , <i>T. varianta</i> , <i>Subbotina triloculinoides</i> , <i>S. trivialis</i> , <i>S. edita</i>
Planktonic Foraminifera Zone: <b><i>Morozovella conicotruncata</i></b> Zone (Thanetian P3B?)	<i>M. angulata</i> , <i>M. tadjikistanensis</i> , <i>M. cubanensis</i> , <i>Igorina pusilla</i> , <i>Turborotalia pseudobulloides</i> , <i>T. varianta</i> , <i>Subbotina triloculinoides</i> , <i>S. trivialis</i>

Planktonic Foraminifera Zone: <b><i>Planorotalites pseudomenardii</i></b> Zone (Thanetian P4)	<i>Planorotalites pseudomenardii</i> , <i>Morozovella occlusa</i> , <i>M. valascoensis</i> , <i>Igorina laevigata</i> , <i>I. convexa</i> , <i>Acarinina intermedia</i> , <i>A. subsphaerica</i> , <i>Subbotina velascoensis</i> , <i>S. nana</i> , <i>S. pileata</i>
Planktonic Foraminifera Zone: <b><i>Morozovella velascoensis</i></b> Zone (Thanetian P5/P6A)	<i>M. velascoensis</i> , <i>M. acuta</i> , <i>M. occlusa</i> , <i>M. aequa</i> , <i>M. apantesma</i> , <i>Acarinina acarinata</i> , <i>A. intermedia</i> , <i>A. subsphaerica</i> , <i>Muricoglobigerina soldadoensis</i> , <i>Subbotina nana</i> , <i>S. velascoensis</i> , <i>S. compressaformis</i> , <i>Planorotalites pseudomenardii</i> (minor, at base)
Planktonic Foraminifera Zone: <b><i>Morozovella subbotinae</i></b> Zone (Ypresian P6B)	<i>M. subbotinae</i> , <i>M. aequa</i> , <i>M. formosa gracilis</i> , <i>Acarinina pseudotopilensis</i> , <i>A. triplex</i> , <i>A. acarinata</i> , <i>A. intermedia</i> <i>Muricoglobigerina soldadoensis</i> , <i>Subbotina compressaformis</i> , <i>S. nana</i> , <i>S. eocaenica</i> <i>Morozovella velascoensis</i> (minor, at base)
Planktonic Foraminifera Zone: <b><i>Morozovella aragonensis</i></b> Zone (Ypresian P8)	<i>M. aragonensis</i> , <i>M. lensiformis</i> , <i>Acarinina interposita</i> , <i>A. triplex</i> , <i>A. pseudotopilensis</i> , <i>Muricoglobigerina soldadoensis</i> , <i>Subbotina pseudoeocaena</i>
Planktonic Foraminifera Zone: <b><i>Acarinina pentacamerata</i></b> Zone (Ypresian P9)	<i>Morozovella aragonensis</i> , <i>Acarinina pentacamerata</i> , <i>A. interposita</i> , <i>A. pseudotopilensis</i> , <i>Subbotina pseudoeocaena</i>
Planktonic Foraminifera Zone: <b><i>Acarinina bullbrooki</i></b> Zone	<i>A. bullbrooki</i> , <i>Globigerapis</i> sp., <i>Subbotina boweri</i>
Planktonic Foraminifera Zone: <b><i>Morozovella lehneri</i></b> Zone (Lutetian P12)	<i>M. lehneri</i> , <i>Acarinina rotundimarginata</i> , <i>A. bullbrooki</i> , <i>A. triplex</i> , <i>Truncorotaloides rohri</i> , <i>T. topilensis</i> , <i>Subbotina boweri</i> , <i>S. frontosa</i> , <i>S. pseudoeocaena</i> , <i>Globigerapis index</i> , <i>Muricoglobigerina senni</i> , <i>Hantkenia liebusi</i> , <i>H. lehneri</i> <i>Turborotalia centralis</i> and <i>Morozovella aragonensis</i> (Occ)
Planktonic Foraminifera Zone: <b><i>Orbulinoides beckmanni</i></b> Zone (Bartonian P13)	None listed

Planktonic Foraminifera Zone: <b><i>Globigerinoides primordius</i></b> – <b><i>Globorotalia kugleri</i></b> Zone (Aquitanian)	<i>Globigerina venezuelana</i> , <i>G. woodi</i> , <i>G. praebuloides</i> , <i>G. connecta</i> , <i>G. juvenilis</i> , <i>Globigerinita dissimilis</i> , <i>G. unicava</i> , <i>Globorotaloides suteri</i> , <i>Globigerinoides primordius</i> and <i>Turborotalia aff. Kugleri</i> (Rare)
Planktonic Foraminifera Zone: <b><i>Globigerinita dissimilis</i></b> and <b><i>Globigerinita stainforthi</i></b> undifferentiated Zone (Upper Aquitanian)	<i>Globigerinoides trilobus</i> , <i>Globoquadrina praedehiscens</i> , <i>Globigerinita unicava</i> , <i>G. dissimilis</i> , <i>G. stainforthi</i> , <i>Globigerina venezuelana</i> , <i>G. juvenilis</i> , <i>G. connecta</i> , <i>G. falconensis</i> , <i>Turborotalia siakensis</i> 500+ species of benthic foraminifers
Planktonic Foraminifera Zone: <b><i>Globigerinoides trilobus</i></b> Zone (Burdigalian)	<i>G. trilobus</i> , <i>G. subquadratus</i> , <i>G. diminutus</i> , <i>Globoquadrina altispira</i> , <i>G. dehiscens</i> , <i>Globigerina bollii</i> , <i>G. falconensis</i> , <i>G. foliata</i> , <i>G. venezuelana</i> , <i>G. angustiumbilitata</i> , <i>Cassigerinella chiplensis</i> , <i>Turborotalia siakensis</i>
Planktonic Foraminifera Zone: <b><i>Praeorbulina glomerosa</i></b> Zone (Langhian)	<i>P. glomerosa glomerosa</i> , <i>P. glomerosa circularis</i> , <i>P. transitoria</i> , <i>Globigerinoides bisphaerica</i> , <i>Globorotalia peripheroronda</i> , <i>Globigerina druryi</i> , Samples show inheritance from underlying unit and contain 600+ benthic foraminifera species
Planktonic Foraminifera Zone: <b><i>Orbulina suturalis</i></b> – <b><i>Globorotalia peripheroronda</i></b> Zone (Early Serravallian)	<i>Orbulina suturalis</i> , <i>Borbulina bilobata</i> , <i>Globigerinella aequilateralis</i> , <i>Globigerina concinna</i> , <i>Globigerinoides obliquus</i> , <i>Turborotalia obesa</i>
Planktonic Foraminifera Zone: <b><i>Globorotalia peripheroacuta</i></b> , <b><i>Globorotalia fohsi</i></b> , <b><i>Globorotalia fohsi lobata</i></b> , <b><i>Sphaeroidinellops subdehiscens</i></b> – <b><i>Globigerina druryi</i></b> Undivided Zones (Serravallian)	<i>Orbulina suturalis</i> , <i>Borbulina bilobata</i> , <i>Globigerinella aequilateralis</i> , <i>Globigerinoides obliquus</i> , <i>G. bollii</i> , <i>G. trilobus</i> , <i>Globoquadrina dehiscens</i> , <i>G. altispira</i> , <i>Globigerina bulloides</i> , <i>G. druryi</i> , <i>G. concinna</i> , <i>G. eamesi</i> , <i>Turborotalia siakensis</i> , <i>T. obesa</i> , <i>Globorotalia linguaensis</i> , <i>G. scitula</i> “The <b><i>Globorotalia fohsi</i></b> group shows only rare specimens of <i>Globorotalia peripheroacuta</i> , marking the lower age limit”
Planktonic Foraminifera Zone: <b><i>Globigerina nepenthes</i></b> – <b><i>Turborotalia siakensis</i></b> Zone (Upper Serravallian)	“Is characterised by a similar complex of planktonic foraminifers (as the above, undivided zone)” <i>Orbulina universa</i> , <i>Globigerina nepenthes</i>

Planktonic Foraminifera Zone: <b><i>Turborotalia</i></b> <b><i>continiosa</i></b> Zone (Upper Miocene)	Possible but very poor microfauna
Planktonic Foraminifera Zone: <b><i>Turborotalia</i></b> <b><i>acostaensis</i></b> Zone (Tortonian)	<i>Globorotalia menardii</i> , <i>G. scitula</i> , <i>Orbulina universa</i> , <i>Globigerinoides obliquus</i> , <i>G. extremus</i> , <i>G. bolli</i> , <i>G. trilobus</i> , <i>Gloigerina nepenthes</i> , <i>G. bulloides</i> , <i>G. decoraperta</i> , <i>G. quinqueloba</i> , <i>G. eamesi</i> , <i>Globigerinella aequilateralis</i> , <i>Globoquadrina dehiscens</i> , <i>G. altispira</i> , <i>Globigerinita glutinata</i> , <i>Borbulina bilobata</i> , <i>Turborotalia acostaensis</i> (few)
Planktonic Foraminifera Zone: Messinian	Mixed planktonic and benthic foraminifers assemblage: <i>Globorotalia apertura</i> , <i>G. involuta</i> , <i>Orbulina universa</i> , <i>Globigerina nepenthes</i> , <i>G. bulloides</i> , <i>Globigerinoides extremus</i> , <i>Globigerinita apennica</i> , <i>Bulimina echinata</i> , <i>B. aculeata</i> , <i>Valvulineria aff. complanata</i> , <i>Elphidium macellum</i> , <i>E. aculeatum</i> , <i>Cymbalopora vitrea</i> , <i>Cibicides lobatulus</i> , <i>C. boueanus</i> , <i>Uvigerina gaudryinoides</i> , <i>Bolivina dilatata</i> , <i>B. dentellata</i> , <i>B. variabilis</i>
Planktonic Foraminifera Zone: <b><i>Sphaeroidinellops</i></b> <b><i>Acme-Zone</i></b> (Basal Pliocene)	<i>Sph. Seminulina</i> , <i>Sph. Subdehiscens</i> , <i>Globigerinoides sacculifer</i> , <i>G. ruber</i> , <i>G. conglobatus</i> , <i>G. obliquus</i> , <i>G. extremus</i> , <i>G. trilobus</i> , <i>Orbulina universa</i> , <i>Globigerina nepenthes</i> , <i>G. bulloides</i> , <i>G. apertura</i> , <i>G. decoraperta</i> , <i>Globorotalia scitula</i> , <i>Globigerinella aequilateralis</i> , <i>Globoquadrina altispira</i>
Planktonic Foraminifera Zone: <b><i>Globorotalia</i></b> <b><i>margaritae evoluta</i></b> Zone (Pliocene)	<i>G. margaritae margaritae</i> , <i>G. margaritae evoluta</i> (both sparse) <i>Globigerinoides</i> , <i>Globigerina</i> , <i>Globoquadrina</i> and <i>Globigerinella</i> (frequent species of each) <i>Sphaeroidinellops</i> (disappears at the end of Lower Pliocene)
Planktonic Foraminifera Zone: Upper Pliocene	<i>Globigerinoides conglobatus</i> , <i>G. sacculifer</i> , <i>Orbulina universa</i> , <i>Globigerina bulloides</i> , <i>G. apertura</i> , <i>G. decoraperta</i> , <i>Globigerinella aequilateralis</i> , <i>Globorotalia scitula</i> , <i>G. inflata</i> (rare) <i>Globoquadrina</i> sp. <i>Globigerina nepenthes</i> and <i>Globorotalia margaritae</i> (missing)



				Planktonic Foraminifera and other biomarkers identified by Marcel BouDagher-Fadel (University College, London)
Cenozoic	Quaternary			No sample recorded
	Pliocene	Late		No sample recorded
		Early		<i>Globigerinoides</i> sp., <i>Orbulina</i> sp., <i>Sphaeroidinellopsis subdehiscens</i> , <i>Sphaeroidinella dehiscens</i> , <i>Dentoglobigerina altispira</i> , <i>Operculinella</i> sp.
	Neogene	Messinian		No sample recorded
		Tortonian		No sample recorded
		Miocene	Serravallian	<i>Globorotalia praemenardii</i> , <i>Orbulina bilobata</i> , <i>Orbulina universa</i> , <i>Orbulina suturalis</i> , <i>Dentoglobigerina altispira</i> , <i>Globigerinoides obliquus</i> , <i>Sphaeroidinellopsis sudehiscens</i> , <i>Globigerina</i> sp., <i>Orbulina</i> sp., <i>Globigerinoides</i> sp., <i>Bulimina</i> sp., <i>Globoquadrina</i> sp., <i>Valvulineria</i> sp., <i>Nodosaria</i> sp., With some small benthic foraminifera; <i>Bulimina</i> sp., <i>Cycloclypeus</i> sp., <i>Amphistegina</i> sp., <i>Elphidium</i> sp. plus ostracod and rodophytes fragments.
			Langhian	<i>Orbulina bilobata</i> , <i>Orbulina universa</i> , <i>Dentoglobigerina altispira</i> , <i>Globigerina decoraperta</i> , <i>Globigerinoides quadrilobatus</i> , <i>Praeorbulina glomerata</i> , <i>Praeorbulina transitoria</i> , <i>Globigerinoides trilobus</i> , <i>Globorotalia peripheroronda</i> , <i>Globorotalia mayeri</i>
			Burdigalian	No sample recorded
			Aquitania	<i>Rotalia</i> sp., <i>Miogypsinella</i> sp., <i>Miogypsinoides</i> sp., <i>Operculina</i> sp., <i>Lepidocyclina stratifera</i> , <i>Lepidocyclina (Nephrolepidina)</i>
	Palaeogene	Oligocene		No sample recorded
			Late	<i>Victoriella</i> sp., <i>Fabiania</i> sp., <i>Discocyclina</i> sp., <i>Rotalia</i> sp., <i>Operculina</i> sp.
		Eocene	Middle	<i>Discocyclina</i> sp., <i>Pellatispira</i> sp., <i>Operculina</i> sp., <i>Miscellanea</i> sp., <i>Globigerina</i> sp., <i>Nummulites</i> sp., <i>Alveolina</i> sp., <i>Turborotalia cerroazulensis</i> , <i>Turborotalia increbescens</i> , <i>Orbulinoides beckmanni</i>
			Early	No sample recorded
		Palaeocene	Late	<i>Morozovella velascoensis</i> , <i>Morozovella uncinata</i> , <i>Planorotalites pseudomenardii</i> , <i>Subbotina pseudobulloides</i> , <i>Globorotalia aequa</i> , <i>Assilina</i> sp.
			Early	No sample recorded
Mesozoic	Cretaceous	Senonian	Maastrichtian	<i>Subbotina pseudobulloides</i> , <i>Morozovella uncinata</i> , <i>Morozovella velascoensis</i> , <i>Globorotalia aequa</i> , <i>Rugoglobigerina rotundata</i> , <i>Planohedbergella</i> sp., <i>Globotruncana</i> sp., <i>Rugoglobigerina</i> sp., <i>Hedbergella</i> sp., <i>Spiroplecta</i> sp., <i>Globotruncana stuarti</i> , plus Ostracods

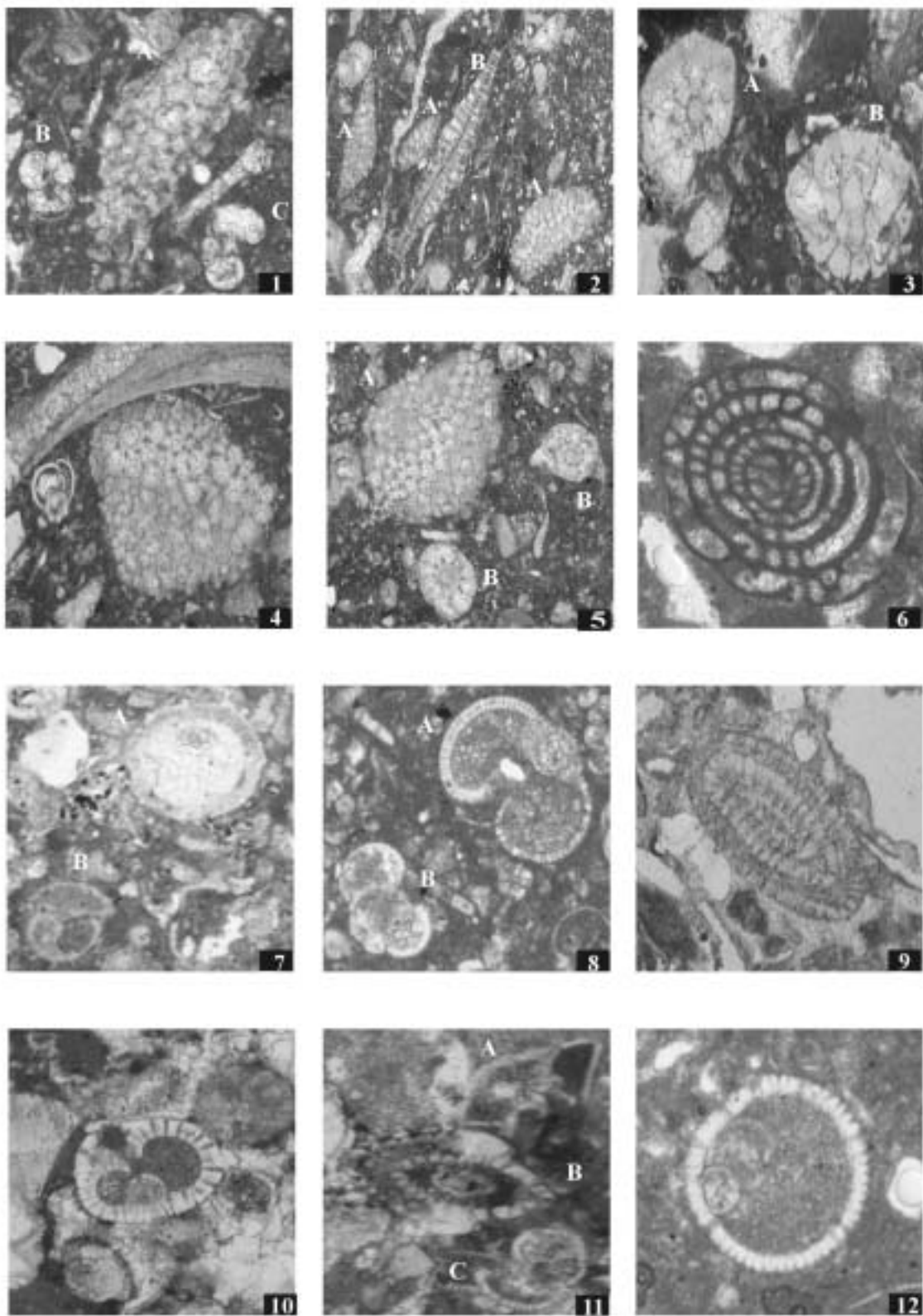
**Appendix 1. Figure 3.** Foraminiferal species identified by Marcel BouDagher-Fadel from samples collected during this project.

**Key to Figure 4** Plate 1 – Miocene/Pliocene photomicrographs of age diagnostic foraminifera (planktonic and benthic), by Marcel BouDagher-Fadel, University College, London.

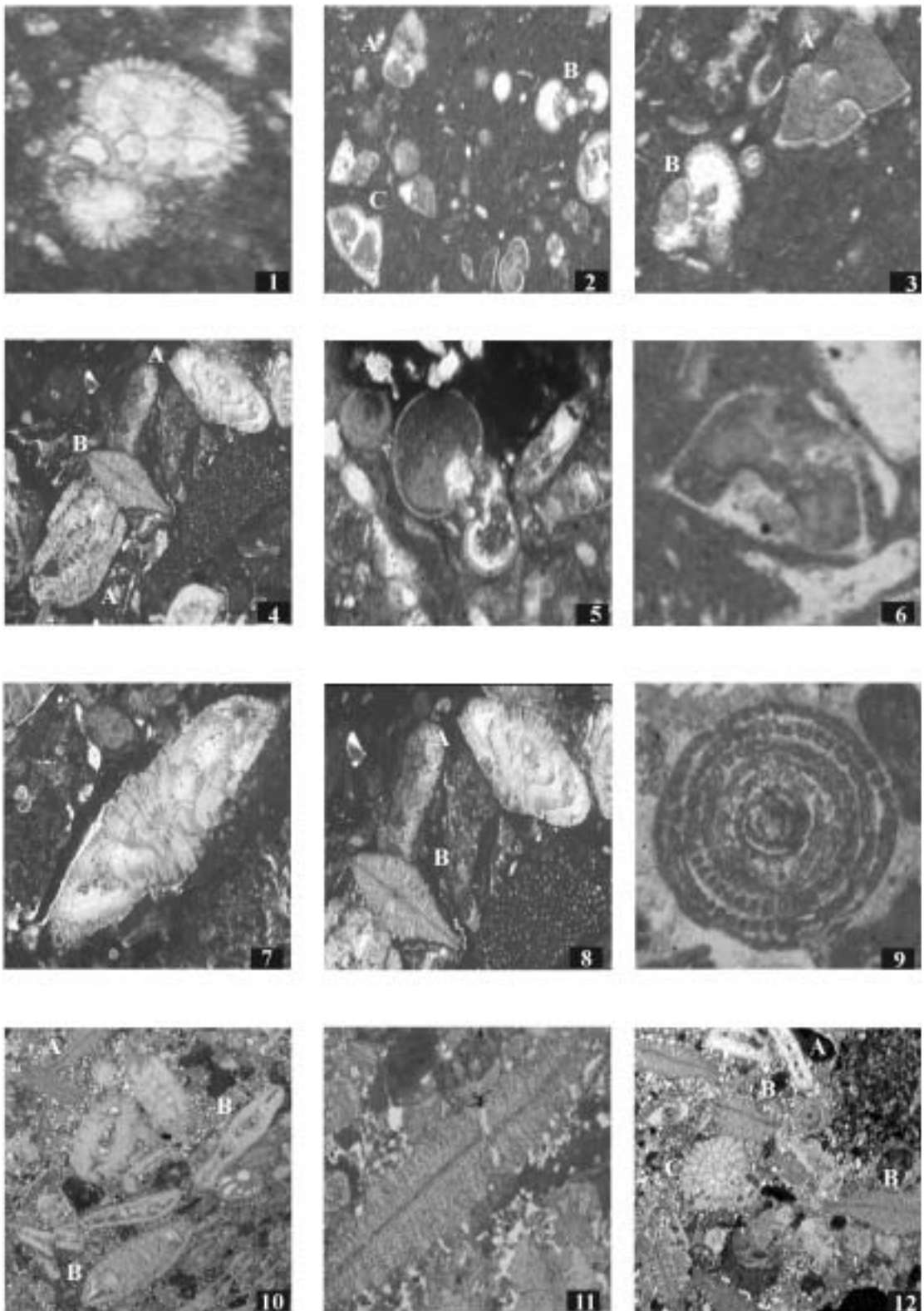
1. Aquitanian, N4. [A] oblique equatorial section of *Miogypsinoidea* sp., [B] *Globigerinoides* sp., [C] *Globorotalia peripheronda* (Blow and Banner), x38.
2. Aquitanian. [A] *Miogypsinoidea* sp., [B] *Lepidocyclina stratifera*?, x15.
3. Aquitanian. [A] equatorial section, [B] vertical section of *Paleomigypsina boninensis* (Matsumaru), x27.
4. Aquitanian. An equatorial section of *Miogypsinoidea* sp., showing the proloculus surrounded by a whorl of embryonic chambers, x27.
5. Aquitanian. [A] *Miogypsinoidea* sp., [B] *Paleomigypsina boninensis* (Matsumaru), x27.
6. Langhian, N9. *Borelis melo* (Fitchel and Moll), x25.
7. Upper Serravallian, N14. [A] *Praeorbulina glomerosa* (Blow), [B] *Globoquadrina* sp., x37.
8. Upper Langhian, N9. *Globorotalia semivera* (Hornibrook), x60.
9. Aquitanian, N4. *Cellanthus craticulatus* (Fitchel and Moll), x27.
10. Upper Serravallian, N13. A vertical section of *Sphaeroidnellops subdehiscens* (Blow), x62.
11. Serravallian, N12. [A] *Globorotalia praemenardii* (Cushman and Stainforth), [B] *Elphidium crispum* (Linné), [C] *Globigerinoides* sp., 0.8mm
12. Lower Pliocene. Vertical section of *Orbulina Universa* (d'Orbigny), x80.

**Key to Figure 5** Plate 2 – Cretaceous/Palaeocene/Eocene photomicrographs of age diagnostic foraminifera (planktonic and benthic), by Marcel BouDagher-Fadel, University College, London.

1. Maastrichtian. *Rugoglobigerina* sp., x90.
2. Upper Palaeocene. [A] *Morozovella velascoensis* (Cushman), [B] *Pseudohastigerina*, [C] *Morozovella aequa* (Cushman and Renz), x32.
3. Upper Palaeocene. [A] *Morozovella uncinata* (Bolli), [B] *Morozovella velascoensis* (Cushman), x50.
4. Upper Middle Eocene. [A] *Nummulites* sp., [B] *Discocyclina* sp., x10.
5. Upper Palaeocene. Vertical section of *Morozovella pseudobulloides* (Plummer), x110.
6. Upper Palaeocene. *Morozovella* cf. *aequa* (Cushman and Renz), x115.
7. Upper Middle Eocene. A vertical section of a megalospheric form of *Pellatispira* sp. x13.
8. Upper Middle Eocene. Vertical sections of [A] *Pellatispira* sp., [B] *Discocyclina* sp., x14.
9. Upper Middle Eocene. *Aveolina* sp., x29.
10. Upper Eocene. [A] *Discyclina* sp., [B] *Operculina* sp., x13.
11. Upper Eocene. A vertical section of *Lepidocyclina* sp., x29.
- Upper Eocene. [A] *Operculina* sp., [B] *Discocyclina* sp., x10.



**Appendix 1, Figure 4.** Plate 1. Project foraminifera identified by Marcelle BouDagher-Fadel. See text for details.



**Appendix 1, Figure 5. Plate 2.** Project foraminifera identified by Marcelle BouDagher-Fadel. See text for details.

<b>Time period</b>	<b>Diagnostic nannofossils</b>	<b>Supplementary fauna and remarks</b>
<b>Early Pliocene</b>	<i>Pseudoemiliana lacunosa</i> , <i>Discoaster calcaris</i> , <i>D. broweri</i> , <i>D. asymmetricus</i> , <i>D. surculus</i> , <i>Syracosphaera pulchra</i> , <i>Calcidiscus macintyreii</i> , <i>Umbilicosphaera rotula</i> . Sphenoliths are absent.	Common reworked Cretaceous and Palaeogene taxa. Ascidian spicules present.
<b>Late Miocene- Early Pliocene</b>	<i>Calcidiscus leptoporous</i> , <i>Calcidiscus mcintyreii</i> , <i>C. tropicus</i> , <i>Helicosphaera mediterranea</i> , <i>Sphenolithus moriformis</i> , <i>S. cf. S. abies</i> , <i>Sciphosphaera apsteini</i> , <i>Discoaster surculus</i> , <i>D. variabilis</i> , <i>D. exilis</i> , <i>Umbilicosphaera jafari</i> , <i>U. rotula</i> , <i>Sphenolithus abies</i> , <i>Sciphosphaera cylindrica</i>	Abundant Ascidian spicules. Reworked nannofossils outnumber those <i>in situ</i> – mainly from Palaeogene (Danian to Late Oligocene). Cretaceous taxa also present.
<b>Late Miocene</b>	<i>Calcidiscus leptoporous</i> , <i>Calcidiscus mcintyreii</i> , <i>C. tropicus</i> , <i>Reticulofenestra gelida</i> , <i>Helicosphaera carteri</i> , <i>Sphenolithus moriformis</i> , <i>Sphenolithus cf. S. abies</i> .	Abundant Ascidian spicules. Common reworked Eocene and Oligocene taxa ; rare reworked Cretaceous taxa. Discoasters absent (unusual), very proximal setting?
<b>Miocene</b>	<i>Calcidiscus leptoporous</i> , <i>Calcidiscus mcintyreii</i> , <i>Helicosphaera carteri</i> , <i>Reticulofenestra gelida</i> , <i>Discoaster exilis</i> group, 6-rays overgrowth <i>discoasters</i> spp.	Rare reworked Cretaceous and Eocene taxa. Coccoliths are very small size – restricted environment?

**Appendix 1. Figure 6.** Nannofossil species identified by Sylvia Gardin, from Nahr El-Kabir Valley samples.

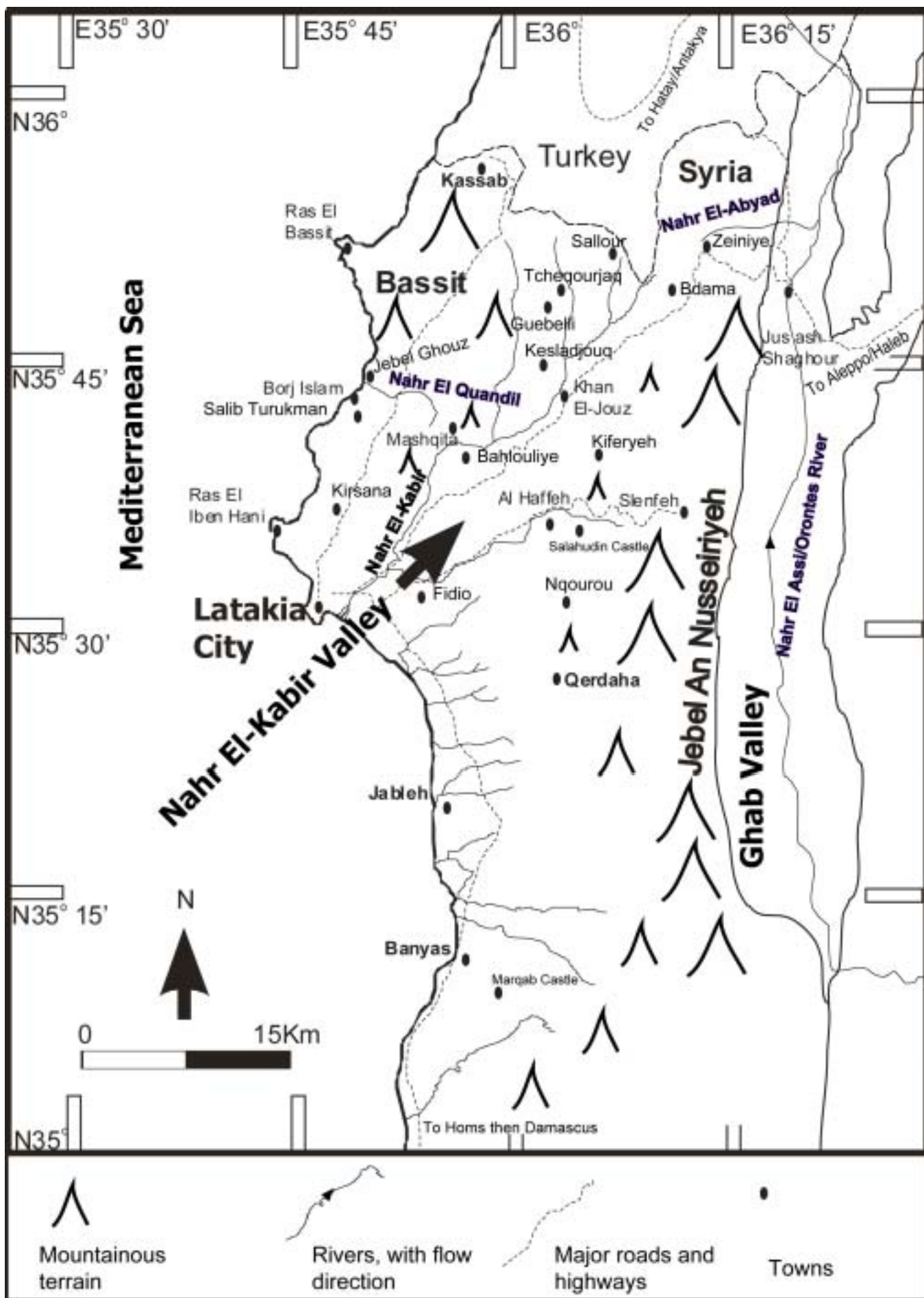
**Ascidian spicules** – from Ascidians or Tunicate, more commonly known as sea-squirts.

Habitats ([www.usgs.gov](http://www.usgs.gov)), full salinity marine conditions in sheltered water with little tidal or wave action. Often found on bedrock or bouldery substrate with silts and encrusting algae. Littoral water depth to a maximum of 50m, more commonly 25m water depth, although not in direct sunlight.

## **Appendix 2**

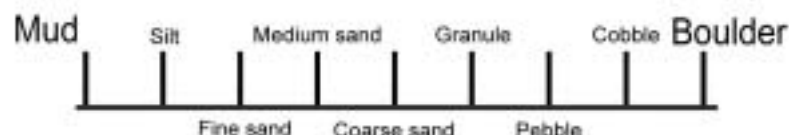
### ***Pull-out maps and figure key***



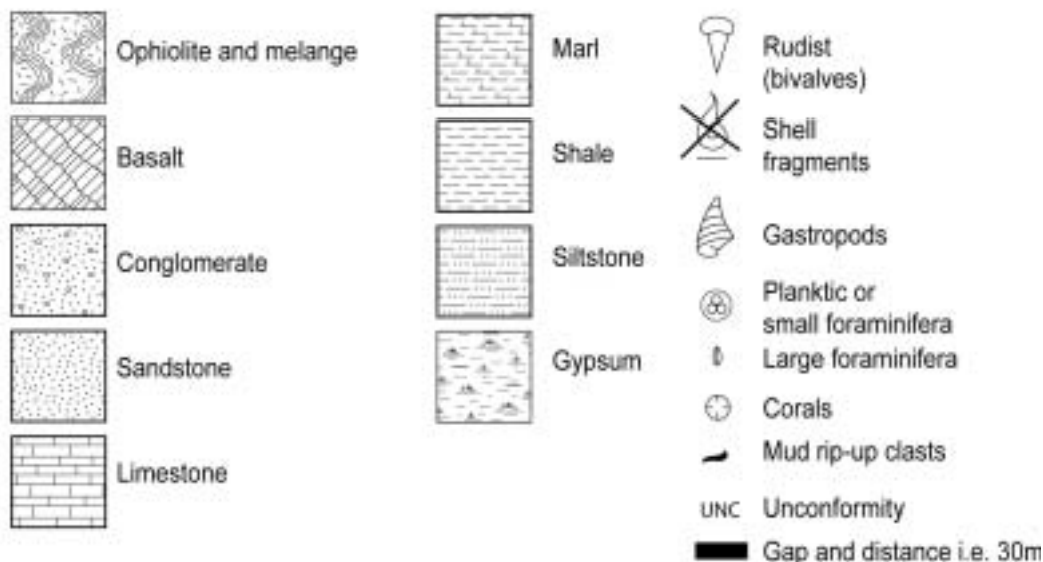


**Pull-out location map -** Project area location map, showing major towns, villages and topography.

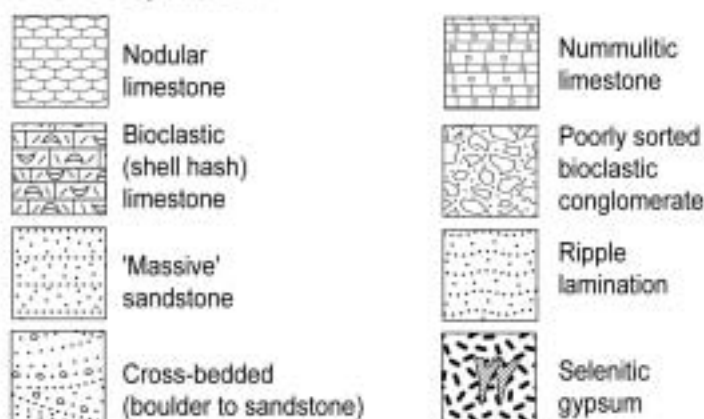
## Grain size



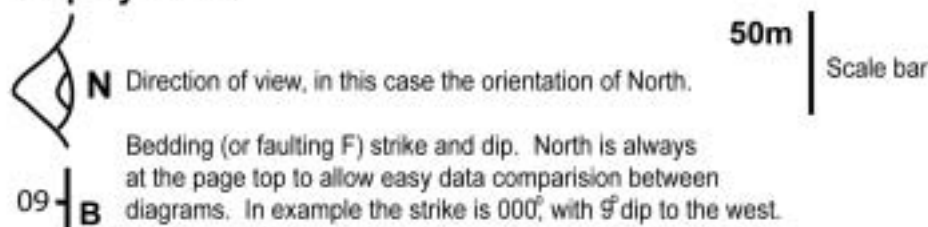
## Lithological symbols



## Facies symbols



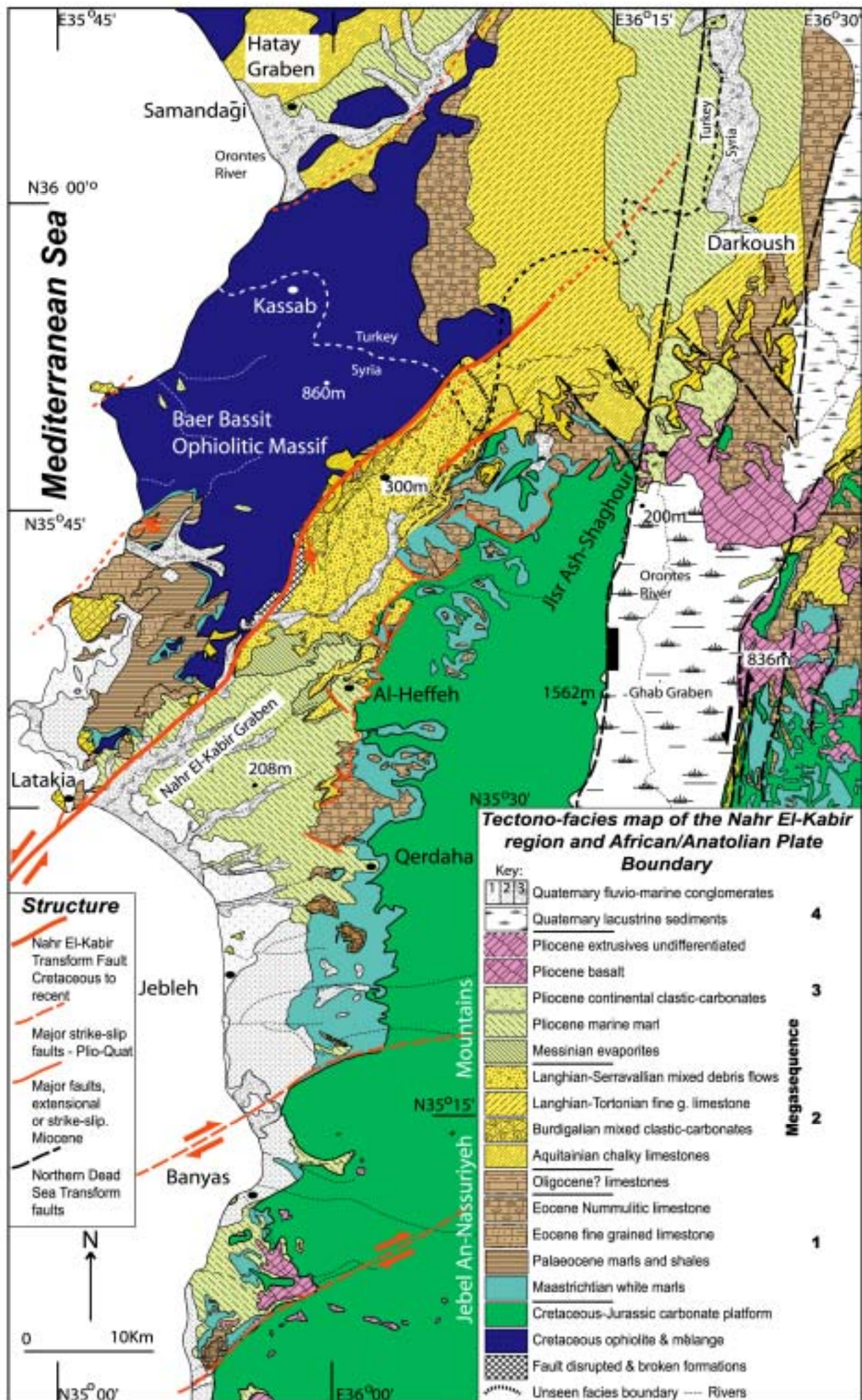
## Map Symbols



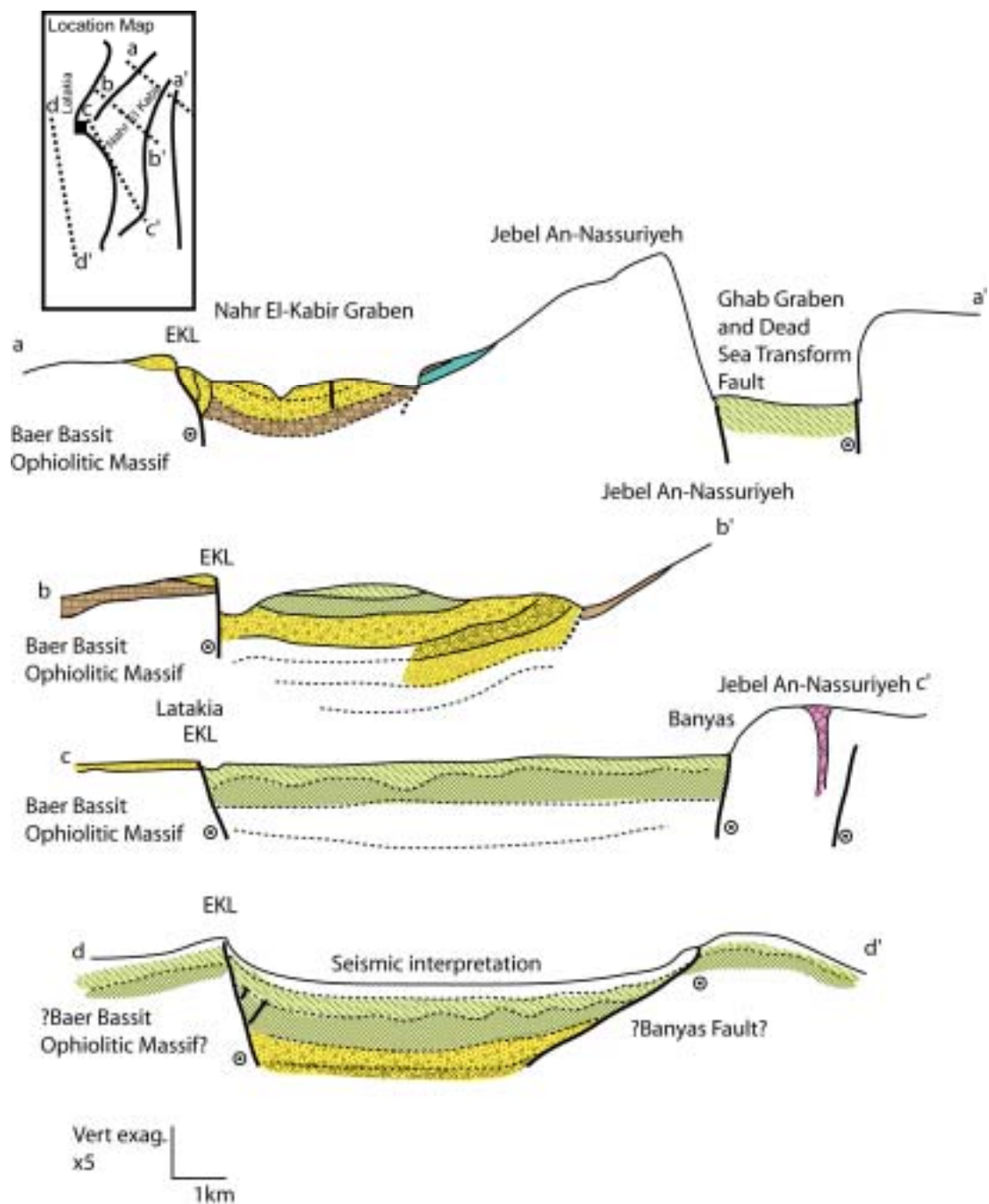
**XPL, PPL** Refer to crossed polarised and plain polarised light microscopy

**Pull-out key.** Key to diagrams, logs and maps used throughout this thesis (unless otherwise given)





**Pull-out Geological Map - interpretation from this study**

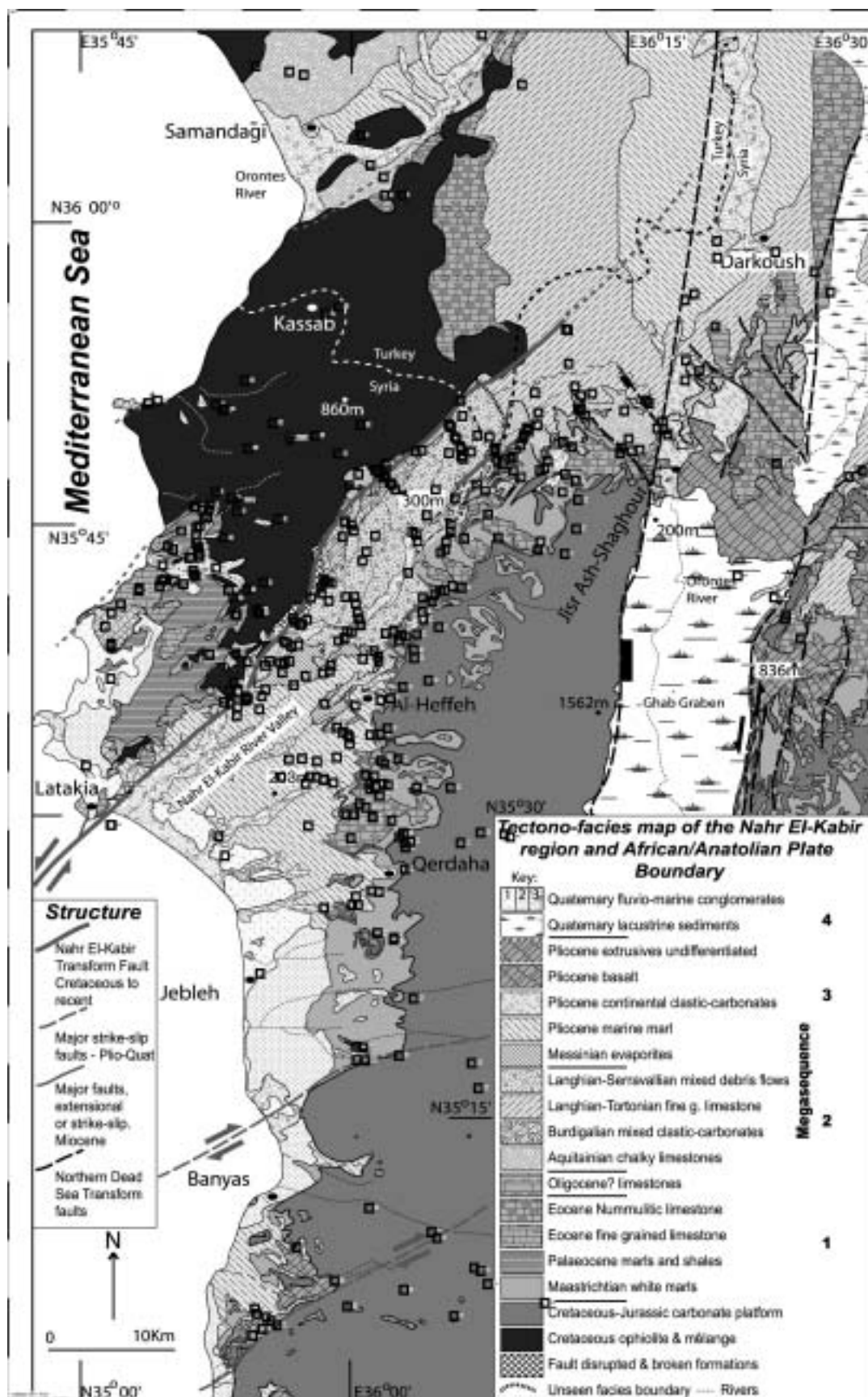


**Pull-out cross sections** of the Nahr El-Kabir Graben and offshore extension.

# **Appendix 3**

## ***Field localities***





**Appendix 3.** Fieldwork localities in the Nahr El-Kabir region utilised during 1999-2001 field-seasons. 410 localities.